Iliya Boguslawsky · Nikolay Korovkin
Masashi Hayakawa

Large A.C. Machines

Theory and Investigation Methods of Currents and Losses in Stator and Rotor Meshes Including Operation with Nonlinear Loads

Springer

Large A.C. Machines

Iliya Boguslawsky · Nikolay Korovkin
Masashi Hayakawa

Large A.C. Machines

Theory and Investigation Methods of Currents and Losses in Stator and Rotor Meshes Including Operation with Nonlinear Loads

Springer

Iliya Boguslawsky
Peter the Great St. Petersburg Polytechnic University
Saint Petersburg
Russia

Nikolay Korovkin
Peter the Great St. Petersburg Polytechnic University
Saint Petersburg
Russia

Masashi Hayakawa
The University of Electro-Communications
Tokyo
Japan

ISBN 978-4-431-56473-7 ISBN 978-4-431-56475-1 (eBook)
DOI 10.1007/978-4-431-56475-1

Library of Congress Control Number: 2016955911

Printed on acid-free paper

This Springer imprint is published by Springer Nature
The registered company is Springer Japan KK
The registered company address is: Chiyoda First Bldg. East, 3-8-1 Nishi-Kanda, Chiyoda-ku, Tokyo 101-0065, Japan

Preface

Modern high-power electrical machines differ in the increased electromagnetic, mechanical, and thermal levels from those of former years. This book will provide progress in the development of heavy electric machine building and raise technical and economic indicators and competitiveness of machines. This is true not only of machines operating in networks of industrial frequency, but also of those in networks with nonlinear elements (in nonlinear networks), for example, with frequency converters.

Practice makes great demands of professional knowledge from their creators, knowledge that should be useful at the modern level of the power industry. Profound academic knowledge only in any single engineering area, for example, in the field of heat transfer, will help an engineer only a little in his production activity. For the solution of a wide complex of problems, an engineer at work is required to have knowledge of electromagnetism, thermal problems of heat transfer and ventilation, durability of structures, insulation of windings, technology, and related areas, all of which are inseparably linked with production.

It should be noted that unfortunately production usually does not give much time to engineers for extensive bibliographic searches and investigations connected with the solution of problems.

For these reasons, an effective link of production with scientific organizations is extremely important (to universities, Russian Academy of Sciences, for instance). For ensuring this link, a factory engineer should be able to:

- formulate correctly problems together with scientists (for example, to be able to correctly formulate boundary conditions if the problem is solved using differential or difference equations describing an investigation process);
- estimate intermediate and end results of solutions and to actively participate in their discussion with experts from scientific organizations;
- use correctly and comprehensively solution results of all these problems in machine construction taking into account factory technological capability.

Let us note that with the use of the results of investigations, factory engineers can make a final decision on the selection of machine construction and its units following the specifications, requests by IEC, and so on.

One of additional peculiarities in the work of modern factory engineers in collaboration with scientists is the search for technological compromises in the solution of production problems, because physical processes are interconnected. The complex solution of engineering problems also has another peculiarity. It is based on the synthesis of factory experience and its use for the generation of uniform investigation, calculation, and design methods for machines of various types produced by a factory.

The contents of this monograph fully meet the requirements of science for engineers at work. The reason is that real problems are solved, connected with the generation and operation of large, modern A.C. machines, including their operation with nonlinear loads.

The monograph shows how to solve specific practical problems. Based on the production and scientific activities of the authors, these problems were solved to the extent they arose in practice. Those results were published in the past 10–15 years and in many articles in domestic [USSR (Russia)] and foreign (Germany, USA, Czech Republic, Poland) journals, and were discussed in a number of international conferences. Their generalization in the form of a monograph allows us to study, in strict and consecutive statements based on uniform positions, the complex problem of creation and operation of motors and generators.

In spite of the fact that many problems studied in this monograph are difficult, much attention is paid to physical processes, so that the contents are illustrated by examples from engineering practice. When writing this book, we have followed the fundamental idea by Dr. Ruedenberg by citing the sentences of the preface of his book (1950) because his intention is exactly the same as ours.

> From experience of more than 30 years as an engineer and still longer as a teacher, I have learned that in the minds of students of engineering those methods of solution for intricate problems survive best, until an opportunity for application occurs, which are of the greatest possible simplicity. All the higher and more involved methods are more suitable for applied mathematicians and theoretical researchers than for engineers in practice, even if they are working scientifically. For engineers the physical understanding of the analysis of the example and the ease of discussion of the result are of greater importance than the mathematical rigor and generality of the method of solution.
>
> Reinhold Ruedenberg, *Transient Performance of Electric Power Systems*. McGraw–Hill Book Company, Inc., 1950 (New York–Toronto–London).

All this allows recommending this monograph to a wide range of experts in the field of development, operation, and repair of heavy motors and generators, as well as in the field of study of physical processes in various modes.

Saint Petersburg, Russia — Iliya Boguslawsky
Saint Petersburg, Russia — Nikolay Korovkin
Tokyo, Japan — Masashi Hayakawa

Acknowledgments

In solving all these problems, and then in starting this edition of the monograph, the authors worked together with experts and teams that always rendered them full assistance and support.

The authors express profound gratitude to:

Academician of the Russian Academy of Sciences, Demirchyan K.S. Owing to his long-term help, actual engineering problems have been solved connected with the development in the operational and reliability increase of new types of high-power turbogenerators, low-voltage diesel generators, and induction and synchronous motors in a wide power range.

The administration of Peter the Great St. Petersburg Polytechnic University (SPbPU) for full support at all stages of the monograph edition.

The staffs of electro-engineering works "Elektrosila" Work, the Stock Company "Power Machines" and LEZ, and the Stock Company "Ruselprom", St. Petersburg, where this work was carried out.

The staffs of Electrical Machines and Theoretical Electrical Engineering departments of SPbPU, where stages of the solutions of a number of problems and obtained results were discussed.

The staff of the "Peterburgskiy Energetik" firm. Many engineering solutions underwent additional testing in this firm, which specializes in repair and service of large machines.

The staff of the All-Russian Research Institute of Power Engineering (VNIIE) (Moscow), where stages of solutions of a number of problems and obtained results were discussed.

The staff of the Laboratory of Power Engineering of Academician RAS. Danilevich Ya. B., the Federal State Institution of the Science Institute of Silicate Chemistry, Russian Academy of Sciences (RAS IHS), St. Petersburg, where stages of solutions of a number of problems and obtained results were discussed.

The staff of the translation agency LITERRA, St. Petersburg. This firm made the translation in a short time and taking into account all wishes of the monograph's authors.

The management and staff of the publisher Springer (Springer-Verlag up to 1999), which intelligently carried out the work with authors of the monograph at all stages of its edition.

The authors hope that the number of scientists and specialists who participate in the creation of new modern A.C. machines for the different branches of industry will increase in the near future. The problems of developing new high-voltage insulation (with increasing values of thermal conductivity) of the electrotechnical sheet with reduced values of specific losses, of the massive rotors, and the ending bell ringing with elevated levels of strength, of the new types of frequency converters, and so on., the increase of efficiency will remain as it currently is.

Contents

1 Problems Formulation 1
1.1 Requirements to High-Power A.C. Motors and Generators 1
1.2 Actual Problems of Modern Electric Machine-Building Industry; Their Solution in the Monograph 4
1.3 Presentation Order of Monograph Contents and Structure 7
1.3.1 Choice of Investigation Methods: Position of Monograph's Authors 7
1.3.2 Presentation Order of Monograph Contents 8
1.3.3 Checking Methods Developed in the Monograph 9
1.3.4 Symbols Accepted in the Monograph 9
1.4 Order of References 10

2 Investigation Methods of Performance Characteristics for Double-Fed Machines with Converter in Rotor Circuit. Summary of Main Investigation Stages of A.C. Machines 13
2.1 Peculiarities of Investigation Methods 13
2.2 Problem Statement 15
2.3 Frequencies and Amplitudes of Voltage and Current First Harmonics in Machine Rotor and Stator Windings 16
2.3.1 Ratio of Frequencies $f_{ROT,1}$ and $f_{ST,1}$ at n_{REV} = var 16
2.3.2 Ratio of Voltages $U_{ROT,1}$ and $U_{st,1}$ at n_{REV} = Var 17
2.4 Frequencies and Amplitudes of Voltage and Current Higher Time Harmonics in Machine Rotor and Stator Windings 18
2.4.1 Ratio of Frequencies $f_{ROT,Q}$ and $f_{ST,Q}$ at n_{REV} = var 19
2.4.2 Ratio of Voltages $U_{ROT,Q}$ and $U_{ST,Q}$ at n_{REV} = var 19
2.5 Method for Solving Both Problems; Two Systems of Equations 21

2.5.1 Magnetization Characteristics Presentations $\boldsymbol{\theta}_{0.1} = \boldsymbol{\theta}\left(F_{M.C.,1}\right)$ in Piecewise Linear Function Form . . . 21
2.5.2 Peculiarities of Solving Both Systems . . . 22
2.6 Check of Methods . . . 23
2.7 Excitation System Peculiarities . . . 24
2.8 Summarizing the Results: Main Stages of A.C. Machine Investigations with Rotor Short Circuited Windings . . . 24
2.8.1 Stator and Rotor Circuits Frequency Voltage. Rotational Speed of Rotor and Stator Fields in Air Gap . . . 24
2.8.2 Ampere's Law Equations . . . 25
2.8.3 Kirchhoff's Second Law Equations for Stator Winding . . . 25
2.8.4 Kirchhoff's Second Law Equations for Rotor Loops. System of Equations . . . 26
Appendix 2.1 . . . 26
A.2.1.1 DFM Rotor Current and MMF Under Load . . . 27
A.2.1.2 Phase Angle Defining Complex Amplitudes Position of MMF $F_{ROT,1}$ and Current $I_{ROT,1}$ (in Stator Coordinates) . . . 29
A.2.1.3 Rotor Winding Voltage, Its Components . . . 29
A.2.1.4 Phase Angle Defining Complex Amplitude Position $U_{ROT,1}$ . . . 30
A.2.1.5 Rotor Winding Power Factor; Active and Reactive Winding Power; Rotor Winding Losses . . . 30
A.2.1.6 DFM Rotor Winding Design Peculiarities . . . 30
Appendix 2.2 . . . 31
Brief Conclusions . . . 32
References . . . 33

3 Stator MMF Harmonics at Non-sinusoidal Machine Power Supply (for M ≥ 1, Q ≥ 1) . . . 37
3.1 Initial Data and Its Representation . . . 37
3.2 Stator Winding Design Peculiarities; Its Number of Phases m_{PH} . . . 39
3.3 MMF Harmonics at $m_{PH} = 3$ . . . 40
3.4 MMF Harmonics at $m_{PH} = 6$ . . . 43
3.5 MMF Harmonic Comparison at $m_{PH} = 3$ and $m_{PH} = 6$ . . . 45
3.6 EMF Frequency in Magnetically Coupled Loops ($m_{EL} \geq 1$, $Q \geq 1$) . . . 47
3.6.1 Salient Pole Machines Operating in Synchronous Speed Modes . . . 47
3.6.2 A.C. Machines in Asynchronous Modes $\left(\omega_{REV} \neq \frac{\omega_1}{p}\right)$ . . . 51

3.7 MMF Harmonics of Magnetically Coupled Loops in Multiphase Stator Winding at Non-sinusoidal Power Supply and their Representation . . . 53
3.8 Magnetically Coupled Loops in Machine Operating with Nonlinear Network Elements . . . 54
Appendix 3.1 . . . 56
Brief Conclusions . . . 57
References . . . 58

4 Peculiarities of Currents Investigation in Magnetically Coupled Circuits for A.C. Machines with Short-Circuited Rotor Windings . . . 61
4.1 General . . . 62
4.2 The Problem Determination and Algorithm of Solution . . . 63
4.3 Method Investigating of Operation Characteristics of Powerful Squirrel Cage Motors with Nonlinear Parameters . . . 68
4.4 Experimental Data and Calculating Results Comparison for the Torque M on the Shaft Depended on Slip S_{SL} for DAZ-Type Motor . . . 72
4.5 Generalized Characteristic of Rotor Current in Cage Elements . . . 73
Appendix 4.1: Screen Calculation Method of Large Low-Frequency Motor Pole Shoe . . . 75
A.4.1.1 Simply Connected Domain . . . 76
A.4.1.2 Multiply Connected Domain . . . 84
A.4.1.3 Irregular Grid with Arbitrary Configuration Elements . . . 85
A.4.1.4 The Screen Element D.C. Resistance Depends on the Temperature Distributed in It (Nonlinear Problem); the Domain Is Simply—Or Multiply Connected . . . 85
A.4.1.5 Screen Element Reactance Accounting . . . 86
Appendix 4.2: Determination of Average Flux Density Point Location by "Mean Value Theorem (Lagrange)" . . . 87
Appendix 4.3: Equivalent Circuit of Powerful Induction Motors Operating in Nonlinear Networks . . . 87
A.4.3.1 Basic Equations of Powerful Asynchronous Machine Substitution Patterns ($Q_{TIM} \geq 1$) . . . 88
A.4.3.2 Machine Circuit Losses Components and Shaft Power . . . 90
A.4.3.3 Additional Losses and Equivalent Circuit Impedances . . . 92
Brief Conclusions . . . 93
References . . . 96

5 Representation of Currents in Rotor Short-Circuited Winding Elements in the Form of Generalized Characteristics 99
5.1 Problem Statement 99
5.2 Initial Data and Its Representation 101
5.2.1 Representation of Resulting Field Harmonics in Air Gap 101
5.2.2 Geometrical Dimensions of Winding Elements. Designation of Loop EMF 103
5.2.3 A.C. Resistances and Reactances, Currents in Winding Elements 103
5.3 System of Equations and Peculiarities of Matrix Structure of Its Coefficients 104
5.4 Solution Results: Currents in Elements of Short-Circuited Rotor Windings. Their Generalized Characteristics 106
5.5 Accounting of "Adjacent" Harmonics Fields by Means of Generalized Characteristics of Currents 109
5.6 Peculiarities of Numerical Realization of System of Equations for Calculation of Generalized Characteristics 110
Brief Conclusions 110
References 112

6 Passive Quadripoles; Recurrent Circuits of Various Structure: Investigation of Their Peculiarities for Modeling Process of Currents Distribution in Short-Circuited Rotor Windings 115
6.1 General Comments 115
6.2 Representation of Short-Circuited Rotor Winding Elements in the Form of Quadripoles and Recurrent Circuits 116
6.3 Passive Symmetrical and Asymmetrical Quadripoles 116
6.4 Structural Features of Passive Symmetrical and Asymmetrical Recurrent Circuits 117
6.5 Methods of Investigation of Passive Symmetrical Recurrent Circuits Described by "Step" or "Lattice" Functions 120
6.5.1 Difference Equations, Methods of Their Solution 120
6.5.2 Pecularities of Currents Distribution in Symmetrical Passive Recurrent Circuits 124
6.6 Open Passive Recurrent Circuits. Constants for Calculation of Currents Distribution Calculation Examples 125
6.6.1 General Comments 125
6.6.2 System of Equations for Constants 126
6.6.3 Calculation Examples 127
6.7 Investigation Methods of Passive Asymmetrical Recurrent Circuits 129
6.7.1 Difference Equations, Methods of Their Solution 129

6.7.2 Constants of Asymmetrical Passive Open Recurrent Circuit; Their Determination 132
6.7.3 Calculation Examples 134
Appendix 6.1 136
Brief Conclusions 136
References. 138

7 Active Symmetrical and Asymmetrical Chain Circuits: Investigation of Their Peculiarities for Modeling Process of Currents Distribution in Short-Circuited Rotor Windings. 139
7.1 Main Definitions. Structural Kinds of Active U-Shaped Chain Circuits and Peculiarities of EMF Distribution of Loops 140
7.2 Methods of Investigation of Active Symmetrical Chain Circuits with EMFs Changing Depending on Number of Link Under the Harmonic Law 142
7.2.1 Difference Equations, Methods of Their Solution 142
7.2.2 Constants for Currents in Active Open Symmetrical Chain Circuits 144
7.2.3 Constants for Currents in Active Closed Symmetrical Chain Circuits 145
7.2.4 Constants for Currents in Regular Closed Chain Circuits 146
7.3 Methods of Currents Investigation in Asymmetrical Active Open and Closed Chain Circuits 150
7.3.1 Method of Investigation of Currents in Active Open Chain Circuits with Asymmetrical (Damaged) Elements. Calculation Example 151
7.3.2 Method of Investigation of Currents in the Active Closed Chain Circuits with Asymmetrical (Damaged) Elements: Calculation Example 154
7.3.3 Modification of the Investigation Method of Currents in the Active Closed Chain Circuits with Asymmetrical (Damaged) Elements: Calculation Examples 158
Appendix 7.1 161
Appendix 7.2 161
Brief Conclusions 162
References. 163

8 EMF Induced by Resulting Field in Short-Circuited Loops of Damper Winding and Squirrel Cage 165
8.1 Initial Data and Its Representation 165
8.1.1 Representation of Resulting Field Harmonics in Air Gap 166

8.1.2 Initial Geometrical Dimensions of Damper Winding, Squirrel Cage, Pole Winding 167
8.2 Two EMF Components in Loops of Short-Circuited Rotor Winding 169
8.2.1 General Problem: EMF in Any Loop of Short-Circuited Winding 169
8.2.2 EMF of Damper Winding Loops Located on Pole . . . 171
8.2.3 EMF of Damper Winding Loops Located on Cross Axis q 172
8.2.4 EMF of Loops in Squirrel Cage 173
8.2.5 Excitation Winding EMF. 175
Brief Conclusions 176
References. 178

9 Investigation Methods of Currents Distribution in Regular Damper Windings and Squirrel Cages 179
9.1 Compliance Between Structures of Recurrent Circuits and Constructions of Short-Circuited Rotor Windings (Damper Winding, Squirrel Cages). 180
9.2 Symmetrical Squirrel Cage of Induction Machine. 181
9.3 Two Definitions in Investigation of Currents in Squirrel Cage Loops; Their Compliance and Areas of Correctness 183
9.4 Damper Winding of Salient Pole Machine 187
9.5 Checking Results: Transformation of Expression for Currents in Elements of Complete Damper Winding of Synchronous Machine in Expression for Currents in Squirrel Cage Elements of Induction Machine 192
9.6 About the Determination of Damper Winding Reactances Based on Solution Obtained in This Chapter on Distribution of Currents in This Winding (Discussion Between L. A. Kilgore, Westinghouse El. Corp. and M. E. Talaat, Elliott Comp.). 194
Appendix 9.1: Method of Calculation of Overheats of Short-Circuited Rotor Winding Elements at Start-Up with Account for Change of the Main and Additional Losses in it from Temperature (with Account of Skin Effect) 197
Brief Conclusions 199
References. 201

10 Investigation Methods of Currents Distribution in Squirrel Cages with Asymmetry 203
10.1 General Comments 204
10.2 Currents in Asymmetrical Squirrel Cages of Induction Machine Rotors 204
10.2.1 Squirrel Cage with Asymmetrical Rotor Bar 205

10.2.2 Squirrel Cage with Two (Not Adjacent) Asymmetrical Bars in Rotor. Additional Currents in Winding Elements . . . 205
10.2.3 General Problem: Squirrel Cage with Several (Not Adjacent) Asymmetrical Bars. Additional Currents in Winding Elements . . . 206
10.2.4 Squirrel Cage with Three Adjacent Asymmetrical Bars (with Damages). Additional Currents in Winding Elements . . . 209
10.2.5 Squirrel Cage with Three Asymmetrical Bars (with Damages): Two Bars Nearby, the Third—Next but One. Additional Currents in Winding Elements . . . 209
10.2.6 Squirrel Cage with Three Asymmetrical Bars: Three Bars, not Adjacent. Additional Currents in Winding Elements . . . 210
10.2.7 Calculation Example . . . 211
Appendix 10.1: Additional Currents in Eq. (10.2) for Squirrel Cage with Two (Not Adjacent) Asymmetrical Bars . . . 211
Appendix 10.2: Additional Currents in Eqs. (10.6) for Squirrel Cage with Three Adjacent Asymmetrical Bars . . . 212
Appendix 10.3: Additional Currents in Eq. (10.7) for Squirrel Cage with Three Asymmetrical Bars: Two Bars Nearby, the Third—Next but One . . . 213
Appendix 10.4: Additional Currents in Eq. (10.8) for Squirrel Cage with Three Asymmetrical Bars: Three Bars, Not Adjacent . . . 213
Brief Conclusions . . . 214
References . . . 216

11 Investigation Methods of Currents Distribution in Irregular Damper Windings . . . 219
11.1 Currents in Damper Windings with Bars of Various Impedance on Each Pole . . . 220
11.1.1 General Comments . . . 220
11.1.2 Initial Data and Calculation Method for Currents in Winding Elements . . . 220
11.2 Currents in Damper Winding with Damaged Bar on Pole . . . 226
11.2.1 General Comments . . . 226
11.2.2 Initial Data and Method of Calculating Currents in Winding Elements . . . 227
Appendix 11.1 . . . 231
Appendix 11.2 . . . 231
Appendix 11.3 . . . 234
Appendix 11.4 . . . 234
Brief Conclusions . . . 235
References . . . 236

12 MMF of Damper Winding, Squirrel Cage (at Asymmetry in Them or at Its Absence) and Excitation Winding. Representation of MMF in the Form of Harmonic Series in Complex Plane 239
12.1 Fundamental Assumptions 239
12.2 Representation of Damper Winding and Squirrel Cage MMFs (at Asymmetry or Its Absence in Them) in the Form of Step Function 241
12.2.1 Initial Data and Their Representation 241
12.2.2 Peculiarities of Representing MMF and Field of Damper Winding and Squirrel Cage Currents in the Form of Step Function 242
12.3 General Method of Calculating MMF Harmonics and Fields of Rotor Currents; Use of Symbolical Method of Representation of Currents in Combination with Complex Form of Harmonic Series Representation (Fourier) 246
12.3.1 Physical Treatment of Method. Calculation Expressions for Terms of Harmonic Series 246
12.3.2 General Expressions for Calculation of Complex Amplitudes of MMF Harmonics in Short-Circuited Winding of Arbitrary Construction 248
12.4 MMF and Field Harmonics in Squirrel Cage with Damages for Induction Machine (General Problem). 249
12.4.1 MMF Harmonics and Fields of Asymmetrical Squirrel Cage (with One Damaged Bar); Its Number Is $N = N_P$ 251
12.4.2 MMF Harmonics and Fields of Asymmetrical Squirrel Cage (Three Adjacent Damaged Bars); Their Numbers Are: $N = 0$, $N = 1$, $N = 2$. 252
12.4.3 MMF Harmonics and Fields of Asymmetrical Squirrel Cage (Three Damaged Bars: Two Are Adjacent, the Third Is Next Nearest; Their Numbers Are: $N = 0$, $N = 2$, $N = 3$). 252
12.4.4 MMF Harmonics and Fields of Asymmetrical Squirrel Cage (Three Damaged Non-adjacent Bars); They Numbers Are: $N = 0$, $N = N_{P2}$, $N = N_{P3}$. 253
12.5 Harmonics of MMF and Fields of Symmetrical Squirrel Cage (Without Damages). Checking Results. 253

12.6 MMF Harmonics of Irregular Damper Windings 256
12.6.1 First Construction Version of Irregular Damper Winding: Bars with Different Impedance Are Located Only on One or on Only Several Poles 256
12.6.2 Second Construction Version of Irregular Damper Winding: Bars with Various Impedances Are Located on Each Pole; They Occupy Identical Position on Each Pole Relative to Its Longitudinal Axis 259
12.7 MMF Harmonics of Regular Damper Windings 262
12.8 MMF Harmonics of Excitation Winding of Salient-Pole Machine and Screen on Polar Shoe 263
12.8.1 MMF Harmonics of Excitation Winding 263
12.8.2 MMF Harmonics of Screen on Pole Shoe of Low-Speed Frequency Controlled Motor 264
Appendix 12.1: Accounting the Finite Width of Rotor Slots in the Calculation of Damper Winding MMF (Regular and Irregular) or Squirrel Cage (Symmetrical and Asymmetrical) 265
Brief Conclusions 266
References 269

13 Field Harmonics in Air Gap of A.C. Machine in Nonlinear Network 271
13.1 Problem Setting 272
13.2 Initial Data and Their Representation 272
13.2.1 Complex Amplitudes (Phasors) of MMF Harmonics of Machine Rotor and Stator Loops and Their Representation 273
13.2.2 Equivalent Gap and Its Representation 273
13.2.3 Rotor Rotation Speed and Slip S_{SL} 274
13.3 Calculation Method of Field Harmonics Excited by Rotor and Stator Winding MMFs 274
13.3.1 Induction Machines 275
13.3.2 Complex Amplitudes (Phasors) of Field Harmonics Excited by Damper Winding MMF and Excitation Winding MMF of Salient-Pole Synchronous Machine 276
13.3.3 Rotation Speeds $\omega_{BOR,R}$ in Air Gap of Field Harmonic Components Excited by Damper Winding MMF and Excitation Winding MMF of Salient-Pole Synchronous Machine 284

13.3.4 Complex Amplitudes (Phasors) of Field Harmonics Excited by Stator Winding MMF with Account of Cross Section Geometry of Salient-Pole Synchronous Machine at Rotor at Standstill ($\omega_{REV} = 0$) and at Its Rotation ($\omega_{REV} \neq 0$) 286
13.3.5 Rotation Speeds $\omega_{BOR,ST}$ in Air Gap of Field Harmonic Components Excited by Stator Winding MMF of Salient-Pole Synchronous Machine 288
13.3.6 Additional Ratios for Calculation of Complex Amplitudes (Phasors) of Stator Windings at $|m| = |n| = |k| = 1$, Their Check 290
Brief Conclusions 291
References 293

14 System of Equations for Magnetically Coupled Loops for A.C. Machine in Nonlinear Network 295
14.1 Problem Setting 295
14.2 Selection Method of Magnetically Coupled Loops for System of Equations 296
14.3 Features of System of Equations for Magnetically Coupled Loops 297
14.4 Basic System of Equations for Magnetically Coupled Loops 298
14.4.1 Formulation of System; Initial Data and Results 298
14.4.2 Calculation Expressions for Flux Density Harmonics Complex Amplitudes Flux Density (Phasors) of Rotor and Stator Loops $|m| = |n| = |k| = 1$ 300
14.4.3 Calculation Expressions for Complex Amplitudes of Rotor Winding Harmonics Flux Density at $|m| = |n| = |k| = 1$ 300
14.4.4 Calculation Expressions for Complex Amplitudes of Stator Winding Harmonics Flux Density at $|m| = |n| = |k| = 1$ 300
14.4.5 Result Summary: Calculation Expressions for Complex Amplitudes; Field Speeds in Air Gap 301
14.4.6 Comparative Assessment of Separate Components of Complex Amplitudes (Phasors) 301
14.5 System of Magnetically Coupled Loops Equations 302
14.5.1 Equations for the First System of Loops Determined by EMF Frequency $\omega_{ST} = Q_1\omega_1$ 302
14.5.2 Equations for the $\omega_{ST}^{(2)} = Q_2\omega_1$ Second System of Loops Determined by EMF Frequency 303

14.5.3 Coupling Equations Between Both Systems of Stator Loops Determined by EMF of These Loops with Frequencies ω_{ST} and $\omega_{ST}^{(2)}$ 304
14.5.4 Peculiarities of Basic System of Equations 305
Appendix 14.1: Accounting Higher Spatial Harmonics in a System of Equations of Magnetically Coupled Loops 306
Brief Conclusions 308
References 309

15 Peculiarities of Operation Modes of A.C. Machine with Short-Circuited Rotor Windings at Nonsinusoidal Power Supply 311
15.1 General Comments 311
15.2 Peculiarities of Squirrel Cage Operation Mode ($\omega_{REV} < \omega_1/p$) 312
15.3 Peculiarities of Damper Winding Operation Mode ($\omega_{REV} = \omega_1/p$) 313
15.4 Additional Measures to Decrease Damper Winding Losses in Salient-Pole Machine 314
Appendix 15.1 314
Brief Conclusions 315
References 316

16 Operation Problems of High-Power AC Machines in Nonlinear Network 317
16.1 General Comments 317
16.2 Admissible Power of AC Machines in Nonlinear Network: Determination Methods; Practical Examples 318
16.2.1 Losses in Stator Winding Carrying Alternating Current Containing a Number of Time Harmonics . . . 319
16.2.2 Losses in Machine Stator and Rotor Core Caused by Mutual Induction Field Containing a Number of Time Harmonics 322
16.2.3 Machine Admissible Total Power P_{ADM} 328
16.2.4 Calculation Examples: Determination of Machine Admissible Power P_{ADM}^{*} 328
16.2.5 Experimental Determination of Screening Factors $S_{N,DIR}$, $S_{N,AD}$ of Asynchronous and Synchronous Salient Pole Machines 330
16.2.6 Checking of Rotor Short-Circuited Winding of Asynchronous and Synchronous Salient Pole Machines Heating Due to Higher Time Harmonics ($N > 1$): Losses for Its Calculation; Their Effect on Load of Operating Machines 335

16.3 Method of Determination Admissible Modes of High-Power Salient-Pole Generator Under Combined Load . . . 337
16.4 About the Level of Electromagnetic Load of Modern Salient-Pole Generators and Their Dynamic Characteristics in Independent Mode . . . 340
16.4.1 General Comments . . . 340
16.4.2 Requirements for Dynamic Modes . . . 340
16.4.3 Transient Deviation of Generator Voltage ΔU, Influence of Its Reactances . . . 341
16.4.4 Inductive Resistances and Their Influence on Generator Weight and Dimensional Indicators . . . 342
16.4.5 Problem Solutions: Offers . . . 343
16.4.6 Additional Requirements to Generators . . . 344
Brief Conclusions . . . 344
References . . . 346

17 Frequency-Controlled Induction Motors in Nonlinear Networks: Assessment Criteria of Higher Harmonics Influence—Method of Criteria Calculation . . . 349
17.1 Higher Harmonics and Need of Their Influence Assessment on Machine Modes in Nonlinear Network . . . 349
17.2 Frequency-Controlled Induction Machines with Short-Circuited Rotor . . . 350
17.2.1 Harmonics $Q_{AD} > 1$ (m = 1): Slip S_{AD}, EMF and Current Frequencies $F_{AD,ROT}$ in Rotor Loops. Power Balance in Secondary Loop . . . 350
17.2.2 Harmonics $Q_{DIR} > 1 = (m = 1)$: Slip S_{DIR}, Frequency of EMF and Currents in Rotor Loops. Power Balance in Secondary Loop . . . 352
17.2.3 Technical and Economic Indicators Frequency-Controlled Induction Motors [22–26] . . . 353
17.2.4 Calculation Peculiarities of Technical and Economic Indicators of Induction Motors in Nonlinear Network . . . 356
Brief Conclusions . . . 358
References . . . 360

18 Method of Minimizing Losses in High-Power Low-Speed Frequency-Controlled Motors in Operation Modes at Nonlinear Dependence of Shaft Torque on Rotation Speed . . . 363
18.1 Application Areas of High-Power Low Speed Frequency-Controlled Motors . . . 363

18.2 Voltage, MMF and Currents in Windings in Operation Modes ($n_{REV} < n_{NOM}$); Mutual Induction Flux in Air Gap 364
18.3 Structure of Losses in Low Speed Frequency-Controlled Motor; Efficiency in Operation Modes ($n_{REV} < n_{NOM}$) 366
Appendix 18.1 367
Appendix 18.2 368
Appendix 18.3 368
Brief Conclusions 368
References 369

19 Methods of Decreasing Nonlinear Distortion Factor in Voltage Curve of Salient-Pole Generator: Investigation of EMF Tooth Harmonics of Its Multiphase Winding with q per Pole and Phase as Integer 371
19.1 Introduction 371
19.2 Tooth Harmonics of Machine with q as Integer: Amplitude of Their Mutual Induction Field in Air Gap in no-Load Mode; Frequency of This Field (Order of Tooth Harmonics) 373
19.2.1 Problem Formulation 373
19.2.2 Solution 374
19.2.3 Field of Harmonics $b_{SLT}(x,t,n)$ in Stator Slot Zone 375
19.2.4 Excitation Field $b_{MI}(x)$ (Rotor Field); Resulting Mutual Induction Field (in Air Gap); Flux Density $b_{Z,0}(x,t,n)$ of Tooth Order 377
19.2.5 Frequencies of Tooth Harmonics $\omega_Z^{(1)}$ and $\omega^{(2)}$; Calculation Expression for Nonlinear Distortion Factor 378
19.3 Rotor Construction with Local Shift of Poles in Tangential Direction 379
19.3.1 Peculiarities of Practical Realization 379
19.3.2 Tooth Harmonics of EMF $e_{Z,0}(t,n)$ in Stator Winding 380
19.3.3 Calculation Example 381
19.4 Rotor Construction with Group Shift of Poles in Tangential Direction 382
19.4.1 Peculiarities of Practical Realization 382
19.4.2 Tooth Harmonics of EMF $e_{Z,0}(t,n)$ in Stator Winding 383
19.4.3 Calculation Example 384
19.5 Generator Construction with Stator Axial Skewing of Stator Core or Rotor Poles 384
19.5.1 Peculiarities of Practical Realization 384

19.5.2 Calculation Example 385
Appendix 19.1 386
Appendix 19.2 386
Brief Conclusions 388
References 389

20 Methods of Decreasing Nonlinear Distortion Factor in Voltage Curve of Double-Fed Machines: Investigation of EMF Tooth Harmonics of Its Multiphase Stator and Rotor Windings with q Per Pole and Phase as Integer 391
20.1 Introduction 391
20.2 Assumptions 392
20.3 Peculiarities of Investigating EMF Tooth Harmonics of ASG Stator and Rotor Three-Phase Windings with Integer Number Q of Slots Per Pole and Phase 393
20.4 Rotor Fields of and Their Harmonics 393
20.4.1 Excitation Winding and Field of Its "Winding" Harmonics 393
20.4.2 Toothed Rotor Form; Fields of Rotor Tooth Harmonics 394
20.4.3 Interaction of the First Harmonic of Mutual Induction Field and Field of Rotor Tooth Harmonics 395
20.5 The First Component of Resulting Mutual Induction Field in Air Gap of Tooth Order 395
20.5.1 Amplitudes of the First Field Component 395
20.5.2 Frequencies $\omega_Z^{(1)}$, $\omega_Z^{(2)}$, $\omega_Z^{(3)}$ and $\omega_Z^{(4)}$ of EMFs Induced in Stator Winding by the First Component of Field Harmonics 397
20.5.3 EMF Amplitudes $e_1^{(1)}$, $e_1^{(2)}$, $e_1^{(3)}$ and $e_1^{(4)}$ Induced in Stator Winding by the First Field Component 397
20.5.4 Nonlinear Distortion Factor $K_{DIST,1}$ of ASG Stator Winding Voltage Caused by the First Component of Mutual Induction Resulting Field in Air Gap of Tooth Order 399
20.5.5 Calculation Example 399
20.6 The Second Component of Resulting Mutual Induction Field in Air Gap of Tooth Order 400
20.6.1 Amplitudes of the Second Field Component 400
20.6.2 Frequencies $\omega_Z^{(1)}$, $\omega_Z^{(2)}$ of the Second Component of Stator Winding EMF Tooth Harmonics 401

20.6.3 EMF Amplitudes $e_2^{(1)}$, $e_2^{(2)}$, Induced in Stator Winding by the Second Component of Pole Harmonics . . . 401
20.6.4 Nonlinear Distortion Factor $K_{DIST,2}$ of ASG Stator Winding Voltage Caused by the Second Component of Mutual Induction Resulting Field in Air Gap of Tooth Order . . . 402
20.6.5 Calculation Example . . . 402
20.7 The Third Component of Resulting Mutual Induction Field in Air Gap . . . 403
20.7.1 Amplitudes of the Third Field Component . . . 403
20.7.2 EMF Frequencies $\omega_{ST,W}$ in Stator Winding Induced by "Winding" Harmonics of Rotor Field . . . 403
20.7.3 EMF Amplitudes in Stator Winding Induced by "Winding" Harmonics of Rotor Field . . . 404
20.7.4 Nonlinear Distortion Factor $K_{DIST,3}$ of ASG Stator Winding Voltage Caused by the Third Component of Mutual Induction Resulting Field in Air Gap . . . 404
20.7.5 Calculation Example . . . 405
20.8 The Fourth Component of Resulting Mutual Induction Field in Air Gap of Tooth Order . . . 405
20.8.1 Amplitudes of the Fourth Field Component; Frequency EMF . . . 405
20.8.2 EMF Amplitudes Induced in Stator Winding by the Fourth Component of Field Harmonics . . . 406
20.8.3 Nonlinear Distortion Factor $K_{DIST,4}$ of ASG Stator Winding Voltage Caused by the Fourth Component of Mutual Induction Resulting Field in Air Gap of Tooth Order . . . 406
20.8.4 Calculation Example . . . 407
Brief Conclusions . . . 407
References . . . 409

21 Method of Determination Stator Winding MMF at Arbitrary Phase Current Waveform and Unequal Width of Phase Zones (for Investigation of Operational Characteristics of Frequency: Controlled Motors) . . . 411
21.1 Introduction: Problem Formulation . . . 411
21.2 Illustration of a Method of Solution for a Particular Case . . . 414
21.2.1 Initial Data . . . 414
21.2.2 Solution Stages . . . 415
21.3 Solution of General Problem . . . 416
21.3.1 Initial Data . . . 417

21.3.2 Step Functions of Stator Current: Representation of Each of Them in the Form of Harmonic Series $\Sigma F(\alpha, m, \Delta t_S = idem)$ 418
21.3.3 Determination of Amplitude and Phase of Stator Current Step Function in the Form of Series $\Sigma F(\alpha, m, \Delta t_S = idem)$ of Spatial Harmonics of Order m 418
21.3.4 Approximation of Stator Current Step Function Harmonics $\Sigma F(\alpha, m, \Delta t_S = idem)$ by Means of Time Harmonious Series; Time Harmonics of Order $Q \geq 1$ 420
21.3.5 Result: MMF Harmonics of Stator Winding 423
21.4 Checking Results: Calculation Example 424
21.4.1 Phase Currents in Stator Winding 424
21.4.2 Three-Phase Six-Zone Single-Layer Stator Winding with Diametral Pitch and Phase Zones of Equal Width $\alpha_A = \alpha_{C'} = \alpha_B = \alpha_{A'} = \alpha_C = \alpha_{B'} = = \pi/3$; Number q = 1. Position of Borders Between Phase Zones Along the Stator Periphery as Per (21.5): $\alpha_A = \pi/3$; $\alpha_{C'} = 2\pi/3$; $\alpha_B = \pi$; $\alpha_{A'} = 4\pi/3$; $\alpha_C = 5\pi/3$; $\alpha_{B'} = 2\pi$. 425
Brief Conclusions 430
References. 432

22 Investigation Method of Transient Modes in Induction Machines with Rotor Cage Asymmetry 433
22.1 Introduction: Problem Formulation 433
22.2 Calculation of Currents Distribution in Asymmetrical Squirrel Cage Elements 434
22.2.1 Additional Aperiodic Current Components in Rotor Loops at Occurrence of Rotor Cage Asymmetry 434
22.2.2 Resultant Currents in Ring Portions $\underline{\underline{I}}_{(N)}$ and Bars $\underline{\underline{J}}_{(N)}$ After Breakage 436
22.3 Calculation of MMF for Asymmetrical Cage Currents 436
22.4 Calculation of Resulting Mutual Induction Fields (Fields in Air Gap) at n = p 437
22.4.1 Direct Field 437
22.4.2 Additional Field. 439
22.5 Determination of Mutual Induction Factors and Parameters of Secondary Loops (Rotor) for the Main and Additional Fields 440
22.5.1 Mutual Induction Factor M_{DIR} and Parameters of Secondary Loop (Rotor) for Direct Field 441

22.5.2 Mutual Induction Factor M_{ADD} and Parameters of Secondary Loop (Rotor) for Additional Field 441
22.5.3 Interrelation of Mutual Induction Factors and Parameters of Secondary Loops (Rotor) for Direct and Additional Fields 442
22.6 Equations for Calculation of Transients in Both Magnetically Coupled Machine Loops 443
22.6.1 Equations for Transient Currents in Stator $I_{STAT,DIR}$ and Rotor $I_{SEC,DIR}$ Caused by Direct Field 443
22.6.2 Equations for Transient Currents in Stator $I_{STAT,DIR}$ and Rotor $I_{SEC,ADD}$ Caused by Additional Field 444
22.7 The Resulting Transient Currents in Windings 446
22.7.1 Currents in Stator Winding 446
22.7.2 Currents in Secondary Loop (in Rotor) 446
22.8 Prospects for Using the Method with Account of Rotor MMF Higher Spatial Harmonics, and also for Calculations of Transient Currents in Synchronous Salient Pole Machines with Damper Winding 446
Brief Conclusions 447
References 450

23 Theory and Methods of Investigation of Eddy Currents and Additional Losses in Stator Windings 453
23.1 Problem Formulation 454
23.2 Losses and Their Distribution in Bar Stator Windings 455
23.2.1 Winding Construction Features 455
23.2.2 Sources of Bar Losses: Fundamental Assumptions While Investigating Losses 457
23.2.3 Problem Setting and Solving Methods 458
23.2.4 General Problem of Eddy Currents and Losses Calculation in Elementary Conductors of the Bar 465
23.2.5 Bars with Solid Conductors (Complete Transposition): Calculation Example 471
23.2.6 Bars with Hollow Conductors (Complete Transposition): Calculation Example 472
23.2.7 Bars with Incomplete Transposition: Calculation Example 475
23.2.8 Bars with Different D.C. Resistance of Elementary Conductors: Calculation Example 485
23.3 Numerical Methods of Eddy Current Investigation in Elementary Conductors of Bar Winding 495
23.3.1 General Observations 495

23.3.2 Problem Statement: Losses in Elements of Hollow and Solid Conductors of Slot Group. 496
23.3.3 System of Equations for Currents in Elements of Slot Group Conductors. Circuits with Flux Linkage 498
23.4 Losses Distribution in Bar Winding 504
23.4.1 Additional Losses Distribution in Winding Turns in Slots 504
23.4.2 Losses in Several Bars of Double-Layer Winding 507
23.4.3 Losses Ratio in Outer Turns in Slot 508
23.4.4 Losses, Overheating and Bar Sizing in Non-standard Design of Stator Double-Layer Winding of Large Modern A.C. Machines 509
23.5 Additional Losses in Coil Winding. 524
23.5.1 Design Features 524
23.5.2 Fundamental Assumptions. 527
23.5.3 Approaches to Solve the Problems of Additional Losses Caused by Slot Leakage Flux 527
23.5.4 Distribution of Circulating Currents. 528
23.5.5 Losses Due to Circulating Currents and Losses Distribution in Winding Turn 534
23.6 Questions for Self-Testing 536
Appendix 1 Method of Skin Effect Computation in Rotor Bars of Large Power Asynchronous Motor with Allowances for Temperature Distribution Therein 538
Appendix 2 Analytical Method of Designing Polyphase ($m_{PH} \geq 3$) Stator Winding with an Arbitrary Fractional Number Q of Slots Per Pole and Phase. 545
Brief Conclusions 548
References. 549

About the Authors

Iliya Boguslawsky is Professor in the Theoretical Electrical Engineering and Electromechanic Department at Peter the Great St. Petersburg Polytechnic University and is a senior member of IEEE. He has spent 50 years' in the electric machine-building industry (calculation and design of large alternating current machines). His work at the "Elektrosila" Works Stock Company was in power machines and the Leningrad Electrical Machine Building Plant.

Nikolay Korovkin is Professor and Head of the Theoretical Electrical Engineering and Electromechanic Department at Peter the Great St. Petersburg Polytechnic University. He has more than 35 years' experience in power engineering.

Masashi Hayakawa is Emeritus Professor of the University of Electro-Communications (UEC), a fellow of The Institute of Electronics, Information and Communication Engineers (IEICE), Japan, and a senior member of the Institute of Electrical Engineers (IEE), Japan. He is the CEO of the Hayakawa Institute of the Seismo Electromagnetics Co. Ltd. (UEC Incubation Center) and a visiting professor at the Advanced Wireless & Communications Research Center (AWCC), UEC, Tokyo. He has more than 45 years' experience in electromagnetics.

The authors gratefully welcome any comments and suggestions (in English, German, or Russian languages) on the contents of this monograph. They should be addressed to Polytechnicheskaya str., 29, Peter the Great St. Petersburg Polytechnic University, Theoretical Engineering and Electromechanic Department, St. Petersburg, 195251, Russia; email: Nikolay.korovkin@gmail.com.

Chapter 1
Problems Formulation

1.1 Requirements to High-Power A.C. Motors and Generators

The main tendency in the creation of modern alternating current (A.C.) motors for various industries and generators for stationary and mobile power plants is growth of their technical and economic level by an increase in their electromagnetic, thermal loads, improvement of construction and production technique. This tendency is caused by the need to increase constantly machine competitiveness.

Modern induction and synchronous motors of industrial frequency find broad application in metallurgy, mining, cement, woodworking industry, transport and agriculture. Generally, in operation practice use is made of two groups of indicators for determination of their technical and economic level: indicators for operation in nominal (rated) mode and in start-up mode.

First group contains motor efficiency, ratio of its nominal (rated) torque to volume of active part, its weight, etc. The second contains motor characteristics: start-up current and torque, maximum and minimum torques, value of admissible dynamic moment of inertia of mechanism coupled with motor shaft; in practice, the value of this dynamic moment is often limited to opportunities of short-circuited winding of motor rotor (damper winding, squirrel cage).

However, with growth of electromagnetic and thermal level of motors and corresponding increase of technical and economic indicators of the first group, there can be problems with some indicators of the second group—with motor torque at start-up, with its maximum torque, etc.; they can decrease negatively affecting motor competitiveness. We note that these indicators are determined considerably by construction and parameters of short-circuited rotor winding of motor (damper winding, squirrel cage), distribution of currents in the elements of this winding induced during its operation. Therefore, investigation of parameters of these windings and distribution of currents in their elements represents a practical interest.

I. Boguslawsky et al., *Large A.C. Machines*,
DOI 10.1007/978-4-431-56475-1_1

For the determination of technical and economic level of modern generators for stationary and mobile power plants of industrial frequency, use is also made of two groups of indicators: indicators for operation in nominal mode and in transient mode.

The first group of indicators for generators and motors is similar. The second contains indicators defining, for example, the degree of dynamic stability of generators for operation in parallel with high-power network, and for generators of autonomous power plants—possibility of preset power induction motor start-up, extent of generator voltage drop at sudden load-on. This load has peculiarities: it differs at start-up by lowered values of power factor ($\cos \varphi = 0.3–0.4$), etc.

However, with growth of electromagnetic and thermal level of generators there can be problems with some indicators of the second group that also negatively affect their competitiveness. These indicators at preset current load to a certain extent are also determined by parameters depending on the construction of generator rotor damper winding.

Modern frequency-controlled electric drives nowadays are widely introduced in those industries, which were traditional for uncontrolled electric drives or for D.C. electric drives used, for example, in metallurgy and shipbuilding. In operation practice, in order to determine technical and economic level of frequency-controlled motors of these electric drives use is made of the same characteristics in nominal mode, as for machines of industrial frequency, especially, if these motors are intended for operation in the modes with sharp load variation. However, current and voltage distortion factors caused by the frequency converter operation in armature circuit have an essential impact on these indicators; they are determined by higher time harmonics in current and voltage curves of this circuit. Fields of these higher time harmonics induce additional EMFs (electro-motive forces) and currents in loops of a frequency-controlled motor, including in its short-circuited winding (damper winding, squirrel cage), especially at sharp load variation. Therefore, physical processes in rotor loops of industrial frequency motor at start-up and frequency-controlled motors in nominal mode and at sharp load variation are similar.

However, unlike the short-term start-up mode of industrial frequency motors, these EMFs and currents are typical for continuous operation mode of frequency-controlled machines. These cause a number of additional physical processes in motor, for example, additional heating of rotor and stator loops in comparison with motor operation in linear networks. Respectively, motor admissible power fed from a frequency converter should be reduced in comparison with the power when fed from a linear network; this admissible power taking into account nonlinear distortion factors needs to be previously calculated and specified in delivery specifications. With growth of machine electromagnetic level, the additional currents, losses and additional heating can also increase in rotor loops (damper winding, squirrel cage). We note that these indicators are considerably determined (as at asynchronous start-up from network) by construction and parameters of short-circuited rotor winding of motor, distribution of currents in the elements of this winding induced during continuous operation. Therefore,

investigation of parameters of short-circuited rotor windings, distribution of currents in their elements represents a practical interest for machines of this class.

Modern generators of stationary and mobile power plants are even more often used in nonlinear networks. In short-circuited loops of their rotors, there appear additional currents and heating; they are similar to additional currents which continuously appear in synchronous motors fed from frequency converters.

Let us note that higher time harmonics caused by stator stepped form, in particular in salient pole machines with a small number of slots per pole and phase as well as in double-fed machines (in generator mode) can result in network nonlinearity; application of known measures to decrease EMF nonlinear distortions for these machines in practice sometimes meet certain difficulties, especially for double-fed machines. Therefore, the solution of these problems represents a practical interest.

It is also necessary to note problems of winding MMF (magneto-motive force) determination at non-sinusoidal power supply, in particular, generally—in asymmetrical modes, and currents in winding phases vary in time under arbitrary periodic (not only harmonic) law, and the winding is implemented with a fractional number of slots per pole and phase so its phase zone width cannot be identical.

Thus, practice puts forward problems of profound studying processes arising in modern A.C. machines with short-circuited rotor loops for operation in a nonlinear network. Its purpose is a further increase in machine technical and economic indicators and their competitiveness.

For this purpose, refinement of investigation methods is necessary for operational characteristics of the following:

- synchronous and induction motors (especially for operation from a network or from a frequency converter in heavy modes, for example, with variable load, etc.);
- synchronous and double-fed machines operating on nonlinear or combined load, and currents in winding phases with a fractional number of slots per pole and phase vary in time under arbitrary (not only harmonic) law.

Besides, practice puts forward problems of developing methods of reduction of EMF nonlinear distortions in high-power salient pole machines not only by skewing of stator slots (rotor poles) in axial direction, but also by shifting poles (group or local) in tangential direction. Similar problems also arise in the production of high-power double-fed machines.

As the solution of these problems, it is necessary to continue investigations on refinement of the following:

- MMF harmonics of time orders Q and spatial m excited by non-sinusoidal currents of stator winding with account of a number of its phases, their connection diagram, etc.;
- MMF harmonics of spatial orders n excited by currents with frequency ω_{ROT} in rotor loops, including short-circuited windings stated above: damper winding of synchronous machine and squirrel cage of induction machine.

- distribution of currents induced by these harmonics in rotor loops, including elements of damper winding of salient pole machine, asymmetrical squirrel cage of induction machine;
- processes in magnetically coupled loops of stator and rotor with account of several time and spatial harmonics;
- fields of higher time harmonics of stator stepped form order for salient pole machines and double stepped form order (stator and rotor)—for double-fed machines;
- circulating and eddy currents in stator windings of various construction (bar, coil), additional losses caused by these currents.

From the statement above it follows that realization of development tendencies for modern high-power electric machine building demands solving a number of problems connected with refinement and extension of theory and investigation methods of A.C. machine processes, improvement of their physical and, respectively, mathematical models. It refers to motors and generators operating not only in linear, but also in nonlinear networks: to frequency-controlled induction and synchronous motors, generators of stationary and mobile power plants, etc.

1.2 Actual Problems of Modern Electric Machine-Building Industry; Their Solution in the Monograph

This monograph generalizes a long-term production and scientific experience of authors on the development of theory and methods of investigation of physical processes in modern high-power A.C. motors and generators of high electromagnetic, mechanical and thermal level. In the last decades, problems of ensuring reliability of these machines in networks with nonlinear elements (in nonlinear networks) were added to those of ensuring their reliable operation in linear networks. These are connected with higher time harmonics causing additional losses in machine loops, shaft torques and, respectively, increased heating of windings, stator and rotor cores, housing vibration. Factory engineers need to solve these problems within their production activity rather often, because a modern converting equipment is implemented in various industries, transport, and agriculture more widely.

In the monograph are investigated the problems connected with the distribution of currents and losses induced in rotor loops of A.C. machines with large electromagnetic loads. For example, these are the processes in damper winding of salient pole machines of various construction, and in squirrel cage of induction machines with asymmetry in it. In addition, we are describing the theory and methods of determining admissible power of these machines in various operational modes. These problems were put forward by practice: In developing high-power frequency-controlled induction and synchronous motors and also diesel generators intended for the operation in nonlinear networks, authors often had to investigate

modes of these machines and to determine their construction with account of field harmonic in air gap. For the first time this problem was solved by them in a developing frequency-controlled drive based on induction motor 500 kW, 660 V, 3000 rpm. («Elektrosila» Work, Stock Company "Power Machines" St.-Petersburg); it was intended for a charger in the first loop of nuclear reactor. Taking into account facility importance, authors considered also construction versions of squirrel cage with possible asymmetry.

However, progress in the development of converting equipments puts forward a problem of introduction into industry high-power frequency-controlled drives based on synchronous salient pole machines as well. Respectively, problems of creation of these drives for mining and cement industry—were solved for nominal power up to 10,000 kW and speed apprx. 10 rpm. (gearless drive of grinding units, shaft torque up to 1000 T m, range of speed regulation 0–120 %, weight up to 500 T, "ring motor"). Operation of the USSR's first high-power frequency-controlled drive (gearless drive for cement mill, shaft torque about 355 T m, speed 16 rpm, regulation range 0–120 %, number of pole pairs p = 30) has proved the correctness of construction solution adopted in its development. They included not only theoretical investigations, but also pilot investigations of drive elements at factory bench («Elektrosila» Work, Stock Company "Power Machines"); in particular, there were investigated problems of currents distribution, additional losses and overheats in machine loops caused by high harmonics. As a prototype, authors used a serial salient pole SDSZ type motor (2000 kW, 100 rpm, number of pole pairs p = 30, Limited Liability Company "Scientific-Production Association" "Leningrad Electrical Machine Building Plant"). Problems of creation of similar drives were at the same time solved for rated power up to 20,000 kW and speed of 110–150 rpm. (system of electric propulsion for ice breakers, shaft torque up to 180 T m, range of speed regulation "up"—to 125 %). When developing motors of these drives, the authors have refined methods created in developing low-frequency motors for gearless drives; in addition, they solved the problem on optimum regulation of these motors for obtaining maximum efficiency.

We examined very carefully the problems of current distribution in the damper winding of the synchronous machines as well as in the cage winding by damage of the asynchronous machines. The results were confirmed on the test bench of work («Elektrosila» Work, Stock Company "Power Machines").

For generators in autonomous (independent) nonlinear networks, for example, ship, there was additionally solved a problem of determining admissible power in the mode, when part of load is linear, for example, vessel lighting network, and part —nonlinear, for example, pump motors fed from a frequency converter. Methods developed by authors, as the solution of these problems, were checked on industrial sample of generator (up to 2000 kW, 750 rpm in factory bench conditions, at «Elektrosila» Work, Stock Company "Power Machines" St. Petersburg). In recent years, the problem of providing dynamic modes for A.C. generators with large electromagnetic loads in autonomous networks has become actual; it is solved by the authors.

All this has demanded to investigate in more detail problems of distribution of currents and losses not only in rotor loops, but also in stator winding; their solution is described in the last part of the monograph.

At present, double-fed machines (DFMs) both in motor and generator mode become widely used in world power industry; rotor winding of machine of this type is connected to frequency converters. Calculation methods of the modes for these machines (with account of magnetic circuit nonlinearity and higher time harmonics from this converter) are solved by the authors.

In several works, the authors investigate the effectiveness of construction solutions necessary for the restriction of nonlinear distortions in voltage curve according to the requirements of GOST (National Industrial Standards of Russia) and IEC (International Electrotechnical Commission) (local and group shift of poles in tangential direction, shift of poles or stator slots in axial direction). For the investigation of operational characteristics of frequency-controlled salient pole motors, the MMF determination method for stator winding is developed for an arbitrary waveform of currents in phases and unequal phase zone width, expanding phase currents into symmetric components is excluded for these machines. Calculation method of transient processes in an induction machine for rotor cage asymmetry is developed in the Chap. 22 of this monograph.

It should be noted that at present the power of motors and generators intended for the operation in nonlinear networks continue to increase. Such machines become not only problems of investigation of their performance characteristics, but also problems of developing assessment criteria of technical and economic indicators similar to known criteria at their operation in linear networks.

Problems connected with the investigation of eddy currents and additional losses in stator winding of modern A.C. machines of various constructions are solved in the last chapter of the monograph. Authors often have to solve these problems for machines of various types. If you adhere to chronology, the start was made by the problem investigation of additional losses in hollow conductors of stator bar winding of new series in high-power turbogenerators over 100 MW with direct cooling. Detailed investigation of this problem led us to its solution by an iterative method, but not by the solution of the known Helmholtz equation usually used in such problems. Further, the authors found modifications of this method. They were applied for the calculation of eddy currents and losses in stator windings with bars of various height in slot, for example, for high-power turbo—and hydrogenerators with bars where hollow and solid conductors differ in resistivity; in stator bar winding with incomplete transposition, for example, for high-power multipolar machines (hydrogenerators, etc.). It appeared that this method could also be applied to modern machines with stator coil winding differing in large number of rectangular elementary conductors in turn height, etc.

The problem of skin effect in the induction motor bar is investigated in Appendix I in extensive Chap. 23 of the monograph; unlike usual investigations of this problem, the distribution of bar temperature at start-up is considered. This solution allows us to specify the shaft torque at start-up of high-power of induction motors with large electromagnetic loads and can be used in the form of CAD

element. Appendix II gives an analytical method of multiphase winding structure with arbitrary number of slots per pole and phase q ($q \geq 1$, $q < 1$), etc.; in practice, the structure of such windings meets sometimes serious difficulties, especially for multipole machines.

Theory and methods developed in the monograph differ in physical presentation and provide simple verification of calculations performed. Tests of manufactured machines and their operation proved correctness of found solutions.

Main contents of the monograph were published in Russia, USA, Germany, Czech Republic, Poland, in materials of international conferences.

The publications of authors are pointed in the reference list in the end part of each chapter.

1.3 Presentation Order of Monograph Contents and Structure

1.3.1 Choice of Investigation Methods: Position of Monograph's Authors

Long-term experience of authors proves that among investigation methods of processes in A.C. machines, in engineering practice more widely are used those differing by clarity of their physical treatment, by opportunity to estimate intermediate results, for example, by reduction of investigated processes in modern machines to similar, but simpler ones (in particular, processes caused by breakage of damper winding in salient pole machine—to similar processes in induction machine with cage asymmetry, etc.). Therefore, despite the complexity of many problems and not traditional character of solving some of them for electric machine industry practice, constant attention is paid to the physical treatment of processes in the monograph. The authors completely share grounds of a famous expert R. Ruedenberg on it (Dr. Ing., Dr. hon., A.M. hon. of Harvard University; formerly Chief Electrical Eng., Siemens Schuckertwerke, Berlin; Cons. Eng. GEC, London), given earlier in the form of epigraph.

Analytic expressions of closed form for currents in structural components have been obtained as the result of studies of damper windings of salient pole synchronous machines:

- with segments between neighboring poles;
- with a bar on each pole whose impedance differs from other ones on it;
- with damaged bar on one of poles;
- asynchronous machines with one or few damaged bars.

Expressions for currents in components of squirrel-cage armature windings have been used to obtain analytic expressions for MMF and air gap flux created by these currents. In terms of salient-pole synchronous machines the air-gap irregularity

(under pole and between poles) is to be considered by complex Fourier expansion of flow step function. Such a presentation of Fourier expansion results allows one to get complex amplitudes (phasors) of MMF and flux rotating around armature both in positive and negative directions. As a result, the currents in structural components of squirrel-cage armature windings, MMF and air-gap flux due to these currents have been obtained in the form of generalized responses specified by machine design, its active part geometrical sizes; such responses are convenient to be studied as transfer functions establishing the relationship between these values and an amplitude of total field gap induction (field mutual induction). An induction amplitude shall be calculated with the use of known equations of flux linkage of circuits.

However, to consider the air-gap irregularity (under pole and between poles) the break-down of MMF and flux may be carried out along orthogonal axes according to known papers of A. Blondel (1895), and R. H. Park (1929, 1933). In this case, the calculation of current distribution through armature structural elements shall be performed (with the use of the method proposed in the above paper) for both components; resulting current shall be calculated for each component in the form of a sum; and this shall make the solution more complicated.

It should be noted that for salient-pole synchronous machines several approaches to avoid the transformation of mutual induction field into orthogonal components have been made in some papers with application of methods similar to that realized in the known paper of R. Ruedenberg (1923) for asynchronous machines. Various modifications of equation systems have been applied for flux linkage of circuits (D. A. Gorodsky "Theory of electrical processes in synchronous machines", Electrotechnical industry reporter, Moscow, 1942; S. Yamamura. "Spiral Vector Theory of A.C. Circuits and Machines", 1992), etc. It is also noteworthy to cite the monograph K.S. Demirchyan, P.A. Butyrin «Modelling and numerical calculations of electrical circuits», Moscow, 1988, in which the authors propose a new efficient method for the analytical investigation of transients in synchronous machines. However, these papers present a damper winding in a simplified form—in the form of lumped impedances; the problem of calculation of current distribution in structural components has not been studied in these papers.

1.3.2 Presentation Order of Monograph Contents

Material of the monograph is stated regularly: At first, are stated foundations of physical processes and phenomena, theory and methods of their investigation; in further statement they are used for the solution of practical problems connected with the creation of high-power A.C. machines. At the same time, sections are given whenever possible independently from each other, with minimum number of references to previous ones. Inevitable repetitions in such statement are avoided in such a way that for practical use of certain chapters and sections there is no need in detail to study contents of the whole monograph. For example, the method and

algorithm of performance characteristics calculation for double-fed machines with account of saturation and higher harmonics in rotor circuits are so stated in the monograph; also is stated a method and algorithm of calculation of performance characteristics of high-power induction motors with nonlinear parameters. The monograph also represents calculation methods and algorithms of currents distribution in asymmetrical closed and open active U-shaped recurrent circuits necessary, for example, in the investigation of currents in damper winding elements of salient pole machine, etc.

1.3.3 Checking Methods Developed in the Monograph

In the monograph, the methods and developed investigation results obtained for the first time are subjected to repeated checks. For example, general methods of investigating passive asymmetrical U-shaped recurrent circuits (with broken elements), developed in the monograph for investigating currents in short-circuited rotor windings, are checked by a number of numerical examples whose solution results can also be estimated based on physical considerations. Calculation equations for currents distribution in active asymmetrical U-shaped recurrent circuits are checked by reducing their structure to that of symmetrical circuits differing in other boundary conditions. Calculation equations for currents distribution in complete damper winding of synchronous machine are checked using equations for currents in squirrel cage of induction machine as special case (at pole overlapping $\alpha = 1$ (relation between the pole width and pole pitch), etc. Also several checks of equations were performed for short-circuited rotor winding MMFs obtained by the representation of harmonic (Fourier) series in complex plane in the form of rotating waves, etc. It allows us to use confidently in engineering practice the results obtained in the monograph. In addition, some of developed methods have passed testing at factory benches («Elektrosila» Work, Stock Company "Power Machines" St.-Petersburg and Limited Liability Company "Scientific-Production Association" "Lenin-grad Electric Machine Building Plant"). This is, for example, the method of determining admissible power for generator operation with nonlinear or combined load, investigation method for double-fed machine modes, investigation method of currents distribution in damper winding, etc.

1.3.4 Symbols Accepted in the Monograph

Current, flux density, MMF, EMF and voltage written in capital letters are complex amplitudes (phasors, time complexes of symbolical method). In some chapters, moduli of these complex amplitudes are used as well. To distinguish designation of this phasor from its modulus, the standard sign of absolute value is used, for example, its voltage modulus is designated as follows: $|U|$. Symbols of these and

many other physical quantities—are usual for technical literature, for example, D—diameter, L—length. Each new designation is explained throughout the presentation of a chapter. Besides, at the end of each chapter, symbols are given in alphabetical order as a list, also there is explanation for each of them; symbols using letters of the Greek alphabet are given in separate list. This is done in order to have the opportunity to learn each chapter separately, without the learning of the previous chapters.

Indices at designations of physical quantities explain, as far as possible, their physical sense, for example, DINN—inner diameter of stator boring, LCOR—core length. Authors hope that all these will facilitate reading each chapter. The whole thing simplifies the access for the engineers to the solution of problems independently on the content of the previous chapters.

1.4 Order of References

The list of references includes the following sections:

I: monographs, general courses, textbooks;
II: induction machines (articles, author's certificate and patents);
III: synchronous machines (articles, author's certificate and patents);
IV: GOST, IEC and other normative documents.

According to it, in the monograph, references in the text have double numeration, for example means: List of references, section II (induction machines), article No. 1 from this list.

For material representation in the monograph, the authors considered necessary to acquaint their readers with works of many foreign experts who played a significant role in the formation and development of power industry including experts of the USSR (Russia), USA, England, Germany, Czech Republic, Hungary, Italy. Authors proceeded, thus, from the following:

- now there exist several rather effective translation means (for example, Lingvo, Multitran, Promt, etc.), and even "speaking" translators (for example, Collins, Companion) considerably facilitate reading publications in languages of specified countries;
- formulas in these publications usually "do not require translation": it is well known that "engineers in articles on their specialty read formulas without translator".

It should be noted that magazines with articles of monograph authors were published not only in the USSR (Russia); at the same time they were translated into English and published in the USA by ALLERTON PRESS, INC publishing house (18 West Street. New York N.Y. 10001): this is "Izvestia RAN. Energetika" magazine; "Elektrotechnika" magazine; "Electrichestvo" magazine.

Authors consider paying expedient attention of readers of the monograph to a number of achievements in power industry of the USSR (Russia) which characterize its scientific and technological level; these are found in publications.

We give here only some of these achievements in the USSR connected with the creation of turbogenerators and A.C. machines for various industries within the period from 1945 (World War II end) till 2014.

In 1946, the world's largest two-pole 50 Hz turbogenerator with indirect hydrogen cooling was manufactured in the USSR. Its development was not only achievement of electric machine industry, but also of metallurgy: Sizes of rotor forging active part were also a record: length—5250 mm, diameter—1000 mm. Since 1957, the USSR started to produce a series of turbogenerators of 60–1200 MW with direct cooling: rotor winding with hydrogen (by 30 psig and more), stator winding—with distillate. A turbogenerator of 1200 MW of this series was put into operation in 1980. At that time, this generator held the position of largest generator in Europe. At the beginning of 60th, the USSR starts the production of turbogenerator new series of 60–1250 MW using direct cooling of windings rotor and stator also rotor and stator cores with distillate; without hydrogen; generators of similar construction are not produced by foreign firms.

Since 1946, the USSR starts production of a series of general-purpose high-power induction and synchronous machines in a wide range of power (to 50 MW) and rotation speed (to 3000 rpm): for mining and cement industry, metallurgy, transport, including electric motion of vessels, agriculture, etc. Each series has some modifications of construction with account of operation in these industries. Now many of machines are used as frequency-controlled (with frequency converters). In addition, production was started for many unique machines, for example, high-speed motors with solid rotor (in the range: 3600 kW at 12,000 rpm–200 kW at 50,000 rpm).

Development in the production of extensive nomenclature of all these machines with high electromagnetic, mechanical and thermal load has become possible thanks to profound scientific-research works whose results were published in domestic and foreign editions. Within the subject of the monograph, its authors also tried to reflect some of these publications in references to each chapter.

However, works of prof., Dr. Sci. Tech. Botvinnik M.M. deserve separate mention. He is not only a famous author of the theory and methods of double-fed machines regulation in various operational modes; his talent also extends to modern theory of chess, not less difficult. Botvinnik M.M.—electrical engineer, the only in the history of electrical equipment, who five times was the world champion in chess (in 1948, 1951, 1954, 1958, 1961). Followers of his school, successfully continue works of Botvinnik M. M. in the field of DFMs. References to his works and works of his followers are given in references to Chap. 2.

Chapter 2
Investigation Methods of Performance Characteristics for Double-Fed Machines with Converter in Rotor Circuit. Summary of Main Investigation Stages of A.C. Machines

This chapter presents investigation methods on operation modes of high-power double-fed machines (DFMs) with frequency converter in rotor circuit. These methods are checked experimentally and are used in modern practice, for example, in production of these machines for operation both in modes of frequency-controlled motors and generators with variable rotation speed.

Main stages of their investigation are noted. Obtained there are equations for calculation of electromagnetic loads of these machines in various operational modes, including equations for calculation of current, voltages and power of rotor winding; they are initial for designing A.C. exciter (exciter EMF frequency is determined by machine slip). Practical examples are given.

As a result of generalization of these stages, it is possible to formulate the main investigation objectives for modern A.C. machines solved in subsequent chapters.

Content of this chapter is development of the methods stated in [14, 20–26].

2.1 Peculiarities of Investigation Methods

Let us consider main peculiarities in investigation methods of performance characteristics for machines of this type; the converter is included into their rotor circuit [21–24].

Summarizing main stages of this investigation, let us also determine basic investigation stages of A.C. machines with squirrel cage rotor windings in nonlinear networks. Investigation methods for these machines modes are more complicated than for DFMs due to the following reasons: rotor winding of DFM is three-phase one. Each phase of such a winding can be considered as the only loop of rotor with lumped parameters: resistance and leakage inductance. Unlike this winding, short-circuited rotor windings of synchronous and induction machines, for example, damper winding of salient-pole machine, squirrel-cage with damaged bars or without damages of induction machine, consist of several loops; these are windings

I. Boguslawsky et al., *Large A.C. Machines*,
DOI 10.1007/978-4-431-56475-1_2

with distributed parameters. Only in the simplest case of short-circuited winding, namely the squirrel cage, consisting of N_0 intact bars, in the theory of induction motors it is considered as a polyphase winding with number of phases m_{PH} equal to the number of those bars $(m_{PH} = N_0)$. In general, currents flowing through rotor short-circuited winding loops differ not only in phase, but also in amplitude. It is more difficult to determine these currents than those in a single current loop—either in one of three phases $(m_{PH} = 3)$ of DFM rotor winding or in one of N_0 squirrel cage phases without any damage.

Note another distinction of short-circuited winding in a salient pole machine rotor (damper winding, asymmetrical cage winding) from three-phase rotor winding of DFM: for a machine with short-circuited winding in nonlinear network, each EMF in rotor loops (E_{ROT}) with frequency ω_{ROT} corresponds in stator winding to two EMFs $\left(E_{ST,1}, E_{ST,2}\right)$ with frequencies ω_1 and ω_2 $\omega_1 \neq \omega_2$; it also refers, in particular, to the first spatial harmonic of the resulting field in the air gap.

Therefore, mode investigation methods of DFMs are easier. There is no need to investigate the current distribution in rotor short-circuited winding loops taking into consideration those two EMFs in stator winding, etc. However, it is also easy to identify main stages of solving more general problems specific to machines with rotor short-circuited windings and to give their physical interpretation.

Note further that the investigation methods of DFMs described in this chapter are of independent practical interest: It has already been pointed out that such machines are used in engineering practice.

DFMs now become more widely used in various industries including power industry. In motor modes, they are used in controlled electric drives, for example, blast furnace blowers, rolling mill converter units, turbochargers, etc.; their maximum rated power has reached 50–60 MW. In generator modes, they are used in power plants providing constant voltage frequency and amplitude at variable rotation speed of drive motors (diesel, turbine). Depending on type, the DFM maximum power is various: it is 5–8 MW for wind power and small hydroelectric power plants; 400 MW for high voltage transmission line generators; DFMs are also used as condensers (with 60 MVA maximum power) [27–31].

Another application field of such machines has become known recently "variable frequency transformers" [32]. This "variable frequency transformer" with 100 MVA rated power was manufactured by General Electric Co. It is used for connecting two power systems different, for example, in their frequency: its stator winding is connected to one of the systems and rotor winding—to another. Actually, such a "variable frequency transformer" is a device converting energy of one frequency to another. It is necessary to rotate a rotor of this machine to provide slip frequency between two systems. It has vertical design taking into consideration the machine high rated power and, correspondingly, its rotor dimensions. In this case, the air gap can be made smaller than in variant with horizontally-arranged machines. Neither advantages nor disadvantages of this trend are discussed as far as the application of DFMs is not concerned. They are not compared with other

technical solutions used in practice [6–9]. It should be noted that the method mentioned below, could also be used for developing such a converter of frequency.

Numerous extensive studies of DFM physical processes, methods of analysis and design, DFM regulation methods for determining optimal power models were launched in 20 s of XX century [10–12]; these were proved by experiments and operation in some European countries and the USA. DFM motor operation mode comprising electric drive (cascades) was considered initially; they differ in their speed regulation principles. DFM quasi steady state and transient processes in generator modes have been researched later. Currently, due to rise of DFM application level and use of frequency converter allowing us to control the rotor winding voltage in amplitude and phase, it is necessary to consider more strictly DFM magnetic circuit saturation, influence of DFM modes on this saturation and flux winding magnitude leakages, to consider the influence of higher time harmonic influence ($Q > 1$) on machine losses and shape of voltage curves [2–4, 6–9, 25].

After these preliminary remarks, let us proceed to investigation methods of performance characteristics for DFMs with frequency converter in rotor circuit. The method is set forth in the equations for two magnetically coupled circuits (stator and rotor); this system takes account of machine magnetic circuit saturation.

2.2 Problem Statement

The calculation methods of DFM modes are shown by examples of the generator mode, so that the original equations would have a univocal form; In references [6–9, 21–23, 25] these generators are sometimes called ASG (asynchronized synchronous generators); This name will be also used in this chapter for short. The equations are written similarly for the motor mode.

There are a number of peculiarities describing the rotational speed variation of DFM rotors:

- the first harmonic voltage at stator winding terminals remains constant in amplitude and frequency: $U_{ST,1} \neq f(n_{REV})$; $f_{ST,1} \neq f(n_{REV})$;
- the first harmonic voltage at rotor winding terminals varies in amplitude and frequency: $U_{ROT,1} = f(n_{REV})$; $f_{ROT,1} = f(n_{REV})$; it is assumed that rotor winding is powered from a frequency converter, for example, via contact rings;
- stator and rotor winding voltage contains a number of higher harmonics: $U_{ST,Q} = f(n_{REV})$; $U_{ROT,Q} = f(n_{REV})$; $f_{ST,Q} = f(n_{REV})$; $f_{ROT,Q} = f(n_{REV})$.

The task is to determine specified relationships.

The assumptions adopted in these equations are standard in A.C. machine theory. They take into account magnetic circuit saturation and higher time harmonic effect. In particular, it is accepted that the resulting flux in ASG air gap is

determined according to the Ampere's law [1, 2]. Magnetic circuit saturation is based on considering the first harmonic of this flux in MMF calculations. If necessary, the higher time harmonics can be registered using an iteration method.

2.3 Frequencies and Amplitudes of Voltage and Current First Harmonics in Machine Rotor and Stator Windings

2.3.1 Ratio of Frequencies $f_{ROT,1}$ and $f_{ST,1}$ at $n_{REV} = var$

In rotor speed variation modes ($n_{REV} = var$) the frequency converter control system should provide:

$$f_{ST,1} \neq f(n_{REV}); \quad f_{ROT,1} = f(n_{REV}).$$

The law of frequency regulation $f_{ROT.1}$ follows from the ratio:

$$f_{ST,1} = \left| \frac{pn_{REV}}{60} + f_{ROT,1}(-1)^{S+1} \right|. \tag{2.1}$$

Here S—sign defining the phase order sequence for the first ($Q_{ROT} = 1$) rotor winding time voltage harmonic or rotor field rotation direction relative to rotor.

Regulation laws of frequency converter are as follows:

- In rotor rotation speed modes at $n_{REV} < 60f_{ST}/p$ a direct phase sequence order (S = 1) should be provided for rotor winding first voltage harmonic; in this case the rotor field rotation direction of the first harmonic ($Q_{ROT} = 1$) and that of rotor coincide;
- In rotor rotation speed modes at $n_{REV} > 60f_{ST}/p$ an opposite phase sequence order (S = 2) should be provided for rotor winding first voltage harmonic; in this case the rotor field rotation direction of the first harmonic ($Q_{ROT} = 1$) and that of the rotor misalign;
- On the practice the modes with $n_{REV} > 60f_{ST}/p$ did not allowed.
- in modes approaching rotor synchronous speed $n_{REV} \approx 60f_{ST}/p$ the frequency of the first voltage harmonic ($Q_{ROT} = 1$) should be $f_{ROT,1} \approx 0$. At the same time, winding overheating in these phases can be different.

2.3.2 Ratio of Voltages $U_{ROT,1}$ and $U_{st,1}$ at n_{REV} = var

In rotor speed variation modes (n_{REV} = var) the frequency converter control system should provide:

$$U_{ST,1} \neq f(n_{REV});\ U_{ROT,1} = f(n_{REV}).$$

The voltage control law $U_{ROT,1}$ follows from the equitation system for magnetically coupled stator and rotor circuits [1, 2, 14, 30, 31]. It is reasonable to present them based on rotating field theory [5, 15, 16] as ASG is a non-salient pole machine. In contrast to the usual equation system of such two circuits, at first, machine magnetic circuit saturation is considered additionally, then influence of higher time harmonics.

In accordance with Kirchhoff's second law, for the first time harmonics of rotor and stator voltage windings we have:

$$I_{ROT,1}\kappa_1 + \Phi_{0,1}\kappa_2 = U_{ROT,1}(-1)^{S+1}, \tag{2.2}$$

$$I_{ST,1}\kappa_4 + \Phi_{0,1}\kappa_3 = U_{ST,1}. \tag{2.3}$$

$$K_1 = Z_{ROT,1} + Z_{F,1(ROT)};\quad Z_{ROT,1} = R_{ROT,1} + j2\pi f_{ROT,1}L_{ROT,1};$$
$$K_2 = j2\pi f_{ROT,1}W_{ROT}K_{W,ROT};\quad K_3 = -\,j2\pi f_{ST,1}W_{ST}K_{W,ST};$$
$$K_4 = -\,Z_{ST,1}\text{-}Z_{F,1(ST)};\quad Z_{ST,1} = R_{ST,1} + j2\pi f_{ST,1}L_{ST,1}.$$

Here $Z_{F,1(ROT)}$, $Z_{F,1(ST)}$—impedance of filter in rotor and stator windings, correspondingly; $Z_{ST,1}$, $Z_{ROT,1}$—impedance of stator winding and rotor correspondingly. In Eqs. (2.2) and (2.3) the impedance values $Z_{F,1(ROT)}$, $Z_{F,1(ST)}$ are calculated at frequencies $f_{ROT,1}$ and $f_{ST,1}$ respectively.

The following is valid for these magnetically coupled circuit windings: $F_{ROT,1} + F_{ST,1} = F_{0,1}$ or

$$I_{ROT,1}K_5 + I_{ST,1}K_6 + F_{0,1}K_7 = 0, \tag{2.4}$$

where

$$K_5 = \frac{m_{ROT}W_{ROT}K_{W,ROT}}{p\pi};\quad K_6 = \frac{m_{ST}W_{ST}K_{W,ST}}{p\pi};\ K_7 = -1;$$
$$F_{0,1} = F_{L,1} + F_{M.C.,1}.$$

Here $F_{ST,1}$, $F_{ROT,1}$—MMF complex amplitudes of stator and rotor respectively, $F_{0,1}$,…, $F_{M.C.,1}$ value—MMF magnetic circuit; $F_{L,1}$—MMF corresponding to $P_{L,1}$ sum of no-load losses and machine additional losses (considering ventilation, mechanical e.g., friction losses and losses in bearings, etc.) [13, 14, 16, 17]:

Table 2.1 Coefficients of the first equation system

$U_{ROT,1}$	$I_{ROT,1}$	$\Phi_{0,1}$	$F_{0,1}$	The right part
$(-1)^{S+1}$	$-K_1$	$-K_2$	0	0
0	0	K_3	0	$U_{ST,1}-I_{ST,1}K_4$
0	K_5	0	K_7	$-I_{ST,1}K_6$
0	0	1	$-E_N$	0

Note: E_N—coefficient (see Sect. 2.5.1)

$$F_{L,1} = I_{L,1}K_6, \text{ where } \left|I_{L,1}\right| \approx \frac{2P_{L,1}}{m_{ST}U_{ST,1}} \tag{2.5}$$

These losses are partially dependent on flux $\Phi_{0,1}$, as well as frequencies $f_{ST,1}$, $f_{ROT,1}$; it is suitable to determine the value $P_{L,1}$ using the iteration method. As an initial approximation, the value $I_{L,1} \approx 0$ can be set; as it has been proved by calculation practice, it is usually sufficient to have three iterations to determine the values $P_{L,1}$ and $I_{L,1}$. The machine magnetic circuit saturation is calculated taking into account the magnetization characteristics according to [13, 16]:

$$\Phi_{0,1} = \Phi\left(F_{M.C.,1}\right). \tag{2.6}$$

Equations (2.1)–(2.6) make up a system for solving the first problem. The followings are set: values $U_{ST,1}$; $I_{ST,1}$; $f_{ST,1}$; $f_{ROT,1}$; impedances $Z_{ST,1}$; $Z_{ROT,1}$; $Z_{F,1(ST)}$; $Z_{F,1(ROT)}$; magnetization characteristic $\Phi_{0,1} = \Phi\left(F_{M.C.,1}\right)$.

There are four unknown values in the system: $U_{ROT,1}$; $I_{ROT,1}$; $\Phi_{0,1}$; $F_{0,1}$. The system coefficients are given in Table 2.1.

It should be noted that in ASG modes at speeds $n_R > 60f_{ST}/p$ rotor winding can correspond to generator mode.

As a result of problem solution given in this paragraph, it is possible to calculate the exciter and frequency converter, thus to determine a series of higher time voltage harmonics in ASG rotor circuit.

2.4 Frequencies and Amplitudes of Voltage and Current Higher Time Harmonics in Machine Rotor and Stator Windings

Amplitude values of higher current harmonics in rotor winding, as well as stator winding voltage and current, are determined by solving the second problem. It allows us to determine a voltage waveform of ASG stator winding, standardized by IEC and GOST (Russian State Standard) [35]; simultaneously the filter options in these windings are determined providing acceptable curve distortion degree.

2.4.1 Ratio of Frequencies $f_{ROT,Q}$ and $f_{ST,Q}$ at $n_{REV} = var$

Now the relation between higher harmonics voltage frequencies ($Q_{ROT} > 1$) in both windings is determined. Similar by to (2.1) we obtain:

$$f_{ST,Q} = \left| \frac{pn_{REV}}{60} + f_{ROT,Q}(-1)^{D+1} \right|, \tag{2.1′}$$

where D—sign defining the phase sequence voltage for rotor winding higher ($Q_{ROT} > 1$) time voltage harmonics or direction of rotor field rotation for this harmonic relative to rotor.

Now, we consider the modes of some practical interest:

In modes at rotor rotation speeds $n_{REV} < 60\frac{f_{ST}}{p}$ (S = 1) the rotor fields of time order $Q_{ROT} = 5, 11, 17,\ldots, 6\,K–1$ (at K = 1, 2, 3…) and rotor rotate in the opposite direction (D = 2), rotor fields of time order $Q_{ROT} = 7, 13, 19,\ldots, 6\,K + 1$ (at K = 1, 2, 3,…) and rotor—in the same direction (D = 1).

In modes at rotor rotation speeds $n_{REV} > 60\frac{f_{ST}}{p}$ (S = 2), rotor fields of time order Q_{ROT} = 5,11,17,.., 6 K–1 (at K = 1,2,3 …) and rotor rotate in the same direction (D = 1), rotor fields of time order Q_{ROT} = 7,13,19,.., 6 K + 1 (at K = 1,2,3…) and rotor—in the opposite direction (D = 2).

Example. Frequency of the first voltage harmonic of ASG stator winding with number of poles 2p = 4 is equal to $f_{ST,1}$ = 50 Hz; let us accept the rotor rotation speed equal to n_{REV} = 1150 rpm. As it follows from Eq. (2.1), the frequency of the first voltage harmonic of rotor winding is equal to $f_{ROT,1}$ = 11.67 Hz (S = 1). Then, harmonic of the order Q_{ROT} = 5 ($f_{ROT,5}$ = 58.33 Hz) according to (2.1′) corresponds to the frequency $f_{ST,5}$ = 20 Hz (D = 2), and harmonic of the order Q_{ROT} = 7 ($f_{ROT,7}$ = 81.67 Hz), to the frequency $f_{ST,7}$ = 120 Hz (D = 1).

Note. It is assumed in the example that the number of rotor winding phases is equal to $m_{ROT} = 3$. In this case, it is possible to reduce the voltage harmonic amplitude of frequency $f_{ST,Q}$ by filters in both windings. However, when the number of phases $m_{ROT} = 6$, the time harmonic rotor fields of order $Q_{ROT} = 5$ and $Q_{ROT} = 7$ do not induce any additional voltages in stator winding.

2.4.2 Ratio of Voltages $U_{ROT,Q}; U_{ST,Q}$ at $n_{REV} = var$

In rotor speed variation modes ($n_{REV} = var$) frequencies of voltages of both windings $f_{ROT,Q}$ and $f_{ST,Q}$, and their amplitudes $U_{ROT,Q}$ and $U_{ST,Q}$ change.

In order to determine ratios of these amplitudes, it is advisable to use the rotating field theory [5, 15] for solving this problem, similar to that of the first problem. At the same time, it is also possible to consider magnetic circuit saturation [5, 17].

In accordance with the Kirchhoff's second law the winding voltages of stator and rotor higher time harmonics are as follows:

$$I_{ROT,Q}\kappa_{1,Q} + \Phi_{0,Q}\kappa_{2,Q} = U_{ROT,Q}, \tag{2.2'}$$

$$I_{ST,Q}\kappa_{4,Q} + \Phi_{0,Q}\kappa_{3,Q} = 0, \tag{2.3'}$$

where $K_{1,Q}$; $K_{2,Q}$; $K_{3,Q}$; $K_{4,Q}$—coefficients similar to those K_1; K_2; K_3; K_4 from the first problem, the impedance values $Z_{ST,Q}$; $Z_{ROT,Q}$; $Z_{F,Q(ST)}$; $Z_{F,Q(ROT)}$, which they contain, are computed for frequencies $f_{ST,Q}$ and $f_{ROT,Q}$, respectively.

For stator winding voltage the following ratio is true: $U_{ST,Q} = I_{ST,Q}Z'_{ST}$; where Z'_{ST} is load impedance, which is external relative to stator winding terminals.

The expression similar to (2.4) is true to magnetically coupled rotor and stator circuits based on Ampere's law:

$$F_{ROT,Q} + F_{ST,Q} = F_{0,Q}$$

or

$$I_{ROT,Q}\kappa_5 + I_{ST,Q}\kappa_6 + F_{0,Q}\kappa_7 = 0, \tag{2.4'}$$

where $F_{0,Q} = F_{1,Q} + F_{MC.,Q}$. Here, $F_{M.C.,Q}$—magnetic circuit MMF depending on mutual flux similar to (2.6) according to the relation:

$$\Phi_{0,Q} = \Phi\left(F_{MC.,Q}\right). \tag{2.5'}$$

$F_{L,Q}$—MMF component corresponding to the sum of machine no-load and additional losses for frequencies $f_{ST,Q}$ and $f_{ROT,Q}$ (without ventilation losses, mechanical losses, for example, friction, in bearings, etc.) [13, 14, 16, 17]:

$$F_{L,Q} = I_{L,Q}K_6, \left|I_{L,Q}\right| \approx \frac{2P_{L,Q}}{m_{ST}U_{ST,Q}} \tag{2.6'}$$

These losses can be calculated using an iteration method.

Equations (2.1′)–(2.6′) make up a system for solving the second problem: where impedances $Z_{ST,Q}$; $Z_{ROT,Q}$; $Z_{F,Q(ST)}$ $Z_{F,Q(ROT)}$; magnetization characteristic $\Phi_{0,Q} = \Phi\left(F_{MC,Q}\right)$.

There are four unknown values in the system: $I_{ROT,Q}$; $I_{ST,Q}$; $\Phi_{0,Q}$; $F_{0,Q}$, and the system coefficients are given in Table 2.2.

It should be noted that voltage and current complex values $\left(U_{ST,1}; I_{ST,1}; U_{ROT,1}; I_{ROT,1}\right)$ in both problems determine the power factor values $\left(\cos\varphi_{ST,1}; \cos\varphi_{ROT,1}\right)$ and, respectively, $\cos\varphi_{ST,Q}$; $\cos\varphi_{ROT,Q}$, as well as values of active and reactive power.

Table 2.2 Coefficients of the second equation system

$I_{ROT,Q}$	$I_{ROT,Q}$	$\Phi_{0,Q}$	$F_{0,Q}$	Right part
$K_{1,Q}$	0	$K_{2,Q}$	0	$U_{ROT,Q}$
0	$K_{4,Q}$	$K_{3,Q}$	0	0
K_5	K_6	0	K_7	0
0	0	1	$-E'_N$	0

Note: $-E'_N$—coefficient (see Sect. 2.5.2)

2.5 Method for Solving Both Problems; Two Systems of Equations

In ASG modes with preset values of power factor and stator current, the first problem can be solved without an iteration method [13, 14, 17]: flux $\Phi_{0,1}$—is determined from Eq. (2.3): $F_{0,1}$ and MMF $F_{M.C.,1}$—from magnetization characteristic (2.6) and from relationship (2.4), herewith, $F_{M.C.,1}$ MMF has the same phase angle as $\Phi_{0,1}$; $I_{ROT,1}$—from (2.4); $U_{ROT,1}$—from (2.2).

However, the given equation systems with their minor modifications remain valid for the calculation of DFM performance characteristics not only in ASG modes, but also in other modes, for example, in frequency controlled motor modes. If the generator power factor (or stator winding current) is not specified, it is also necessary to modify the equations of both systems for ASG.

Let us consider in more detail a method of calculation of DFM modes with account of magnetic circuit saturation for this general case: ASG or motor.

2.5.1 Magnetization Characteristics Presentations $\theta_{0.1} = \theta(F_{M.C.,1})$ in Piecewise Linear Function Form

Both systems are nonlinear: they take into account magnetic circuit saturation in accordance with (2.6) and (2.6′). To solve them, it is advisable to introduce the characteristic (2.6) as a piecewise linear function.

In the simplest case, this feature could be presented as a straight line drawn from the origin of coordinates. In this case, the magnetic circuit impedances would not be dependent on the flux.

In a general case, this characteristic can be presented as consisting of S discrete points at the intersections of magnetization curve (2.6) and straight lines drawn from the origin of coordinates.

With account of Table 2.3, the relation between flux $\Phi_N(\Phi_N \in \Phi_{0,1})$ in the portion with number N = 1, 2,…, S and MMF $F_{M.C.,N}$ in the same portion takes the form [14] $\Phi_N = E_N \cdot F_{M.C.,N}$.

Table 2.3 Angular coefficient E_N for approximation of elation between flux in portion with number N and MMF in the same portion

N	E_N	Portions Φ_N
1	E_1	$0 \le \Phi_N < \Phi_1$
2	E_2	$\Phi_1 \le \Phi_N < \Phi_2$
⋮	⋮	⋮
N	E_N	$\Phi_{N-1} \le \Phi_N < \Phi_N$
⋮	⋮	⋮
S–1	E_{S-1}	$\Phi_{S-2} \le \Phi_N < \Phi_{S-1}$
S	E_S	$\Phi_{S-1} \le \Phi_N < \Phi_S$

Thus, the only parameter, namely, the angular coefficient E_N corresponds to each straight line drawn from the origin of coordinates. Its value at N = 1 corresponds to unsaturated magnetic circuit.

For this representation of curve, the equation system (2.1)–(2.6) is quasilinear for all values N = 1, 2,…, S. The system can be considered solved provided the calculated values of field in air gap and MMF respond to the value of coefficient E_N in Table 2.3, for which they were determined.

2.5.2 *Peculiarities of Solving Both Systems*

The algorithm for solving the first system $(Q_{ROT} = 1)$ can be represented by the following calculation sequence:

(a) Magnetization characteristic calculation (2.6) as per [5, 17];
(b) This characteristic should be presented as it is shown in Table 2.3. In practical calculations, the portion $0 < \Phi_N < \frac{1}{2}\left[\Phi_{0,1}\right]_{NOM}$ can be represented as a single line with coefficient E_N (for N = 1), where $\left[\Phi_{0,1}\right]_{NOM}$ is the flux approximate value in nominal (rated) mode;
(c) Numerical solution of quasilinear system of Eqs. (2.1)–(2.6) at $E_N (1 \le N \le S)$. Coefficient E_N (for N = 1) is assumed as the initial approximation.
Results of system solution: $U_{ROT,1}$; $I_{ROT,1}$; $\Phi_{0,1}$; $F_{0,1}$ and $F_{M.C.,1}$;
(d) Analysis of these results: the angular coefficient value E_{N+K} (at $K \ge 0$) is determined according to Table 2.3 for flux $\Phi_{0.1}$. If this value is equal to E_N (K = 0), the results are the desired system solution (the end of the first problem solution);
(e) Otherwise, the following coefficient value E_N (assign $N = N + 1$) should be selected from Table 2.3 and computation of algorithm items: (c), (d), (e) are repeated.

This method can be used for an arbitrary curve form (2.6). The only requirement for this curve is as follows: the first derivative for angular coefficient $E'_N = \frac{\partial \Phi_{0,1}}{\partial F_{M.C.,1}}$ in

Table 2.4 Results of mode calculation for ASG 1250 kW

n_{REV}, rpm	$f_{ROT,1}$, Hz	$U_{ROT,1}$, V	$\cos \varphi_{ROT,1}$
1300	6.67	120	0.635
1350	5.0	94.5	0.65
1400	3.34	63.0	0.68
1450	1.67	35.0	0.755
1550	1.67	19.5	0.36

Note: $f_{ST,1} = 50°Hz$; $I_{ST,1} = 145A \neq f(n_{REV})$; $I_{ROT,1}A \neq f(n_{REV})$

Table 2.5 Influence of higher order time harmonics Q = 5 and Q = 7

Q	$f_{ST,Q}$, Hz	$f_{ROT,Q}$, Hz	$I_{ST,Q}$, A	$I_{ROT,Q}$, A	$U_{ROT,Q}$, V	$\cos \varphi_{ROT}$
5	20	25	37	181	19.0	0.115
7	80	35	19	93	13.5	0.105

the calculation area of magnetization curve should be continuous. This requirement is always satisfied in practical calculations.

The algorithm of the second system solution in addition should be based on that the saturation degree of machine magnetic circuit is already determined as a result of first problem solution. Mutual induction flux $\Phi_{0,Q}$ and $F_{M.C.,Q}$ MMF in the calculation area can be approximately presented as [18]:

$$\Phi_{0,Q} \approx E'_N F_{M.C.,Q}; \quad \text{here} \quad E'_N = \frac{\partial \Phi_{0,1}}{\partial F_{M.C.,1}} \quad (**).$$

The sign (**) shows that the derivative is taken at the point of machine magnetization characteristic (2.6) corresponding to the flux $\Phi_{0,1}$ determined in the first problem.

Results of mode calculation for ASG 1250 kW, 6.3 kV; 2p = 4 are given in Table 2.4. The effect of higher order time harmonics of EMF and of the rotor currents for Q = 5 and Q = 7 for speed n_{REV} = 1350 rpm is taken into account in Table 2.5.

2.6 Check of Methods

Calculation methods have been tested experimentally by the bench test at « Elektrosila » Work, Stock Company "Power Machines" St.-Petersburg. An induction motor with phase-wound rotor 630 kW, 6 kV, 2p = 12 was used for ASG mode. Excitation was performed with the use of a converter that included a D.C. motor and a synchronous generator [20]. It provided voltage variation in amplitude and frequency. When rotor winding is fed with voltage of higher harmonic order

Q_{ROT} = 5, 11, 17, the reverse phase sequence (A, C, B) was chosen, and for harmonics of order Q_{ROT} = 7, 13, 19—the direct one (A, B, C); thus, rotor rotation speed was $n_R < 500$ rpm. Discrepancy between calculated and tested values of currents in windings did not exceed 6 %.

It should be noted that in practice, when using serial induction motors with phase-wound rotor as ASG, their rated power needs to be lowered by 15–20 % to keep rotor winding overheat at the same level as for motors.

2.7 Excitation System Peculiarities

For DFMs as well as for synchronous machines two exciter versions [3, 4] are possible: brushless or static (with slip rings). In production and operation each of them has advantages and disadvantages. Brushless exciters are traditionally used for synchronous machines. Recently, the works for DFMs have been under way to improve brush assembly operational reliability of brushes and slip rings unit [33, 34] to avoid brushless versions of exciters. Some peculiarities of exciters for DFMs should be noted. Unlike synchronous machine exciters, its dimensions are determined by two apparent power components $P_{TOT,1}$ of rotor winding: $P_{TOT,1} = P_{AC,1} + jP_{R,1}$; the active power $P_{AC,1}$ is determined by machine electromagnetic power and its slip (with account of winding skin effect); reactive power $P_{R,1}$ depends on the rotor winding inductance and slip; that is, on its impedance (also with account of skin effect) [3, 4, 13, 16]. Hence, dimensions of exciter active part and converter in its circuit for DFM are more than for synchronous machine of the same power. The difference is determined by the speed control range in operating conditions.

2.8 Summarizing the Results: Main Stages of A.C. Machine Investigations with Rotor Short Circuited Windings

2.8.1 Stator and Rotor Circuits Frequency Voltage. Rotational Speed of Rotor and Stator Fields in Air Gap

The ratio between the first harmonic voltage circuit frequencies of rotor and stator loops is determined for DFMs in Sect. 2.3.1 with using (2.1), and the ratio between higher time harmonic frequencies at the first spatial harmonics ($|m| = |n| = 1$) is determined using Eq. (2.1′) (see Sect. 2.4.1). These fields cause the resultant field in air gap and torque on machine shaft.

As it follows from equations for a DFM, each time harmonic of frequency EMF ω_{ROT} in rotor loop corresponds to one frequency EMF ω_1 in stator loop, and,

therefore, one resulting field in air gap, one torque on machine shaft torques. This is true for spatial harmonics of order $(|m| = |n| \geq 1)$. However, the calculation method mentioned in this chapter takes into account only first spatial harmonic.

Let us designate in this paragraph for short the machines operating in nonlinear networks and with short-circuited loops in rotor in the form of damper winding, squirrel cage with asymmetry as: machines type (*). As it has already been noted, there are some differences in DFMs and machine type (*). In particular, to each EMF harmonic in rotor loops (E_{ROT}) with frequency ω_{ROT} of (*) type machines, in stator winding there correspond to two EMFs $\left(E_{ST,1}, E_{ST,2}\right)$ with frequencies ω_1 and ω_2. Two stator fields and two rotor fields with ω_{ROT} frequency currents correspond to them. These fields produce two resultant fields in air gap different in their amplitudes, rotation direction and speed and two–machine shaft torques. This regularity is true for spatial harmonics of any order $(|m| = |n| \geq 1)$ for (*) type machines. Ratio of EMF frequencies in rotor and stator loops of these machines is given in Chap. 3.

They allow us to determine rotor and stator magnetically coupled circuits of (*) type machines.

2.8.2 *Ampere's Law Equations*

The ratio between the first time harmonics of MMF stator and rotor windings is determined by Eq. (2.4) for a DFM in Sect. 2.3.2. Both summands of this equation correspond to the fields of the stator and rotor first time harmonics mutually fixed in air gap generating one resulting field. The same is true for fields of each stator and rotor higher time harmonic, their MMFs correspond to Eq. (2.4′) in Sect. 2.4.2; they are also mutually fixed in air gap and generate one resulting field.

Each of these two equations contains expressions for MMF stator and rotor windings. MMF equations are known [3, 4] and given in the above-mentioned paragraphs for multiphase stator windings (usually three-phase, rarely six-phase) and three-phase rotor winding.

However, the problem is more complicated for type (*) machines. It is necessary to investigation preliminarily the current distribution in bars and ring portions of these short-circuited windings in order to write down expressions for MMF of damper winding or squirrel cage with damages. This investigation is an independent problem, and it is solved in subsequent chapters.

2.8.3 *Kirchhoff's Second Law Equations for Stator Winding*

Ratio between the first time harmonics of EMFs, voltages and stator loop currents is determined in Sect. 2.3.2 for DFMs using Eq. (2.3). Ratio between their time higher harmonics is determined in Sect. 2.4.2 using Eq. (2.3′). Stator winding in these

equations is considered as a lumped circuit (with A.C. resistance and leakage inductance), set up in solving the problem. Each of these two equations is based on the assumption that the expression for resultant mutual induction fluxes $\Phi_{0,1}$ and, respectively, $\Phi_{0,Q}$ are determined by Eqs. (2.6) and (2.6′).

However, for (*) type machines, determination of these mutual induction fluxes is connected with a need to find the rotor winding MMF requiring the previous investigation of the distribution of currents in elements of damper winding or squirrel cage with damages. It has already been noted that this investigation makes up a separate problem, and it is solved in the following chapters.

2.8.4 *Kirchhoff's Second Law Equations for Rotor Loops. System of Equations*

The ratio between the first time harmonics of EMFs, voltages and rotor circuit currents is determined in the same paragraphs for DFMs using Eq. (2.2) and the ratio between their higher harmonics—using Eq. (2.2′). The rotor winding in these equations as well as the stator winding are considered as a lumped circuit (with A. C. resistance and leakage inductance) given in solving the problem.

However, rotor winding unlike stator winding is a circuit with distributed parameters for (*) type machine. It consists of a series of short-circuited loops. Therefore, the system of equations, whose order responds to the number of loops, should be written instead of a single equation as in (2.2) or (2.2′). It should also include the equation of the form (2.3) or (2.3′) for stator in addition to rotor circuit equations according to Kirchhoff's second law. At the same time, EMFs, voltages and currents in stator loops, which differ in frequency [1, 2], should be considered in the system. This numerical solution modification is given in Chap. 5. A system of equations for short-circuited rotor loops is given as a part of this modification. It allows reducing the order for system of equations for magnetically coupled loops.

The above-stated confirms additionally that it is necessary to solve preliminarily the problem of currents distributions in short-circuited rotor winding elements: damper winding or squirrel cage with damages. When solving this problem, it is suitable to use generalized current and MMF characteristics of rotor windings.

Appendix 2.1

A general method of calculating DFM operating characteristics outlined above (in Sects. 2.2–2.7) allows one to calculate the mode characteristics of frequency-controlled motor, condenser, generator and frequency inverter. It is reduced to solving systems of equations of the fourth order in the complex plane. However, in

practice, it appears appropriate to develop additionally a DFM calculation method similar to factory methods [13, 17, 19] for calculating non-salient pole machines (turbogenerators, turbomotors and induction machines). It allows the engineer under production conditions to consider the experience of developing traditional designs of these non-salient pole machines. Key elements of this methodology are given below in Sects. A.2.1.1–A.2.1.5 as applied to DFM "overexcitation" in motor, condenser, generator modes.

A.2.1.1 DFM Rotor Current and MMF Under Load

Now, let us use the Ampere's law according to Eq. (2.4). The first summand in the expression for $F_{0,1} = F_{1,1} + F_{M.C.,1}$ can be neglected. Magnetic circuit MMF amplitude $F_{M.C.,1}$ contains two summands [13, 17]:

$$F_{M.C.,1} = F_{M.C.ST,1} + F_{M.C.ROT,1}. \tag{A.2.1.1}$$

First of them $F_{M.C.ST,1} = F_{M.C.GAP,1} + F_{M.C.TOOTH,1} + F_{M.C.YOKE,1}$ contains three components: MMF of air gap, teeth and stator yoke, respectively. These components in (A.2.1.1) are determined by air gap, stator magnetic circuit geometry and mutual induction flux $\Phi_{0,1}$ in air gap [1, 13, 19]:

$$\left|\Phi_{0,1}\right| = \left|\frac{j}{\omega_1 W_{ST} K_{WST}} E_v U_{0,1}\right|, \quad E_v = \sqrt{\cos^2\varphi + \left(X_{ST,1} + \sin\varphi\right)^2}, \tag{A.2.1.2}$$

where ω_1—network angular frequency; E_V—internal EMF [13, 19]; $X_{ST,1}$—stator winding leakage inductance (in per units system, p.u.); we accept that it exceeds A. C. resistance $R_{ST,1}$; $\cos\varphi$—power factor on DFM stator terminals.

The second summand in (A.2.1.1) $F_{M.C.ROT,1} = F''_{M.C.TOOTH,1} + F''_{M.C.YOKE,1}$ contains two components respectively, MMF of rotor teeth and yoke [13, 17, 19]. Both components are determined by the sum $\Phi'_{MI,1}$ of mutual flux $\Phi_{0,1}$ in (A.2.1.2) and rotor slot leakage fluxes $\Phi_{M.C.LEAK,1}$:

$$\left|\Phi'_{MI,1}\right| = \left|\Phi_{0,1}\right| + \left|\Phi_{M.C.LEAK,1}\right|. \tag{A.2.1.3}$$

Here $\Phi_{M.C.LEAK,1} = \left|F_{GEN.EQ,1}\right| \cdot \Lambda_{SLOT.LEAK}$, where $\Lambda_{SLOTLEAK}$,—rotor slot leakage conductivity [13, 17, 19]; $F_{GEN.EQ,1}$—equivalent generator MMF. Based on the calculation method for turbogenerators and turbomotors, let us determine it in the form of sum of two complex amplitudes [19]:

$$F_{GEN.EQ,1} = F_{ST,1} + F_{M.C.ST,1}. \tag{A.2.1.4}$$

where $F_{ST,1}$—MMF of stator winding (phasor).

In practical calculations, it is convenient to calculate complex amplitude module in (A.2.1.4) $F_{GEN.EQ,1}$ in the form:

$$\left|F_{GEN.EQ,1}\right|^2 = \left|F_{ST,1}\right|^2 + \left|F_{M.C.ST,1}\right|^2 + 2\frac{\left|F_{ST,1}\right| \cdot \left|F_{M.C.ST,1}\right|}{\sqrt{1 + \left(\frac{\cos\varphi}{X_{ST,1} + \sin\varphi}\right)}} \tag{A.2.1.5}$$

After determination of $F_{GEN,EQ,1}$ according to (A.2.1.4) or (A.2.1.5), $\Phi'_{MI,1}$ according to (A.2.1.3), we obtain consistently MMF of $F''_{M.C.TOOTH,1}$, $F''_{M.C.YOKE,1}$ and $F_{M.C.ROT,1}$. As a result we obtain the component in (A.2.1.1) $F_{M.C,1}$—MMF of DFM magnetic circuit.

The required complex amplitude of rotor MMF at load $F_{ROT,1}$ is calculated according to (A.2.1.6) and (A.2.1.7).

First, let us determine complex amplitude components in stator coordinates (real axis is aligned with complex phase voltage, and imaginary one makes the angle $+\pi/2$):

$$\begin{aligned} \mathrm{Re}\left(F_{ROT,1}\right) &= -\left|F_{M.C.,1}\right| \cdot \sin\psi - \left|F_{ST,1}\right| \cdot \cos\varphi; \\ \mathrm{Im}\left(F_{ROT,1}\right) &= \left|F_{M.C.,1}\right| \cdot \cos\psi + \left|F_{ST,1}\right| \cdot \sin\varphi. \end{aligned} \tag{A.2.1.6}$$

Here MMF phase angle $F_{M.C.,1}$ is equal to $\psi = \arccos\frac{X_{ST,1} \cdot \sin\varphi + 1}{E_v} + \frac{\pi}{2}$; angle φ—corresponds to DFM power factor. Let us note that according to (A.2.1.6) in the adopted coordinate system, the MMF complex $F_{M.C.,1}$ is positioned so that the angle ψ is within the range: $\frac{\pi}{2} \le \psi < \pi$. In practical calculations, the complex module $F_{ROT,1}$ for check is calculated similarly (A.2.1.5):

$$\begin{aligned} \left|F_{ROT,1}\right|^2 &= \mathrm{Re}^2\left(F_{ROT,1}\right) + \mathrm{Im}^2\left(F_{ROT,1}\right) \\ &= \left|F_{ST,1}\right|^2 + \left|F_{M.C.,1}\right|^2 + 2\frac{\left|F_{ST,1}\right| \cdot \left|F_{M.C.,1}\right|}{\sqrt{1 + \left(\frac{\cos\varphi}{X_{ST,1} + \sin\varphi}\right)^2}} \end{aligned} \tag{A.2.1.7}$$

As it follows from the ratio (A.2.1.7), for DFM: $\left|F_{ROT,1}\right| > \left|F_{ST,1}\right|$.

The rotor current under load $I_{ROT,1}$ is determined according to (A.2.1.7) from the known ratios [13, 17] used for MMF polyphase winding.

A.2.1.2 Phase Angle Defining Complex Amplitudes Position of MMF $\mathbf{F_{ROT,1}}$ and Current $\mathbf{I_{ROT,1}}$ (in Stator Coordinates)

Using Eq. (A.2.1.6), the following is obtained:

$$\beta = \pi - \operatorname{arctg}\left|\frac{\mathrm{IM}\left(F_{ROT,1}\right)}{\mathrm{RE}\left(F_{ROT,1}\right)}\right|. \tag{A.2.1.8}$$

Let us note that according to (A.2.1.6) in the adopted coordinate system, the MMF complex $F_{ROT,1}$ is positioned, so that the angle β is within the range: $\frac{\pi}{2} < \beta < \pi$.

A.2.1.3 Rotor Winding Voltage, Its Components

Now, the Eq. (2.2) for complex $U_{ROT,1}$ is transformed to find out its real and imaginary components. They determine the phase angle γ in this complex. To do it, the following ratio is preliminarily calculated:

$$Z_{EQ,1} = \Phi_{0,1}\frac{j2\pi f_{ROT,1} \cdot W_{ROT} \cdot K_{W,ROT}}{I_{ROT}} = \left|Z_{EQ,1}\right|e^{j\delta} = R_{EQ,1} + jX_{EQ,1}, \tag{A.2.1.9}$$

Taking into account Eq. (A.2.1.9), the following is obtained:

$$\begin{aligned}\mathrm{Re}\left(U_{ROT,1}\right) &= \mathrm{Re}\left(I_{ROT,1}\right) \cdot \left(R_{ROT,1} + R_{EQ,1}\right) - \mathrm{Im}\left(I_{ROT,1}\right) \cdot \left(X_{ROT,1} + X_{EQ,1}\right),\\ \mathrm{Im}\left(U_{ROT,1}\right) &= \mathrm{Re}\left(I_{ROT,1}\right) \cdot \left(X_{ROT,1} + X_{EQ,1}\right) + \mathrm{Im}\left(I_{ROT,1}\right) \cdot \left(R_{ROT,1} + R_{EQ,1}\right),\end{aligned} \tag{A.2.1.10}$$

where $X_{ROT,1} = j2\pi f_{ROT,1} \cdot L_{ROT,1}; X_{ST,1} = j2\pi f_{ST,1} \cdot L_{ST,1}$. According to (A.2.1.10), the complex amplitude modulus of this phase voltage is equal to:

$$\left|U_{ROT,1}\right| = \sqrt{\mathrm{Re}^2\left(U_{ROT,1}\right) + \mathrm{Im}^2\left(U_{ROT,1}\right)}. \tag{A.2.1.11}$$

In practical calculations, the complex amplitude module $U_{ROT,1}$ is calculated as a check as follows:

$$\left|U_{ROT,1}\right| = \left|I_{ROT,1}R_{ROT,1} + jI_{ROT,1}X_{ROT,1} + j2\pi f_{ROT,1}\Phi_{0,1}W_{ROT}K_{WROT}\right|. \tag{A.2.1.12}$$

A.2.1.4 Phase Angle Defining Complex Amplitude Position $U_{ROT,1}$

In stator coordinates, the angle defining position of rotor voltage complex $U_{ROT,1}$ is equal to,

$$\gamma = \pi + \operatorname{arctg}\left|\frac{\operatorname{Im}(U_{ROT,1})}{\operatorname{Re}(U_{ROT,1})}\right|. \tag{A.2.1.13}$$

A.2.1.5 Rotor Winding Power Factor; Active and Reactive Winding Power; Rotor Winding Losses

It is necessary to maintain the rotor winding power factor $\cos \varphi_{ROT,1}$ by means of an exciter (frequency converter) to ensure DFM operational characteristics for operation in network (including its given active and reactive power values, etc.).

It is determined with the help of phase angle values β as per (A.2.1.8) and γ as per (A.2.1.13)

$$\varphi_{ROT,1} = \gamma - \beta. \tag{A.2.1.14}$$

The angle $\varphi_{ROT,1}$ should be maintained by DFM control system in real time [6–9].

From the obtained expressions for $U_{ROT,1}, \varphi_{ROT,1}$ for rotor windings, we calculate [13, 17] apparent, active and reactive powers of exciter (frequency converter), and also rotor winding losses.

A.2.1.6 DFM Rotor Winding Design Peculiarities

First, let us consider design peculiarities of bar winding [5, 13, 16]. The Field's factor value for DFM high power winding is estimated. The DFM rotor slot height is assumed to be H = 200 mm, the copper height in it is $H_{CU} = 150$ mm, and the Field's coefficient for transposed bars at frequency $f_{50} = 50$ Hz is equal to $K_{F,50} \approx 1.25$. At frequency $f_{ROT,1} = 2.5$ Hz (slip 0.05) we obtain:$K_{F,S} \approx 1.0$. Now this coefficient is determined at first for the same equivalent bar with $f_{ROT,1} = 2.5$ Hz without any transposition. A "reduced height" is to be found for this bar [1, 2] $H_{RED} = K' \cdot H_{CU}$ at industrial frequency (50 Hz):

$$H_{RED,50} = \sqrt{\frac{\omega_{50}\mu_0\Delta}{2\rho_{CU}}} \cdot H_{CU} = 0.085 \cdot H_{CU} = 12.5$$

where μ_0—air magnetic permeability, $\Delta \approx 0.8$—copper width in slot/slot width ratio, ρ_{CU}—specific resistance (at the temperature 75°C); hence, at frequency $f_{ROT,1} = 2.5$ Hz we obtain: $H_{RED,ROT,1} = 2.8$. It is assumed that the ratio of bar slot part to its length is equal to $\lambda \approx 0.75$. Then, for non-transposed bar, the Field's coefficient at $f_{ROT,1} = 2.5$ Hz is equal to $K'_{F,S} \approx 2.1$. This practically eliminates a possibility to use bars without any transposition in the design of bar winding for DFM.

Now, the coil winding design peculiarities are considered [13, 14, 17]. For this winding at H = 200 mm and $f_{ROT,1} = 2.5$ Hz:$K'_{F,S} \approx 1.0$. Hence, the coil winding does not cause any problems with additional losses and in overheating for DFM at slip $S \leq 0.05$.

Appendix 2.2

Generalized current characteristic of three-phase rotor winding of DFM.

As an example of DFMs, let us determine the concept of rotor winding generalized current characteristic [14, 26] in relation to the first time harmonics ($Q_{ROT} = 1$) of current and EMF also to the first spatial harmonic (m = 1) of the resulting field in air gap (mutual induction field); in this winding the resulting field in air gap induces EMF with slip frequency ω_{ROT}.

Let us name the current relation in rotor three-phase winding $I_{ROT,1}$ from Eq. (2.2) to flux density amplitude by m = 1, $Q_{ROT} = 1$ as current generalized characteristic. The flux and the flux density amplitude relation is determined at first as:

$$\Phi_{0,1} = \frac{1}{\pi} T_1 \cdot L \cdot B(m = 1, Q_{ROT} = 1).$$

Then, the EMF induced in winding by this current at the frequency ω_{ROT} is equal to:

$$E_{ROT,1} = -\frac{j\omega_{ROT}}{\pi} T_1 \cdot L_{COR} \cdot W_{ROT} \cdot K_{W,ROT} \cdot B_{0,1}.$$

Here $B_{0,1} = B\,(m = 1,\, Q_{ROT} = 1)$. Generalized characteristic of rotor winding current for the first current time harmonics and EMF and the first resultant field spatial harmonic in air gap can be determined as:

$$I_{ROT,1} = \left[I_{ROT,1}\right] \cdot B_{0,1}.$$

Physically, this generalized current characteristic in rotor three-phase winding at the frequency $\omega_{ROT} = \text{idem}$ can be considered as a similarity criterion. It determines in flux density scale $B(m = 1, Q_{ROT} = 1)$ the amplitude and current phase in this winding. In subsequent calculations, a similar concept of generalized MMF winding characteristics is introduced. It will be used to form a system of equitation of magnetically coupled rotor and stator loops.

Brief Conclusions

1. Calculation methods for DFMs allow us to make calculations of the following with account of magnetic circuit saturation: voltages and currents in windings caused by the first time harmonic; voltages and currents of higher time harmonics caused by operation of frequency converter in rotor circuit.
2. Results of mode calculation are initial for further calculations:
   - of exciter in rotor circuit;
   - of filter impedance in stator and rotor windings providing a voltage waveform as per IEC and GOST [35].
3. Generalized characteristic of rotor winding currents is determined by its number of turns and winding factor as well as geometrical dimensions of machine active part.

List of Symbols

$f_{ROT,1}; f_{ST,1}$	Frequencies of the first voltage harmonic of rotor and stator windings
$f_{ROT,Q}; f_{ST,Q}$	Frequencies of higher voltage harmonics of rotor and stator windings
$F_{ROT,1}; F_{ROT,Q}; F_{ST,1}; F_{ST,Q}; F_{M.C.,1}; F_{M.C.,1}$	MMF complex amplitudes (phasors) of rotor, stator windings and machine magnetic circuit
$I_{ROT,1}; I_{ROT,Q}; I_{ST,1}; I_{ST,Q}; I_{M.C.,1}; I_{M.C.,Q}$	Complex amplitudes (phasors) of currents in rotor (stator) windings and magnetization current
$K_{W,ROT}; K_{W,ST}$	Winding factors for rotor and stator windings
L_{COR}	Active core length
$L_{ROT}; L_{ST}$	Leakage inductance of rotor and stator windings
m	Order of stator MMF spatial harmonic
$m_{ROT}; m_{ST}$	Number of phases of rotor and stator windings
n	Order of rotor MMF spatial harmonic
n_{REV}	Rotor rotation speed
P	Power
p	Number of pole pairs
$Q_{ROT}; Q_{ST}$	Orders of time voltage harmonics of rotor and stator windings
$R_{ROT,1}; R_{ROT,Q}; R_{ST,1}; R_{ST,Q}$	A.C. resistance of rotor and stator windings
S	Slip

T_1	Period of the first flux harmonic
$U_{ROT,1}; U_{ROT,Q}; U_{ST,1}; U_{ST,Q}$	Complex amplitudes of phase voltages of rotor and stator windings
$W_{ROT}; W_{ST}$	Number of turns in phase of rotor and stator windings
$X_{ROT,1}; X_{ROT,Q}; X_{ST,1}; X_{ST,Q}$	Inductive leakage reactances of rotor and stator windings
$\Phi_{0,1}; \Phi_{0,Q}$	Complex amplitudes of mutual induction resulting fluxes
$\varphi_{ROT,1}; \varphi_{ROT,Q}; \varphi_{ST,1}; \varphi_{ST,Q}$	Phase angles between voltage and current of rotor (stator) windings

References

I. Monographs, General Courses, Textbooks

1. Demirchyan K.S., Neyman L.R., Korovkin N.V., Theoretical Electrical Engineering. Moscow – St.Petersburg: Piter, 2009. Vol. 1, 2. (in Russian).
2. Kuepfmueller K., Kohn G., Theoretische Elektrotechnik und Elektronik. 15 Aufl. Berlin, N. Y.: Springer, 2000. (in German).
3. Mueller G., Ponick B., Elektrische Maschinen, N.Y.: John Wiley, 2009. (in German).
4. Voldek A.I., Electrical Machines. Leningrad: Energiya, 1974. (in Russian).
5. Schuisky W., Berechnung elektrischer Maschinen. Wien: Springer, 1960. (in German).
6. Botvinnik M.M., Forced regulation and excitation of the double power supplied machines. Moscow: Torus-Press, 2011. (in Russian).
7. Botvinnik M.M., Shakaryan Yu.G., Controlled A.C. Machine. Moscow: Nauka, 1969. (in Russian).
8. Zagorskiy A.E., Shakaryan Yu.G., Control of Transients in A.C. Machines. Moscow: Energoatomizdat, 1986. (in Russian).
9. Radin V.I., Zagorskiy A.E., Shakaryan Yu.G., Controllable Electric Generators Under Variable Frequency. Moscow: Energiya, 1978. (in Russian).
10. Dreyfuss L., Kommutatorkaskaden und Phasenverschieber. Berlin: Springer, 1931. (in German).
11. Walker M., The Control of the Speed and Power Factor of Induction Motors. London: Pittman, 1924.
12. Onistchenko G.B., The asynchronous gate stages and the double power supplied machines. Moscow. Energiya, 1979. (in Russian).
13. Mueller G., Vogt K., Ponick B., Berechnung elektrischer Maschinen. Berlin: Springer, 2007. (in German).
14. Boguslawsky I.Z., A.C. motors and generators. The theory and investigation methods by their operation in networks with non linear elements. Monograph. TU St.Petersburg Edit., 2006. Vol. 1; Vol.2. (in Russian).
15. Ruedenberg R., Elektrische Schaltvorgaenge. Berlin, Heidelberg, N.Y.: Springer, 1974. (in German).

16. Richter R., Elektrische Maschinen. Berlin: Springer. Band I, 1924; Band II, 1930; Band III, 1932; Band IV, 1936; Band V, 1950. (in German).
17. Construction of Electrical Machines. Edited by of Kopylov, I.P. Moscow: Energiya, 1980. (in Russian).
18. Korn G., Korn T., Mathematical Handbook., N.Y.: McGraw – Hill, 1961.
19. Turbogenerators. The calculation and constructing. Edited by Ivanov N.P. and Lyuter R.A. Leningrad, Energiya, 1967. (in Russian).

II. Induction Machines. Papers, Inventor's Certificates

20. Antonov V.V., Boguslawsky I.Z., Kochetkova E.Yu., Rogachevskiy V.S., Method of steady state modes calculating of asynchronized synchronous generator. Elektrotechnika, #2, 1992. (in Russian).
21. Boguslawsky I.Z., Danilevich Ya.B., Popov V.V., Features of the calculation of electromagnetic loads and the power factor of the rotor of asynchronized synchronous generator at different slips. Proceedings of the Russian Academy of Sciences. Energetika. #6, 2011. (in Russian).
22. Boguslawsky I.Z., Danilevich Ya.B., Popov V.V., Rogachevskiy V.S., Features of the calculation of electromagnetic loads of double power supplied machines with take into account the saturation and high harmonics. Proceedings of the Russian Academy of Sciences. Energetika. #6, 2013. (in Russian).
23. Boguslawsky I.Z., Double power supplied asynchronous machine with converter in the rotor winding performance investigation method. Proceedings of the Int. Symp.UEES-01. Helsinki. 2001.
24. Boguslawsky I.Z., Berechnung der Zusatzverluste in den Staenderwicklungen von modernen Wechselstrommaschinen. Archiv fuer Elektrotechnik (El. Eng.), #5, 1994, Springer Verlag, Berlin. (in German).
25. Boguslawsky I.Z., Dubitsky S.D., Korovkin N.V., Research Methods for the Slot-Ripple EMF in Large Double-Fed Machines. IEEE Russia (Northwest) Section. December, 2012. St. Petersburg.
26. Demirchyan K.S., Boguslawsky I.Z., The calculation of the currents and the losses in the rotor short-circuited induction motor using the generalized characteristics of the rotor MMF. Electrichestvo, #5, 1980 (in Russian).
27. Dir R., Neuffer J., Schlueter W., Waldmann H., Neuartige Elektronische Regeleinrichtungen Fuer Doppelgespeiste Asynchronmotoren von Stromrichterkaskaden. Wiss. Z. Elektrotechnik, 1971, #5 (in German).
28. Kuwabara T., Shibuya A., Furuta H., Kita E., Design and dynamic response characteritics of 400 MW adjustable speed pumped storage unit. IEEE Transactions on Energy Conversion. 1996, Vol. 11, #2.
29. Aguro K., Kato M., Kichita F., Machino T., Mukai K., Nagura O., Sekiguchi S., Shiozaki T., Rich operation experience and new technologies on adjustable speed pumped storage systems in Japan. SIGRE. 2008.
30. Boguslawsky I.Z., Danilevich Ya. D., Wind – power and small hydrogenerators designing problems. Proceedings of the IEEE Russia (Northwest Section). Int. Symp. "Distributed Generation Technology", October 2003.
31. Shakaryan Yu.G., Electromachin-gates complexes in power engineering. Proceedings of the III-th Int. Symp. Interelectromach (IEM) "Electrical Machines in the New Century". Moscow, 2000. (in Russian).
32. Journal "Modern Systems". 2002. April. Page 23.

33. Kim K.K., Izotov A.M., Kolesov L.S., To the question of the use of solid lubricants in the moving current-collecting systems. Elektrotechnika, #3, 2000. (in Russian).
34. Zaboin V.N., Methodology for optimizing the parameters of the current-collecting systems of electrical machines. Electrichestvo, #1, 1999. (in Russian).

III. State Standards (IEC, GOST and so on)

35. GOST (Russian State Industrial Standard) R – 52776 (IEC 60034-1). Rotating Electrical Machines. (in Russian).

Chapter 3
Stator MMF Harmonics at Non-sinusoidal Machine Power Supply (for M ≥ 1, Q ≥ 1)

This chapter presents investigation methods of MMF harmonics of time orders Q and spatial m excited by currents of stator multiphase winding for various connection schemes (star, with separate phase power supply, etc.). When developing these methods, practical results are obtained for three- and six-phase machines most often used in practice. Peculiarities in operation of machines of both types at non-sinusoidal power supply are compared; not only advantages are noted, but also shortcomings of machines with six-phase windings. Stated are practical ways to decrease the influence of higher time harmonics fields in air gap for machines operating in networks with modern frequency converters. Results of investigation performed in this chapter are a stage for determination of magnetically coupled loops in A.C. machine stator when operating in nonlinear network. Practical examples are given.

The content of this chapter is development of the methods stated in [1, 2, 8–12].

3.1 Initial Data and Its Representation

Main investigation stages of A.C. machines in nonlinear networks are outlined in previous chapter. One of these stages is determination of stator MMF harmonics at non-sinusoidal machine power supply, EMF frequencies in stator and rotor magnetically coupled loops, as well as field rotation speeds of these loops in the air gap. These problems are the part of a more general problem discussed in this chapter. Conventional assumptions adopted in A.C. machine theory for steady-state mode analysis are used in their solution [3–5]. In particular, it is assumed that stator and rotor core saturation is determined by the first order time and spatial harmonics;

I. Boguslawsky et al., *Large A.C. Machines*,
DOI 10.1007/978-4-431-56475-1_3

if it is necessary to take into account higher harmonic influence, it is refined with the help of iteration method.

The following initial parameters are accepted for solving these problems:

- Currents flowing in stator winding phases; they vary in time according to non-sinusoidal periodic law. Network voltage over phases is non-sinusoidal and symmetrical; its instantaneous value for one of the phases u(t) is as follows:

$$u(t) = U_1 \cos(\omega_1 t - \varphi_{1,U}) + \cdots + U_Q \cos(\omega_Q t - \varphi_{Q,U}) + \cdots, \tag{3.1}$$

where

$$\omega_Q = \omega_1 Q. \tag{3.2}$$

Here t—time; $U_1, \ldots, U_Q$—harmonic amplitudes; $\omega_1, \ldots, \omega_Q$—circular frequencies of current harmonics; Q—order of time harmonics; $\varphi_{1,U}, \ldots, \varphi_{Q,U}$—initial phase angles of voltage harmonics for short, initial harmonic phases are usually taken equal to zero by expanding into function series (voltage, current, MMF, etc.) in further description;

- Number of stator winding phases is equal to m_{PH}; winding is distributed over the stator slots; it generates a stepped form field in air gap. The order of MMF harmonics of this field is equal to m. Winding has W_{PH} turns in phase, the winding factor for order m field harmonic is equal to $K_W(m)$;
- Rotor speed is equal to ω_{REV};
- Number of poles in machine is equal to 2p.

Note. We note representation peculiarity of MMF and stator winding fields in the air gap. When expanding the waveform of current distribution in slots (current load) to harmonic (Fourier) series [3–7] with period $T = \pi D$ (D—boring diameter), the harmonic order is designated by letter m. However, in investigation of air gap field, it is often sufficient to take $T_{EL} = \pi D/p$ as expansion period, then the order of the same harmonic is equal to $m_{EL} = \frac{m}{p}$, as $\frac{m_{EL}}{T_{EL}} = \frac{m}{T}$. For example, the harmonic of order $m_{EL} = 1$ at expansion to harmonic series with period T_{EL} corresponds to that of order m = p at expansion to series with period T.

Determinations of MMFs and fields with period T_{EL} and order of harmonic m_{EL} are often used in engineering practice. However, it is connected with certain difficulties in some cases. For example, when defining MMF harmonics of order $m < p$ for windings with fractional slot number per pole and phase q [3–5], some of them are of order $m_{EL} < 1$ using the expansion period T_{EL}. Therefore, they are called "fractional", as it does not correspond to MMF mathematical expansion procedures in harmonic series. Their order must be an integer number equal to or greater than one [7]. In this chapter, we will investigate a step function distribution

of stator winding MMF using harmonic series containing harmonics of order $m_{EL} = 1, 3, 5, 7, \ldots$.

The same also refers to rotor MMF harmonics; their order is designated in the monograph by letter n. The same designations are accepted in subsequent chapters for investigation of rotor MMF harmonics of order n: $\frac{n_{EL}}{T_{EL}} = \frac{n}{T}$.

General problems of winding MMF expansion are investigated further, for example, MMF of asymmetric squirrel cage of induction machine. For solution of these tasks, it is necessary to use expansion period $T = \pi D = T_{EL} p$.

3.2 Stator Winding Design Peculiarities; Its Number of Phases m_{PH}

A.C. machine stator winding is usually made double-layer, of coil or bar type and with shortened pitch. For induction and non-salient pole synchronous machines, the number of slots per winding pole and phase, as a rule, is selected equal to an integer; however, for synchronous salient pole machines (motors and generators) it can be also fractional [6].

Basic regularities distinguishing this type of polyphase windings, winding diagram plotting methods used by these regularities (including those at $q < 1$) are set forth in [3–5, 8–11]. Peculiarities of single-layer winding with fractional number q are given there as well.

Number of winding phases is usually taken to be equal $m_{PH} = 3$, but for high power machines in networks with frequency converters and also for brushless exciters armature windings with number of phases $m_{PH} > 3$, for example, with number of phases $m_{PH} = 6$ are sometimes used. Phase windings usually are star connected; the null point is usually isolated in domestic practice. However, in networks with frequency converters in some cases use is made of circuits with separate phase power supply. At the same time, time harmonics of order $Q = 3$ and their multiples may appear in the stator current curve.

Winding with phase numbers $m_{PH} = 6$ is sometimes considered as a system of two three-phase windings shifted in space relative to each other at an angle of 30 electrical degrees (30 el. degr.); it can be considered in such a conception that one winding system voltage is shifted relative to another in time at the angle of 30 electrical degrees (30 el. degr.). In engineering practice, the stator winding with $m_{PH} = 6$ is often called as: “winding with two stars under thirty electrical degrees (30 el. degr.)”.

Modern windings are usually made with the phase zone number M equal to double phase number ($M = 2m_{PH}$). It helps to obtain better usage of stator tooth zone spacing than at $M = m_{PH}$ [5]. According to (3.1), a non-sinusoidal current flows in the stator winding phases m_{PH}. For example, the instantaneous current value $i_Z(t)$ in one phase of polyphase winding (two stars with the shift on 30 el. degr.) is as follows:

$$i_Z(t) = \left|I_{Z,1}\right|\cos(\omega_1 t - \sigma_Z) + \cdots + \left|I_{Z,Q}\right|\cos Q(\omega_1 t - \sigma_Z) + \cdots. \tag{3.3}$$

Here z—phase name, for example, A′; $\left|I_{Z,Q}\right|$—phase current amplitude; σ_Z—phase angles of current harmonics.

3.3 MMF Harmonics at $m_{PH} = 3$

According to the Ampere's law [1, 2], each phase of six-zone stator winding with phase number $m_{PH} = 3$ generates M = 6 pulsating fields in air gap. Their appearance is caused by the non-sinusoidal current in phases in accordance with (3.1) and non-sinusoidal field distribution in air gap (along the stator surface) [5]. Therefore, with account of this expression, the phase MMF can be represented as (Table 3.1):

$$\begin{aligned} &f_Z(t,x,m_{EL},Q) = \left|F_{m_{EL,Q}}\right|\cos m_{EL}(a - \varphi_Z)\cdot\cos Q(\omega_1 t - \sigma_Z) \\ &\text{where } a = \frac{2\pi x}{T_{EL}};\quad 0 \le x \le T_{EL};\quad \varphi_Z, \sigma_Z - \text{according}\quad \text{Table 3.1} \end{aligned} \tag{3.4}$$

$F_{m_{EL,Q}}$—amplitude of MMF of spatial harmonics with number m_{EL} and time harmonics with number Q:

$$F_{m_{EL,Q}} = \frac{2I_Q W_{PH} K_W(m_{EL})}{\pi\, m_{EL} p} \tag{3.5}$$

We calculate the MMF of three-phase winding; for this purpose it is necessary to summarize $f_Z(t, x, m_{EL}, Q)$ MMF of all its phases determined as per (3.4). The orders m_{EL} of spatial and time harmonics Q should be considered. As a result, the following is obtained:

$$f_{ST,RES}(t, x, m_{EL}, Q) = f_A(t, x, m_{EL}, Q) + f_B(t, x, m_{EL}, Q) + f_C(t, x, m_{EL}, Q).$$

For example, if the value $m_{EL} = 7$, Q = 5 according to Eqs. (3.4) and (3.5), the following is obtained for three-phase MMF [3–5]:

$$\begin{aligned} f_A(t,x,m_{EL} = 7, Q = 5) &= \left|F_{7,5}\right|\cos 7a\cdot\cos(5\omega_1 t), \\ f_B(t,x,m_{EL} = 7, Q = 5) &= \left|F_{7,5}\right|\cos(7(a - 120))\cdot\cos(5(\omega_1 t - 240)), \\ f_C(t,x,m_{EL} = 7, Q = 5) &= \left|F_{7,5}\right|\cos(7(a - 240))\cdot\cos(5(\omega_1 t - 120)). \end{aligned}$$

Table 3.1 Phase angles σ_Z for currents and φ_Z for MMF

z	Phase A	Phase B	Phase C
σ_Z, φ_Z el. degr.	0	120	240

In this particular case (at $m_{EL} = 7$, Q = 5, $m_{PH} = 3$), three-phase stator winding MMF is obtained after summing in the form:

$$f_{ST,RES}(t,x,m_{EL} = 7, Q = 5) = \frac{1}{2} m_{PH} \left| F_{7,5} \right| \cos\left(5\omega_1 t + 7\frac{2\pi x}{T_{EL}} \right). \qquad (3.5')$$

At any values of orders of time harmonics $Q \neq 3k_1$ and spatial $m_{EL} \neq 3k_2 (k_1, k_2 = 1, 3, 5, \ldots)$ MMF of three-phase stator winding is equal to,

$$f_{ST,RES}(t,x,m_{EL}, Q) = \frac{1}{2} m_{PH} \left| F_{m_{EL},Q} \right| \cos\left[Q\omega_1 t + (-1)^S m_{EL} \frac{2\pi x}{T_{EL}} \right], \qquad (3.6)$$

where S = 1 or S = 2. It depends on harmonic order combinations Q and m_{EL} is determined below. Physically, Eq. (3.6) corresponds to the field of mutual induction in the machine air gap rotating relative to stator winding in the direction of rotor rotation (S = 1) or in the opposite direction (S = 2).

The value of linear rotation speed V_{BOR} of these field relative to stator winding is equal to, $V_{BOR}(m_{EL}, Q) = (-1)^{(S+1)} Q\omega_1 \frac{T_{EL}}{m_{EL} 2\pi}$.

Angular rotation speed magnitude $\omega_{BOR}(m_{EL}, Q)$ of these fields relative to stator winding correspondingly is equal to:

$$\omega_{BOR}(m_{EL}, Q) = (-1)^{(S+1)} Q \frac{\omega_1}{m_{EL} p}.$$

In the particular case, the following is obtained for the main field angular speed $(m_{EL} = 1, Q = 1)$ according to (3.6):

$$\omega_{BOR}(m_{EL} = 1, Q = 1) = \frac{\omega_1}{p}.$$

In machine synchronous operation mode, this speed is equal to rotor rotation speed $\omega_{REV} = \omega_{BOR}$. The ratio of linear speed for an arbitrary order Q field harmonics and m_{EL} to the field linear speed with Q = 1 and $m_{EL} = 1$ is equal to:

$$\frac{V_{BOR}(m_{EL}, Q)}{V_{BOR}(m_{EL} = 1, Q = 1)} = \frac{\omega_{BOR}(m_{EL}, Q)}{\omega_{BOR}(m_{EL} = 1, Q = 1)}.$$

For various orders of time Q and spatial m_{EL} harmonics $(Q \neq 1, m_{EL} \neq 1)$ in fractions from the main field speed (Q = 1, $m_{EL} = 1$) these relations are given in Appendix 3.1. The minus sign in Table 3.7 of Appendix 3.1 corresponds to the direction of field rotation against that of rotor rotation.

A symbolic method is used to represent the sinusoidal currents [1, 2]. The expression obtained for MMF stator winding is as follows:

$$F_{ST,RES}(x,m_{EL},Q) = |F_{ST}(m_{EL},Q)|e^{j(-1)^{Sm}_{EL}\frac{2\pi x}{\tau_{EL}}}, \tag{3.7}$$

where $F_{ST}(m_{EL},Q) = \frac{1}{2}m_{PH}\left|F_{m_{EL,Q}}\right|e^{jQ\omega_1 t}$. Here $F_{ST}(m_{EL},Q)$—complex amplitude (phasor) of stator winding MMF.

The results of MMF stator winding analysis are as follows:

For $m_{EL} = 1,7,13,\ldots,6k_1+1;$ $Q = 1,7,13,\ldots,6k_2+1;$ $(k_1,k_2 = 0,1,3,5,\ldots)$ the value of S is equal to:

$$S = 1. \tag{3.7'}$$

- For $m_{EL} = 5,11,17,\ldots,6k_1+5;$ $Q = 1,7,13,\ldots,6k_2+1;$, where $k_1,k_2 = 0,1,3,5,\ldots$ or for $Q = 5,11,17,\ldots,6k_1+5;$ $m_{EL} = 1,7,13,\ldots,6k_2+1,$

  where $k_1,k_2 = 0,1,3,5,\ldots$, the value of S is equal to:

$$S = 2 \tag{3.8}$$

- For $m_{EL} = 5,11,17,\ldots.6\cdot_1 +5;$ $Q = 5,11,17,\ldots.6k_2+5,$

.

  where $k_1,k_2 = 0,1,3,5,\ldots$, the value of S is equal to:

$$S = 1. \tag{3.9}$$

Let us consider the MMF of three-phase winding taking into account time and spatial harmonics, multiple of three, also including a separate power supply of its phases from the frequency converter.

For calculation of three-phase winding MMF in these cases also, as well as for $Q \neq 3k$ and $m_{EL} \neq 3k$ (k = 1, 3, 5,…) it is necessary to add MMFs $f_Z(t,x,m_{EL},Q)$ of all phases determined as per (3.4).

As a result, the following is obtained:

- for Q = 3, 9 ,15, …, 3 k; m_{EL} = 1,5,7,11,…,

  or

- for Q = 1,5,7,11,…; m_{EL} = 3,9,15,…, 3 k (k = 1,3,5,…):

$$f_{ST,RES}(t,x,m_{EL},Q) = 0. \tag{3.10}$$

Equation (3.10) shows that the stator winding currents of these harmonics do not excite any fields in machine air gap (mutual induction fields). In calculations of machine processes in this case, only leakage fields are considered: of slot and end parts of winding.

- for Q = 3,9,15,…, $3k_1$, m_{EL} = 3,9,15,…, $3k_2$,

  where k_1, k_2 = 1,3,5,…, we obtain:

$$f_{ST,RES}(t, x, m_{EL} = 3k_2, Q = 3k_1) = 3\left|F_{m_{EL,Q}}\right| \cos(3k_1\omega_1 t) \cdot \cos\frac{3k_2 2\pi x}{T_{EL}}. \quad (3.11)$$

This expression indicates the pulsating field in machine air gap. It is possible to represent [5] in the form of the sum of two components similarly to (3.7) (at S = 2 and S = 1):

$$\begin{aligned} f'_{ST,RES}(t, x, Q = 3k_1, m_{EL} = 3k_2) &= \frac{3}{2}\left|F_{m_{EL,Q}}\right| \cos\left(3k_1\omega_1 t - 3k_2\frac{2\pi x}{T_{EL}}\right), \\ f''_{ST,RES}(t, x, Q = 3k_1, m_{EL} = 3k_2) &= \frac{3}{2}\left|F_{m_{EL,Q}}\right| \cos\left(3k_1\omega_1 t + 3k_2\frac{2\pi x}{T_{EL}}\right). \end{aligned} \quad (3.12)$$

Both of these components have identical amplitudes and rotate relative to stator winding with equal speed in opposite directions. Note that in a particular case at $k_1 = k_2 = 1$ being of the greatest practical interest, the first field component does not induce any EMF in synchronous machine rotor loops in continuous operation mode $\left(\omega_{REV} = \frac{\omega_1}{p}\right)$.

Only a limited number of resulting field components are taken into account in solving practical problems. The numbers of spatial harmonics are usually limited to the order $m_{EL} \leq 11 - 13$. Ratio between amplitudes of these harmonic field is substantially determined by winding factors $K_W(m_{EL})$. The number of time harmonics depends on the current waveform (3.3).

3.4 MMF Harmonics at $m_{PH} = 6$

MMF expressions for $m_{PH} = 6$ and $m_{PH} = 3$ are derived similarly. MMF phase amplitudes of six-phase winding are also calculated using Eq. (3.5), and MMF distribution in the boring – using Eq. (3.7).

When representing winding as "two-star machine winding at thirty electrical degrees (30 el. degr.)", each phase zone of three phase windings (A, B, C) can be considered as subdivided into two $[(A', A''); (B', B''); (C', C'')]$. Then phase angles σ_Z for currents and φ_Z for MMF (Table 3.2) are as follows:

Table 3.2 Phase angles σ_Z for currents and φ_Z for MMF

Z	Phase A'	Phase A"	Phase B'	Phase B"	Phase C'	Phase C"
σ_Z, φ_Z, el. degr.	0	30	120	150	240	270

From Table 3.2 it follows that angles of currents in phases of the first system are equal to,$\sigma_{A'} = 0$ el. el. degr., $\sigma_{B'} = 120$ el. el. degr., $\sigma_{C'} = 240$ el. degr., and for currents of the second: $\sigma_{A''} = 30$ el. degr., $\sigma_{B''} = 150$ el. degr., $\sigma_{C''} = 270$ el. degr., so the phase shift between currents is equal in each of systems 120 el. degr., and between currents of adjacent phases, for example, of B' and B'', it is equal to 30 el. degr.

A method of winding factors calculation $K_W(m_{EL})$ for twelve-zone six-phase winding with fractional number of slots per pole and phase is given in [9, 10].

It should be noted some peculiarities of winding at the number of phases $m_{PH} = 6$, representing the most practical interest:

- for Q = 1, m_{EL} = 7,19,31,…, 6 k + 1, where k = 1,3,5,… and m_{EL} = 5,17,29, …, 6 k + 5, where k = 0,2,4,…:

$$f_{ST,RES}(t, x, m_{EL}, Q = 1) = 0. \tag{3.13}$$

- for m_{EL} = 1, Q = 7,19,31,… 6 k + 1, where k = 1,3,5,… and Q = 5,17,29,… 6 k + 5, where k = 0,2,4, ..:

$$f_{ST,RES}(t, x, m_{EL} = 1, Q) = 0. \tag{3.14}$$

Other ratios of time harmonic orders Q and spatial harmonics m_{EL} excluding stator field emergence in air gap (fields of mutual inductance) are given in Appendix 3.1.

We consider six-phase stator winding MMF with account of time and spatial harmonics, multiple of three, including separate power supply of its phases from the frequency converter.

- For Q = 3,9,15,… 3 k (k = 1,3,5,…); m_{EL} = 1,5,7,11,..,

  or

- for Q = 1,5,7,11,… m_{EL} = 3,9,15,…, 3 k (k = 1,3,5,7,11,…):

$$f_{ST,RES}(t, x, m_{EL}, Q) = 0. \tag{3.14'}$$

In calculations of machine processes in this case, as well as for three-phase machine (m_{PH} = 3), only leakage fields are considered: of slot and end parts of winding.

- For Q = 3; m_{EL} = 3 (the greatest practical interest)

$$f_{ST,RES}(t, x, Q = 3, m_{EL} = 3) = 3\left|F_{m_{EL,Q}}\right| \cos\left(3\omega_1 t - 3\frac{2\pi x}{T_{EL}}\right). \tag{3.11'}$$

Here we have two three-phase systems shifted by an angle of 90 electrical degrees (90 el. degr.). Unlike fields in three-phase machine, for considered combination of time and spatial harmonics in six-phase machine air gap ($m_{PH} = 6$), there arises rotating (but not pulsating) field; in that specific case, at $Q = m_{EL} = 3$ the angular rotation speed of this field is equal to the synchronous rotor rotation speed.

We note that at $Q = m_{EL} = 3$ this field does not induce any EMF in synchronous machine rotor loops in continuous operation mode ($\omega_{REV} = \omega_1/p$).

Besides, only a limited number of resultant field harmonics are taken into account in solving practical problems for windings with $m_{PH} = 6$. For spatial harmonics it is usually limited to the order $m_{EL} \leq 17 - 19$; it is no more than for windings with $m_{PH} = 3$, since for harmonics of orders of $m_{EL} = 5$, $m_{EL} = 7$ it is not necessary to consider the resulting fields in the gap.

Number of time harmonics depends on the current waveform (3.3).

We note that the expressions for rotation speeds of separate harmonics obtained earlier for number of phases $m_{PH} = 3$ are still true for $m_{PH} = 6$.

3.5 MMF Harmonic Comparison at $m_{PH} = 3$ and $m_{PH} = 6$

a. $Q > 1$, $m_{EL} > 1$.

MMF and field amplitudes in air gap at $m_{PH} = 3$ are practically determined by all odd current time harmonics of order Q and spatial harmonics—of order m_{EL}.

However, at $m_{PH} = 6$, fields in air gap determined by odd harmonics with rather high amplitudes ($Q = 1$ at $m_{EL} = 5$; $Q = 1$ at $m_{EL} = 7$; $Q = 5$ at $m_{EL} = 1$; $Q = 7$ at $m_{EL} = 1$) are absent.

b. $Q = 1$, $m_{EL} = 1$.

The expression for MMF main harmonic can be represented as:

$$|F_{ST}(m_{EL} = 1, Q = 1)| = \frac{1}{2} m_{PH} \left|F_{m_{EL,Q}}\right| \sim AS \frac{DK_W}{p},$$

where $\left|F_{m_{EL,Q}}\right|$—as per (3.5), current load $AS = \frac{|I_{PH}| Z_{SLT} S_N}{a\pi D}$; $|I_{PH}|$—phase current; D—stator boring diameter; a—number of parallel paths in phase; Z_{SLT}–number of slots, S_N—number of effective conductors in slot.

We compare two machines with identical power, voltage, frequency and rotation speed, but with the number of phases: $m_{PH} = 3$ and $m_{PH} = 6$. Both machines are assumed to have AS = idem, the boring diameter D = idem., p = idem.

Ratio of MMF amplitudes is equal ceteris paribus to:

$$\frac{[F_{ST}]_{m_{PH}=3}}{[F_{ST}]_{m_{PH}=6}} = \frac{K_W(m_{PH}=3)}{K_W(m_{PH}=6)}.$$

Thus, at $m_{PH} = 6$ the absence of fields determined by spatial harmonics of order m_{EL} satisfying Eq. (3.13), and the absence of time harmonics fields of order Q satisfying Eq. (3.14) makes expedient using this winding for machines fed from the frequency converter. Thus, it becomes possible to design their stator winding with shortening β_6 a little larger $(0.833 < \beta_6 \leq 1)$ than in three-phase winding with shortening $\beta_3 (0.75 < \beta_3 \leq 0.833)$.

Let us continue a comparison of two machines with identical power, voltage, frequency and rotation speed with number of phases $m_{PH} = 3$ and $m_{PH} = 6$ under conditions: AS = idem, D = idem, p = idem. Machine active part length at $m_{PH} = 6$ and pitch shortening β_6 is 5–6 % less than for machines with winding at number of phases $m_{PH} = 3$ and pitch shortening β_3 [4, 6]. In induction machines due to the complicated winding design and its terminal, the winding with $m_{PH} = 6$ is usually not used. In synchronous machines design at pitch shortening $0.833 < \beta_6 \leq 1$ has the following peculiarities:

a. Increase of end part length. It results in the following differences from three-phase winding:

   - Leakage reactance of this winding end part is more; this fact may be important for machines operating in networks with frequency converters;
   - Increased winding insulation consumption;
   - Machine axial length (between bearing shields) is also increased with equal axial length of active part, particularly, for high-voltage machines.

b. MMF armature reaction is increased at pitch shortening β_6. It is greater than for pitch shortening β_3. When setting values of maximum torque M_{MAX} = const for synchronous machine [13], the excitation winding MMF should be also increased by 5–6 %; respectively, the rotor winding overheat for pitch shortening β_6 will be by 10–12 % more than for β_3 (the excitation windings are identical and $m_{PH} = 3$, $m_{PH} = 6$ accordingly).

Let us turn our attention to other means of reducing additional losses in rotor loops of modern machines in circuits with frequency converters: on the use of frequency converters operating in pulse-width modulation system (PWM)), and on the influence of these frequency converters on its isolation in stator winding circuit.

As it is shown in practice, when using frequency converters operating on this principle, the higher harmonics with order typically $Q > 19$ are present in the voltage converter curve. For fundamental frequency voltage converter 50 Hz, its higher harmonic frequency usually exceeds 1 kHz. At the same time, this voltage waveform differs in local portions with high slope. The experiments prove that the uneven voltage distribution takes place with these converters: it is higher in the first

stator winding circuits (counting from line terminals). Partial discharges in coil insulation are also registered. Its damage and, correspondingly, short circuits in winding are possible after a long operation term (typically after two years of operation). Currently, harmonic filters are usually installed to extend machine life. Some manufacturers additionally enhance insulation of the first winding turns; however, it causes additional overheating of these turns, sometimes close to permitted value or even exceeding it, being undesirable: this overheating can also cause reduction of insulation life.

Note that the higher order harmonics in the voltage curve influence the electrical device operation located near the electric machine. For example, they interfere in the operation of modern means of motor protection, metering devices, etc.

It is an actual scientific-technical challenge to study comprehensively the effect of these harmonics on the stator winding machine insulation and operation of nearby electrical devices. Its solution allows formulating practical recommendations for designing modern winding insulation fed by frequency converters of this type.

3.6 EMF Frequency in Magnetically Coupled Loops ($m_{EL} \geq 1$, $Q \geq 1$)

3.6.1 Salient Pole Machines Operating in Synchronous Speed Modes

In this mode, the rotor angular speed ω_{REV} is determined by the first time ($Q = 1$) and the first spatial ($m_{EL} = 1$) harmonics:

$$\omega_{REV} = \omega_{BOR}.$$

It is assumed that the rotor angle positive direction coincides with its rotation direction.

a. EMF frequencies in rotor loops.

First, we consider EMF frequencies induced in the air gap by rotating fields in magnetically coupled rotor loops; these fields are determined by MMF $f_{ST,RES}(t, x, m_{EL}, Q)$.

EMF frequencies induced in magnetically coupled rotor loops by air gap pulsating fields will be considered additionally.

Let us designate harmonics of orders Q, m_{EL}, having numbers: 1,7,13,…, $6k + 1$, with indices (DIR), i.e. Q_{DIR} and m_{DIR} are marked; respectively, the harmonics having orders (numbers) 5,11,17,…, $6k + 5$ ($k = 0,1,2,3,\ldots$)—with indices (AD), that is Q_{AD} and m_{AD}.

The fields determined by MMF harmonics Q_{DIR}, m_{DIR} at $S = 1$, according to (3.7) induces EMF in rotor loops of the following frequency:

$$\omega_{ROT}(Q_{DIR}, m_{DIR}) = \omega_1 |Q_{DIR} - m_{DIR}|. \tag{3.15}$$

For example, when $Q_{DIR} = 1, m_{DIR} = 7$, as well as $Q_{DIR} = 7, m_{DIR} = 1$ the following is obtained:

$$\omega_{ROT} = 6\omega_1. \tag{3.15'}$$

Equation (3.15) is also valid for time and spatial harmonics of higher orders, such as $Q_{DIR} = 7; m_{DIR} = 13$, etc.

The field determined by MMF harmonics of orders Q_{AD}, m_{DIR} at S = 2, according to (3.8) induces EMF in rotor loops with frequency:

$$\omega_{ROT}(Q_{AD}, m_{DIR}) = \omega_1 (Q_{AD} + m_{DIR}). \tag{3.16}$$

For example, when $Q_{AD} = 5, m_{DIR} = 1$, the following is obtained:

$$\omega_{ROT} = 6\omega_1. \tag{3.16'}$$

As it follows from Eqs. (3.15) and (3.16), two fields determined by time harmonics of various orders Q_{DIR} and Q_{AD}, and spatial harmonic of order m_{DIR} induce EMF of the same frequency in rotor loops.

$$\omega_{ROT}(Q_{DIR}, m_{DIR}) = \omega_{ROT}(Q_{AD}, m_{DIR}). \tag{3.17}$$

provided that the orders (numbers) of both time harmonics (Q_{AD}, Q_{DIR}) satisfy the ratio:

$$|Q_{DIR} - Q_{AD}| = 2m_{DIR}. \tag{3.17'}$$

Both rotating fields determined by MMF harmonics of orders (Q_{DIR}, m_{DIR}) and (Q_{AD}, m_{DIR}) are characterized by the same period over the stator boring T_{EL}. They should be taken into consideration in the general equation system for magnetically coupled machine loops.

The field determined by MMF harmonics of orders Q_{DIR}, m_{AD} at S = 2, according to (3.8) induces EMF in rotor loops with frequency:

$$\omega_{ROT}(Q_{DIR}, m_{AD}) = \omega_1 (Q_{DIR} + m_{AD}). \tag{3.18}$$

For example, when $Q_{DIR} = 1, m_{AD} = 5$ the following is obtained:

$$\omega_{ROT} = 6\omega_1. \tag{3.18'}$$

The field determined by MMF harmonics of orders Q_{AD}, m_{AD} at S = 1, according to (3.9) induces EMF in rotor loops with frequency:

$$\omega_{ROT}(Q_{AD}, m_{AD}) = \omega_1 |Q_{AD} - m_{AD}|. \tag{3.19}$$

For example, when $Q_{AD} = 11, m_{AD} = 5$ the following is obtained:

$$\omega_{ROT} = 6\omega_1. \tag{3.19'}$$

As it follows from Eqs. (3.18) and (3.19), two fields determined by MMF time harmonics of various orders Q_{DIR} and Q_{AD}, and spatial harmonic of order m_{AD} induce EMF of the same frequency in rotor loops.

$$\omega_{ROT}(Q_{DIR}, m_{AD}) = \omega_{ROT}(Q_{AD}, m_{AD}) \tag{3.20}$$

provided that numbers of both MMF time harmonics (Q_{AD}, Q_{DIR}) satisfy the ratio:

$$|Q_{DIR} - Q_{AD}| = 2m_{AD}. \tag{3.21}$$

As it follows from the aforementioned equations, in synchronous mode two fields appear simultaneously in the machine air gap. They are induced by MMF time harmonics of order Q_{DIR} and Q_{AD} having similar spatial order (m_{DIR} or m_{AD}). These fields rotate in opposing directions relative to stator winding. These MMF time harmonics can be named "adjacent" ones, for example, at $m_{AD} = 5$ we obtain: $Q_{DIR} = 1$ and $Q_{AD} = 11$, and also $Q_{DIR} = 7$ and $Q_{AD} = 17$.

However, besides these fields in a machine air gap there is a number of other fields rotating in opposite directions relative to rotor and in the same direction relative to stator winding. They induce EMF with the same frequency in rotor circuits. For example, at $m_{DIR} = 7$ we obtain: $Q'_{DIR} = 1$ and $Q''_{DIR} = 13$ or for $m_{AD} = 11 : Q'_{AD} = 5$ and $Q''_{AD} = 17$.

There is the following frequency ratio for these fields:

$$\omega_{ROT}(Q'_{DIR}, m_{DIR}) = \omega_{ROT}(Q''_{DIR}, m_{DIR}) \tag{*}$$

provided that numbers of both MMF time harmonics of orders (Q'_{DIR}, Q''_{DIR}) satisfy the ratio: $Q'_{DIR} + Q''_{DIR} = 2m_{DIR}$, or the following frequency ratio takes place:

$$\omega_{ROT}(Q'_{AD}, m_{AD}) = \omega_{ROT}(Q''_{AD}, m_{AD}) \tag{**}$$

provided that numbers of both MMF time harmonics of orders (Q'_{AD}, Q''_{AD}) satisfy the ratio: $Q'_{AD} + Q''_{AD} = 2m_{AD}$.

It should be noted that fields with such peculiarities have spatial order $m_{EL} \geq 7$, therefore, practically they sometimes can be neglected.

Equations (3.15)–(3.21') confirm that for calculation of currents induced in magnetically coupled rotor loops, it is necessary to consider also the fields differing in order of time and spatial harmonics.

Earlier it was already noted that several MMFs and fields in the air gap correspond to currents in rotor loops of synchronous machines with symmetrical or

asymmetrical cage and induction machines with asymmetrical cage; these current fields in rotor loops with frequency $\omega_{ROT}(Q, m_{EL})$ has spatial orders n = 1,3,5,…, 2·k + 1 (k = 0,1,2, …). They rotate in opposite directions relative to rotor. In this paragraph, EMF frequencies inducing these fields in stator winding are determined.

b. EMF frequencies in stator loops.

The fields rotating in a positive direction induce EMF in stator winding with frequency:

$$\omega_Q(m_{EL}, Q, n) = \omega_{ROT}(Q, m_{EL}) + n\omega_1. \tag{3.22}$$

Similarly, fields of order n of the same rotor currents induce EMF with the following frequency in stator winding:

$$\omega_Q(m_{EL}, Q, n) = |-\omega_{ROT}(Q, m_{EL}) + n\omega_1|, \tag{3.23}$$

if they rotate in negative direction relative to rotor.

The ratio for calculating EMF frequency in stator loops (Table 3.3) is obtained using Eqs. (3.22) and (3.23).

For practice only the case $|m| = |n|$ is important, correspondingly $|m_{EL}| = |n_{EL}|$.

Notes to Table 3.3.

1. Positive and negative rotation directions of field components relative to rotor are given in the Table
2. Stator winding field harmonic effects of orders Q_{DIR}, Q_{AD} m_{DIR}, m_{AD}, are taken into account in the Table. The influence of stator winding field harmonics of orders Q = 3,9,15,…,$3k_1$, m_{EL} = 3,9,15,…,$3k_2$ (k_1, k_2 = 1,3,5, …) for separate power supply of its phases can be considered similarly.
3. Some expressions for frequency $\omega_Q(m_{EL}, Q, n)$ in the Table can be simplified because the difference of the space harmonics numbers is equal to zero. Nevertheless, to keep the structure of all expressions for $\omega_Q(m_{EL}, Q, n)$ we omitted this simplification.

Table 3.3 EMF frequencies in stator loops (synchronous speed operation mode)

Frequency ω_{ROT}	Direction of rotor MMF component	Frequency
		$\omega_Q(Q, m_{EL}, n)$
According to (3.15)	Positive	$\omega_1(n + \lvert Q_{DIR} - m_{DIR}\rvert)$
	Negative	$\lvert\omega_1(n - \lvert Q_{DIR} - m_{DIR}\rvert)\rvert$
According to (3.16)	Positive	$\omega_1(n + Q_{AD} + m_{DIR})$
	Negative	$\lvert\omega_1(n - Q_{AD} - m_{DIR})\rvert$
According to (3.18)	Positive	$\omega_1(n + Q_{DIR} + m_{AD})$
	Negative	$\lvert\omega_1(n - Q_{DIR} - m_{AD})\rvert$
According to (3.19)	Positive	$\omega_1(n + \lvert Q_{AD} - m_{AD}\rvert)$
	Negative	$\lvert\omega_1(n - \lvert Q_{AD} - m_{AD}\rvert)\rvert$

For example, as it follows from the equations given in Table 3.3, the harmonic field of orders $Q_{DIR} = 7, m_{DIR} = 1$, n = 1 induces two EMFs of various frequency in stator loops: $\omega_Q = 7\omega_1$ and $\omega_Q = 5\omega_1$. From these equations it also follows that the harmonic Q_{AD} = 5, m_{DIR} = 1, n = 1 also induces in stator loops two EMFs of the same frequency: $\omega_Q = 5\omega_1$ and $\omega_Q = 7\omega_1$. Thus, loops with EMF frequency $\omega_Q = 7\omega_1$ and $\omega_Q = 5\omega_1$ are magnetically coupled; these two frequencies in stator loops correspond to the uniform frequency $\omega_{ROT} = 6\omega_1$ in rotor loops.

4. Some expressions for frequencies $\omega_Q(m_{EL}, Q, n)$ in the table can be simplified, since the difference in numbers of space orders between them is zero. However, in order to keep in the table the same structure formulas for frequencies $\omega_Q(m_{EL}, Q, n)$, the simplification is not made.

Note that EMF with frequency ω_Q in stator loops induced by positive or negative field component (Table 3.3) may have different phase sequence orders. This sequence order can be easily determined with account of frequency values ω_{ROT}, ω_1 and harmonic order Q; m_{EL}; n.

As it follows from equations given in Table 3.3, the frequency of any additional EMFs can coincide with that of other EMF in the series (3.1) in synchronous speed operation mode ($\omega_{REV} = \omega_1/p$). It is also necessary to consider these magnetically coupled loops in calculating machine modes.

3.6.2 A.C. Machines in Asynchronous Modes $\left(\omega_{REV} \neq \frac{\omega_1}{p}\right)$

a. EMF frequencies in rotor loops (incl. asymmetrical cage winding).

EMF frequencies in rotor loops induced by rotating field harmonics of orders $Q_{DIR}, Q_{AD}, m_{DIR}, m_{AD}$ are obtained from Eqs. (3.15)–(3.20):

$$\omega_{ROT}(Q_{DIR}, m_{DIR}) = |Q_{DIR}\omega_1 - pm_{DIR}\omega_{REV}|. \tag{3.24}$$

$$\omega_{ROT}(Q_{AD}, m_{DIR}) = Q_{AD}\omega_1 + pm_{DIR}\omega_{REV}. \tag{3.25}$$

$$\omega_{ROT}(Q_{DIR}, m_{AD}) = Q_{DIR}\omega_1 + pm_{AD}\omega_{REV}. \tag{3.26}$$

$$\omega_{ROT}(Q_{AD}, m_{AD}) = |Q_{AD}\omega_1 - pm_{AD}\omega_{REV}|. \tag{3.27}$$

Rotating fields of six-phase winding machine determined by harmonics of orders Q = 3, m_{EL} = 3 induce in rotor loops EMF with frequency:

$$\omega_{ROT}(Q, m_{EL}) = |3\omega_1 - 3p\omega_{REV}|. \tag{3.21'}$$

Pulsating fields of three phase winding machine determined by harmonics of orders Q = 3,9,15,…,$3k_1$, m_{EL} = 3,9,15,…,$3k_2$, where k_1, k_2 = 1,3,5,…, induce in rotor loops EMF with frequency:

$$\omega_{ROT}(Q, m_{EL}) = |3k_1\omega_1 \pm 3k_2 p\omega_{REV}|.$$

b. EMF frequencies in stator loops.

Similarly to machine synchronous operation mode, in its asynchronous mode currents in rotor loops with frequency $\omega_{ROT}(Q, m_{EL})$ [Eqs. (3.24)–(3.27)] also generate fields in air gap; their component of spatial order n rotating in positive direction relative to rotor induces EMF in stator winding with frequency:

$$\omega_Q(Q, m_{EL}, n) = \omega_{ROT}(Q, m_{EL}) + pn\omega_{REV}. \tag{3.28}$$

Accordingly, EMF frequency for current field component in rotor loops rotating relative to it in negative direction is equal to:

$$\omega_Q(Q, m_{EL}, n) = |-\omega_{ROT}(Q, m_{EL}) + pn\omega_{REV}|. \tag{3.28'}$$

Using Eqs. (3.28) and (3.28'), we obtain ratios (Table 3.4) for calculating EMF frequencies in stator loops in asynchronous mode ($\omega_{REV} \neq \omega_1/p$). For practice only the case $|m| = |n|$ is important, that is, $|m_{EL}| = |n_{EL}|$.

EMF with frequency ω_Q in stator loops induced by positive or negative field component (Table 3.4) may have different phase sequence orders. This sequence order can be easily determined with account of frequency values ω_{ROT}, ω_1 and harmonic orders Q; m_{EL}; n, as in synchronous mode.

From Table 3.4 it follows that in asynchronous mode at certain rotor rotation speed $\omega_{REV} \neq \omega_1/p$ it can appear that any of additional EMF frequencies $\omega_Q(Q, m_{EL}, n)$ coincides with EMF frequency ω_Q from the series (3.1). Such magnetically coupled loops should also be considered in the computation of machine asynchronous mode.

Table 3.4 EMF frequencies in stator loops (asynchronous mode)

Frequency ω_{ROT}	Direction of rotor component	Frequency $\omega_Q(Q, m_{EL}, n)$
As per (3.24)	Positive	$pn\omega_{REV} + \|Q_{DIR}\omega_1 - p\omega_{REV}m_{DIR}\|$
	Negative	$\|pn\omega_{REV} - \|Q_{DIR}\omega_1 - p\omega_{REV}m_{DIR}\|\|$
As per (3.25)	Positive	$Q_{AD}\omega_1 + p\omega_{REV}(n + m_{DIR})$
	Negative	$\|-Q_{AD}\omega_1 + p\omega_{REV}(n - m_{DIR})\|$
As per (3.26)	Positive	$Q_{DIR}\omega_1 + p\omega_{REV}(n + m_{AD})$
	Negative	$\|-Q_{DIR}\omega_1 + p\omega_{REV}(n - m_{AD})\|$
As per (3.27)	Positive	$pn\omega_{REV}\|Q_{AD}\omega_1 - p\omega_{REV}m_{AD}\|$
	Negative	$\|pn\omega_{REV} - \|Q_{DIR}\omega_1 - p\omega_{REV}m_{AD}\|\|$

3.7 MMF Harmonics of Magnetically Coupled Loops in Multiphase Stator Winding at Non-sinusoidal Power Supply and their Representation

In the previous para we obtained that under certain conditions two fields in the air gap corresponding to two MMF harmonics determined by time orders of Q_1 and Q_2 $(Q_1 \neq Q_2)$ and spatial order of m_{EL} = idem, induce EMF of the same frequency in rotor loops; these harmonics are called "adjacent". Two "adjacent" time harmonics of stator winding MMF form two loops; both of these loops are interconnected by their common rotor loops, their EMF frequency is equal, for example, to $\omega_{ROT} = 6\,\omega_1$.

MMFs of these two stator loops have the same spatial order (m_{EL} = idem), and differ in amplitude, direction and speed of rotation relative to stator.

The calculated expression for these MMF harmonics is obtained in the form of (3.6). With account of values $S_1 \neq S_2$ it can be presented as:

$$F_{ST,RES}(x, m_{EL}, Q_1) = F_{ST}(m_{EL}, Q_1)e^{j(-1)^{S_1}\frac{m_{EL}2\pi x}{T_{EL}}}, \tag{3.29}$$

$$F_{ST,RES}(x, m_{EL}, Q_2) = F_{ST}(m_{EL}, Q_2)e^{j(-1)^{S_2}\frac{m_{EL}2\pi x}{T_{EL}}}, \tag{3.30}$$

where $F_{ST}(m_{EL}, Q_1) \neq F_{ST}(m_{EL}, Q_2)$—complex amplitudes (phasors) of stator MMF corresponding to two "adjacent" time harmonics of orders Q_1 and Q_2; $S_1 \neq S_2$—attributes depending on the combination of orders of harmonics Q_1 and m_{EL}, Q_2 and m_{EL}. These attributes are determined in para 3.3.

Now, we slightly simplify Eqs. (3.29) and (3.30) for these MMFs. It is assumed for specificity that the sign S in combination of MMF harmonics of orders m, Q_1 gets the value S = 1, and in combination of MMF harmonics of orders m, Q_2—gets the value S = 2. Then, it is convenient to represent stator MMF in the form (index "EL" for harmonic order m and period T is omitted):

$$\begin{aligned} F_{ST,RES}(x, m, Q_1) &= F_{ST}(m, Q_1)e^{-j\frac{2pmx}{T}}; \\ F_{ST,RES}(x, m, Q_2) &= F_{ST}(m, Q_2)e^{j\frac{2pmx}{T}}. \end{aligned} \tag{3.31}$$

Taking into account the accepted designations in further statement for short, we will also use the following designations of complex amplitudes (phasors) in the expressions as (3.31):

$$F_{ST}(m, Q_1) \text{ or simply } F_{ST}(m, Q); F_{ST}(m, Q_2), F_{ST}(-m, Q_2), \text{ or simply } F_{ST}(-m, Q).$$

As it follows from the aforementioned investigations, two MMFs in Eq. (3.31) determine the following magnetically coupled loops in salient-pole machine with non-sinusoidal power supply:

- Two "adjacent" loops in stator with EMF frequencies equal to $\omega_1 Q_1$ and $\omega_1 Q_2$;
- Some rotor loops (damper winding, excitation winding), where EMF of the same frequency ω_{ROT} is induced.

3.8 Magnetically Coupled Loops in Machine Operating with Nonlinear Network Elements

Chapter 2 presented investigations of DFM operation modes with account of two magnetically coupled loops, one in stator, the second – in rotor. In this consideration we determined stator and rotor winding MMFs, limiting only to the first spatial harmonic; para 2.3 accounts for the first voltage time harmonic, and para 2.4 for higher harmonics generated by the frequency converter in rotor circuit.

In this chapter, we determined stator winding MMF, corresponding to harmonics of various time order Q and spatial m, and also EMFs induced by fields of these harmonics in machine loops. This allows us to generalize the concept of machine magnetically coupled loops operating in nonlinear network.

This generalization is restricted by operation mode of salient-pole machine in this network; harmonic orders are restricted by values $Q \leq 13$, $m \leq 11$.

We choose for example those orders of harmonics from this series corresponding to EMF with frequency $\omega_{ROT} = 6\,\omega_1$ in rotor loops (damper winding, excitation winding). The results are given in Table 3.5.

From Table 3.5 it follows that EMFs in rotor loops with frequency $\omega_{ROT} = 6\,\omega_1$ are induced at $Q \leq 13$, $m \leq 11$ by fields forming four groups of magnetically coupled loops.

Table 3.5 System of four magnetically coupled loops with common rotor loop (EMF frequency $\omega_{ROT} = 6\,\omega_1$)

Stator loop. EMF frequency ω_Q	$m_{DIR} = 1$ $Q_{DIR} = 7$	$m_{DIR} = 1$ $Q_{AD} = 5$	$m_{DIR} = 7$ $Q_1 = 1$	$m_{DIR} = 7$ $Q_{DIR} = 13$
Rotor loops. EMF frequencies ω_{ROT}	$\omega_{ROT} = 6\,\omega_1$	$\omega_{ROT} = 6\,\omega_1$	$\omega_{ROT} = 6\,\omega_1$	$\omega_{ROT} = 6\,\omega_1$
Group number of magnetically coupled loops	No. 1	No. 2	No. 3	No. 4

Table 3.6 System of three magnetically coupled loops with common stator loop (EMF frequency $\omega_Q = 13\,\omega_1$)

Stator loop. EMF frequency ω_Q	$m_{DIR} = 7 = n$ $Q_{DIR} = 13$	$m_{DIR} = 1 = n$ $Q_{DIR} = 13$	$m_{AD} = 5 = n$ $Q_{DIR} = 13$
Rotor loops. EMF frequency ω_{ROT}	$\omega_{ROT} = 6\,\omega_1$	$\omega_{ROT} = 12\,\omega_1$	$\omega_{ROT} = 18\,\omega_1$
Group number of magnetically coupled loops	No. 4	No. 5	No. 6

Let us note that in this Table each group of magnetically coupled loops in stator and rotor (Nos. 1–4) has the following peculiarities:

- Identical orders of spatial harmonics of stator and rotor fields in air gap;
- Identical rotation speeds of these fields relative to stator boring.

One of them is the group of loops No. 4 $(m_{DIR} = 7, Q_{DIR} = 13)$. EMF frequency in stator loop of this group is equal to $\omega_Q = 13\,\omega_1$; this loop cannot be considered in isolation from other stator loops with other spatial orders $(m_{DIR} \neq 7)$, but with the same frequency of EMF $\omega_{ROT} = 6\,\omega_1$. As a result, we obtain an additional system from two groups of magnetically coupled loops (at $Q \leq 13$, $m \leq 11$). The results are given in Table 3.6.

Note that each group of magnetically coupled loops in stator and rotor (Nos. 5, 6) has peculiarities similar to those of groups Nos. 1–4 in this Table. However, there are also differences between groups in both tables: in Table 3.6 groups Nos. 4, 5 and 6 have different spatial order.

As it follows from Table 3.6, EMFs in stator loops with frequency $\omega_Q = 13\,\omega_1$ are induced at $m \leq 11$ by the fields forming a system of three groups of magnetically coupled loops.

From both Tables, the following can be taken as a basis for setting a system of magnetically coupled loops for a machine operating in nonlinear network:

- either stator loops with different EMF frequency, which corresponds to rotor loops with the same frequency (ω_{ROT} = idem.). See, e.g., Table 3.5;
- or stator loops with different EMF frequency, which corresponds to stator loops with the same frequency (ω_Q = idem.). See, e.g., Table 3.6.

This generalization can be extended to induction machines operating in nonlinear network.

As it is found out for DFMs in Chap. 2, the MMF of stator and rotor windings are included in the system of equations for magnetically coupled loops. This system

is used for calculating DFM modes, determination of EMF harmonics and currents in loops, as well as of resulting field harmonics in the air gap. Note that only one group of magnetically coupled loops for such a machine is taken into account.

In general case, A.C. machine modes in nonlinear networks are also calculated using a similar equation system. However, it comprises equations for several groups of magnetically coupled loops unlike system of equations for DFMs. Such groups of magnetically coupled loops are given in Tables 3.5 and 3.6. Harmonics of EMF and currents in loops, and those of resulting field in air gap are also determined from this system. Structure and peculiarities of these systems are given in Chap. 14.

Harmonic numbers in nonlinear networks were practically limited by values $Q \leq 13$, $m \leq 11$ in order to make the data more concrete and suitable for presenting in Tables; they may be limited to other values if confirmed by practical need. Selection order of harmonics for a system of equations for magnetically coupled loops is given in detail in Chap. 14.

Appendix 3.1

See Table 3.7.

Table 3.7 Field rotation speeds V_{BOR} in the air gap relative to stator winding

m_{EL}	Q = 1	Q = 5	Q = 7	Q = 11	Q = 13	Q = 17
1	1	–5*	7*	–11	13	–17*
5	–1/5*	1	–7/5	11/5*	–13/5*	17/5
7	1/7*	–5/7	1	–11/7*	13/7*	–17/7
11	–1/11	5/11*	–7/11*	1	–13/11	17/11*
13	1/13	–5/13*	7/13*	–11/13	1	–17/13*
17	–1/17*	5/17	–7/17	11/17*	–13/17*	1

1. Speeds in the air gap are given in fractions of synchronous value corresponding to harmonic orders $m_{EL} = 1$; Q = 1
2. Field speeds rotating relative to stator in the direction opposite to its rotor rotation are marked with “minus” sign
3. In the table are given field speeds for three- and six-phase windings. At certain combinations of orders, m_{EL} and Q for six-phase winding, fields in air gap are absent, for example, fields characterized by harmonics $m_{EL} = 7$, Q = 1. These fields are indicated in corresponding table cells with (*) sign

Brief Conclusions

1. A number of mutual induction fields different in their periods and rotation speeds occur in A.C. machine air gap at non-sinusoidal power supply. The fields inducing EMF of the same frequency in rotor loops can be determined in them. Loops generating these fields are magnetically coupled, for instance, loops of rotor and stator (in Table 3.4). Except them, there are mutual induction fields inducing EMF of identical frequency in stator loops, but differing in order of spatial harmonics; loops corresponding to them are also magnetically coupled, for instance loops of rotor and stator (in Table 3.5). The machine processes are determined taking into account the interaction of these loops in the general system of Eqs.
2. Two fields determined by time harmonics of various orders Q containing in expansion (3.1) and spatial harmonics of order m in expansion (3.4) at certain combination of these orders induce in rotor loops EMF of identical frequency, for example, at $m_{AD} = 5$: $Q_{DIR} = 1$ and $Q_{AD} = 11$, and also $Q_{DIR} = 7$ and $Q_{AD} = 17$.
3. Unlike fields in air gap of three-phase machine, fields in air gap of six-phase machine, determined by time harmonics of orders $Q = 3$ and spatial of order $m_{EL} = 3$ form rotating (but not pulsating) fields; in that specific case, the angular rotation speed of this fields is equal to rotor synchronous rotation speed. Consequently, this field does not induce any EMF in synchronous machine rotor loops in continuous operation mode $(\omega_{REV} = \omega_1/p)$.
4. For non-sinusoidal power supply it is possible to avoid the influence of series higher time harmonics on rotor loops using the stator winding scheme with phase number $m_{PH} > 3$. However, there are some drawbacks in winding with increased phase numbers.

List of Symbols

a	Number of parallel branches in phase
b_P	Width of pole shoe
AS	Stator current load
D	Stator boring diameter
$F_1, \ldots, F_m$	Amplitudes of spatial harmonics of stator winding phase MMF
$F_{ST}(m_{EL}, Q)$, $F_{ST,RES}(x, m_{EL}, Q)$	Respectively, complex amplitude (phasor) and amplitude (modulus) of spatial harmonic of order of m_{EL} and time harmonic of order Q of all winding phases m_{PH}
I_Q	Harmonic amplitude of order Q for stator phase current
$K_W(m)$	Winding factor for m order field harmonic

k_Q	Relation of stator current harmonic amplitude of order $Q > 1$ to harmonic amplitude of order $Q = 1$
m, m_{EL}	Orders of MMF spatial harmonics of MMF and stator fields
m_{PH}	Number of stator winding phases
Q	Order of time harmonics
Q_{DIR}, m_{DIR}	Order of time and spatial harmonics of direct field
Q_{AD}, m_{AD}	Order of time and spatial harmonics of additional field
n, n_{EL}	Orders of spatial harmonics of MMF and rotor fields
S_N	Number of effective conductors in slot
T	Time
P	Number of machine pole pairs
Q	Number of slots per pole and phase of stator winding
T, T_{EL}	Expansion periods of MMF and mutual induction field to harmonic series
$U_1, \ldots, U_Q$	Amplitudes of time harmonics
W_{PH}	Number of turns in stator winding phase
Z_1	Number of stator slots
β	Pitch shortening of stator winding
$\varphi_{1,U}, \ldots, \varphi_{Q,U}$	Initial phase angles of voltage harmonics
τ	Pole pitch
$\omega_1, \ldots, \omega_Q$	Stator current circular frequencies
ω_{REV}	Angular rotation speed of rotor
ω_{BOR}	Angular rotation speed of MMF and stator field in air gap
ω_{ROT}	Circular frequency of EMF and rotor current

References

I. Monographs, general courses, textbooks

1. Demirchyan K.S., Neyman L.R., Korovkin N.V., Theoretical Electrical Engineering . Moscow, St.Petersburg: Piter, 2009. Vol. 1, 2 (In Russian).
2. Kuepfmueller K., Kohn G., Theoretische Elektrotechnik und Elektronik. 15 Aufl. Berlin, N. Y.: Springer, 2000. (In German).
3. Mueller G., Ponick B., Elektrische Maschinen, N.Y.:, J. Wiley, 2009. (In German).
4. Schuisky W., Berechnung elektrischer Maschinen. Wien: Springer, 1960. (In German).

5. Richter R., Elektrische Maschinen. Berlin: Springer. Band I, 1924; Band II, 1930; Band III, 1932; Band IV, 1936; Band V, 1950. (In German).
6. Mueller G., Vogt K., Ponick B., Berechnung elektrischer Maschinen. Berlin: Springer, 2007. (In German).
7. Korn G., Korn T., Mathematical Handbook, N.Y.: McGraw-Hill, 1961.

II, III. Asynchronous and synchronous machines. Papers, inventor's certificates, patents

8. Boguslawsky I.Z., Kuss G., Investigation of the structure m-phase stator winding with a fractional number q. Proceedings of the Russian Academy of Sciences. Energetika, #5, 1998.
9. Boguslawsky I.Z., Twelve – zone stator winding with fractional number of slots per pole and phase for large slow–speed machines. Elektrotechnika, #1, 1978. (In Russian).
10. Boguslawsky I.Z., Winding factors of the 12-phase winding with fractional q for the synchronous slow-moving machines. Elektrotechnika, #7, 1976. (In Russian).
11. Boguslawsky I.Z., Features six-phase armature winding machines with non-sinusoidal power supply. Proceedings of the Russian Academy of Sciences. Energetika. #5, 1997. (In Russian).
12. Boguslawsky I.Z., The harmonics of armature field and frequencies of rotor loops currents of multiphase synchronous motor under nonsinusoidal feeding. Research Institute of Electric Machine Industry of Russian Academy of Science (Elektromach). No. 2, 1998. (In Russian).

IV. State Standards (IEC, GOST and so on)

13. GOST (Russian State Standard) R-52776 (IEC 60034-1). Rotating Electrical Machines. (In Russian).

Chapter 4
Peculiarities of Currents Investigation in Magnetically Coupled Circuits for A.C. Machines with Short-Circuited Rotor Windings

This chapter states peculiarities of investigation methods of magnetically coupled loops in A.C. machine with short-circuited rotor windings. Noted here are solutions of general problem on currents distribution in these windings: stated here is the solution algorithm for a system of equations, the concept is introduced on generalized characteristics of currents in rotor loops elements (for example, in elements of damper winding of salient pole machine). As practical usage an example of generalized characteristics of currents and MMF of short-circuited rotor loops is given with the calculation method of performance characteristics of high-power induction motors with nonlinear parameters (with account of skin effect in squirrel cage and magnetic circuit saturation). It is checked experimentally and is used in industry for calculation of machines with power up to 12–15 MW.

The appendix to this chapter presents a method of currents calculation for pole electromagnetic screen as one more example of generalized characteristics application; it is developed for low-frequency high-power salient pole machines (with torque over 50 T m). This screen carries out the same role as standard damper winding, however, in comparison with it, for low-frequency machines it has a number of advantages. The solution is reduced to realization of Saint-Venant's problem [1] on vector electric potential; thus, it was expedient to use the mesh current method. In developing the calculation method for this screen, a link is established between apparent current in loop of arbitrary form (mesh current) and vector potential averaged (according to Lagrange's mean value theorem) within the same loop [2, 3].

The content of this chapter is development of the methods stated in [15–18, 22–26].

I. Boguslawsky et al., *Large A.C. Machines*,
DOI 10.1007/978-4-431-56475-1_4

4.1 General

The main investigation stages of A.C. machines operating in non-linear networks with short-circuited rotor windings are listed in Chap. 2; it is noted that one of the main stages is the problem of current distribution calculation in these winding construction elements, namely, in damper windings and squirrel cage winding, when damaged.

The magnetically coupled circuits determined in previous chapter allow formulating the methods necessary for solving this problem. To use these methods physically reasonable, it is advisable to present the currents in generalized characteristic forms of the windings [15]; a special case of calculating expressions for generalized current in a DFM rotor winding is obtained in Chap. 2.

These concepts can be easily introduced for some other rotor winding constructions used in practice. At first, it is necessary to consider the current calculation features in several rotors magnetically-coupled circuits with lumped parameters; every circuit current is determined considering its induced EMF and its impedance (D.C. resistance and leakage inductance). Then, the results are extended to the current calculation methods, EMF and MMF rotor branch circuits with distributed parameters, for example, to the current calculation methods in bars, short-circuited ring portions and etc. at non-sinusoidal power supply.

Some forms representing the equation system for magnetically-coupled circuit currents and, accordingly, its solution methods are known in the electrical machine theory. First, one of them is considered using the following problem as an example: the currents in three magnetically-coupled circuits with A.C. machine lumped parameters are determined.

It is sufficient to consider only one time harmonic, for example, the first (Q = 1). Only the first space harmonic (m = 1) is taken into account in calculations. Two machine circuits are located on a rotor, and one—on a stator. Its operational mode is asynchronous. The machine is connected to A.C. networks with frequency ω_1 and rotates at $\omega_{REV} \neq \omega_1/p$ speed. Therefore, the EMF frequency induced in rotor circuits is equal to $\omega_{ROT} = \omega_1 S_{SL} \neq \omega_1$ (sleep at $S_{SL} \neq 0$).

To make the current calculation methods simple, it is assumed that the rotor windings are multiphase as the stator winding is. Suppose, for example, the phase numbers of all the windings are identical and equal to m_{PH}. This means in practice that the damper winding with the distributed parameters and short-circuited single-phase excitation winding in a salient pole machine are replaced with two equivalent circuits. It is not our task to determine the equivalent parameters of these multi-phase rotor short-circuits.

The correspondence of two magnetically coupled rotor circuits to real salient pole synchronous machine windings is stipulated to clarify the physical problem under consideration. Now, the iteration method [3, 15] of determining the currents in a stator winding and in two equivalent rotor circuits of the machine is considered with use of generalized characteristics of the currents, MMF and EMF.

Note additionally that this problem (as applied to one rotor winding phase and one stator winding phase of a DFM) is solved earlier taking into account the magnetic circuit saturation.

Here, the problem of determining the currents in two circuits on a rotor using the iterative method, if the number of circuits on the rotor $N_0 \gg 1$, is investigated.

4.2 The Problem Determination and Algorithm of Solution

It is assumed that we know:

- phase circuit voltage U_{PH} is with frequency ω_1;
- EMF frequency in rotor circuits is ω_{ROT};
- machine pole numbers are 2p;
- circuit A.C. resistances are R_1, R_2, R_3, respectively.
- circuit inductance leakages are $L_{1,S}, L_{2,S}, L_{3,S}$ respectively;
- circuit turn numbers and winding coefficients are $W_1, K_{W_1}; W_2, K_{W_2}; W_3, K_{W_3}$;
- no load characteristic is $|\Phi_0| = f(|F_0|)$.

where Φ_0—mutual flux complex amplitude (phasor) in an air gap, F_0—MMF magnetic circuit complex amplitude (phasor) corresponding to the flux Φ_0 in an air gap

It is required to calculate the currents in three magnetically coupled circuits including both short-circuited rotor ones.

The equation system for calculating currents can be written as follows.

The equation for stator winding voltage is:

$$U_{PH} = \left(R_1 + j\omega_1 L_{1,s}\right) I_1 + j\omega_1 W_1 K_{W_1} \Phi_0. \tag{4.1}$$

The equations for EMF of both rotor short-circuits are:

$$0 = \left(R_2 + j\omega_{ROT} L_{2,S}\right) I_2 + j\omega_{ROT} W_2 K_{W_2} \Phi_0. \tag{4.2}$$

$$0 = \left(R_3 + j\omega_{ROT} L_{3,S}\right) I_3 + j\omega_{ROT} W_3 K_{W_3} \Phi_0. \tag{4.3}$$

The fourth equation corresponds to Ampere's law:

$$F_1 + F_2 + F_3 = F_0. \tag{4.4}$$

where F_1, F_2, F_3—MMF complex amplitudes of three circuits; the flux Φ_0 is determined by no load characteristic $|\Phi_0| = f(|F_0|)$ while the complex amplitude phases of the flux Φ_0 and MMF F_0 coincide.

The fifth equation, namely the dependence $\Phi_0 = f(F_0)$ can also be expressed analytically as:

$$\Phi_0 = \frac{F_0 T_{EL} L_{COR} \mu_0}{\delta \pi k_{CART} k_{SAT}} = \frac{(F_1 + F_2 + F_3) T_{EL} L_{COR} \mu_0}{\delta \pi k_{CART} k_{SAT}}. \quad (4.5)$$

where μ_0—air magnetic permeability ($\mu_0 = 4\pi 10^{-7}$ Hn/m); $T_{EL} = \frac{\pi D}{p}$—MMF expansion period; L_{COR}—stator core active length; δ—equivalent air gap; k_{CART}, k_{SAT}—Carter's coefficient [4–6] and the magnetic circuit saturation coefficient, respectively.

This system contains five unknown values: three currents I_1, I_2, I_3; the flux Φ_0; MMF F_0. The equation connecting the complex flux density amplitude B_1 and the flux Φ_0 is as follows (the flux density complex amplitude of resulting field in a gap B(m = 1, Q = 1) for short, it is indicated as $B(m = 1, Q = 1) = B_1$):

$$B_1 = \frac{\Phi_0 \pi}{T_{EL} L_{COR}}.$$

It is assumed that the equations connecting MMF and the phase current for lumped phase winding are known [4, 5, 7, 8]. For example, the MMF F_1 for stator phase windings and the current I_1 are $F_1 = \frac{m_{PH} W_1 I_1 K_{W_1}}{\pi p}$. Therefore, the MMF F_1, F_2, F_3 are not listed among the unknowns, and these connecting equations are not included in the system.

If the rotor windings are short-circuited, it is convenient to use the iterative solution method regardless of the rotor short-circuit numbers, while presenting the equation systems for magnetically coupled circuits in (4.1)–(4.5).

As a result, it is possible to avoid difficulties implementing higher-order equation systems in (4.1)–(4.5) relative to the unknown currents using direct calculation methods [2, 3].

The iterative algorithm for realizing this system can be presented in the following calculation sequence:

1. The arbitrary value of the flux density amplitude B_1 (in the form of real or complex numbers) is set.
2. The flux $\Phi_0 = \frac{T_{EL} L_{COR}}{\pi} B_1$ is calculated.
3. The currents in rotor circuits are calculated using Eqs. (4.2)–(4.3): the current I_3—using Eq. (4.3), the current I_2—using Eq. (4.2). The resulting MMF F_0 is determined by the machine no load characteristics; $|\Phi_0| = f(|F_0|)$ the phase angle of the flux Φ_0, i.e. the flux density B_1 is assigned for this MMF.
4. The MMF F_1 and the stator current I_1 are determined using Eq. (4.4).
5. The voltage U is calculated using Eq. (4.1).
6. If the value $|U| \neq |U_{PH}|$, it is necessary to adjust the amplitude of B_1 using one of root determination methods for nonlinear equations, such as Newton's method [2, 3].

6.1 If the value $|U| < |U_{PH}|$, it is necessary to increase the flux density amplitude B_1 and see Item 2.

6.2 If the value $|U| > |U_{PH}|$, it is necessary to reduce the flux density amplitude B_1 and see Item 2, as well.

6.3 If the value $\frac{|U-U_{PH}|}{|U_{PH}|} \leq \varepsilon$, five unknown values are the currents I_1, I_2, I_3, the flux density amplitude B_1 and MMF F_0 are desired values (here the value ε is a preset computational accuracy of the root algorithm $U = f(B_1)$.

Now, the physical interpretation of the above algorithm 1–6.3 is considered.

Firstly, the Item 3 of the algorithm is examined.

The second term in Eq. (4.3) of the EMF in the third machine rotor circuit is indicated as follows: $E_3 = -j\omega_{ROT} W_3 K_{W_3} \Phi_0$. This EMF can also be represented otherwise:

$$E_3 = [E_3]B_1 \quad \text{where} \quad [E_3] = \frac{-j\omega_{ROT} W_3 K_{W_3} T_{EL} L_{COR}}{\pi} \tag{4.6}$$

– generalized characteristic of the EMF.

The result is that the expression for $[E_3]$ is determined by geometrical dimensions of the machine active part (T_{EL}, L_{COR}), winding data (W_3, K_{W_3}), frequency (ω_{ROT}) of the circuit, EMF and it is independent of any electromagnetic loads. The expressions for calculating $[E_2], [E_1]$ are written similarly. The expressions $[E_1], [E_2], [E_3]$ remain constant in the process of calculating over the algorithm 1–6.3.

The current in the third shorted circuit on the rotor is expressed using the EMF $[E_3]$. The following is obtained from Eq. (4.3):

$$\begin{aligned} I_3 &= \frac{-j\omega_{ROT} W_3 K_{W_3} \Phi_0}{R_3 + j\omega_{ROT} L_{3,S}} = j\omega_{ROT} W_3 K_{W_3} \frac{\frac{T_{EL} L_{COR} B_1}{\pi}}{R_3 + j\omega_{ROT} L_{3,S}} \\ &= \frac{[E_3]}{R_3 + j\omega_{ROT} L_{3,S}} B_1 = [I_3]B_1. \end{aligned} \tag{4.7}$$

where $[I_3] = \frac{[E_3]}{R_3 + j\omega_{ROT} L_{3,S}}$—generalised charactersitic of the current; $[E_3]$—over (4.6)

The expression for current I_2 is written similarly: $I_2 = [I_2]B_1$. Thus, if the shorted circuits are arranged on a rotor, the currents therein are determined up to the amplitude B_1.

Now, the Items 4 and 5 of the algorithm are considered. When submitting currents in short-circuits in the form (4.7), the MMF values F_2, F_3 take the form:

$$F_2 = \frac{m_{PH} W_2 K_{W_2}}{\pi p}[I_2] = \frac{m_{PH} W_2 K_{W_2}}{\pi p}[I_2]B_1 = [F_2]B_1; \quad [F_2] = \frac{m_{PH} W_2 K_{W_2}[I_2]}{\pi p} \tag{4.8}$$

$$F_3 = \frac{m_{PH} W_3 K_{W_3}}{\pi p} [I_3] B_1 = [F_3] B_1; \quad [F_3] = \frac{m_{PH} W_3 K_{W_3} [I_3]}{\pi p} \tag{4.9}$$

where $[F_2], [F_3]$ are generalized characteristics of MMF

Therefore, the MMF rotor short-circuits are also determined accurately within the amplitude value B_1.

Note that expressions for calculating $[I_2], [I_3], [F_2], [F_3]$, as well as $[E_2], [E_3]$ are determined by geometrical dimensions of the machine active part (T_{EL}, L_{COR}), winding data, frequency (ω_{ROT}) of the EMF rotor circuits and the circuit impedance. They are not dependent on electromagnetic loads and they are constant at EMF frequency in rotor circuits ω_{ROT}.

Similarly imagine the resulting MMF F_0:

$$F_0 = \frac{B_1 \delta k_{CART} k_{SAT}}{\mu_0}.$$

The MMF F_0 depends on the flux Φ_0 or flux density B_1. It is determined by the machine no load characteristic $|\Phi_0| = f(|F_0|)$. Hence, it depends on the saturation degree of its magnetic circuit (the saturation ratio k_{SAT}). So, it is written in the form of:

$$F_0 = \frac{\delta k_{CART} k_{SAT}}{\mu_0} B_1 = [F_0(k_{SAT})] B_1. \quad \text{Here} [F_0(k_{SAT})] = \frac{\delta k_{CART} k_{SAT}}{\mu_0} \tag{4.10}$$

Using this expression and Eq. (4.4), the stator winding current I_1 is determined:

$$I_1 = \pi p \frac{[F_0(k_{SAT})] - [F_2] - [F_3]}{m_{PH} W_1 K_{W_1}} B_1. \tag{4.11}$$

Finally, item 6 of the algorithm is considered. It deals with Eq. (4.1). The calculated expression for voltage U taking into consideration the above ratios takes the following form:

$$U = \pi p \frac{[F_0(k_{SAT})] - [F_2] - [F_3]}{m_{PH} W_1 K_{W_1}} \left(R_1 + j\omega_1 L_{1,S}\right) B_1 + \frac{j\omega_1 W_1 K_{W_1} T_{EL} L_{COR}}{\pi} B_1. \tag{4.12}$$

It is obtained from this equation that the desired flux density amplitude B_1 is determined analytically in a closed form for a machine with an unsaturated magnetic circuit $(k_{SAT} = 1)$. Respectively, the desired currents in three circuits are determined. As far as the saturated machine is concerned, it is necessary to carry out several iterations in order to determine this saturation degree, i.e., the coefficient $k_{SAT} > 1$ [with take in account (4.10)].

The obtained researching results are summarized using the iterative current method in three magnetically coupled circuits (meshes), two of which are short-circuited and located on a rotor. The research results have confirmed that the current distribution problem can be divided into several stages.

First stage: to calculate the currents in shorted rotor circuits accurately within the flux density amplitude B_1 of the resulting field in an air gap. It is given by an arbitrary value.

Second stage: to calculate the MMF created by these currents accurately within the flux density amplitude B_1 of the resulting field in an air gap.

Third stage: to calculate the stator winding current and the flux density amplitude B_1. The equation for this phase voltage of motor is used. This voltage U_{PH} is set in it.

Note that Eq. (4.4) contains the MMF current complex amplitudes (phasors). Consequently, in general, it is supposed to expand into harmonic series a number of current distribution curves in rotor and stator windings. The MMF determination methods for a salient-pole machine damper winding and an asynchronous machine squirrel cage (asymmetric or symmetric) are described in Chap. 12.

It is appropriate to extend the aforementioned solution stages to a rotor design with distributed parameters, such as the damper winding design. Indeed, the MMF generalized characteristic of rotor short-circuited windings $[F_2], [F_3]$ are obtained using Eqs. (4.8) and (4.9). It is carried out without solving the system (4.1)–(4.5), as these characteristics are determined by geometrical dimensions of the machine active part (T_{EL}, L_{COR}), winding, frequency (ω_{ROT}) of EMF rotor circuits, as well as the circuit impedance. They are constant at the permanent frequency ω_{ROT} of EMF in rotor circuits. Therefore, the generalized characteristics $[F_2], [F_3]$ can be determined in advance. Using them, the equation system can be modified. The system is reduced to the following two equations.

$$\left(R_1 + j\omega_1 L_{1,S}\right) I_1 + \frac{j\omega_1 W_1 K_{W_1} T_{EL} L_{COR}}{\pi} B_1 = U. \tag{4.12'}$$

$$\frac{m_{PH} W_1 K_{W_1} I_1}{\pi p} + [F_2] B_1 + [F_3] B_1 - [F_0(k_{SAT})] B_1 = 0 \tag{4.4'}$$

It contains two unknown values: the current I_1 and the flux density B_1. After determining the flux density B_1, the MMF $F_2 = [F_2]B_1; F_3 = [F_3]B_1$ are determined. It is easy to determine the rotor winding currents in terms of the MMF. If it turns out that $k_{SAT} > 1$ after determining B_1, then it is required to clarify the values k_{SAT} and, correspondingly, $[F_0(k_{SAT})]$. The system is linear, if the value $k_{SAT} = 1$.

However, the reduction of unknown values is not so important in comparison with the system (4.1)–(4.5). It is more important that this system is valid not only for the rotor winding design with lumped parameters. It indicates the way to calculate magnetically coupled circuits. Some of them correspond to short-circuited windings on the rotor with distributed parameters, for example, the damper

winding. In order to solve such a system, it is necessary to determine the generalized characteristics summarized above.

As a practical example, the method of large induction motors performance investigating is presented in Sect. 4.3. It is developed for powerful asynchronous motors [16, 19, 20] with nonlinear parameters (including the skin effect in squirrel cage bars and the magnetic circuit saturation). It is based on the generalized characteristics of EMF, currents and MMF. While working on this problem, it turned out to be necessary to develop additionally the method of determining nonlinear algebraic equation roots. Compared with the method commonly used [3], for example, the modification of the Newton's method and "regula falsi" method, the equivalent curve method developed in [21] for solving similar problems allow determining the nonlinear function roots assigned in the form of an algorithm, and when this function is "not smooth". It is necessary to apply this method in algorithms used for electrical machine calculations. The appearance of "non-smooth" ratios is dependent, for example, on discrete sizes of strand conductors, experimental magnetization curves, etc. An additional advantage of the developed method determining the nonlinear algebraic equation roots [16, 21] is to reduce the iteration numbers, thus accelerating the solution convergence.

This method has been verified experimentally. It is used in industrial practice for investigating the operations of asynchronous machines with the rated power up to 12–15 MW [19, 20].

Another example of using generalized characteristics of EMF and currents is presented in Appendix 4.1. This is the method for calculating the damper winding unconventional design of powerful salient frequency—controlled machines [22–24]. This design is expedient for frequency—controlled salient-pole machines (with the torque on the shaft more than 50 T m at rotational speed up to 50–60 rpm).

4.3 Method Investigating of Operation Characteristics of Powerful Squirrel Cage Motors with Nonlinear Parameters

The practice of designing modern, powerful asynchronous motors with squirrel-cage rotors raises the problem of verifying the calculation methods of their characteristics. This is important in cases, where the motors are designed for heavy-duty operation (in metallurgy, mining industry, etc.). This is applied both to the industrial frequency machines and frequency-controlled machines. At the same time it is necessary to take into account the motor nonlinear reactance. This nonlinearity is caused by the machine magnetic circuit saturation and by slip depending parameters, etc. The calculations of parameters of powerful modern induction machines, in which capacitive elements are included in the secondary circuit, are referred to the problem of non-linear parameter registration.

Now, the problem of calculating the currents in stator and rotor windings and the torque on the shaft on a large asynchronous machine shaft, as well as the power factor of other performance characteristics for a given slip value S_{SL} is considered. Basic equations for the A.C. machine asynchronous mode with nonlinear parameters, reduced to the primary circuit, have the form [16]:

$$I_0 = I_1 + I'_2. \tag{4.13}$$

$$I'_2 Z'_2 = E. \tag{4.14}$$

$$U = I_1 Z_1 - E. \tag{4.15}$$

$$I_0 = I_A + I_\mu. \tag{4.16}$$

$$|I_A| \approx \frac{P_{COR} + P_{MECH} + P_{AD}}{1.5|U|}. \tag{4.17}$$

$$I_\mu = |f(|E|)|. \tag{4.18}$$

They correspond to the T-shape circuit for m = 1 [4–8] written for the effective current values, EMF and voltages. In these equations:

E	magnetizing circuit EMF
I_0	magnetizing circuit current
I_1, I'_2	primary and secondary circuit currents, respectively
I_A	active component of no load magnetizing current
I_μ	reactive component of magnetizing current
P_{COR}	losses in stator and rotor cores
P_{MECH}	mechanical losses
P_{AD}	additional losses
U	Primary circuit voltage
Z_1, Z'_2	primary and secondary circuit impedances depending on slip S_{SL} (taking into account the skin effect)

Note: The secondary circuit currents and impedances are reduced [4–8] to the primary circuit and marked by a "prime" on.

The given values are assumed in this system as: U, Z_1, Z'_2; the dependences as: $|I_\mu| = f(|E|)$, $P_{COR} = f(|E|)$, $P_{MECH} = f(S_{SL})$, $P_{AD} = f(|E|)S_{SL}$; ε—voltage calculation accuracy. Its analytical expression as well as the analytic expression for Z'_2 considering the skin effect in general case are rather complicated. That is why some certain difficulties appear in solving the closed-form system and it is practically inexpedient. The iterative numerical methods suitable for practical implementation are developed below.

It is convenient to reduce the system solution (4.13)–(4.18) to solving a nonlinear algorithm [2, 3]

$$U = f\left(I'_2\right) \tag{4.19}$$

or any type

$$U = f(B_1). \tag{4.20}$$

Here the root of each algorithm is $U = U_{PH}$, where B_1—air gap flux density amplitude,U_{PH}—phase voltageNote that the phase angles of current I_μ and flux density B_1 coincide.

The following feature is a peculiarity of using the root search method in the nonlinear algorithm (4.19). In practical calculations, it is more convenient not to set the secondary circuit current by a complex number, but that of the real form $I'_2 = I'_2 e^{j\Psi_2}$ at $\Psi_2 \neq 0$, where Ψ_2—angle between the positive direction of the vector I'_2 and real axis. It is necessary that the real axis positive direction in the coordinate system (+1, + j) coincides with the vector positive direction. Correspondingly, the EMF of stator winding phase is assumed in this case to be not a real number, but a complex form $E = E_M e^{j\psi_E}$, where ψ_E—angle between positive direction of vector E and real axis. It is necessary to multiply the system left and right parts (4.13)–(4.18) over the complex $e^{j(\pi+\psi_E)}$ in order to obtain the expression for I'_2 and E in the indicated form. That means the turn at the angle $\pi + \psi_E$ all vectors of vector diagram. Such transformation of the equation system (4.13)–(4.18) allows solving nonlinear algorithms of the form (4.19) for the real I'_2 at a given phase voltage value U_{PH}.

Now, the solution of nonlinear algorithm $U = f\left(I'_2\right)$ using an equivalent curve method [16, 21] is considered. It is suitable to present this method as a sequence of computations performed for each slip value S_{SL}. The iteration number is denoted with the letter K.

1. The real number $I_2^{\prime(K)} = I_{2L}^{\prime(K)}$ is designated and calculated using the system (4.13)–(4.18): $U_L^{(K)} = f\left[I_{2L}^{\prime(K)}\right]$.
2. The real number $I_2^{\prime(K)} = I_{2R}^{\prime(K)}$ is designated and calculated using the system (4.13)–(4.18): $U_R^{(K)} = f\left[I_{2R}^{\prime(K)}\right]$.
3. The real number $I_2^{\prime(K)} = I_{2M}^{\prime(K)}$ is designated and calculated using the system (4.13)–(4.18): $U_M^{(K)} = f\left[I_M^{(K)}\right]$.
4. The equivalent curve coefficients are calculated:

$$C^{(K)} = \frac{U_R^{(K)} I_{2M}^{\prime(K)} - U_M^{(K)} I_{2R}^{\prime(K)}}{I_{2M}^{\prime(K)} \cdot I_{2R}^{\prime(K)} \left(U_R^{(K)} - U_M^{(K)}\right)}; \quad F^{(K)} = \frac{U_M^{(K)} U_R^{(K)} \left(I_{2R}^{\prime(K)} - I_{2M}^{\prime(K)}\right)}{I_{2M}^{\prime(K)} \cdot I_{2R}^{\prime(K)} \left(U_R^{(K)} - U_M^{(K)}\right)}.$$

5. The value $I_2'^{(K)} = \frac{U_{PH}}{U_{PH}C^{(K)} + F^{(K)}}$ is calculated; this value is the following approximation of the secondary current values; this approximation is denoted with number K.
6. The voltage $U = f\left[I_2'^{(K)}\right]$ is calculated using the system (4.13)–(4.18).
7. If $\left|\frac{U - U_{PH}}{U_{PH}}\right| < \varepsilon$, the calculation is over, otherwise see Item 8.
8. If $U - U_{PH} \le 0$ and $I_2'^{(K)} - I_{2L}'^{(K)} - I_{2R}'^{(K)} + I_{2M}'^{(K)} > 0$, it is necessary to see Item 9, otherwise—Item 10.
9. The value $I_{2L}'^{(K+1)} = I_{2M}'^{(K)}$; $I_{2M}'^{(K+1)} = I_2'^{(K)}$; $I_{2R}'^{(K+1)} = I_{2R}'^{(K)}$ is specified; Items 1–8-repeated.
10. The value $I_{2L}'^{(K+1)} = I_{2L}'^{(K)}$; $I_{2M}'^{(K+1)} = I_{2M}'^{(K)}$; $I_{2R}'^{(K+1)} = I_{2R}'^{(K)}$ is specified and Items 1–7-repeated.

The voltage U of the system (4.13)–(4.18) is determined as follows: the EMF $E(I_\mu) = Ee^{j\psi_E}$ is calculated over (4.14); the currents I_A and I_μ—over (4.17) and (4.18); the current $I_0 = (\dot{I}_A + \dot{I}_\mu)e^{j(\pi + \psi_E)}$—over (4.16); the current $I_1 = I_0 - I_2'$—over (4.13); the voltage $U = Ue^{j\psi_E}$—over (4.15).

It is not difficult to determine the interval, in which the desired root $I_2'^{(Find)}$ is found: $0 \le I_2'^{(Find)} \le \left|\frac{U_{PH}}{Z_2}\right|$.

It is convenient to choose these minimum and maximum values of current I_2' as initial approximations for $I_{2L}'^{(0)}$ and $I_{2R}'^{(0)}$, and to calculate the value $I_{2M}'^{(0)}$ using the ratio: $I_{2M}'^{(0)} = 0.5I_{2R}'^{(0)}$.

Similarly, the "regula falsi" method [2, 3] can be realized for the non-linear algorithm intersection $U = f(I_2')$.

The iteration numbers corresponding to both methods are compared in Table 4.1.

The nonlinear algorithm solution $U = f(B_1)$ now is considered, which is described as a sequence of computations performed for each value S_{SL} using the "regula falsi" method:

Table 4.1 Iteration numbers for implementing nonlinear algorithms using numerical methods

S_{SL}	"Regula falsi"	Equivalent curve method	"Regula falsi"
	$U = f(B_1)$	$U = f(I_2')$	$U = f(B_1)$
0.2	2	1	2
0.4	2	1	2
0.6	2	2	2
0.8	2	1	2
1.0	2	1	2

1. The complex number $B_1^{(K)} = B_1^{(0)}$ is specified.
2. The value $E^{(K)} = \omega_1 W_1 K_{W_1} \frac{T_{EL} L_{COR}}{\pi} B_1^{(K)} e^{-j\frac{\pi}{2}}$; where ω_1—network angular frequency; W_1—number of turns in rotor winding phase (for short-circuited winding $W_1 = 0.5$); K_{W_1}—winding factor (for short-circuited winding $K_{W_1} = 1$);

   T_{EL}—first space harmonic period $\left(T_{EL} = \frac{\pi D}{p}\right)$.
3. The current $I_2'^{(k)}$ is calculated with (4.14).
4. The currents $I_A^{(K)}$ and $I_\mu^{(K)}$ are calculated with (4.17) and (4.18). The value $I_0^{(K)}$ is calculated with (4.16), $I_1^{(K)}$—with (4.13), $U^{(K)}$—with (4.15).
5. If $\left|\frac{U_{PH} - U^{(K)}}{U_{PH}}\right| < \varepsilon$, the calculation is over, otherwise Steps 2–5 are repeated for $B_1^{(K+1)}$; where ε—voltage calculation accuracy.

The following can be taken as an initial approximation B_1^0 :

$$B_1^0 \approx \frac{\pi U_{PH}}{\omega_1 W_1 K_{W_1} T_{EL} L_{COR}}.$$

Calculation results present the performance parameter calculations of DAZ-type («Elektrosila» Work, Stock Company "Power Machines" St.-Petersburg and Limited Liability Company "Scientific-Production Association" Leningrad Electrical Machine Building Plant") powerful induction motor rating power (1250–2500) kW [16, 19, 20]. The calculation accuracy is accepted as: $\varepsilon < 0.01$. The number of iterations is compared corresponding to the "regula falsi" method and the equivalent curve method implementing nonlinear algorithms (4.19) and 4.20). The calculation practice confirms that less time is required for adjusting it, when the "regula falsi" method is used for implementing the nonlinear algorithm (4.20). By comparison, the use of the equivalent curve method for the nonlinear algorithm solution (4.19) can result in reducing computer time, especially with the parameters distinguished by their significant nonlinearity.

4.4 Experimental Data and Calculating Results Comparison for the Torque M on the Shaft Depended on Slip S_{SL} for DAZ-Type Motor

The comparison of experimental and estimated data on DAZ-type motor is presented in Table 4.2.

It is shown in the table that the calculation algorithm constitutes a match with experimental data sufficient for practical calculations.

Table 4.2 Experimental and calculated results comparison of DAZ-type motor

S_{SL}	Calculating according [16]		Experiment	
	$S_{SL} = 0.02$	$S_{SL} = 1$	$S_{SL} = 0.02$	$S_{SL} = 1$
S_{SL}	Calculating according [16]		Experiment	
	$S_{SL} = 0.02$	$S_{SL} = 1$	$S_{SL} = 0.02$	$S_{SL} = 1$
I_1, A	406.2	1474.5	412	1470
I_2, A	956.4	1421	–	–
Cosφ	0.8348	0.1382	0.834	0.139
I_0, A	129.5	54.1	135	55
E, V	5605	3308	5650	3310

The above current calculation method used in T—equivalent structure of an asynchronous motor is simple. It is based on the root-finding method of nonlinear algebraic equations [2, 3, 16, 21].

In the design of high-power induction motors with heavy-duty (sudden change of load, etc.) this method can be supplemented by a subroutine of the refinement of the impedance of rotor bars. In the subroutine we realized the method for impedance calculation with take into account simultaneously the skin effects in the rotor bar and the temperature distribution along its height. This method is given in Appendix 1 of Chap. 23.

4.5 Generalized Characteristic of Rotor Current in Cage Elements

It is important to note the following peculiarities of this method for further description of each slip S_{SL}.

- Three values can be consistently identified setting arbitrary the flux density amplitude value in an air gap (or the current in a secondary circuit): the secondary circuit EMF, the secondary circuit current and the circuit magnetizing current. The primary circuit current is determined on the basis of Ampere's law, taking into account MMF of magnetically coupled machine circuits. There are only two MMFs for a squirrel cage machine—one for a multiphase stator winding, the second—for a multiphase rotor winding. These values are sufficient to calculate the primary circuit voltage and to compare it with those specified in the problem;
- the EMF, currents and MMF are linearly dependent on the flux density amplitude B_1 in an air gap for the secondary circuit. These dependencies subject to squirrel cage structural peculiarities [4–8] are as follows:
- for the EMF amplitude bar (E_B):

$$E_B = \left[\frac{-j\omega_{ROT} W_{PH} K_W T_{EL} L_{COR}}{\pi}\right] B_1 = \left[\frac{-j\omega_{ROT} T_{EL} L_{COR}}{2\pi}\right] B_1 = [E_B] B_1;$$

- for the bar current amplitude (J_B):

$$J_B = \frac{E_B}{Z_2} = -\frac{\frac{j\omega_{ROT} T_{EL} L_{COR}}{2\pi}}{Z_B + \frac{Z_R}{2\sin^2 \frac{\pi p}{N_0}}} B_1 = [J_B] B_1;$$

here Z_B, Z_R—impedances of bar and portion of rings between two bars, N_0—number of bars;

- for the current amplitude in a ring portion between two bars (I_R):

$$I_R = \frac{J_B}{2\sin \frac{\pi p}{N_0}} = -\frac{-j\omega_{ROT} T_{EL} L_{COR}}{2\pi} \cdot \frac{1}{2Z_B \sin \frac{\pi p}{N_0} + \frac{Z_R}{\sin \frac{\pi p}{N_0}}} B_1 = [I_R] B_1; \quad (4.21)$$

- for MMF amplitude of a squirrel cage (F_2): $F_2 = \frac{1}{2}\frac{N_0 J_B}{\pi p} = [F_2] B_1$;
- It is found out that the proportionality coefficients $[E_B], [J_B], [I_R], [F_2]$ are not dependent on winding currents. They are determined by the following main factors:
- the machine geometrical dimensions, for example, the length L_{COR};
- the winding parameters, for example, its impedances Z_B and Z_R calculated for a certain slip S_{SL} considering the skin effect;
- machine pole numbers 2p.

These proportionality coefficients can be designated $[E_B], [F_2], [J_B], [I_R]$, namely, the generalized characteristics of EMFs, MMF, bar currents and, respectively, currents in squirrel cage ring portions.

Physically, these generalized characteristics of EMF, MMF, squirrel cage currents for specifying the slip S_{SL} (or for rotor current frequency ω_{ROT} = idem) and the selected winding structure can be regarded as the similarity criteria. They characterize the amplitudes of EMF, MMF, cage currents in the flux density amplitude scale B_1. They determine the relationship between the EMF, MMF, squirrel cage currents and the flux in a gap, i.e. the reaction of a rotor winding exposed to flux density amplitude B_1 in the steady-state mode.

Appendix 4.1: Screen Calculation Method of Large Low-Frequency Motor Pole Shoe

General The problem of field current distribution in a damper system of a powerful salient pole low-frequency motor (with shaft torque more than 50 T m) is of some interest in practical work. This system is designed as a screen (a rectangular conductive plate) and it is located at the rotor pole shoe [22–24]. Currents are induced by the mutual magnetic field in air gap. This design is effective for powerful low frequency machines. It is distinguished by its low level leakage flux between the poles [7–10] from the conventional design of damper system. The requirements to screen fields of higher order time harmonics generated by a stator circuit frequency inverter, as well as a field of negative phase-sequence in case of motor emergency modes (with its stator winding phase asymmetry, etc.) are only produced to the low-frequency motor damper system unlike the industrial frequency motor damper system. The synchronous starting is carried out for these motor types, so the damper winding is not used as a starting one.

Methods of calculating the screens at the poles, as set out in this appendix, can be used as a subroutine in the design of low speed high-power frequency-controlled motors with large values of the distortion factor of voltage and current waveforms.

Problem of determination. The screen dimensions are assumed to be specified parameters (Fig. 4.1): width FK = A = 2a; length FC = L = 2b; the screen thickness is assumed to be equal to h, where h << A; h << L. The origin of coordinates is located as follows: $0 \le X \le 2a$; $0 \le y \le 2b$. Note that the Y-axis direction coincides with the machine axis rotation direction. To simplify the design, no jumpers between the poles are installed. This screen is similar to incomplete damper winding of a salient-pole machine. The screen resistivity is equal to ρ, and the magnetic permeability—to μ_0. The ferromagnetic base (pole) resistivity is equal to

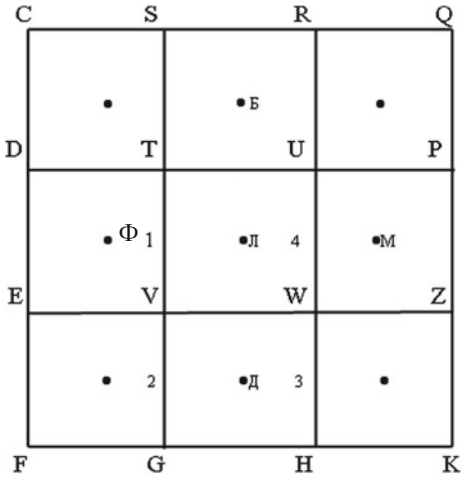

Fig. 4.1 The rectangular grid

ρ_{FE} and its magnetic permeability—μ_{FE}, while $\rho_{FE} \gg \rho$. The mutual induction field lines in an air gap are taken as orthogonal to the screen surface and its ferromagnetic base. Stray fields of the screen laid on the ferromagnetic pole shoe surface are initially neglected unlike ordinary stray fields of a conventional damper winding, whose bars are laid in the semi-closed slots. Their accounting is described in Sect. 4.1.5.

The mutual flux coupled with a screen varies in an air gap sinusoidal. Now, the symbolic method [7, 8] is used. The flux density distribution in a gap of rotor coordinates can be presented as follows:

$$b(x,t) = |B_1| e^{j\left(\omega_{ROT} t - \frac{\pi x}{\tau}\right)} = B_1 e^{-\frac{jx}{\tau}}; \quad B_1 = |B_1| e^{j\omega_{ROT} t}. \tag{A.4.1.1}$$

where $|B_1|$ and B_1—amplitude and the corresponding complex flux density amplitude (phasor); τ—pole pitch, ω_{ROT}—screen current frequency; t—time; the flux density complex amplitude B_1 is determined using the generalized MMF rotor characteristic from the magnetically coupled circuit theory [4–8, 15, 25, 26].

Now, the distributions of current I induced by the screen magnetic field (A.4.1.1): I = I(x, y) are found out. It is assumed in Sects. 4.6.1 and 4.6.2 that the screen element resistance does not depend on the temperature distribution in it. This dependence is taken into account in Sect. 4.6.4.

It is convenient to calculate the current distribution I using generalized characteristics, since the screen is a shorted circuit disposed on a rotor. Therefore, the currents I are determined with the help of the method outlined previously in this chapter with the accuracy up to the complex flux density value of the resulting field in an air gap. These currents I = I(x, y) are not enclosed in square brackets in order to make the notation simpler.

A.4.1.1 Simply Connected Domain

The method of solving this problem for a simply connected domain is considered: for the screen, made of a material with only one resistivity ρ, for example, without any- or additional soldered-in parts in it or structural openings; in this case:

$$\rho \neq \rho(x,y) \tag{A.4.1.1′}$$

The computational domain is subdivided into elements of the loop. Their number is chosen in such a way that it provides the practical calculation required accuracy of currents in a screen.

Regular grid

At first, the rectangular circuit elements with $N_{EQ} = N_L N_W$ are chosen, where N_L, N_W—number of elements along the screen length and width, correspondingly. It is expedient to subdivide the computational domain for this problem. Current components directed along the machine rotation axis (along the axis Y) are of the

most practical interest. They form a flux in an air gap interacting with the stator winding flux.

The Maxwell equation [7, 8, 11, 12] is true for each element loop:

$$\oint \mathrm{edl} = -\int_{Q} \frac{\mathrm{db}(x,t)}{\mathrm{dt}} \mathrm{dQ}, \qquad (A.4.1.2)$$

where e—electric field intensity; l—element part (the integration path); $Q = \frac{4AL}{N_{EQ}}$—rectangular element area.

If the mutual induction flow is changed according to (A.4.1.1), this equation is as follows:

$$\oint \mathrm{Edl} = -\mathrm{j}\omega \int_{Q} \mathrm{Be}^{-\frac{\mathrm{j}\pi x}{\tau}} \mathrm{dQ}; \qquad (A.4.1.2')$$

(Hereinafter, the subscript "1 (one)" is omitted in the complex amplitude flux density B_1).

Now the "mean value theorem (Lagrange)" [2, 3] is used. The right part of this equation can be presented for the arbitrary circuit TVWUT (Fig. 4.1) as follows:

$$-\mathrm{j}\omega \int_{Q} \mathrm{Be}^{-\frac{\mathrm{j}\pi x}{\tau}} \mathrm{dQ} = -\mathrm{j}\omega B^{*} Q_{\Lambda}. \qquad (A.4.1.3)$$

where $B^{*} = \mathrm{Be}^{-\frac{\mathrm{j}\pi x^{*}_{\Pi}}{\tau}}$—average value of flux density complex amplitude of arbitrary rectangular area element Q_{Λ}, for example, TVWUT; x^{*}_{Λ}—abscissa of point "Λ", where the flux density is equal to B^{*}. This point is within the TVWUT circuit. Its position is determined according to the equation in Appendix 4.2. As it follows from the analysis, the point "Λ" can be combined with the gravity circuit center in practical calculations of the screen current field. Equation (A.4.1.2′) with (A.4.1.3) for TVWUT loop can be presented as

$$\oint \mathrm{Edl} = -\mathrm{j}\omega B^{*} Q_{\Lambda} \qquad (A.4.1.4)$$

Similar equations are true for other screen circuits.

Now, the concept of the current vector electric potential in the screen is used. The electric field intensity E in the element through the vector electric potential A^{E} [7, 8] can be presented as:

$$E = \mathrm{rot} A^{E}. \qquad (A.4.1.5)$$

The ratio (A.4.1.5) is valid because the screen line currents are continuous and closed, so [7, 8]:

$$\mathrm{div} E = 0. \qquad (A.4.1.6)$$

The vector components E in the chosen coordinate system are as follows:

$$(E)_X = \frac{\partial A^E}{\partial y}; \quad (E)_Y = -\frac{\partial A^E}{\partial x}. \tag{A.4.1.7}$$

Now, the difference approximation of Eqs. (A.4.1.4) and (A.4.1.7) is considered. The discrete vector values A^E are assigned to the screen element gravity centers (circuits), but not to the grid nodes, as it is sometimes taken in the numerical field calculations [13], for example in FEM (finite element method) [11–13].

One of the circuits, for example, the average TVWUT (Fig. 4.1) is chosen arbitrarily. The intensity vector components E along the axes X, Y are found for these circuit (mesh) portions TU, VW, VT, WU. They are required for making a line integral along these portions in accordance with (A.4.1.4). According to (A.4.1.7), the following is obtained:

For the portions TU: $(E)_X = (E)_{TU} = \frac{A^E_Б - A^E_Л}{\Delta y}; \ (E)_Y = 0.$

For the portions VW: $(E)_X = (E)_{VW} = \frac{A^E_Л - A^E_Д}{\Delta y}; \ (E)_Y = 0.$

For the portions TV:

$$(E)_Y = (E)_{TV} = -\frac{A^E_Л - A^E_Г}{\Delta x}; \ (E)_X = 0. \tag{A.4.1.8}$$

For the portions WU: $(E)_Y = (E)_{WU} = -\frac{A^E_M - A^E_Л}{\Delta x}; \ (E)_X = 0.$

The parts along the axis are equal to: $\Delta x = \frac{2a}{N_W}; \quad \Delta y = \frac{2b}{N_L}.$

Subject to the obtained Eq. (A.4.1.8) for tension components, Eq. (A.4.1.4) for an arbitrary circuit TVWUT is as follows:

$$(E)_{VW}\Delta x + (E)_{WU}\Delta y - (E)_{TU}\Delta x - (E)_{TV}\Delta y = -j\omega B^*_Л Q_Л. \tag{A.4.1.9}$$

After the conversing Eq. (A.4.1.9) for this arbitrary circuit TVWUT taking into account the tension component expressions presented in Eq. (A.4.1.8), the following equation is obtained:

$$2A^E_Л\left(\frac{\Delta y}{\Delta x} + \frac{\Delta x}{\Delta y}\right) - A^E_Б\frac{\Delta x}{\Delta y} - A^E_Г\frac{\Delta y}{\Delta x} - A^E_Д\frac{\Delta x}{\Delta y} - A^E_M\frac{\Delta y}{\Delta x} = -j\omega B^*_Л Q_Л. \tag{A.4.1.10}$$

The equations similar to (A.4.1.10) are written for other circuits belonging to the screen, for example, STURS, DEVTD,…. The number of such equations N_{EQ} is equal to that of circuits $N_{EQ} = N_L N_W$. They form a linear equation system with the imaginary right part, the unknown values of vector electric potentials, such as $A^E_Л, A^E_Б, A^E_Д, \ldots$ are contained in the left part N_{EQ}. The methods for solving such systems are widely used in engineering practice [7, 8].

Boundary conditions for the problem solution can be the electric potential vector invariant of the screen outer circuit CFKQC: A^E_{CFKQC} = const. Such a constant value can be “zero”.

Now, the physical interpretation of the obtained results can be considered in detail. The arbitrary portion (the rectangle side) of one of the circuits, for example, is the portion VW of circuit TVWUT. The first summand in Eq. (A.4.1.9) corresponds to this portion:

$$(U)_{VW}=(E)_{VW}\Delta x=\left(A^{E}_{Л}-A^{E}_{Д}\right)\frac{\Delta x}{\Delta y}.$$

where $(U)_{VW}$—voltage between V and W nodes. Now, this expression is transformed as follows:

$$(U)_{VW}=\left(A^{E}_{Л}\frac{h}{\rho}-A^{E}_{Д}\frac{h}{\rho}\right)\frac{\rho\Delta x}{\Delta yh}, \tag{A.4.1.11}$$

or

$$(U)_{VW}=\left(A^{E}_{Л}\frac{h}{\rho}-A^{E}_{Д}\frac{h}{\rho}\right)R_{Л,Д}. \tag{A.4.1.11′}$$

where $R_{Л,Д}=\frac{\rho\Delta x}{h\Delta y}$—circuit D.C. resistance limited by points 1234 in Fig. 4.1. This circuit has the length Δy, width Δx; its thickness is equal to h, and the resistivity —ρ. It must be assumed from the last expression analysis that both first cofactor terms in Eq. (A.4.1.11′)

$$I_{VW}=A^{E}_{Л}\frac{h}{\rho}-A^{E}_{Д}\frac{h}{\rho} \tag{A.4.1.12}$$

have the current dimension.

Now, dimension of the first summand in (A.4.1.12) is verified. It can be presented in the form of:

$$\left[A^{E}_{Л}\frac{h}{\rho}\right]=\left[A^{E}_{Л}\right]\frac{[h]}{[\rho]}=\frac{[U][L]}{[R][L]}=\frac{[U]}{[R]}=[I]. \tag{A.4.1.13}$$

The second term dimension in (A.4.1.12) is similar. As a result, it is confirmed that the expression for I_{VW} in Eq. (A.4.1.12) also has the current dimension. Each of its terms is a vector. The first of them coincides in its direction with the vector $A^{E}_{Л}$, the second—with the vector $A^{E}_{Д}$, correspondingly. The first summand is described as:

$$I^{K}_{Л}=A^{E}_{Л}\frac{h}{\rho} \tag{A.4.1.14}$$

The vector of loop TVWUT as the mesh current. This vector has the current dimension. It characterizes physically the electric potential vector value $A^{E}_{Л}$ in the circuit (element) TVWUT. Similarly with (A.4.1.11′), the expression for the circuit VGHWV is valid as follows:

$$I^{K}_{Д}=A^{E}_{Д}\frac{h}{\rho}. \tag{A.4.1.14′}$$

Thus, the branch current in the portion VW according to Eq. (A.4.1.12) is expressed in terms of the relations obtained for vectors (mesh currents) as follows:

$$I_{VW}=A^{E}_{Л}\frac{h}{\rho}-A^{E}_{Д}\frac{h}{\rho}=I^{K}_{Л}-I^{K}_{Д}. \qquad (A.4.1.15)$$

The expressions for these mesh currents are used and the estimated equation for the selected circuit TVWUT is written down. Similar to (A.4.1.10), there is:

$$I^{K}_{Л}\left(R_{ЛБ}+R_{ЛГ}+R_{ЛД}+R_{ЛМ}\right)-I^{K}_{Б}R_{ЛБ}-I^{K}_{Г}R_{ЛГ}-I^{K}_{Д}R_{ЛД}-I^{K}_{М}R_{ЛМ}=-j\omega B^{*}_{L}Q_{L}. \qquad (A.4.1.16)$$

Here the D.C. resistance portion are calculated similarly (A.4.1.11′) for . They are equal to:

$$R_{ЛБ}=\frac{\rho\Delta x}{\Delta yh};\ R_{ЛГ}=\frac{\rho\Delta y}{\Delta xh};\ R_{ЛМ}=\frac{\rho\Delta y}{\Delta xh}. \qquad (A.4.1.16')$$

Equations (A.4.1.15) and (A.4.1.16) are the formulation of the mesh current method [7, 8]. They can serve as a proof of its existence applied to this problem.

Two conditions are to be pointed out:

– Equation (A.4.1.6) is carried out for an arbitrary grid point. It corresponds to the first Kirchhoff's law at difference approximation of Eqs. (A.4.1.4) and (A.4.1.7). For example, there is an identity for the node T:

$$\left(I^{K}_{Ф}-I^{K}_{Б}\right)+\left(I^{K}_{Л}-I^{K}_{Г}\right)+\left(I^{K}_{Г}-I^{K}_{Ф}\right)+\left(I^{K}_{Б}-I^{K}_{Л}\right)\equiv 0; \qquad (A.4.1.6')$$

– for near-boundary areas (portions), for example, for the portion CD (Fig. 4.1), the D.C. resistance is calculated as follows: $R_{CD}=\frac{2\rho\Delta x}{h\Delta y}$, and for the portion GH: $R_{GH}=\frac{2\rho\Delta y}{\Delta xh}$.

Equations for other circuits, e.g., STURS, DEVTD, are similar (A.4.1.16). Their numbers are equal to the circuit numbers N_{EQ}. They form a linear equation system with an imaginary right part containing in the left part some unknown mesh current values N_{EQ}, as well as the equation system for vector electric potential. Branch currents in the screen portions are calculated using the expressions similar to (A.4.1.15).

The same mesh current value on the outer boundary of the screen CFKQC: I_{CFKQCK} = const can serve as a boundary condition for solving the current distribution problem. Such a constant value can be "zero".

Note that in practice the mesh current method is generally set forth [7, 8] as a calculation sequence for a specific circuit selected as an example. At the same time we take all the assignments with regard to the circuit calculation method; pre-selection "direction of path tracing" and the assignment on dependence of sign of the "mutual impedance" (impedance of the branch between two adjacent meshes) of the circuits; use of Kirchhoff's equations for mesh currents, instead for branch

currents; sequence of calculations branch currents using mesh currents etc.). They are all derived from the Maxwell equations according (A.4.1.1)–(A.4.1.16).

Now, we will sum up the results obtained in this section:

- the branch current distribution in the screen is set on the basis of equations linear system solutions with the imaginary right part either for the electric current vector potential of the type (A.4.1.10) or for mesh currents of the type (A.4.1.16);
- the assumptions taken in the mesh current calculation sequence [7, 8] are confirmed for the problem under consideration by Eqs. (A.4.1.15), (A.4.1.16), (A.4.1.11′) and (A.4.1.16′).

Irregular triangular grid

Now, for the screen current distribution problem we use an irregular grid, e.g., consisting of triangular elements. The portions, bounding each triangle in the grid can be not only straight, but also curved. It is expedient in practice to use such grids instead of rectangular ones, when it is necessary to specify the current distribution in certain screen parts, or when some computational domain section forms are different from the square ones. The triangular grid consisting of N_{EQ} circuits (loops) is shown in Fig. 4.2. The circuits are limited by straight portions.

Now, one of its elements, such as BEDB is chosen. Equation (A.4.1.4) for this circuit have a form similar to (A.4.1.9)

$$(E)_{BE}\,BE+(E)_{ED}\,ED+(E)_{DF}\,DF+(E)_{FB}\,FB=-j\omega B^{*}_{Л}Q_{Л}. \qquad (A.4.1.17)$$

where $B^{*}_{Л}$—average value of flux density complex amplitude at the point "Л" of arbitrary triangular circuit BEDB of area according to Eq. (A.4.1.3).

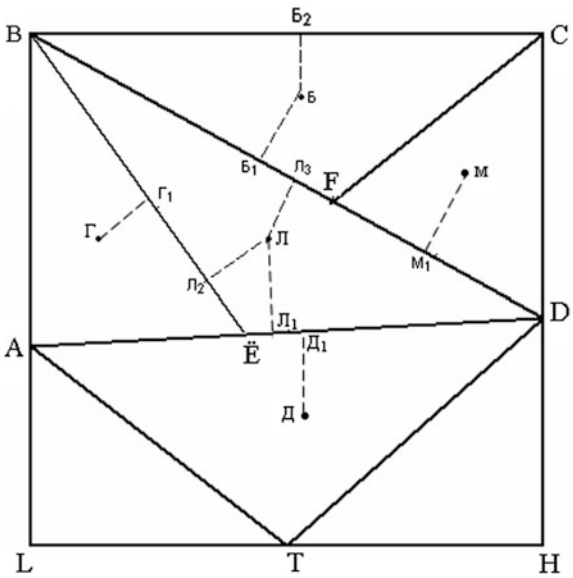

Fig. 4.2 The triangular grid

It is easy to show in practical screen current field calculations that the point "Л" by $N_{EQ} \to \infty$ can be combined with the triangular circuit gravity center, as well as the rectangular one discussed earlier. Equation (A.4.1.5) for the vector electric potential A^E applied to the triangular grid is written similar to Eq. (A.4.1.8) for the rectangular one:

$$\begin{aligned}
&\text{For the portion BE:} \quad (E)_{BE} = \frac{A^E_Л - A^E_Г}{ЛГ},\\
&\text{For the portion ED:} \quad (E)_{ED} = \frac{A^E_Л - A^E_Д}{ЛД},\\
&\text{For the portion DF:} \quad (E)_{DF} = \frac{A^E_Л - A^E_M}{ЛМ},\\
&\text{For the portion FB:} \quad (E)_{FB} = \frac{A^E_Л - A^E_E}{ЛБ}.
\end{aligned} \tag{A.4.1.18}$$

Here $ЛГ = ЛЛ_2 + ГГ_1$; $ЛД = ЛЛ_1 + ДД_1$; $ЛМ = ЛЛ_3 + ММ_1$; $ЛБ = ЛЛ_3 + Б_1Б$. .

After conversing Eq. (A.4.1.17) with taking into account Eq. (A.4.1.18), the following is obtained:

$$\frac{h}{\rho}\left[\left(A^E_Л - A^E_Г\right)R_{BE} + \left(A^E_Л - A^E_Д\right)R_{ED} + \left(A^E_Л - A^E_M\right)R_{DF} + \left(A^E_Л - A^E_Б\right)R_{FB}\right] = -j\omega B^*_Л Q_Л. \tag{A.4.1.19}$$

The D.C. resistances of the triangular grid portion in Eq. (A.4.1.19) are equal to:

$$R_{BE} = \frac{\rho BE}{ЛГh};\ R_{ED} = \frac{\rho ED}{ЛДh};\ R_{DF} = \frac{\rho DF}{ЛМh};\ R_{FB} = \frac{\rho FB}{ЛБh} \tag{A.4.1.20}$$

with ЛГ, ЛД, ЛМ,ЛБ—according (A.4.1.18).

The number of these resistances is equal to that of triangle portions in the calculated area. Note that the resistance for the "border portion", for example, the portion BC is calculated as follows:

$$R_{BC} = \frac{\rho BC}{ББ_2 h}. \tag{A.4.1.20'}$$

Now, the vectors of electric potentials in Eq. (A.4.1.19) are called as mesh currents. This is similar to Eq. (A.4.1.14) for a rectangular grid:

$$I^K_Л = A^E_Л \frac{h}{\rho};\ I^K_Г = A^E_Г \frac{h}{\rho};\ I^K_Д = A^E_Д \frac{h}{\rho};\ I^K_Q = A^E_Q \frac{h}{\rho};\ I^K_R = A^E_R \frac{h}{\rho}. \tag{A.4.1.21}$$

After transforming Eq. (A.4.1.19) and considering (A.4.1.21), one of the equations of the mesh current calculation system is obtained:

$$I^K_Л\left(R_{BE} + R_{ED} + R_{DF} + R_{FB}\right) - I^K_Г R_{BE} - I^K_Д R_{ED} - I^K_M R_{DF} - I^K_Б R_{FB} = -j\omega B^*_Л Q_Л. \tag{A.4.1.22}$$

The equations similar to (A.4.1.22) are also valid for the remaining triangular circuits, for example, BAEB, BFCB,…. The number of such equations N_{EQ} is equal to that of circuits (meshes). They form a linear equation system with the imaginary right part, containing N_{EQ} vectors of electric potential unknown values in the left part, such as $A^{E}_{Л}, A^{E}_{Г}, A^{E}_{Д}, \ldots$ or the corresponding mesh currents $I^{K}_{Л}, I^{K}_{Г}, I^{K}_{Д}, \ldots$.

Equation (A.4.1.6) is valid for a grid arbitrary node, as well as the rectangular or triangular one. It corresponds to the first Kirchhoff's law at difference approximation of Eqs. (A.4.1.4) and (A.4.1.7). For example, there is the following identity for the node F:

$$\left(I^{K}_{Б}-I^{K}_{M}\right)+\left(I^{K}_{M}-I^{K}_{Л}\right)+\left(I^{K}_{Л}-I^{K}_{Б}\right)\equiv 0\,. \qquad (A.4.1.6'')$$

The use of a triangular mesh does not affect the boundary condition formulation for solving the current distribution problem, as it is the same used for a rectangular grid. For example, the conditions for the area shown in Fig. 4.2 are as follows: $I^{K}_{BLHCB} = \text{const}$. This constant value can be "zero".

The branch currents are calculated after solving this linear equation system N_{EQ} in accordance with ratios arising from (A.4.1.19) and (A.4.1.21):

$$\begin{aligned} I_{BE}&=A^{E}_{Л}\frac{h}{\rho}-A^{E}_{Г}\frac{h}{\rho}=I^{K}_{Л}-I^{K}_{Г}; \quad I_{ED}=A^{E}_{Л}\frac{h}{\rho}-A^{E}_{Д}\frac{h}{\rho}=I^{K}_{Л}-I^{K}_{Д};\\ I_{DF}&=A^{E}_{Л}\frac{h}{\rho}-A^{E}_{M}\frac{h}{\rho}=I^{K}_{Л}-I^{K}_{M}; \quad I_{FB}=A^{E}_{Л}\frac{h}{\rho}-A^{E}_{Б}\frac{h}{\rho}=I^{K}_{Л}-I^{K}_{Б}. \end{aligned} \qquad (A.4.1.23)$$

Thus, the following additional results are obtained using the triangular grid (as compared to rectangular grid):

- the calculation expressions for estimating branch currents in screen grid portions through the electric circuits vector potential values or through the mesh current values remain unchanged;
- also, the equations expressing mesh currents in grid elements through the vector electric potential values at their gravity centers also remain unchanged;
- the assumptions usually made in the mesh current method are confirmed by Eqs. (A.4.1.21), (A.4.1.22) and (A.4.1.23).

Consequently, the use of vector electric potential and its value assignment (or the mesh current value) not to the nodes, but to the grid circuit mesh gravity centers allows reducing it to the electric circuit calculations for solving screen current problems numerically.

This requires solving the linear equation system. It helps prevent the variational problem implementation [11–13], as it is accepted in the FEM.

The electric circuit calculation methods are widely used in engineering practice. It allows us to use the experience gained in dealing with similar problems.

A.4.1.2 Multiply Connected Domain

Now, the method of solving this problem for multiply connected domains is considered: for the screen made of different resistivity materials, for example, with some additional soldered-in parts or structural holes. In this case,

$$\rho = \rho(x, y). \tag{A.4.1.24}$$

The computational domain is subdivided into elements (circuits). Their number is determined in order to provide the necessary accuracy of screen current calculations.

Regular grid

The elements in the rectangular circuit forms similar to those described in Sect. 4.6.1.1 for a simply connected domain (A.4.1.1′) are chosen. The obtained results can be used in this section for multiply connected domains (A.4.1.24), provided that the equivalent resistive portions for the coefficients (resistivity) of the unknown mesh currents in the system consisting of Eq. (A.4.1.16) are calculated from the ratios of the type

$$\rho_{ЛД}^{EQ}=\frac{2\rho_{Л}\rho_{Д}}{\rho_{Л}+\rho_{Д}};\ \rho_{ЛБ}^{EQ}=\frac{2\rho_{Л}\rho_{Б}}{\rho_{Л}+\rho_{Б}};\ \rho_{ЛГ}^{EQ}=\frac{2\rho_{Л}\rho_{Г}}{\rho_{Л}+\rho_{Г}};\ \rho_{ЛМ}^{EQ}=\frac{2\rho_{Л}\rho_{М}}{\rho_{Л}+\rho_{М}}. \tag{A.4.1.25}$$

Similarly, the coefficients are calculated for the remaining resistivity equation system of the type (A.4.1.16). Note that the resistivities are calculated for near-boundary areas, for example, the segment CD, thus: $\rho_{Ф}^{EQ} = 2\rho_{Ф}$ and for the segment GH:

Irregular grid with triangular elements

The elements in the form of triangular circuits are similarly chosen to those described in Sect. 4.1.1 for a simply connected domain (A.4.1.1′). The results obtained therein may be used in this section provided that the coefficients (resistance) in the system consisting of Eq. (A.4.1.22) calculated taking into account the equivalent resistivity circuit domains are as follows

$$\begin{gathered}\rho_{BE}^{EQ}=\frac{\rho_{Л}\dfrac{BE}{ЛЛ_2}\rho_{Г}\dfrac{BE}{ГГ_1}}{\rho_{Л}\dfrac{BE}{ЛЛ_2}+\rho_{Г}\dfrac{BE}{ГГ_1}};\ \rho_{ED}^{EQ}=\frac{\rho_{Л}\dfrac{ED}{ЛЛ_1}\rho_{Д}\dfrac{ED}{ДД_1}}{\rho_{Л}\dfrac{ED}{ЛЛ_1}+\rho_{Д}\dfrac{ED}{ДД_1}};\\ \rho_{DF}^{EQ}=\frac{\rho_{Л}\dfrac{DF}{ЛЛ_3}\rho_{М}\dfrac{DF}{ММ_1}}{\rho_{Л}\dfrac{DF}{ЛЛ_3}+\rho_{М}\dfrac{DF}{ММ_1}};\ \rho_{FB}^{EQ}=\frac{\rho_{Л}\dfrac{FB}{ЛЛ_3}\rho_{Б}\dfrac{FB}{ББ_1}}{\rho_{Л}\dfrac{FB}{ЛЛ_3}+\rho_{Б}\dfrac{FB}{ББ_1}}.\end{gathered} \tag{A.4.1.26}$$

Similarly, the coefficients are calculated for the remaining D.C. resistance equations system in (A.4.1.22).

Note that the D.C. resistance of these portions is calculated in the same way as in Sect. 4.1.1 for a simply connected domain (Eq. A.4.1.20′) for the near-border portions, for example, the portion BC, forming the simply connected circuit domain, for example, the circuit BFCB.

A.4.1.3 Irregular Grid with Arbitrary Configuration Elements

The results obtained in previous sections for the vector electric potential, mesh currents and circuit resistances can also be used to calculate the current distribution in a screen divided not only into rectangular or triangular elements, but also into other configuration elements. It is assumed that the part of these elements can be not only straight, but also curved, e.g., the parabolic portions.

The principal point of using these results is Eq. (A.4.1.3), which determines the flux density B* estimated value of each mesh with the help of the Lagrange's mean value theorem [2, 3].

A.4.1.4 The Screen Element D.C. Resistance Depends on the Temperature Distributed in It (Nonlinear Problem); the Domain Is Simply—Or Multiply Connected

When the screen is flown around by the currents, induced by the mutual induction field in an air gap, the temperature θ distribution in screen elements is not uniform. Accordingly, the resistivity of these elements is not the same even for a simply connected domain, so $\rho = \rho(x, y, \theta)$, wherein the dependence of circuit resistivity ρ on temperature is expressed by the ratio: $\rho_\Theta = \rho_0(1 + \rho^*\theta)$, where ρ_0—circuit conductor resistivity at $\theta = 0°C$, ρ^*—high-resistivity temperature coefficient. Therefore, it is necessary to find simultaneously the temperature distribution in screen elements (circuits) in the steady state thermal mode in order to calculate the current distributions.

Practically, it is expedient to determine the steady state temperature and current elements as asymptotes to which they aspire in their transient thermal mode during the time $t \to \infty$. It is assumed that in initial state the screen is not flown by currents initially (no mutual induction field), the temperature of all the elements is equal to the ambient temperature θ_{AMB}.. Then the screen is exposed to the mutual induction

field (A.4.1.1), and various resistivity and temperature value are fixed in all elements at $t \to \infty$.

The temperature rise process in the screen circuits (elements) can be presented as a differential equation system of the type [14] for each mesh, for example for mesh Л:

$$\frac{d\theta_{Л}}{dt} = \frac{Q_{Л}^{EL} - Q_{Л}^{CNV} - Q_{Л}^{COND}}{cG_{Л}^{EL}}. \qquad (A.4.1.27)$$

where

$\theta_{Л}$ element overheating

$Q_{Л}^{EL}$ losses evolved in time t

$Q_{Л}^{CNV}$ losses allocated from the element by convection

$Q_{Л}^{COND}$ losses allocated to the adjacent element (entering the element) by thermal conductivity

c screen element specific heat

$G_{Л}^{EL}$ screen element weight (Figs. 4.1 and 4.2)

The initial conditions for this system from N_{EQ} first order differential equations are formulated as follows: the temperature of all screen elements is $\theta = \theta_{AMB}$ at $t = 0$. Note that there are known solutions [24] of selecting the system integration step Δt from Eq. (A.4.1.27), its stability and convergence problems associated with choosing this step.

The determination of steady state screen temperature elements (circuits) as the transient thermal mode asymptotes assumes an alternate solution of two problems for each time t: the current distribution problem using the equation systems (A.4.1.16) or (A.4.1.22); the temperature distribution problems using the equation system of type (A.4.1.27).

A.4.1.5 Screen Element Reactance Accounting

The following should be noted formulating the current calculation problems. Unlike ordinary damper winding stray fields, whose bars are laid in the semi-closed slots, the stray fields of conductive screen laid on the pole shoe ferromagnetic surface are initially neglected.

The D.C. resistance is only taken into account, for example, the D.C. resistance R_{BE} of the triangular grid portion BE (Fig. 4.2).

However, it is expedient to consider these fields in general, for example, at high screen current frequency ω_{ROT}. Note that the symbolic method [7, 8] is used in Sects. 4.1.1 and 4.1.2 presenting the harmonic functions of mutual flux, electric field intensity, and screen currents. If necessary, these peculiarities allow taking into account the leakage field data and corresponding screen reactance circuits (elements).

If it is used, the equations for both Kirchhoff's laws remain valid in general case, when each part of the chain domain contains not only the D.C. resistance, but also

the complex one. For example, the triangular grid portion BE is complex and equal to the impedance Z_{BE} [7, 8].

Without any additional assumptions, these symbolic method features allow writing the linear equation system value N_{EQ} derived in Sects. 4.1.1 and 4.1.2 as follows:

Using a rectangular grid in the form of:

$$I_{Л}^{K}\left(Z_{ЛБ}+Z_{ЛГ}+Z_{ЛД}+Z_{ЛМ}\right)-I_{Б}^{K}Z_{ЛБ}-I_{Г}^{K}Z_{ЛГ}-I_{Д}^{K}Z_{ЛД}-I_{М}^{K}Z_{ЛМ}=-j\omega B_{Л}^{*}Q_{Л}. \qquad (A.4.1.16'')$$

Using a triangular grid in the form of:

$$I_{Л}^{K}\left(Z_{BE}+Z_{ED}+Z_{DF}+Z_{FB}\right)-I_{Г}^{K}Z_{BE}-I_{Д}^{K}Z_{ED}-I_{М}^{K}Z_{DF}-I_{Б}^{K}Z_{FB}=-j\omega B_{Л}^{*}Q_{Л} \qquad (A.4.1.22'')$$

Appendix 4.2: Determination of Average Flux Density Point Location by "Mean Value Theorem (Lagrange)" [2, 3]

The original equation is:

$$\Delta yB\int_{N\Delta x}^{(N+1)\Delta x} e^{-\frac{j\pi x}{\tau}}dx=\Delta y\Delta xB*e^{-j\pi\Delta x\frac{N+\alpha}{\tau}}.$$

where $1<N\le N_W; 0<\alpha<1$. The ratio for determining the number α is obtained from the equation:

$$\frac{2\tau}{\Delta x\pi}\sin\frac{\Delta x\pi}{2\tau}e^{\frac{-j\Delta x\pi}{2\tau}}=e^{\frac{-j\alpha\Delta x\pi}{\tau}}.$$

The analyzed equation results are as follows: at the $\frac{\Delta X}{\tau}\le 0.01$ value $\alpha\approx 0.5$ is obtained. Thus, the point "Л" coincides with the rectangular circuit gravity center.

Appendix 4.3: Equivalent Circuit of Powerful Induction Motors Operating in Nonlinear Networks

Additional indications:

m_{ST}, m_{ROT}—stator and rotor winding phase numbers, respectively;
P_1—network consumed power;
P_2—motor shaft power;
$\sum Q$—amount of losses for calculating magnetization current active component I_A;
$Q_{1,OHM}, Q_{2,OHM}$—stator and rotor winding D.C. losses;

$R_{1,OHM}, R'_{2,OHM}$—D.C. resistance of stator winding phase and rotor winding equivalent phase.

Problem statement A number of assumptions [4, 6–8] are used when calculating electromagnetic loads and performance of industrial frequency powerful motors operating in linear networks. In these assumptions we take into account neither mechanical losses (for ventilation, in bearings) very significant for powerful motors, nor consider them approximately.

The losses in stator winding A.C. resistance are taken approximately within the frameworks of these assumptions. It is approximately assumed in calculating the inductive current component I_μ of the magnetizing circuit and the secondary circuit current I'_2 that the EMF at its terminals is $E \approx (0.93 - 0.97)U_{PH}$ depending [9, 10] on pole numbers (2p = 4–10). The active magnetizing circuit component I_A is also calculated using approximate ratios derived on the basis of some assumptions.

All the assumptions are based on the experience of serial motor design and operation. However, these assumptions lead to errors in current calculation results loses and motor shaft power losses in circuits with increasing electromagnetic load levels of industrial motor use. For example, the power balance is disturbed when a rotor is locked $(S_{SL} = 1)$: power consumption turns out to be not equal to the estimated amount of losses dissipated in its circuits [10]. This contradicts the problem physical conditions, etc. These assumptions lead to additional errors in calculation results of powerful frequency-controlled asynchronous motors and induction generators operating with frequency converters.

So, the practical task is to clarify the magnetizing circuit parameters, as well as parameters of stator and rotor circuits at powerful asynchronous machine with an increased level of electromagnetic load by accounting the distribution of main and additional losses in it.

A.4.3.1 Basic Equations of Powerful Asynchronous Machine Substitution Patterns $(\mathbf{Q_{TIM} \geq 1})$

Note preliminarily that the procedure of EMF time harmonic and current order is denoted by the letter Q_{TIM} unlike other sections. This is due to the fact that the machine losses are marked here with the letter Q.

Now, we consider the equation system for calculating electromagnetic loads and performance characteristics of powerful frequency-controlled induction machines in motor mode for the harmonic order $Q_{TIM} \geq 1$ of the supply voltage. They correspond to the T-shape circuit for m = 1 [4–8] written for the effective current values, EMF and voltages.

The expression for network consumed total power is written additionally to the equation system (4.13)–(4.18) for magnetically coupled stator and rotor circuits. The following is obtained for the power P'_1 consumed by the primary winding (stator) phase and the secondary stator-reduced winding (rotor) phase at $Q_{TIM} = 1$:

$$\begin{aligned} P'_1 = U_{PH}(I_1)^* &= (I_1Z_1 - E)(I_1)^* = I_1Z_1(I_1)^* - E\left(I_0 - I'_2\right)^* \\ &= I_1Z_1(I_1)^* - E(I_0)^* + E\left(I'_2\right)^*. \end{aligned} \tag{A.4.3.1}$$

where $(I_1)^*$—complex conjugated with complex I_1; the conjugated complexes $(I_0)^*$, $\left(I'_2\right)^*$ are marked similarly.

Note that the real part of the component expression P'_1 is equal to the active component $\left(P'_1\right)_A$ of network power consumption and its imaginary part—to the reactive component $\left(P'_1\right)_R$ of this power:

$$P'_1 = \left(P'_1\right)_A + j\left(P'_1\right)_R. \tag{A.4.3.2}$$

Now, three summands in (A.4.3.1) of network totally-consumed power P'_1 are considered in detail.

The first of them corresponds to the total power consumed by the primary circuit phase (stator):

$$P'_{1,1} = I_1Z_1(I_1)^* = |I_1|^2(R_1 + jX_1) = |I_1|^2R_1 + j|I_1|^2X_1 = \left(P'_{1,1}\right)_A + j\left(P'_{1.1}\right)_R. \tag{A.4.3.3}$$

The second summand in (A.4.3.1) corresponds to the total power consumed by the magnetizing circuit. Considering Eq. (4.16), the following is obtained:

$$P'_{1,2} = -E(I_0)^* = \left(P'_{1,2}\right)_A + j\left(P'_{1,2}\right)_R. \tag{A.4.3.4}$$

The third term in (A.4.3.1) corresponds to the total power consumed by the secondary circuit phase (rotor) reduced to a stator winding:

$$P'_{1,3} = E(I_2)^* = \left(\frac{|E|}{|Z'_2|}\right)^2 \frac{R'_2}{S_{SL}} + j\left(\frac{|E|}{|Z'_2|}\right)^2 X'_2 = \left(P'_{1,3}\right)_A + j\left(P'_{1,3}\right)_R. \tag{A.4.3.5}$$

where $|Z'_2| = \sqrt{\left(\frac{R'_2}{S_{SL}}\right) + \left(X'_2\right)^2}$.

Note that the total power $P_{1,3}$ consumed by the m_{ST} phases of secondary circuit reduced to a stator winding can be presented as [4–6, 9]:

$$\begin{aligned} P_{1,3} = m_{ST}P'_{1,3} &= m_{ST}\left|I'_2\right|R'_2 + m_{ST}\left|I'_2\right|^2R'_2\frac{1 - S_{SL}}{S_{SL}} + jm_{ST}\left|I'_2\right|^2X'_2 \\ &= \left(P_{1,3L}\right)_A + \left(P_{1,3SH}\right)_A + j\left(P_{1,3}\right)_R. \end{aligned} \tag{A.4.3.5′}$$

where

$$\left(P_{1,3L}\right)_A = m_{ST}\left|I_2'\right|^2 R_2' = m_{ROT}\left|I_2'\right|^2 R_2 - \text{the losess in rotor winding},$$

$$\left(P_{1,3SH}\right)_A = m_{ST}\left|I_2'\right|^2 R_2' \frac{1 - S_{SL}}{S_{SL}} = m_{ROT}\left|I_2'\right|^2 R_2 \frac{1 - S_{SL}}{S_{SL}} - \text{the power on motor shaft.}$$

As a result, the expression for active power $(P_1)_A$ consumed by the machine from network (with phase numbers of stator winding m_{ROT} and rotor winding m_{ROT}) is obtained:

$$\begin{aligned}(P_1)_A &= \left(P_{1,1}\right)_A + \left(P_{1,2}\right)_A + \left(P_{1,3L}\right)_A + \left(P_{1,3SH}\right)_A \\ &= m_{ST}|I_1|^2 R_1 + m_{ST}|E||I_A| + m_{ROT}|I_2|^2 R_2 + m_{ROT}|I_2|^2 R_2 \frac{1 - S_{SL}}{S_{SL}}.\end{aligned} \tag{A.4.3.6}$$

Accordingly, the expression for the reactive power $(P_1)_R$ is as follows:

$$\begin{aligned}(P_1)_R &= \left(P_{1,1}\right)_R + \left(P_{1,2}\right)_R + \left(P_{1,3}\right)_R \\ &= m_{ST}|I_1|^2 X_1 + m_{ST}|E|\left|I_\mu\right| + m_{ROT}|I_2|^2 X_2.\end{aligned} \tag{A.4.3.6'}$$

Note. According with (3.1) in the basic system (4.13)–(4.18) we have to, instead of the value $U = U_{PH} = U_1$ ($Q_{TIM} = 1$), use the value $U = U_Q$ for high time harmonics ($Q_{TIM} > 1$).

A.4.3.2 Machine Circuit Losses Components and Shaft Power

Now, the power balance is discussed. The condition is when the motor-consumed network power is equal to the sum of losses dissipated in its circuits and the developed motor shaft power should be found out analytically by $Q_{TIM} = 1$.

For the beginning, the first special case, namely the mode $S_{SL} = 1$ is considered. As it follows from the obtained Eq. (A.4.3.6), the calculated power value $\left(P_{1,3SH}\right)_A$ is equal to "zero" at $S_{SL} = 1$. The expression for the machine network-consumed active power $(P_1)_A$ at $S_{SL} = 1$, $Q_{TIM} = 1$ is as follows:

$$\begin{aligned}(P_1)_A(\text{at } S_{SL} = 1) &= \left(P_{1,1}\right)_A + \left(P_{1,2}\right)_A + \left(P_{1,3L}\right)_A \\ &= m_{ST}|I_1|^2 R_1 + m_{ST}|E||I_A| + m_{ROT}|I_2|^2 R_2.\end{aligned} \tag{A.4.3.7}$$

As it follows from a comparison of Eqs. (A.4.3.6) and (A.4.3.7):

(a) The power balance is achieved at $S_{SL} = 1$ in (A.4.3.7): the calculated machine network-consumed active power $(P_1)_A$ (at $S_{SL} = 1$) is equal to the amount of losses $(P_{1,1})_A$; $(P_{1,2})_A$; $(P_{1,3L})_A$ scattered in its circuits only with a proviso that the component $(P_{1,2})_A$ is calculated from the ratio:

$$(P_{1,2})_A = m_{ST}\left(P'_{1,2}\right)_A = m_{ST}|E||I_A|. \tag{A.4.3.8}$$

As it follows from (4.17), this component is equal to the sum of losses $\sum Q{:}(P_{1,2})_A = \sum Q$. This amount includes the losses that are not proportional to the machine circuit currents square I_1 and I'_2, for example, no-load losses in stator and rotor cores;

In practical calculations we usually accept in the basic system (4.13)–(4.18) for high time harmonics ($Q_{TIM} > 1$):

$$\sum Q = Q_{COR} + Q_{AD(NO\,LOAD)}. \tag{A.4.3.8'}$$

(b) The regularities obtained in the equation analysis (A.4.3.7) for $S_{SL} = 1$ are preserved at $S_{SL} \neq 1$ in (A.4.3.6). The power balance takes place in this mode, when the following additional conditions are observed:

- for $Q_{TIM} = 1$ the mechanical losses (for ventilation, in bearings), whose value is also not proportional to the machine circuit currents square I_1 and I'_2, should be included in the amount of losses $\sum Q$ in addition to the above-mentioned losses. These losses are dissipated as heat energy as well as the winding losses. It can be assumed conditionally that:
- the component $(P_{1,3SH})_A = m_{ROT}|I_2|^2 R_2 \frac{1-S_{SL}}{S_{SL}}$ corresponds to the power available at the machine shaft: $(P_{1,3SH})_A = P_2$.

Thus, expanding the equation system (4.13)–(4.18) for magnetically coupled circuits with Eq. (A.4.3.6) for the network-consumed motor total power, the conditions are derived analytically, under which the arbitrary slip power balance S_{SL} is fulfilled: the active network-consumed power $(P_1)_A$ is equal to the sum of losses dissipated in the motor circuits and the power $(P_{1,3SH})_A = P_2$ developed on the shaft.

The error arises in determining the magnetizing current effects on the calculation results of the currents distributions I_1 and I'_2 and, consequently, on the calculated values of losses and on the motor efficiency, as well as the power P_2. Besides, this error affects the estimated value of the magnetizing circuit reactance X_μ and, hence, the motor power factor cosφ.

A.4.3.3 Additional Losses and Equivalent Circuit Impedances

The following ratios for the equation system parameter calculations are obtained from Eqs. (A.4.3.6) and (A.4.3.7):

- the methods of A.C. resistance calculation taking into account the skin effect [4–6, 9] (Field's factor) are given for different constructions of stator windings in Chap. 23, for different constructions of rotor bars—in appendix of Chap. 23;
- the active current magnetization value $|I_A|$ is determined for $Q_{TIM} = 1$ with the losses according to Eq. (4.17), for $Q_{TIM} > 1$—with the losses based on Eq. (A.4.3.8′).

At $Q_{TIM} > 1$ the relationship between the magnetizing circuit EMF $|E|_{Q_{TIM}=1}$ and the magnetization current $\left|I_\mu\right|_{Q_{TIM}=1}$ is convenient to present [3] in the form:

$$|E|_{Q_{TIM}} \approx F'_{Q_{TIM}=1} \left|I_\mu\right|_{Q_{TIM}}, \quad F'_{Q_{TIM}=1} = \left(\frac{\partial |E|_{Q_{TIM}=1}}{\partial \left|I_\mu\right|_{Q_{TIM}=1}}\right)^{**}$$

The asterisk (**) denotes the derivative at the main magnetization characteristics $(Q_{TIM} = 1)$ corresponding to the EMF $|E|_{Q_{TIM}=1}$.

As for large asynchronous machines, their losses Q_{AD} at $Q_{TIM} = 1$ are estimated by the method commonly used in practice [10]:

$$Q_{AD} \approx 0.005 P_{2,RAT}. \tag{A.4.3.9}$$

where $P_{2,RAT}$—rated motor power.

The test results of powerful serial asynchronous motors confirm that additional losses QAD are usually close in rated mode to the estimated values calculated from (A.4.3.9). The rated mode is understood as the mode with rated shaft power, rated network frequency and rated torque.

Note that the aforementioned condition is met in (A.4.3.9): the estimated losses QAD do not depend on the machine circuit currents squares I_1 and I'_2.

In recent years, it is required to clarify the calculated value QAD in (A.4.3.9) due to the increased level of electromagnetic load of modern machines including the frequency-controlled motors. This is especially applied to modern frequency-controlled motors: it is necessary to calculate the following operational modes for such motors:

– with a rated torque supported throughout the control range. The machine power and frequency are not retained rated in this range;
– with rated power maintained throughout the control range. The machine torque and frequency are not retained rated in this range.

Note that the losses QAD are not the same in these operating modes and they do not remain constant with frequency network changes, so it is impossible to use Eq. (A.4.3.9) for their calculations: it is not confirmed by the test results.

Researching the components included in the losses QAD, it is taken into account that they are actually determined by MMF and the magnetic flux in air gap [4–6].

These components are as follows:

- no load losses determined by the harmonics of magnetic flux in air gap, for example, the rotor circuit losses caused by stator tooths;
- load losses determined by MMF currents of stator and rotor circuit harmonics, for example, magnetic flux leakage losses in stator and rotor cores, in stator winding and in rotor bars.

It is necessary to separate the additional losses in this case:

- no load losses $Q_{AD(NO\ LOAD)}$. To determine the value $\sum Q$ they are summed up to the main losses in stator and rotor cores, and at $Q_{TIM} = 1$—also with the mechanical losses (for ventilation, in bearings);
- current dependent losses $Q_{AD(ST)}$ and $Q_{AD(ROT)}$ in stator and rotor windings (from the leakage field $Q_{TIM} \geq 1$ [4–6, 10]). These losses determine the operation mode overheating; they are considered during the calculation of the impedances of these windings. It should be noted that there are some additional losses in rotor bars under load (with account of the skew slots) comprising two components [10], one of which is dependent on the stator current square, and the second—on the rotor current square at the slot skewing of rotor short-circuited winding.

Brief Conclusions

1. The equation system can be used for magnetically coupled circuits, whose solution is expedient to be performed by the iteration method for calculating the A.C. machine mode, and whose design foresees several short-circuited windings lumped on a rotor.
2. The method feature is that the EMF currents, MMF rotor shorted circuits are calculated in the form of generalized characteristics, i.e., to the resultant field induction amplitude in air gap. The flux density itself is calculated by iteration on the basis of the stator winding specified voltage.
3. These generalized characteristics of EMFs, currents, MMF of squirrel cage for a specific slip S_{SL} and the chosen rotor design can be regarded physically as the similarity criteria. They characterize the amplitudes of EMF, currents and MMF in the flux density scale amplitude B_1. They determine the rotor winding reaction, when it is subjected by the flux density amplitude equal to B_1 in steady state mode.

4. The current distribution calculation method in the screen on the low-frequency motor pole has the following features:
   - The current distribution is determined subject to its parameters (the screen conduction, its thickness, etc.) of the linear equation system solution either for the vector electric potential or mesh currents.
   - The method enables us to solve the current distribution problems in the screen, in which A.C. resistance depends on its temperature. It is convenient to obtain the solution as the thermal transient process asymptote.
   - The following is obtained with the help of the vector electric potential using electromagnetic field equations in the integral form. The assumptions accepted in the mesh current calculation method are valid for calculating the current screen for a computational grid of arbitrary shape. At the same time the relationship between the fictitious current circuit of arbitrary shape (mesh current) and the vector potential averaged within the same circuit is established.
5. The conditions are found out analytically under which the power balance for the arbitrary slip S_{SL} is carried out for powerful asynchronous motors powered from the linear network or the frequency inverter. These conditions are obtained on the basis of the magnetically coupled circuit equations and the additional equation for the power, consumed by the motors from the power network.

List of Symbols

A^E	Vector electric potential
A	Width of screen
L	Length of screen
h	Thickness of screen
B^1	Magnetic flux density amplitude of mutual flux in air gap
E	Electric field intensity
$E_{N+1,N}$	EMF of loop
F_0	MMF magnetic circuit complex amplitude (phasor) corresponding to the flux Φ_0
F_1, F_2, F_3	MMF of loops on the rotor according to the currents I_1, I_2, I_3
I_A, I_μ	Active and reactive components of magnetization current
I_0, I_1, I_2'	Currents in the equivalent T-shape circuit
I_2'	Reduced to stator winding
J_B, I_R	Currents in elements of short-circuits winding on the rotor
k	Number of iteration
k_{CART}, k_{SAT}	Carter's factor and saturation factor accordingly
$L_{1,S}$, $L_{2,S}$, $L_{3,S}$	Leakage inductance of rotor loops

L_{COR}	Core length
m	Number of spatial harmonic
$m_{PH,ST}$, $m_{PH,ROT}$	Stator an rotor winding phases number accordingly
N_0	Number of rotor meshes
p	Number of pole pairs
P_1	Power consumed from network
P_2	Power on the motor shaft
P_{COR}, P_{MECH}, P_{AD}	Losses in core, mechanical and additional losses accordingly
Q	Value of screen mesh square
Q_{TIM}	Number of time harmonic
$Q_{1,OHM}$, $Q_{2,OHM}$	D.C. losses in stator and rotor respectively
ΣQ	Summarized losses for the calculation value of I_A
R_1, R_2, R_3	A.C. resistance of rotor circuits
$R_{1,OHM}$, $R'_{2,OHM}$	D.C. resistances of stator and rotor phase windings
X_μ	Magnetizing circuit inductance
S_{SL}	Slip
T_{EL}	MMF expansion period
U_{PH}	Phase circuit voltage
W_1, K_{W1}; W_2, K_{W2}; W_3, K_{W3}	Number of circuit turns of three contours and their winding coefficients
Z_1, Z'_2	Primary and secondary circuit impedances
Z_B, Z_R	Impedances of bar and portion of short-circuited ring
δ	Equivalent air gap
ε	Accuracy of iteration method
μ_0	Air magnetic permeability
ρ	Specific resistivity of shield
τ	Pole pitch
Φ_0	Flux complex amplitude (phasor) in an air gap
$\psi 2$	Angle between positive direction of vector I'_2 and real line
ψ_E	Angle between positive direction of vector E and real line
ω_{REV}	Angular frequency of rotor rotation
ω_1	Circular frequency of network

References

I. Monographs, General Courses, Textbooks

1. Luriye A.I., The Theory of Elasticity. Moscow: Nauka. 1974. (in Russian).
2. Jeffris H., Swirles B., Methods of Mathematical Physics. Third Edition, Vol. 1–Vol. 3, Cambridge: Cambridge Univ. Press, 1966.
3. Korn G., Korn T., Mathematical Handbook, N.Y.: McGraw-Hill, 1961.
4. Mueller G., Ponick B., Elektrische Maschinen, N.Y., J. Wiley, 2009. (in German).
5. Schuisky W., Berechnung elektrischer Maschinen. Wien: Springer, 1960. (in German).
6. Richter R., Elektrische Maschinen. Berlin: Springer. Band I, 1924; Band II, 1930; Band III, 1932; Band IV, 1936; Band V, 1950. (in German).
7. Demirchyan K.S., Neyman L.R., Korovkin N.V., Theoretical Electrical Engineering. Moscow, St. Petersburg: Piter, 2009. Vols. 1, 2 (In Russian).
8. Kuepfmueller K., Kohn G., Theoretische Elektrotechnik und Elektronik. 15 Aufl. Berlin, New York: Springer, 2000. (in German).
9. Mueller G., Vogt K., Ponick B., Berechnung elektrischer Maschinen. Springer, 2007. (in German).
10. Electrical machines design. Edited by Kopylov O.P. Moscow: Energya. 1980. (in Russian).
11. ELCUT User Manual. Version 5.2. Private firm "TOR". St.-Petersburg. 2005. (in Russian).
12. Binns K., Lawrenson P., Analysis and Computation of Electric and Magnetic Field Problems. Oxford: Pergamon Press, 1963.
13. Zienkiewicz O.C., Finite Element Method in Engineering Science. London; N.Y.: McGraw-Hill, 1971.
14. Gotter G., Erwaermumg und Kuehlung elektrischer Maschinen. Berlin, Goettingen, Heidelberg: Springer, 1954. (in German).

II. Induction Machines. Papers, Inventor's Certificates, Patents

15. Demirchyan K.S., Boguslawsky I.Z., The calculation of the currents and the losses in the rotor short-circuited induction motor using the generalized characteristic of the rotor MMF. Electrichestvo, #5, 1980. (in Russian).
16. Antonov V.V., Boguslawsky I.Z., Savelyeva, M.G., Calculation of the characteristics of a powerful induction motor with non-linear parameters. In the book: Elektrosila, #35, 1984. (in Russian).
17. Antonov V.V., Boguslawsky I.Z., Kochetkova E.Yu., Rogachevskiy V.S., Method of steady state modes calculating of asynchronized synchronous generator. Elektrotechnika, #2, 1992. (in Russian).
18. Boguslawsky I.Z., Double power supplied asynchronous machine with converter in the rotor winding performance investigation method. Proceedings of the Int. Symp. UEES-01. Helsinki. 2001. (in Russian).
19. Korchagin N.V., Stepanov A.I., Boguslawsky I.Z., Veynger A.M., Ryabova T.S., Tsatskin A. Y., Problems of creating powerful four poles induction motors. Russian Engineering Research. 4. # 2008. (in Russian).
20. Antonov V.V., Boguslawsky I.Z., Lesokhin A.Z., Novik J.A., Semenov M.R. Asynchronous frequency controlled motor to drive the supercharger. In the book: Elektrosila, # 35, 1984. (in Russian).

21. Boguslawsky I.Z., Sikiryavy I.J., Method for solving nonlinear algebraic equations for the calculation of electric machines. In the book: Elektrosila, # 28, 1974.(In Russian).

III. Synchronous Machines. Papers, Inventor's Certificates, Patents

22. Boguslawsky I.Z., Demirchyan K.S., Jigulin Yu.V., Lesokhin A.Z., The Pole of Synchronous Motor, Inventor's certificate #817866, 1981. (in Russian).
23. Boguslawsky I.Z., Demirchyan K.S., Jigulin Yu.V., Lesokhin A.Z. The Armature of Synchronous Motor, Inventor's certificate #915171, 1982. (in Russian).
24. Boguslawsky I.Z., The method of calculation of the screen on the pole shoe of low-frequency motor. Elektrotechnika, #8, 2004. (in Russian).
25. Boguslawsky I.Z., Generalized characteristics of currents and MMF of magnetically loops of rotor in A.C. machines. Proceedings of the Russian Academy of Sciences. Energetika, #5, 1995. (in Russian).
26. Boguslawsky I.Z., Magnetically coupled loops in A.C. machines under nonsinusoidal supply. Proceedings of the Russian Academy of Sciences. Energetika, #2, 1995. (in Russian).

Chapter 5
Representation of Currents in Rotor Short-Circuited Winding Elements in the Form of Generalized Characteristics

This chapter still deals with the investigation of generalized characteristics of MMF and rotor currents. It is obtained that currents in short-circuited rotor loop elements can be represented in the form of generalized characteristics without any restrictions in the structure of such windings (complete or incomplete damper winding with broken bars or without them, etc.). Two versions of concept physical interpretation on generalized characteristics introduced in previous chapters are given here.

The content of this chapter is development of the methods stated in [1, 2, 8–14].

5.1 Problem Statement

In the previous chapter, the iterative method of currents determination in A.C. machine loops was given based on the assumption that there are two short-circuited windings with lumped parameters, located in the rotor. In its realization, it is convenient to use generalized current characteristics of these windings and their MMFs in the air gap. An important result in solving the system of equations for magnetically coupled loops by this method is the fact that this system is true not only for rotor winding structure with lumped parameters; this result determines solutions of system of equations for magnetically coupled loops, some of which correspond to windings with distributed parameters, for example, damper winding consisting of a number of short-circuited loops. However, it is true if it is possible to prove that the following can be presented in the form of generalized characteristics:

- currents in rotor short-circuited winding elements regardless of the number of loops in it;
- MMFs of these short-circuited loops or the whole winding.

Let us note that for short-circuited rotor winding it is practically not necessary to calculate MMF generalized characteristic of its each short-circuited loop as it was given in Chap. 4 for generalized characteristics [F2], [F3]. The method given in

I. Boguslawsky et al., *Large A.C. Machines*,
DOI 10.1007/978-4-431-56475-1_5

Chap. 12 allows one to find MMF generalized characteristic of damper winding (regular or irregular) or squirrel cage (with broken bars) as a sum of MMF generalized characteristics of separate loops forming such winding, if generalized current characteristics are found in these loops.

In the same Chap. 4 based on the method of investigation of performance data of high power induction motors with nonlinear parameters (with account of skin effect in cage bars and magnetic circuit saturation), the expediency of using current and MMF generalized characteristics in a secondary loop is confirmed in practical calculations. Physical validity of iterative method is combined thus with simplicity of its realization.

In this chapter, we shall go on with consideration of current generalized characteristics of rotor windings with distributed parameters, for example of salient pole machine damper winding.

We formulate in this regard the following problem: Let us show that rotor winding currents with distributed parameters irrespective of its structure (regular or irregular damper winding, squirrel cage with broken bars) and numbers of loops in it can be represented by means of generalized characteristics. It will serve us as substantiation in solving main problems connected with analytical research of currents in short-circuited rotor loops of A.C. machines fed with non-sinusoidal current. By development of investigation methods of passive and active U-shaped recurrent circuits of various structure, this monograph presents analytical calculation methods of currents distribution in structural elements of these short-circuited rotor windings, and also we find regularities of their distribution and formulate practical recommendations.

To prove a possibility of representation of currents in winding with distributed parameters in the form of generalized characteristics, we will compile a system of equations for rotor winding with N_0 short-circuited loops, herewith, geometrical dimensions, impedance (incl. A.C. resistance and reactance) of separate loop elements can differ from each other. This system of equations is similar to that for magnetically coupled loops from the previous chapter and is its more general version. Thereby, we get generality of problem solution: its results become possible to extend to various structures of squirrel cage damper winding (for example, with broken bars and without them), etc. At the same time, the use of system of equations given in this chapter also represents an independent practical interest, thus, it is possible:

- to carry out additional checking of the results obtained from analytical solutions in the following chapters;
- to obtain numerical values of generalized characteristics of resulting currents of irregular damper winding or asymmetrical squirrel cage, without stating concepts on their components: main and additional currents [8, 10, 11].

5.2 Initial Data and Its Representation

Initial data accepted:

- resulting field in air gap with complex induction amplitude (phasor) B(m, Q);
- geometrical dimensions of winding elements;
- impedances (incl. A.C. resistances and leakage reactances) of winding elements;
- rotation speed ω_{REV} (slip S_{SL}) and number of poles 2p;

At first, let us consider some initial data in more detail.

5.2.1 Representation of Resulting Field Harmonics in Air Gap

Harmonics of the first order for this field (Q = 1, m = 1) for a special case—DFMs—were already determined by corresponding systems of equations. They are calculated according to the Ampere's law [1, 2] using two summands: of the first spatial harmonics of stator winding MMF and rotor winding MMF. These MMFs were determined by currents in multiphase stator winding and in three-phase rotor winding. Both currents are calculated from a system of equations for two magnetically coupled loops in stator and rotor.

However, in solving the problem of currents distribution calculation in damper winding and squirrel cage structural elements fed with non-sinusoidal current, $(Q \geq 1, m \geq 1)$, MMF values of these windings are still unknown: these MMFs are found with account of currents distribution in windings and their structure. In Chap. 8, proceeding from harmonics of resulting field in air gap, we obtain expressions for EMF necessary for calculation of this distribution. In the following chapters there is realized a method for determination of currents and MMF of these resulting field harmonics; for its realization use is made of generalized characteristics properties [9, 12].

In Chap. 3 it was determined that among stator and rotor fields harmonics there can be found those differing in identical spatial periods in air gap and identical EMF frequency in rotor loops. For example, for salient pole machines when fed with non-sinusoidal current, in air gap it is possible to allocate two resulting fields meeting the following conditions: T = idem, ω_{ROT} = idem, where ω_{ROT}—EMF frequency in rotor loops. These resulting fields of each group of the "adjacent" harmonics differ in the direction of rotation relative to rotor, rotation speed relative to stator and in amplitude. They form a system of magnetically coupled loops. EMF frequencies induced in stator loops by both these fields in air gap are obtained in Chap. 3. Such two resulting fields with "adjacent" frequencies, are, for example,

the fields determined by time harmonics of orders $Q_{DIR} = 7, Q_{ADD} = 17$ and spatial of order $m_{ADD} = 5$, or fields of loops N = 1 and N = 2, N = 3 and N = 4 in Table 3.4.

Considering features of these physical processes of occurrence of resulting fields fed with non-sinusoidal current, we will assume in this chapter that in the A.C. machine air gap for operation in a network with nonlinear elements each couple of such conditions (T = idem, ω_{ROT} = idem) corresponds to two resulting fields with specified differences.

We assign $B_{DIR}(m, Q)$ as the flux density amplitude of resulting field whose direction in air gap coincides with that of rotor rotation, and amplitude $B_{AD}(m, Q)$ —field rotating in air gap in direction, opposite to the direction of rotor rotation.

It is more convenient to consider these two resulting fields in air gap as two components of the uniform resulting field which meets the condition common to both of them: T = idem, ω_{ROT} = idem. Then flux density b(x, t, m, Q) in air gap in any point x and at any timepoint t has the following form: [3, 4, 13, 14]:

$$b(x,t,m,Q) = |B_{DIR}(m,Q_1)|\cos\left(\omega_{ROT}t - \frac{2\pi mx}{T}\right) + |B_{AD}(m,Q_2)|\cos\left(\omega_{ROT}t + \frac{2\pi mx}{T}\right).$$

Here x—coordinate along boring in tangential direction; t—time; $Q_1 \neq Q_2$—order of time harmonics corresponding to criteria S = 1 or S = 2 according to Chap. 3. It was already noted that the current frequency in rotor loops ω_{ROT} is determined in Chap. 3 depending on harmonics orders m and Q, and also from the speed of rotor rotation ω_{REV} and from machine operating mode (synchronous or asynchronous).

We use a symbolical method for representation of resulting field in air gap. Then, the flux density b(x, m, Q) in air gap takes the form:

$$b(x,m,Q) = B_{DIR}(m,Q_1)\cdot e^{-j\frac{2\pi mx}{T}} + B_{AD}(m,Q_2)\cdot e^{j\frac{2\pi mx}{T}}.$$

Here $B_{DIR}(m,Q_1), B_{AD}(m,Q_2)$—complex amplitudes (phasors):

$$B_{DIR}(m,Q_1) = |B_{DIR}(m,Q_1)|\cdot e^{j(\omega_{ROT}t+\varphi_{DIR})},$$
$$B_{AD}(m,Q_2) = |B_{AD}(m,Q_2)|\cdot e^{j(\omega_{ROT}t+\varphi_{AD})},$$

where $\varphi_{AD}, \varphi_{DIR}$—initial phase angles.

In further statement, we will omit indices for flux density values and orders of time harmonics for both summands in this expression for record simplification and write down as follows:

$$b(x,m,Q) = B(m,Q)\cdot e^{-j\frac{2\pi mx}{T}} + B(-m,Q)\cdot e^{j\frac{2\pi mx}{T}}. \tag{5.1}$$

5.2.2 Geometrical Dimensions of Winding Elements. Designation of Loop EMF

Let us designate initial geometrical dimensions of loops of damper winding or squirrel cage as follows: $G_{N+1,N}$. Here, both indices mean that a loop is formed by bars with numbers N + 1, N and corresponding ring portions (segment) with number N; this loop is designated: (N + 1, N). It is supposed that, in general, geometrical dimensions of loops forming short-circuited rotor winding differ from each other: $G_{N+1,N}$ = var; it is true, for example, for geometrical dimensions of damper winding loops on pole and between poles.

EMF induced by means of the first component of induction in each of short-circuited rotor loops, for example, in loop (N + 1, N) we represent in the form:

$$E_{N+1,N} = -j\omega_{ROT} G_{N+1,N} B(m, Q). \tag{5.2}$$

The similar expression for the EMF corresponds to the second component of the induction B(−m, Q).

5.2.3 A.C. Resistances and Reactances, Currents in Winding Elements

Those sets are impedances $Z_{B,0}$; $Z_{B,1}$; $Z_{B,2}$;…; $Z_{B,N}$ of bars in slots of short-circuited winding accordingly with numbers 0, 1, 2, …, N, … $(0 \le N \le N_0 - 1)$ and impedances of one ring portions (segment) $Z_{R,0}$; $Z_{R,1}$; $Z_{R,2}$;…; $Z_{R,N}$ between axes of adjacent bars; numbers of these portions are designated respectively 0,1,2, …, N, … (Fig. 5.1). All these impedances are calculated for a certain slip S_{SL} or rotor current frequency ω_{ROT} with account of skin effect in rotor bars.

It is generally supposed that the winding is asymmetrical, so

$$Z_{B,0} \neq Z_{B,1} \neq Z_{B,2} \cdots \neq \cdots Z_{B,N}; Z_{R,0} \neq Z_{R,1} \neq Z_{R,2} \cdots \neq \cdots Z_{R,N}.$$

We designate currents in bars and ring portions (segments) respectively with letters “J” and “I”, and their “current values” that are dependent on number N, respectively, $J_{(N)}$ and $I_{(N)}$. In this chapter for simplification of writing down systems of equations, brackets for indices are omitted.

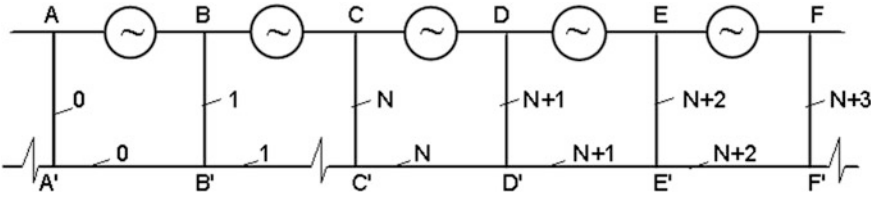

Fig. 5.1 Element of short-circuited rotor winding

5.3 System of Equations and Peculiarities of Matrix Structure of Its Coefficients

Let us consider an element of A.C. machine short-circuited rotor winding, for example, of pole damper winding (Fig. 5.1).

This winding element consists of a number of loops with set bar impedances (for example: $AA', BB', \ldots, FF'$) and ring portions, (for example, AB, BC,…, EF).

We write down for clarity the following system of equations as per the second Kirchhoff's law for three adjacent loops in rotor:

$$J_{N+2} \cdot Z_{B,N+2} - J_{N+1} \cdot Z_{B,N+1} - 2I_{N+1} \cdot Z_{R,N+1} = E_{N+2,N+1} \quad \text{for loop } (N+2, N+1).$$

$$J_{N+3} \cdot Z_{B,N+3} - J_{N+2} \cdot Z_{B,N+2} - 2I_{N+2} \cdot Z_{R,N+2} = E_{N+3,N+2} \quad \text{for loop } (N+3, N+2).$$

$$J_{N+4} \cdot Z_{B,N+4} - J_{N+3} \cdot Z_{B,N+3} - 2I_{N+3} \cdot Z_{R,N+3} = E_{N+4,N+4} \quad \text{for loop } (N+4, N+3).$$

Relation between current J_N in bar number N and currents in adjacent ring portions I_N, I_{N-1} (Fig. 5.1) with numbers N and N − 1 is determined by the first Kirchhoff's law:

$$J_N = I_N - I_{N-1}. \tag{5.3}$$

Taking into account this ratio, we transform this system of equations to the following:

$$\begin{aligned}
&I_{N+2}Z_{B,N+2} - I_{N+1}\left(Z_{B,N+2} + Z_{B,N+1} + 2Z_{R,N+1}\right) + I_{N+0}Z_{B,N+1} = E_{N+2,N+1} \quad \text{for loop } (N+2, N+1).\\
&I_{N+3}Z_{B,N+3} - I_{N+2}\left(Z_{B,N+3} + Z_{B,N+2} + 2Z_{R,N+2}\right) + I_{N+1}Z_{B,N+2} = E_{N+3,N+2} \quad \text{for loop } (N+3, N+2).\\
&I_{N+4}Z_{B,N+4} - I_{N+3}\left(Z_{B,N+4} + Z_{B,N+3} + 2Z_{R,N+3}\right) + I_{N+2}Z_{B,N+3} = E_{N+4,N+3} \quad \text{for loop } (N+4, N+3).
\end{aligned} \tag{5.4}$$

When checking this system, it should be noted that instead of currents in the ring it is possible to assume a concept on the current in each loop (mesh current [1, 2]).

This system should be still added with equation as per second Kirchhoff's law for excitation winding:

$$I_{EX}Z_{EX} = E_{EX}. \tag{5.4'}$$

Here E_{EX}—EMF induced in this winding by the resulting field in air gap, I_{EX}—current in winding, $Z_{EX} = R_{EX} + jX_{EX}$—accordingly its impedance, A.C. resistance and inductive leakage reactances including the impedance in excitation system circuit.

As for the screening influence of rotor excitation winding in modern machines, the following should be noted:

- semiconductor elements of excitation system usually partly or completely "cut off" a negative half wave of alternating current induced by fields of higher time harmonics; it depends on the winding inductance.
- impedance of this winding is more than that of rotor damper winding. In this regard, the screening influence of excitation winding in comparison with damper winding is small.

We note that regularities in the structure of both of these systems of equations are simple that allows to to check easily in practical calculations correctness of equation formation; for each subsequent equation in the system it is necessary to change by unit the index numeration for currents, impedances and EMFs.

Let us designate the sum of three impedances in the left part of system of Eq. (5.4):

$$\begin{aligned} &Z_{B,N+2} + Z_{B,N+1} + 2 \cdot Z_{R,N+1} = Z_{N+2,N+1}; Z_{B,N+3} + Z_{B,N+2} + 2 \cdot Z_{R,N+2} \\ &\quad = Z_{N+3,N+2}; Z_{B,N+4} + Z_{B,N+3} + 2 \cdot Z_{R,N=3} = Z_{N+4,N+3}; \ldots. \end{aligned} \tag{5.5}$$

We set out coefficients for currents in the system (5.4) in Table 5.1 taking into account designations (5.5).

Table 5.1 Table of coefficients for unknowns in the system of equations for calculation of currents in short-circuited winding

I_{N+0}	I_{N+1}	I_{N+2}	I_{N+3}	I_{N+3}	…	EMF
$Z_{B,N+1}$	$-Z_{N+2,N+1}$	$Z_{B,N+2}$			…	$E_{N+2,N+1}$
	$Z_{B,N+2}$	$-Z_{N+3,N+2}$	$Z_{B,N+3}$		…	$E_{N+3,N+2}$
		$Z_{B,N+3}$	$-Z_{N+4,N+3}$	$Z_{B,N+4}$	…	$E_{N+4,N+3}$
…	…	…	…	…	…	…

Sum of impedances $Z_{N+2,N+1}$ in (5.5) is in the left part of system of Eq. (5.4). Index of this impedance corresponds to that at EMF $E_{N+2,N+1}$ in the right part of equation; the same refers to indices of the sum of impedances $Z_{N+3,N+2}$ and EMF $E_{N+3,N+2}$, sum of impedances $Z_{N+4,N+3}$ and EMF $E_{N+4,N+3}$, ….

Entering coefficients in this table is quite simple, and it can be easily checked in practical calculations. Its peculiarities are as follows:

- the number of impedances in each line equals three;
- these three impedances for each next line are shifted by one column to the right, towards increase of indices for currents;
- numbering of indices at these three impedances for each next line changes by unit;
- each group of impedances differing by unit, for example, from those $Z_{B,N+1}$, $Z_{B,N+2}$, $Z_{B,N+3}$, etc., is located in the table diagonally.

The number of equations in the system and, respectively, number of lines in Table 5.1 is determined by that of loops in short-circuited rotor winding. This number of loops depends on its construction. For example, incomplete damper winding with N_0 bars on pole has $N_0 - 1$ loops; respectively, for calculation of currents in this winding it is necessary to solve a system of N_0 equations including Eq. (5.4′), and to determine $N_0 - 1$ currents in ring elements (segments). Currents in bars are calculated according to (5.3). However, squirrel cage in induction machine contains N_0 bars and N_0 loops; respectively, system (5.4) consists of N_0 equations with N_0 unknown currents in ring elements (segments). Currents in N_0 bars are also calculated according to (5.3), Eq. (5.4′) for rotor excitation winding is excluded.

5.4 Solution Results: Currents in Elements of Short-Circuited Rotor Windings. Their Generalized Characteristics

It is convenient to present solution results of the system of Eq. (5.4) in the form:

$$I_{N+0} = \frac{D_{N+0}}{D_{SYST}};\ I_{N+1} = \frac{D_{N+1}}{D_{SYST}};\ I_{N+2} = \frac{D_{N+2}}{D_{SYST}};\ I_{N+3} = \frac{D_{N+3}}{D_{SYST}};\ I_{N+4} = \frac{D_{N+4}}{D_{SYST}}; \ldots.$$

Here D_{SYST}—system determinant dependent on the impedance of loops given in Table 5.1; D_{N+0}; D_{N+1}; D_{N+2}; D_{N+3}; D_{N+4};…—algebraic adjunct [5].

Let us consider the expression for one of algebraic adjuncts in more detail, for example, for D_{N+2}. In its calculation, the column from the system coefficients (5.4), that is the column of cage elements impedances $Z_{B,N+2,}; -Z_{N+3,N+2}; Z_{B,N+3}; \ldots$

corresponding in Table 5.1 to the current I_{N+2}, we replace [5] with the column from cage loops EMF $E_{N+2,N+1}; E_{N+3,N+2}; E_{N+4,N+3}; \ldots$. We expand the determinant obtained in this way in this column. Result of calculations is also an expression for algebraic adjunct D_{N+2}; for further calculations it is expedient to present it in the form:

$$\begin{aligned} D_{N+2} &= E_{N+2,N+1}A + E_{N+3,N+2}B + E_{N+4,N+3}C + \cdots \\ &= [-j\omega_{ROT}B(m,Q)]T_{N+2}. \end{aligned} \tag{5.6}$$

Here A, B, C….,—matrices of coefficients (impedances); order of these matrices is one unit less than that of the system of equations; T_{N+2}—proportionality coefficient determined by the impedance from Table 5.1 calculated taking into account geometrical dimensions of machine active part (D, L_{COR}) and loops $G_{N+1,N}$. It follows from Eq. (5.2) that EMF of each loop of short-circuited winding contains the same factor: $[-j\omega_{ROT}B(m,Q)]$. It is taken into account in Eq. (5.6) for the algebraic adjunct D_{N+2}.

Similar expressions from a system of equations for unknown currents can be also obtained in the calculation of other algebraic adjuncts: $D_{N+0}; D_{N+1}; D_{N+3}; D_{N+4}; \ldots$.

As a result of transformations performed, the expression for currents in elements of short-circuited ring (in segments) of damper winding or squirrel cage takes the following form:

$$\begin{gathered} I_{N+0} = \frac{-j\omega_{ROT}T_{N+0}}{D_{SYST}}B(m,Q); \\ I_{N+1} = \frac{-j\omega_{ROT}T_{N+1}}{D_{SYST}}B(m,Q);\ I_{N+2} = \frac{-j\omega_{ROT}T_{N+2}}{D_{SYST}}B(m,Q); \\ I_{N+3} = \frac{-j\omega_{ROT}T_{N+3}}{D_{SYST}}B(m,Q);\ I_{N+4} = \frac{-j\omega_{ROT}T_{N+4}}{D_{SYST}}B(m,Q); \ldots. \end{gathered} \tag{5.7}$$

It is easy to show that the system determinant $D_{SYST} \neq 0$, and it is convenient to present these currents as:

$$\begin{gathered} I_{N+0} = [I_{N+0}]B(m,Q); I_{N+1} = [I_{N+1}]B(m,Q); \\ I_{N+2} = [I_{N+2}]B(m,Q); I_{N+3} = [I_{N+3}]B(m,Q); \\ I_{N+4} = [I_{N+4}]B(m,Q); \ldots. \end{gathered} \tag{5.8}$$

In the last expressions we have:

$$\begin{gathered} [I_{N+0}] = \frac{-j\omega_{ROT}T_{N+0}}{D_{SYST}}; [I_{N+1}] = \frac{-j\omega_{ROT}T_{N+1}}{D_{SYST}}; \\ [I_{N+2}] = \frac{-j\omega_{ROT}T_{N+2}}{D_{SYST}}; [I_{N+3}] = \frac{-j\omega_{ROT}T_{N+3}}{D_{SYST}}; \\ [I_{N+4}] = \frac{-j\omega_{ROT}T_{N+4}}{D_{SYST}}; \ldots. \end{gathered}$$

Similarly, in Eq. (5.8) currents in bars can be represented as:

$$\begin{gathered} J_{N+0} = [J_{N+0}]B(m,Q); J_{N+1} = [J_{N+1}]B(m,Q); \\ J_{N+2} = [J_{N+2}]B(m,Q); J_{N+3} = [J_{N+3}]B(m,Q); \\ J_{N+4} = [J_{N+4}]B(m,Q); \ldots . \end{gathered} \tag{5.9}$$

They are obtained from the ratio following from (5.3).

We name proportionality coefficients obtained in (5.8) and (5.9).

$$[I_{N+0}]; [I_{N+1}]; [I_{N+2}]; [I_{N+3}]; [I_{N+4}]; \ldots, \tag{5.10}$$

$$[J_{N+0}]; [J_{N+1}]; [J_{N+2}]; [J_{N+3}]; [J_{N+4}]; \ldots . \tag{5.11}$$

as generalized characteristics of currents in ring portions of damper winding or squirrel cage and, respectively, in bars.

Thus, as a result we obtain that currents in short-circuited rotor winding elements can be represented in the form of generalized characteristics without any restrictions in the structure of such windings (complete or incomplete damper winding with broken bars or without them, etc.).

For three-phase rotor winding of DFMs the concept of generalized characteristics of currents was given in appendix of Chap. 2. Also, physical treatment of this concept was given and calculation expressions for generalized characteristics of currents were obtained in Chap. 2.

For symmetrical squirrel cage of induction machine the concept of generalized characteristics of currents was given in Chap. 4. These generalized characteristics for currents in elements of its cage are a special case characterizing short-circuited rotor winding, in which:

- impedances of all bars are equal; the same refers to those of ring portions;
- EMFs of loops are equal in amplitude, but differ in phase angles φ_N, herewith, the difference of phase angles of two EMFs of adjacent loops is constant: $\Delta\varphi = \varphi_{N+1} - \varphi_N = \varphi_{N+2} - \varphi_{N+1} = \varphi_{N+3} - \varphi_{N+2} = \cdots$.

For damper winding of salient pole machine and squirrel cage induction machine at the occurrence of damage in it, both or one of these conditions are not met. Therefore, for the calculation of A.C. machines modes fed with non-sinusoidal current, it was also necessary to proceed to a more complex problem formulated in the form of system of equations for magnetically coupled loops.

Physically, these generalized current characteristics for currents in elements of damper winding or squirrel cage (symmetrical or asymmetrical) with frequency ω_{ROT} = idem can be considered, as well as for three-phase rotor winding of DFMs, as criteria of similarity: they determine in the scale of flux density B(m, Q) current amplitudes and phases in all elements of these short-circuited windings.

Generalized characteristics of currents can be considered also as transfer functions; in steady-state operation mode (Heaviside's operator $j\omega_{ROT} = p_1$) [1, 2] they determine the relation between currents in short-circuited winding elements and resulting flux in air gap, that is the winding reaction affected by this flux.

5.5 Accounting of "Adjacent" Harmonics Fields by Means of Generalized Characteristics of Currents

In the previous para, we obtained general expressions for generalized characteristics of currents in short-circuited rotor winding elements used in practice (in damper winding, squirrel cage). In their calculation, it was supposed that in air gap there is resulting field with complex amplitude of flux density B (m, Q). We designate the corresponding generalized characteristics of currents obtained from a system of equations for currents in short-circuited ring portion, for example, with number N + 0 in the form $[I_{N+0}]$ and in the adjacent bar, for example, with the same number, in the form $[J_{N+0}]$.

The system of equations for currents in short-circuited winding elements and in excitation winding induced by the field with complex amplitude of flux density B (−m, Q) is given similarly; we designate their generalized characteristics of currents as follows: $\left[I'_{N+0}\right], \left[I'_{N+1}\right], \left[I'_{N+2}\right], \ldots$ and $\left[J'_{N+0}\right], \left[J'_{N+1}\right], \left[J'_{N+2}\right], \ldots$. We note that these generalized characteristics are determined with the same frequency ω_{ROT} of rotor EMF. Therefore, in their calculation the values of impedances are still true (taking into account skin effect) specified in Table 5.1.

Then, currents induced by resulting field of "adjacent" harmonics can be calculated from the ratios:

$$
\begin{aligned}
I_{N+0} &= [I_{N+0}] \cdot B(m,Q) + \left[I'_{N+0}\right] \cdot B(-m,Q);\\
I_{N+1} &= [I_{N+1}]B(m,Q) + \left[I'_{N+1}\right]B(-m,Q);\\
&\vdots\\
J_{N+0} &= [J_{N+0}]B(m,Q) + \left[J'_{N+0}\right]B(-m,Q);\\
J_{N+1} &= [J_{N+1}]B(m,Q) + \left[J'_{N+1}\right]B(-m,Q);\\
&\vdots
\end{aligned}
$$

In further statement (Chaps. 4–13) the generalized characteristics of currents in short-circuited rotor winding elements, and also generalized characteristics of MMF and field of these currents in air gap are not put into square brackets for the purpose to simplify designations: in these chapters the theory and methods of their investigation are stated. However, in Chap. 14, para (14.5), these generalized characteristics are used for the formation of system of equations for magnetically coupled loops; therefore we will return to designations of these characteristics using square brackets.

5.6 Peculiarities of Numerical Realization of System of Equations for Calculation of Generalized Characteristics

Let us note the following peculiarities of Table 5.1 with system coefficients usually to be considered in practical calculations.

One of these is as follows: its every line contains only three impedances (coefficients under three unknown currents). It is accepted to name matrices of sparsity structures. Realization of systems of equations with similar matrices has peculiarities. There are several methods of their solution [6, 7] that allow one to obtain the result with minimum calculation error, that is with minimum losses of accuracy of the result. The second peculiarity is connected with the change of A.C. resistances and reactances of damper winding or squirrel cage bars depending on slip S_{SL}. For high values of slip $S_{SL} \approx 1$, the inductive reactance of short-circuited windings bars is usually maximum, despite sharp manifestation of skin effect; it tends to zero as slip reduces. A.C. resistance of bars at slips $S_{SL} \approx 1$ is also maximum in connection with sharp manifestation of skin effect; it tends to the value of D.C. resistance as slip decreases. Therefore, for small slips (usually at $S_{SL} < 0.2$) often in practice of calculations of similar systems difficulties arise in numerical methods; in order to avoid them, sometimes calculation is performed with "doubled accuracy".

Brief Conclusions

1. Currents in short-circuited rotor winding elements can be represented in the form of generalized characteristics without any restrictions in the structure of such windings (complete or incomplete damper winding with broken bars or without them, etc.). As a result of this research it is obtained that generalized characteristics of currents $[I_2]$, $[I_3]$ and MMFs $[F_2]$, $[F_3]$ obtained in previous chapter are a special case of generalized characteristics for short-circuited rotor winding. To use an iterative method of calculation of magnetically coupled loops for rotor having windings with distributed parameters (for example, damper winding), it is necessary to determine previously:
   - EMF generalized characteristics of each short-circuited rotor loop; for this purpose in the previous chapter equations used are similar to (4.6);
   - generalized characteristics of currents in short-circuited winding elements; for this purpose the system of equations of magnetically coupled loops or the equations similar to (4.7) were used in the previous chapter;
   - MMF generalized characteristics, proceeding from generalized characteristics of currents in the previous chapter for this purpose there were used equations in the form of (4.8)–(4.9).

2. Generalized characteristics of currents in elements of damper winding or squirrel cage (symmetrical or asymmetrical) with frequency w_{ROT} = idem can be considered, as well as for three-phase rotor winding of DFMs, as criteria of similarity: they determine in the scale of the flux density B(m, Q) or B(−m, Q) the current amplitudes and phases in all elements of these short-circuited windings. Generalized characteristics of currents can be also considered as transfer functions; in steady-state operation mode (Heaviside's operator $p = j\omega_{ROT}$) they determine the relation between currents in short-circuited winding elements and resulting flux in air gap, that is the winding reaction affected by this flux.
3. Regularities in the structure of systems of equations for calculation of currents are simple that allows us to check easily in practical calculations correctness of equation formation.
4. The system of equations for calculation of currents has peculiarities: each equation contains only three impedances (coefficients under three unknown currents). In practice, for numerical realization of systems of equations with similar sparse matrices in the area of small slips (usually at $S_{SL} < 0.2$) there often arise difficulties: inductive and A.C. resistance of bars for these slips sharply decrease in comparison with the mode at $S_{SL} \approx 1$.
5. Numerical calculation method of currents unlike analytical, does not allow us to determine general regularities of current distribution in its elements for specific structures of short-circuited rotor windings. At the same time, its development along with analytical methods, represents a practical interest: the method allows us to carry out additional investigation of results, to obtain calculated values of generalized current characteristics, not stating concepts on the main and additional currents [8, 10, 11] of irregular damper winding or asymmetrical squirrel cage.

List of Symbols

A, B, C…	Matrices of coefficients (impedances) of system of equations
B(m, Q)	Flux density resulting field complex amplitude (phasor) in air gap
B_{DIR}(m, Q)	Complex amplitude (phasor) of flux density of direct field
B_{AD}(m, Q)	Complex amplitude (phasor) of flux density of additional field
b(x, t, m, Q)	Instantaneous value of flux density of resulting field in air gap
$D_{N+0}; D_{N+1}; D_{N+2}; D_{N+3}; D_{N+4}; \ldots$	Algebraic adjuncts of system of equations
D_{SYST}	Determinant of system of equations
$E_{N+1,N}$	EMF of short-circuited loop
$G_{N+1,N}$	Geometrical dimensions of loops of damper winding or squirrel cage

J_N and I_N	Currents in bars and ring portions
$[J_{N+0}]; [J_{N+1}]; [J_{N+2}]; [J_{N+3}]; [J_{N+4}]; \ldots;$ $[I_{N+0}]; [I_{N+1}]; [I_{N+2}]; [I_{N+3}]; [I_{N+4}]; \ldots$	Generalized characteristics of currents in bars and, respectively, in ring portions of damper winding or squirrel cage
m	Order of spatial harmonic
N, N + 1, …	Bar (ring portions) numbers of short-circuited rotor winding
p	Number of pole pairs
Q	Order of time harmonic
S_{SL}	Slip
T	Spatial period
t	Time
T_{N+2}	Proportionality coefficient determined by machine impedance
$Z_{B,0}; Z_{B,1}; Z_{B,2}; \ldots; Z_{B,N};$	Impedances of bars in slots of short-circuited rotor winding
$Z_{R,0}; Z_{R,1}; Z_{R,2}; \ldots; Z_{R,N};$	Impedances of ring portions between rotor bars
ω_{REV}	Angular speed of rotor rotation
ω_{ROT}	Circylar frequency of rotor EMF and current
$\varphi_{AD}, \varphi_{DIR}$	Initial phase angles

References

I. Monographs, general courses, textbooks

1. Demirchyan K.S., Neyman L.R., Korovkin N.V., Theoretical Electrical Engineering. Moscow, St. Petersburg: Piter, 2009. Vol. 1, 2 (In Russian).
2. Kuepfmueller K., Kohn G., Theoretische Elektrotechnik und Elektronik. 15 Aufl. Berlin, N. Y.: Springer. 2000. (In German).
3. Mueller G., Ponick B., Elektrische Maschinen, N.Y., J. Wiley, 2009. (In German).
4. Richter R., Elektrische Maschinen. Berlin: Springer. Band I, 1924; Band II, 1930; Band III, 1932; Band IV, 1936; Band V, 1950. (In German).
5. Korn G., Korn T., Mathematical Handbook., N.Y.: McGraw-Hill, 1961.
6. Brameller A., Allan R., Haman, Y., Sparsity Structures of the Matrices. London: Pitman, 1976.
7. Jeffris H., Swirles B., Methods of Mathematical Physics. Third Edition, Vol. 1-3, Cambridge: Cambridge Univ. Press, 1966.

II. Induction machines. Papers, inventor's certificates

8. Boguslawsky I.Z., Currents in a asymmetric short-circuited rotor cage. Proceedings of the Russian Academy of Sciences. Energetika i Transport, 1982, #1. (In Russian).
9. Demirchyan K.S., Boguslawsky I.Z., The calculation of the currents and the losses in the rotor short-circuited induction motor using the generalized characteristics of the rotor MMF. Electrichestvo, #5, 1980. (In Russian).

III. Synchronous machines. Papers, inventor's certificates, patents

10. Boguslawsky I.Z., Currents and harmonic MMFs in a damper winding with damaged bar at a pole. Proceedings of the Russian Academy of Sciences. Energetika i Transport, 1985, #1. (In Russian).
11. Demirchyan K.S., Boguslawsky, I.Z., Current flowing in damper winding bars of different resistivity in a heavy- duty low speed motor. Proceedings of the Russian Academy of Sciences. Energetika i Transport, 1980, #2. (In Russian).
12. Boguslawsky I.Z., Generalized characteristics of currents and MMF of magnetically loops of rotor in A.C. machines. Proceedings of the Russian Academy of Sciences. Energetika, #5, 1995. (In Russian).
13. Boguslawsky I.Z., Magnetically coupled loops in A.C. machines under nonsinusoidal supply. Proceedings of the Russian Academy of Sciences. Energetika, 1995, #2 (In Russian).
14. Boguslawsky I.Z., Korovkin N.V., Unsymmetrical modes of polyphase machine ($m_{PH} \geq 3$): determinattion of MMF harmonics of armature reaction. Proceedings of the Russian Academy of Sciences. Energetika, 2013, #4. (In Russian).

Chapter 6
Passive Quadripoles; Recurrent Circuits of Various Structure: Investigation of Their Peculiarities for Modeling Process of Currents Distribution in Short-Circuited Rotor Windings

This chapter develops methods of current investigation in elements of U-shaped passive recurrent circuits with various structure of their links (symmetric, asymmetrical, etc.) in relation to the design of short-circuited rotor windings of large A. C. machines; peculiarities of investigation methods for asymmetrical recurrent circuits are described in detail. This chapter establishes a basis for the investigation of currents in elements of active U-shaped recurrent circuits used in subsequent chapters for distribution of currents in short-circuited rotor windings. Methods are proved with numerical examples.

The content of this chapter is development of the methods stated in [1, 2, 11–14].

6.1 General Comments

Generalized characteristics allow using analytical methods to solve problems of currents distribution in damper winding elements of salient pole synchronous machines and in squirrel cages (with broken bars)—of induction machines. Practical advantages of these methods in solution of the problem considered, in comparison with numerical are known; they allow us to determine general regularities of currents distribution in various constructions of short-circuited rotor windings, including operation in nonlinear circuit. For this purpose, peculiarities of investigation methods of symmetrical recurrent circuits are stated in detail in this chapter, methods of investigation of asymmetrical recurrent circuits of various structure with account of various constructions of machine short-circuited rotor windings of specified types are developed.

In the following chapters, these methods for the first time in engineering practice were used to solve the problems of currents distribution in elements of modern winding constructions in nonlinear networks of A.C. machines; it demanded a number of additional checks of validity of results. Methods differ in description

I. Boguslawsky et al., *Large A.C. Machines*,
DOI 10.1007/978-4-431-56475-1_6

completeness of physical processes, strictness of their solution and clarity of physical interpretation of results based on common ground.

Earlier, these methods were successfully used practically in investigation of eddy currents and losses in modern constructions of stator coil windings in A.C. machines. They will be given in Chap. 23.

In relation to problems considered, the structure of recurrent circuits has a number of peculiarities determined by specific features of various constructions of short-circuited windings found in practice.

6.2 Representation of Short-Circuited Rotor Winding Elements in the Form of Quadripoles and Recurrent Circuits

It is convenient to consider a loop of short-circuited rotor winding in A.C. machine formed by two adjacent bars and two ring portions concluded between them as a quadripole. A number of such quadripoles makes a recurrent circuit.

For more accurate representation of peculiarities in investigation methods of quadripoles and recurrent circuits developed in this monograph, let us begin with stating results of their development with quadripoles and passive recurrent circuits. Such quadripoles feature the absence of power sources (EMF) inside each of them.

Let us note that real problems to be investigated in the following chapters are more difficult: in each loop of short-circuited rotor winding of A.C. machines in operational modes there are EMFs induced by resulting field in machine air gap. For their investigation, we will use methods, typical for active quadripoles; each containing power sources (EMF) inside. Methods of investigation of these recurrent circuits with EMF in every loop differing in amplitude and phase, are developed in the following chapters on the basis of results obtained in this chapter.

6.3 Passive Symmetrical and Asymmetrical Quadripoles

Let us designate the voltage and current at passive quadripole input as U_1, I_1, and at output—U_2, I_2. We use one of notations for equations of this quadripole which establish the relation between U_1, I_1 and U_2, I_2:

$$\begin{aligned} U_1 &= AU_2 + BI_2, \\ I_1 &= CU_2 + DI_2. \end{aligned} \tag{6.1}$$

Here A, B, C, D—constants determined by quadripole impedances [1, 2]. We note that between the constants in Eq. (6.1) the following relation takes place: $AD - BC = 1$. Thus, passive quadripole is characterized by only three independent

constants. With their help, the quadripole can be represented with one of two equivalent circuits: T-shaped (two longitudinal elements with impedances Z_{R_1}, Z_{R_3} and one cross element with impedance Z_{B_1} are star connected) or U-shaped (two cross elements with impedances Z_{B_1}, Z_{B_3} and one longitudinal element with impedance Z_{R_1} are delta connected). T-shaped equivalent circuit is symmetrical if $Z_{R_1} = Z_{R_3}$, otherwise $(Z_{R_1} \neq Z_{R_3})$ it is asymmetrical. Similarly, U-shaped equivalent circuit is symmetrical if $Z_{B_1} = Z_{B_3}$, otherwise $(Z_{B_1} \neq Z_{B_3})$ it is asymmetrical.

In further statement, we will use these both equivalent circuits.

6.4 Structural Features of Passive Symmetrical and Asymmetrical Recurrent Circuits

If we have a number of quadripoles and output terminals (2′, 2″) of one (Fig. 6.1) are connected to input terminals (3′, 3″) of the following, we obtain the recurrent circuit (Fig. 6.2) consisting of N_0 cross elements; its component quadripoles are links of such a circuit. In further statement, we will differentiate the following types of passive recurrent circuits:

- on the ratio of values of longitudinal or cross elements: symmetrical and asymmetrical;
- in the structure: open and closed.

Let us consider in more detail, primarily, the first type of recurrent circuits (symmetrical and asymmetrical):

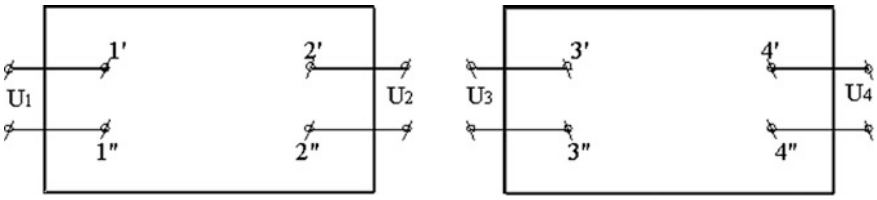

Fig. 6.1 Quadripoles and recurrent circuit

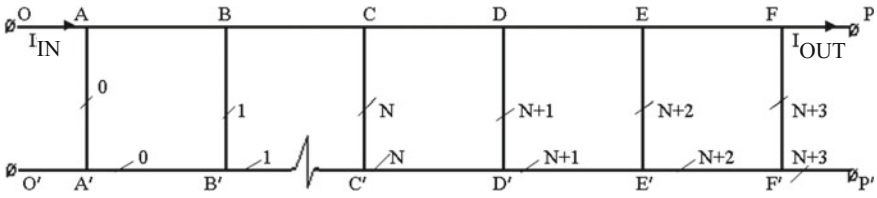

Fig. 6.2 Passive recurrent circuit

- symmetrical circuits; in such a circuit all quadripoles forming it are symmetrical: impedance of all cross elements, for example, AA′, BB′, . . ., FF′ satisfies the following ratio:

$$Z_B = \text{idem} \tag{6.2}$$

and all longitudinal elements, for example, AB, BC,…, EF—to the ratio:

$$Z_R = \text{idem} \tag{6.3}$$

- asymmetrical circuits; in such a circuit one or several elements satisfy the ratios:

$$Z_R \neq \text{idem or } Z_B \neq \text{idem} \tag{6.4}$$

In asymmetrical circuits we allocate one class naming it as asymmetrical regular or for simplicity—regular. In this recurrent circuit, groups as $A_1A_1', B_1B_1', F_1F_1'$ (Fig. 6.3) can be allocated consisting of $N_0 \gg 1$ symmetrical cross elements meeting the condition (6.2) and groups, for example, A_1B_1, B_1F_1, consisting of $N_0 - 1$ symmetrical longitudinal elements meeting the condition (6.3).

However, there are asymmetrical longitudinal elements between these groups of elements, for example, F_1A_2, F_2A_1, satisfying one of conditions (6.4). Such a circuit corresponds to damper winding.

In asymmetrical circuits, we allocate one more class naming it as asymmetrical irregular or for simplicity—irregular. In such a recurrent circuit unlike asymmetrical regular, groups of cross elements can be allocated, for example; B_1B_1', F_1F_1' (Fig. 6.3) not meeting the condition (6.2). Such a circuit corresponds to damper winding, for example, with damaged bar.

Let us proceed to the second type of recurrent passive circuits (open and closed):

- open circuits; in such circuits consisting of N_0 (N = 0, 1, 2,…) cross elements and N_{0-1} longitudinal, the following ratios for currents are satisfied: currents in the first (N = 0) cross element and the first longitudinal are equal in amplitude and phase; currents in the last cross ($N = N_{0-1}$) and in the last longitudinal

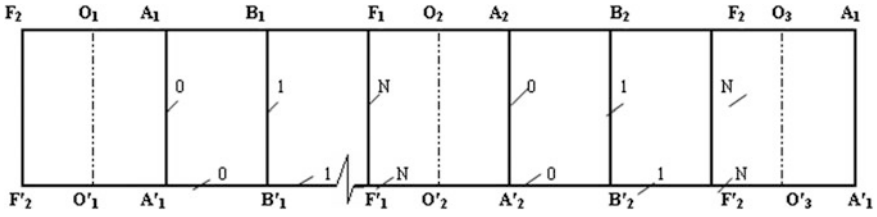

Fig. 6.3 Asymmetrical regular passive recurrent circuit

($N = N_{0-2}$) element are equal in amplitude, but are opposite in phase. There are not a EMF in elements of passive chain open circuits; the currents are created by the external voltage sources. An example is the circuit in Fig. 6.3 if the voltage (current) source is not connected to these elements (voltage (current) source on element N = 0);

- closed circuits; in this circuit consisting of N_0 cross elements and N_0 longitudinal, the following ratios for currents are satisfied: difference of currents in longitudinal elements with numbers $N = N_{0-1}$ and N = 0 is equal to the current in cross element with number N = 0. An example is the same circuit in Fig. 6.2 if terminals OO′ and PP′ are galvanically connected if the voltage (current) source is not connected to these elements. There are not a EMF in elements of passive chain closed circuits; the currents are also created by the external voltage sources. In some cases it is more convenient to set out this circuit as "closed" (Fig. 6.4). In further statement when investigating closed recurrent circuits both passive and active we will use both forms of closed circuits.

Let us note that from the methods of investigation of passive asymmetrical recurrent circuits given in this chapter it follows that they are reduced to investigation of symmetrical circuits with account of a number of additional boundary conditions determined by degree of circuit asymmetry.

About the features of differencial and difference equations: currents in passive recurrent circuit (Fig. 6.5a) and in equivalent current—carrying plate (Fig. 6.5b).

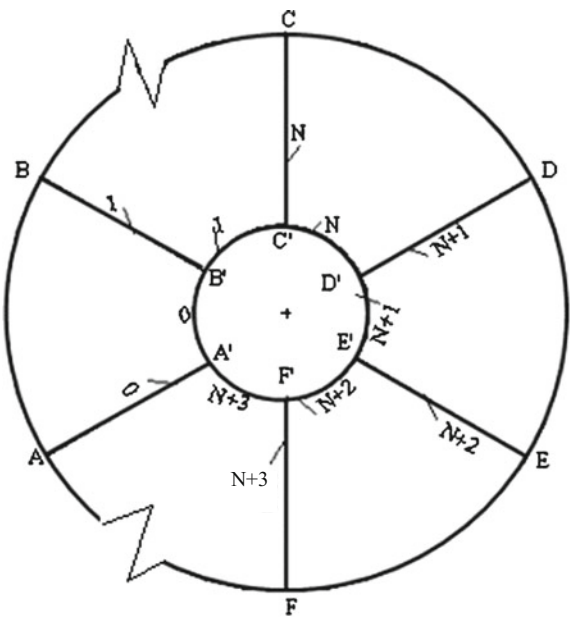

Fig. 6.4 Passive closed recurrent circuit

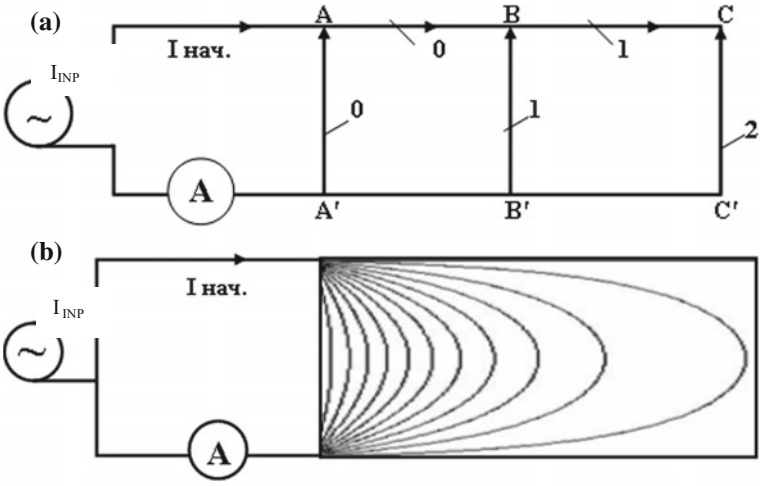

Fig. 6.5 Currents in passive recurrent circuit (**a**), and in equivalent current carrying plate (**b**)

6.5 Methods of Investigation of Passive Symmetrical Recurrent Circuits Described by "Step" or "Lattice" Functions

6.5.1 Difference Equations, Methods of Their Solution

We proceed to the statement of calculation methods of current distribution in passive recurrent circuits.

Thus, we will accept as initial:

- impedances in longitudinal elements—as per (6.2);
- impedances in cross elements—as per (6.3);
- voltage applied to one or several elements of recurrent circuit.

Let us consider some links (elements) of symmetrical passive recurrent circuit presented in Figs. 6.2, 6.3 or 6.4.

As well as in the previous chapter, let designate serial numbers of cross elements of the circuit as follows: N = 0, 1, 2, …, N − 1, …, N_{0-1}; Let us assign number N to each longitudinal element bounded between two cross elements with numbers N and N + 1. Respectively, the loop bounded between cross elements with numbers N + 1 and N and longitudinal elements with number N will be designated: (N + 1, N). Currents in longitudinal element with number N will be designated as I[N], and in cross element with the same number—J[N]; unknown dependence of these currents on element number N will be designated respectively $\mathbf{I}_{(N)}$ and $\mathbf{J}_{(N)}$.

Further, let us consider a loop formed by cross elements with numbers N + 2, N + 1 and longitudinal elements with number N + 1. For this loop we will write down the equation as per second Kirchhoff's law [1, 2]:

$$(J[N+2] - J[N+1])Z_B - 2 \cdot I[N+1]Z_R = 0. \tag{6.5}$$

According to the first Kirchhoff's law we have the following relations between these currents:

$$J[N+2] = I[N+2] - I[N+1]; \quad J[N+1]I[N+1] - I[N+0]. \tag{6.6}$$

After transformation (6.5) taking into account (6.6), we get:

$$I[N+2] - (2+\sigma) \cdot I[N+1] + I[N+0] = 0. \tag{6.7}$$

$$\text{where coefficient} \quad \sigma = 2 \cdot \frac{Z_R}{Z_B} \tag{6.7'}$$

is determined by the relation of impedance of longitudinal and cross elements of symmetrical recurrent circuit; generally it is a complex number. It is easy to show that this coefficient physically corresponds to the distribution coefficient from the theory of transmission lines [3–6].

Equation (6.7) describes the distribution of currents in all elements of recurrent circuit. It belongs to the class of linear difference equations with constant coefficients [4–7] and has the order equal to two. Equations of this kind correspond to processes described by so-called "step" or "lattice" functions. Features of such a function are, in particular, that its argument changes discretely; respectively, and this function accepts only discrete values [6, 7].

Unlike it—functions describing processes by means of differential equations change continuously, as well as their arguments (except for special discontinuity points not considered here).

In the task class considered, such "step" or "lattice" functions are currents in longitudinal I[N] and in cross elements J[N]; they are connected by the ratio (6.6). Argument of these functions as stated above changes discretely: N = 0, 1,2, …, N − 1,….

Distinction between "step" functions describing processes by means of difference equations, and continuous functions describing processes by means of differential equations has clear physical interpretation. It is necessary for sure to use step functions and methods of their analysis in engineering practice.

Let us consider for example the following two physical problems; for simplicity we select two receivers (Fig. 6.5a, b). In the first example it is necessary to find the distribution of currents in longitudinal and cross elements of passive circuit connected to terminals A, A′ of alternating current source; let us designate the impedance measured between these terminals as Z_{EQ}.

In the second—it is necessary to find the distribution of current in a conducting plate (for example, copper) connected to terminals AA′ of the same source and with the same impedance between these terminals: $Z_{EQ} = \text{idem}$. Let us note that provided that ($Z_{EQ} = \text{idem}$) we replace ("equalize") the circuit with discrete longitudinal and cross impedances of its elements—by conducting plate. Spreading of currents in such a plate (their continuous distribution) is described by Laplace differential equation, and in each point of this plate the Ohm law in differential form $\Delta = \gamma \cdot E$ is true, where Δ—current density in plate element, γ—its specific conductivity, E—electric field intensity. Unlike this continuous distribution of currents in plate, currents in elements of recurrent circuit are distributed discretely according to the solution of corresponding difference equation.

Difference equations can be solved by several methods.

In practice, besides classical [6–8] the method of solution of difference equations by means of Laplace discrete transformation is widely used (Z-transformations). This method [4–7] is similar to that of differential equations solution by means of operational calculation and is especially convenient when solving difference equations or their systems of high order [3].

In the analysis of currents distribution in considered recurrent circuits we will use classical method.

In practical calculations within this method, some modifications of difference equation solution are used as (6.7). Let us consider one of these.

Let us set out the solution of uniform difference Eq. (6.7) in the form:

$$I_{(N)} = C_1 \cdot e^{k_1 N} + C_2 \cdot e^{k_2 N} + \ldots C_M \cdot e^{k_M N} \tag{6.8}$$

Here $C_1, C_2, \ldots, C_M$—constants determined by boundary conditions of problem; $k_1, k_2, \ldots, k_M$—coefficients determined by parameters of recurrent circuit (impedances of its elements).

Therefore, the solution of difference Eq. (6.8) is found if the following are determined:

- constants $C_1, C_2, \ldots, C_M$ from boundary conditions depending on peculiarities of recurrent circuit structure;
- coefficients $k_1, k_2, \ldots, k_M$ from ratios containing recurrent circuit parameters.

Index M in summation determines the number of summands in (6.8); it corresponds to the order of difference equation and is equal for Eq. (6.7) to two, so M = 1; 2. Let us substitute solution (6.8) to initial Eq. (6.7). After these transformations, we get:

$$e^{2k_M} - (2 + \sigma) \cdot e^{k_M} + 1 = 0. \tag{6.9}$$

Equation (6.9) is one of forms of characteristic equation corresponding to difference Eq. (6.7). Let us represent it as:

$$\left(e^{\frac{k_M}{2}} - e^{-\frac{k_M}{2}}\right)^2 = \sigma.$$

From this expression we calculate $k_M \in k_1; k_2$.:

$$\text{sh}\frac{k_1}{2} = +\frac{\sqrt{\sigma}}{2}; \quad \text{sh}\frac{k_2}{2} = -\frac{\sqrt{\sigma}}{2}. \tag{6.10}$$

When transforming Eq. (6.9) it is supposed that $e^{\frac{k_M}{2}} \neq 0$; this condition is always satisfied in the considered class of tasks. Equations (6.10) implicitly determine both coefficients $k_M : k_1$ and k_2. However, such a type of coefficient representation is inconvenient: inverse hyperbolic functions complicate the type of calculation equation for currents in a closed form. It practically excludes a possibility to use calculation equations in such a form for their joint solution, for example, if they form a system made under both Kirchhoff's laws or if it is necessary to generalize the analysis results of currents distribution in recurrent circuit.

In some tasks, for example, when designing grounding cables for power transmission line supports [6], when studying the distribution of waves along recurrent circuits modeling processes in high voltage lines it is possible to accept [6]:

$$k_1 \approx +\sqrt{\sigma}; \quad k_2 \approx -\sqrt{\sigma}.$$

Thus, it is supposed that when expanding function $\text{sh}\frac{k_1}{2}$ into a series, only the first term of series is considered. $\text{sh}\frac{k_1}{2} \approx \frac{k_1}{2}$; similarly, $\text{sh}\frac{k_2}{2} \approx \frac{k_2}{2}$. However, these approximate expressions are true only for $\sigma << 0.1$ and for short-circuited rotor windings of A.C. machines usually are not satisfied.

In practice, for the investigation of distribution of currents in elementary conductors (conductor strands) of stator winding [9] or in rotor winding construction elements [13] other modification of solution by any classical method of difference equation as (6.7) has revealed to be more convenient. Its advantage is that it allows obtaining the solution of difference Eq. (6.7) in a closed form. Now we consider it in more detail. Let us perform previously the following additional transformations. Let us designate the value e^{k_M} in (6.9) as: $e^{k_M} = a_M$, and, as before, for considered class of tasks index M = 1;2. Then Eq. (6.9) takes the form:

$$a_M^2 - (2 + \sigma) \cdot a_M + 1 = 0. \tag{6.11}$$

It is also a form of representation of characteristic equation corresponding to difference Eq. (6.7). From its decision we obtain complex values a_1 and a_2 in an explicit form:

$$a_{1,2} = \frac{2 + \sigma \pm \sqrt{\sigma^2 + 4\sigma}}{2}. \tag{6.12}$$

Thus, coefficients a_1, a_2 are determined by parameters of recurrent circuit elements.

Let us note that according to Vieta's theorem [10] the following ratios are true:

$$a_1 \cdot a_2 = 1; \quad a_1 \cdot a_2 = 2 + \sigma. \tag{6.12'}$$

These both ratios can be obtained directly using Eq. (6.12) for a_1 and a_2. Ratios (6.12) and (6.12) will be repeatedly used in further calculations.

As a result of transformations (6.11)–(6.12), we obtain the solution of uniform difference Eq. (6.7) in a closed form:

$$I_{(N)} = C_1 \cdot a_1^N + C_2 \cdot a_2^N, \tag{6.13}$$

where C_1, C_2—constants determined by boundary conditions; for open and closed recurrent circuits they differ. Let us note that rightness of solution (6.13) can be easily confirmed also directly substituting each of summands into Eq. (6.7), composing Eq. (6.13); number of summands and constants at them (two) are equal thus to the order of difference equation: M = 2.

Equation (6.13) describes the distribution of currents in longitudinal elements of passive recurrent circuit.

Distribution of currents in its cross elements is determined from (6.13) using the first Kirchhoff's law (6.6):

$$J_{(N)} = C_1 \cdot a_1^{N-1} \cdot (a_1 - 1) + C_2 \cdot a_2^{N-1} \cdot (a_2 - 1). \tag{6.14}$$

Thus, from the analysis of the obtained Eqs. (6.13) and (6.14) we can draw an important practical conclusion: currents in elements of passive recurrent circuit are distributed under aperiodic law.

We use obtained solution (6.13) of uniform difference Eq. (6.7) in a closed form further for the investigation of currents distribution not only in symmetrical, but also in asymmetrical passive recurrent circuits, as well as in active recurrent circuits of various structure.

Let us note also that results of this analytical investigation of recurrent circuits will also allow us to obtain expressions for MMF of short-circuited rotor windings of A.C. machines (synchronous and induction), to formulate a system of equations for the calculation of modes of these machines, including their operation in non-linear network.

6.5.2 *Pecularities of Currents Distribution in Symmetrical Passive Recurrent Circuits*

Let us perform an analysis of some peculiarities of solution (6.13) of difference Eq. (6.7) for currents in relation to the open recurrent circuit. Let us accept for

clarity that plus sign in Eq. (6.12) refers to the value of a_1, and minus sign—to value a_2, so $|a_2| < |a_1|$, herewith, $|a_1| > 1$, a $|a_2| < 1$. Let us represent these both complex values as follows:

$$a_1 = \mathrm{Re}(a_1) + j \cdot \mathrm{Im}(a_1) = |a_1| \cdot e^{j\varphi_1}; a_2 = \mathrm{Re}(a_2) + j \cdot \mathrm{Im}(a_2) = |a_2| \cdot e^{j\varphi_2}.$$

Here, φ_1, φ_2—phase angles (generally $\varphi_1 \neq \varphi_2$).

Then the expression for current (6.13) can be represented as:

$$I_{(N)} = C_1 \cdot |a_1|^N \cdot e^{jN\varphi_1} + C_2 \cdot |a_2|^N \cdot e^{jN\varphi_2}. \tag{6.15}$$

Therefore, in Eq. (6.15), current summands $I_{(N)}$ in different ways change their amplitudes and phases with change of loop number N. For the first current summand $I_{(N)}$ with growth number N the amplitude increases, however, for the second summand with increase of N it decreases; for both current summands $I_{(N)}$ with growth number N, phases also change, however the law of their change is various: it was already noted that $\varphi_1 \neq \varphi_2$.

Ratios between constants C_1 and C_2 determine the following possible versions of dependence of longitudinal current $I_{(N)}$ in elements of recurrent circuit on the loop number N:

- with $|C_1| \gg |C_2|$ amplitude of this current with growth number N increases under the exponential law;
- with $|C_1| << |C_2|$ its amplitude with growth of N is attenuated under the exponential law;
- for other combinations of constants C_1 and C_2 and phase angles φ_1, φ_2 of both summands, maximum or minimum current amplitude can be reached with growth of N.

6.6 Open Passive Recurrent Circuits. Constants for Calculation of Currents Distribution Calculation Examples

6.6.1 General Comments

It is noted above that constants C_1, C_2 are determined by boundary conditions, and these conditions depend on structural features of recurrent circuit. Previously, however, we can note the following:

- usually in the theory of passive quadripoles it is accepted that voltages U_1, U_2 and currents I_1, I_2 contained in Eq. (6.1) characterize respectively "input (index 1)" and "output (index 2)" of this quadripole; the same refers to recurrent

circuits formed by several quadripoles. This condition (existence of "input" and "output") is generally not obligatory; further, we will consider boundary conditions for the solution of recurrent circuits which have two "input (indices 1 and 2)"; physically it, for example, means that the recurrent circuit is connected to two independent voltage (current) sources of identical frequency differing in both amplitudes and phase angles.

6.6.2 System of Equations for Constants

Let us consider (Fig. 6.2) a passive symmetrical open recurrent circuit consisting of N_0 cross and, respectively, N_{0-1} longitudinal elements (N = 0,1,2,… $N_0 - 1$). Set in values in this circuit are:

- impedances of cross elements Z_B and longitudinal Z_R;
- boundary conditions to determine the constants C_1, C_2 in calculation equations for currents (6.13) and (6.14):

$$\begin{aligned} &\text{at } N = -1 : I_{(-1)} = I_{INP} \cdot e^{j\varphi_{INP}}; \\ &\text{at } N = N_0 - 1 : I_{(N_0-1)} = I_{OUT} \cdot e^{j\varphi_{OUT}}. \end{aligned} \tag{6.16}$$

Here $I_{INP}; I_{OUT}$—complex amplitudes of currents (phasors), $\varphi_{INP}, \varphi_{OUT}$—corresponding phase angles of these currents.

Let us find the distribution of currents in all elements of this recurrent circuit.

Such formulation of boundary conditions is based on the assumption that recurrent circuit is connected from both sides to sources of sinusoidal voltage (Fig. 6.2). Let us turn our attention to two special cases of such a recurrent circuit:

(a) At phase angles $\varphi_{INP} = 0^\circ, \varphi_{OUT} = 0^\circ$ the recurrent circuit has "input" and "output" as currents $I_{(-1)}$ and $I_{(N_0-1)}$ coincident in phase, and their complex amplitudes have the same sign:

$$I_{(-1)} = +I_{INP}; I_{(N_0-1)} = +I_{OUT}.$$

(b) At phase angles $\varphi_{INP} = 0^\circ, \varphi_{OUT} = 180^\circ$ the recurrent circuit has two "inputs" as currents $I_{(-1)}$ and $I_{(N_0-1)}$ in opposite phase, and their complex amplitudes have opposite signs:

$$I_{(-1)} = +I_{INP}; I_{(N_0-1)} = -I_{OUT}.$$

Generally, at difference of phase angles

$$\varphi = \varphi_{OUT} - \varphi_{I_{NP}}, \tag{6.17}$$

lying within $0^{\circ} < \varphi < 180^{\circ}$, the concepts "input" and "output" of recurrent circuit become less distinct; the recurrent circuit can be characterized in these cases also as a circuit with "double-ended power supply".

Taking into account Eq. (6.17), boundary conditions can be presented in the form:

$$\begin{array}{c} \text{at} \quad N = -1 : I_{(-1)} = I_{NP}; \\ \text{at}\, N = N_0 - 1 : I_{(N_0-1)} = I_{OUT} \cdot e^{j\varphi}. \end{array} \tag{6.16'}$$

Let us proceed to calculation of constants C_1 and C_2 in Eq. (6.13).

Proceeding from boundary conditions, by means of Eq. (6.13) we get:

$$I_{(-1)} = C_1 \cdot a_2 + C_2 \cdot a_1; \quad I_{(N_0-1)} = C_1 \cdot a_1^{N_0-1} + C_2 \cdot a_2^{N_0-1}. \tag{6.18}$$

From the solution of the system of Eq. (6.18) it follows:

$$C_1 = \frac{I_{INP} \cdot a_2^{N_0-1} - I_{OUT} \cdot e^{j\varphi} \cdot a_1}{a_2^{N_0} - a_1^{N_0}}; \quad C_2 = \frac{I_{OUT} \cdot e^{j\varphi} \cdot a_2 - I_{INP} \cdot a_1^{N_0-1}}{a_2^{N_0} - a_1^{N_0}} \tag{6.19}$$

Here a_1, a_2 are calculated according to Eq. (6.12), and φ—is determined according to initial data and Eq. (6.17).

6.6.3 *Calculation Examples*

Example 1 In a passive recurrent circuit with $N_0 = 6$ cross and, respectively, five longitudinal elements (N = 0, 1, K, 5) the followings are assumed as given:

- impedances of cross elements $Z_B = 5$ Ohm and longitudinal $Z_R = 3$ Ohm
- boundary conditions for calculation of currents in the circuit: $|I_{INP}| = |I_{OUT}| = 100$ A.

Let us find the distribution of currents in all elements of this recurrent circuit for two limit values of phase angle difference φ as per (6.17):

$$\text{a)}\ \varphi = 0^{\circ}; \text{b)}\ \varphi = 180^{\circ}.$$

With setting out these two limit values of phase angles φ and values of cross and longitudinal impedances, it is possible to obtain the distribution of currents in the recurrent circuit in extremely clear physical interpretation. Thus, it is possible to simply validate the calculated expressions.

According to the obtained Eqs. (6.13)–(6.19) taking into account values of recurrent circuit parameters we have:

$a_1 = 2.849; a_2 = 0.351$; respectively, constants of C_1, C_2, are determined as follows:

(a) at $\varphi = 0^\circ$: $C_1 = 0.5318$. $C_2 = 35.0345$
(b) at $\varphi = 180^\circ$: $C_1 = -0.5338$. $C_2 = 35.1658$.

Calculation results of currents distribution are given in Tables 6.1 and 6.2.

Let us analyze the obtained results.

At $\varphi = 0^\circ$ we have: $J_{(0)} + J_{(1)} + J_{(2)} + J_{(3)} + J_{(4)} + J_{(5)} = I_{(N_0-1)} - I_{(-1)} = 0$.

At $\varphi = 180^\circ$ we have: $J_{(0)} + J_{(1)} + J_{(2)} + J_{(3)} + J_{(4)} + J_{(5)} = I_{(N_0-1)} - I_{(-1)} = -200\text{A}$.

Thus, both sums of currents in cross elements (at $\varphi = 0^\circ$ and $\varphi = 180^\circ$) taking into account boundary conditions satisfy the Kirchhoff's first law and prove the validity of stated method for passive recurrent circuit calculation.

It should be noted that methods of closed symmetrical recurrent circuits analysis are similar to those of open circuit analysis and differ only in formulation of boundary conditions. They will be considered in the following chapters in relation to active recurrent circuits.

Example 2 In a passive recurrent circuit in Fig. 6.5a with $N_0 = 3$ (N = 0, 1, 2) cross and, respectively, two longitudinal elements, the followings are assumed as given:

Table 6.1 Distribution of currents in recurrent circuit elements ($\varphi = 0^\circ$)

N	$I_{(N)}$	$J_{(N)}$
−1	100.0 (boundary condition)	–
0	35.57	−64.43
1	13.81	−21.75
2	8.63	−5.18
3	13.81	5.18
4	35.57	21.75
5	100.0 (boundary condition)	64.43

Table 6.2 Distribution of currents in recurrent circuit elements ($\varphi = 180^\circ$)

N	$I_{(N)}$	$J_{(N)}$
−1	100.0 (boundary condition)	–
0	34.63	−65.37
1	10.82	−23.81
2	0	−10.82
3	−10.82	−10.82
4	−34.63	−23.81
5	−100.0 (boundary condition.	−65.37

Table 6.3 Distribution of currents in elements of recurrent circuit

N	$I_{(N)}$	$J_{(N)}$
−1	100.0 (boundary condition)	–
0	17.143	−82.856
1	2.856	−14.287
2	0	−2.856

- impedances of cross elements Z_B = 5 Ohm and longitudinal Z_R = 10 Ohm;
- boundary conditions for calculation of currents in circuit: $I_{INP} = 100A$.

Let us find the distribution of currents in all elements of this recurrent circuit.

According to obtained Eqs. (6.13)–(6.19) taking into account values of recurrent circuit parameters, we have:

$a_1 = 5.8284$; $a_2 = 0.1716$; constants of C_1, C_2 are determined as follows: $C_1 = 0.0015$; $C_2 = -1.7158$.

Calculation results of currents distribution are given in Table 6.3.

It is easy to check the obtained results using both Kirchhoff's laws [1, 2]. Comparing them with results of solution of two-dimensional Laplace Equation (Fig. 6.5b), we obtain an additional proof of the validity of both solutions: values of currents when the distance increases from voltage source (from terminals AA') and attenuation that corresponds to physical meaning of task.

6.7 Investigation Methods of Passive Asymmetrical Recurrent Circuits

The methods of analysis of passive asymmetrical circuits developed in this monograph do not depend on their structure and are equally applicable to closed and open circuits including regular.

6.7.1 Difference Equations, Methods of Their Solution

Let us proceed to the statement of calculation methods of currents distribution in asymmetrical recurrent circuits. Thus, we will consider impedances in longitudinal and cross elements.

Let us accept that the impedance Z_{Np} of one of cross elements with number N_P, for example, element CC' of asymmetrical recurrent circuit (Fig. 6.2), differs from the impedance of Z_B of other cross elements:

$$Z_{N_P} = Z_B + \Delta Z. \tag{6.20}$$

The value ΔZ can be generally both positive and negative; in case of circuit break in the element: $\Delta Z \to \infty$. The method also remains true in case of asymmetrically longitudinal impedance of recurrent circuit. If it has several asymmetrical impedances (cross, longitudinal or cross and longitudinal) the method also remains true, and in its realization some modifications are possible; they will be stated in the investigation of calculation features of currents distribution in damper winding elements of synchronous machines and squirrel cages of induction machines.

Let us introduce the following assumption:

- all impedances of recurrent circuit do not depend on currents in its elements, that confirm the recurrent circuit is linear.

Taking into account this assumption, the increment of currents in its elements at the occurrence of asymmetry $(\Delta Z \neq 0)$ is convenient to present in the form:

$$\underline{\underline{\mathbf{I}}}_{(N)} = \mathbf{I}_{(N)} + \Delta\mathbf{I}_{(N)}; \quad \underline{\underline{\mathbf{J}}}_{(N)} = \mathbf{J}_{(N)} + \Delta\mathbf{J}_{(N)}. \tag{6.21}$$

Here $\underline{\underline{\mathbf{I}}}_{(N)}, \mathbf{J}_{(N)}$—resulting currents in circuit elements after the occurrence of asymmetry, $I_{(N)}, J_{(N)}$—currents in symmetrical circuit (before the occurrence of asymmetry), let us name them as main; let us name increments $\Delta I_{(N)}, \Delta J_{(N)}$ as additional currents. Further it will be shown that in the absence of asymmetry, additional currents are equal to zero;

at $\Delta Z = 0 : \Delta I_{(N)} = 0$ and $\Delta J_{(N)} = 0$.

Let us note that in Eq. (6.21) all currents are time complex values (phasors). Let us write down equations under the second Kirchhoff's law [1, 2] for a number of loops of asymmetrical recurrent circuit; at first, let us allocate in it loops only with symmetrical elements $(Z_B = \text{idem.}, Z_R = \text{idem.})$ they satisfy the ratio: $(N_{P+1}, N_P) < N < (N_P, N_{P-1})$. For these loops, the following is true:

$$\underline{\underline{J}}_{(N)} \cdot Z_B - \underline{\underline{J}}_{(N-1)} \cdot Z_B - 2 \cdot \underline{\underline{I}}_{(N-1)} \cdot Z_R = 0.$$

With account of (6.20) and (6.21), we have:

$$J_{(N)}Z_B - J_{(N-1)} \cdot Z_B - 2I_{(N)}Z_R + \left[\Delta J_{(N)} - \Delta J_{(N-1)}\right]Z_B - 2\Delta I_{(N-1)}Z_R = 0. \tag{6.22}$$

Let us note that in Eq. (6.22) for these loops the first three summands correspond to the distribution of currents in a passive symmetrical circuit; their sum is equal to zero: EMF sources in loop are absent.

This important result allows us to subdivide calculation problem of currents distribution in asymmetrical recurrent circuit into two problems:

- calculation of main currents distribution $I_{(N)}$ and $J_{(N)}$ in a symmetrical recurrent circuit before the occurrence of asymmetry in it $(\Delta Z = 0)$;

- calculation of additional currents distribution $\Delta I_{(N)}$ and $\Delta J_{(N)}$ in an asymmetrical recurrent circuit after the occurrence of asymmetry in it ($\Delta Z \neq 0$);

resulting currents $\underline{\underline{\mathbf{I}}}_{(N)}$ and $\underline{\underline{\mathbf{J}}}_{(N)}$ are determined by their addition as per (6.21).

Other summands in (6.22) form the equation:

$$\left[\Delta J_{(N)} - \Delta J_{(N-1)}\right] \cdot Z_B - 2 \cdot \Delta I_{(N-1)} \cdot Z_R = 0. \tag{6.23}$$

Relation between additional currents ΔJ and ΔI is determined by the first Kirchhoff's law similarly to Eq. (6.6):

$$\Delta J[N] = \Delta I[N] - \Delta I[N-1]; \Delta J[N-1] = \Delta I[N-1] - \Delta I[N-2]. \tag{6.6'}$$

As a result, we obtain the following difference equation of the second order:

$$\Delta I[N+2] - (2+\sigma) \cdot \Delta I[N+1] + \Delta I[N+0] = 0 \tag{6.7''}$$

It is similar to Eq. (6.7), but describes the distribution of additional currents caused by asymmetry in recurrent circuit. The solution of this difference equation after transformations has the form:

for circuit elements with numbers $N < N_P$:

$$\Delta I_{(N)} = C_1 \cdot a_1^N + C_2 \cdot a_2^N, \tag{6.24}$$

for circuit elements with numbers $N \geq N_P$:

$$\Delta I_{(N)} = C_3 \cdot a_1^N + C_4 \cdot a_2^N. \tag{6.25}$$

Here C_1, C_2, C_3, C_4—constants determined by boundary conditions for additional currents of recurrent circuit; therefore, they depend on its structure and damage rate of its elements (asymmetry degree). Coefficients a_1, a_2 are determined by parameters of recurrent circuit elements before damage and do not depend on the asymmetry degree; they are found according to Eq. (6.12).

Equations (6.24) and (6.25) correspond to the distribution of additional currents in longitudinal elements. Equations for additional currents in cross elements:

for circuit elements with numbers $N < N_P$:

$$\Delta J_{(N)} = C_1 \cdot a_1^{N-1} \cdot (a_1 - 1) + C_2 \cdot a_2^{N-1} \cdot (a_2 - 1), \tag{6.26}$$

for circuit elements with numbers $N > N_P$:

$$\Delta J_{(N)} = C_3 \cdot a_1^{N-1} \cdot (a_1 - 1) + C_4 \cdot a_2^{N-1} \cdot (a_2 - 1), \tag{6.27}$$

for circuit elements with numbers $N = N_P$:

$$\Delta J_{(N)} = C_3 \cdot a_1^{N_P} - C_1 \cdot a_1^{N_P-1} + C_4 \cdot a_1^{N_P} - C_2 \cdot a_2^{N_P-1}. \tag{6.28}$$

6.7.2 Constants of Asymmetrical Passive Open Recurrent Circuit; Their Determination

6.7.2.1 General Case of Asymmetry: $0 < \Delta Z < \infty$

Let us allocate in recurrent circuit loops containing asymmetrical cross elements with number Np; its impedance corresponds to Eq. (6.20).

In order to determine the constants C_1, C_2, C_3, C_4 from boundary conditions and expressions for calculation of additional currents in the circuit, let us use the following four equations:

(a) It is easy to obtain two equations under the second Kirchhoff's law for two loops containing asymmetrical element with number N_P;

for circuit loop with number (N_P, $N_P - 1$):

$$\begin{aligned} &J_{(N_P)}Z_B - J_{(N_P-1)}Z_B - 2I_{(N_P-1)}Z_R + \Delta J_{(N_P)}Z_{N_P} - \Delta J_{(N_P-1)}Z_B \\ &\quad - 2\Delta I_{(N_P)}Z_R + J_{(N_P)}\Delta Z \\ &\quad = 0; \end{aligned} \tag{6.29}$$

for circuit loop with number (N_{P+1}, N_P):

$$\begin{aligned} &J_{(N_P+1)}Z_B - J_{(N_P)}Z_B - 2I_{(N_P)}Z_R + \Delta J_{(N_P+1)}Z_B - \Delta J_{(N_P)}Z_{N_P} - 2\Delta I_{(N_P)}Z_R \\ &\quad - J_{(N_P)}\Delta Z \\ &\quad = 0. \end{aligned} \tag{6.30}$$

After transformation of these equations, we get:

$$\Delta I_{(N_P)}\left(1 + \frac{\Delta Z}{Z_B}\right) - \Delta I_{(N_P-1)}\left(2 + \sigma + \frac{\Delta Z}{Z_B}\right) + I_{(N_P-1)} = -J_{(N_P)}\frac{\Delta Z}{Z_B}; \tag{6.31}$$

$$\Delta I_{(N_P+1)} - \Delta I_{(N_P)}\left(2 + \sigma + \frac{\Delta Z}{Z_B}\right) + I_{(N_P-1)}\left(1 + \frac{\Delta Z}{Z_B}\right) = J_{(N_P)}\frac{\Delta Z}{Z_B}; \tag{6.32}$$

(b) Two other equations result from the recurrent circuit structure. For closed and open recurrent circuits they are different.

Let us consider the determination of constants for an open circuit containing N_0 cross elements. For such a circuit the following two equations under the first Kirchhoff's law are true:

$$\begin{gathered}\Delta I_{(0)} = \Delta J_{(0)}; \Delta I_{(N_0-2)} = -\Delta J_{(N_0-1)} \text{ or} \\ C_1 \cdot a_2 + C_2 \cdot a_1 = 0. \quad C_3 \cdot a_1^{N_0-1} + C_4 \cdot a_2^{N_0-1} = 0.\end{gathered} \tag{6.33}$$

To obtain calculation expressions for additional currents in elements of open recurrent circuit, it is necessary to determine constants C_1, C_2, C_3, C_4.

Equations (6.31)–(6.33) form a system for their determination.

After transformation of these equations, the system takes the form:

$$\begin{gathered}M \cdot C_1 + T \cdot C_2 + A \cdot C_3 + B \cdot C_4 = -J_{(N_P)} \frac{\Delta Z}{Z_B}; \\ (M+H) \cdot C_1 + (T+K) \cdot C_2 + (A+F) \cdot C_3 + (B+S) \cdot C_4 = 0; \\ N \cdot C_1 + P \cdot C_2 = 0; \quad Q \cdot C_3 + R \cdot C_4 = 0.\end{gathered} \tag{6.34}$$

Values of system coefficients are given in Appendix 6.1.

The order of this system (r = 4) does not depend on the number of links of recurrent circuit being the advantage of method in practical calculations.

From this system we obtain constants for calculation of algebraic adjuncts for currents:

$$C_i = J_{(N_P)} \cdot \frac{\Delta Z}{Z_B} \cdot \frac{D_i}{D_S}.$$

Here D_S—system determinant, D_i—corresponding algebraic adjuncts; i = 1, 2, 3, 4.

System determinant ($N_B = N_{0-2}$):

$$\begin{aligned}D_S = {} & a_1^{N_B+1}\left(a_1^2 - 1 + 2a_1\frac{\Delta Z}{Z_B} - 2\frac{\Delta Z}{Z_B}\right) + a_2^{N_B+1}\left(a_2^2 - 1 + 2a_2\frac{\Delta Z}{Z_B} - 2\frac{\Delta Z}{Z_B}\right) \\ & + \frac{\Delta Z}{Z_B}\left(a_1^{2N_P-N_B-1} + a_2^{2N_P-N_B-1}\right)(2 - a_1 - a_2).\end{aligned} \tag{6.35}$$

Let us note that the third multiplier in the last summand, in brackets, according to Vieta theorem (6.12) equals: $2 - a_1 - a_2 = -2\frac{Z_R}{Z_B}$.

Algebraic adjuncts of system:

$$\begin{gathered}D_1 = \left(a_1^{N_B-N_P-1} + a_1^{N_B-N_P+2}\right)(a_1 - 1), \quad D_2 = \left(a_1^{N_B-N_P} + a_1^{N_P-N-3}\right)(1 - a_1), \\ D_3 = \left(a_1^{N_P-N_B-1} + a_1^{-N_B-N_P-2}\right)(a_1 - 1), \quad D_4 = \left(a_1^{N_P+N_B+1} + a_1^{N_B-N_P}\right)(1 - a_1).\end{gathered} \tag{6.36}$$

We obtained that the system determinant D_S linearly depends on the asymmetry ΔZ of recurrent circuit, and additions D_1, D_2, D_3, D_4 do not depend on ΔZ.

The obtained calculation Eqs. (6.35) and (6.36) prove that in a symmetrical recurrent circuit (at $\Delta Z = 0$) the additional currents in its elements are absent. It proves the validity of developed calculation method of asymmetrical open recurrent circuits.

6.7.2.2 Asymmetry Limit Case: Circuit Break ($\Delta Z \to \infty$)

Checking results

Calculation expressions for currents in asymmetrical recurrent circuits in relation to short-circuited rotor loops are obtained for the first time [13], and, therefore, they require additional checks.

Let us consider one of them: at $\Delta Z \to \infty$ the resulting current in element with number $N = N_p$ should be obtained from equations equal to zero.

At circuit break in the element ($\Delta Z \to \infty$) the calculation expression for currents follows from the obtained expressions by passage to the limit [8–10]. As a result, we have:

$$C_i = J_{(N_P)} \cdot \frac{D_i}{D_\infty} \text{ for } i = 1, 2, 3, 4. \tag{6.37}$$

Here, D_i—as per (6.36) for i = 1, 2, 3, 4.

$$\begin{aligned} D_\infty = {} & 2a_1^{N_B+1}(a_1 - 1) + 2a_2^{N_B+1}(a_2 - 1) \\ & + \left(a_1^{2N_P - N_B - 1} + a_2^{2N_P - N_B - 1}\right)(2 - a_1 - a_2). \end{aligned} \tag{6.38}$$

It follows from this equation that at $N = N_P$ and $\Delta Z \to \infty$ the absolute value of additional current in cross element is equal to the main one, but opposite in sign $\Delta J_{(N_P)} = -J_{(N_P),}$, so the resulting current $\underline{J}_{=(N_P)}$ in the element with this number is equal to zero as per (6.21). This result is an additional proof of the method developed.

It should be noted that analysis methods of closed asymmetrical recurrent circuits are similar to those of open circuits and differ only in formulation of boundary conditions. They will be considered in the following chapters in relation to active recurrent circuits.

6.7.3 Calculation Examples

Let us continue the consideration of examples given in the previous paragraph for angle $\varphi = 180°$. Distribution of currents in symmetrical recurrent circuit for this case is given in Table 6.2.

6.7.3.1 Asymmetry $\Delta Z_{N_P} = 2$

Let us accept in addition that in cross elements with number $N = N_P = 2$ of this circuit there is an asymmetry: $\Delta Z = 2$; circuit asymmetry degree $\frac{\Delta Z}{Z_B} = 0.4$. Then we find the distribution of currents in this asymmetrical circuit.

System determinant according to Eq. (6.35) is equal to: $D_S = 1611.749$; algebraic adjuncts according to Eq. (6.36) are equal to: $D_1 = 121.896$; $D_2 = -15.018; D_3 = 0.0804; D_4 = -2831.989$.

Calculation results of distribution of additional currents in recurrent circuit elements are given in Table 6.4

Calculation results of resulting currents distribution in recurrent circuit elements are given in Table 6.5.

From calculation results, it follows:

- at asymmetry $\left(\Delta Z = 2; \quad \frac{\Delta Z}{ZB} = 0.4\right)$ in comparison with the symmetrical recurrent circuit (Table 6.2), the cross element with number $N = N_P = 2$ is unloaded, however, the currents passing through adjacent cross elements increase, and the extent of distortion decreases with an increase in the distance from asymmetrical element;

Table 6.4 Distribution of additional currents $(\varphi = 180^\circ)$

N	$\Delta I_{(N)}$	$\Delta J_{(N)}$
0	−0.2879	−0.2879
1	−0.9186	−0.631
2	0.9354	1.854
3	0.3239	−0.612
4	0.1012	−0.2227
5	$-7.7236 \cdot 10^{-6} \approx 0$	−0.1012

Table 6.5 Distribution of resulting currents in recurrent circuit elements $(\varphi = 180^\circ)$

N	$\underline{I}_{(N)}$	$\underline{J}_{(N)}$
−1	100.0 (boundary condition)	
0	34.3449	−65.655
1	9.9038	−24.4411
2	0.9354	−8.9684
3	−10.4994	−11.4348
4	−34.5331	−24.0337
5	−100.0 (boundary condition)	−65.4733

- the sum of currents in cross elements satisfies the first Kirchhoff's law and proves validity of developed calculation method for asymmetrical passive recurrent circuits:

$$\underline{\underline{J}}_{(0)} + \underline{\underline{J}}_{(1)} + \underline{\underline{J}}_{(2)} + \underline{\underline{J}}_{(3)} + \underline{\underline{J}}_{(4)} + \underline{\underline{J}}_{(5)} = \underline{\underline{I}}_{(N_0-1)} - \underline{\underline{I}}_{(-1)} = -200(A).$$

6.7.3.2 Limiting Case

Limit case: circuit break $(\Delta Z \to \infty)$ in cross element with number $N = N_P = 2$.

Checking results.

According to Eqs. (6.37) and (6.38) we have:

$D_S = 690.269$; constants are equal to $C_1 = -1.9112$; $C_2 = 0.2354$; $C_3 = -1.2605 \cdot 10^{-3}$; $C_4 = 44.4014$.

The additional current in the element with number $N = N_P = 2\,(\Delta Z \to \infty)$ is equal to: $\Delta J_{(N)} = 10.82$; resulting current according to Table 6.2 is equal to: $\underline{\underline{J}}_{(N)} = 0$. This result also proves the validity of developed calculation method.

Appendix 6.1

System coefficients to determine the constants C_1, C_2, C_3, C_4.

$$M = -a_1^{N_P-1}\left(a_1 + \frac{\Delta Z}{Z_B}\right); \quad A = a_1^{N_P}\left(1 + \frac{\Delta Z}{Z_B}\right); \quad H = a_1^{N_P-1}\left(1 + \frac{\Delta Z}{Z_B}\right);$$

$$F = -a_1^{N_P}\left(a_2 + \frac{\Delta Z}{Z_B}\right); \quad N = a_2; \quad Q = a_1^{N_B+1}.$$

Coefficients T, B, K, S, P, R can be obtained respectively from those M, A, H, F, N, Q by replacement a_1 by a_2 and, respectively, a_2 by a_1.

Brief Conclusions

1. In passive symmetrical recurrent circuits ($\Delta Z = 0$) equations for calculation of currents distribution in elements contain two components; both vary depending on the element number (N) under the aperiodic law.

2. In passive asymmetrical recurrent circuits ($\Delta Z \neq 0$) calculation of currents distribution in elements can be reduced to the solution of two problems:
   - calculation of distribution of the main currents in elements of symmetrical recurrent circuits ($\Delta Z = 0$);
   - calculation of distribution of additional currents which depends on the distribution of the main;
   - calculation of distribution of resulting currents is reduced to the summation of the main and additional currents for the same elements.
3. Equations for calculation of distribution of additional currents contain two components in elements of an asymmetrical recurrent circuit; both vary depending on the element number (N) under the aperiodic law.
4. For limiting case—cross element break ($\Delta Z \rightarrow \infty$)—the main and additional currents are equal in amplitude and are opposite in phase so the resulting current is equal to zero. It proves validity of the obtained equations.
5. Numerical examples also prove validity of the obtained calculation expressions.

List of Symbols

A, B, C, D	Constants determined by quadripole impedances;
C_1, C_2, …, C_M	Constants for calculation of currents determined by boundary conditions of recurrent circuit;
I[N], J[N]	Currents in longitudinal and cross element of recurrent circuit with number N by solution of difference equations;
$I_{(N)}$ and $J_{(N)}$	Dependence of currents in recurrent circuit elements on element number N;
I_{INP}, I_{OUT}	Complex amplitudes of currents at recurrent circuit input and output;
$\Delta I_{(N)}, \Delta J_{(N)}$	Additional currents in longitudinal and cross elements of asymmetrical recurrent circuit;
k_1, k_2, …, k_M	Coefficients determined by impedances of recurrent circuit elements;
N	Element number of recurrent circuit;
N_0	Number of elements in recurrent circuit;
N_P	Asymmetrical element number;
U_2, I_1	Voltage and current at passive quadripole input;
U_2, I_2	Voltage and current at passive quadripole output;
$Z_{B_1}, Z_{B_3}, Z_{R_1}, Z_{R_3}$	Impedances of recurrent circuit elements;
Z_{NP}	Impedance of asymmetrical element;
ΔZ	Additional impedance of asymmetrical element;
σ	Relation determined by impedances of elements of symmetrical recurrent circuit;
$\varphi_{INP}, \varphi_{OUT}$	Phase angles of currents at recurrent circuit input and output

References

I. Monographs, general courses, textbooks

1. Demirchyan K.S., Neyman L.R., Korovkin N.V., Theoretical Electrical Engineering Moscow, St. Petersburg: Piter, Vol. 1, 2, 2009. (In Russian).
2. Kuepfmueller K., Kohn G., Theoretische Elektrotechnik und Elektronik. 15 Aufl. Berlin, N. Y.: Springer. 2000. (In German).
3. Carson J.R., Elektrische Ausgleichvorgaenge und Operatorenrchnung. Berlin: Springer, 1929. (In German).
4. Doetsch G., Handbuch der Laplace – Transformation. Baende 1,2,3. Basel: Verlag Birkhaeuser, 1973. (In German).
5. Doetsch G., Einfuehrung in Theorie und Anwendung der Laplace – Transformation. Basel: Verlag Birkhaeuser, 1976. (In German).
6. Ruedenberg R., Elektrische Schaltvorgaenge. Berlin, Heidelberg, N.-Y.: Springer, 1974. (In German).
7. Gardner M., Barnes J., Transients in Linear Systems Studied by the Laplace Transformation, N. Y.: J. Wiley, 1942.
8. Jeffris H., Swirles B., Methods of Mathematical Physics. Third Edition, Vol. 1 – Vol. 3, Cambridge: Cambridge Univ. Press, 1966.
9. Boguslawsky I.Z., A.C. motors and generators. The theory and investigation methods by their operation in networks with non linear elements. Monograph. TU St. Petersburg Edit., 2006. Vol. 1; Vol.2. (In Russian).
10. Korn G., Korn T., Mathematical Handbook, N. Y.: McGraw – Hill, 1961.

II. Asynchronous machines. Papers, inventor's certificates, patents

11. Boguslawsky I.Z., Methods of MMF investigation for the cage rotor damaged bars. Proc.: The problems of development and operation of new types of power equipment. Department of electrical power problems in Russian Academy of Science. St. Petersburg. 2003. (In Russian.).
12. Boguslawsky I.Z., Demirtschian K.S., Stationaere Stromverteilung in unregelmaessigen und unsymmetrischen kurzgeschlossenen Laeuferwicklungen von Wechselstrommaschinen. Archiv fuer Elektrotechnik, 1992, № 6 (In German).

III. Synchronous machines. Papers, inventor's certificates, patents

13. Demirchyan K.S., Boguslawsky I.Z., Current flowing in damper winding bars of different resistivity in a heavy- duty low speed motor. Proceedings of the Russian Academy of Sciences. Energetika i Transport, 1980, #2. (In Russian).
14. Boguslawsky I.Z., Currents and harmonics MMFs in a damper winding with damaged bar at a pole. Power Eng. (New York), 1985, #1.

Chapter 7
Active Symmetrical and Asymmetrical Chain Circuits: Investigation of Their Peculiarities for Modeling Process of Currents Distribution in Short-Circuited Rotor Windings

This chapter develops investigation methods for active U-shaped chain (recurrent) circuits of various structures in relation to designs of short-circuited rotor windings of large A.C. machines; EMFs of links vary with link number under a certain law, for example, harmonic one. The solution for a general problem and for a number of special cases is found for this distribution of EMF in links, regularities of distribution of currents in elements of symmetrical closed and open chain circuits, and also elements of asymmetrical chain circuits of the same structure follow these solutions. It is obtained that the current in elements of these chain circuits is distributed under some complicated law: current contains three components which vary with number N of U-shaped chain circuit link as follows:

- one of them varies depending on this number under the harmonic law;
- two others—under aperiodic.

For checking solution results, it is confirmed that in that specific case calculation expressions for currents in active regular chain circuit and in open symmetric chain circuit coincide. Analysis methods for active chain circuits of various structure investigated in the monograph are used to solve the problems of currents distribution in elements of short-circuited rotor windings of various design (damper regular and irregular, squirrel cages with damage one or several bars). Methods are proved with numerical examples.

The content of this chapter is development of the methods stated in [1, 2, 8–12].

I. Boguslawsky et al., *Large A.C. Machines*,
DOI 10.1007/978-4-431-56475-1_7

7.1 Main Definitions. Structural Kinds of Active U-Shaped Chain Circuits and Peculiarities of EMF Distribution of Loops

For investigation of real constructions of A.C. machines in nonlinear networks or with sharply variable loads, it was necessary to develop calculation methods of currents distribution in active chain circuits; occurrence of EMF source is supposed in each link of such a circuit.

In further statement, among active chain circuits we will distinguish the same versions as for passive circuits. Their determination is given in Chap. 6.

Let us repeat them briefly. Active chain circuits differ:

- in the ratio of values of longitudinal and cross elements: symmetrical and asymmetrical; In asymmetrical circuits we will distinguish between regular and irregular circuits;
- in structure: open and closed.

In this monograph from a variety of active chain circuits of various structure, we will consider only one type of symmetrical and asymmetrical circuits representing practical interest for investigation of currents distribution in short-circuited rotor loops of A.C. machines. Let us turn our attention to peculiarities of this type and mathematical formulation of problem on calculation of currents distribution in active chain circuit elements.

Let us consider some links (elements) of a symmetrical active chain circuit given in Fig. 7.1. Let us designate, as for a passive chain circuit, serial numbers of circuit cross elements as follows: N = 0, 1, 2, …, N − 1, …, N + 1….; we will assign number N to each longitudinal element set between two cross element with numbers N + 1 and N. Respectively, to the loop set between cross elements with numbers N + 1 and N and longitudinal element with number N we will assign number: (N + 1, N). We will assign this number also to loop EMF: $E_{N+1,N}$.

Peculiarities of symmetrical chain circuits of this type are as follows:

- EMFs of all links vary with time under the harmonic law;
- amplitudes of EMF of all links are identical;
- EMF phase angles φ_N vay linearly with number N, so

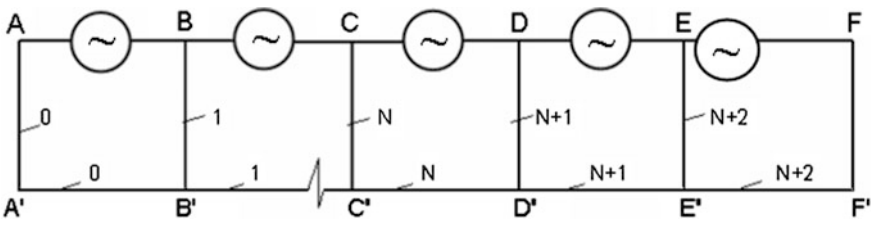

Fig. 7.1 Active open chain circuit

$$\varphi_N = \varphi_0 + kN, \tag{7.1}$$

where φ_0—initial phase angle, k—proportionality coefficient.

Then, EMF amplitude $E_{N+1,N}$ in the loop (N + 1, N) of this circuit (Fig. 7.1) is equal to:

$$E_{N+1,N} = |E_M| e^{j(\omega t - \varphi_N)} = E_M e^{-jk_N}, \quad \text{where } E_M = |E_M| e^{j(\omega t - \varphi_0)}. \tag{7.2}$$

Here E_M—complex amplitude (phasor) of EMF, $|E|_M$—its value, ω—current angular frequency, t—time.

Let us determine, at first, physical conception of coefficient k. We find a difference between EMF phase angles of links with number N + 1 and N:

$$\Delta\varphi_N = \varphi_{N+1} - \varphi_N = k \tag{7.1'}$$

Therefore, the coefficient k characterizes a phase shift angle between EMF of adjacent elements of chain circuit; according to the determination of symmetrical active chain circuit we obtain: k = idem. This is one of peculiarities of considered type of symmetrical chain circuits: EMF changes depending on link number under the harmonic law.

Using the ratios (7.2) and (7.1′), let us write down calculation expressions for EMF of symmetrical chain circuit links as follows $(\Delta\varphi_N = \Delta\varphi)$:

$$\begin{aligned} &E_{2,1} = E_M e^{-j\Delta\varphi}; \quad E_{3,2} = E_M e^{-j2\Delta\varphi}; \quad E_{4,3} = E_M e^{-j3\Delta\varphi}; \ldots; \\ &E_{N+2,N+1} = E_M e^{-j(N+1)\Delta\varphi}; \quad E_{N+3,N+2} = E_M e^{-j(N+2)\Delta\varphi}; \ldots. \end{aligned} \tag{7.3}$$

Let us note peculiarities of asymmetrical active chain circuit. Generally:

- amplitudes of EMF of its links E_M are not identical;
- shift angle of adjacent links $\Delta\varphi_N$ does not remain constant:

$$E_M \neq \text{idem}; \quad \Delta\varphi_N = k \neq \text{idem}\cdot \tag{7.4}$$

In that specific case, conditions (7.1) and (7.2) can persist in an asymmetrical chain circuit for group of loops, true for symmetrical circuits, and for some of them —conditions (7.4). This active asymmetrical chain circuit in addition to the formulation given in Chap. 6 we will name regular. It corresponds to the construction of salient pole machine damper winding.

To study the currents in these windings, the method based on finite-difference equations [3–5] is developed in this monograph. Solution for currents in active chain circuits in comparison with that for currents in passive circuits has peculiarities as the right parts of difference equations contain EMFs other than zero and changing under a certain law.

Let us find an analytical expression for currents distribution in symmetrical chain circuit elements; they satisfy Eqs. (7.1) and (7.2).

7.2 Methods of Investigation of Active Symmetrical Chain Circuits with EMFs Changing Depending on Number of Link Under the Harmonic Law

7.2.1 Difference Equations, Methods of Their Solution

For calculation of currents in active symmetrical chain circuits, we will accept as initial the following:

- impedances of longitudinal elements Z_R;
- impedances of cross elements Z_B;
- EMF in each circuit link.

Let us consider elements of symmetrical active chain circuit (Fig. 7.1).

Let us allocate the loop (N + 2, N + 1) formed by cross elements with numbers N + 2, N + 1 and longitudinal with number N + 1. For this loop we will write down the second Kirchhoff's equation [1, 2]:

$$(J[N+2] - J[N+1])Z_B - 2I[N+1]Z_R = E_{N+2,N+1}, \tag{7.5}$$

where J, I—respectively currents in cross and longitudinal elements, and EMF $E_{N+2,N+1}$—as per (7.3):

$$E_{N+2,N+1} = E_M \cdot e^{-jk(N+1)} = E_M \cdot e^{-jk} \cdot e^{-jkN}, \tag{7.6}$$

where E_M—as per (7.2).

Let us use the ratios between currents in longitudinal and cross elements according to the first Kirchhoff's law (6.6).

After transformation (7.5) we obtain:

$$I[N+2] - (2+\sigma)I[N+1] + I[N+0] = \frac{E_M}{Z_B} e^{-jk-jkN}, \tag{7.7}$$

where $\sigma = 2\frac{Z_B}{Z_R}$.

Let us represent the solution of difference Eq. (7.7) in the form of two summands [3–5]:

$$I_{(N)} = I'_{(N)} I''_{(N)}. \tag{7.8}$$

The first summand in (7.8) is calculated from the homogeneous uniform difference equation [3–5]:

$$I[N+2] - (2+\sigma) \cdot I[N+I] + I[N+0] = 0. \tag{7.9}$$

It corresponds to currents distribution in a passive chain circuit and is already obtained in Chap. 6 earlier:

$$I'_{(N)} = C_1 a_1^N + C_2 a_2^N,$$

where C_1, C_2—constants determined by boundary conditions. These conditions are formulated taking into account concrete peculiarities of active chain circuits structure; for example, for closed and open circuits they are differ.

Values a_1 and a_2 are determined from the solution of characteristic equation obtained earlier in the same Chap. 6: $a_{1,2} = \frac{2+\sigma \pm \sqrt{\sigma^2+4\sigma}}{2}$.

Second summand I''_N in (7.8) is a particular solution of Eq. (7.7).

This solution, unlike the general one, corresponds to the right part of difference equation; physically this compliance means that currents in chain circuit loops determined by partial solution vary depending on number N under the same law, as EMF. Therefore, the partial solution should represent a function changing depending on number N under the harmonic law unlike currents $I'_{(N)}$ of general solution which change depending on number N under the aperiodic law. According to methods of solution of difference equations, let us previously find a partial solution in the form:

$$I''_{(N)} = \frac{E_M}{Z_B \cdot K_B} \cdot e^{-jkN}. \tag{7.10}$$

Here K_B factor—proportionality coefficient to be determined; partial solution of Eq. (7.7) is considered found if the calculation expression for this coefficient is determined.

It is easy to find it directly from Eq. (7.7) if we substitute Eq. (7.10) for $I''_{(N)}$ into this equation. After transformations we get:

$$K_B = \left[1 - (2+\sigma)e^{-jk} + e^{-j2k}\right]e^{jk}. \tag{7.11}$$

As a result, we obtain the solution of difference Eq. (7.7) and the expression for calculation of currents distribution in longitudinal elements of chain circuit:

$$I_{(N)} = I'_{(N)} + I''_{(N)} = C_1 a_1^N + C_2 a_2^N + \frac{E_M}{Z_B \cdot K_B} \cdot e^{-jkN}. \tag{7.12}$$

The expression for currents in cross elements of chain circuit is given by:

$$J_{(N)} = C_1 a_1^{N-1}(a_1 - 1) + C_2 a_2^{N-1}(a_2 - 1) + \frac{E_M}{Z_B K_B}\left(1 - e^{jk}\right)e^{j(-kN)}.$$

In practical calculations, it is sometimes convenient to represent the third current summand in cross elements a little differently. For this purpose, let us transform factor $1 - e^{jk}$ in the last equation:

$$1 - e^{jk} = e^{j\frac{k}{2}}\left(e^{-j\frac{k}{2}} - e^{j\frac{k}{2}}\right) = -j2e^{j\frac{k}{2}}\sin\frac{k}{2}.$$

As a result, we obtain the expression for calculation of currents distribution in longitudinal elements of chain circuit:

$$J_{(N)} = C_1(1 - a_2)a_1^N + C_2(1 - a_1)a_2^N - 2j + \frac{E_M}{Z_B K_B}e^{j\frac{k}{2}}\sin\frac{k}{2}e^{-jkN}. \tag{7.13}$$

Let us note that the solution of Eq. (7.7) has also the same appearance, if we represent EMF $E_{N+1,N}$ unlike (7.2) as follows:

$$E_{N+1,N} = |E_M| \cdot e^{j(\omega t - \varphi_N)} = |E_M|e^{-jkN} \cdot e^{-j\varphi_0}, \tag{7.14}$$

where φ_N—as per (7.1) and $E_M = |E_M|e^{j\omega t}$.

Let us proceed to the calculation of constants C_1, C_2 determined by specific peculiarities of chain circuit structure.

7.2.2 *Constants for Currents in Active Open Symmetrical Chain Circuits*

To determine the constants C_1, C_2 in Eqs. (7.12) and (7.13) let us formulate the following two boundary conditions, as well as for passive chain circuit:

$$J[0] = I[0]; \quad J[N-1] = -I[N-2]. \tag{7.15}$$

The first boundary condition (7.15) takes the form:

$$C_1 a_2 + C_2 a_1 = \frac{E_M}{Z_B \cdot K_B}e^{jk}. \tag{7.16}$$

The second boundary condition taking into account the same equations gives:

$$C_1 a_1^{N_0-1} + C_2 a_2^{N_0-1} = -\frac{E_M}{Z_B \cdot K_B} e^{j(k-kN_0)}. \tag{7.17}$$

Equations (7.16) and (7.17) form a system linear relative to constant C_1, C_2. Its solution is as follows:

$$\begin{aligned} C_1 &= \frac{E_M}{Z_B K_B} e^{jk} \frac{a_1 e^{-jkN_0} - a_2^{N_0-1}}{a_2^{N_0} - a_1^{N_0}}; \\ C_2 &= \frac{E_M}{Z_B K_B} e^{jk} \frac{a_1^{N_0-1} - a_2 e^{-jkN_0}}{a_2^{N_0} - a_1^{N_0}}. \end{aligned} \tag{7.18}$$

Thus, constant C_2 can be obtained from C_1 by substitution of a_2 by a_1 and, respectively, a_1 by a_2.

From an analysis of the obtained Eqs. (7.7)–(7.13) and (7.18), we can draw the following practical conclusion: unlike currents in elements of passive open chain circuit, currents in active circuit contain three components. From these components:

- two vary with number N under the aperiodic law,
- the third vary under the harmonic law.

7.2.3 *Constants for Currents in Active Closed Symmetrical Chain Circuits*

For determination of constants C_1, C_2, let us formulate the following boundary conditions:

$$I[0] - I[N_0 - 1] = J[0]; \quad I[N_0] = I[0]. \tag{7.19}$$

These boundary conditions are satisfied, if

$$C_1 = 0; \quad C_2 = 0. \tag{7.20}$$

These ratios are confirmed also by analytical computations given below.

Thus, currents in longitudinal elements of closed chain circuit are calculated from the ratio:

$$I_{(N)} = \frac{E_M}{Z_B K_B} e^{-jkN}. \tag{7.21}$$

Currents in its cross elements are calculated according to (7.6):

$$J_{(N)} = \frac{-2jE_M}{Z_B K_B} e^{j\frac{k}{2}} \sin\frac{k}{2} e^{-jkN}. \tag{7.22}$$

From analysis of the equations obtained (7.19) and (7.20) we can draw the following practical conclusion:

- currents in elements of symmetrical active closed chain circuit have one component; it changes with number N under the harmonic law.

7.2.4 *Constants for Currents in Regular Closed Chain Circuits*

These circuits belong to an asymmetrical class, and calculation expressions in their elements are more complicated than for symmetrical. Distribution of currents in regular closed chain circuit elements can be obtained, using general methods of investigation of asymmetrical chain circuits developed in the previous chapter. For this purpose it is sufficient to represent the impedance of asymmetrical longitudinal element of regular circuit as the sum as per (6.20) and to write down equations according to both Kirchhoff's laws for calculation of additional currents.

However, in this para is developed other method. It is not requiring representation of the current in elements of regular circuit as the sum of two components: of the main and additional currents. It is made with account of future research problem of currents in elements of irregular damper winding synchronous machine, which can be represented as irregular closed chain circuit. When using for its solution general methods of investigation of asymmetrical active chain circuits, we are required to have two types of additional impedance (ΔZ_R for longitudinal asymmetrical element and ΔZ_B—for cross one); respectively, we have for each element two types of additional currents: longitudinal and cross currents caused by the asymmetry in cross element (ΔI_B and ΔJ_B), but also longitudinal and cross currents caused by the asymmetry in longitudinal element (ΔI_R and ΔJ_R). Preliminary calculations show that the problem solution does not meet any essential difficulties, but considerably complicates checking intermediate results important in engineering practice for confident use of the method.

Let us consider a chain circuit, where EMF changes phase angle determined in limits: $0 \leq \varphi \leq 2\pi$. For this purpose, it is possible to use Fig. 6.3, if in addition we consider that:

- between two cross elements A_1A_1' and B_1B_1'; B_1B_1' and F_1F_1'; …; A_2A_2' and B_2B_2'; B_2B_2' and F_2F_2'; …; there are EMF sources changing under the harmonious law;
- terminals O_1O_1' are superimposed with terminals O_3O_3'.

When the phase angle varies within $0 \leq \varphi \leq 2\pi$, it would be possible to assume that currents in longitudinal elements of chain circuit in portions $A_1B_1F_1$ and $A_2B_2F_2$ at N = idem are respectively equal in value and opposite in sign, that is are shifted in time by angle $\varphi = \pi$. The same assumption can be also formulated for cross elements. These assumptions are obvious to one of three components of currents in Eqs. (7.12) and (7.13): it varies with number N under the harmonic law. However, for other two components of currents in Eqs. (7.12) and (7.13) which vary with number N under the aperiodic law, this assumption demands an additional proof.

Taking into account this remark, let us write down for determination of constants for currents a system of equations according to both Kirchhoff's laws [8–10]. From its solution we will also determine constants for aperiodic components of currents.

Let us represent the equation for currents in longitudinal elements in portions $A_1B_1F_1$ for convenience in the form (index N at all currents I, J is omitted):

$$I^{C_p} = C_0 \cdot a_0^N + C_1 \cdot a_1^N + C_2 \cdot a_2^N. \tag{7.23}$$

Here, in all expressions for currents in chain circuit elements the results of particular solution of difference equation are designated as follows:

$$C_0 = \frac{E_M}{Z_B K_B}; \quad a_0 = e^{-jk}.$$

It simplifies checking results, when performing algebraic transformations as all three summands for currents in Eq. (7.23) take the similar form.

Respectively, the equation for currents in cross elements in portion $A_1B_1F_1$ take the form:

$$J^{C_p} = C_0 a_0^N \left(1 - a_0^{-1}\right) + C_1 a_1^N (1 - a_2) + C_2 a_2^N (1 - a_1). \tag{7.24}$$

The equation for currents in longitudinal elements in portion $A_2B_2F_2$ is similar to (7.23):

$$I^{S_p} = C_0' a_0^N + C_1' a_1^N + C_2' a_2^N. \tag{7.25}$$

Here constants C_0, C_1, C_2 (current with index C_p) corresponds to currents in elements in portion $A_1B_1F_1$, and constants C_0', C_1', C_2' (current with index S_p)—in portion $A_2B_2F_2$.

The equation for currents in cross elements in portion $A_2B_2F_2$ is similar to (7.24):

$$J^{S_p} = C_0' a_0^N \left(1 - a_0^{-1}\right) + C_1' a_1^N (1 - a_2) + C_2' a_2^N (1 - a_1). \tag{7.26}$$

For the last two equations by determination the following is true:

$$C'_0 = -C_0. \tag{7.27}$$

Now, let us use both Kirchhoff's laws. According to the second Kirchhoff's law for loops $F_1F'_1A_2A'_2F_1$ and $F_2F'_2A'_1A_1F_2$ we have (terminals $O_1O'_1$ are superimposed with terminals $O_3O'_3$):

$$\left(J_0^{S_P} - J_{N_0-1}^{C_P}\right)Z_B - 2I_{N_0-1}^{C_P}Z_{F_1A_2} = E_{F_1A_2}. \tag{7.28}$$

$$\left(J_0^{C_P} - J_{N_0-1}^{S_P}\right)Z_B - 2I_{N_0-1}^{S_P}Z_{F_2A_1} = E_{F_2A_1}. \tag{7.29}$$

Here $Z_{F_1A_2} = Z_{F'_1A'_2} = Z_{F_2A_1} = Z_{F'_2A'_1}$—impedance of corresponding portions $\left(F_1A_2; F'_1A'_2; F_2A_1; F'_2A'_1\right)$. $E_{F_1A_2}$ and $E_{F_2A_1}$ EMFs correspond to EMF in loops $F_1F'_1A'_2A_2F_1$ and $F_2F'_2A'_1A_1F_2$. Let us note that for the type of active chain circuits considered, the following relation takes place: $E_{F_1A_2} = -E_{F_2A_1}$.

For the same loops according to the first Kirchhoff's law:

$$I_{N_0-2}^{C_P} + J_{N_0-1}^{C_P} = I_0^{S_P} - J_0^{S_P}, \tag{7.30}$$

$$I_{N_0-2}^{S_P} + J_{N_0-1}^{S_P} = I_0^{C_P} - J_0^{C_P}. \tag{7.31}$$

Equations (7.28)–(7.31) form a system, where four constants C_1, C_2, C'_1, C'_2 are unknown. Let us note that between currents in longitudinal and cross elements entering Eqs. (7.28)–(7.31), the following relations are true:

$$J_0^{S_P} = I_0^{S_P} - I_{-1}^{S_P}; \quad J_{N_0-1}^{C_P} = I_{N_0-1}^{C_P} - I_{N_0-2}^{C_P}. \tag{7.32}$$

After algebraic transformations of system Eqs. (7.28)–(7.31) taking into account relations for currents (7.32) we obtain this system as follows:

$$\begin{cases} C_1 \cdot D + C_2 \cdot E + C'_1 \cdot A + C'_2 \cdot B = \prod_1; \\ C_1 \cdot A + C_2 \cdot B + C'_1 \cdot D + C'_2 \cdot E = -\prod_1; \\ C_1 \cdot F + C_2 \cdot G + C'_1 \cdot H + C'_2 \cdot K = \prod_2; \\ C_1 \cdot H + C_2 \cdot K + C'_1 \cdot F + C'_2 \cdot G = -\prod_2. \end{cases} \tag{7.33}$$

Here coefficients in the left part of system equations:

$$A = Z_B(1 - a_2); B = Z_B(1 - a_1); D = Z_B a_1^{N_0-2}(1 - a_1) - 2a_1^{N_0-1}Z_{F_1A_2};$$
$$E = Z_B a_2^{N_0-2}(1 - a_2) - 2a_2^{N_0-1}Z_{F_1A_2}; F = a_1^{N_0-1}; G = a_2^{N_0-1}; H = -a_2; K = -a_1.$$

Right parts of system equations:

$$\prod_1 = E_{F_1A_2} + C_0 Z_B\left(1 - a_0^{-1}\right) + C_0\left[Z_B a_0^{N_0-2}(a_0 - 1) + 2Z_{F_1A_2} a_0^{N_0-1}\right]; \prod_2 = -C_0\left(a_0^{N_0-1} + a_0^{-1}\right).$$

Let us find unknowns $C_1; C_2; C_1'; C_2'$ of this system. By a general rule of its solution they are equal to [5, 6]:

$$C_1 = \frac{D_1}{D_0}; \quad C_2 = \frac{D_2}{D_0}; \quad C_1' = \frac{D_1'}{D_0}; \quad C_2' = \frac{D_2'}{D_0}.$$

Here: D_0– system determinant, D_1, D_2, D_1', D_2'—its algebraic adjuncts.

Let us expand the determinant. For algebraic adjuncts D_1 and D_1' we obtain:

$$D_1 = [(A + D)(G + K) - (B + E)(H + F)] \cdot [(G - K)\prod_1 - (E - B)\prod_2]$$
$$D_1' = [(A + D)(G + K) - (B + E)(H + F)] \cdot [-(G - K)\prod_1 + (E - B)\prod_2]$$

Now, let us find the sum of these algebraic adjuncts: $D_1 + D_1' = 0$.

Similarly, the sum of algebraic adjuncts D_2 and D_2' is also obtained equal to zero. From the analysis of system (7.33), it is easy to show that its determinant $D_0 \neq 0$. Therefore, in this system coefficients of unknowns satisfy the relation:

$$C_1 = -C_1'; \quad C_2 = -C_2'. \tag{7.34}$$

Then, from this, we obtain a system of equations only of the second order with unknown coefficients C_1, C_2:

$$\begin{cases} C_1(D - A) + C_2(E - B) = \prod_1; \\ C_1(F - H) + C_2(G - K) = \prod_2. \end{cases}$$

Constants C_1 and C_2 take the form: $C_1 = D_3/D_S; \quad C_2 = D_4/D_S$. Here, as before: D_s—system determinant, D_3, D_4—its algebraic adjuncts.

$$D_S = 2(a_2 - a_1) + a_1^{N_0}(a_2 - 2 - \sigma') - a_1^{N_0}(a_1 - 2 - \sigma') + a_1^{N_0-1} - a_2^{N_0-1},$$
$$D_3 = \left(C_0 K_{\sigma_0} - \frac{E_{F_2A_1}}{Z_B}\right)\left(a_2^{N_0-1} + a_1\right) + C_0\left(e^{-j\cdot k(N_0-1)} + e^{jk}\right)K_{\sigma_2}.$$
$$K_{\sigma_0} = 1 + (2 + \sigma')e^{-jk(N_0-1)} - e^{-jk(N_0-2)}; \sigma' = 2\frac{Z_{F_1A_2}}{Z_B}; K_{\sigma_2} = a_2^{N_0-2} - (2 + \sigma')a_2^{N_0-1} - 1. \tag{7.35}$$

To obtain calculation expressions for (C_2), it is necessary in the expression for D_3 to replace a_1 by a_2 and, respectively a_2 by a_1.

From an analysis of obtained Eqs. (7.34) and (7.35), we can draw the following practical conclusion: currents in regular active chain circuit elements have the same

peculiarities, as currents of open symmetrical one. They contain three components, from which:

- two vary depending on number N under the aperiodic law,
- the third varies depending on number N under the harmonic law.

Special case: circuit break $Z_{F_2A_1} \to \infty$, $Z_{F_1A_2} \to \infty$ Checking of results.

To obtain a symmetrical open chain circuit shown in Fig. 7.1 from an asymmetrical regular closed chain circuit shown in Fig. 6.3 (taking into account additional remarks provided in para 7.2.4) it is sufficient to set in the second of them impedances between groups of regular links $Z_{F_2A_1} \to \infty$ and $Z_{F_1A_2} \to \infty$. Let us show that in this case expressions for currents in longitudinal and cross elements coincide with Eq. (7.18) determined earlier as the solution of this simpler problem.

Let us find a limit to which D_s system determinant tends if the impedance $Z_{F_1A_2} \to \infty$ and, $\sigma' = 2\frac{Z_{F_1A_2}}{Z_B} \to \infty$ respectively. To determine this limit we divide in the expression D_s all terms by σ'. Then the expression for D_s takes the form: $\lim\limits_{\sigma' \to \infty} \frac{D_s}{\sigma'} = \frac{-\sigma' a_1^{N_0} + \sigma' a_2^{N_0}}{\sigma'} = a_2^{N_0} - a_1^{N_0}$.

Similarly, the expression for D_3:

$$\lim_{\sigma' \to \infty} \frac{D_3}{\sigma'} = C_0\left(a_2^{N_0-1} + a_1\right)e^{-jk(N_0-1)} + C_0 e^{jk}\left(1 + e^{-jkN_0}\right)\left(-a_2^{N_0-1}\right).$$

After reduction of similar term of equations, we obtain for constant C_1:

$$C_1 = C_0 \cdot e^{jk}\frac{a_1 e^{-jkN_0} - a_2^{N_0-1}}{a_2^{N_0} - a_1^{N_0}} = \frac{E_M}{Z_B K_B} \cdot e^{jk}\frac{a_1 e^{-jkN_0} - a_2^{N_0-1}}{a_2^{N_0} - a_1^{N_0}}. \tag{7.36}$$

This expression coincides with Eq. (7.18) for C_1 obtained earlier for an open symmetrical chain circuit. Constant C_2 can be calculated similarly to C_1.

Therefore, results of solution of this special problem (for $Z_{F_2A_1} \to \infty$ and $Z_{F_2A_2} \to \infty$) proves the validity of expressions for constant C_1, C_2 obtained earlier in this chapter.

7.3 Methods of Currents Investigation in Asymmetrical Active Open and Closed Chain Circuits

Now let us proceed in this para to the solution of general problem: peculiarities of currents distribution in asymmetrical active chain circuits. Its solution is based on results of investigation of passive asymmetrical chain circuits developed in Chap. 6.

Investigation of currents distribution in active open and closed chain circuits at occurrence of asymmetry (damage) in them has much in common: fundamental difference consists in the formulation of boundary conditions determined by

peculiarities in the structure of open and closed chain circuits. However, in practice, open and closed chain circuits have various applications: to open chain asymmetrical circuit corresponding to incomplete (without jumper between poles) damper winding, and to closed one—squirrel cage and complete damper winding. Therefore, let us state calculation methods of currents distribution in these circuits so that the content of one of these paragraphs could be used without sorting the content of another.

It should be noted that the method developed in this para is also true for calculation of additional currents in asymmetrical active chain circuits, for which EMFs of chain circuit elements can differ both in amplitude and phase, and some of them can be equal to zero that corresponds to condition (7.4). This method of calculation of asymmetrical chain circuits does not demand that EMFs of all links of chain circuit were equal in amplitude and differ in phase angle, herewith, the difference of these phase angles of adjacent links would be constant. In this regard, the method can be used for investigation of asymmetrical active circuits having except problems of electric machine industry, also other practical applications.

7.3.1 *Method of Investigation of Currents in Active Open Chain Circuits with Asymmetrical (Damaged) Elements. Calculation Example*

Let us consider a chain circuit of active U-shaped links containing $N_0 - 1$ longitudinal and N_0 cross elements. For this purpose let us use Fig. 7.1. Complex amplitudes (phasors) of links' EMF correspond to Eqs. (7.1) and (7.2). Let us accept that the impedance Z_R of all longitudinal elements of links is identical, and among cross elements there is one with number N_p, for example, element CC′ which the impedance Z_{N_p} differs from the others. Let us represent it in the form of two summands as it was already made in the (6.20) in the investigation of currents in passive asymmetrical chain circuits:$Z_{N_p} = Z_B + \Delta Z$.

Modifications of this method can also used in the presence of several asymmetrical (damaged) elements; at circuit break: $\Delta Z \to \infty$.

Let us write down for each link of the equation under the second Kirchhoff's law [1, 2]: for one of circuit loops with numbers $(N_p + 1, N_p) < N < (N_p, N_p - 1)$.

$$\begin{aligned} &\underline{\underline{J}}_{(N)}Z_B - \underline{\underline{J}}_{(N-1)}Z_B - 2\underline{I}_{(N-1)}Z_R = E_{(N-1)}, \\ &\text{or} \\ &J_{(N)}Z_B - J_{(N-1)}Z_B - 2I_{(N-1)}Z_R + \left(\Delta J_{(N)} - \Delta J_{(N-1)}\right)Z_B - 2\Delta I_{(N-1)}Z_R = E_{(N-1)}; \end{aligned} \tag{7.37}$$

In the last Eq. (7.37) the first three summands on the left part (voltage drops in symmetrical circuit elements) are equal to EMF on the right. This fact allows us to reduce the problem of calculation of currents distribution in asymmetrical active

open chain circuit to those of calculation of currents in the following two open chain circuits:

- in an active symmetrical chain circuit; its solution was given in paras 7.2.1 and 7.2.2;
- in a passive asymmetrical chain circuit; its solution was given in paras 6.7.1 and 6.7.2. It should be noted that boundary conditions for calculation of four constants in asymmetrical active open chain circuit are set in the same way as for asymmetrical passive open circuit in Chap. 6. Two equations under the second Kirchhoff's law are written for the first and last of its loops, and two others—for two loops containing asymmetrical (damaged) element with number N_p:

  for circuit loop with number (N_p, $N_p - 1$):

$$\begin{aligned} &J_{(N_P)}Z_B - J_{(N_P-1)}Z_B - 2I_{(N_P-1)}Z_R + \Delta J_{(N_P)}Z_{(N_P)} - \Delta J_{(N_P-1)}Z_B \\ &\quad - 2\Delta I_{(N_P-1)}Z_R + J_{(N_P)}\Delta Z \\ &\quad = E_{(N_P-1)}; \end{aligned}$$

for circuit loop with number ($N_p + 1$, N_p):

$$\begin{aligned} &J_{(N_P+1)}Z_B - J_{(N_P)}Z_B - 2I_{(N_P)}Z_R + \Delta J_{(N_P+1)}Z_B - \Delta J_{(N_P)}Z_{(N_P)} - 2\Delta I_{(N_P)}Z_R \\ &\quad - J_{(N_P)}\Delta Z \\ &\quad = E_{(N_P)}. \end{aligned} \tag{7.38}$$

Therefore, all calculation relations for additional currents in open active chain circuit elements are still true for additional currents in open passive circuit. These were obtained in Chap. 6; let us use the results obtained in this chapter including expressions for constants C_1, C_2, C_3, C_4 for calculation of currents.

Calculation examples

Given:

(a) Relation of impedances $\sigma = 2.32 \cdot e^{-j23.13}$; $N_0 = 6$; $N_P = 3$.
(b) Distribution of currents before the asymmetry occurrence is obtained from equations for symmetrical active open chain circuit and is given in Table 7.1.

To find currents distribution in a chain circuit.

Table 7.1 Distribution of currents before asymmetry occurrence

N	$I_{(N)}$	$J_{(N)}$
0	$0.3116 \cdot e^{j47.19}$	$0.3116 \cdot e^{j47.19}$
1	$0.3835 \cdot e^{j41.92}$	$0.07864 \cdot e^{j20.62}$
2	$0.3967 \cdot e^{j33.79}$	$0.05677 \cdot e^{-j33.79}$
3	$0.3941 \cdot e^{j24.4}$	$0.06595 \cdot e^{-j63.33}$
4	$0.3756 \cdot e^{j14.13}$	$0.070178 \cdot e^{-j85.91}$
5	$0.3000 \cdot e^{j3.37}$	$0.09835 \cdot e^{j228.9}$

Variant 1: circuit break in cross element.$N_p = 3(\Delta Z \to \infty)$

Variant 2: asymmetry $\frac{\Delta Z}{Z_B} = 1 \cdot e^{-j53.13}$ in cross element with number $N_p = 3$.

Solution: Calculated:;$a_1 = 4.0111 \cdot e^{-j14.02}$; $a_2 = 0.2493 \cdot e^{-j14.02}$;

Checked: $a_2 \cdot a_1 = 1$; $D_1 = 387.53 \cdot e^{-j74.65}$; $D_2 = 49.076 \cdot e^{-j133.33}$; $D_3 = 4.72590 \cdot 10^{-2} \cdot e^{j23.49}$; $D_4 = 819.864 \cdot 10^3 \cdot e^{j35.25}$;

Variant 1: $D_S = D_\infty = 25398 \cdot 06 \cdot e^{j257 \cdot 3}$.

Distribution of resulting currents at circuit break in cross element $N_p = 3$ is given in Table 7.2.

$\underline{\underline{I}}_6 = -\underline{\underline{I}}_5$. Results proves the validity of the obtained calculation expressions.

Variant 2: $D_S = 86813.8 \cdot e^{-j127.64}$.

Distribution of currents after the occurrence of asymmetry in cross element $N_p = 3$ is given in Table 7.3.

From results of calculation it follows: at the asymmetry the cross element with number $N = N_p = 3$ unloads in comparison with symmetrical chain circuit (Table 7.1), however, there increase currents flowing through adjacent cross elements and the extent of distortion decreases with an increase in the distance from asymmetrical element; These regularities are similar to those obtained for asymmetrical passive chain circuits.

Practical interest presents a comparison of losses in chain circuit before and after the break for variants 1 and 2:

Table 7.2 Distribution of resulting currents $\underline{\underline{I}}_{(N)}$ and $\underline{\underline{J}}_{(N)}$ at circuit break in cross element $N_p = 3$

N	$\underline{\underline{I}}_{(N)}$	$\underline{\underline{J}}_{(N)}$
0	$0.3121 \cdot e^{j46.82}$	$0.3121 \cdot e^{j46.82}$
1	$0.3834 \cdot e^{j40.7}$	$0.08066 \cdot e^{j16.34}$
2	$0.3940 \cdot e^{j29.05}$	$0.07960 \cdot e^{-j47.51}$
3	$0.3940 \cdot e^{j29.05}$	0
4	$0.37202 \cdot e^{j15.26}$	$0.09438 \cdot e^{-j81.16}$
5	$0.2985 \cdot e^{j3.61}$	$0.09989 \cdot e^{j232.4}$

Table 7.3 Distribution of resulting currents $\underline{\underline{I}}_{(N)}$ and $\underline{\underline{I}}_{(N)}$ after occurrence of asymmetry in cross element $N_P = 3$

N	$\underline{\underline{I}}_{(N)}$	$\underline{\underline{J}}_{(N)}$
0	$0.3113 \cdot e^{j47.08}$	$0.3113 \cdot e^{j47.08}$
1	$0.3823 \cdot e^{j41.6}$	$0.07827 \cdot e^{j19.31}$
2	$0.3911 \cdot e^{j32.65}$	$0.06106 \cdot e^{-j44.6}$
3	$0.3985 \cdot e^{j25.57}$	$0.04928 \cdot e^{-j52.3}$
4	$0.3765 \cdot e^{j14.52}$	$0.07794 \cdot e^{-j86.92}$
5	$0.2998 \cdot e^{j3.48}$	$0.09989 \cdot e^{j229.7}$

Before break:		100 %
After break:	Variant 1	99.5 %
	Variant 2	99.89 %

7.3.2 *Method of Investigation of Currents in the Active Closed Chain Circuits with Asymmetrical (Damaged) Elements: Calculation Example*

7.3.2.1 General Problem

Let us consider a closed chain circuit of active U-shaped links containing N_0 longitudinal and N_0 cross elements. Let us use Fig. 7.1 again. Let us consider in addition that terminals AA′ are superimposed with terminals FF′. Longitudinal elements of this circuit contain EMF $E_N(0 \le N < N_0 - 1)$. Complex amplitudes (phasors) of link EMFs correspond to Eqs. (7.1) and (7.2). Let us accept that originally the impedance Z_R of all longitudinal elements in links is identical, cross elements Z_B—also identical. Let us find the distribution of currents in chain circuit in case when one of its elements, for example, cross element with number N_p has become asymmetrical (damaged), that is its impedance Z_{N_p} differs from other Z_B: $Z_{N_p} = Z_B + \Delta Z$.

Let us write down equations under the second Kirchhoff's law for $N_0 - 2$ loops not containing a damaged element $(\Delta Z = 0)$ and two equations for two adjacent loops containing this element. They completely coincide with Eqs. (7.37) and (7.38), also true for open active chain circuit. In these equations as it was noted, the first three summands on the left part (voltage drops in circuit elements) are equal to EMF on the right. It allows one to reduce the problem of calculation of distribution of additional currents in asymmetrical active closed chain circuit to the same task for closed asymmetrical passive circuit.

Let us write down calculation expressions for additional currents of closed circuit in the form:

(a) at $0 \le N \le N_p - 1$: $\Delta I_N = C_1 \cdot \alpha_1^N + C_2 \cdot \alpha_2^N$;
(b) at $N_p - 1 < N \le N_0 - 1$: $\Delta I_N = C_3 \cdot \alpha_1^N + C_4 \cdot \alpha_2^N$.

To compute the of distribution of additional currents we need to write down boundary conditions and to calculate their C_1, C_2, C_3, C_4.

Two boundary conditions correspond to Eq. (7.38) and were already used in the investigation of open passive chain circuits:

$$\Delta I_{(N_p)}\left(1+\frac{\Delta Z}{Z_B}\right)-\Delta I_{(N_p-1)}\left(2+\sigma+\frac{\Delta Z}{Z_B}\right)+I_{(N_p-2)}=-J_{(N_p)}\frac{\Delta Z}{Z_B},$$
$$\Delta I_{(N_p+1)}-\Delta I_{(N_p)}\left(2+\sigma+\frac{\Delta Z}{Z_B}\right)+I_{(N_p-1)}\left(1+\frac{\Delta Z}{Z_B}\right)=J_{(N_p)}\frac{\Delta Z}{Z_B}$$

Two other boundary conditions follow from the definition of closed circuit given earlier; they follow from both Kirchhoff's laws. For example, for loop (1, 0) it is as follows:

$$\Delta I_1-\Delta I_0(2+\sigma)+\Delta I_{(N_0-1)}=0$$
$$\text{or} \qquad (7.39)$$
$$C_1[a_1-(2+\sigma)]+C_2[a_2-(2+\sigma)]+C_3a_1^{N_0-1}+C_4a_2^{N_0-1}=0.$$

Equation (7.39) makes a simple physical sense. As according to Vieta's theorem [6]: $a_1+a_2=(2+\sigma)$, $a_1\cdot a_2=1$, this equation takes the form:

$$-C_1a_2-C_2a_1+C_3a_1^{N_0-1}+C_4a_2^{N_0-1}=0.$$

It reflects the following physical fact in this form: functions of currents in ring portions $I_{(N)}$ and in bars $J_{(N)}$—are continuous for loops (1, 0) and ($N_{0\text{-}1}$, 0) of closed chain circuit.

Equation for loop (N_{0-1}, 0) is formed similarly:

$$C_1+C_2+C_3\left[-a_1^{N_0-1}(2+\sigma)+a_1^{N_0-2}\right]+C_4\left[-a_2^{N_0-1}(2+\sigma)+a_2^{N_0-2}\right]=0.$$

It is also convenient to transform it by means of Vieta's theorem and to present in the form:

$$C_1+C_2-C_3a_1^{N_0}-C_4a_2^{N_0}=0. \qquad (7.39')$$

As a result, we obtain a system of four equations with four unknown constants. It is as follows:

$$\begin{cases} C_1+C_2+QC_3+RC_4=0; \\ LC_1+MC_2+NC_3+PC_4=0; \\ HC_1+KC_2+FC_3+SC_4=J_{(N_p)}=\frac{\Delta Z}{Z_B}; \\ DC_1+TC_2+AC_3+BC_4=-J_{(N_p)}=\frac{\Delta Z}{Z_B}. \end{cases}$$

Values of system coefficients are given in Appendix 7.1.

It was already noted that the order of this system (four) does not depend on the number of chain circuit links that is the advantage of this method in practical calculations.

Equations for calculation of additional currents in chain circuit elements after determination of constants C_1–C_4 are reduced to the following form:

(a) currents in longitudinal elements:

$$\Delta I_{(N)} = \frac{J_{(N_P)}}{D_S} \cdot \frac{\Delta Z}{Z_B} \cdot \left(D_i a_1^N + D_{i+1} a_2^N\right), \tag{7.40}$$

herewith, $i = 1$ at $0 \le N \le N_p - 1$; $i = 3$ at $N_p \le N \le N_0 - 1$

(b) currents in cross elements (except $N = N_p$):

$$\Delta J_{(N)} = \frac{J_{(N_P)}}{D_S} \cdot \frac{\Delta Z}{Z_B} \cdot \left[D_i a_1^{N-1}(a_1 - 1) + D_{i+1} a_2^{N-1}(a_2 - 1)\right], \tag{7.41}$$

herewith, $i = 1$ at $0 < N \le N_p - 1$; $i = 3$ at $N_p - 1 < N \le N_0 - 1$;

(c) current in cross element $N = N_p$:

$$\Delta J_{(N)} = \frac{J_{(N_P)}}{D_S} \cdot \frac{\Delta Z}{Z_B} \cdot \left[(D_3 a_1 - D_1) a_1^{N_p - 1} + (D_4 a_2 - D_2) a_2^{N_p - 1}\right]; \tag{7.42}$$

here D_1–D_4—algebraic adjuncts.

Let us generalize the developed method: let us consider the problem of calculation of current distribution, if the number of asymmetrical cross links $P > 1$.

Let us accept that these links are not adjacent. In this problem the number of unknowns C_1; C_2; C_3; C_4… in the equations for additional currents respectively increases; also the order of system of in the equations for their determination increases. It is caused by an increase in the number of equations under the second Kirchhoff's law containing asymmetrical links $P > 1$. Generally, (at $P > 1$) the order [8, 9] of such systems is equal to the number of unknowns in equations for currents $\Delta I_{(N)}$ (according Kirchhoff's laws). There is no analytical expression for the determinant of the DS and for algebraic adjuncts D1–D4; these expressions and numerical values for a particular chain-circuits easily to obtain using for example MATCAD [13] with the coefficients from Appendix 7.1.

A closed chain circuit with three asymmetrical non-adjoining links is given for example in Fig. 7.2 (BB', CC', DD'); its image is similar to Fig. 6.4 in the form of two coaxial rings. At $P = 3$ the equations for additional currents $\Delta I_{(N)}$ have appearance ($N_{P_1} = 2$; $N_{P_2} = 4$; $N_{P_3} = 6$—numbers of damaged bars):

- in portions with numbers $N = 0; 1; \ldots; N_{P_1} - 1$ (portions AB and $A'B'$) $\Delta I_{(N)} = C_1 a_1^N + C_2 a_1^N$;

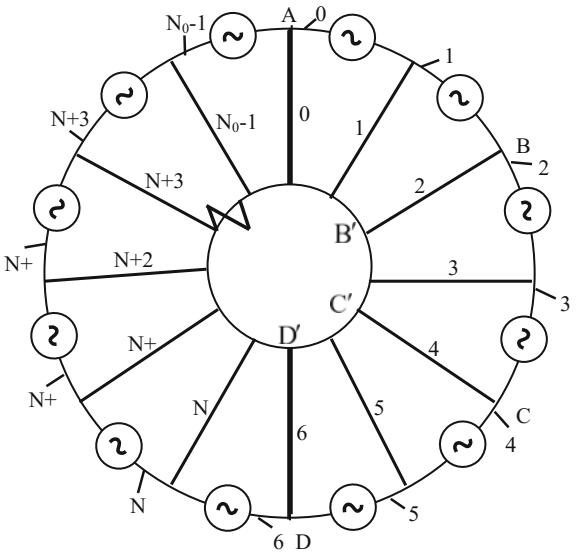

Fig. 7.2 Active closed chain circuit

- in portions with numbers $N = N_{P_1}; N_{P_1} + 1; N_{P_1} + 2; \ldots;\quad N_{P_2} - 1$(portions BC and B′C′);$\Delta I_{(N)} = C_3 a_1^N + C_4 a_1^N$;
- in portions with numbers $N = N_{P_2}; N_{P_2} + 1; N_{P_1} + 2; \ldots;\quad N_{P_3}$ - 1 (portions CD and C′D′);$\Delta I_{(N)} = C_5 a_1^N + C_6 a_1^N$;
- in portions with numbers $N = N_{P_3}; N_{P_3} + 1; N_{P_3} + 2; \ldots; N_0$ - 1 (portions DA and D′A′) $\Delta I_{(N)} = C_7 a_1^N + C_8 a_1^N$.

As a result we have the system with r = 8 unknown coefficients. The problems of calculating such closed circuits will be shown in Chap. 10. This chapter examines the construction of the cage windings with several damaged bars for induction machines.

Let us note that the developed method can be also used for calculation of currents distribution in a closed chain circuit, where asymmetrical elements are adjacent. This problem will be considered in Chap. 10.

7.3.2.2 Special Case—Circuit Break $(\Delta Z \to \infty)$

Checking results.

At the break of element $(\Delta Z \to \infty)$ currents are calculated from the same ratios (7.40)–(7.42); practically, for calculation in this case it is enough to set $\frac{\Delta Z}{Z_B} = 100 - 150$.

Calculations prove that at $\Delta Z \to \infty$ and N = N_P additional current according to (7.42) is equal to; $\Delta J_{(N_P)} =$ - $J_{(N_P)}$ as a result we obtain that the resulting current $\underline{J}_{(N_P)} = 0$, that proves the validity of obtained relations.

Table 7.4 Distribution of currents in cross elements of closed active chain circuit

N	0	1	2	3	4	5
$\left\lvert \underline{J}_{(N)} \right\rvert$	0.1597	0.1607	0.16147	0.1622	0.16297	0.0328
φ, °el. degr.	272.94	264.0	255.5	246.4	237.7	227.0
N	6	7	8	9	10	11
$\left\lvert \underline{J}_{(N)} \right\rvert$	0.16295	0.1622	0.16142	0.16066	0.1599	0.1592
φ, °el. degr.	220.4	211.6	202.8	194.0	185.1	176.1

Note: φ—phase angle

Calculation example

Let us find the distribution of currents in a closed active chain circuit.

Given:

(a) Asymmetry in cross element with number $N_p = 5 : \frac{\Delta Z}{Z_{\widehat{A}}} = 4$; relation value of impedances $\sigma = 9.818.10^{-2} + j \cdot 7.482 \cdot 10^{-6}$ (closed chain circuit corresponds to parameters of rotor squirrel cage of high-power induction motor);

(b) Distribution of currents in cross elements before the occurrence of asymmetry (damage) corresponds to equation: $J_{(N)} = 0.15691 \cdot e^{j(274-9.N)}$.

To find the distribution of currents

Solution for 12 cross elements adjacent to asymmetrical (damaged) is given in Table 7.4.

It follows that the value of resulting current $\underline{J}_N$ in cross element with number $N = N_P = 5$ after damage makes about 20 % of its value before damage. Values of currents in elements adjacent with damaged, increase in comparison with more remote ones; respectively their phase angles change.

7.3.3 *Modification of the Investigation Method of Currents in the Active Closed Chain Circuits with Asymmetrical (Damaged) Elements: Calculation Examples*

Note. The general method described in Sect. 7.3.2 establishes the relationship between calculations of current distribution in an asymmetric ladder circuit of various structure: closed and open. To calculate the current distribution in a closed circuit its input and output terminals are combined with each other. Two boundary conditions are relevant to such a combination of terminals: that one for circuit (1, 0) and (N_{0-1}, 0); they take the form of Eqs. (7.39) and (7.39′). Thus, the described method does not consider the combination of reference mark of closed circuit elements (N = 0) containing the number of one of damaged elements; in this case the number of constants r

to specify additional currents $\Delta I_{(N)}$ and $\Delta J_{(N)}$ is equal to $r \leq 2P + 2$ (as a function of a relative position of damaged elements in closed circuit).

However, to reduce the number of these constants one may combine the reference mark of circuit elements (N = 0) with the number of one of damaged elements. Then the number of constants is $r \leq 2P$.

Now let us consider the peculiarities of this method for calculation of additional currents $\Delta I_{(N)}$ and $\Delta J_{(N)}$ for closed ladder circuit with one damaged element $(0 \leq N \leq N_0 - 1)$; the number of cross damaged element with impedance $Z_{N_p} = Z_B + \Delta Z$ is N_p = N=0. Let us assume that there is one damaged element AA′ in Fig. 7.2. Then additional currents for longitudinal elements $(0 \leq N \leq N_0 - 1)$ may be written as

$$\Delta I_{(N)} = C_5 \alpha_1^N + C_6 \alpha_2^N, \tag{7.43}$$

while for cross elements they should be

$$\Delta J_{(N)} = C_5 \alpha_1^{N-1}(\alpha_1 - 1) + C_6 \alpha_2^{N-1}(\alpha_2 - 1) \tag{7.44}$$

besides, the constants C_5 and C_6 may be calculated with the use of a set of equations obtained for both circuits (1, 0) and $(N_0 - 1)$by virtue of Kirchhoff's law:

$$\begin{cases} C_5 A_0 + C_6 B_0 = J_0 \frac{\Delta Z}{Z_B} \\ C_5 D_0 + C_6 E_0 = -J_0 \frac{\Delta Z}{Z_B} \end{cases}. \tag{7.45}$$

The values of coefficients A_0, B_0, D_0, E_0 are given in Appendix 7.2.

The determinant of system (7.45) may be written as:

$$D_S = D_{S_1} + \frac{\Delta Z}{Z_B} D_{S_2}. \tag{7.46}$$

and algebraic adjuncts D_{C_5} and D_{C_6} as:

$$D_{C_5} = J_0 \frac{\Delta Z}{Z_B} D'_{C_5}, \quad D_{C_6} = J_0 \frac{\Delta Z}{Z_B} D'_{C_6}. \tag{7.46′}$$

The values of coefficients $D_{S_1}, D_{S_2}, D_{C_5}, D_{C_6}$ are given in Appendix 7.2. Then, the expression for additional currents $\Delta I_{(N)}$ in longitudinal elements is as follows:

$$\Delta I_{(N)} = \frac{D'_{C_5} \alpha_1^N + D'_{C_6} \alpha_2^N}{D_{S_1} + \frac{\Delta Z}{Z_B} D_{S_2}} J_0 \frac{\Delta Z}{Z_B}. \tag{7.43′}$$

The expression of additional currents $\Delta J_{(N)}$ in cross elements will be according to (7.44).

Calculation equations of currents in asymmetric active circuits as applied to squirrel-cage rotor have been obtained for the first time and require additional checks. Here are two of them.

Check 1.

At $\Delta Z \to \infty$ the resulting current $\underline{J}_0$ in element with number $N = N_p = 0$ should be equal to zero obtained from Eqs. (7.43)–(7.46′). From these equations, we shall have (Fig. 7.2)

$$\Delta J_0 = \Delta I_{(0)} - \Delta I_{(N_B-1)} = J_0 \frac{\Delta Z}{Z_B} \frac{F}{D_{S_1} + \frac{\Delta Z}{Z_B} D_{S_2}}$$

at that, we have obtained from equations for D_{S_1} and D_{S_2}, that $F = -D_{S_2}$. Then, at $\Delta Z \to \infty \lim_{\Delta Z \to \infty} \Delta J_0 = \frac{J_0 F}{D_{S_2}} = -J_0$.

Therefore, the resulting current is: $\underline{J}_0 = J_0 + \Delta J_0 = 0$.

The result proves the validity of obtained calculation data.

Check 2.

Let it be given that a closed active circuit contains $N_0 = 12$ elements.

An asymmetry in cross element with number $N = N_p = 0$ is equal to $\frac{\Delta Z}{Z_B} = 0.5$, the impedance ratio is $\sigma = 0.9$.

The currents in longitudinal elements are distributed before the damage according to equation $I_{(N)} = 100e^{j\Delta\varphi \times N}$ at $\Delta\varphi = 30$ el. degr.

To find out the current distribution in three circuit elements that neighbor the damaged one.

Solution.

Equation determinant $D_S = -1.8476 \cdot 10^5$.

Algebraic adjuncts $D_{C_5} = -38.823e^{j75} \times 10^{-4}$, $D_{C_6} = -5.0096e^{j75}$.

The results of current calculation are shown in Table 7.5.

From Table 7.5 it follows that the currents $\underline{J}_{(N)}$ in cross elements neighboring a damaged element (at $N = 11$ and $N = 1$) are much equal in amplitude and increase when damaged $\sim$by 5.5%, while the current in damaged element (at $N = 0$) decreases by $\sim$20%. The result agrees with physical representation of current distribution in this circuit.

Table 7.5 Current distribution in elements of closed active circuit neighboring the damaged element

NI, J	10	11	0	1
$\Delta I_{(N)}$	$2.1072\ e^{j75}$	$5.2691\ e^{j75}$	$-5.0094\ e^{j75}$	$-2.0033\ e^{j75}$
$J_{(N)}$	–	$51.764\ e^{j45}$	$51.764\ e^{j75}$	$51.764\ e^{j105}$
$\underline{I}_{(N)}$	$98.5708\ e^{-j59.136}$	$98.7674\ e^{-j27.0462}$	$98.822\ e^{-j2.8065}$	$98.5936\ e^{j29.176}$
$\underline{J}_{(N)}$	–	$54.524\ e^{-j46.661}$	$41.4854\ e^{j75}$	$54.390\ e^{j103.416}$

Appendix 7.1

Values of coefficients for calculation of constants C_1, C_2, C_3, C_4.

$$Q = -a_1^{N_0}; L = a_1^{-1}; N = -a_1^{N_0-1}; H = a_1^{N_p-1}\left(1 + \frac{\Delta Z_{N_P}}{Z_B}\right); F = a_1^{N_p}\left(-a_2 - \frac{\Delta Z_{N_P}}{Z_B}\right);$$
$$D = a_1^{N_p}\left(-2a_2 + a_2^2 - a_2\sigma - a_2\frac{\Delta Z_{N_P}}{Z_B}\right) = -a_1^{N_p}\left(1 + a_2\frac{\Delta Z_{N_P}}{Z_B}\right); A = a_1^{N_p}\left(1 + \frac{\Delta Z_{N_P}}{Z_B}\right).$$

Coefficients R, M, P, K, S, T, B can be obtained from those Q, L, N, H, F, D, A by replacement a_2 by a_1 and, respectively a_1 by a_2.

Appendix 7.2

Coefficients of a set of Eq. (7.45)

$$A_0 = \alpha_1^{N_0-1}\left(1 + \frac{\Delta Z}{Z_B}\right) - \alpha_2 - \frac{\Delta Z}{Z_B}, \quad B_0 = \alpha_2^{N_0-1}\left(1 + \frac{\Delta Z}{Z_B}\right) - \alpha_1 - \frac{\Delta Z}{Z_B},$$
$$D_0 = 1 - \alpha_1^{N_0} + \frac{\Delta Z}{Z_B}\left(1 - \alpha_1^{N_0-1}\right), \quad E_0 = 1 - \alpha_2^{N_0} + \frac{\Delta Z}{Z_B}\left(1 - \alpha_2^{N_0-1}\right).$$

Determinant of system (7.45) and (7.46)

$$D_{S_1} = -\alpha_1^{N_0+1} + \alpha_2^{N_0+1} + \alpha_1^{N_0-1} - \alpha_2^{N_0-1} + 2\alpha_1 - 2\alpha_2,$$
$$D_{S_2} = 2\left(-\alpha_1^{N_0} + \alpha_2^{N_0} + \alpha_1^{N_0-1} - \alpha_2^{N_0-1} + \alpha_1 - \alpha_2\right).$$

Algebraic adjuncts of a set of Eq. (7.46′)

$$D'_{C_5} = -\alpha_2^{N_0} + \alpha_2^{N_0-1} - \alpha_1 + 1, \quad D'_{C_6} = \alpha_1^{N_0} - \alpha_1^{N_0-1} + \alpha_2 - 1.$$

List of Symbols

E_M	Link EMF amplitude
$\underline{I}_N, \underline{J}_N$	Resulting currents in cross and longitudinal elements of links at occurrence of asymmetry (damage)
J, I	Currents in cross and longitudinal elements of symmetrical chain circuit links
$\Delta I_{(N)}$, $\Delta J_{(N)}$	Additional currents in longitudinal and cross elements of asymmetrical chain circuit
N	Element number of the chain circuit
N_p	Asymmetrical element number
t	Time

Z_B, Z_R, Z_F	Impedance of cross and longitudinal elements
Z_{N_P}	Impedance of asymmetrical element
ΔZ	Additional impedance of asymmetrical element
σ, σ'	Relations determined by impedances of symmetrical chain circuit elements
φ_N	Phase angle of link EMF

Brief Conclusions [7]

1. In active symmetrical chain circuits of considered type, EMF has the following peculiarities:
   - EMF amplitudes of all links remain constant,
   - difference of EMF phase angles of adjacent links also remains constant.
2. Currents in elements of active closed and open symmetrical chain circuits with such EMFs in each link contain three components:
   - two of them vary depending on element number (N) under the aperiodic law,
   - the third—under the harmonic law.
3. Distribution of currents in an active regular chain circuit has the same regularity. For checking results of its investigation, it is obtained that in specific case calculation expressions for currents in it and in active open symmetrical chain circuit coincide; it confirms the validity of obtained results.
4. Currents in elements of active closed and open asymmetrical chain circuits, as well as in elements of passive chain circuits, similar in structure, can be found from the solution of the following two problems:
   on the distribution of main currents in elements of active symmetrical chain circuit $(\Delta Z = 0)$;
   on the distribution of additional currents depending on distribution of the main ones; Calculation of the distribution of resulting currents is reduced to summation of the main and additional currents for the same elements.
5. The problem on the distribution of additional currents in elements of active asymmetrical chain circuit is similar to that for passive chain circuit of the same structure; additional currents contain two components, both vary depending on element number (N) under the aperiodic law.
6. Solution of limit problems—on the break of cross element $(\Delta Z \to \infty)$—confirms that the main and additional currents are equal and opposite in phase so the resulting current is equal to zero; it confirms the validity of obtained results.
7. Numerical examples also prove the validity of the obtained calculation expressions.

References

I. Monographs, general courses, textbooks

1. Demirchyan K.S., Neyman L.R., Korovkin N.V., Theoretical Electrical Engineering Moscow, St. Petersburg: Vol. 1, 2, Piter, 2009. (In Russian).
2. Kuepfmueller K., Kohn G., Theoretische Elektrotechnik und Elektronik. 15 Aufl. Berlin, N. Y.: Springer. 2000. (In German).
3. Ruedenberg R., Elektrische Schaltvorgaenge. Berlin, Heidelberg, N.-Y.: Springer, 1974. (In German).
4. Gardner M., Barnes J., Transients in Linear Systems Studied by the Laplace Transformation, N. Y., J. Wiley, 1942.
5. Jeffris H., Swirles B., Methods of Mathematical Physics. Third Edition, Vol. 1–Vol. 3, Cambridge: Cambridge Univ. Press, 1966.
6. Korn G., Korn T., Mathematical Handbook, N.-Y.: McGraw-Hill, 1961.
7. Boguslawsky I.Z., A.C. motors and generators. The theory and investigation methods by their operation in networks with non linear elements. Monograph. TU St. Petersburg Edit., 2006. Vol. 1; Vol.2. (In Russian).

III. Synchronous machines. Papers, inventor's certificates, patents

8. Demirchyan K.S., Boguslawsky I.Z., Current flowing in damper winding bars of different resistivity in a heavy-duty low speed motor. Proceedings of the Russian Academy of Sciences. Energetika i Transport, 1980, #2. (In Russian).
9. Demirchyan K.S., Boguslawsky I.Z., Methods of analytical study of currents in the rotor's short-curcuit windings of A.C. machines. Proceedings of the Russian Academy of Sciences. Energetika i Transport, 1992, #4. (In Russian).
10. Boguslawsky I.Z., Korovkin N.V., Unsymmetrical modes of polyphase machine ($m_{PH} \geq 3$): determination of MMF harmonics of armature reaction. Proceedings of the Russian Academy of Sciences. Energetika, 2013, #4. (In Russian).
11. Boguslawsky I.Z., The calculation method of the active chain-circuits with damaged chains. Electrichestvo, #4, 1984. (In Russian).
12. Boguslawsky I.Z. Nonsymmetrical active chain-circuits: calculation methods. Electrichestvo, #8, 1988. (In Russian).
13. Anastassiou G. A, Itan I., Intelligent Routines: Solving Mathematical Analysis with Matlab, Mathcad, Mathematica and Maple (Intelligent Systems Reference Library), Edition: 2013th, Springer.

Chapter 8
EMF Induced by Resulting Field in Short-Circuited Loops of Damper Winding and Squirrel Cage

This chapter deals with calculation expressions for EMF in loops of short-circuited rotor windings (of damper winding, squirrel cage) used in designs of modern A.C. machines when operating in nonlinear network. It is previously noted that for non-sinusoidal power supply of synchronous machines it is convenient to determine EMF in rotor loops induced by resulting field if this field contains two components formed by "adjacent" time harmonics of stator current; thus, both components of stator current field meet two conditions: spatial period T = idem, current frequency ω_{ROT} = idem.

Both these components differ in rotation direction relative to rotor, rotation speed relative to stator and in amplitudes.

For this problem setting on determination of EMF in rotor loops and corresponding currents, it is expedient (from viewpoint of skin effect and its influence on A.C. resistance and leakage reactance of rotor winding elements) to use a method of superposition: to calculate EMF in loop induced by one of these resulting field components irrespective of the second. Thus, generality of results is preserved.

Obtained here are calculation expressions for EMFs induced by these field components as a general problem: Origin of coordinates—arbitrarily, and pitch between bars does not remain constant (the last takes place, for example, in damper winding of salient pole machine). EMFs in winding loops used in practice are obtained as special cases of these calculation expressions.

The content of this chapter is development of the methods stated in [1, 2, 10–14].

8.1 Initial Data and Its Representation

In first chapters of the monograph it is noted that one of important investigation phases of A.C. machines in nonlinear networks with rotor short-circuited windings is the problem of calculation of currents distribution in construction elements of these windings: in damper winding and squirrel cage (in case of asymmetry in it).

I. Boguslawsky et al., *Large A.C. Machines*,
DOI 10.1007/978-4-431-56475-1_8

In Chap. 7 problems of currents distribution in active U-shaped recurrent circuits (chain circuits) were in detail investigated, provided that EMF of each link vary depending on its number under the harmonic law. Investigation objective of these recurrent circuits of various structure (symmetrical and asymmetrical, open and closed) is modeling process of currents distribution in rotor short-circuited windings of various construction (in damper winding, asymmetrical squirrel cages, etc.).

To use results of this investigation for calculation of performance characteristics of A.C. machines fed by non-sinusoidal current, let us establish a link between EMF in elements of active recurrent circuits and EMF induced in rotor loops of these machines. For this purpose, in this chapter let us find analytical expressions for EMF in various structures of damper winding and squirrel cage. This problem is solved most simply, if assumed that harmonics of resulting field in air gap are set out.

This assumption was already used in proving a possibility of representation of currents in short-circuited rotor winding loops in the form of generalized characteristics (Chap. 5); for this proof use was made of the system of equations with order determined by the number of short-circuited loops in machine rotor. It is realized by numerical methods. However, analytical expressions, available for obtaining from investigation results of active recurrent circuits of various structure, describe regularities of current distribution in various structures of these windings; it allows us to establish the extent of influence of winding parameters on currents distribution process in it, important in engineering practice.

Derivation of analytical expressions for EMF in various structures of damper winding and squirrel cage is the first stage of search of analytical regularities of current distribution in short-circuited rotor winding loops.

As the solution of problem on determination of EMF in damper winding and squirrel cage loops (at absence or at occurrence of asymmetry in them) let us accept as initial the following:

- Harmonics of resulting field in air gap;
- Geometrical dimensions of this winding elements;
- Rotor rotation speed (slip);
- Number of machine poles 2p.

Assumptions for the solution of this problem are given in [3–5] and let us consider at first some initial data in more detail.

8.1.1 Representation of Resulting Field Harmonics in Air Gap

Representation form of resulting field harmonics in air gap was already considered in Chap. 5, when solving a problem on generalized current characteristics in short-circuited rotor winding elements, generally, for any structure. Respectively,

geometrical dimensions of these loops and their impedance (A.C. resistance and leakage reactance) for this general case were accepted as arbitrary.

In this chapter we will obtain calculation expressions for EMF in rotor loops of specific types of short-circuited rotor windings used in modern practice.

Harmonics of resulting field in air gap are initial data for derivation of these expressions. Therefore, we will repeat briefly physical treatment and equations for complex amplitudes (phasor) of flux density (phasor) of this resulting field, given in Chap. 5.

For salient pole machines and induction machines with asymmetry in cage fed by non-sinusoidal current, for each time voltage harmonic in air gap it is possible to determine two resulting fields meeting the following conditions:

$$T = \text{idem},\ \omega_{ROT} = \text{idem},\ \text{where}\ \omega_{ROT} - \ \text{EMF frequency in rotor loops.}$$

T = idem, ω_{ROT} = idem, where ω_{ROT}—EMF frequency in rotor loops.

These resulting fields differ in rotation direction relative to rotor, rotation speed relative to stator and in amplitudes.

- For salient pole machines in synchronous operating mode fed by non-sinusoidal current, these both conditions (T = idem, ω_{ROT} = idem), correspond to two resulting fields formed by time voltage higher harmonics. These fields are called "adjacent" as they meet a certain condition obtained in Chap. 3. They form a system of equations of magnetically coupled loops; this question was also considered in Chap. 3.
- Flux density b(x,t,m,Q) of resulting field in air gap in any point x and at any timepoint t has the form according to (5.1):

$$b(x,m,Q) = B(m,Q) \cdot e^{-2j\pi m\frac{x}{\tau}} + B(-m,Q) \cdot e^{2j\pi m\frac{x}{\tau}}. \tag{8.1}$$

8.1.2 *Initial Geometrical Dimensions of Damper Winding, Squirrel Cage, Pole Winding*

Short-circuited winding construction is assumed to be set out with slot pitch in general case not constant. For such representation we also consider peculiarities of damper winding structure with pitch b between slot axes on the pole is not equal to the distance b_F between axes of edge slots in adjacent poles, and $\frac{b_F}{b} > 1$.

Figure 8.1 shows a portion of such a short-circuited rotor winding with EMF in its each loop; bar numbering is also specified there (N = 0,1,2,3,4,…, N − 1, N, …). Designation of each loop is the same: for example, loop (N,N–1) is formed by two bars with numbers N and N−1 (their impedance are equal accordingly to $Z_{B,N}, Z_{B,N-1}$) and two ring portions (segments) with number N − 1 (impedance of each is equal $Z_{R,N-1}$). Position of axis of each bar on rotor relative to arbitrarily chosen origin of coordinates (0 point) takes the form:

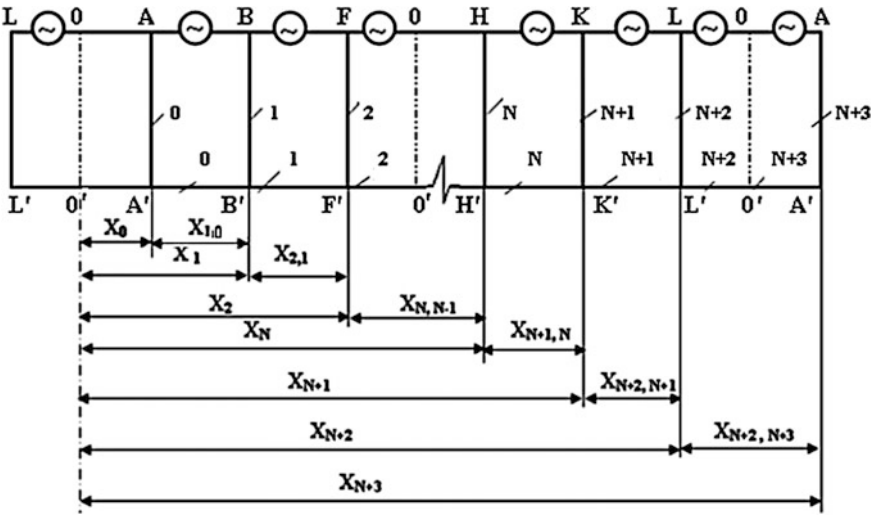

Fig. 8.1 Position of elements of short-circuited winding relative to origin of coordinates (general problem)

$$\begin{aligned}
&\text{for bar} \quad N = 0: \quad x = x_0;\\
&\text{for bar} \quad N = 1: \quad x = x_1 = x_0 + x_{1,0};\\
&\text{for bar} \quad N = 2: \quad x = x_2 = x_0 + x_{1,0} + x_{2,1};\\
&\qquad\vdots\\
&\text{for bar} \quad N: \qquad x = x_N = x_0 + x_{1,0} + x_{2,1} + \ldots + x_{N,N-1};\\
&\qquad\vdots
\end{aligned} \tag{8.2}$$

Here x_0—distance from arbitrarily chosen origin of coordinates to axis of the first slot (bar), $x_{1,0}; x_{2,1}; \ldots; x_{N,N-1}$—distance along rotor periphery between axes of adjacent slots (bars) accordingly with numbers N = 1 and N = 0; N = 2 and N = 1, …, N and N − 1. For generality, it is accepted that geometrical dimensions of loops are different:

$$x_{1,0} \neq x_{2,1} \neq \ldots \neq x_{N,N-1} \neq \ldots. \tag{8.3}$$

For determination of excitation winding EMF the followings are set out:

- pole shoe width $b_P = \alpha \cdot \tau$, where α—pole arc, τ—pole pitch [6–9];
- Z_{EX}—impedance of excitation winding and equivalent impedance of exciter.

8.2 Two EMF Components in Loops of Short-Circuited Rotor Winding

According to conditions (T = idem ω_{ROT} = idem), both resulting field components (8.1) in air gap correspond to EMF and currents in rotor loops of the same frequency. Therefore, the problem on determination of these EMFs and corresponding currents from the view point of skin effect and its influence on impedance and inductance of rotor winding elements can be considered for each of these field components independently using a method of superposition. Proceeding from it, in this chapter without losses of generality of results, let us obtain calculation expressions for EMF in rotor loops induced by flux density b(x,m,Q). This EMF can be determined in two ways: in scale of complex amplitude (phasor) B(m,Q) of the first flux density component in (8.1):

$$b'(x,m,Q) = B(m,Q) \cdot e^{-2j\pi m\frac{x}{T}}; \tag{8.4}$$

or in scale of complex amplitude (phasor) B(–m,Q) of the second flux density component in (8.1):

$$b''(x,m,Q) = B(-m,Q) \cdot e^{2j\pi m\frac{x}{T}}. \tag{8.4'}$$

For this formulation it is not difficult to change from EMF calculation expressions for the first flux density component to the second one. For specificity, Eq. (8.4) is used in further calculations.

8.2.1 General Problem: EMF in Any Loop of Short-Circuited Winding

Let us find previously the EMF induced by field (8.4) in loop (N,N–1) of this winding. It is equal to [1, 2]:

$$\begin{aligned} E_{1,0} &= -j\omega_{ROT}\Phi_{1,0}, \\ &\vdots \\ E_{N+2,N+1} &= -j\omega_{ROT}\Phi_{N+2,N+1}. \end{aligned} \tag{8.5}$$

Here $\Phi_{1,0}, \ldots, \Phi_{N+2,N+1}$—resulting fluxes linked accordingly with loop (1, 0) and loop (N + 2, N + 1). These fluxes are equal to:

$$\begin{aligned}\Phi_{1,0} &= \int_{x_0}^{x_0+x_{1,0}} B(m,Q)e^{-2j\pi m\frac{x}{T}}L_{COR}dx \\ &= B(m,Q)\frac{TL_{COR}}{\pi m}\sin\frac{\pi m x_{1,0}}{T}e^{-j\pi m\frac{x_{1,0}}{T}}e^{-2j\pi m\frac{x_0}{T}}, \\ &\vdots \\ \Phi_{N+2,N+1} &= \int_{x_0+x_{1,0}+\cdots+x_{N+1,N}}^{x_0+x_{1,0}+\cdots+x_{N+2,N+1}} B(m,Q)e^{-2j\pi m\frac{x}{T}}L_{COR}dx \\ &= B(m,Q)\frac{TL_{COR}}{\pi m}\sin\frac{\pi m x_{N+2,N+1}}{T}e^{-j\pi m\frac{x_{N+2,N+1}}{T}}e^{-2j\pi m\frac{x_0+x_{1,0}+\cdots+x_{N+1,N}}{T}}.\end{aligned} \tag{8.6}$$

Expressions for resulting flux magnetically coupled with any loop (N + 2, N + 1) and with loop (1,0) completely correspond to each other. They contain four factors. Let us consider their physical sense:

- the first factor determines loop flux amplitude;
- the second—determines pitch chording of this loop and, therefore, affects its EMF amplitude;
- the third and fourth—determine phase angle of flux and EMF.

It should be noted that the third factor depends on geometrical dimensions $(x_{N+2,N+1})$ of loop (N + 2, N + 1) considered, and the fourth—on the position of this loop relative to the origin of coordinates, that is on the sum of geometrical dimensions of previous loops, counting from the origin of coordinates: $(x_0 + x_{1,0} + \cdots + x_{N+1,N})$.

From Eqs. (8.5) and (8.6) for EMF $E_{N+1,N}$ it follows that this EMF is a function both of time harmonic order Q, and spatial harmonic m. These both harmonic orders (m, Q) are not part of upper or lower indices for flux $\Phi_{N+2,N+1}$ and EMF $E_{N+2,N+1}$, not to complicate their designation. For transition from obtained calculation expression for EMF (8.5) to EMF induced by the second flux density component in (8.4'), it is necessary in (8.5) to substitute complex amplitude (phasor) B(m,Q) by B(–m,Q) and sign m by (–m).

Let us note that EMF of loop (N + 2, N + 1) linearly depends on complex amplitude (phasor) of flux density B(m,Q), therefore, in subsequent calculations of EMF $E_{N+2,N+1}$ from (8.5) it is sometimes convenient to represent taking into account (8.6) in the following form of generalized characteristic:

$$E_{N+2,N+1} = [E_{N+2,N+1}] \cdot B(m,Q). \tag{8.5'}$$

Here,

$$[E_{N+2,N+1}] = -j\omega_{ROT}\frac{TL_{COR}}{\pi m}\sin\frac{\pi m x_{N+2,N+1}}{T}e^{-j\pi m\frac{x_{N+2,N+1}}{T}}e^{-2j\pi m\frac{x_0+x_{1,0}+\cdots+x_{N+1,N}}{T}}.$$

Now let us consider some special cases being of separate practical interest. Results of their solution will be required for calculations in the following chapters.

Let us solve them irrespective of the result obtained in this paragraph; we use it for additional checking validity of special tasks' solution.

8.2.2 EMF of Damper Winding Loops Located on Pole

Let us use Fig. 8.1. We consider that the portion ABF corresponds to rotor damper winding portion with EMF in each its loop. Numbering of bars is also specified there (N = 0, 1, 2,…, N,…); number of bars on each of two poles equals N_0 (bars $AA', BB', \ldots, FF'$ are located on poles of similar polarity; bars $HH', KK', \ldots, LL'$ are located on poles of opposite polarity). Distance between edge bars of adjacent poles (LA, FH) is accepted equal to b_F, and between adjacent bars on pole—equal to b [6–8]. Position of axis of each bar on rotor relative to machine cross axis (axes q, O point) takes the form:

$$\begin{array}{lll} \text{for bar} & N = 0: & x_0 = 0.5b_F; \\ \text{for bar} & N = 1: & x_1 = 0.5b_F + b; \\ \text{for bar} & N = 2: & x_2 = 0.5b_F + 2b; \\ & \vdots & \\ \text{for bar} & N: & x_N = 0.5b_F + Nb; \\ & \vdots & \end{array} \tag{8.7}$$

Let us find EMF induced by field (8.4) in loop (N + 2, N + 1) of this winding located on the pole. It is equal to:

$$E_{N+2,N+1} = -j\omega_{ROT}\Phi_{N+2,N+1}.$$

Here $\Phi_{N+2,\,N+1}$—resulting flux linked with loop (N + 2, N + 1).

This flux is equal to:

$$\begin{aligned} \Phi_{N+2,N+1} &= \int_{0.5b_F+b(N+1)}^{0.5b_F+b(N+2)} B(m,Q)e^{-2j\pi m\frac{x}{T}}L_{COR}dx \\ &= B(m,Q)\frac{TL_{COR}}{\pi m}\sin\frac{\pi mb}{T}e^{-j\pi m\frac{b}{T}}e^{-2j\pi m\frac{0.5b_F+b(N+1)}{T}}. \end{aligned} \tag{8.8}$$

In Chap. 7, Eqs. (7.3) for calculation of EMF in loops are given in the form $\left(\Delta\varphi = 2\pi m\frac{b}{T}\right)$:

$$E_{N+2,N+1} = E_M e^{-j\Delta\varphi(N+1)}; \quad E_{N+3,N+2} = E_M e^{-j\Delta\varphi(N+2)}; \ldots.$$

From a comparison of Eqs. (7.3) and (8.8) it follows that complex amplitude (phasor) for calculation of EMF E_M of damper winding loops located on the pole is equal to:

$$E_M = -j\omega_{ROT} B(m,Q) \frac{TL_{COR}}{\pi m} \sin\frac{\pi m b}{T} e^{-j\pi m\frac{b}{T}} e^{-j\pi m\frac{b_F}{T}}. \qquad (8.8')$$

Expression for the flux in any loop (N + 2, N + 1) on the pole completely corresponds to that obtained earlier (8.6). It confirms validity of results. It contains 4 factors, and their physical sense is similar to factors in Eq. (8.6).

8.2.3 *EMF of Damper Winding Loops Located on Cross Axis q*

Problem 1 Let us find EMF in loop $LL'A'AL$ (Fig. 8.1); it is formed by portions of short-circuited rings (segments)$LA, L'A'$ between poles and axes of edge bars $LL', A'A$ on adjacent poles. Let us keep the origin of coordinates for determination of bars' position as in Sect. 8.2.2.
EMF induced by field (8.4) in the loop $LL'A'AL$, is equal to:

$$E_{LL'A'AL} = -j\omega_{ROT}\Phi_{LL'A'AL}.$$

Flux linked with loop $LL'A'AL$ is equal to:

$$\Phi_{LL'A'AL} = \int_{-x_0}^{x_0} B(m,Q) e^{-2j\pi m\frac{x}{T}} L_{COR} dx = B(m,Q) \frac{TL_{COR}}{\pi m} \sin\frac{\pi m b_F}{T}. \qquad (8.9)$$

We obtained that flux $\Phi_{LL'A'AL}$ is a real quantity and is determined by loop geometrical dimensions $(2x_0 = b_F)$.

Let us note that Eq. (8.9) for $\Phi_{LL'A'AL}$ completely corresponds to Eq. (8.8) for $\Phi_{N+1,N}$ taking into account the accepted numbering of bars and damper winding peculiarities.

Problem 2 Let us find EMF in a loop $FF'H'HF$ (Fig. 8.1); it is also formed by portions of short-circuited rings (segments) $FH, F'H'$ between poles and axes of edge bars $FF', H'H$ on adjacent poles, but shifted relative to loop from the previous problem ($LL'A'AL$) by half of the period. Let us keep the origin of coordinates for definition determination of bars' position as in Sect. 8.2.2. Expression for EMF of such a loop will be required in subsequent chapters for determination of currents in damper winding elements.

It is natural to assume that EMF in this loop is equal in amplitude to EMF in loop LL′A′AL and is shifted relative to it in phase by angle of 180 electrical degrees (el. degr.). Let us check this assumption.

$$E_{FF'H'HF} = -j\omega_{ROT}\Phi_{FF'H'HF}.$$

Flux linked with loop FF′H′HF is equal taking into account designations accepted in (8.7):

$$\Phi_{FF'H'HF} = \int_{0.5T-x_0}^{0.5T+x_0} B(m,Q)e^{-2j\pi m\frac{x}{T}}L_{COR}dx = B(m,Q)\frac{TL_{COR}}{\pi m}\sin\frac{\pi m b_F}{T}\cdot e^{-j\pi m} \tag{8.9'}$$

For odd $m = 1, 3, 5$, we have: $e^{-j\pi m} = -1$.

We have obtained that for odd harmonics of any order the assumption is proved.

Let us note that both last relations can be also obtained directly from general Eq. (8.6) that proves validity of given calculations.

8.2.4 EMF of Loops in Squirrel Cage

a. General case. The flux density machine squirrel cage is presented in Fig. 8.2 and in Fig. 7.2; its image similar to Fig. 6.4 in the form of two coaxial rings is more expedient than in the form of recurrent circuit developed on the plane as it was accepted for regular damper winding. Portions of both rings AB, BC, …,A′B′, B′C′ in Fig. 8.2 correspond to the impedance of cage short-circuited rings, and radial portions between them AA′, BB′, …, FF′, to bars in its slots. Expediency of such representation is explained simply: bars of two poles of regular damper winding are laid within period $T_{EL} = \pi\frac{D}{p}$ (Fig. 8.1). However, squirrel cage bars are not laid within this period T_{EL}; for its investigation it should be taken equal to $T = pT_{EL} = \pi D$. Squirrel cage correspond in this regard to stator winding with fractional number of slots per pole and phase [3–8].

Rotor contains N_0 squirrel cage bars ($(N = 0; 1; 2; \ldots, N_0 - 1)$, Fig. 8.2). Distance between axes of bars (slots), as well as for damper winding on pole, is equal to b.

Let us find EMF in loop (N + 2, N + 1) of rotor cage for a case if the origin of coordinates is chosen so that for bar N = 0:X = X_0 (Fig. 8.2).

Position of axis for each bar on the rotor relative to arbitrarily chosen origin of coordinates (0 point) takes the form:

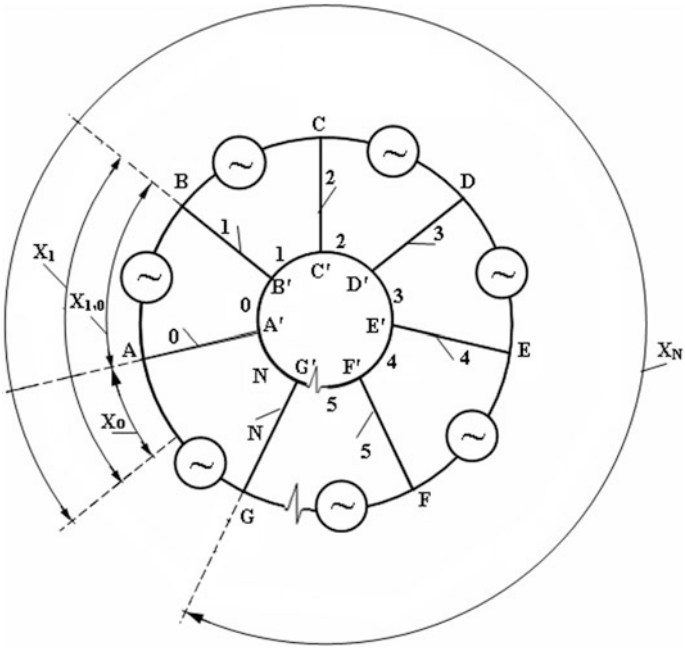

Fig. 8.2 Position of squirrel cage elements relative to arbitrary origin of coordinates

$$\begin{aligned}
&\text{for bar} \quad N = 0: \quad x_0;\\
&\text{for bar} \quad N = 1: \quad x_1 = x_0 + b;\\
&\text{for bar} \quad N = 2: \quad x_2 = x_0 + 2b;\\
&\qquad\vdots\\
&\text{for bar} \quad N: \qquad x_N = x_0 + Nb;\\
&\qquad\vdots
\end{aligned} \tag{8.10}$$

EMF induced by field (8.4) in loop (N + 2, N + 1) is equal to:

$$E_{N+2,N+1} - j\omega_{ROT}\Phi_{N+2,N+1}. \tag{$*$}$$

Resulting flux $\Phi_{N+2,N+1}$ coupled with loop (N + 2, N + 1), is equal to:

$$\begin{aligned}
\Phi_{N+2,N+1} &= \int_{x_0+(N+1)b}^{x_0+(N+2)b} B(m,Q)e^{-2j\pi m\frac{x}{T}}L_{COR}\,dx\\
&= B(m,Q)\frac{TL_{COR}}{\pi m}\sin\frac{\pi mb}{T}e^{-j\pi m\frac{b}{T}}e^{-2j\pi m\frac{x_0+b(N+1)}{T}}.
\end{aligned} \tag{8.11}$$

b. Special case: let us find EMF in loop (N + 2, N + 1) of rotor cage if the origin of coordinates coincides with the axis of zero bar AA′ (Fig. 8.2): $x_0 = 0$.

Resulting flux $\Phi_{N+2,N+1}$ coupled with loop (N + 2, N + 1), is given by:

$$\Phi_{N+2,N+1} = B(m,Q)\frac{TL_{COR}}{\pi m}\sin\frac{\pi mb}{T}e^{-j\pi m\frac{b}{T}}e^{-2j\pi m\frac{b(N+1)}{T}}. \tag{8.12}$$

From a comparison of Eqs. (7.3) and (8.12) it follows that the complex amplitude (phasor) E_M to compute EMF of squirrel cage loops $(\text{at } x_0 = 0)$, is equal to:

$$E_M = -j\omega_{ROT}B(m,Q)\frac{TL_{COR}}{\pi m}\sin\frac{\pi mb}{T}e^{-j\pi m\frac{b}{T}}. \tag{8.12'}$$

c. Special case: let us find EMF in the loop (N + 2, N + 1) of rotor cage, when the origin of coordinates is spaced from zero bar axis (Fig. 8.2) by a value: $x_0 = 0.5T$.

Resulting flux $\Phi_{N+2,N+1}$ linked with loop (N + 2, N + 1) is obtained:

$$\begin{aligned}\Phi_{N+2,N+1} &= \int_{0.5T+(N+2)b}^{0.5T+(N+2)b} B(m,Q)e^{-2j\pi m\frac{x}{T}}L_{COR}dx \\ &= -B(m,Q)\frac{TL_{COR}}{\pi m}\sin\frac{\pi mb}{T}e^{-j\pi m\frac{b}{T}}e^{-2j\pi m\frac{b(N+1)}{T}}.\end{aligned} \tag{8.13}$$

EMF $E_{N+2,N+1}$ − according(∗)

Relations (8.8)–(8.9'), (8.11)–(8.13) can be also obtained directly from the general Eq. (8.6) that proves the validity of given calculations.

8.2.5 *Excitation Winding EMF*

Similarly to (8.6) let us write down the equation for flux coupled with excitation winding on the pole:

$$\Phi_{EX} = \int_{0.5\tau(1+\alpha)}^{0.5\tau(1+\alpha)} B(m,Q)e^{-2j\pi m\frac{x}{T}}L_{COR}dx = B(m,Q)\frac{TL_{COR}}{\pi m}\sin\frac{\pi m_{EL}\alpha}{2}e^{-j\frac{\pi m}{2}}. \tag{8.14}$$

Here $\tau = \frac{\pi D}{2p}$.

Respectively, the calculation expression for excitation winding EMF on the pole takes the form: $E_{EX} = -j\omega_{ROT} W_{EX} \Phi_{EX}$; here, W_{EX}—number of turns per pole.

EMF on excitation winding terminals of $E_{EX,RES}$ is determined with account of coils' connection diagram on machine poles. Usually, they are connected in series: EMF for such connection of pole coils, as a rule, does not exceed several hundreds of volts. Then, $E_{EX,RES} = E_{EX} 2p$. From the obtained expressions it follows that field harmonics rotating in the direction opposite to rotor rotation, for example, m = 5, 11, 17… or, respectively, Q = 5, 11, 17… (at S = 2 according to Chap. 3), flux signs, EMF of excitation winding change to the opposite.

Brief Conclusions

1. For A.C. machine fed by non-sinusoidal current, it is convenient to determine EMF in short-circuited rotor loops (damper winding, squirrel cage) induced by resulting field in air gap meeting conditions: T = idem, ω_{ROT} = idem. This field has two components, which differ in rotation direction relative to rotor, rotation speed relative to stator and in amplitudes. For this problem setting on determination of EMF in rotor loops and currents corresponding to them, it is possible (from viewpoint of skin effect and its influence on A.C. resistance and inductance of rotor winding elements) to use a method of superposition: to calculate the EMF in loop induced by one of these resulting field components irrespective of the second.
   Without losses of generality of results, it is sufficient to obtain calculation expressions for EMF in rotor loops induced by resulting field

$$b(x,m,Q) = B(m,Q) \cdot e^{-2j\pi m \frac{x}{T}}.$$

2. Expression for the flux coupled with any loop (N + 2, N + 1) contains 4 multipliers. The first of them determines loop flux amplitude; the second—loop pitch chording and, therefore, affects its EMF amplitude; the third and fourth—determine phase angle of flux and EMF, herewith, the third factor depends on geometrical dimensions $\left(x_{N+2,N+1}\right)$ of the loop considered (N + 2, N + 1), and the fourth—on the sum of geometrical dimensions of previous loops, counting from the origin of coordinates: $\left(x_0 + x_{1,0} + \ldots + x_{N+1,N}\right)$.
3. Calculation expressions for EMF of damper winding loops (for longitudinal and cross axes), of squirrel cage are special cases of calculation expression in general problem of EMF calculation for any short-circuited winding loop. It proves the validity of the obtained calculation expressions for EMF.

List of Symbols

b	Pitch between axes of pole slots
b_F	Distance between axes of edge slots on adjacent poles
$b(x,t,m,Q)$	Instantaneous value of resulting field flux density in air gap
$B(m,Q)$	Flux density amplitude of resulting field in air gap
D	Diameter of stator boring
E_{EX}	EMF on excitation winding terminals
E_M	Rotor loop EMF amplitude
$E_{N+2,N+1}$	EMF of the loop formed by bars with numbers N = 1 and N = 2
I_{EX}	Excitation winding current
L_{COR}	Stator core active length
m	Spatial harmonic order
N	Bar (ring portion) number of damper winding or squirrel cage
N_0	Number of bars in damper winding on rotor pole or in squirrel cage
p	Number of pole pairs
Q	Order of time harmonic
t	Time
T	Series expansion periods of MMF and fields of mutual induction to harmonic series
W_{EX}	Number of excitation winding turns on pole
x	Current coordinate along stator boring (in tangential direction)
x_0	Distance from the origin of coordinates to axis of the first slot (bar)
Z_B, Z_R, Z_F	Impedance of bar, ring portion between bars on pole, ring portion between edge bars of adjacent poles
Z_{EX}	Impedance of excitation winding and equivalent impedance of exciter
α	Pole arc, $\alpha = \frac{b_p}{\tau}$, where b_p—width of pole shoe, τ—pole pitch
$\Phi_{1,0}, \ldots, \Phi_{N+2,N+1}$	Mutual induction resulting fluxes linked accordingly with loop (1,0) and loop (N + 2, N + 1)
Φ_{EX}	Flux linked with excitation winding
ω_{ROT}	Circylar frequency of EMF and current in rotor loops

References

I. Monographs, Textbooks

1. Demirchyan K.S., Neyman L.R., Korovkin N.V., Theoretical Electrical Engineering. Moscow, St. Petersburg: Piter, 2009. Vol. 1, 2. (In Russian).
2. Kuepfmueller K., Kohn G., Theoretische Elektrotechnik und Elektronik. 15 Aufl. Berlin, New–York: Springer. 2000. (In German).
3. Mueller G., Ponick B., Elektrische Maschinen. N.Y., J. Wiley, 2009. (In German).
4. Richter R., Elektrische Maschinen. Berlin: Springer. Band I, 1924; Band II, 1930; Band III, 1932; Band IV, 1936; Band V, 1950. (In German).
5. Kostenko M.P., and Piotrovskiy L.M., Electrical Machines. Vol. 2. - Leningrad: Energiya. 1965. (In Russian).
6. Mueller G., Vogt, K., Ponick B., Berechnung elektrischer Maschinen. Springer, 2007. (In German).
7. Schuisky W., Berechnung elektrischer Maschinen. Wien: Springer, 1960. (In German).
8. Construction of Electrical Machines. Edited by of Kopylov, I.P., Moscow: Energiya, 1980. (In Russian).
9. Concordia Ch. Synchronous Machines, Theory a. Performance. N.Y., J. Wiley, 1951.

III. Synchronous Machines. Papers, Inventor's Certificates, Patents

10. Boguslawsky I.Z., Calculating the current distribution on the damper winding of large slow–speed synchronous motors in asynchronous operation. Power Eng. N.Y, 1979, No. 3.
11. Demirchyan K.S., Boguslawsky I.Z., Current flowing in damper winding bars of different resistivity in a heavy- duty low speed motor. Power Eng. N.-Y, 1980, No. 2.
12. Boguslawsky I.Z., Currents in a Asymmetric Short – Circuited Rotor Cage. Power Eng. N.-Y, 1982, No. 1.
13. Boguslawsky I.Z., Currents and harmonic MMFs in a damper winding with damaged bar at a pole. Power Eng. N. Y, 1985, No. 1.
14. Boguslawsky I.Z., Demirtschian K.S. Stationaere Stromverteilung in unregelmaessigen und unsymmetrischen kurzgeschlossenen Laeuferwicklungen von Wechselstrommaschinen. Archiv fuer Elektrotechnik, 1992, No. 6. (In German).

Chapter 9
Investigation Methods of Currents Distribution in Regular Damper Windings and Squirrel Cages

This chapter presents methods of investigation of currents in regular damper winding elements of various design (complete, incomplete) caused by influence of the first and higher harmonics ($Q \geq 1$, $|m| = |n| \geq 1$) of resulting field in air gap. They are based on investigation results for currents in U-shaped recurrent circuits of various structure. Obtained here are regularities of currents distribution in construction elements of regular damper winding in operational modes of salient pole machine.

Additional proof of results correctness is obtained by aggregation of obtained calculation expressions for complete damper winding to expressions for squirrel cage of induction machine (at pole overlapping $\alpha = b_p/\tau = 1$).

For currents in damper winding the following regularity of currents distribution is obtained:

- besides the current of regular damper winding there is an additional current which contains two components;
- both these components vary depending on bar or ring portion number under aperiodic law.
- Methods are checked in bench conditions on pilot motor type SDSZ 2.000 kW, 6 kV, 100 rpm (LEZ, Stock Company "Ruselprom").

Calculation method of adiabatic overheat of short-circuited rotor windings with account of the dependence of skin effect on temperature is given in appendix to the chapter.

The content of this chapter is development of the methods stated in [1, 2, 12–16].

I. Boguslawsky et al., *Large A.C. Machines*,
DOI 10.1007/978-4-431-56475-1_9

9.1 Compliance Between Structures of Recurrent Circuits and Constructions of Short-Circuited Rotor Windings (Damper Winding, Squirrel Cages)

This chapter presents analytical methods of investigation of currents distribution induced by mutual induction field harmonics in construction elements of damper winding of salient pole synchronous machines and squirrel cages of induction machines.

In the previous chapters a detailed analysis was performed for this investigation of U-shaped passive and active recurrent circuits of various construction representing practical interest for analysis of processes in A.C. machines (symmetrical and asymmetrical, open and closed); methods of analytical calculation of currents distribution in elements of these circuits are stated. In investigation of currents distribution of elements in active recurrent circuits it was accepted that EMF of each link varies depending on its number under the harmonic law.

Let us establish a relationship between the main types of short-circuited rotor winding construction (damper winding and squirrel cages) and types of recurrent circuits investigated in Chaps. 6 and 7. This relationship is given in Table 9.1.

However, at first, let us give the list of main peculiarities of short-circuited rotor winding construction (damper winding and squirrel cages) found in modern practice [3–7].

(A) Damper windings of salient pole machine.

(A_1) Complete damper winding. In this construction, equal number of bars is laid in slots on each pole; all bars are connected from both rotor sides at its ends by short-circuited rings (segments) both within poles, and in space between poles. Pitch between bars located on poles is identical.

Table 9.1 Compliance between short-circuited rotor windings and active recurrent circuits of various construction

No.	Winding	Recurrent circuit	
–	–	On ratio of impedances	In construction
1.	Complete damper winding	Asymmetrical	Closed
1.1	Regular	Asymmetrical, regular	Closed
1.2	Irregular	Asymmetrical	Closed
2.	Incomplete damper	Symmetrical or asymmetrical	Open
2.1	Regular	Symmetrical	Open
2.2	Irregular	Asymmetrical	Open
3.	Squirrel cage	Symmetrical or asymmetrical	Closed
3.1	Symmetrical	Symmetrical	Closed
3.2	Asymmetrical	Asymmetrical	Closed

(A_2) Incomplete damper winding. In this construction unlike complete damper winding, all bars are connected from both rotor sides on its ends by short-circuited rings (segments) only within pole shoe.
We will distinguish the following kinds of damper winding constructions given above from the viewpoint of symmetry of bars and short-circuited ring portions (segments).
(A_3) Regular damper winding. In this winding construction, all bars on poles have equal impedance in whole working range of frequencies; the same also belongs to impedance of all portions of both rings (segments) between bars, as well as to impedance of all portions of both rings (segments) between poles.
(A_4) Irregular damper winding. In this winding construction, there is one or several bars with various impedance, for example:

- on one or several poles there are damage bars (in limit case—with break);
- or on each pole there are in addition to bars made of copper, bars made of brass or bronze.

(B) Squirrel cages of induction machine. Let us distinguish the following types of squirrel cage construction.
(B_1) Symmetrical squirrel cage. In this winding construction all bars have equal impedance in whole working range of frequencies; the same also belongs to impedance of all portions of both short-circuited rings between bars.
(B_2) Asymmetrical squirrel cage. In this winding construction there are bars with various impedance, for example, there are bars with damage (in limit case—with break); the same also belongs to impedance of some portions of both short-circuited rings between bars.

Let us consider methods of analytical investigation of currents in short-circuited rotor winding constructions found in modern practice beginning with simplest problem: squirrel cage of induction machine.

9.2 Symmetrical Squirrel Cage of Induction Machine [12, 13]

In analysis of recurrent circuits, the peculiarities of symmetrical active closed circuit were considered in Chap. 7.

Distribution of currents in its longitudinal elements with account of values of constants $C_1 = 0, C_2 = 0$ was obtained in the form:

$$I_{(N)} = \frac{E_M}{Z_B K_B} e^{-jkN}.$$

Respectively, currents in cross elements:

$$J_{(N)} = \frac{E_M}{Z_B K_B}(1 - e^{jk})e^{-jkN}.$$

According to Table 9.1, let us assign a symmetrical squirrel cage of induction machine rotor to this recurrent circuit. Then, longitudinal elements of the circuit correspond to ring portions with impedance Z_R (A.C. resistance and leakage reactance), and cross ones—winding bars with impedance Z_B. To find currents in these squirrel cage structural elements, previously, let us determine the following in expressions for currents:

- coefficient k;
- EMF amplitude E_M;
- coefficient K_B.

In Chap. 7 we determined physical sense of the coefficient k: it is equal to phase shift angle $\Delta\varphi_N$ between EMF of adjacent elements of recurrent circuit, for example, with numbers N + 1 and N. If the circuit is symmetrical, according its determination: $k = \Delta\varphi_N = \text{const}$. For induction machine squirrel cage, this coefficient does not depend on N and is calculated from the ratio:

$$\Delta\varphi_N = \Delta\varphi = 2\pi m\frac{b}{T} \neq f(N).$$

Here, $T = \pi D$—EMF period; D—stator boring diameter; m—order of spatial harmonic; m = 1p, 3p, 5p ….

Let us proceed to the determination of EMF E_M. Calculation expressions for squirrel cage EMF are obtained in Chap. 8. When we selected the origin of coordinates coinciding with axis of zero bar ($x_0 = 0$, Fig. 8.2), we obtained the EMF induced by the resulting field in loop (N + 2, N + 1):

$$E_{N+2,N+1} = -j\omega_{ROT}\Phi_{N+2,N+1} \tag{9.1}$$

Flux $\Phi_{N+2,+1}$, linked with loop (N + 2, N + 1) is obtained:

$$\Phi_{N+2,N+1} = B(m,Q)\frac{T}{\pi m}L_{COR} \cdot \sin\frac{\pi mb}{T} \cdot e^{-j\pi m\frac{b}{T}} \cdot e^{-2j\pi m\frac{b(N+1)}{T}},$$

therefore

$$E_M = -j\omega_{ROT}B(m,Q)\frac{T}{\pi m}L_{COR} \cdot \sin\frac{\pi mb}{T} \cdot e^{-j\pi m\frac{b}{T}}.$$

Let us proceed to coefficient K_B determined by the expression:

$$K_B = [1 - (2+\sigma)e^{-jk} + e^{-2jk}]e^{jk}.$$

With taking account of parameters of squirrel cage it is equal to:

$$K_B = \left[1 - (2+\sigma)e^{-2j\pi m\frac{b}{T}} + e^{-4j\pi m\frac{b}{T}}\right]e^{2j\pi m\frac{b}{T}}. \tag{9.2}$$

Here $\sigma = \frac{2Z_R}{Z_B}$.

So, we obtained the expression for calculation of currents in ring portions:

$$I_{(N)} = \frac{E_M e^{-2j\pi mb\frac{N}{T}}}{Z_B K_B}. \tag{9.3}$$

Respectively, currents in bars: $J_{(N)} = I_{(N)} - I_{(N-1)}$ or

$$J_{(N)} = E_M\left(1 - e^{2j\pi m\frac{b}{T}}\right)\frac{e^{-2j\pi mb\frac{N}{T}}}{Z_B K_B}. \tag{9.4}$$

From these expressions we obtain generalized characteristics of currents in structural elements of induction machine short-circuited rotor winding.

For currents in ring portions it takes the form:

$$\left[I_{(N)}\right] = -j\omega_{ROT}\frac{T}{\pi m}L_{COR}e^{-j\pi m\frac{b}{T}}\frac{e^{-2j\pi mb\frac{N}{T}}}{Z_B K_B}\sin\frac{\pi mb}{T}. \tag{9.5}$$

for currents in bars:

$$\left[J_{(N)}\right] = -j\omega_{ROT}\frac{T}{\pi m}L_{COR}e^{-j\pi m\frac{b}{T}}\frac{e^{-2j\pi mb\frac{N}{T}}}{Z_B K_B}\left(1 - e^{2j\pi m\frac{b}{T}}\right)\sin\frac{\pi mb}{T}. \tag{9.6}$$

Here, K_B—as per (9.2).

9.3 Two Definitions in Investigation of Currents in Squirrel Cage Loops; Their Compliance and Areas of Correctness

In previous paras, currents in rotor squirrel cage elements are obtained by the solution of symmetrical active closed recurrent circuit using difference equations [12].

In setting these equations it is supposed that the object of calculation are squirrel cage loops formed by two adjacent bars and short-circuited ring portions corresponding to them on both rotor ends; currents in these loops are induced by resulting rotating field in air gap. Such concept allows us to investigate the

distribution of currents in symmetrical squirrel cage, to extend the calculation results obtained for it to general case—asymmetrical cages, for example, with damages arising during operation. Therefore, this concept needs to be confirmed in addition, if we suppose to use it in calculation of induction machine performance characteristics, frequency-controlled or general purpose application in case of damages in its cage. It can be made, for example, by a comparison of results:

- obtained in this paragraph for special case—symmetrical squirrel cage;
- obtained from the theory of induction machines [3–6] widely used in practice.

Unlike the method stated, in the theory of induction machines the problem of calculation of currents in symmetrical cage and determination of performance characteristics of these machines is solved differently: rotor cage is considered as multiphase winding with number of equivalent phases equal to number of rotor bars N_0. All these equivalent phases are accepted symmetrical, therefore, the equations for induction machine and corresponding equivalent circuit are assumed for one rotor phase and one stator phase. Equivalent rotor phase is formed by one bar (with impedance Z_B) and two equivalent short-circuited ring portions (each with impedance Z'_R) located between axes of adjacent bars on both rotor ends. It is supposed that these equivalent phases of rotor winding are connected in star. One of these rings serves as zero point of this star. It is convenient to consider each of N_0 portions of the second ring as external impedance between these phases (with equivalent impedance $2Z'_R$). This method was given in Chap. 4 and is successfully used in long-term practice of designing induction machines. It was stated in relation to the first spatial harmonic (m = 1p). Let us repeat its basic provisions for general case ($m \geq 1p$). At the same time, we assume that the period T of expansion into a series MMF of stator and rotor windings is equal to πD.

Peculiarity of calculation of this multiphase rotor parameters (with N_0 equivalent phases) is that the impedance [3–6] of equivalent ring portion Z'_R is not equal to the actual impedance Z^R of this portion; they differ by "reduction coefficient of equivalent impedance of cage ring" K_{RED}:

$$\kappa_{RED} = \frac{Z_R}{Z'_R} = 4\sin^2\frac{\pi mb}{T}. \tag{9.7}$$

This coefficient means that the current in bar and current in adjacent ring portions differ in amplitude and phase, but both vary in space along the rotor periphery under the harmonic law. It is obtained from the condition that the energy dissipated in active component of impedance Z_R of short-circuited ring element carrying real current is equal to that dissipated by current in active component of equivalent impedance Z'_R; current in this equivalent impedance is equal to that in bar. The same condition is satisfied for reactive energy stored in inductance of real and equivalent ring portions.

As it follows from Eq. (9.7), each spatial harmonic of m order corresponds to its own "reduction coefficient" κ_{RED}. This fact is important for practical calculations of induction machines fields using two-dimensional (2D) software packages, for example, by FEM (finite element method).

Thus, the method widely used in general theory of induction machines [3–9] does not assume its application for solution of tasks on currents distribution in asymmetrical cage elements: rotor loops are calculated based on its single equivalent phase. For setting equations for currents in squirrel cage rotor of induction machine, the expressions for equivalent impedance of rotor phase, resulting flux Φ in air gap linked with it, and for phase EMF, and also for currents in it have other appearance, as compared with those obtained earlier for recurrent circuit elements:

- equivalent impedance of rotor phase [3–5, 8]:

$$Z_{EQ,PH} = Z_B + \frac{Z_R}{2\sin^2\frac{\pi m b}{T}}; \tag{9.8}$$

- resulting flux in air gap:

$$\Phi = \int_{x_0}^{x_0+\frac{T}{2}} B(m,Q)e^{-2j\pi m\frac{x}{T}}L_{COR}dx = B(m,Q)\frac{TL_{COR}}{\pi jm}e^{-2j\pi m\frac{x_0}{T}}. \tag{9.9}$$

Let us note that for $x_0 = -\frac{T}{4p}$ and for values of order m = 1p; 3p; 5p… we obtain the known expression [3–6]: $\Phi = \left|B(m,Q)\frac{TL_{COR}}{\pi m}\right|$.

- EMF phase amplitude:

$$E_{M,PH} = -j\omega_{ROT}W_{PH}K_W(m)\Phi. \tag{9.10}$$

In calculation of EMF $E_{M,PH}$, it is supposed that the calculation unit (equivalent phase) for any spatial harmonic m has the number of turns $W_{PH} = 0.5$ and winding factor $K_W(m) = 1$;

- currents in rotor phase:

$$J_{PH} = \frac{E_M}{Z_B + \frac{Z_R}{2\sin^{2\pi}\frac{mb}{T}}}. \tag{9.11}$$

After transformations, we get:

$$J_{PH} = [J_{PH}]B(m,Q), \quad \text{where} \quad [J_{PH}] = \frac{j\omega_{ROT} T L_{COR} \frac{1}{\pi m}}{Z_B + \frac{Z_R}{2\sin^2 \frac{\pi m b}{T}}}. \tag{9.12}$$

Let us note that Eqs. (9.8–9.12) coincide with those given in Chap. 4 for a special case: m = 1p.

Thus, we obtained two calculation expressions different by kind for generalized characteristics of currents (9.5), (9.6), (9.12) in elements of induction machine rotor symmetrical squirrel cage:

- Equations (9.5) and (9.6) are obtained proceeding from the distribution of currents in symmetrical recurrent circuits and solutions of difference equations; we assume that the calculation unit in their setting is N_0 loops of rotor winding, each of which is formed by two adjacent bars and two portions of short-circuited rings at both rotor ends; portions of both rings are located between these two bars. "Reduction coefficient of equivalent impedance of cage ring" for derivation of expressions is not required;
- Equations (9.12) are obtained proceeding from the assumption of harmonic distribution of currents in multiphase symmetrical system [5, 6, 9]; we assume that the calculation unit is one equivalent phase of squirrel cage with number of turns $W_{PH} = 0.5$ and winding factor $K_W(m) = 1$. When deriving calculation expressions for currents in its elements, the "reduction coefficient of equivalent impedance of cage ring" is used for each spatial harmonic of m order.

To prove identity

$$\left|\left[J_{(N)}\right]\right| = |[J_{PH}]| \tag{9.13}$$

Let us determine at first the module of complex number in expressions for currents (9.3) and (9.4): $M_1 = |Z_B K_B|$:

$$\begin{aligned} M_1 &= \left|Z_B\left[e^{j\Delta\varphi} - (2+\sigma) + e^{-j\Delta\varphi}\right]\right| = |Z_B[2\cos\Delta\varphi - (2+\sigma)]| \\ &= \left|4Z_B \sin^2\frac{\Delta\varphi}{2} + 2Z_R\right|. \end{aligned} \tag{9.14}$$

Here $\Delta\varphi$—according to expression in Sect. 9.2.

We determine the module of complex number in expressions for currents (9.3) and (9.4): $M_2 = \left|1 - e^{2j\pi m\frac{b}{T}}\right|$,

$$M_2 = |1 - \cos\Delta\varphi - j\,\sin\Delta\varphi| = 2\,\sin\frac{\Delta\varphi}{2}. \tag{9.15}$$

Using Eqs. (9.14) and (9.15) we proceed to the identity (9.13) for currents in bars.

As a result, we get:

- rotor symmetrical squirrel cage can be investigated as symmetrical multiphase winding (with number of phases $m_{Ph} = N_0$ and "reduction" of impedance of its end part to slot part for each harmonic of m order), or as a set of N_0 magnetically coupled loops within recurrent circuit.

Let us consider task solutions on currents distribution in asymmetrical squirrel cage.

Within the method used in the general theory of induction machines, it is possible to present rotor asymmetrical squirrel cage in the form of multiphase system [11] and to investigate this system by a method of symmetrical components [1, 2]. This method is usually used for analysis of the modes in A.C. high voltage lines and other electrical power systems, devices and installations, including A.C. machines at asymmetrical short circuits in stator winding [9]. Investigations prove that using the method of symmetrical components for these purposes meets serious computing difficulties [1, 17, 19] even in the solution of elementary tasks with squirrel cage asymmetry, thus, clarity of physical treatment is lost. For example, application of method of symmetrical components for investigation of typical asymmetrical cage [20] with number of slots $N_0 > 36-40$ requires preliminary calculation of currents in each of these symmetrical components; let us note that "reduction coefficients" for impedance of short-circuited ring element to bar impedance for spatial harmonics of various orders of m differ. Therefore, its use for investigation of damper winding (even without damages) is especially unpromising.

In this monograph for investigation of currents in asymmetrical squirrel cages other method is developed, given in previous chapters for investigation of currents in asymmetrical passive and active recurrent circuits. Its advantage over the method of symmetrical components consists not only in simplicity of realization and clarity of physical treatment, but also in the fact that it is extended for investigation of the whole class of rotor short-circuited windings including damper winding.

9.4 Damper Winding of Salient Pole Machine [14–16]

In an analysis of active recurrent circuits we considered peculiarities of regular active closed circuit. For deriving calculation expressions, we used Fig. 6.3 with the following additions:

- between two cross elements $A_1A'_1$ and $B_1B'_1$; $B_1B'_1$ and $F_1F'_1$; …; $A_2A'_2$ and $B_2B'_2$; $B_2B'_2$ and $F_2F'_2$; … there are EMF sources which vary depending on number of link N under the harmonic law;
- terminals $O_1O'_1$ are superimposed with terminals $O_3O'_3$.

We will also use the same additions to Fig. 6.3 in the analysis of damper winding with these changes: cross elements $A_1A'_1, \ldots, F_2, F'_2$ in Fig. 6.3 will present winding bars with impedance Z_B, longitudinal $A_1B_1, \ldots, B_2F_2$—portions of short-circuited rings (segments) with impedance ZF; longitudinal $F_1A_2, \ldots, F_2A_1$—portions of short-circuited rings (segments) between poles with impedance ZF; loops $F_1F'_1A'_2A_2F_1; F_2F'_2A'_1A_1F_2$—correspond to the space between poles.

Let us designate pole with bars $A_1A'_1; B_1B'_1; \ldots; F_1F'_1$ as CP, and pole of opposite polarity with bars $A_2A'_2; B_2B'_2; \ldots; F_2F'_2$—as letter S_P.

Equation for currents in its longitudinal elements, for example, A_1B_1 in portion $A_1B_1F_1$ was obtained in Chap. 7 in the form (index N in all currents I, J is omitted):

$$I^{C_P} = C_0a_0^N + C_1a_1^N + C_2a_2^N. \tag{9.16}$$

Here, in expressions for currents in recurrent circuit elements the results of partial solution of difference equation are designated as follows:

$$C_0 = \frac{E_M}{Z_B K_B}; \quad a_0 = e^{-jk}. \tag{9.17}$$

It was already noted that this designation facilitates checking results when performing algebraic transformations; C_1, C_2—constants determined from boundary conditions.

Respectively, equation for currents in cross elements, for example, $F_1F'_1$ in portion $A_1B_1F_1$ was obtained as follows:

$$J^{C_P} = C_0a_0^N(1 - a_0^{-1}) + C_1a_1^N(1 - a_2) + C_2a_2^N(1 - a_1). \tag{9.18}$$

Equation for currents in longitudinal elements, for example, A_2B_2 in portion $A_2B_2F_2$:

$$I^{S_P} = C'_0a_0^N + C'_1a_1^N + C'_2a_2^N. \tag{9.19}$$

Equation for currents in cross elements, for example, F_2, F'_2 in portion $A_2B_2F_2$:

$$J^{S_P} = C'_0a_0^N(1 - a_0^{-1}) + C'_1a_1^N(1 - a_2) + C'_2a_2^N(1 - a_1). \tag{9.20}$$

According to the results obtained in Chap. 8 the following ratio takes the form: $C'_0 = -C_0$. For constants C'_1, C'_2 in the last equations the following relationships were proved in Chap. 7:

$$C'_1 = -C_1; C'_2 = -C_2. \tag{9.21}$$

According to Table 9.1, let us assign this regular active closed recurrent circuit to regular damper winding of synchronous machine rotor.

To find currents in all these structural elements of damper winding, let us previously determine the following in Eqs. (9.17)–(9.20):

- Coefficient k;
- EMF amplitude E_M;
- Constants C_1 and C_2;
- Coefficient K_B;

We already considered the similar task for squirrel cage in this chapter. For this task, EMF period of loops was chosen equal to $T = \pi D$.

However, in the analysis of fields excited by some types of windings (for example, in the analysis of fields of regular damper winding or stator windings with integer number of slots per pole and phase), it is sufficient to select other value of period: $T_{EL} = T/p$; respectively, the order of spatial harmonic becomes equal to $m_{EL} = m/p$.

Earlier, we determined physical sense of coefficient k of active recurrent circuit: it is equal to the phase shift angle $\Delta\varphi_N$ between EMF of adjacent elements of active recurrent circuit, for example, of elements with numbers N + 1 and N; it was already noted that if the circuit is symmetrical, then by its determination: $k = \Delta\varphi_N = \text{const}$. For damper winding construction this shift angle $\Delta\varphi_N$ remains constant only within loops located on the pole:

$$\Delta\varphi_N = \Delta\varphi = 2\pi m_{EL}\frac{b}{T_{EL}} = \pi m_{EL}\frac{b}{\tau_{EL}} \neq f(N)$$

Here $\tau_{EL} = \tau = \pi\frac{D}{2p}$—pole pitch [3, 4, 7].

Shift angle $\Delta\varphi F$ between axes of edge slots on adjacent poles is equal to:

$$\Delta\varphi_F = 2\pi m_{EL}\frac{b_F}{T_{EL}} = \pi m_{EL}\frac{b_F}{\tau_{EL}}. \tag{9.22}$$

Let us proceed to the determination of EMF E_M.

It was already obtained in Chap. 8 earlier. Here, when setting this expression for EMF, let us take into account the selected period T_{EL}, its change and consider that $\frac{m}{T} = \frac{m_{EL}}{T_{EL}} = \frac{m_{EL}}{2\tau_{EL}}$. Then expression for EMF takes the form:

$$E_{N+2,N+1} = -j\omega_{ROT}B(m,Q)\frac{2\tau_{EL}}{\pi m_{EL}}L_{COR}\sin\frac{\pi m_{EL}b}{2\tau_{EL}}\cdot e^{-j\pi m_{EL}\frac{b_F}{2\tau_{EL}}}e^{-j\pi m_{EL}\frac{b_F}{2\tau_{EL}}}e^{-j\pi m_{EL}\frac{b(N+1)}{\tau_{EL}}}. \tag{9.23}$$

$$E_M = -j\omega_{ROT}B(m,\,Q)\frac{2\tau_{EL}}{\pi m_{EL}}L_{COR}\sin\frac{\pi m_{EL}b}{2\tau_{EL}}\cdot e^{-j\pi m_{EL}\frac{b_F}{2\tau_{EL}}}\cdot e^{-j\pi m_{EL}\frac{b}{2\tau_{EL}}}. \tag{9.23′}$$

Let us write down calculation expressions for constants C_1 and C_2. Constants C_1, C_2 were calculated earlier from boundary conditions using equations according

to both Kirchhoff's laws. The system was derived from these equations; these constants are obtained from its solution

$$C_1 = \frac{D_1}{D_0}; \quad C_2 = \frac{D_2}{D_0}.$$

Here D_0—system determinant, D_1, D_2—its algebraic adjuncts.

As a result, currents are determined in longitudinal and cross elements of damper winding.

In Chap. 7, expressions for them are obtained in the form (7.35). We will present expressions for calculation of these constants in this paragraph in an expanded form. Such representation is more convenient for checking calculation expressions obtained: in further statement they will be used for one limit task whose solution in addition allows us to prove their validity.

Let us transform additions D_1, D_2 in Eq. (7.35) and present them as:

$$\begin{aligned} D_1 = {} & E_{F1A2}\left(a_2^{N_0-1} + a_1\right) + C_0\left[Z_B\left(a_2^{N_0-1} - 2a_2^{N_0-1}a_0^{-1}\right.\right. \\ & + a_0^{N_0-1}a_2^{N_0-2} + a_1 + 2a_1a_0^{N_0-1} - a_0^{N_0-2}a_1 + a_2^{N_0-2}a_0^{-1} - a_0^{N_0-1} \\ & \left.\left. - a_0^{-1} - a_0^{N_0-2}a_2^{N_0-1}\right) + Z_{F1A2}\left(2a_1a_0^{N_0-1} - a_0^{N_0-2}a_2^{N_0-1} - 2a_2^{N_0-1}a_0^{-1}\right)\right]. \end{aligned} \tag{9.24}$$

Here $Z_{F1A2} = Z_F$. Constant $(-C_2)$ can be obtained from C_1 by substitution of a_2 by a_1 and, respectively, a_1 by a_2.

Let us also transform the expression for system determinant D_0 in (7.35) and present it in the form:

$$D_0 = 2Z_B\left[(a_2 - a_1) + \left(a_2^{N_0} - a_1^{N_0}\right) - \left(a_2^{N_0-1} - a_1^{N_0-1}\right)\right] + 2Z_{F1A2}\left(a_2^{N_0} - a_1^{N_0}\right). \tag{9.25}$$

At first, let us perform an analysis of expression for D_0. In the determinant, we have the relation $\sigma = \frac{2Z_B}{Z_R} \neq 0$; coefficients $a_2 \neq a_1$, and for clarity it was accepted that $a_2 < a_1$. As a result we come to an important conclusion: always system determinant $D_0 \neq 0$.

To find currents in all these elements of damper winding, it is necessary to write down in (9.24) the expression for EMF E_{F1A2} induced by resulting rotating field in air gap. It was obtained in Chap. 8 in the form (8.9′):

$$E_{F1A2} = -j\omega_{ROT}B(m, Q)\frac{T}{\pi m}L_{COR}\sin\frac{\pi m b_F}{T}e^{-j\pi m_{EL}}. \tag{9.26}$$

Thus, from investigation results we obtain that the current in damper winding elements as well as in recurrent circuit elements corresponding to it, is determined under the complicated law:

- its two components vary with element number N under the aperiodic law,
- one—under harmonic law.

In operation of salient pole machine in nonlinear network, for example, from a frequency converter or in an industrial network with variable load, this fact leads to uneven distribution of currents in bars and portions of short-circuited rings (segments). With sharp load variation, for example, at start-up, middle bars on pole pass the current of smaller amplitude than end ones; also currents in ring portions (segments) are distributed respectively. It should be noted that motor start-up is limited in time by only some tens seconds, however, it is characterized by high current amplitudes in damper winding elements and, respectively, intensive emission of losses in them. Practical methods of calculating overheats in short-circuited rotor winding elements at variable load with account of bar temperature influence on skin effect, that is a variation of main and additional losses from the temperature are given in Appendix 9.1.

Uneven distribution of currents in elements of damper winding and, therefore, uneven distribution of temperature causes appearance of additional temperature deformations and corresponding stresses, and sometimes also damages in bars (breaks).

For balancing currents distribution, temperatures and corresponding deformations, damper winding bars of motors in some constructions are made of metals with different resistivity. However, this action causes appearance of several additional fields in air gap and corresponding torques on motor shaft that is undesirable. In more detail, the problem of currents distribution calculation in this damper winding construction at asymmetry in it, is considered in Chap. 11.

Operating modes of salient pole machine in nonlinear network, for example, of generator or frequency-controlled motor, have peculiarities distinguishing them from modes of asynchronous start:

- these modes are long-term;
- currents in damper winding elements are less in amplitude;
- stator winding field in air gap at T = idem is created by two “adjacent” harmonics and has two components differing in amplitude; they rotate relative to rotor in opposite direction, but induce in its loops EMF and currents of equal frequency ω_{ROT}. These field peculiarities are given in Chaps. 3, 12 and 13. Influence of these harmonics leads to the fact that distribution of currents and losses in bars and ring portions, when machine operates in nonlinear network, can differ from their distribution in asynchronous mode; peculiarities of distribution of currents and losses are considered in Chap. 15.

9.5 Checking Results: Transformation of Expression for Currents in Elements of Complete Damper Winding of Synchronous Machine in Expression for Currents in Squirrel Cage Elements of Induction Machine

Calculation expressions for distribution of currents in damper winding elements are obtained for the first time, therefore in several paragraphs of the monograph they are subjected to numerous checks.

In Chap. 7 for this purpose we already considered one special case of transformation of asymmetrical regular active closed recurrent circuit into symmetrical active open; this transformation proves solution validity of difference equations for currents in both recurrent circuits and obtained calculation expressions for currents in their elements.

In this para we will consider one more transformation which also proves validity of calculating expressions for currents and EMF in damper winding elements of salient pole machine obtained in previous para. This fact allows us to use confidently calculation expressions for currents in damper winding elements in engineering practice.

Let us consider a limit case: damper winding construction with length b_F equal to the portion between bar axes on the pole b; also their impedances are respectively equal to:

$$b_F = b; \quad Z_R = Z_F. \tag{9.27}$$

If we assume additionally that the space between poles is filled with ferromagnetic material with the same properties as pole steel, practically, it means that for this pole we have pole arc α (in p.u.) equal to $\alpha = 1$ (it means $b_p = \tau$). This damper winding is equivalent to the squirrel cage of induction machine rotor; number of its slots per pole N_0 would be equal to $N_0 = \frac{Z_2}{2p}$, where Z_2—number of slots of equivalent rotor in induction machine.

Let us remind at first that in this paragraph the following designation was accepted: $a_0 = e^{-j\Delta\varphi}$. Then, taking into account conditions (9.27) for this winding, the following transformations are true:

$$\begin{gathered} a_0^{-1} = e^{j\Delta\varphi}; a_0^{N_0-1} = e^{-j\Delta\varphi(N_0-1)} = -e^{j\Delta\varphi}, \quad \text{as} \\ e^{-j\Delta\varphi N_0} = -1; a_0^{N_0-2} = e^{-j\Delta\varphi(N_0-2)} = -e^{j2\Delta\varphi}. \end{gathered} \tag{9.28}$$

We show that in this case taking into account (9.28) both constants in equations for currents $C_1 = D_1/D_0$ and $C_2 = D_2/D_0$ are identically equal to zero and do not depend on the number of bars per pole N_0.

Let us present the algebraic adjunct D_1 in the form of two summands:

$$\begin{aligned} D_1 &= D_{1,1} + D_{1,2}. \\ \text{Here } D_{1,1} &= E_{F1A2}\left(a_2^{N_0-1} + a_1\right); \\ D_{1,2} &= C_0\left[Z_B\left(a_2^{N_0-1} - 2a_2^{N_0-1}\cdot e^{j\Delta\varphi} + a_2^{N_0-1}\cdot e^{2j\Delta\varphi}\right.\right. \\ &\quad \left.\left. -2a_1e^{j\Delta\varphi} + a_1 + a_1e^{2j\Delta\varphi}\right) - Z_{F1A2}\left(2a_1e^{j\Delta\varphi} + a_2^{N_0-1}e^{j\Delta\varphi}\right)\right]. \end{aligned} \tag{9.29}$$

Let us consider the first summand. We use Eq. (9.26) for EMF EF2A1 (Fig. 6.3) and present $D_{1,1}$ in the form:

$$D_{1,1} = E_{F1A2}\left(a_2^{N_0-1} + a_1\right) = j\omega_{ROT}B(m, Q)\frac{2\tau_{EL}}{\pi m_{EL}}L_{COR}\sin\frac{\pi m_{EL}b}{2\tau_{EL}}\left(a_2^{N_0-1} + a_1\right).$$

In this transformation it was considered that $b_F = b$ according to conditions (9.27).

After transformation of second summand taking into account the ratios (9.28) we have:

$$D_{1,2} = C_0Z_B\left[\left(a_2^{N_0-1} + a_1\right) - (2+\sigma)\left(a_2^{N_0-1} + a_1\right)e^{j\Delta\varphi} + \left(a_2^{N_0-1} + a_1\right)e^{2j\Delta\varphi}\right].$$

Expression for C_0 is given in the previous paragraph: $C_0 = \frac{E_M}{Z_BK_B}$. EMF E_M is already obtained earlier in (9.23′).

As a result, for the second summand $D_{1,2}$ we get:

$$\begin{aligned} D_{1,2} &= -j\omega_{ROT}B(m, Q)\frac{2\tau_{EL}}{\pi m_{EL}}L_{COR}e^{-j\pi m_{EL}\frac{b}{2\tau_{EL}}}\cdot e^{-j\pi m_{EL}\frac{b}{2\tau_{EL}}}\sin\frac{\pi m_{EL}b}{2\tau_{EL}}\left(a_2^{N_0-1} + a_1\right)\cdot \\ &\cdot e^{j\Delta\varphi}\frac{1-(2+\sigma)e^{j\Delta\varphi} + e^{2j\Delta\varphi}}{1-(2+\sigma)e^{j\Delta\varphi} + e^{2j\Delta\varphi}} = -j\omega_{ROT}B(m, Q)\frac{2\tau_{EL}}{\pi m_{EL}}L_{COR}\sin\frac{\pi m_{EL}b}{2\tau_{EL}}\left(a_2^{N_0-1} + a_1\right). \end{aligned}$$

In this transformation it was considered that as per (9.22) $\Delta\varphi = \pi m_{EL}\frac{b}{\tau_{EL}}$, and coefficient K_B is equal to:

$$K_B = \left[1-(2+\sigma)e^{-j\Delta\varphi} + e^{-2j\Delta\varphi}\right]e^{j\Delta\varphi} \text{ or } K_B = \left[1-(2+\sigma)e^{j\Delta\varphi} + e^{2j\Delta\varphi}\right]e^{-j\Delta\varphi}.$$

We obtained both summands $D_{1,1}$ and $D_{1,2}$ of algebraic adjunct D_1; they are equal in value and are opposite in sign, so their sum is identically equal to zero: $D_1 = D_{1,1} + D_{1,2} \equiv 0$.

Similar identity is also true for the algebraic adjunct D_2.

In the previous paragraph we analyzed the expression for D_0. From this it follows that at $b_F = b$; $D_0 \neq 0$.

Thus, we came to the conclusion that in limit task, under conditions $b_F = b$; $Z_R = Z_{F1A2} = Z_F$ constants C_1, C_2 are identically equal to zero, so currents in elements of this damper winding vary with bar number N under the harmonic law as in squirrel cage of induction machine.

This conclusion proves additionally the validity of the obtained calculation expressions for currents in damper winding elements.

9.6 About the Determination of Damper Winding Reactances Based on Solution Obtained in This Chapter on Distribution of Currents in This Winding (Discussion Between L. A. Kilgore, Westinghouse El. Corp. and M. E. Talaat, Elliott Comp. [21, 22])

In previous paragraphs of this chapter, we obtained an analytical solution for distribution of currents in construction elements of damper winding. On the basis of this distribution it is possible to solve one more actual practical problem: to specify parameters of rotor loops necessary for calculation of synchronous machine transient performances. Let us turn our attention to one of known publications [21] devoted to the solution of this problem. It is followed by substantial discussion with participation of leading experts of the USA from firms of manufactures of power machines (Westinghouse, General Electric and Elliott Company).

In the publication [21], its author M. Talaat made an attempt to specify equations for calculation of reactances in salient pole synchronous machine. Earlier, these equations were obtained by Kilgore [22], confirmed by extensive experimental material and were widely used in engineering practice by experts not only in the USA, but also in Europe. In [21] M. Talaat set the task to prove that Kilgore's [22] work is incorrect, as the expression obtained by L. Kilgore for subtransient reactance does not meet the limit condition: it does not coincide with the expression for reactance of secondary loop of induction machine rotor (squirrel cage) if we assume that pole arc $\alpha = 1$, or in the designations accepted in this monograph: $b_F = b$.

At the same time, the expression obtained in [21] by M. Talaat, meets this condition; in the derivation he accepted the assumption of sinusoidal distribution of currents in bars of damper winding.

L. Kilgore in discussion proved the solution obtained by him, having noted:

> … As to method, the author (M. E. Talaat) claims his assumed sinusoidal distribution of currents in the damper to be better than my attempt to proportion the currents at least in the pole—tip bars depending on the permeance. The chief argument is that, in a round rotor machine with open field this distribution is approached. This does not prove that it is accurate in practical salient—pole machines since, even with uniform bar materials and permeances, the pole—tip bars have quite a different current distribution. Actually, neither method of dealing with the damper is very accurate, if applied to too wide a variety of machines. I feel there is still room for some good work by one interested in the true

distribution of the currents who has a facility of boiling dawn exact solutions to usable design approximation.

Let us proceed to assessment of the assumptions accepted by both authors, using the results obtained in this monograph:

- equations for currents in damper winding elements;
- solution results of limit task: expressions for currents in damper winding of salient pole machine for pole arc, equal to unity ($\alpha = 1$), that is under condition: $b_F = b$.
- It is methodically convenient to subdivide problems of determination of synchronous machine reactance into two:
- problem of distribution of currents in damper winding bars;
- problem of MMF determination of rotor and stator loops for calculation of reactance, proceeding from distribution of currents.

(a) Let us consider the first of these problems: distributions of currents in damper winding bars.

In his work, Talaat [21] set the harmonic distribution of currents in damper winding bars of synchronous machine as the basis for determination of reactance. He gives no validity proof for this assumption, but it is only mentioned that this distribution is characteristic for induction machine squirrel cage, and squirrel cage, in his opinion, is in this case a limit task (at pole arc $\alpha = 1$, that is under condition: $b_F = b$).

Contrary to this assumption, L. Kilgore proceeded from physical process of occurrence of EMF and current in damper winding from the mutual field harmonics in the air gap. He fairly considered that currents in damper winding bars should not distribute under the harmonic law, and current amplitude in pole edge bars should exceed those in middle ones; currents in these edge bars were approximately determined by him. It is natural that harmonic distribution of currents in bars could not be assumed by him as a basis for calculation of reactance.

Let us estimate the correctness of solution of both authors, using the solution obtained in this monograph for currents in damper winding structural elements.

M Talaat's assumption on harmonic distribution of currents in damper winding considers only one summand in (9.16–9.20); both aperiodic components were not considered. However, these components lead to considerable distortion of currents distribution picture, and at their expense, the current amplitudes in edge bars exceed those in middle one that is also confirmed experimentally. At the same time, the results of task solution obtained in this monograph for currents in damper winding (9.19–9.20) do not contradict to solution results of task on currents in squirrel cage (9.3–9.4) and to their harmonic distribution in bars. The solution results obtained in the previous para for limit task confirmed that at $\alpha = 1$ both aperiodic components of damper winding currents become equal to zero.

L. Kilgore's approximate solution that currents in damper winding should not be distributed under the harmonic law, and current amplitudes in pole edge bars

exceed those in middle ones, is correct, is confirmed by results obtained in this monograph and reflects physical condition of the process.

Thus, solution of the first problem—distribution of currents in damper winding bars—is more correctly executed by L. Kilgore; unfortunately, this solution belongs only to pole edge bars, but not to all construction elements of damper winding.

b) Let us consider the second problem: determination of MMF of rotor and stator loops for calculation of reactances, based on distribution of currents.

Calculation of these reactances assumes that in machine rotor and stator there are magnetically coupled loops which generate in the operational modes mutually moveless fields in air gap; these fields form the resulting field. In the problem considered for determination of damper winding reactance such loops are: in stator —loops of three phases forming field of stator reaction in the air gap; in rotor—loops of damper winding also forming in the operational modes field in the air gap. When rotor rotates with set slip, magnetically coupled stator and damper winding fields are those which have equal periods and rotation speeds relative to stator.

Results of investigation of MMF and fields in the air gap excited by currents in stator loops were obtained in Chap. 3 for general case (non-sinusoidal currents in phases) at a number of phases in winding $m_{PH} = 3$ and $m_{PH} = 6$ and for various connection circuits (star, separate phase power supply, etc.).

General method of harmonic analysis of MMF of currents in loops of short-circuited rotor winding (damper winding, asymmetrical squirrel cage), convenient for practical application, is given in Chap. 12. Using the results obtained, it is easy to show that the rotor field MMF amplitude considerably is determined by currents in damper winding edge bars: they exceed currents in its middle bars.

From the results obtained in this chapter, it follows: In M. Talaat's work, it could be just for clarification (in comparison with L. Kilgore's work) of MMF amplitudes with account of distribution of currents in damper winding bars. However, this substantiation cannot be executed with M. Talaat's assumption on harmonic distribution of currents in its bars.

Thus, solution of the second problem—MMF determination of rotor damper winding loops is performed by Talaat [21] with several considerable errors not reflecting real physical processes. It is connected with unreasonable assumption on harmonic distribution of currents in damper winding bars. In such an assumption, M. Talaat does not consider the following circumstances:

- MMF amplitude of damper winding is determined not only by harmonic component of current (9.19)–(9.20), but also by two aperiodic components in these expressions;
- In MMF curve of damper winding there should appear besides the first spatial harmonic some more higher harmonics; their assessment was not made by M. Talaat;
- Accounting of actual currents only in pole edge bars performed by L. Kilgore reflects physical condition of problem more fully: amplitudes of these currents in operational modes exceed current amplitudes in pole middle bars and considerably determine MMF amplitude in damper winding.

As a result, solution of the second problem—determination of MMF of rotor loops for calculation of machine reactance—is also more correctly done by L. Kilgore; unfortunately, when determining MMF he considered only currents in pole edge bars, but not currents in all its bars that is associated with an error in MMF value.

Appendix 9.1: Method of Calculation of Overheats of Short-Circuited Rotor Winding Elements at Start-Up with Account for Change of the Main and Additional Losses in it from Temperature (with Account of Skin Effect)

In calculation practice, when determining admissible short-term overloads of stator winding made of copper elementary conductors, the following relation is usually applied [3, 4, 10]:

$$\frac{d\Theta(t)}{dt} = \frac{j_{EQ}^2 K_F}{175}. \tag{A.9.1.1}$$

Here $\Theta(t)$—winding temperature (overheat); t—time; j_{EQ}—mean square value of current density in winding element during T_{TR} of transient thermal performance (A/mm^2), K_F—Field's factor [3, 4, 7]:

$$j_{EQ}^2 = \frac{1}{T_{TR}} \int_0^{T_{TR}} j^2(t)\, dt$$

and j_{EQ}—corresponds to the effective value of current. From this ratio the stator winding temperature is obtained:

$$\Theta(t) = \Theta(t = 0) + j_{EQ}^2 K_F \frac{T_{TR}}{175}. \tag{A.9.1.2}$$

Here $\Theta(t = 0)$—stator winding temperature in the set mode before overload, for example, at no-load or before machine commissioning.

This expression is an approximate solution of thermal balance equation for adiabatic heating [10]:

$$Pdt = CGd\,\Theta(t). \tag{A.9.1.3}$$

Here designated: P—electric losses dissipated in winding; $\Theta(t)$—temperature (overheat); C—specific heat; G—winding weight.

Calculation Equation (A.9.1.2) is obtained from (A.9.1.3) without account of temperature for conductor specific impedance; it is true for copper elementary conductors with resistivity calculated at their average temperature in transient thermal mode, equal to $\Theta \approx 50\,^{\circ}\mathrm{C}$.

However, unlike admissible temperatures of stator winding [3, 7] temperature of short-circuited rotor winding bars of A.C. machines (damper winding, squirrel cages) in the operational modes reaches $\Theta < 300\,^{\circ}\mathrm{C}$ [3, 4, 7]; in such modes for calculation of bar temperature it is also necessary to consider an increase in conductor resistivity with temperature increase.

At first, let us consider an increase from temperature of D.C. bar losses (ohmic). For small power machines (with bar height in rotor slot at most 15–20 mm) we can approximately consider that K_F factor with temperature increase remains invariable; then from the solution of differential equation (A.9.1.3) we obtain:

$$\Theta(t) \approx \frac{[\Theta(t=0)\rho^* + 1]e^{tA\rho^*} - 1}{\rho^*}. \qquad \text{(A.9.1.4)}$$

Here ρ*—temperature factor of conductor resistivity, $A = j_{EQ}^2 \frac{K_F}{B}$; values B and ρ* are given in Table 9.2.

Let us consider an increase in not only D.C. losses (ohmic) in bar, but also additional losses from temperature: for high power A.C. machines (with bar height in slot over 25–30 mm) it is necessary to consider additionally a change of K_F factor with temperature increase. Let us note that for each bar shape (rectangular, round, trapezoidal, bottle, etc.) this relation for specified dimensions is considered only by conductor "reduced height" [1, 2].

As a result, for high-power A.C. machines fr K_F om the solution of Equation (A.9.1.3) we obtain [23]:

$$T_{TR} \approx \frac{2}{A_1\rho^*}\left[\sqrt{1+\rho^*\Theta(t)} - \sqrt{1+\rho^*\Theta(t=0)}\right]. \qquad \text{(A.9.1.5)}$$

Here, $A_1 = j_{EQ}^2 \frac{K_{F,0}}{B}$. $K_{F,0}$—value of bar Field's factor at resistivity for temperature Θ(t = 0).

Let us note that for motor mode the overheat is calculated at each step of numerical integration of start-up differential equation; thus, dynamic moment of inertia and torque on the shaft of mechanism are considered. The refined method for calculating the overheating at the start, or due to sudden change of the mode of cage

Table 9.2 Values B and ρ*

Conductor	B	ρ*
Copper	210	1/235
Aluminum	85	1/245
Brass (manganous)	35	1/500
Bronze (phosphorous)	28	1/333

rotor cores with the account of the skin effect is set out in the appendix to Chap. 23. It can be used as an element of CAD when calculating of the powerful induction motors (see Chap. 4).

Brief Conclusions

1. Processes of currents distribution in active recurrent circuits (open and closed) are identical to those in construction elements of short-circuited rotor windings used in modern practice (damper winding, squirrel cages). Methods of investigation of these circuits developed in previous chapters allow obtaining regularities of currents distribution, important for practice, in these windings. In particular, we obtain the following regularity of currents distribution in construction elements of regular damper winding in asynchronous operating mode of salient pole machine and for operation in nonlinear network. Current contains three components which vary with the number N as follows:

- one of them varies depending on bar or ring portion number under the harmonic law;
- two others—under the aperiodic law, one of which with increase in this number fades in amplitude, the other—decreases.
- The solution obtained for currents distribution in regular damper winding elements is confirmed:
- by coincidence of calculation expressions for currents in elements of complete and incomplete damper winding (in limit case at $Z_F \to \infty$);
- by coincidence of calculation expressions for currents in elements of complete and squirrel cage (in limit case at $b_F = b$ and respectively, $Z_F = Z_R$);

2. With sharp load variation in frequency-controlled salient pole motors or industrial motors, the current components vary with damper winding loop number under the aperiodic law, and result in uneven distribution of resulting current in bars: pole middle bars pass current considerably of smaller amplitude, than edge ones; also currents in ring portions (segments) are respectively distributed. Uneven distribution of currents in elements of damper winding causes uneven distribution of their temperature, appearance of additional temperature deformations and corresponding stresses, and sometimes damages (breaks) in bars.

Stator winding field, when operating in non-linear network at T = idem, is created by two "adjacent" harmonics and has two components differing in amplitude; they rotate relative to rotor in opposite direction, but induce in its loops EMF and currents of equal frequency ω_{ROT}. A result of influence of these harmonics, the processes of currents distribution and losses in bars and damper winding ring portions can differ from those in asynchronous mode.

Representation of squirrel cage in the form of symmetrical multiphase winding with "reduction" of short-circuited ring element impedance to bar impedance is a special case of its representation in the form of symmetrical active closed recurrent circuit. In case of damages in cage, investigation of currents in it by the method of symmetrical components (as in asymmetrical multiphase system) meets considerable computing difficulties [21] and is unpromising; at the same time, the methods of investigation of asymmetrical active recurrent circuits developed in the monograph allow us to investigate also more difficult rotor windings constructions: irregular damper winding, squirrel cages with damage.

List of symbols

b	Pitch between pole slot axes;
b_P	Width of pole;
b_F	Distance between axes of edge slots on adjacent poles;
B(m, Q)	Flux density amplitude of resulting field in air gap;
C	Specific heat;
D	Stator boring diameter;
E_M	Rotor loop EMF amplitude;
G	Winding weigth;
j_{EQ}	Mean square value of current density in rotor winding element;
J, I	Currents in bars and ring portions of symmetrical short-circuited rotor winding;
K_F	Field's factor;
$K_{F,0}$	Value of bar Field's factor at resistivity for temperature $\Theta(t = 0)$;
L_{COR}	Active length of stator core;
m, m_{EL}	Spatial harmonic order;
N	Bar (ring portion) number of damper winding or squirrel cage;
N_0	Number of bars of damper winding on pole or squirrel cage on the rotor;
N_p	Asymmetrical bar number;
p	Number of pole pairs;
P	Electric losses dissipated in winding;
Q	Time harmonic order;
t	Time;
T, T_{EL}	Serial expansion periods of MMF and of mutual field to harmonic series;
T_{TR}	Time of transient thermal performance;
x	Current coordinate along stator boring (in tangential direction);
x_0	Distance from origin of coordinates to first rotor slot (bar) axis;

Z_B, Z_R, Z_F	Impedances of bar, ring portion between pole bars, of ring portion between edge bars of adjacent poles;
Z_{N_p}	Impedance of asymmetrical bar;
ΔZ	Additional impedance of asymmetrical bar;
α	Pole arc $(\alpha = b_p/\tau)$;
σ, σ'	Relations determined by impedances of symmetrical recurrent circuit elements;
τ	Pole pitch;
$\Phi_{1,0}, \ldots, \Phi_{N+2,N+1}$	Mutual resulting fluxes linked accordingly with loop (1, 0) and loop (N + 2, N + 1);
φ_N	Phase angle of loop EMF with number N;
$\Theta(t)$	Winding temperature (temperature rise);
ρ^*	Temperature factor of conductor resistivity;

References

I. Monographs, Textbooks

1. Demirchyan K.S., Neyman L.R., Korovkin N.V., Theoretical Electrical Engineering. Moscow, St. Petersburg: Piter, 2009. Vol. 1, 2. (In Russian).
2. Kuepfmueller K., Kohn G., Theoretische Elektrotechnik und Elektronik. 15 Aufl., Berlin, New York: Springer. 2000. (In German).
3. Schuisky W., Berechnung elektrischer Maschinen. Wien: Springer, 1960. (In German).
4. Construction of Electrical Machines. Edited by of Kopylov, I.P., Moscow: Energiya, 1980. (In Russian).
5. Richter R., Elektrische Maschinen. Berlin: Springer. Band I, 1924; Band II, 1930; Band III, 1932; Band IV, 1936; Band V, 1950. (In German).
6. Mueller G., Ponick B., Elektrische Maschinen. N. Y., J. Wiley, 2009. (In German).
7. Mueller G., Vogt, K., Ponick B., Berechnung elektrischer Maschinen. Springer, 2007. (In German).
8. Mueller G., Ponick B., Grundlagen elektrischer Maschinen. Springer, 2005. (In German).
9. Kostenko M.P., and Piotrovskiy L.M., Electrical machines. Vol. 2. Leningrad: Energiya. 1965. (In Russian).
10. Gotter G., Erwaermumg und Kuehlung elektrischer Maschinen. Berlin (Goettingen), Heidelberg: Springer, 1954. (In German).

II. Induction Machines. Papers, Inventor's Certificates

11. Vaš P., Analysis of space–harmonics effects in induction motors using N – phase theories. – International Conference of Electrical Machines. Brussel, 1978.

III. Synchronous Machines. Papers, Inventor's Certificates, Patents

12. Boguslawsky I.Z., Demirtschian K.S., Stationaere Stromverteilung in unregelmaessigen und unsymmetrischen kurzgeschlossenen Laeferwicklungen von Wechselstrommaschinen. Archiv fuer Elektrotechnik, 1992. № 6. (In German).
13. Boguslawsky I.Z., Currents in a asymmetric short – circuited rotor cage. Power Eng., N. Y, 1982, № 1.
14. Boguslawsky I.Z., Calculating the current distribution on the damper winding of large slow–speed synchronous motors in asynchronous operation. Power Eng. N. Y, 1979. № 3.
15. Demirchyan K.S., Boguslawsky I.Z., Current flowing in damper winding bars of different resistivity in a heavy- duty low speed motor. Power Eng., N. Y, 1980, № 2.
16. Boguslawsky I.Z., Currents and harmonic MMFs in a damper winding with damaged bar at a pole. Power Eng., N. Y, 1985, № 1.
17. Boguslawsky I.Z., The calculation method of short-term stress of the damper winding. – In book: Electrotechnical Industry. Electrical machines, Issue. 2, 1983. (In Russian).
18. Ambrosini M., Sacceti R., Circuiti aquivalenti di machine asincroni alimentate con tensioni in sequenze generalizzate di Fortescue. L'Energia Electrica, 1980, №11. (In Italian).
19. Ambrosini M., Filipetti F., Il metodo dei circuiti equivalente parziale nello studio dei regimi di quasto nei motori asincroni a gabbia. L'Energia Elettrica, 1981, №1. (In Italian).
20. Saccetti R., Troili R., Una tecnica unitaria nello studio dei circuiti a delle motori il metodo dei circuiti equivalente parziale. L'Energia Electrica, 1980, №3. (In Italian).
21. Schuisky W., Ueber die Stromverteilung im Anlaufkaefig eines Synchronmotors. E. u M., 1940, №9/10. (In German).
22. Talaat M.E., A new approach to the calculation of synchronous machine reactances. Power Apparatus and Systems. 1955, № 17; 1956, № 24.
23. Kilgor L.A., Calculation of synchronous machine constants reactances and time constants affecting transient characteristics. Trans. AIEE, 1931, v. 50.

Chapter 10
Investigation Methods of Currents Distribution in Squirrel Cages with Asymmetry

This chapter generalizes investigation methods of asymmetrical active U-shaped chain circuits (open and closed) developed in previous chapters. On their basis we obtained important results for practice regularities of currents distribution in asymmetrical squirrel cages (with breakages) induction machines:

- besides currents in symmetrical squirrel cage elements there are additional currents with two components;
- both components vary depending on the number of bar ring portion under the aperiodic law, one of which fades with increase of this number in amplitude, and another—increases.

The general problem on the calculation of currents distribution in rotor squirrel cage with P asymmetrical bars is considered; it is obtained as being reduced to the solution of an algebraic system of linear equations. Its order is determined only by number P of these asymmetrical bars; it does not depend on total number of N_0 bars in the cage. This method has essential advantages in comparison with numerical methods based on the solution of a system of Kirchhoff's equations for N_0 loops. In practical problems $N_0 \leq 70$, and $P \leq 3 - 4$. For small slips, real and imaginary parts of some system coefficients differ in some tens times, therefore, the solution of systems of high order N_0 with complex coefficients meets difficulties. Besides the general problem, its special cases representing independent practical interest are considered:

- asymmetrical squirrel cage with two (not adjacent) damage bars;
- asymmetrical squirrel cage with three adjacent damage bars;
- asymmetrical squirrel cage with three damage bars: two bars nearby, the third—next but one;
- asymmetrical squirrel cage with three damage bars: three bars, not adjacent.

Prospects of investigating rotor asymmetrical short-circuited windings by means of active closed chain circuit of various structure [7, 8] are noted: investigation of

I. Boguslawsky et al., *Large A.C. Machines*,
DOI 10.1007/978-4-431-56475-1_10

currents is not cumbersome and differs in clarity of physical representations. Unlike this method, the use for this purpose of traditional analytical method (symmetric components) leads to difficult calculations even for a number of elementary problems [9–11]. It is also noted that for investigating currents in the design of damper winding, this traditional analytical method (of symmetric components) cannot be practically used.

An example is given to calculate the distribution of currents in elements of squirrel cage of DAP type motor (1250 kW, 6000 V, 1500 rpm) in case of breakages in it («Elektrosila» Work, Joint-Stock Company "Power Machines" St. Petersburg).

The content of this chapter is development of the methods stated in [1, 2, 12–14, 18–21].

10.1 General Comments

Let us start consideration of investigation methods of currents in asymmetrical constructions of short-circuited rotor windings found in modern practice with induction machine squirrel cage; in this structure, impedance of one or several bars differs from the others. The results obtained in the investigation of passive and active chain circuits of various structures are the basis for this investigation. Compliance between short-circuited windings of rotor and these circuits is given in Table 9.1 of the previous chapter.

10.2 Currents in Asymmetrical Squirrel Cages of Induction Machine Rotors

An asymmetry in short-circuited rotor of induction motors can arise both in machine manufacturing and in operation. In manufacturing of high-power induction machine rotors, additional impedance in bar-end ring joint can appear (due to low-quality soldering or welding), and in manufacturing of low and average power machines with cast cage—due to defects in molding process. Severe operation conditions from a network or from a frequency converter, especially with sharp load variation, sometimes lead to bar or ring damages, including their break (due to cage temperature deformations) [7–17].

Practice puts forward the problem of developing methods for calculating performance characteristics of such motors with rotor asymmetry. The purpose of this development: determination of admissible modes of machine operation.

Methods of analytical investigation of asymmetrical active open and closed chain circuits were developed in Chap. 7; these chain circuits differ in that the EMF of each loop varies depending on its number under harmonic law.

In these investigations, it is obtained that resulting currents $\underline{\underline{I}}_N, \underline{\underline{J}}_N$ in asymmetrical chain circuit elements ($\Delta Z \neq 0$) have two components

$$\underline{\underline{I}}_N = I_N + \Delta I_N, \quad \underline{\underline{J}}_N = J_N + \Delta J_N,$$

where J_N, I_N—main currents in symmetrical chain circuit elements (without damages); $\Delta J_N, \Delta I_N$ additional currents caused by the asymmetry in chain circuit. According to the first Kirchhoff's law [1, 2]: $\underline{\underline{J}}_N = \underline{\underline{I}}_N - \underline{\underline{I}}_{N-1}$, and, therefore, $J_N = I_N - I_{N-1}, \Delta J_N = \Delta I_N - \Delta I_{N-1}$.

The peculiarity of developed investigation method is that additional currents of asymmetrical active chain circuit are expressed through currents of symmetrical circuit (main currents) corresponding to it, and the order of system of equations for calculation of constants determining additional currents is minimum. It is determined only by the number of asymmetrical bars.

Investigation methods of closed asymmetrical chain circuits [18] developed in Chaps. 6, 7 are used for investigating damper winding of various structure and asymmetrical squirrel cages [12, 13, 19–21].

10.2.1 Squirrel Cage with Asymmetrical Rotor Bar

Ratios obtained in Chap. 7 for the calculation of distribution of additional currents in asymmetrical active closed chain circuit with one damaged cross element ($\Delta Z \neq 0$) remain true for squirrel cage with one damaged bar.

Calculation expressions for squirrel cage MMF with this damage will be given in Chap. 12.

10.2.2 Squirrel Cage with Two (Not Adjacent) Asymmetrical Bars in Rotor. Additional Currents in Winding Elements

Let us use Fig. 8.2 to illustrate this construction. We accept that squirrel cage contains two (not adjacent) asymmetrical bars: bars AA′ (with number N_{P_1}) and EE′ (with number N_{P_2}), moreover $N_{P_2} > N_{P_1}; N = 0, 1, 2, \ldots, N_0 - 1$. Let us accept for clarity that $N_{P_1} = 0$.

Additional currents in ring portions a $N_{P_2} \leq N < N_0$ are as follows:

for portions with numbers (portions of segment EFA, Fig. 8.2):

$$\Delta I_{(N)} = C_3 a_1^N + C_4 a_2^N, \tag{10.1}$$

for portions with numbers $N_{P_1} \le N < N_{P_2}$ (portions of segment ADE, Fig. 8.2):

$$\Delta I_{(N)} = C_5 a_1^N + C_6 a_2^N, \tag{10.1'}$$

where a_1, a_2—as per (6.12): $a_{1,2} = \frac{2+\sigma \pm \sqrt{\sigma^2+4\sigma}}{2}$; $\sigma = 2\frac{Z_R}{Z_B}$.

Expressions for additional currents in bar(s) with number(s) are as follows:

$$\begin{aligned}
&N_{P_1} < N < N_{P_2} : \cdots \Delta J_{(N)} = C_5 a_1^N (1 - a_2) + C_6 a_2^N (1 - a_1);\\
&N_{P_2} < N < N_0 : \cdots \Delta J_{(N)} = C_3 a_1^N (1 - a_2) C_4 a_2^N (1 - a_1);\\
&N = N_{P_1} : \cdots \Delta J_{N=N_{P_1}} = a_1^{N_{P_1}} (C_5 - C_3 a_2) + a_2^{N_{P_1}} (C_6 - C_4 a_1);\\
&N = N_{P_2} : \cdots \Delta J_{N=N_{P_2}} = a_1^{N_{P_2}} (C_3 - C_5 a_2) + a_2^{N_{P_2}} (C_4 - C_6 a_1).
\end{aligned} \tag{10.2}$$

If the number of bars with asymmetry is more than two, the number of constants increases correspondingly [12, 13]. The solution of this general problem is considered in the following paragraph.

Let us consider a method of calculating constants C_3, C_4, C_5, C_6 in more detail. We designate constants for currents in ring portions for $N_{P_2} \le N < N_0$ as C_3, C_4 [segment portions EFA, Fig. 8.2], and for $N_{P_1} \le N < N_{P_2}$ (segment portions ADE) as C_5, C_6, herewith, N_{P_1} and N_{P_2}—numbers of asymmetrical bars $AA'EE'$. To determine four constants $C_3 - C_6$ we will write down four equations according to Kirchhoff's laws: two equations for loops $(N_{P_1} + 1, N_{P_1})$, $(N_{P_1}, N_{P_1} - 1)$ and two—for loops $(N_{P_2} + 1, N_{P_2})$ $(N_{P_2}, N_{P_2} - 1)$. As a result, we obtain a system of four equations. Coefficients of this system and its right parts are given in Appendix 10.1.

10.2.3 *General Problem: Squirrel Cage with Several (Not Adjacent) Asymmetrical Bars. Additional Currents in Winding Elements*

Let us consider an asymmetrical short-circuited rotor cage of N_0 bars; numbers of bars and corresponding ring portions are as follows (Fig. 8.2): $N = 0, 1, 2, \ldots, \ldots, N_0 - 1$. Let us accept bars with numbers $N = 0, \ldots, N_P, \ldots, N_R, \ldots, N_S, \ldots$ as asymmetrical; for example, in Fig. 8.2 these bars are AA', CC', EE'.

Let their number be equal to P, and the impedance of each of them is equal to $(N_P < N_R < N_S)$:

$$\begin{aligned}
Z_0 = Z_B + \Delta Z_0, \ldots, Z_{N_P} = Z_B + \Delta Z_{N_P}, \ldots, Z_{N_R} = Z_B + \Delta Z_{N_R}, \ldots, Z_{N_S}\\
= Z_B + \Delta Z_{N_S}, \ldots
\end{aligned}$$

Here Z_B impedance of undamaged (symmetrical) bars; in calculating Z_B, with taking account of skin effect [1–6]; $\Delta Z_0, \ldots, \Delta Z_{N_P}, \ldots, \Delta Z_{N_R}, \ldots, \Delta Z_{N_S}$—additional impedances; each varying in a wide range of values:

$$0 \le \Delta Z_0 < \infty, \ldots, 0 \le \Delta Z_{N_S} < \infty.$$

Breaks of bars are also possible. In this limit case, for example, for damage bar with number N_S, we have: $\Delta Z_{N_S} \to \infty$.

Calculation methods of main currents in symmetric cage elements were given in Chap. 9. These currents vary depending on the number of bar N under harmonic law. Unlike the main, additional currents in cage elements with asymmetrical bars vary depending on bar number N under aperiodic, but not under harmonic law. At the emergence of asymmetry in several rotor bars, it is expedient to subdivide a squirrel cage into corresponding number of portions; on each of them additional currents vary under aperiodic law:

$$\begin{array}{ll} 0 \le N < N_P: & \Delta I_N = C_0 a_1^N + D_0 a_2^N; \\ N_P \le N < N_T: & \Delta I_N = C_{N_P} a_1^N + D_{N_P} a_2^N \\ N_T \le N < N_S: & \Delta I_N = C_{N_T} a_1^N + D_{N_T} a_2^N \end{array} \tag{10.3}$$

Here $C_0, \ldots, C_{N_T}, \ldots, D_0, \ldots, D_{N_T}, \ldots$—constants determined from both Kirchhoff's laws; their number is $r \le 2P + 2$. Let us note that coefficients a_1 and a_2 are determined by impedances of symmetrical cage elements (bar Z_B and short-circuited ring portion Z_R).

We proceed to the calculation of additional currents distribution in squirrel cage elements and, therefore, to the method of calculating constants $C_0 \ldots, D_{N_T}$. Let us consider for generality the loop formed by bars with numbers $N_P, N_P - 1$ and ring portion with the number $N_P - 1$. Let us write down for loop $(N_P, N_P - 1)$ the equation according to Kirchhoff's second law:

$$\underline{I}_{N_P} Z_{N_P} - \underline{I}_{N_P - 1} Z_B - 2\underline{I}_{N_P - 1} Z_R = E_{N_P, NP-1},$$

where $E_{N_P.N_P-1}$—EMF in the loop $(N_P, N_P - 1)$ induced by resulting field in the air gap.

After simple transformations, the last equation takes the form:

$$\Delta J_{N_P}(Z_B + \Delta Z_{N_P}) - \Delta J_{N_P - 1} Z_B - 2I_{N_P - 1} Z_R = -J_{N_P} \Delta Z_{N_P}.$$

According to Kirchhoff's first law [1, 2]:

$$\Delta I_{N_P}\left(1 + \frac{\Delta Z_{N_P}}{Z_B}\right) - \Delta I_{N_P - 1}\left(a_1 + a_2 + \frac{\Delta Z_{N_P}}{Z_B}\right) + \Delta I_{N_P - 2} = -J_{N_P}\frac{\Delta Z_{N_P}}{Z_B}. \tag{10.4}$$

In setting Eq. (10.4), the following identity is taken into account: $2 + \sigma = a_1 + a_2$.

From Eq. (10.4) it follows that additional currents $\Delta I_{N_P}, \Delta I_{N_P-1}, \Delta I_{N_P-2}$ are determined ceteris paribus by degree of asymmetry $\left(\frac{\Delta Z_{N_P}}{Z_B}\right)$ of bar with number N_P, and also by current $J_{N\,p}$ in it before asymmetry emergence.

Then, let us write down an equation according to Kirchhoff's second law for the adjacent loop (N_{P+1}, N_P), also containing this asymmetrical impedance $Z_{N\,P}$:

$$\underline{J}_{N\,P+1} Z_B - \underline{J}_{N_p} Z_{N_p} - 2\underline{I}_{N_p} Z_R = E_{N_p^{+1,N_p}}.$$

After transformations, we obtain for loop (N_{P+1}, N_P):

$$\Delta I_{N_{p+1}} - \Delta I_{N_P}\left(a_1 + a_2 + \frac{\Delta Z_{N_p}}{Z_B}\right) + \Delta I_{N_{P-1}}\left(1 + \frac{\Delta Z_{N_p}}{Z_B}\right) = J_{N_p}\frac{\Delta Z_{N_p}}{Z_B}. \qquad (10.5)$$

Similarly, we get equations for each two loops containing asymmetrical impedances $Z_0, \ldots, Z_{N_P}, \ldots, Z_{N_R}, \ldots, Z_{N_S}, \ldots$.

From the ratios similar to (10.4) and (10.5) it is easy to obtain a system of equations, linear relative to unknown coefficients $C_0, \ldots, C_{N_T}, \ldots, D_0, \ldots, D_{N_T}, \ldots$. The number of equations in the system is equal to that of these coefficients, i.e. 2P. With account of constants $C_0, \ldots, D_{N_T}, \ldots$ and parameters of symmetrical cage a_1, a_2, additional currents in short-circuited ring elements and bars, and, therefore, resulting currents in cage can be calculated.

This method of calculating the currents distribution in asymmetrical rotor cage has a number of advantages compared to the numerical method given in Chap. 5. For example, in realization of the problem by this numerical method, it is necessary to solve the system from $r = N_0$ linear equations with complex coefficients. Unlike this method, in the realization of the problem by the method stated in this paragraph, the system consists only of in general case $r \leq 2P + 2$ linear equations. Let us note that in practical problems $N_0 \leq 70$, and $P \leq 3 - 4$. At small slips, i.e. with small frequencies ω_{ROT}, real and imaginary parts of some system coefficients differ in several dozen times, therefore the numerical solution of systems of high order $(r = N_0)$ with complex coefficients (or $r' = 2N_0$—with real coefficients) meets difficulties; they were already stated in Chap. 5.

Constants $C_0, \ldots, D_{N_T}$ as per (10.3), (10.4) and (10.5) linearly depend on the main currents $J_0, \ldots, J_S$ (currents in symmetrical cage) and, therefore, linearly depend on the complex amplitude (phasor) of resulting field in the air gap.

Therefore, additional currents can also be represented in the form of generalized characteristics, as well as the main.

In setting equations for determination of additional currents, it was accepted that asymmetrical bars with impedance differing from the others are not adjacent. Using both Kirchhoff's laws it is easy to obtain a system of linear equations like (10.4) and (10.5) and for case of adjacent bars with asymmetry.

With applying this general method to calculating additional currents, we consider some special cases of practical interest.

10.2.4 Squirrel Cage with Three Adjacent Asymmetrical Bars (with Damages). Additional Currents in Winding Elements

Let us consider, as example, in more detail a problem of calculating additional currents in cage with three asymmetrical bars: three bars located nearby. Their numbers N = 0; N = 1; N = 2; for example, we will accept that in Fig. 8.2 these bars are AA', BB', CC'.

Equations for additional currents in ring (N—numbers of ring portions):

$$\begin{gathered} N = 0 \ : \ \Delta I = C_1; \\ N = 1 \ : \ \Delta I = C_2; \\ 2 \le N \le N_0 - 1 : \Delta I = C_3 a_1^N + C_4 a_2^N. \end{gathered} \tag{10.6}$$

The system of four equations for calculating constants C_1, C_2, C_3, C_4, is given in Appendix 10.2.

Calculation expressions for squirrel cage MMF with this damage will be given in Chap. 12.

10.2.5 Squirrel Cage with Three Asymmetrical Bars (with Damages): Two Bars Nearby, the Third—Next but One. Additional Currents in Winding Elements

Their numbers: N = 0, N = 2, N = 3; for example, we will accept that in Fig. 8.2 such bars are bars AA', CC', DD'.

Equations for additional currents in ring (N—numbers of ring portions):

$$\begin{gathered} 0 \le N < 2 : \ \Delta I = C_1 a_1^N + C_2 a_2^N; \\ N = 2 : \ \Delta I = C_3; \\ 3 \le N < N_0 - 1 : \ \Delta I = C_4 a_1^N + C_5 a_2^N. \end{gathered} \tag{10.7}$$

The system of five equations for calculating constants C_1, C_2, C_3, C_4, C_5 is given in Appendix 10.3.

Calculation expressions for squirrel cage MMF with this damage will be given in Chap. 12.

10.2.6 Squirrel Cage with Three Asymmetrical Bars: Three Bars, not Adjacent. Additional Currents in Winding Elements

Their numbers are $N = 0$, $N = N_{P_1}, N = N_{P_2}$; for example, we will accept that in Fig. 8.2 such bars are AA', CC', EE'.

The general problem of calculating additional currents in an asymmetrical squirrel cage is solved by the numerical method in Sect. 10.2.3. In this paragraph due to the limited number of asymmetrical bars (only three), its analytical solution is found.

Equations for additional currents in ring (N—numbers of ring portions):

$$\begin{array}{c} 0 \le N < N_{P_1}: \Delta I = C_1 a_1^N + C_2 a_2^N; \\ N_{P_1} < N < N_{P_2}: \Delta I = C_3 a_1^N + C_4 a_2^N; \\ N_{P_2} < N < N_0 - 1: \Delta I = C_5 a_1^N + C_6 a_2^N. \end{array} \tag{10.8}$$

The system of six equations for calculation of six constants $C_1, C_2, C_3, C_4, C_5, C_6$ is given in Appendix 10.4.

The distribution of current amplitudes in cage bars of high-power DAP type motor (1600 kW, 6.3 kV, 1500 rpm; "Elektosila Work", Stock Company "Power Machines" St. Petersburg) calculated by the method stated in this paragraph are given in Table 10.1. In the table, the bars located in asymmetry zone are specified. Calculation expressions for squirrel cage MMF with this damage will be given in Chap. 12.

Table 10.1 Distribution of currents in rotor bars of DAP type motor ($N_0 = 64$) at «Elektrosila» Work, Stock Company "Power Machines" St.-Petersburg. Variant: three bars side by side ($\Delta Z_0 = 0.8Z_B; \Delta Z_1 = 0.9Z_B; \Delta Z_2 = 10Z_B$)

N_0	Amplitude of currents with asymmetry, $\underline{J}$ (A)	Phase angle φ (e1.deg.)
0*	6763.95	195.275
1*	6446.83	184.608
2*	1115.21	173.946
3	12,071.24	163.048
4	11,993.87	152.119
5	10,865.25	141.19
16	10,865.25	16.083
24	11,528.27	285.104
32	11,146.63	195.33
40	11,638.28	105.954
49	11,907.41	4.063
63	12,050.29	206.008

Bars with numbers N = 0, 1, 2 are damaged; they are marked by sign (*)
For rotor winding without damages the phase shift between currents of bars $\Delta\varphi = 11.25°$el. degr., the current amplitude in bars calculated by the method [14] and checked by the method in Chap. 4 is equal to J = 10.9 kA

10.2.7 Calculation Example

From calculation results, it follows:

- currents in bars, adjacent with damaged, increase; this increase leads to an additional increase in overheat of undamaged bars, to additional thermal stresses in cage elements;
- fluctuations of current amplitude have physical substantiation: they are caused by emergence in the air gap of additional field rotating relative to the rotor in the direction opposite to the main field. This field is caused by one of MMF components in air gap; it causes also EMFs in stator winding whose frequencies differ from that of network frequency.

Let us note that ratios obtained in appendices can be used with asymmetry (damage) in one or two bars including their break. For example, at the break of two (not adjacent) bars it is sufficient to set in the equations given in the last appendices: $\frac{\Delta Z_0}{Z_B} \geq 100; \quad \frac{\Delta Z_{N_{P_1}}}{Z_B} \geq 100.$

Appendix 10.1: Additional Currents in Eq. (10.2) for Squirrel Cage with Two (Not Adjacent) Asymmetrical Bars

The system of equations is given by:

$$\sum_{i,j} a_{i,j} C_{j+2} = \ddot{I}_i \quad \text{at} \quad i,j = 1,2,3,4.$$

Coefficients of system of equations (at $N_{P_1} = 0$, $N_{P_2} = N_P$):

$$a_{1,1} = -a_2 - \frac{\Delta Z_0}{Z_B}; \quad a_{1,3} = a_1^{N_0-1}\left(1 + \frac{\Delta Z_0}{Z_B}\right); \quad a_{2,1} = a_1^{N_{P-1}}\left(1 + \frac{\Delta Z_{N_P}}{Z_B}\right);$$

$$a_{2,3} = -a_1^{N_P-1}\left(1 + a_1\frac{\Delta Z_{N_P}}{Z_B}\right);$$

$$a_{3,1} = -a_1^{N_P}\left(1 + a_2\frac{\Delta Z_0}{Z_B}\right); \quad a_{3,3} = a_1^{N_P}\left(1 + \frac{\Delta Z_{N_P}}{Z_B}\right); \quad a_{4,1} = 1 + \frac{\Delta Z_0}{Z_B};$$

$$a_{4,3} = -a_1^{N_0-1}\left(a_1 + \frac{\Delta Z_0}{Z_B}\right).$$

Right parts of the system of equations:

$$\Pi_1 = J_0 \frac{\Delta Z_0}{Z_B}; \quad \Pi_2 = J_{N_P} \frac{\Delta Z_{N_P}}{Z_B}; \quad \Pi_3 = -J_{NP} \frac{\Delta Z_{NP}}{Z_B}; \quad \Pi_4 = -J_0 \frac{\Delta Z_0}{Z_B}.$$

Note: Let us designate for generality the first index at system coefficients $a_{i,j}$ as i, and the second—as j. At values of i = 1, 2, 3, 4 and at even values j = 2k (for k = 1, 2,…) each coefficient $a_{i,j}$ can be obtained from the previous value $a_{i,j}$ (for j = 2k–1), if we replace a_1 by a_2 and, respectively, a_2 by a_1, for example $a_{1,2}$—from $a_{1,1}$, $a_{4,4}$—from $a_{3,4}$, etc.

Appendix 10.2: Additional Currents in Eqs. (10.6) for Squirrel Cage with Three Adjacent Asymmetrical Bars

The system of equations is expressed by:

$$\sum_{ij} a_{i,j} C_j = \Pi_i \text{ at } i, j = 1, 2, 3, 4.$$

Coefficients in the system of equations (see Note to Appendix 10.1):

$$a_{1,2} = 1 + \frac{\Delta Z_2}{Z_B}; \quad a_{1,3} = -a_1 - a_1^2 \frac{\Delta Z_2}{Z_B}; \quad a_{1,4} = -a_2 - a_2^2 \frac{\Delta Z_2}{Z_B}; \quad a_{2,1} = 1 + \frac{\Delta Z_1}{Z_B};$$

$$a_{2,2} = -a_1 - a_2 - \frac{\Delta Z_1}{Z_B} - \frac{\Delta Z_2}{Z_B}; \quad a_{2,3} = a_1^2 \left(1 + \frac{\Delta Z_2}{Z_B}\right); \quad a_{2,4} = a_2^2 \left(1 + \frac{\Delta Z_2}{Z_B}\right);$$

$$a_{3,1} = -a_1 - a_2 - \frac{\Delta Z_1}{Z_B} - \frac{\Delta Z_0}{Z_B}; \quad a_{3,2} = a_{2,1}; \quad a_{3,3} = a_1^{N_0 - 1} \left(1 + \frac{\Delta Z_0}{Z_B}\right);$$

$$a_{3,4} = a_2^{N_0 - 1} \left(1 + \frac{\Delta Z_0}{Z_B}\right); \quad a_{4,1} = 1 + \frac{\Delta Z_0}{Z_B}; \quad a_{4,3} = -a_1^{N_0 - 1} \left(a_1 + \frac{\Delta Z_0}{Z_B}\right);$$

$$a_{4,4} = -a_2^{N_0 - 1} \left(a_2 + \frac{\Delta Z_0}{Z_B}\right); \quad a_{1,1} = a_{4,2} = 0.$$

Right parts of the system of equations:

$$\Pi_1 = J_2 \frac{\Delta Z_2}{Z_B}; \quad \Pi_2 = -J_2 \frac{\Delta Z_2}{Z_B} + J_1 \frac{\Delta Z_1}{Z_B}; \quad \Pi_3 = -J_1 \frac{\Delta Z_1}{Z_B} + J_0 \frac{\Delta Z_0}{Z_B};$$

$$\Pi_4 = -J_0 \frac{\Delta Z_0}{Z_B}.$$

Appendix 10.3: Additional Currents in Eq. (10.7) for Squirrel Cage with Three Asymmetrical Bars: Two Bars Nearby, the Third—Next but One

The system of equations:

$$\sum_{i,j} a_{i,j} C_j = \Pi_i \quad \text{at} \quad i,j = 1,2,3,4,5.$$

Coefficients in the system of equations (see Note to Appendix 10.1):

$$a_{1,3} = a_{2,4} = a_{2,5} = 1 + \frac{\Delta Z_3}{Z_B}; \quad a_{1,4} = -a_1^2 - a_1^3 \frac{\Delta Z_3}{Z_B}; \quad a_{1,5} = -a_2^2 - a_2^3 \frac{\Delta Z_3}{Z_B};$$

$$a_{2,1} = a_{2,2} = a_{3,3} = 1 + \frac{\Delta Z_2}{Z_B}; \quad a_{2,3} = -a_1 - a_2 - \frac{\Delta Z_2}{Z_B} - \frac{\Delta Z_3}{Z_B};$$

$$a_{3,1} = -a_1\left(a_1 + \frac{\Delta Z_2}{Z_B}\right); \quad a_{3,2} = -a_2\left(a_2 + \frac{\Delta Z_2}{Z_B}\right); \quad a_{4,1} = -a_2 - \frac{\Delta Z_0}{Z_B};$$

$$a_{4,2} = -a_1 - \frac{\Delta Z_0}{Z_B}; \quad a_{4,4} = a_{5,1} a_1^{N_0 - 1};$$

$$a_{4,5} = a_{5,1} a_2^{N_0 - 1}; \quad a_{5,1} = 1 + \frac{\Delta Z_0}{Z_B} = a_{5,2}; \quad a_{5,4} = -a_1^{N_0 - 1}\left(a_1 + \frac{\Delta Z_0}{Z_B}\right);$$

$$a_{5,5} = -a_2^{N_0 - 1}\left(a_2 + \frac{\Delta Z_0}{Z_B}\right); \quad a_{1,1} = a_{1,2} = a_{3,4} = a_{3,5} = a_{4,3} = a_{5,3} = 0.$$

Right parts of the system of equations:

$$\Pi_1 = J_3 \frac{\Delta Z_3}{Z_B}; \quad \Pi_2 = -J_3 \frac{\Delta Z_3}{Z_B} + J_2 \frac{\Delta Z_2}{Z_B}; \quad \Pi_3 = -J_2 \frac{\Delta Z_2}{Z_B}; \quad \Pi_4 = J_0 \frac{\Delta Z_0}{Z_B};$$
$$\Pi_5 = -\Pi_4.$$

Appendix 10.4: Additional Currents in Eq. (10.8) for Squirrel Cage with Three Asymmetrical Bars: Three Bars, Not Adjacent

The system of equations:

$$\sum_{i,j} a_{i,j} C_j = \Pi_i \text{ at } i,j = 1,2,3,4,5,6.$$

Coefficients in the system of equations (see Note to Appendix **10.1**):

$$a_{1,1} = a_{1,2} = 1 + \frac{\Delta Z_0}{Z_B}; \quad a_{1,5} = -a_1^{N_0}\left(a_1 + \frac{\Delta Z_0}{Z_B}\right); \quad a_{1,6} = -a_2^{N_0-1}\left(a_2 + \frac{\Delta Z_0}{Z_B}\right);$$

$$a_{2,1} = -a_2 - \frac{\Delta Z_0}{Z_B}; \quad a_{2,2} = -a_1 - \frac{\Delta Z_0}{Z_B}; \quad a_{2,5} = a_1^{N_0-1}a_{1,1}; \quad a_{2,6} = a_2^{N_0-1}a_{1,1};$$

$$a_{3,1} = a_1^{N_P-1}\left(1 + \frac{\Delta Z_{N_{P_1}}}{Z_B}\right); \quad a_{3,2} = a_2^{N_{P_1}-1}\left(1 + \frac{\Delta Z_{N_{P_1}}}{Z_B}\right);$$

$$a_{3,3} = -a_1^{N_{P_1}-1}\left(1 + a_1\frac{\Delta Z_{N_{P_1}}}{Z_B}\right); \quad a_{3,4} = -a_2^{N_{P_1}-1}\left(1 + a_2\frac{\Delta Z_{N_{P_1}}}{Z_B}\right);$$

$$a_{4,1} = -a_1^{N_{P_1}}\left(1 + a_2\frac{\Delta Z_{N_{P_1}}}{Z_B}\right); \quad a_{4,2} = -a_2^{N_{P_1}}\left(1 + a_1\frac{\Delta Z_{N_{P_1}}}{Z_B}\right); \quad a_{4,3} = a_1^{N_{P_1}}\left(1 + \frac{\Delta Z_{N_{P_1}}}{Z_B}\right)$$

$$a_{4,4} = -a_2^{N_{P_1}}\left(1 + \frac{\Delta Z_{N_{P_1}}}{Z_B}\right); \quad a_{5,3} = -a_1^{N_{P_2}}\left(1 + a_2\frac{\Delta Z_{N_{P_2}}}{Z_B}\right); \quad a_{5,4} = -a_2^{N_{P_2}}\left(1 + a_1\frac{\Delta Z_{N_{P_2}}}{Z_B}\right)$$

$$a_{5,5} = a_1^{N_{P_2}}\left(1 + \frac{\Delta Z_{N_{P_2}}}{Z_B}\right); \quad a_{5,6} = a_1^{N_{P_2}}\left(1 + \frac{\Delta Z_{N_{P_2}}}{Z_B}\right); \quad a_{6,3} = a_2 a_{5,5}; \quad a_{6,4} = -a_1 a_{5,6}$$

$$a_{6,5} = -a_1^{N_{P_2}}\left(a_2 + \frac{\Delta Z_{N_{P_2}}}{Z_B}\right); \quad a_{6,6} = -a_2^{N_{P_2}}\left(a_1 + \frac{\Delta Z_{N_{P_2}}}{Z_B}\right);$$

$$a_{1,3} = a_{1,4} = a_{2,3} = a_{2,4} = a_{3,5} = a_{3,6} = a_{4,5} = a_{4,6} = a_{5,1} = a_{5,2} = a_{6,1} = a_{6,2} = 0.$$

Right parts of the system of equations:

$$\Pi_1 = -J_0\frac{\Delta Z_0}{Z_B}; \quad \Pi_2 = J_0\frac{\Delta Z_0}{Z_B}; \quad \Pi_3 = J_{N_{P_1}}\frac{\Delta Z_{N_{P_1}}}{Z_B};$$

$$\Pi_4 = -J_{N_{P_1}}\frac{\Delta Z_{N_{P_1}}}{Z_B}; \quad \Pi_5 = -J_{N_{P_2}}\frac{\Delta Z_{N_{P_2}}}{Z_B}; \quad \Pi_6 = J_{N_{P_2}}\frac{\Delta Z_{N_{P_2}}}{Z_B}.$$

Brief Conclusions

1. Investigation methods of symmetrical active open and closed chain circuits are generalized and used to study asymmetrical chain circuits class (open and closed). As a result of their generalization it has become possible to obtain regularities of currents distribution, important for practice, in asymmetrical squirrel cages (with damages). In particular, the following regularities of currents distribution in asymmetrical squirrel cage elements of induction machine are obtained:

- besides currents for symmetrical squirrel cage elements there are additional currents with two components;
- both components vary depending on the number of bar ring portion under the aperiodic law, one of which fades with increase of this number in amplitude, and another—increases.

2. The general problem to compute currents distribution in short-circuited rotor cage with P asymmetrical bars is reduced to the solution of algebraic system in general case of r linear equations ($r \leq 2P + 2$); its order does not depend on total number N_0 of bars in cage. This method has essential advantages in comparison with numerical methods based on the solution of a system of Kirchhoff's equations for N_0 loops. In practical problems $N_0 \leq 70$, and $P \leq 3 - 4$. For small slips, real and imaginary parts of some system coefficients differ in several dozen times, therefore in practice, the solution of systems of high order N_0 with complex coefficients using numerical methods meets difficulties.
3. Besides the general problem, its special cases representing independent practical interest are solved:

- asymmetrical squirrel cage with one and two damaged bars;
- asymmetrical squirrel cage with three adjacent damaged bars;
- asymmetrical squirrel cage with three damaged bars: two bars nearby, the third—next but one;
- asymmetrical squirrel cage with three damaged bars: three bars, not adjacent.

List of Symbols

$C_1, \ldots, C_{N_T}, \ldots, D_0, \ldots, D_{N_T}, \ldots$	Constants for calculating currents determined from both Kirchhoff's laws;
$E_{N_P, N_P - 1}$	EMF in the loop $(N_P, N_P - 1)$, induced by the resulting field in air gap;
$\underline{\underline{I}}_N, \underline{\underline{J}}_N$	Currents in ring portions (segments) and in bars of squirrel cage at emergence of asymmetry (damage);
I_N, J_N	Currents in ring portions (segments) and in bars of squirrel cage before asymmetry emergence;
$\Delta I_{(N)}, \Delta J_{(N)}$	Additional currents in bars and ring portions of asymmetrical squirrel cage;
N	Bar (ring portion) number of squirrel cage;
N_0	Number of squirrel cage bars;
N_{P_1}, N_{P_2}	Numbers of asymmetrical bars of squirrel cage;
Z_B	Impedance of the symmetrical (undamaged) bar;

Z_R	Impedance of the ring portion between two adjacent bars;
$Z_{N_P}, \ldots, Z_{N_R}, \ldots, Z_{N_S}$	Impedances of asymmetrical (damaged) bars;
$\Delta Z_{N_P}, \ldots, \Delta Z_{N_R}, \ldots, \Delta Z_{N_S}$	Additional impedances of asymmetrical (damaged) bars

References

I. Monographs, Textbooks

1. Demirchyan K.S., Neyman L.R., Korovkin N.V., Theoretical Electrical Engineering. Moscow, St. Petersburg: Piter, 2009. Vol. 1, 2. (in Russian).
2. Kuepfmueller K., Kohn G., Theoretische Elektrotechnik und Elektronik. 15 Aufl., Berlin, N. Y: Springer. 2000. (in German).
3. Richter R., Elektrische Maschinen. Berlin: Springer. Band I, 1924; Band II, 1930; Band III, 1932; Band IV, 1936; Band V, 1950. (in German).
4. Mueller G., Ponick B., Elektrische Maschinen. N.Y: J. Wiley. 2009. (in German).
5. Mueller G., Ponick B., Grundlagen elektrischer Maschinen. Springer. 2005. (in German).
6. Schuisky W., Berechnung elektrischer Maschinen. Wien: Springer. 1960. (in German).

II. Induction Machines. Papers, Inventor's Certificates

7. Braun R., Brüche an Käfigwicklungen von Drehfelmaschine. Maschinenschaden, 1959, № 9/10. (in German).
8. Hiller U., Einfluß fehlender Laeuferstaebe auf die elektrischen Eigenschaften von Kurzschlußlaeufermotoren. ETZ "A", 1962. №4. (in German).
9. Ambrosini M., Sacceti R., Circuiti aquivalenti di machine asincroni alimentate con tensioni in sequenze generalizzate di Fortescue. L'Energia Electrica, 1980. №11. (in Italian).
10. Ambrosini M., Filipetti F., Il metodo dei circuiti equivalente parziale nello studio dei regimi di quasto nei motori asincroni a gabbia. L'Energia Electrica, 1981, №1. (in Italian).
11. Saccetti R., Troili R., Una tecnica unitaria nello studio dei circuiti a delle motori il metodo dei circuiti equivalente parziale. L'Energia Electrica, 1980, №3. (in Italian).
12. Boguslawsky I.Z., Currents in a asymmetric short-circuited rotor cage. Power Eng., NY, 1982. № 1.
13. Boguslawsky I.Z., Demirtschyan K.S., Stationaere Stromverteilung in unregelmaessigen und unsymmetrischen kurzgeschlossenen Laeuferwicklungen von Wechselstrommaschinen. Archiv fuer Elektrotechnik, 1992. №6. (in German).
14. Antonov V.V., Boguslavsky I.Z., Savelyeva M.G., Calculation of the characteristics of a powerful induction motor with non-linear parameters. In the book. Elektrosila, #35, 1984. (in Russian).
15. Schuisky W., Brueche im Kurzschlusskaefig eines Induktionsmotors und ihre Einfluesse auf das Verhalten des Motors. Archiv fuer Elektrotechnik, 1941, № 5. (in German).
16. Williamson S., Smith A.C., Steady – state analysis of 3 – phase cage motors with rotor bar and end ring faults. Proceed. IEE, 1982, №3 (Part B).
17. Rusek J., Sila electromotoryczna i strumien sprzezony z cewkami pomiarowymi jako wskaznik uszkodzen wirnika silnikow indukcyjnych. Zesz. naukowe Akad. Gorniczo-hutniczej (Krakow), 1988, № 13. (in Polish).

III. Synchronous Machines. Papers, Inventor's Certificates, Patents

18. Boguslawsky I.Z., Method of calculating of the active chain-circuits with damaged elements. Electrichestvo, 1984. № 4; 1988. № 8. (in Russian).
19. Boguslawsky I.Z., Calculating the current distribution on the damper winding of large slow – speed synchronous motors in asynchronous operation. Power Eng. N.Y, 1979. № 3.
20. Demirchyan K.S., Boguslawsky I.Z., Current flowing in damper winding bars of different resistivity in a heavy- duty low speed motor. Power Eng. N.Y, 1980. № 2.
21. Boguslawsky I.Z., Currents and harmonic MMFs in a damper winding with damaged bar at a pole. Power Eng., N.Y, 1985. № 1.

Chapter 11
Investigation Methods of Currents Distribution in Irregular Damper Windings

In this Chapter, investigation methods of asymmetrical active recurrent circuits (open and closed) developed in Chap. 7, are used for calculation of currents distribution in irregular damper windings of salient pole machines.

If in damper winding on each pole there is one bar with impedance differing from the others, calculation of currents distribution is reduced to determination of main and additional currents, similar to currents in asymmetrical squirrel cage. Calculation of distribution of additional currents is reduced to that of only four constants included in a system of difference equations. The order of this system ($r = 4$) does not depend on number of bars N_0 on pole. In solving the problem by a numerical method, the system order is determined by the product $r' = 2pN_0$.

If in damper winding on one pole there is a bar with impedance different from the others, calculation of currents distribution is reduced as in previous design to the solution of two problems: Constants of calculation expressions for currents are calculated from a system of linear equations whose order is determined only by the number of machine poles and does not depend on the number of bars per pole: In solving the problem by the numerical method, the system order is determined as in previous design by product $r' = 2pN_0$. Developed methods allow calculating currents distribution for several bars or ringing portions whose impedance differ from the others. These methods are proved by results of experimental bench investigation of pilot motor type SDSZ (2000 kW, 6 kV, $2p = 60$), at LEZ, Stock Company "Ruselprom".

The content of this chapter is development of the methods stated in [1, 2, 6–11].

I. Boguslawsky et al., *Large A.C. Machines*,
DOI 10.1007/978-4-431-56475-1_11

11.1 Currents in Damper Windings with Bars of Various Impedance on Each Pole

11.1.1 General Comments

Let us begin with the consideration of this problem with a short description of damper winding design of SDSZ type motor (2000 kW, 6 kV, 100 rpm, 50 Hz). This motor is intended for grinding unit drives in mining and cement industry. To obtain more uniform distribution of current in damper winding bars at sharp load variation, its middle bar on each pole is made of copper, and other four—of brass; short-circuited rings (segments)—of copper. This damper winding design is also expedient for high-power frequency-controlled machines intended for similar operational modes, for example, for drive motors of rolling mills. As determined in Chap. 9 it is irregular because bars with various impedances are located on poles. However, in investigation of currents in construction elements and MMF in air gap for this class of irregular damper windings, as well as regular damper winding it is sufficient to assume the period equal to $T_{EL} = \frac{\pi D}{p}$. This circumstance facilitates investigation of currents and MMF of such winding.

11.1.2 Initial Data and Calculation Method for Currents in Winding Elements

The method is based on results of investigation of asymmetrical active chain circuits obtained in Chap. 7 [6].

In Chap. 9 we already used Fig. 6.3 for investigation of currents distribution in damper winding elements. The following changes and additions were entered into Fig. 6.3:

- cross elements $A_1A'_1, \ldots, F_2F'_2$ in Fig. 6.3 represent winding bars with impedance Z_B;
- longitudinal elements $A_1B_1, \ldots, B_2F_2$ represent portions of short-circuited rings (segments) with impedance Z_R;
- longitudinal elements $F_1A_2, \ldots, F_2A_1$ represent portions of short-circuited rings (segments) between poles with impedance Z_F;
- loops $F_1F'_1A'_2A_2F_1$, $F_2F'_2A'_1A_1F_2$—correspond to the space between poles;
- between bars $A_1A'_1$ and $B_1B'_1$; $B_1B'_1$ and $F_1F'_1$; … there are EMF sources changing depending on the number of link N under the harmonic law;
- terminals $O_1O'_1$ are superimposed with terminals $O_3O'_3$;
- Let us assign index "C_P" to pole with bars $A_1A'_1, \ldots, F_1F'_1$, and index "S_P" to pole with bars $A_2A'_2, \ldots, F_2F'_2$.

Let us also enter an addition: Let us accept that bars $B_1B'_1$ and $B_2B'_2$ are asymmetrical.

Let us list initial data to solve the considered problem. Set in values are: currents in elements of regular damper winding, number of machine poles 2p, number of bars N_0 on each of poles, impedance Z_B of symmetrical bars and Z_R—impedance of portions of short-circuited rings (segments), and also impedance Z_F of jumper between poles. Asymmetrical bars of damper winding has the number Z_P, herewith, $0 < N_P < N_0 - 1$, i.e. it is not an edge one on the pole; Let us designate its impedance as Z_{N_P}.

Let us find the distribution of currents in elements of such winding.

At first, we consider the case with the only bar on each pole and different impedance ($\Delta Z_{N_P} = \Delta Z$).

Let us write down equations for EMF and currents in loops (1, 0), …,

$$(N_P, N_P + 1), (N_P + 1, N_P), \ldots, (N_B + 1, N_B); \text{ here } N_B = N_0 - 2.$$

For pole C_P, we have:

$$\begin{cases} \left(\underline{\underline{J}}_1^{C_P} - \underline{\underline{J}}_1^{C_P}\right) Z_B - 2\underline{\underline{I}}_0^{C_P} Z_R = E_1; \\ \vdots \\ \underline{\underline{J}}_{N_P}^{C_P} Z_{N_P} - \underline{\underline{J}}_{N_P-1}^{C_P} Z_B - 2\underline{\underline{I}}_{N_P-1}^{C_P} Z_R = E_1 e^{-j\Delta\varphi(N_P-1)}; \\ \underline{\underline{J}}_{N_P+1}^{C_P} Z_{N_P} - \underline{\underline{J}}_{N_P}^{C_P} Z_{N_P} - 2\underline{\underline{I}}_{N_P}^{C_P} Z_R = E_1 e^{-j\Delta\varphi N_P}; \\ \vdots \\ \left(\underline{\underline{J}}_{N_B+1}^{C_P} Z_{N_B}^{C_P}\right) Z_B - 2\underline{\underline{I}}_{N_B}^{C_P} Z_R = E_1 e^{-j\Delta\varphi N_B}, \end{cases} \tag{11.1}$$

where $\underline{\underline{I}}_N$—currents in winding ring portions (segments); $\underline{\underline{J}}_N$—currents in winding bars; Z_B—impedance of symmetrical bar slot part; Z_R—impedance of ring portion between bars, $\Delta\varphi$—phase angle between EMF of bars on pole, E_1 − EMF amplitude; it is induced by resulting field in air gap in pole loops.

For each node we have:

$$\underline{\underline{I}}_{N-1}^{C_P} + \underline{\underline{J}}_N^{C_P} = \underline{\underline{I}}_N^{C_P}. \tag{11.2}$$

For ring segment between poles C_P and S_P we have:

$$\begin{aligned} &\left(\underline{\underline{J}}_0^{S_P} - \underline{\underline{J}}_{N_B+1}^{C_P}\right) Z_B - 2\left(\underline{\underline{J}}_{N_B}^{C_P} + \underline{\underline{J}}_{N_B+1}^{C_P}\right) Z_F = E_F; \\ &\underline{\underline{I}}_{N_B}^{C_P} + \underline{\underline{J}}_{N_B+1}^{C_P} + \underline{\underline{J}}_0^{S_P} = \underline{\underline{I}}_0^{S_P}, \end{aligned} \tag{11.3}$$

where E_F − EMF in loop $F_1F'_1A'_2A_2F_1$.

Equations are similar for pole S_P and second ring portion between poles. They can be obtained from Eqs. (11.2) and (11.3) replacing index C_p by S_P at currents $\underline{\underline{J}}_N, \underline{\underline{I}}_N$ and multiplying E_1 and E_F EMFs by coefficient: $e^{j\pi} = -1$.

System of equations for currents in damper winding elements is linear with constant coefficients. Let us represent currents in these elements on both poles in the form of two components:

$$\underline{\underline{J}}_N = J_N + \Delta J_N, \tag{11.4}$$

$$\underline{\underline{I}}_N = I_N + \Delta I_N. \tag{11.5}$$

These ratios are true if we represent the bar impedance with number Np according to (6.20) in the form:

$$Z_{N_P} = Z_B + \Delta Z.$$

Let us consider at first the equations for loops formed by identical (symmetrical) bars; let an arbitrary loop (N + 1, N) be one of them. The equation corresponding to it from system (11.2) to (11.5) takes the form:

$$\left[\left(J_{N+1}^{C_P} - J_N^{C_P}\right)Z_B - 2I_N^{C_P}Z_R - E_1 e^{-j\Delta\varphi N}\right] + \left[\left(\Delta J_{N+1}^{C_P} - \Delta J_N^{C_P}\right)Z_B - 2\Delta I_N^{C_P}Z_R\right] = 0. \tag{11.6}$$

Let us note that the first sum on the left part concluded in square brackets is identically equal to zero. It is the formulation of Kirchhoff's second law [1, 3] for regular damper winding loops with all bars identical. Method of calculating currents distribution in elements of this design is given in Chap. 9.

Let us consider a loop formed by bars with various impedance, for example $(N_P, N_P - 1)$. The equation corresponding to it from system (11.1) to (11.6) takes the form:

$$\begin{aligned}\left[\left(J_{N_P}^{C_P} - J_{N_P-1}^{C_P}\right)Z_B - 2I_{N_P-1}^{C_P}Z_R - E_1 e^{-j\Delta\varphi(N_P-1)}\right] + \left[\left(\Delta J_{N_P}^{C_P} - \Delta J_{N_P}^{C_P}\right)Z_B\right. \\ \left. + \Delta J_{N_P}^{C_P} - \Delta Z + J_{N_P}^{C_P}\Delta Z - 2\Delta I_{N_P-1}^{C_P}Z_R\right] = 0.\end{aligned} \tag{11.7}$$

Similarly as stated above, here the first sum on the left part concluded in braces is also identically equal to zero. From this equation it also follows that additional currents ΔJ_{N_P}, ΔJ_{N_P-1}, ΔI_{N_P-1}, subject to determination are calculated from current J_{N_P} .

Thus, we obtain from Eqs. (11.1) to (11.7) that both for considered winding design and for asymmetrical squirrel cage, the problem of calculating currents distribution can be physically subdivided into two problems.

The first one, whose solution method was given in Chap. 9 consists in calculation of the main currents for regular damper winding (main currents at Z_B = idem), and the second consists in calculation of distribution of additional currents.

For calculation of additional currents, we obtain the following system of equations using the initial system (11.1)–(11.7). It is easy to check the left parts of this system: they follow directly from (11.1) to (11.7) if instead of resulting currents $\underline{\underline{J}}_{(N)}, \underline{\underline{I}}_{(N)}$ we write down their increments $\Delta J_{(N)}, \Delta I_{(N)}$ caused by asymmetrical bar on the pole.

For pole C_P: ($N_B = N_0 - 2$)

$$\begin{cases} \left(\Delta J_1^{C_P} - \Delta J_0^{C_P}\right) Z_B - 2\Delta I_0^{C_P} Z_R = 0, \\ \vdots \\ \Delta J_{N_P}^{C_P} Z_{N_P} - \Delta J_{N_P-1}^{C_P} Z_B - 2\Delta I_{N_P-1}^{C_P} Z_R = -\Delta J_{N_P}^{C_P} \Delta Z, \\ \Delta J_{N_P+1}^{C_P} Z_B - \Delta J_{N_P}^{C_P} Z_{N_P} - 2\Delta I_{N_P}^{C_P} Z_R = \Delta J_{N_P}^{C_P} \Delta Z, \\ \vdots \\ \left(\Delta J_{N_B+1}^{C_P} - \Delta J_{N_B}^{C_P}\right) Z_B - 2\Delta I_{N_B}^{C_P} Z_R = 0. \end{cases} \tag{11.8}$$

For each node we have:

$$\Delta I_{N-1}^{C_P} + \Delta J_N^{C_P} = \Delta I_N^{C_P}. \tag{11.8'}$$

For ring portion between poles:

$$\begin{aligned} &\left(\Delta J_0^{S_P} - \Delta J_{N_B+1}^{C_P}\right) Z_B - 2\left(\Delta I_{N_B}^{C_P} + \Delta J_{N_B+1}^{C_P}\right) Z_F = 0, \\ &\Delta I_{N_B}^{C_P} + \Delta J_{N_B+1}^{C_P} + \Delta J_0^{S_P} = \Delta I_0^{S_P}. \end{aligned} \tag{11.9}$$

For pole S_P and second ring portion between poles, the equations are similar. They can be obtained by replacement of index C_P by S_P at currents ΔJ_N and ΔI_N .

Let us show that the solution of this system can be reduced to that of system of equations only of the fourth order (r = 4) at any number of pole bars, if we use the obtained result of analytical solution of difference equations [6–9].

At first, let us consider the first equation of system (11.8). It corresponds to the loop formed by bars with numbers N = 1 and N = 0, that is to bars with numbers $0 \le N < N_P$. Let us express additional currents in bars through currents in ring portions (segments). As a result we obtain the following ratio between additional currents in ring portions (segments) with numbers N = 1, N = 0, N = −1:

$$\Delta I_1^{C_P} Z_B - 2\Delta I_0^{C_P} (Z_B + Z_R) + \Delta I_{(-1)}^{C_P} Z_B = 0. \tag{11.10}$$

Similar ratios are also true for other additional currents in ring portions with numbers $0 \le N < N_P$. It is convenient to write down these ratios in the form of one difference equation [3]:

$$\Delta I^{C_P}[N+2] - (2+\sigma)\Delta I^{C_P}[N+1] + \Delta I^{C_P}[N] = 0, \quad \text{here } \sigma = 2\frac{Z_R}{Z_B}. \tag{11.11}$$

Let us consider the last equation of system (11.8). It corresponds to the loop on the pole formed by bars with numbers N = N_B + 1 and N = N_B, that is bars with numbers $N_P < N \le N_B + 1$. Similarly, we obtain the same difference Eq. (11.11) for additional currents in ring portions (segments) with the same numbers $N_P \le N \le N_B + 1$. Difference equations like (11.11) can be also easily obtained for currents in ring portions (segments) of pole S_P.

Let us write down the solution of these difference equations.

For pole C_P currents in ring portions $0 \le N < N_P$:

$$\Delta I_N^{C_P} = D_1 a_1^N + D_2 a_2^N. \tag{11.12}$$

For pole C_P currents in ring portions $N_P \le N \le N_B + 1$:

$$\Delta I_N^{C_P} = D_3 a_1^N + D_4 a_2^N. \tag{11.13}$$

For pole S_P currents in ring portions $0 \le N < N_P$:

$$\Delta I_N^{S_P} = D'_1 a_1^N + D'_2 a_2^N. \tag{11.14}$$

For pole S_P currents in ring portions $N_P \le N \le N_B + 1$:

$$\Delta I_N^{S_P} = D'_3 a_1^N + D'_4 a_2^N. \tag{11.15}$$

Here $D_1 - D_4; D'_1 - D'_4$—constants determined by boundary conditions.

Calculation of distribution of additional currents is reduced to that of these eight constants. It is convenient to determine them from boundary conditions determined by Kirchhoff's laws for damper winding loops.

For a loop formed by jumpers between poles C_P, S_P and bars with numbers N = N_B + 1 (on pole C_P) and N = 0 (on pole S_P), two equations corresponding to both Kirchhoff's laws are given in (11.9). Two similar equations are true for the loop formed by jumpers between poles S_P, C_P and bars with numbers N = 0 (on pole C_P) and N = N_B + 1 (on pole S_P).

For loops (N_P + 1, N_P) and (N_P, N_P − 1) two equations corresponding to the second Kirchhoff's law are given in (11.8) for pole C_P. Two similar equations can be written down for corresponding loops of pole S_P. As a result, we obtain a system of eight equations for determination of constants $D_1, D_2, D_3, D'_1, D'_2, D'_3, D'_4$.

Using (11.13)–(11.16), it is convenient to represent this system in the form:

$$\begin{cases} MD_1 + GD_2 + PD'_1 + RD'_2 = -J^{C_P}_{N_P}\frac{\Delta Z}{Z_B}; \\ QD_1 + TD_2 + FD'_1 + WD'_2 = -J^{C_P}_{N_P}\frac{\Delta Z}{Z_B}; \\ MD'_3 + GD'_4 + PD_3 + RD_4 = J^{S_P}_{N_P}\frac{\Delta Z}{Z_B}; \\ QD'_3 + TD'_4 + FD_3 + WD_4 = J^{S_P}_{N_P}\frac{\Delta Z}{Z_B}; \end{cases} \tag{11.16}$$

$$\begin{cases} AD_1 + BD_2 + VD_3 + CD_4 = 0; \\ AD'_3 + BD'_4 + VD'_1 + CD'_2 = 0; \\ HD_3 + LD_4 + SD_1 + KD_2 = 0; \\ HD'_1 + LD'_2 + SD'_3 + KD'_4 = 0. \end{cases} \tag{11.17}$$

Values of system coefficients are given in Appendix 11.1.

It is early proved that for main currents in bars with identical number, for example, of N_P located on adjacent poles, the following ratio is satisfied:

$J^{C_P}_{N_P} = -J^{S_P}_{N_P}$ [7]; it is true for all three components of the main current, including its two aperiodic components. It is possible to show that for the system (11.17) the following ratios are satisfied:

$$D_1 = -D'_3;\ D_2 = -D'_4;\ D'_1 - D_3;\ D'_2 - D_4.$$

They allow us to represent this system in the form:

$$\begin{cases} MD_1 + GD_2 - PD_3 - RD_4 = -J^{C_P}_{N_P}\frac{\Delta Z}{Z_B}; \\ (Q + M)D_1 + (T + G)D_2 - (F + P)D_3 - (W + R)D_4 = 0; \\ AD_1 + BD_2 + VD_3 + VD_4 = 0; \\ S_0D_1 + KD_2 + HD_3 + LD_4 = 0. \end{cases} \tag{11.18}$$

Using it, we obtain the following calculation formulas for additional currents.

Pole C_P.

Currents in ring portions $(N_P \le N \le N_B + 1)$:

$$\Delta I^{C_P}_{(N)} = \frac{\Delta_1 a_1^N + \Delta_2 a_2^N}{\Delta}. \tag{11.19}$$

Currents in bars $(N_P < N \le N_B + 1)$:

$$\Delta J^{C_P}_{(N)} = \frac{\Delta_1 (a_1 - 1) a_1^N + \Delta_2 (a_2 - 1) a_2^N}{\Delta}. \tag{11.19'}$$

Pole S_P.

Currents in ring portions $(0 \le N < N_P)$:

$$\Delta I_{(N)}^{S_P} = \frac{\Delta_3 a_1^N + \Delta_4 a_2^N}{\Delta}. \tag{11.20}$$

Currents in bars $(0 \le N < N_P)$:

$$\Delta J_{(N)}^{S_P} = \frac{\Delta_3 (a_1 - 1) a_1^N + \Delta_4 (a_2 - 1) a_2^N}{\Delta}. \tag{11.20'}$$

Current in bar $N = N_P$ of pole C_P:

$$\Delta J_{(N_P)}^{C_P} = \frac{\left(\Delta_1 + \Delta_3 a_1^{-1}\right) a_1^N + \left(\Delta_2 + \Delta_4 a_2^{-1}\right) a_2^N}{\Delta}. \tag{11.21}$$

Here Δ—system determinant (11.18), $\Delta_1, \Delta_2, \Delta_3, \Delta_4$—algebraic adjuncts corresponding to required constants $D_1 - D_4$ (11.18);

$$D_1 = \frac{\Delta_1}{\Delta}; D_2 = \frac{\Delta_2}{\Delta}; D_3 = \frac{\Delta_3}{\Delta}; D_4 = \frac{\Delta_4}{\Delta}.$$

As a result, we obtain the distribution of additional current in winding bars.

Let us note that in the presence of several asymmetrical bars, the problem is solved similarly; number of constants for calculation of additional currents respectively increases.

Experimental and calculation distribution of currents in damper winding elements of SDSZ type motor obtained in bench conditions on the manufacturing work is compared in Appendix 11.2. Difference between experimental and calculation current values in bars does not exceed 11% that is acceptable for engineering calculations.

11.2 Currents in Damper Winding with Damaged Bar on Pole

11.2.1 General Comments

Let us proceed to the investigation of currents distribution in elements of one more class of irregular damper winding. According to Chap. 9, in construction of such winding only in several rotor poles, there are one or several bars with different impedance, for example, bars with damage (break).

Change of impedance of one of damper winding bars can be caused by production defect, for example, due to low-quality soldering or welding in

bar-short-circuited ring (segment) joint, violations in connections between segments in rotor assembly.

Severe operation conditions for a network or a frequency converter, especially with sharp load variation (for example, for the motors of rolling mills), sometimes lead to damages of bar or ring, including their break. Usually, the reason of these damages is the temperature deformation of winding elements and mechanical stresses in them caused by these deformations.

Practice determines the problem of developing methods for calculating performance characteristics of machines with this asymmetry in damper winding. Purpose of this development: determination of admissible modes of their operation.

11.2.2 Initial Data and Method of Calculating Currents in Winding Elements

The method is based on results of investigation of asymmetrical chain circuits obtained in Chaps. 6 and 7. It does not require any additional assumptions, besides those used for calculation of currents in short-circuited symmetrical (without damages) rotor winding of induction motor or regular damper winding of salient-pole machine.

The same values as in previous problem are assumed as given.

Let us list them: currents in elements of regular damper winding, number of machine poles 2p, number of bars N_0 on each pole, impedance Z_B of undamaged (symmetrical) bars and Z_R—of short-circuited ring portions (segments) between adjoining bars, and also impedance Z_F of jumper between poles; number of damper winding damaged bar N_P on pole number $q(q \in S; 1 \leq S \leq 2p)$. Impedance of this bar $Z_{N_P} : Z_{N_P} = Z_B + \Delta Z$. Let us note that at bar break $\Delta Z \to \infty$.

At first, let us consider the problem on currents calculation in damper winding with one damaged bar on pole number q on the assumption that the impedance of all other $2pN_0$-1 bars of winding is the same. This circumstance leads to the fact that in investigation of currents and MMFs in this winding, unlike the problem solved in the previous paragraph [9], it is necessary to assume the period $T = \pi D = pT_{EL}$.

Let us note that in the previous problem all poles from the viewpoint of design and material of bars, their arrangements on pole shoe repeat each other [4], [5]; in the considered problem [8] only one pole from this viewpoint differs from all others.

According to this method at $\Delta Z \neq 0$, currents in damper winding elements of bars $\underline{\underline{J}}_N$ and short-circuited ring portions (segments) $\underline{\underline{I}}_N$ of each pole with number S can be represented in the form of two components: of main current J_N,I_N and additional $\Delta J_N, \Delta I_N$, herewith [6, 11]

$$\underline{\underline{J}}_N^{(S)} = J_N^{(S)} + \Delta J_N^{(S)}; \underline{\underline{I}}_N^{(S)} = I_N^{(S)} + \Delta I_N^{(S)}. \tag{11.22}$$

In previous chapters it is obtained that the main currents $J_N^{(S)}, I_N^{(S)}$ correspond to currents of regular damper winding, impedance of all bars $2pN_0$ is the same and is equal to Z_B. In the considered problem, these currents are assumed as given; their calculation method is stated above [7]. Additional currents in ring portions on each pole satisfy the homogeneous difference equation of the second order:

$$\begin{aligned} &\Delta I[N+2] - (2+\sigma)\Delta I[N+1] + \Delta I[N+1] = 0, \\ &\text{here } \sigma = 2\frac{Z_R}{Z_B}. \end{aligned} \tag{11.23}$$

Solution of Eq. (11.23) for pole ring portions, where $\Delta Z = 0$:

$$\Delta I_{(N)} = C^{(S)} a_1^N + D^{(S)} a_2^N. \tag{11.24}$$

Respectively, currents in bars on these poles:

$$\Delta J_{(N)} = C^{(S)} a_1^{N-1} + D^{(S)} a_2^{N-1}(a_2 - 1), \tag{11.25}$$

where $N = 0,1,\ldots,N_0 - 1; a_{1,2} = \frac{2+\sigma(\sigma+4)}{2}; C^{(S)}, D^{(S)}$—constants, calculated for currents of each pole, proceeding from boundary conditions.

At first, let us obtain calculation expressions for the general case when damaged damping bar is not the edge on the pole, i.e. its number

$$N_P \neq N_0 - 1 \text{ or } N_P \neq 0.$$

Let us designate constants $C^{(S)}, D^{(S)}$ for the current in ring portions located on both sides of damper pole bar number q respectively as $C_L^{(q)}, D_L^{(q)}$ and $C_R^{(q)}, D_R^{(q)}$.

Thus, to determine the current in damper winding structural elements, it is necessary to calculate r = 4p + 2 constants whose number does not depend on the number N_0 of pole bars; for example, for machine with 2p = 6 the number of constants r = 14, and for machine with 2p = 60 this number and, respectively, the order of system for their determination is equal to r = 122.

We consider a system of r = 4p + 2 linear equations for calculation of these constants. These equations are obtained from both Kirchhoff's laws [1, 3] for corresponding loops and joints.

(a) Equations for two loops (N_P, $N_P - 1$) and ($N_P + 1$, N_P), containing damaged bars. For the loop (N_P, $N_P - 1$) according to the second Kirchhoff's law we have:

$$\Delta J_{N_P}^{(q)} Z_{N_P} - \Delta J_{N_P-1}^{(q)} Z_B - 2\Delta I_{N_P-1}^{(q)} Z_R = -J_{N_P} \Delta Z, \tag{11.26}$$

where J_{N_P}—current in bar with number N_P before its damage (at $\Delta Z = 0$).

Using the first Kirchhoff's law and Eqs. (11.24), (11.25) of (11.26), we have:

$$AC_R^{(q)} + BD_R^{(q)} + EC_L^{(q)} + FD_L^{(q)} = -J_{N_P} \frac{\Delta Z}{Z_B}. \tag{11.27}$$

For loop (N_P + 1, N_P) similarly

$$GC_R^{(q)} + HD_R^{(q)} + KC_L^{(q)} + LD_L^{(q)} = J_{N_P} \frac{\Delta Z}{Z}. \tag{11.28}$$

Values of coefficients A, B, E, F, G, H, K, L are given in Appendix 11.3.

(b) Equations for 2p loops limiting the space between poles. We use the expression for the current in jumper between poles with numbers S and S + 1. Proceeding from the first Kirchhoff's law, we obtain:

$$\begin{aligned} &\Delta J_{N_B+1}^{(S)} + \Delta I_{N_B}^{(S)} = \Delta I_0^{(S+1)} - \Delta J_0^{(S+1)} \\ \text{or} \quad &C^{(S)} a_1^{N_B+1} + D^{(S)} a_2^{N_B+1} - C^{(S+1)} a_1^{-1} - D^{(S+1)} a_2^{-1} = 0, \end{aligned} \tag{11.29}$$

where $N_B = N_0 - 2$.

For the loop (0,N_B + 1) formed by bar with number N_B + 1 of pole S and bar with number N = 0 of pole S + 1 according to the second Kirchhoff's law we have:

$$\begin{aligned} &\Delta J_0^{(S+1)} Z_B - \Delta J_{N_B+1}^{(S)} Z_B - 2\Delta I_{N_B+1}^{(S)} Z_F = 0, \\ \text{or} \quad &MC^{(S+1)} + PD^{(S+1)} + QC^{(S)} + RD^{(S)} = 0. \end{aligned} \tag{11.30}$$

Values of coefficients M, P, Q, R are given in Appendix 11.3.

Equations like (11.29) and (11.30) are true for all 2p poles with damper winding (S = l, 2, …, 2p), including loops between poles q − 1, q and q + 1.

For the loop between poles q − 1 and q both equations are as follows:

$$\begin{cases} C^{(S)} a_1^{N_B+1} + D^{(S)} a_2^{N_B+1} - C_L^{(q)} a_1^{-1} - D_L^{(q)} a_2^{-1} = 0, \\ MC_L^{(q)} + PD_L^{(q)} + QC^{(S)} + RD^{(S)} = 0, \end{cases} \tag{11.31}$$

where S = q − 1. For the loop between poles q and q + 1:

$$\begin{cases} C_R^{(q)} a_1^{N_B+1} + D_R^{(S)} a_2^{N_B+1} - C^{(S)} a_1^{-1} - D^{(S)} a_2^{-1} = 0, \\ MC^{(S)} + PD^{(S)} + QC_R^{(q)} + RD_R^{(q)} = 0, \end{cases} \tag{11.32}$$

where S = q +1 .

Thus, we obtained the system of r = 4p + 2 linear equations for determination of currents in damper winding construction elements with a damaged bar. Currents are calculated from the following ratios:

- currents $\Delta I_N^{(S)}$ in ring portions on poles at $S \neq q$—as per (11.24);
- currents $\Delta J_N^{(S)}$ in bars on poles at $S \neq q$—as per (11.25);
- currents $\Delta I_N^{(q)}$ in ring portions on pole S = q

$$\text{at } 0 \le N \le N_P - 1,\ \Delta I_{(N)} = C_L^{(q)} a_1^N + D_L^{(q)} a_2^N; \tag{11.33}$$

$$\text{at: } N_P \le N \le N_B + 1,\ \Delta I_{(N)} = C_R^{(q)} a_1^N + D_R^{(q)} a_2^N; \tag{11.34}$$

- currents $\Delta J_N^{(q)}$ in bars on pole S = q

$$\text{at } 0 \le N \le N_P - 1:\ \Delta J_{(N)} = C_L^{(q)} a_1^{N-1}(a_1 - 1) + D_L^{(q)} a_2^N (a_2 - 1); \tag{11.35}$$

$$\text{at } N_P + 1 \le N \le N_B + 1:\ \Delta J_{(N)} = C_R^{(q)} a_1^{N-1}(a_1 - 1) + D_R^{(q)} a_2^N (a_2 - 1); \tag{11.36}$$

- current ΔJ_{N_P} in damaged bar on pole S = q:

$$\Delta J_{N_P} = \left[C_R^{(q)} - C_L^{(q)} a_2\right] a_1^{N_P} + \left[D_R^{(q)} - D_L^{(q)} a_1\right] a_2^{N_P}. \tag{11.37}$$

In the presence of several damaged bars located on one or different poles, the problem is solved similarly. It is possible to show that in limit case—at bar break ($Z = \infty$), the system of r = 4p + 2 equations has a solution for coefficients; in practical calculations it is enough to set the value ΔZ by 1–2 orders more, than Z_B. Thus, the problem in Appendix 11.4 is solved.

Expressions for calculation of additional currents (11.24), (11.25), (11.33)–(11.37) are found, proceeding from the distribution of the main currents in constructions with bars of identical impedance on all poles. In the previous paragraph it is obtained [7] that if there is a bar on each pole, for example, a middle one made of metal with other resistivity, then other bars of the same pole, then for solution of this problem it is also necessary to calculate previously the main currents in construction with identical bars. Thus, in case of bar damage in more complicated structures the following currents in its elements are calculated:

(a) Main, corresponding to regular winding, impedance of all $2pN_0$ bars that is identical,
(b) Additional, caused by existence of bar made of metal with other resistivity on each pole [9],
(c) Additional, caused by bar damage on pole q (calculated by stated method) [8].

Calculation method of additional currents for special case, when damaged bar is edge one on pole, is similar.

Appendix 11.1

Values of coefficients A, V, H, S, M, P, Q, F, B, C, L, K, G, R, T, W for determination of constants from systems (11.17) and (11.18).

$$A = a_1^{N_B+1}; V = -a_1^{-1}; H = a_1^{-1}(a_1 - 1)Z_B;$$
$$S_0 = a_1^{N_B}(1 - a_1)Z_B - 2a_1Z_F; M = a_1^{N_P}\left(1 + \frac{\Delta Z}{Z_B}\right);$$
$$P = a_1^{N_P-2} - a_1^{N_P-1}\left(2 + \sigma + \frac{\Delta Z}{Z_B}\right);$$
$$Q = a_1^{N_P}\left[a_1 - \left(2 + \sigma + \frac{\Delta Z}{Z_B}\right)\right]; F = a_1^{N_P-1}\left(1 + \frac{\Delta Z}{Z_B}\right).$$

Coefficients B, C, L, K, G, R, T, W can be obtained respectively from coefficients A, V, H, S_0, M, P, Q, F by replacement of a_1 by a_2.

Appendix 11.2

Investigation of currents in damper winding elements of SDSZ type motor; a comparison with experimental data (Table 11.1).

Research objective—determine the currents distribution in damper winding elements of SDSZ type motor (2000 kW, 6 kV, 100 rpm, 50 Hz.) with power supply from a frequency converter. Brief description of damper winding construction for this motor is given in para 11.1.1. Investigations were performed at voltage U supplied to a motor from frequency converter in the range of $5\ \text{Hz} < f < 20\ \text{Hz}$ under the condition: $\frac{U}{f} = \text{const}$,where f—frequency. Investigation results are given in Table 11.1 for frequency f = 6.25 Hz; this frequency is selected proceeding from the following assumptions:

- for determining bar impedances Z_B and bar impedance Z_{N_P}, skin effect with this rather low frequency can be neglected that eliminates possible additional calculation errors in results;
- for low frequency, signal transmission to "analog-digital" converter is connected with smaller distortions.

Table 11.1 Calculated val $\Delta R = -0.2875 \times 10^{-3}$ ues of resulting currents distribution with frequency f = 6.25 Hz; a comparison with experimental data

No.	0	1	2	3	4
$\underline{J}_{(N)}$	1.405	1.31	1	1.214	1.456
$J_{(N),EXP}$	1.36	1.34	1.12	1.3	1.5
ε_1, %	3.5	−2.2	−11	−7.0	−3.0

Investigations were carried out within development of the USSR's first high-power frequency controlled motor of SDT type [10] for gearless drive (Fig. 11.1) of cement mill with productive capacity of 100 tons of cement per hour (5500 kW, 900 V, 16 rpm, 8 Hz; shaft toque apprx. 350 T m). SDSZ type motor was used as the model. In bench conditions (Fig. 11.2), at investigation of SDSZ type motor, the following problems were solved:

Fig. 11.1 The USSR's first high-power low-frequency SDT type motor for gearless drive of cement mill with productive capacity of 100 tons of cement per hour (5500 kW, 16 rpm, 8 Hz, shaft toque apprx. 350 tm) at "Elektrosila" Work, Stock Company "Power Machines" St. Petersburg

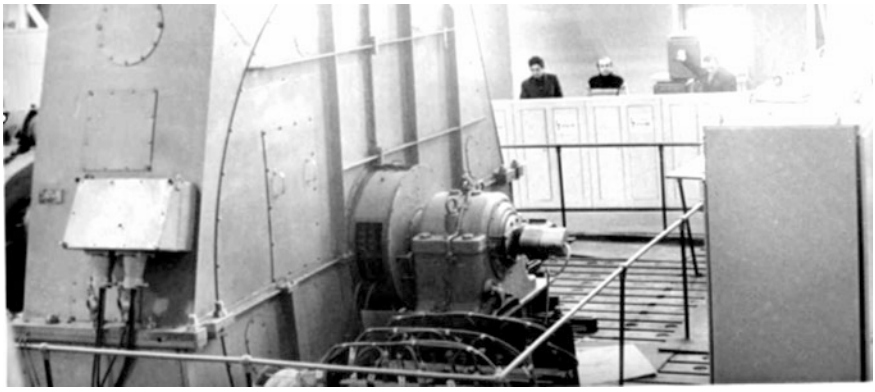

Fig. 11.2 SDSZ type motor in bench; investigations of electromagnetic processes at operation from frequency converter at LEZ, Stock Company "Ruselprom"

- choice of optimum rotor sensor design (sensor of torque angle Θ in salient-pole machine);
- working set of electric equipment with frequency converter, exciter and rotor sensor; purpose: minimization of current and voltage distortion factors;
- investigations of additional losses from higher time harmonics in resulting field and currents distribution in damper winding construction elements, when operating from frequency converter.

To study the currents distribution in damper winding construction elements, its bars from both end faces at slot exit were equipped with Rogowski sensor and thermocouples. Bars were previously drilled for thermocouples, after installation of thermocouples, holes were thoroughly calked. Signals from sensors arrived at the "analog-digital" converter, and then were processed in real time in Argus system (ICL Company, England). The decipherment of thermocouples data is carried out according to Ross method [12].

Results

Distribution of resulting currents in bars $\underline{J}_{(N)}$ for the mode f = 6.25 Hz at $\Delta R = -0.2875.10^{-3}$Ohms $\left(\frac{\Delta R}{R_B} = -0.75\right)$ are specified in Table 11.1. Current in middle bar (N = 2) is taken for unity. These values of currents $\underline{J}_{(N)}$ compared with experimental $J_{(N)EXP}$, are also given in Table 11.1. Here is given the difference ε_1 between $J_{(N)}$ and $J_{(N),EXP}$.

Appendix 11.3

Values of coefficients A, B, E, F, G, H, K, L for determination of constants $C^{(S)}, D^{(S)}, C_R^{(q)} C_L^{(q)}, D_R^{(q)}, D_L^{(q)}$ from systems (11.27) to (11.32).

$$A = a_1^{N_P}\left(1 + \frac{\Delta Z}{Z_B}\right); E = -a_1^{N_P-1}\left(2 + \sigma + \frac{\Delta Z}{Z_B}\right);$$
$$G = a_1^{N_P+1} - a_1^{N_P}\left(2 + \sigma + \frac{\Delta Z}{Z_B}\right); K = a_1^{N_P-1}\left(1 + \frac{\Delta Z}{Z_B}\right);$$
$$M = (1 - a_2)Z_B;\ Q = \left(a_1^{N_B} - a_1^{N_B-1}\right)Z_B - 2a_1^{N_B+1}Z_F.$$

Coefficients B, F, H, L, P, R can be obtained respectively from coefficients A, E, G, K, M, Q replacing a_1 by a_2 and, respectively, a_2 by a_1.

Appendix 11.4

Calculation example: dependence of additional current in the damaged bar of SBGD type generator (6 MW, 1000 rpm, 10.5 kV "Elektrosila" Work, Stock Company "Power Machines" St. Petersburg) on impedance ΔZ_B.

$$\text{Given: } Z_B = (1.62 + j1.995) \times 10^{-4}, Z_R = (1.814 + j2.165) \times 10^{-4}$$
$$Z_F = (7.514 + j8.967) \times 10^{-6};\ N_0 = 8;\ N_P = 3;\ J_3 = 4e^{-j25.5}$$

Variants for

$$\Delta Z_B : A).\ \Delta Z_B = 2Z_B; B).\ \Delta Z_B = 20Z_B; C).\ \Delta Z_B = 80Z_B; D).\ \Delta Z_B = 100Z_B.$$

To find for $N_P = 3 : \Delta J_3, J_3, \frac{\left|\underline{J}_{=3}\right|}{J_3}$

The solution is obtained from the system (11.27) to (11.32) and Eq. (11.37) and tabulated in Table 11.2

Note. When designing powerful synchronous motors with severe operating conditions (load change, etc.), the values of overheating of damper winding bars and Field's factor may be clarified by the method stated in Appendix 1 of Chap. 23.

Table 11.2 Dependence of additional current in damaged bar of damper winding on impedance ΔZ_B of SBGD type generator

Variants for ΔZ_B	ΔJ_3	$\underline{J}_{=3}$	$\frac{\left\|\underline{J}_{=3}\right\|}{\left\|J_3\right\|}$
A	$1.787e^{j154.84}$	$2.212e^{-j25.78}$	0.553
B	$3.559e^{j154.57}$	$0.4404e^{-j25.51}$	0.110
C	$3.879e^{j154.52}$	$0.1204e^{-j26.09}$	0.030
D	$3.9036e^{j154.48}$	$0.0964e^{-j26.1}$	0.024

This method provides the calculation of skin effect in the bars of the rotor, taking into account the temperature distribution on its height.

Brief Conclusions

1. If in damper winding on each pole there is one bar with impedance differing from the others, calculation of currents distribution is reduced to the solution of two problems: for main and additional currents.
2. For this design of damper winding, calculating distribution of additional currents (the second problem) is reduced to the computation of only four constants as part of difference equations. The order of this system does not depend on the number of bars N_0 on the pole and is equal to r = 4. In solving the problem by a numerical method the system order is determined by the product $r' = 2pN_0$.
3. At emergence of damage in damper winding bar on one of poles, calculation of currents distribution in its elements is reduced, as well as in previous design, to the solution of two problems. Constants of calculation expressions for additional currents are calculated from the system of linear equations whose order is determined only by the number of machine poles and does not depend on the number of bars per pole: $r \leq 4p + 2$. In solving the problem the system order is determined as well as in previous design by product $r' = 2pN_0$. Note that the methods presented in [13–20] do not provide a solution to this problem.
4. The method allows one to calculate the distribution of currents in the presence of several bars or ring portions whose impedances differ from the others.

List of Symbols

$D_1, D_2, D_3, D_4, D'_1, D'_2, D'_3, D'_4$	Constants for determination of currents of both poles of opposite polarity
E_1	EMF amplitude induced by air gap resulting field in rotor loops on pole
E_F	EMF in loop formed by edge bars of adjacent poles
$\underline{\underline{I}}_N, \underline{\underline{J}}_N$	Currents in ring portions (segments) and in damper winding bars at emergence of asymmetry (damage)
I_N, J_N	Currents in ring portions (segments) and in damper winding bars before asymmetry emergence
$\Delta I_{(N)}, \Delta J_{(N)}$	Additional currents in bars and ring portions of asymmetrical damper winding
$\Delta J_{N_P}, \Delta I_{N_P}$	Additional currents of asymmetrical (damaged) bar and ring portions in the loop containing this bar

N	Bar (ring portion) number of damper winding or squirrel cage
N_0	Number of damper winding bars on pole
N_p	Asymmetrical bar number
p	Number of pole pairs
q	Pole number with asymmetrical (damaged) bar
T, T_{EL}	Expansion period of MMF and mutual fields in air gap to harmonic series
Z_B, Z_R, Z_F	Impedances of bar, ring portion between bars on pole, ring portion between bars of adjacent poles
ΔZ_{N_P}	Additional impedance of asymmetrical (damaged) bar
$\Delta\varphi$	Phase angle between EMF of adjacent bars on pole

References

I. Monographs, textbooks

1. Demirchyan K.S., Neyman L.R., Korovkin N.V., Theoretical Electrical Engineering. Moscow, St.Petersburg: Piter, 2009. Vol. 1, 2. (In Russian).
2. Kuepfmueller K., Kohn G., Theoretische Elektrotechnik und Elektronik. 15 Aufl., Berlin, N. Y.: Springer. 2000. (In German).
3. Gardner M., Berns D., Transients in Linear Systems Studied by Laplace Transformation. N. Y.: J. Wiley, 1942.
4. Richter R., Elektrische Maschinen. Berlin: Springer. Band I, 1924; Band II, 1930; Band III, 1932; Band IV, 1936; Band V, 1950. (In German).
5. Mueller G., Ponick B., Grundlagen elektrischer Maschinen. Springer, 2005. (In German).

III. Synchronous machines. Papers, inventor's certificates, patents

6. Boguslawsky I.Z., Calculating the current distribution on the damper winding of large slow – speed synchronous motors in asynchronous operation. Power Eng. (New York), 1979, № 3.
7. Boguslawsky I.Z., Currents and harmonic MMFs in a damper winding with damaged bar at a pole. Power Eng. (New York), 1985, № 1.
8. Demirchyan K.S., Boguslawsky I.Z., Current flowing in damper winding bars of different resistivity in a heavy-duty low speed motor. Power Eng. (New York), 1980, № 2.
9. Boguslawsky I.Z., Method of calculating of the active chain-circuits with damaged elements. Electrichestvo, 1984. № 4; 1988. № 8. (In Russian).
10. Fomin B.I., Makarov N.I., Boguslawsky I.Z., Datzkowskiy L.Kh., Gigulin Yu.V., Krol N.M., Lesokhin A.Z., Powerful synchronous motors for controlled electric A.C. drive. Elektrotechnika, 1984, #8. (In Russian).

11. Boguslawsky I.Z., Demirtschian K.S. Stationaere Stromverteilung in unregelmaessigen und unsymmetrischen kurzgeschlossenen Laeuferwicklungen von Wechselstrommaschinen. Archiv fuer Elektrotechnik, 1992. № 6. (In German).
12. Ross M.D., Time – temperature tests to determine machine losses. Electrical Engineering (USA). 1935. Vol. 54, #10; 1936. Vol. 55, #3.
13. Schuisky W., Ueber die Stromverteilung im Anlaufkaefig eines Synchronmotors. E. u M., 1940, № 9/10 (In German).
14. Kleinrath H., Die Synchronmaschine im asynchronen Betrieb, betrachtet als Doppelkaefigmotor aus dem Blickwinkel der Zweiachsentheorie. Archiv fuer Elektrotechnik, 1963. № 4 (In German).
15. Lorenzen H., Jordan H., Der Einfluß einzelner Maschinengrößen auf das Anlaufverhalten geblechter Schenkelpolsynchronmaschinen. Archiv für Elektrotechn., 1966. Vol. 51 (In German).
16. Bausch H., Jordan H., Weiss M., Zur digitalen Berechnung des asynchronen Betriebsverhaltens von Drehfeldmaschinen mit anisotropem Läufer. Archiv für Elektrotechn., 1968. №3 (In German).
17. Nicolaide A., Untersuchung des Daempferwicklung und des natuerlichen Daempfersystems der Schenkelpolmaschinen. Archiv fuer Elektrotechnik, 1969. Vol. 54 (In German).
18. Nicolaide A., Untersuchung der Charakteristiken des asynchronen Betriebes der Synchronmaschine mit Schenkelpolen und Daempferwicklung. Archiv fuer Elektrotechnik, 1975. Vol. 60 (In German).
19. Saccetti R., Troili R., Una tecnica unitaria nello studio dei circuiti a delle motori il metodo dei circuiti equivalente parziale. L'Energia Electrica, 1980. № 3 (In Italian).
20. Fritz W., Hyrenbach M., Sehneckmann W., The behavior of damper cages. ETEP, Vol. 8, №1, Januar/Februar, 1998. (In German).

Chapter 12
MMF of Damper Winding, Squirrel Cage (at Asymmetry in Them or at Its Absence) and Excitation Winding. Representation of MMF in the Form of Harmonic Series in Complex Plane

This chapter deals with investigation methods of MMF harmonics of spatial orders n ($|m|=|n| \geq 1$) excited by the currents with frequency ω_{ROT} in rotor loops, included in short-circuited windings: damper winding of synchronous machines and squirrel cage of induction machines (also in asymmetrical). When developing these methods, an expansion into harmonic series (Fourier) in complex form is applied; it allowed us to obtain without additional transformations complex amplitudes (phasors) of main and additional components of resultant MMF and fields in air gap and to give them clear physical interpretation. Thus, currents in rotor structural elements are represented by means of a symbolic method in the form of time complexes (phasors). Expansion period T is accepted in the investigation equal to $T = \pi D$; as a result it was possible to consider not only MMF higher spatial harmonics and fields in air gap, but also the lower; here D—calculation diameter of stator boring. Obtained here are calculation expressions for MMF complex amplitudes (phasors):

- damper winding (regular and irregular);
- asymmetrical squirrel cage (general problem) and its special cases, whose calculation of currents was investigated in the previous chapter; they are listed above.
- excitation winding of salient-pole machines;

The content of this chapter is development of the methods stated in [1, 2, 10–13].

12.1 Fundamental Assumptions

Among the problems of investigating A.C. machines in nonlinear networks and with short-circuited rotor windings, the problem determining MMF of these windings was given in Chap. 2. It was noted that the solution of this problem should

I. Boguslawsky et al., *Large A.C. Machines*,
DOI 10.1007/978-4-431-56475-1_12

be based on the real distribution of currents in elements of damper winding and squirrel cage (in the absence or emergence of asymmetry). Therefore, let us use investigation results of currents in structural elements of short-circuited windings obtained in the previous chapters.

Besides general assumptions listed in them and used here, the following should be noted.

Let us accept that the current in rotor bars is concentrated on the slot symmetry axis. In damper winding of salient-pole machines, the bars are usually laid in slots from rotor end face, so that the slot opening width in slot makes $b_{OP} = 2-4^{\circ}$mm, and its relation to pitch t_{SLT} over slots is small: $\frac{b_{OP}}{t_{SLT}} < 0.05-0.1$. The same refers also to squirrel cages if in their structure provision is made for laying bars from end face or filling slots with aluminum; then $\frac{b_{OP}}{t_{SLT}} < 0.1-0.15$. For all these constructions it is possible to assume that MMF in the air gap has a step form distributed along the period $T = \pi D$. The next MMF surge by a current value in the slot takes place when reaching the slot symmetry axis in the process of its number increase.

In high-power induction machines slots are sometimes made open, then bars in them are laid from the top, from the side of wedge zone. Investigations of such a design indicates that even in case of sharp manifestation of skin effect the current density in a bar is admissible to consider as constant along the entire slot width. Therefore, the step form of MMF distribution somewhat changes: within a slot, the MMF curve rises not stepwise, but linearly, and also by a current value in the slot, and remains constant until reaching a wall of the next slot in the process of its number increase.

Assessment of these assumptions indicates that taking into account of the linear variation of MMF curve along the slot width even for open slots practically does not influence the amplitude of lower MMF harmonics representing the greatest practical interest; therefore, for open slots, with accuracy sufficient for practice, it is possible to consider that the current is concentrated on the slot symmetry axis, if we limit the calculation to spatial harmonics maximum in amplitude (n = 5, 7, 11). Accounting of this linear variation of MMF curve along the slot width is usually necessary for the solution of special tasks caused by reducing machine vibrations, noise, etc. Peculiarities of rotor windings MMF calculation method with account of final slot width are given in Appendix 12.1.

Let us state at first the method of MMF calculation in relation to short-circuited rotor windings taking into account an assumption that the current in rotor bars is concentrated on the slot symmetry axis.

12.2 Representation of Damper Winding and Squirrel Cage MMFs (at Asymmetry or Its Absence in Them) in the Form of Step Function

12.2.1 Initial Data and Their Representation

The following initial data are accepted for solving this problem:

- currents distribution in structural elements of these windings;
- geometrical dimensions of windings;
- rotor rotation speed (slip);
- number of machine poles 2p.

Let us consider at first some initial data in more detail.

(a) Currents distribution in structural elements of these windings;

As obtained in the previous chapters, it is supposed that currents are set in the form of generalized characteristics, i.e. with accuracy of flux density complex amplitudes of resulting field in air gap. Determination methods of these complex amplitudes are stated below, when forming equations and the solution algorithm of a system of magnetically coupled loops.

(b) Geometrical dimensions of damper winding and squirrel cage.

These dimensions are selected the same as for calculation of EMF in damper winding and squirrel cage loops. They were given in Chap. 8 (Figs. 8.1 and 8.2). Let us note only that the derivation of calculation expressions for MMF is made for general task: the distance x from the origin of coordinates to the axis of the first slot (bar) is assumed arbitrary and equal to $x = x_0$. For generality, it is accepted also that distances along the rotor periphery between axes of adjacent slots (bars) with numbers: $N = 1$ and $N = 0$; $N = 2$ and $N = 1$; …; N and $N - 1$ designated respectively, $x_{1,0}; x_{2,1}; \ldots; x_{N,N-1}$, are accepted not identical:

$$x_{1,0} \neq x_{2,1} \neq \cdots \neq x_{N,N-1} \neq \cdots. \tag{12.1}$$

For such a representation, we also consider peculiarities of damper winding construction with pitch b between slot axes on the pole not equal to distance b_F between axes of edge slots in adjacent poles, and $\frac{b_F}{b} > 1$.

12.2.2 Peculiarities of Representing MMF and Field of Damper Winding and Squirrel Cage Currents in the Form of Step Function

Harmonics of MMF and fields of rotor winding currents for a special case—DFMs—were already determined by Eqs. (2.4) and (2.4′), based on the current in three-phase rotor winding of this machine. Calculation expressions for these MMF harmonic of three-phase winding were obtained in Chap. 3.

Unlike rotor winding of DFMs, short-circuited rotor winding structures of synchronous and induction machines represent a set of loops shifted in space along the rotor periphery by a certain phase angle $\Delta\varphi$ electrical degrees; respectively, EMF of each subsequent loop is shifted relative to that of previous one in time by the same phase angle $\Delta\varphi$. Currents in rotor loops induced by any harmonic of mutual induction field, generate for each period T the only rotating field in the air gap [2, 3] of order $n \ll \frac{Z_2}{p}$ in case if:

- phase angle between each two adjacent loops remains constant: $\Delta\varphi = \text{const}$; air gap $\delta = \text{const}$;
- impedance of all Z_2 winding bars are equal; the same refers also to the impedance of short-circuited ring portions (segments).

Here Z_2—number of slots in squirrel cage; for salient-pole machines $\frac{Z_2}{2p} = N_0$, where N_0—number of pole bars.

Damper winding structure (with asymmetry or without it) and squirrel cage (with damage) meet these requirements only partially, and squirrel cage without damages —completely. Therefore, it is necessary to expect that the field of currents in short-circuited A.C. machine rotor windings generally [3, 4] for every period T can be represented in the form of two components rotating relative to the rotor winding with these currents directed in opposite sides. The field components rotating in the direction opposite to the rotor rotation will be so intensive, because this short-circuited winding structure meets the listed above requirements. For example, in the construction of complete damper winding both requirements are not met: Bars are not installed in space between poles. In linear induction motors, the first requirement is not met: the rotor winding is open. When the squirrel cage bar or ring portion is damaged, the second requirement is not met.

Let us consider a general method of analysis of MMFs and fluxes in air gap created by currents in short-circuited winding; it provides both observance of the requirements listed above and deviation from them.

As is described in [1, 2], the magnetic flux in the air gap and MMF corresponding to it meets the law of continuity. In a differential form it is determined as follows:

$$\operatorname{div} b(x,t) = 0; \quad \operatorname{div} f(x,t) = 0, \tag{12.2}$$

and in an integral form

$$\int_{-\frac{T}{2}}^{\frac{T}{2}} b(x,t) L_{COR} dx = 0; \quad \int_{-\frac{T}{2}}^{\frac{T}{2}} f(x,t) L_{COR} dx = 0. \tag{12.2'}$$

Here, $b(x,t), f(x,t)$ correspondingly values of flux density and MMF, $T = \pi D$—period of flux or MMF variation, D—stator boring calculation diameter, L_{COR}—core calculation length.

For regular damper winding it is sufficient to assume as the period $T_{EL} = \pi \frac{D}{p}$, if poles are made without shift and, therefore, pole pitch $\tau = \pi \frac{D}{p} = \text{const}$; this construction common for medium power generators and motors, is accepted for further MMF investigation. Let us note that the same period is enough to be selected in the analysis of MMF and three-phase stator winding with an integer number of slots per pole and phase.

For damper irregular winding in which, for example, there is a bar damage in one of poles, it is necessary to select $T = \pi D$ as a period.

In squirrel cage the number of bars N_0 is usually selected such that its relation to the number of pole pairs—is fractional [5, 6]. Therefore, for a squirrel cage without damage of its elements, as well as at their emergence, the period T is selected equal to $T = \pi D$. Let us note that the same period is necessary to assume in the analysis of MMF and three-phase stator winding with fractional number of slots per pole and phase.

Let us use Fig. 8.2 for descriptive reasons and illustrations of the general method of MMF determination. We already reused it: in Chap. 8 in the calculation of EMF of squirrel cage loops and in Chap. 10 in the calculation of currents with different types of squirrel cage asymmetry.

We consider rotor winding in Fig. 8.2 as generalized (arbitrary) construction of short-circuited rotor cage whose particular versions are damper winding (regular or irregular) or squirrel cage (symmetrical or asymmetrical). We consider a method of MMF determination of this short-circuited rotor winding.

Let us proceed to the mathematical formulation of this general problem: Let us represent short-circuited rotor winding MMF of any design in the form of step function (Table 12.1); for this purpose, we use the Ampere's law [1, 2]. Then, let us determine this step function of MMF in the form of a number of rotating waves.

In the first column of Table 12.1 a serial number of portion between symmetry axes of adjacent slots (step number) throughout which the current function keeps its

Table 12.1 MMF step function of short-circuited rotor winding of arbitrary construction (Fig. 8.2)

Serial number of step (portion between adjacent slots)	Step extent.	Function of current ("heights of steps under teeth") $F_{ROT}(x)$
1	$x_0 \le x < x_0 + x_{1,0}$	J_0
2	$x_0 + x_{1,0} \le x < x_0 + x_{1,0} + x_{2,1}$	$J_0 + J_1$
3	$x_0 + x_{1,0} + x_{2,1} \le x < x_0 + x_{1,0} + x_{2,1} + x_{3,2}$	$J_0 + J_1 + J_2$
4	$x_0 + x_{1,0} + x_{2,1} + x_{3,2} \le x < x_0 + x_{1,0} + x_{2,1} + x_{3,2} + x_{4,3}$	$J_0 + J_1 + J_2 + J_3$
5	$x_0 + x_{1,0} + x_{2,1} + x_{3,2} + x_{4,3} \le x < x_0 + x_{1,0} + x_{2,1} + x_{3,2} + x_{4,3} + x_{5,4}$	$J_0 + J_1 + J_2 + J_3 + J_4$
⋮	⋮	⋮
N	$x_0 + x_{1,0} + \cdots + x_{N,N-1} \le x < x_0 + x_{1,0} + \cdots + x_{N+1,N}$	$J_0 + J_1 + \cdots + J_{N-1} = I_{N-1} - I_{-1}$

The currents $\underline{J}_N$ the bars and currents $\underline{I}_{N-1}$ in segments of ring are resultant currents; in the table the underline is omitted

invariable value till meeting with an axis of the following slot (in the process of slot number increase) where it increases stepwise by the current value in this slot.

In the second column of Table 12.1 the extent of each step is specified; Let us note that according to the condition accepted earlier, dimensions of these steps are generally not identical; it takes place, for example, in the construction of damper winding.

In the third column the values of current function are specified for short-circuited winding $F_{ROT}(x)$ or MMF ("heights of steps under teeth") obtained based on the Ampere's law. These are designated as functions $F_{ROT}(x)$ of spatial coordinate x along the boring periphery; Let us note that currents in short-circuited winding elements are time dependent complexes.

Table 12.1 represents all necessary parameters for MMF investigation, for example, its harmonic analysis.

However, we perform simple mathematical transformations over current function $F_{ROT}(x)$ ("heights of steps under teeth"). These transformations have a simple physical sense and at the same time represent practical interest in the construction of damper winding or squirrel cages. For this purpose let us transform the current function of each step, using the first Kirchhoff's law [1, 2]; current in bars will be expressed through currents in adjacent portions of short-circuited rings (segments), for example, $J_0 = I_0 - I_{-1}; J_1 = I_1 - I_0; J_2 = I_2 - I_1; \ldots$.

As a result, we obtain expressions for current function $F_{ROT}(x)$ in the form.

$$\begin{aligned}
&\text{For step } 1 : F_{ROT}(x) = I_0 - I_{(-1)};\\
&\text{For step } 2 : F_{ROT}(x) = I_1 - I_{(-1)};\\
&\text{For step } 3 : F_{ROT}(x) = I_2 - I_{(-1)};\\
&\text{For step } 4 : F_{ROT}(x) = I_3 - I_{(-1)};\\
&\text{For step } 5 : F_{ROT}(x) = I_4 - I_{(-1)};\\
&\qquad\vdots\\
&\text{For step } (N - K) : F_{ROT}(x) = I_{N-K-1} - I_{(-1)};\\
&\qquad\vdots
\end{aligned} \tag{12.3}$$

One notes a practical conclusion [5, 6] following from these expressions connected with the selection of ring (segment) section q_R between poles for damper winding bar section q_B selected: $q_R = (0.4{-}0.5)q_B N_0$, where N_0—number of bars on the pole.

Step function given in Table 12.1 is periodic; as noted earlier, its period is equal to $T = \pi D$. Let us represent it in the form of a number of rotating waves. For this purpose, we use the expansion of a step function into harmonic series (Fourier).

12.3 General Method of Calculating MMF Harmonics and Fields of Rotor Currents; Use of Symbolical Method of Representation of Currents in Combination with Complex Form of Harmonic Series Representation (Fourier)

12.3.1 Physical Treatment of Method. Calculation Expressions for Terms of Harmonic Series

Some forms of representation of this harmonic series [7, 8] are known. However, one of them has an interesting feature for the investigation of field in air gap allowing us to give it a simple physical interpretation: it gives an opportunity without any additional transformations to represent step curves of MMF and magnetic field in air gap in the form of several rotating waves, when using a symbolic method of representation of harmonic functions and expanding into a series in complex plane.

Let us write down at first mathematical formulation of harmonic series in complex form [7, 8] for some function $F_{ROT}(x)$:

$$F_{ROT}(x) = \sum \left[C(-n)e^{-2j\pi\frac{nx}{T}} + C(n)e^{2j\pi\frac{nx}{T}}\right] + C_0.$$

In this expression, summation of terms of series is made over the numbers of rotor harmonics (n); expansion coefficients are equal to,

$$C(-n) = \frac{1}{T}\int_{-\frac{T}{2}}^{\frac{T}{2}} F_{ROT}(x)e^{2j\pi\frac{nx}{T}}dx; \quad C(n) = \frac{1}{T}\int_{-\frac{T}{2}}^{\frac{T}{2}} F_{ROT}(x)e^{-2j\pi\frac{nx}{T}}dx;$$
$$C_0 = \frac{1}{T}\int_{-\frac{T}{2}}^{\frac{T}{2}} F_{ROT}(x)dx. \tag{12.4}$$

Here, $F_{ROT}(x)$—according to Table 12.1 (the third column) or with Eq. (12.3).

With account of magnetic field properties in the air gap (12.2') or (12.2), we obtain the coefficient $C_0 = 0$.

Let us consider in more detail the rotor MMF component harmonic of order n according to the first summand in Eq. (12.4):

$$F_{ROT,1}(x, n) = C(-n)e^{-2j\pi\frac{nx}{T}}. \tag{12.5'}$$

We assume that the coefficient C(−n) for this harmonic is a complex amplitude of symbolic method [1, 2] and has the form:

$$C(-n) = |C(-n)|e^{j\omega_{ROT}t},$$

Here $|C(-n)|$—modulus of complex amplitude, ω_{ROT}—EMF frequency.

Then, this summand for harmonic of order n can take the following form:

$$f_{ROT,1}(x,t,n) = |C(-n)|e^{j\left(\omega_{ROT}t - 2\pi\frac{nx}{T}\right)}. \quad (12.4')$$

Similarly, the rotor harmonic of an order according to the second summand in Eq. (12.4) is as follows:

$$f_{ROT,2}(x,t,n) = |C(n)|e^{j\left(\omega_{ROT}t + 2\pi\frac{nx}{T}\right)}. \quad (12.4'')$$

Equation (12.4′) for $f_{ROT.1}(x, t, n)$ describes the rotating wave with amplitude $|C(-n)|$; its rotation direction—towards positive values of x coordinate, that is, in the direction of rotor rotation. Its rotation speed V relative to rotor is equal to,

$$V_{ROT,1} = \frac{dx}{dt} = \omega_{ROT}\frac{T}{2\pi n} = \omega_{ROT}\frac{D}{2n}\omega_{ROT}\frac{R}{n}.$$

Here, $R = \frac{D}{2}$—calculation radius of stator boring. Thus, wave speed relative to the rotor increases with frequency ω_{ROT} of EMF and currents in rotor loops; it is inversely proportional to the order of spatial harmonic n.

Similarly, Eq. (12.4″) for $f_{ROT.2}(x, t, n)$ with amplitude $|C(n)|$ also describes the rotating wave; but unlike the first, its rotation direction—towards negative values of x coordinate; that is, against the direction of rotor rotation. Its rotation speed V relative to rotor is equal to,

$$V_{ROT,2} = \frac{dx}{dt} == -\omega_{ROT}\frac{T}{2\pi n} = -\omega_{ROT}\frac{D}{2n} - \omega_{ROT}\frac{R}{n}.$$

As a result, we obtain an expression for instantaneous values of step function given in Table 12.1 in the form of series:

$$\begin{aligned} f_{ROT}(x,t) &= \sum\left[|C(-n)|e^{j\left(\omega_{ROT}t - 2\pi\frac{nx}{T}\right)} + |C(n)|e^{j\left(\omega_{ROT}t + 2\pi\frac{nx}{T}\right)}\right] \\ &= \sum f_{ROT,1}(x,t,n) + \sum f_{ROT,2}(x,t,n). \end{aligned} \quad (12.5)$$

In Eq. (12.5) summation of series terms is made over the rotor harmonics numbers (n). Let us note that both fields correspond to rotor currents with frequency ω_{ROT}.

Thus, using the representation of harmonic series (Fourier) in complex plane and the symbolic method for current harmonic functions, we obtain a possibility to make a clear physical interpretation of both summands of this series in relation to

MMF and fields in the air gap of A.C. machines. Let us use designations accepted for MMF:

$$\sum C(-n) = \sum F_{ROT,1}(n, \omega_{ROT}); \quad \sum C(n) = \sum F_{ROT,2}(n, \omega_{ROT});$$

with account of (12.5) we obtain:

$$F_{ROT}(x) = \sum F_{ROT,1}(n, \omega_{ROT}) e^{-2j\pi\frac{nx}{T}} + \sum F_{ROT,2}(n, \omega_{ROT}) e^{2j\pi\frac{nx}{T}}. \qquad (12.5'')$$

Summation is made over the harmonics numbers of order n. One of these two summands corresponds to field harmonics of order n rotating in the same direction with rotor, and the second of the same order n rotating in the opposite direction.

12.3.2 *General Expressions for Calculation of Complex Amplitudes of MMF Harmonics in Short-Circuited Winding of Arbitrary Construction*

We use Table 12.1 and expressions from (12.4) to find expansion coefficients and complex amplitudes of MMF harmonics of short-circuited winding of arbitrary construction in Fig. 8.2. In their calculation let us consider that the function $F_{ROT}(x)$ within each step keeps its value invariable. So, in the integration as per (12.4) it is expedient to subdivide the period T into separate segments corresponding to these steps; then the current function within each step can be taken out the integration sign. These segments ("step extents") are specified in the second column of Table 12.1. Let us note that unlike calculation expressions for coefficients C(n), C(−n) given in the previous paragraph, here we take different integration limits: 0, T [7, 8].

For coefficient C (−n) with account of the last, we have [7, 8]:

$$C(-n) = \frac{1}{T}\int_0^T F_{ROT}(x) e^{2j\pi\frac{nx}{T}} dx = \frac{I_0}{T}\int_{x_0}^{x_1} e^{2j\pi\frac{nx}{T}} dx + \frac{I_1}{T}\int_{x_1}^{x_2} e^{2j\pi\frac{nx}{T}} dx + \frac{I_2}{T}\int_{x_2}^{x_3} e^{2j\pi\frac{nx}{T}} dx + \cdots + \frac{I_N}{T}\int_{x_{N-1}}^{x_N} e^{2j\pi\frac{nx}{T}} dx + \cdots \qquad (12.6)$$

Note $N \leq N_0$.

To obtain an expression for coefficient C(n), it is necessary to substitute the value (−n) by (n) and vice versa in Eq. (12.6).

In Eq. (12.6) currents $I_0, I_1, I_2, \ldots, I_N, \ldots$ are resultant; at asymmetry in short-circuited winding they have some components and according to accepted designations should be double underlined. However, for simplification of the text hereinafter these currents are represented without underlining.

Let us note that in this Eq. (12.6) there is no current $I_{(-1)}$: in integration ranging from 0 to T it remains invariable, and the integral corresponding to it is equal to zero.

In Eq. (12.6) we will not substitute the upper and lower limits for each step into the exponential function $e^{2j\pi\frac{nx}{T}}$: this operation is rather obvious.

Let us regularize amplitude designations of MMFs in rotor loops. Amplitudes of MMF stator harmonics in Chap. 3 were designated as: $F_{STAT}(m, Q)$ or $F_{STAT}(-m, Q)$. Unlike the symbol of stator winding MMF amplitudes with stator time harmonic order Q, for rotor loops instead of time harmonic order is more convenient to specify its frequency ω_{ROT}: in Chap. 3 it is obtained that it is not always possible to express its order as integer.

Complex amplitudes of rotor $F_{ROT,1}(n, \omega_{ROT})$ and $F_{ROT,2}(n, \omega_{ROT})$ in the equations can be indicated more simply, omitting indices. We will designate the first of them as $F_{ROT}(n, \omega_{ROT}) = F_{ROT,1}(n, \omega_{ROT})$. Similarly, the second of them: $F_{ROT}(-n, \omega_{ROT}) = F_{ROT,2}(n, \omega_{ROT})$. These symbols are similar to those of stator MMF complex amplitudes.

Let us find complex amplitudes of MMF harmonics for the construction of short-circuited rotor winding representing practical interest now.

12.4 MMF and Field Harmonics in Squirrel Cage with Damages for Induction Machine (General Problem)

Let us apply the obtained results of step curve expansion, at first, to MMF and field harmonics in squirrel cage at any degree of its asymmetry. We consider the squirrel cage consisting of N_0 bars, with distance between their axes equal to $b(x_{1,0} = x_{2,1} = \cdots = x_{N,N-1} = b)$. Let us superimpose the origin of coordinates with the bar axis having serial number N = 0, that is, we accept $x_0 = 0$. We use investigation results obtained in the previous paragraph for the general calculation problem of rotating MMF waves in the air gap.

We find complex amplitudes $F_{CAG}(n, \omega_{ROT}), F_{CAG}(-n, \omega_{ROT})$. According to Eq. (12.6) we obtain:

$$F_{CAG}(n,\omega_{ROT}) = \frac{1}{T}\int_0^T F_{CAG}(x)e^{2j\pi\frac{nx}{T}}dx = \frac{I_0}{T}\int_0^b e^{2j\pi\frac{nx}{T}}dx + \frac{I_1}{T}\int_b^{2b} e^{2j\pi\frac{nx}{T}}dx + \frac{I_2}{T}\int_{2b}^{3b} e^{2j\pi\frac{nx}{T}}dx + \cdots + \frac{I_{N_0-2}}{T}\int_{T-b}^{T} e^{2j\pi\frac{nx}{T}}dx. \quad (12.7)$$

This expression is true for any arbitrary current distribution in cage elements along the boring, including the presence of current aperiodic components caused by its damage. In Eq. (12.7) as in (12.6), we will not substitute upper and lower limits for each step into exponential function $e^{2j\pi\frac{nx}{T}}$: Matter is not only in cumbersome expressions obtained after algebraic transformations, but also in the practice of calculations and investigations of A.C. machines accepted now:

(a) Transformation of the expression like (12.7) to obtain in the closed form an analytical ratio between key parameters of asymmetrical rotor winding would be reasonable, if it is possible to obtain from its recommendations connected, for example, with rational selection of MMF waveform. However, such a result can be obtained only for squirrel cage without damages (para 12.5). Emergence of aperiodic summands for damper winding or asymmetrical squirrel cages in distribution curves of resulting current caused by its additional components $\left[\Delta J_{(N)}, \Delta I_{(N)}\right]$, considerably complicates calculation expressions. They are given as an example for squirrel cage with one damaged bar, with two bars, with three bars, as well as for irregular damper winding; these cumbersome expressions also substantiate the stated approach for MMF calculation. The presence of aperiodic components in the obtained analytical expressions for MMF of these short-circuited windings did not allow the authors to formulate any additional practical recommendations concerning MMF waveform. We succeeded in formulating these recommendations only for symmetrical squirrel cage, as a special case of asymmetrical (at asymmetry $\Delta J_{(N)} = 0$) to prove [3, 4] validity of the stated MMF determination method. They are given in para 12.5;

(b) Thus, analytical expressions for MMF of asymmetrical squirrel cages obtained in paragraphs of this chapter have no advantages before the given calculation expressions like (12.6), (12.7): these analytical expressions are cumbersome, they cover only special cases of asymmetry, and require some efforts for their algorithmization. At the same time, the given calculation expressions like (12.6), (12.7) are general, cover the whole class of symmetrical and asymmetrical windings and with account of tables like 12.1 are convenient for algorithmization.

Design formulations of practical interest are given as an example in the following four sections of the chapter for asymmetrical squirrel cage construction with one damaged bar (basic task) and with three damaged bars with their different location (three adjacent; two close, the third—next nearest; three—non-adjacent).

12.4.1 MMF Harmonics and Fields of Asymmetrical Squirrel Cage (with One Damaged Bar); Its Number Is $N = N_P$

Equations for resulting currents in components of such a cage have been presented in Chap. 10. It follows from these equations that MMF for harmonic components of principal current $F_{CAG}(n, \omega_{ROT}), F_{CAG}(-n, \omega_{ROT})$ and for its aperiodic components $\Delta F_{CAG}(n, \omega_{ROT}), \Delta F_{CAG}(-n, \omega_{ROT})$ may be calculated independently. The amount of both MMF components gives the value of MMF resulting component respectively for spatial and complementary waves:

$$\underline{\underline{F}}_{RES,CAG}(n, \omega_{ROT}) = F_{CAG}(n, \omega_{ROT}) + \Delta F_{CAG}(n, \omega_{ROT});$$
$$\underline{\underline{F}}_{RES,CAG}(-n, \omega_{ROT}) = F_{CAG}(-n, \omega_{ROT}) + \Delta F_{CAG}(-n, \omega_{POT}).$$

In this section we shall give design expressions for MMF complex amplitudes corresponding to aperiodic components. Expressions for MMF complex amplitudes which correspond to harmonic components of principal current (for symmetrical squirrel cage) may be obtained in the following section as for special case of asymmetrical squirrel cage.

Let us use expressions for aperiodic components in the elements of cage ring and Eq. (12.7). After a series of transformations we shall have the following for MMF complex amplitudes

$$\Delta F_{CAG}(n, \omega_{ROT}) = \frac{1}{2j\pi n} S_2 \left[C_1 \frac{(a_1 S_1)^{N_P} - 1}{a_1 S_1 - 1} + C_2 \frac{(a_2 S_1)^{N_P} - 1}{a_1 S_1 - 1} + C_3 (a_1 S_1)^{N_P} \frac{(a_1 S_1)^{N_0 - N_P} - 1}{a_1 S_1 - 1} + C_4 (a_2 S_1)^{N_P} \frac{(a_2 S_1)^{N_0 - N_P} - 1}{a_2 S_1 - 1} \right]. \tag{12.8}$$

Here C_1, C_2, C_3, C_4—are constants for calculation of aperiodic currents; they were previously determined in Chap. 7;

$$S_1 = e^{2j\pi \frac{nb}{T}}; \quad S_2 = e^{2j\pi \frac{nb}{T}} - 1.$$

Complex amplitudes of additional field MMF $\Delta F_{CAG}(-n, \omega_{ROT})$ may be obtained from (12.8) while substituting n by $(-n)$.

12.4.2 MMF Harmonics and Fields of Asymmetrical Squirrel Cage (Three Adjacent Damaged Bars); Their Numbers Are: N = 0, N = 1, N = 2

The design expression for auxiliary current MMF:

$$\Delta F_{CAG}(-n, \omega_{ROT}) = \frac{1}{2j\pi n} S_2 \left\{ C_1 + C_2 a_1 S_1 + C_3 (a_1 S_1)^2 \frac{(a_1 S_1)^{N_0 - 2} - 1}{a_1 S_1 - 1} + C_4 (a_2 S_1)^2 \frac{(a_2 S_1)^{N_0 - 2} - 1}{a_2 S_1 - 1} \right\} \tag{12.9}$$

Here C_1, C_2, C_3, C_4—are constants for the calculation of auxiliary currents; which were previously determined in Chap. 10.

Complex amplitudes of additional field MMF $\Delta F_{CAG}(-n, \omega_{ROT})$ may be obtained from (12.9) while substituting n by (−n).

12.4.3 MMF Harmonics and Fields of Asymmetrical Squirrel Cage (Three Damaged Bars: Two Are Adjacent, the Third Is Next Nearest; Their Numbers Are: N = 0, N = 2, N = 3)

The design expression for auxiliary current MMF:

$$\Delta F_{CAG}(n, \omega_{ROT}) = \frac{1}{2j\pi n} S_2 \left\{ C_1 (1 + a_1 S_1) + C_2 (1 + a_2 S_1) + C_3 S_1^2 + C_4 (a_2 S_1)^3 \frac{(a_1 S_1)^{N_0 - 3} - 1}{a_1 S_1 - 1} + C_5 (a_2 S_1)^3 \frac{(a_2 S_1)^{N_0 - 3} - 1}{a_2 S_1 - 1} \right\}. \tag{12.10}$$

Here C_1, C_2, C_3, C_4, C_5—are constants for calculation of auxiliary currents; they were previously determined in Chap. 10.

Complex amplitudes of additional field MMF $\Delta F_{CAG}(-n, \omega_{ROT})$ may be obtained from (12.10) while substituting n by (−n).

12.4.4 MMF Harmonics and Fields of Asymmetrical Squirrel Cage (Three Damaged Non-adjacent Bars); They Numbers Are: N = 0, N = N_{P2}, N = N_{P3}

The design expression for auxiliary current MMF:

$$\Delta F_{CAG}(n,\omega_{ROT}) = \frac{1}{2j\pi n} S_2 \left\{ C_1 \frac{(a_1 S_1)^{N_{P_2}} - 1}{a_1 S_1 - 1} + C_2 \frac{(a_2 S_1)^{N_{P_2}} - 1}{a_2 S_1 - 1} \right.$$
$$+ C_3 (a_1 S_1)^{N_{P_2}} \frac{(a_1 S_1)^{N_{P_3} - N_{P_2}} - 1}{a_1 S_1 - 1} + C_4 (a_2 S_1)^{N_{P_2}} \frac{(a_2 S_1)^{N_{P_3} - N_{P_2}} - 1}{a_2 S_1 - 1}$$
$$\left. + C_5 (a_1 S_1)^{N_{P_3}} \frac{(a_1 S_1)^{N_0 - N_{P_3}} - 1}{a_1 S_1 - 1} + C_6 (a_2 S_1)^{N_{P_3}} \frac{(a_2 S_1)^{N_0 - N_{P_3}} - 1}{a_2 S_1 - 1} \right\}. \tag{12.11}$$

Here $C_1, C_2, C_3, C_4, C_5, C_6$—are constants for calculation of aperiodic currents; they were previously determined in Chap. 10.

Complex amplitudes of additional field MMF $\Delta F_{CAG}(-n,\omega_{ROT})$ may be obtained from (12.11) while substituting n by (−n).

12.5 Harmonics of MMF and Fields of Symmetrical Squirrel Cage (Without Damages). Checking Results [9]

If there are no cage damages, currents in its elements change along the boring under the harmonic law. The expression for MMF calculation in squirrel cage without damages is known and is widely used in practice [3, 4]. Therefore, the purpose of this paragraph is the use of this known problem to check the developed method of determining MMF of irregular and asymmetrical rotor windings, to obtain calculation expressions for MMF of symmetrical cage as for special case; to formulate practical recommendations for the construction of symmetric squirrel cages following from them and to compare them with the known ones.

Let us use the expressions obtained in Chap. 8 for EMF and Eq. (12.7) for MMF and substitute in it expressions for periodic currents in short-circuited ring elements $(I_0, I_1, I_2, \ldots, I_{N_0-2})$. As a result, we have:

$$F_{CAG}(n,\omega_{ROT}) = \frac{I_0}{2j\pi n}\left(e^{2j\pi\frac{nb}{T}} - 1\right)\left[1 + e^{2j\pi\frac{(n-m)b}{T}}\right.$$
$$\left. + e^{2j\pi\frac{2(n-m)b}{T}} + e^{2j\pi\frac{3(n-m)b}{T}} + \cdots + e^{2j\pi\frac{(n-m)(T-2b)}{T}} + e^{2j\pi\frac{(n-m)(T-b)}{T}}\right]. \tag{12.12}$$

Here n—order of MMF harmonic and field of squirrel cage, m—stator fields.

MMF complex amplitudes of additional field $F_{CAG}(-n, \omega_{ROT})$ can be obtained from (12.12) by substitution of n by (−n).

Let us note as previously that terms of series in braces of Eq. (12.12) make a geometrical progression with common ratio of progression:

$$q_1 = e^{2j\pi\frac{b}{T}(n-m)}.$$

To draw practical conclusions from this ratio, let us find the sum of terms of geometrical progression in Eq. (12.12). As a result, we have:

$$F_{CAG}(n,\omega_{ROT}) = \frac{I_0}{2j\pi n}\left(e^{2j\pi\frac{b}{T}} - 1\right)\frac{1 - e^{2j\pi\frac{b(n-m)}{T}N_0}}{1 - e^{2j\pi\frac{b(n-m)}{T}}}. \qquad (12.12')$$

Let us note now that the factor in the numerator can be simplified:

$$q_2 = 1 - e^{2j\pi\frac{b(n-m)N_0}{T}} = 1 - e^{2j\pi(n-m)}, \text{ since}\frac{bN_0}{T} = 1.$$

Then expression for $F_{CAG}(n, \omega_{ROT})$ also becomes simpler:

$$F_{CAG}(n, \omega_{ROT}) = \frac{I_0}{2j\pi n}\left(e^{2j\pi\frac{nb}{T}} - 1\right)\frac{1 - e^{2j\pi(n-m)}}{1 - e^{2j\pi\frac{b(n-m)}{T}}}. \qquad (12.13)$$

Let us analyze the obtained expression $F_{CAG}(n, \omega_{ROT})$.

(a) Orders of harmonics of $|m| = |n|$. At such a ratio of spatial orders we obtain an uncertainty in Eq. (12.13) for MMF $F_{CAG}(n, \omega_{ROT})$ as both in the numerator and denominator expressions in braces are equal to zero. Expansion of uncertainty [7, 8] gives for amplitude of squirrel cage direct field at $|m| = |n|$:

$$F_{CAG}(n, \omega_{ROT}) = \frac{I_0}{2j\pi n}\left(e^{2j\pi\frac{nb}{T}} - 1\right)N_0. \qquad (12.14)$$

Let us compare this obtained expression with that for MMF amplitude of stator multiphase winding obtained in Chap. 3:

$$F_{ST,RES}(m_{EL}, Q) = \frac{m_{PH}K_Q I_1 W_{PH}K_W(m_{EL})}{\pi m_{EL}P}. \qquad (12.15)$$

Here $K_Q I_1$—amplitude of stator current Q time harmonic, m_{EL}—order of MMF spatial harmonic and stator field for expansion into harmonic series with period $T_{EL} = \frac{\pi D}{P}$; m_{PH}—number of winding phases, p—number of pole pairs, $W_{PH}, K_W(m_{EL})$—number of turns in winding phase and its winding factor for harmonic of m_{EL} order.

It can be applied also to MMF calculation in squirrel cage, as to winding with number of phases $m_{PH} = N_0$, $W_{PH} = 0.5$ and $K_W(m_{EL}) = 1$.

Let us turn our attention to Eq. (12.14) for $F_{CAG}(n, \omega_{ROT})$; Let us represent one of factors in the form:

$$S = e^{2j\pi\frac{nb}{T}} - 1 = \cos\frac{2\pi nb}{T} - 1 + j\sin\frac{2\pi nb}{T};$$

Therefore, its modulus:

$$|S| = 2\sin\frac{\pi nb}{T}. \tag{12.16}$$

This factor S is known in the theory of induction machines as "factor of reduction of currents in the ring to those in the bar" [3, 4], which determines the relationship between currents in short-circuited ring and bar: $|J_N| = |I_N||S|$. As a result of these transformations, we obtain identical expressions:

$$|F_{CAG}(n, \omega_{ROT})| = \left|F_{ST,RES}(m_{EL}, Q)\right|,$$

that proves validity of the obtained Eq. (12.14).

(b) Orders of harmonics $n - m \neq 0$, and $n - m \neq N_0$.

In this case as per (12.13) $F_{CAG}(n, \omega_{ROT}) = 0$ as in the numerator of this expression we obtain: $e^{2j\pi(n-m)} = 1$.

Let us consider in more detail inequality $n - m \neq N_0$. We divide both of its parts by number of pole pairs p, and as a result, we have: $n_{EL} \neq \frac{N_0}{P} + m_{EL}$.

In particular, complex amplitude $F_{CAG}(n, \omega_{ROT}) = 0$ for harmonics of MMF and rotor fields of order $n_{EL} \neq \frac{N_0}{P} + 1$ (at $m_{EL} = 1$ that represents the greatest practical interest [3, 4]). Therefore, in the air gap there are no rotor fields whose order is not equal to tooth one.

(c) Orders of harmonics $n = m + N_0$.

At such a ratio of spatial orders we obtain an uncertainty in Eq. (12.13) for MMF $F_{CAG}(n, \omega_{ROT})$ as both in the numerator and denominator both expressions in braces are equal to zero. Expansion of uncertainty [7, 8] gives:

$$F_{CAG}(n, \omega_{ROT}) = \frac{I_0}{2j\pi n}\left(e^{2j\pi\frac{nb}{T}} - 1\right)N_0 \neq 0. \tag{12.17}$$

The comparison of complex amplitudes (12.13) and (12.17) for harmonics of order $|m| = |n| = p$ and accordingly harmonics of order $n = N_0 + m$ confirms that in (12.17) it is n times less. In particular, at $m_{EL} = 1$ we obtain that currents in bars of symmetrical squirrel cage generate fields of higher harmonics, the most intensive of which have tooth order [3, 4]: $n_{EL} = \frac{N_0}{p} + 1$.

Let us analyze the obtained expression $F_{CAG}(-n, \omega_{ROT})$. To obtain the calculation expression for complex amplitude $F_{CAG}(-n, \omega_{ROT})$, it is necessary in (12.13) to substitute n order by (−n). Analysis of the expression $F_{CAG}(-n, \omega_{ROT})$ gives the results:

(d) Orders of harmonics $n + m \neq 0$, and $n - m \neq N_0$.

The result coincides with that in item b): $F_{CAG}(-n, \omega_{ROT}) = 0$.

(e) Orders of harmonics $n + m = N_0$.

The result coincides with that in item (c): $F_{CAG}(-n, \omega_{ROT}) \neq 0$.

The most intensive fields of higher rotor harmonics have tooth order: $n_{EL} = \frac{N_0}{P} - 1$.

The conclusions given here on properties of symmetrical squirrel cage are known [3, 4] and in addition prove the validity of the general calculation method for MMF of various short-circuited rotor winding structures.

12.6 MMF Harmonics of Irregular Damper Windings [9]

Chapter 9 provided the definition of such windings. The following versions of their construction are possible:

- on one or several poles there are damaged bars.
- on each pole there are one or several bars with various D.C. resistance, for example, there are bars both from copper, and from brass or bronze. These bars on each pole have identical position relative to its longitudinal axis.

12.6.1 First Construction Version of Irregular Damper Winding: Bars with Different Impedance Are Located Only on One or on Only Several Poles

The construction of such machine winding intended for nonlinear networks as it was already noted earlier, can practically appear due to defects in the process of production (low-quality soldering or welding in bar–short-circuited ring (segment) joint, at violations in the process of rotor installation, etc. For salient-pole motors, violations in the construction of damper winding arise in the operation usually during sharp load variation.

In such constructions, currents in damaged bars with identical numbers on adjacent poles differ not only in phase, but also in amplitude. In practice this last circumstance is externally (visually) particularly noticeable, when comparing heating level of damaged bars and those located near them.

In investigation of such irregular winding MMF for the expansion period as it was noted, it is necessary to select the value $T = \pi D$, where D—stator boring diameter [10].

Let us designate the number of bars on each of 2p poles, as usual, as N_0, so that the total number of rotor bars is equal to $N_0 2p$, and serial numbers of bars on each pole $N = 0, 1, 2, 3, \ldots, N_0 - 1$.

In order to represent damper winding of the class considered, let us use Fig. 6.3 again. We already used this figure in Chap. 6 when investigating regular passive recurrent circuits. Let us use it for representation of irregular windings. We consider that in each loop of this circuit there are EMFs, and that in this figure there are two poles; on one pole (C_p) are located bars $A_1A_1'; B_1, B_1'; \ldots; F_1, F_1', \ldots$, on the pole of opposite polarity (S_p)—bars $A_2A_2'; B_2, B_2'; \ldots; F_2, F_2', \ldots$, Segments $F_1A_2 = F_2A_1 = F_1'A_1' = F_2'A_1' = b_F$—distances between edge bars of adjacent poles. Let us superimpose cross axis (q) with point "0_1", so the segment $X_0 = \frac{b_F}{2}$. Positive direction, as usual, is accepted to be the direction towards bars $A_1A_1'; B_1, B_1'; \ldots..$

Let us consider two adjacent poles of such winding: one on pole with bars $A_1A_1'; B_1, B_1'; \ldots; F_1, F_1', \ldots$, and the second on pole with bars $A_2A_2'; B_2, B_2'; \ldots; F_2, F_2', \ldots$, Number of bars on each pole is equal to N_0, and their serial numbers, as well as earlier, $N = 0, 1, 2, \ldots, N_0 - 1$. We consider that in irregular damper winding of this type, the bar number N on pole number No. 2 is damaged.

We proceed to the mathematical formulation of the problem: We present MMF of this version of irregular damper winding structure in the form of step function (Table 12.2); for this purpose, we use the Ampere's law [1, 2], similar to the "general" construction of short-circuited windings in Table 12.1. Then, let us represent this step function of MMF in the form of several rotating waves.

Structures of Tables 12.1 and 12.2 are similar. The difference is that in Table 12.2 currents in bars of other poles are added; the number of poles in Table 12.2 is limited only by two. The algorithm of table formation for other poles with numbers 3, …, 2p becomes clear from its contents.

In the first column of Table 12.2 are specified serial numbers of pole and portion between symmetry axes of adjacent slots (step number) on this pole; within this portion the current function keeps its invariable value till meeting with an axis of the following slot (in the process of slot number increase), where it increases stepwise by the current value in this slot.

In the second column of Table 12.2 the extent of each step is specified; thus the following geometrical ratios are used as in Fig. 6.3:

$$A_1F_1 = (N_0 - 1)b; \quad A_1F_1 + b_F = O_1O_2 = \frac{T_{EL}}{2}. \qquad (12.18')$$

In the third column are specified values of current function $F_D(x)$ or MMF ("heights of steps under teeth of each pole") obtained based on the Amper's law.

Table 12.2 represents all necessary parameters for MMF investigation, for example, its harmonic analysis.

Table 12.2 MMF step function of irregular rotor damping winding (Fig. 8.1)

Pole no. 1:	Step extent	Function of current ("heights of steps under teeth") $F_D(x)$
Serial number of step (portion between adjacent slots) on pole no. 1	–	–
1	$\frac{b_F}{2} \le x \le \frac{b_F}{2} + b$	$J_0^{(1)}$
2	$\frac{b_F}{2} + b \le x \le \frac{b_F}{2} + 2b$	$J_0^{(1)} + J_1^{(1)}$
3	$\frac{b_F}{2} + 2b \le x \le \frac{b_F}{2} + 3b$	$J_0^{(1)} + J_1^{(1)} + J_2^{(1)}$
4	$\frac{b_F}{2} + 3b \le x \le \frac{b_F}{2} + 4b$	$J_0^{(1)} + J_1^{(1)} + J_2^{(1)} + J_3^{(1)}$
⋮	⋮	⋮
$N_0 - 1$	$\frac{b_F}{2} + (N_0 - 1)b \le x \le \frac{b_F}{2} + \frac{T_{EL}}{2}$	$J_0^{(1)} + J_1^{(1)} + \cdots + J_{N_0-1}^{(1)} = I_{N_0-1}^{(1)} - I_{(-1)}^{(1)}$
Pole no. 2:		
Serial number of step (portion between adjacent slots) on pole no. 2	–	–
1	$\frac{b_F}{2} + \frac{T_{EL}}{2} \le x \le \frac{b_F}{2} + \frac{T_{EL}}{2} + b$	$J_0^{(2)} + I_{N_0-1}^{(1)} - I_{(-1)}^{(1)}$
2	$\frac{b_F}{2} + \frac{T_{EL}}{2} + b \le x \le \frac{b_F}{2} + \frac{T_{EL}}{2} + 2b$	$J_0^{(2)} + J_1^{(2)} + I_{N_0-1}^{(1)} - I_{(-1)}^{(1)}$
3	$\frac{b_F}{2} + \frac{T_{EL}}{2} + 2b \le x \le \frac{b_F}{2} + \frac{T_{EL}}{2} + 3b$	$J_0^{(2)} + J_1^{(2)} + J_2^{(2)} + I_{N_0-1}^{(1)} - I_{(-1)}^{(1)}$
4	$\frac{b_F}{2} + \frac{T_{EL}}{2} + 3b \le x \le \frac{b_F}{2} + \frac{T_{EL}}{2} + 4b$	$J_0^{(2)} + J_1^{(2)} + J_2^{(2)} + J_3^{(2)} + I_{N_0-1}^{(1)} - I_{(-1)}^{(1)}$
⋮	⋮	⋮
$N_0 - 1$	$\frac{b_F}{2} + \frac{T_{EL}}{2} + (N_0 - 1)b \le < x \le \frac{b_F}{2} + T_{EL}$	$J_0^{(2)} + J_1^{(2)} + \cdots + J_{N_0-2}^{(2)} + I_{N_0-1}^{(1)} - I_{(-1)}^{(1)}$

However, as previously, we performed simple mathematical transformations over current function ("heights of steps under each tooth") as it was already made for the general case of short-circuited windings earlier. For this purpose, one transforms current functions of each step, using the first Kirchhoff's law [1, 2].

As a result, we obtain expressions for current function $F_D(x)$ in the form.

$$\begin{aligned}
&\text{For pole No.1}: \\
&\text{For step 1}: F_D(x) = I_0^{(1)} - I_{(-1)}^{(1)}. \\
&\text{For step 2}: F_D(x) = I_1^{(1)} - I_{(-1)}^{(1)}. \\
&\text{For step 3}: F_D(x) = I_2^{(1)} - I_{(-1)}^{(1)}. \\
&\text{For step 4}: F_D(x) = I_3^{(1)} - I_{(-1)}^{(1)}. \\
&\qquad\vdots \\
&\text{For step } N_0 - 1: F_D(x) = I_{N_0-2}^{(1)} - I_{(-1)}^{(1)}.
\end{aligned} \tag{12.18}$$

For pole No. 2 expressions for currents in bars and current functions $F_D(x)$ are determined similarly.

In Table 12.2 and in Eq. (12.18) upper indices at currents in bars and ring portions indicate the pole number. The current $I^{(1)}_{(-1)}$ corresponds to that in the ring with number $N_0 - 1 (N = 0, 1, \ldots, N_0 - 1)$ on the pole with number equal to 2p (that is, to the current in the last ring of the last pole); for simplicity, it is supplied with index (–1); in further calculations this current is not necessary to use.

Let us present MMF of step form (step function) in the form of several rotating waves. For this purpose, we use the expansion of step function into harmonic series (Fourier); for pole No. 1 it is determined as:

$$F_D(n, \omega_{ROT}) = \frac{1}{T}\int_0^T F_D(x) e^{2j\pi\frac{nx}{T}} dx = \frac{I_0^{(1)}}{T}\int_{\frac{b_F}{2}}^{\frac{b_F+b}{2}} e^{2j\pi\frac{nx}{T}} dx + \frac{I_1^{(1)}}{T}\int_{\frac{b_F}{2}+b}^{\frac{b_F}{2}+2b} e^{2j\pi\frac{nx}{T}} dx + \frac{I_2^{(1)}}{T}\int_{\frac{b_F}{2}+b}^{\frac{b_F}{2}+3b} e^{2j\pi\frac{nx}{T}} dx + \frac{I_3^{(1)}}{T}\int_{\frac{b_F}{2}+3b}^{\frac{b_F}{2}+4b} e^{2j\pi\frac{nx}{T}} dx + \cdots + \frac{I_{N_0-1}^{(1)}}{T}\int_{\frac{b_F}{2}+(N_0-1)b}^{\frac{b_F+T_{EL}}{2}} e^{2j\pi\frac{nx}{T}} dx + \cdots + . \quad (12.19)$$

For poles with numbers 2, 3, …, 2p, summands of this series are determined similarly.

In Eq. (12.19) we will not substitute the upper and lower limits for each step into the exponential function $e^{2j\pi\frac{nx}{T}}$: Results of such substitution are obvious in this step function, as well as in the step function given in Table 12.1. It is made further in the derivation of calculation expressions for MMF of some specific constructions of damper winding used in practice.

12.6.2 Second Construction Version of Irregular Damper Winding: Bars with Various Impedances Are Located on Each Pole; They Occupy Identical Position on Each Pole Relative to Its Longitudinal Axis

In this paragraph, we investigate MMF of one more class of irregular damper windings. An example of such irregular winding is the damper winding of motor briefly described in the previous chapter.

Let us use Fig. 6.3 again. We present by means of this figure irregular damper winding with asymmetrical bar number N_P on each pole. Let us superimpose, as before, cross axis (q) with point "O_1", so that as before, the segment $x_0 = \frac{b_F}{2}$. We consider methods of MMF determination of this short-circuited rotor winding.

Irregular damper winding of this type has the following differences from the damper winding considered in para 12.6.1:

- for the investigation of its MMF it is sufficient to select as the period $T_{EL} = \pi\frac{D}{p}$ or $\frac{T_{EL}}{2} = \tau$;
- on each pole of this winding the bar with different impedance has the same position, that is, N_P = idem, for example,—middle;
- respectively, currents in winding elements in adjacent poles with identical serial numbers N = idem. are equal in amplitude and opposite in sign. For example, for bars with numbers N = 2 on adjacent poles the following is true: $\underline{I}_2^{S_p} = -\underline{I}_2^{C_p}$.

Method 1. Within this method, let us use calculation expressions for complex amplitudes obtained earlier in this chapter for arbitrary structure of short-circuited winding and for its special case—irregular damper winding with bars of different impedance located only on one or only on several poles (para 12.6.1). According to Eqs. (12.6) and (12.19) we have:

$$\begin{aligned}
F_D(n_{EL},\omega_{ROT}) = \frac{1}{2j\pi n_{EL}}\Bigg\{&\left[I_0\left(e^{2j\pi n_{EL}\frac{0.5b_F+b}{T_{EL}}} - e^{2j\pi n_{EL}\frac{0.5b_F}{T_{EL}}}\right)\right]\\
&+ I_1\left(e^{2j\pi n_{EL}\frac{0.5b_F+2b}{T_{EL}}} - e^{2j\pi n_{EL}\frac{0.5b_F+b}{T_{EL}}}\right) + I_2\left(e^{2j\pi n_{EL}\frac{0.5b_F+3b}{T_{EL}}} - e^{2j\pi n_{EL}\frac{0.5b_F+2b}{T_{EL}}}\right)\\
&+ \cdots + I_{N_0-1}\left[e^{2j\pi n_{EL}\frac{0.5(b_F+T_{EL})}{T_{EL}}} - e^{2j\pi n_{EL}\frac{0.5b_F+(N_0-1)b}{T_{EL}}}\right]\Bigg\}\\
&+ \frac{1}{2j\pi n_{EL}}\Bigg\{I_0'\left[e^{2j\pi n_{EL}\frac{0.5b_F+0.5T_{EL}+b}{T_{EL}}} - e2j\pi n_{EL}^{\frac{0.5(b_F+T_{EL})}{T_{EL}}}\right]\\
&+ I_1'\left(e^{2j\pi n_{EL}\frac{0.5b_F+0.5T_{EL}+2b}{T_{EL}}} - e^{2j\pi n_{EL}\frac{0.5b_F+0.5T_{EL}+b}{T_{EL}}}\right)\\
&+ I_2'\left(e^{2j\pi n_{EL}\frac{0.5b_F+0.5T_{EL}+3b}{T_{EL}}} - e^{2j\pi n_{EL}\frac{0.5b_F+0.5T_{EL}+2b}{T_{EL}}}\right)\\
&+ \cdots + I_{N_0-1}'\left[e^{2j\pi n_{EL}\frac{b_F+0.5T_{EL}+(N_0-1)b}{T_{EL}}} - e^{2j\pi n_{EL}\frac{0.5b_F+0.5T_{EL}+(N_0-1)b}{T_{EL}}}\right]\Bigg\}.
\end{aligned} \tag{12.20′}$$

Here, $I_0, I_1, I_2, \ldots, I_{N_0-1}; I_0' = -I_0; I_1' = -I_1; I_2' = -I_2; \ldots; I_{N_0-1}' = -I_{N_0-1}$—currents in elements of short-circuited rings (segments) of adjacent poles. By means of these ratios between currents and geometrical ratios (12.18′), Eq. (12.20′) can be simplified a little.

MMF complex amplitudes of additional field $F_{AD}(-n_{EL},\omega_{ROT})$ can be obtained from (12.20′) by substitution of n by $(-n_{EL})$.

Method 2. The investigated class of irregular damper winding allows us to realize one more method of determination of MMF complex amplitudes.

To represent the damper winding of the class considered, let us use Fig. 6.3 again. Let us use the peculiarity of currents distribution, noted already, in such winding: currents in winding elements in adjacent poles with identical serial numbers are equal in amplitude and are opposite in sign. Taking into account this regularity we obtain that MMF step distribution curve can be determined differently from that made earlier in previous method. It can be obtained also in the form of number of rectangles of identical width; for example, the first of them formed by currents $J_1^{S_p}$ and $J_1^{C_p}$ has a width $A_1A_2 = \frac{T_{EL}}{2}$, where T_{EL}—period of EMF and MMF: $T_{EL} = \frac{\pi D}{p}$. The same is also true for other MMF steps formed by currents $J_2^{S_p}$ and $J_2^{C_p}; J_2^{S_p}$ and $J_3^{C_p}; \ldots J_{N_0-1}^{S_p}$ and $J_{N_0-1}^{C_p}$. The similar method is usually used in the analysis of turbogenerator rotor winding MMF. It is reduced to the analysis of several rectangles whose number is equal to that of coils on rotor pole. Let us note, however, that in steady-state operation mode the turbogenerator excitation current—is D.C. current so it is not necessary to present MMF of its rotor in the form of several rotating waves in complex plane.

We write down an expression for complex amplitudes of direct and additional MMF waves of irregular damper winding of this class:

$$F_D(n_{EL}, \omega_{ROT}) = \frac{J_0}{T_{EL}} \int_{\frac{b_F}{2}}^{\frac{b_F}{2}+\frac{T_{EL}}{2}} e^{2j\pi\frac{n_{EL}x}{T_{EL}}}dx + \frac{J_1}{T_{EL}} \int_{\frac{b_F}{2}+b}^{\frac{b_F}{2}+b+\frac{T_{EL}}{2}} e^{2j\pi\frac{n_{EL}x}{T_{EL}}}dx + \frac{J_2}{T_{EL}} \int_{\frac{b_F}{2}+2b}^{\frac{b_F}{2}+2b+\frac{T_{EL}}{2}} e^{2j\pi\frac{n_{EL}x}{T_{EL}}}dx + \cdots + \frac{J_{N_0-1}}{T_{EL}} \int_{\frac{b_F}{2}+b(N_0-1)}^{\frac{b_F}{2}+b(N_0-1)+\frac{T_{EL}}{2}} e^{2j\pi\frac{n_{EL}x}{T_{EL}}}dx. \tag{12.20}$$

Here b—portion between axes of adjacent bars on pole. Let us transform the expression for $F_D(n, \omega_{ROT})$:

$$F_D(n_{EL}, \omega_{ROT}) = -\frac{e^{j\pi\frac{n_{EL}b_F}{T_{EL}}}}{j\pi n_{EL}}\left[J_0 + J_1 e^{2j\pi\frac{n_{EL}b}{T_{EL}}} + J_2 e^{2j\pi\frac{2n_{EL}b}{T_{EL}}} + \cdots + J_{N_0-1} e^{2j\pi\frac{n_{EL}(N_0-1)b}{T_{EL}}}\right]. \tag{12.21}$$

MMF complex amplitudes of additional field $F_D(-n_{EL}, \omega_{ROT})$, can be obtained from (12.21) replacing n_{EL} by $-n_{EL}$.

12.7 MMF Harmonics of Regular Damper Windings [9]

Analytical expressions for currents in bars of this winding are obtained in Chap. 9:

$$J_{(N)} = C_0 a_0^N \left(1 - a_0^{-1}\right) + C_1 a_1^N (1 - a_2) + C_2 a_2^N (1 - a_1). \tag{12.22}$$

Here $C_0 = \frac{E_M}{Z_B K_B}$, $a_0 = e^{-j\Delta\varphi}$, $\Delta\varphi = 2\pi n_{EL} \frac{b}{T_{EL}}$; expressions for calculation of coefficients a_1 and a_2 are given in (6.12): $a_{1,2} = \frac{2+\sigma \pm \sqrt{\sigma^2+4\sigma}}{2}$; $\sigma = 2\frac{Z_R}{Z_B}$.

Let us transform the obtained Eq. (12.21) for MMF taking into account a change of currents in bars according to (12.22).

$$F_D(n_{EL}, \omega_{ROT}) = \sum \frac{-C_K}{j\pi n_{EL}} e^{j\pi n_{EL} \frac{b_F}{T_{EL}}} (a_K - 1) a_K^{-1} \left[1 + a_K e^{2j\pi n_{EL} \frac{b}{T_{EL}}} + a_K^2 e^{2j\pi n_{EL} \frac{b}{T_{EL}}} + a_K^3 e^{2j\pi n_{EL} \frac{3b}{T_{EL}}} + \cdots + a_K^{N_0 - 1} e^{2j\pi n_{EL} (N_0 - 1) \frac{b_F}{T_{EL}}}\right].$$

Here, summation is made over the parameter (K), and it accepts values: K = 0, 1, 2, for example, for coefficients a_K we have: $a_K \in \{a_0, a_1, a_2\}$. The expression in braces is geometrical progression with common ratio: $q = a_K e^{2j\pi n_{EL} \frac{b}{T_{EL}}}$. Let us find its sum; then the complex amplitude $F_D(n_{EL}, \omega_{ROT})$ takes the form:

$$F_D(n_{EL}, \omega_{ROT}) = \sum \frac{-C_K}{j\pi n_{EL}} e^{j\pi n_{EL} \frac{b_F}{T_{EL}}} (a_K - 1) a_K^{-1} \frac{1 - \left(a_K e^{2j\pi n_{EL} \frac{b}{T_{EL}}}\right)^{N_0}}{1 - a_K e^{2j\pi n_{EL} \frac{b}{T_{EL}}}}. \tag{12.23}$$

Here summation is also made over the parameter (K) which accepts the same values: K = 0, 1, 2.

The expression for complex amplitude $F_D(-n_{EL}, \omega_{ROT})$ is obtained from $F_D(n_{EL}, \omega_{ROT})$ by replacement (n_{EL}) by $(-n_{EL})$.

From analysis of the obtained expressions, it follows that:

- for a harmonic component of current in rotor bars which in Eq. (12.22) is equal to the summand $C_0 a_0^N \left(1 - a_0^{-1}\right)$, conclusions obtained in MMF analysis of squirrel cage remain true.
- aperiodic components do not allow us to draw any general conclusions on the influence of rotor and stator harmonics order on MMF complex amplitudes: their dependence on the ratio of impedance $\sigma = \frac{2Z_R}{Z_B}$ (also dependence on coefficients a_1, a_2) is non-linear. These conclusions are influenced also by the ratio of amplitudes C_0, C_1, C_2 included in (12.22).

12.8 MMF Harmonics of Excitation Winding of Salient-Pole Machine and Screen on Polar Shoe [9]

12.8.1 MMF Harmonics of Excitation Winding

Then, we find a calculation expression for MMF harmonics of excitation winding located on salient-pole machine rotor. In its loop, the resulting flux in gap induces EMF of the same frequency as in damper winding.

At stationary operating mode in a nonlinear network the excitation winding is constantly closed on the exciter impedance. In this mode, EMFs of several frequencies determined by orders of time and spatial harmonics of stator winding currents field are induced in this winding. These EMFs and corresponding currents in excitation winding are invariable within the entire period of machine operation.

Excitation current is equal to,

$$I_{EX} = |I_{EX}|e^{j\omega_{ROT}t}. \tag{12.24}$$

Here I_{EX}—complex amplitude of current with frequency ω_{ROT} of excitation winding, the calculation expression for current I_{EX} was given in Chap. 8.

Let us obtain an expression for MMF on spatial coordinate φ into harmonic series in complex form. The expansion period is taken equal to T_{EL}, and we locate the axis of angles origin φ fixed in space. Let the cross axis q coincide with the reference origin of angles $(\varphi = 0)$.

Mathematical statement of harmonic series was provided earlier:

$$F_{EX}(\varphi, n_{EX}) = F_{EX}^{DIR}(n_{EX}, \omega_{ROT})e^{-j\varphi n_{BX}} + F_{EX}^{AD}(n_{EX}, \omega_{ROT})e^{-j\varphi n_{BX}}. \tag{12.25}$$

Here $F_{EX}^{DIR}(n_{EX}, \omega_{ROT}) = \frac{2}{\pi n_{EX}} jI_{EX}W_{EX}\sin\frac{\pi n_{EX}\alpha}{2}\sin\frac{\pi n_{EX}}{2}$,

n_{EX}—order of spatial harmonic of excitation winding MMF. To obtain the calculation expression for F_{EX}^{AD}, it is necessary in (12.25) to replace n_{EX} by $(-n_{EX})$; as a result we obtain:

$$F_{EX}^{AD}(n_{EX}, \omega_{ROT}) = -F_{EX}^{DIR}(n_{EX}, \omega_{ROT}). \tag{12.26}$$

In further statement we designate complex amplitude $F_{EX}^{DIR}(n_{EX}, \omega_{ROT})$ for simplification as $F_{EX}(n, \omega_{ROT})$, that is without upper index "DIR", and complex amplitude $F_{EX}^{AD}(n_{EX}, \omega_{ROT})$ as: $F_{EX}(-n_{EX}, \omega_{ROT})$.

Let us note that this ratio is true regardless of whether we calculate field MMF characterized by sign S = 1 or sign S = 2; these signs characterize the direction of field rotation in the gap and were given in Chap. 3.

12.8.2 MMF Harmonics of Screen on Pole Shoe of Low-Speed Frequency Controlled Motor

Appendix 4.1 gave main advantages of damper winding construction in the form of screen of motor with large shaft torque in comparison with usual construction of damper winding in low speed salient-pole machines. There is stated the calculation method of currents induced in it by the resulting field in the air gap [10–13].

These currents for each screen point are obtained in the form of two components determined by the type of selected calculation grid: regular or irregular. Let us consider for clarity of problem solution peculiarities of MMF calculation for regular grid in Fig. 4.1.

For MMF calculation we need to have on the periphery of the screen (on X axis) the current component coinciding in the direction with machine rotation axis (Y axis). According to Fig. 4.1 these components are:

- for screen segment FC: $I_{FE}, I_{ED}, \ldots, I_{DC}$;
- for screen segment GS: $I_{GV}, I_{VT}, \ldots, I_{TS}$;
- for screen segment HR: $I_{HW}, I_{WU}, \ldots, I_{UR}$;
- for screen segment KQ: $I_{KZ}, I_{ZP}, \ldots, I_{PQ}$.

Peculiarity of the distribution of these components within this problem consists in the fact that currents along the machine rotation axis are distributed under the certain law [12], and in the middle part (in zone DPZED) they are higher than in face zones (CQPDC) and (EZKFE). Hence, for strict solution of this problem it is necessary to determine the screen MMF, with considering the distribution of currents in it along both coordinates (X, Y). For an approximate solution, we will reduce the problem of MMF calculation to one-dimensional; Let us determine average values of currents $\left(N_D = \frac{FC}{FE}\right)$:

for screen segment FC: $I_{FC} = \frac{I_{FE} + I_{ED} + \cdots + I_{DC}}{N_D}$;

for screen segment GS: $I_{GS} = \frac{I_{GV} + I_{VT} + \cdots + I_{TS}}{N_D}$;

for screen segment HR: $I_{FC} = \frac{I_{HW} + I_{WU} + \cdots + I_{UR}}{N_D}$;

Now it is possible to fill in Table 12.3 similar to Table 12.1 of para 12.2 and to use the general method of MMF calculation stated in para 12.3 ($N_R = FK/FG$).

Appendix 12.1: Accounting the Finite Width of Rotor Slots in the Calculation of Damper Winding MMF (Regular and Irregular) or Squirrel Cage (Symmetrical and Asymmetrical)

Figure 12.1 represents an example of MMF distribution in rotor slots. Numbers of slots with currents $J_1, J_2, J_3, \ldots, J_N, \ldots$ are designated respectively as 1;2;3; …; N. Generally, currents are not equal in amplitude and are shifted in time by some phase angles not equal to each other ($\varphi_1 \neq \varphi_2 \neq \varphi_3 \neq \cdots \neq \varphi_6$). Therefore, MMF distribution diagram in Fig. 12.1 has only qualitative character; actually, currents in slots are complex, but not real values, therefore, to represent MMF distribution diagram reflecting its quantitative variation along the boring the following is required:

- to consider the current phase angle in the bar of each N_0 slot;
- to represent the distribution diagram separately for its real and imaginary part of this current.

However, it is not required for illustrating a method of accounting the finite slot width because we apply a symbolic method for representing currents.

Let us use the general method stated in para 12.3; Let us find the complex amplitude C(−n), using the ratio (12.4). It is convenient to superimpose the origin of coordinates with the side of the first slot.

One proceeds to the mathematical statement of this general problem: We represent MMF of rotor short-circuited winding with account of the finite slot width in the form of step function, similar to Table 12.1. Then, using the ratios (12.4), it is easy to represent it in the form of several rotating waves. For calculation of separate steps we will determine, as previously, the concept of slot current estimated density: $S_N = \frac{J_N}{b_{SLT}h}$; here J_N, b_{SLT}, h respectively, current amplitude of N^{th} slot, its width

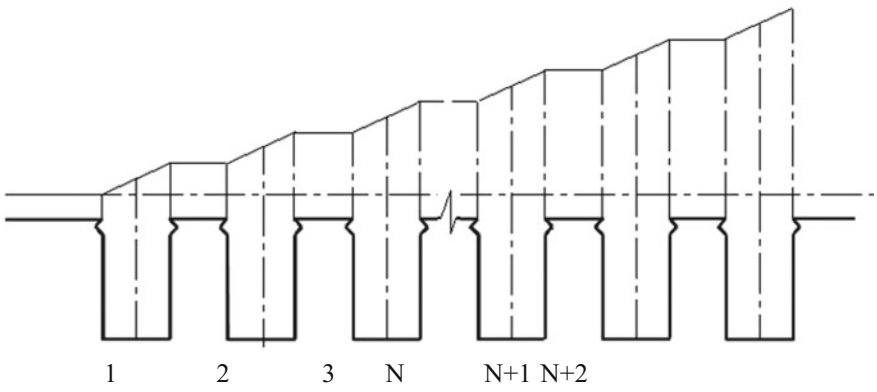

Fig. 12.1 MMF distribution diagram with account of finite width of slots

Table 12.3 MMF step function of pole screen

Designation of step (screen portion along X axis)	Step extent	Function of current ("heights of steps on screen portion") $F_{SCR}(x)$
FG	$0 < x \leq \Delta X$	I_{FC}
GH	$0X < x \leq 2\Delta X$	$I_{FC} + I_{GS}$
HK	$(N_R - 1)\Delta X < x \leq N_R \Delta X$	$I_{FC} + I_{GS} + I_{HR}$
⋮	⋮	⋮

Table 12.4 MMF step function of short-circuited rotor winding with account of finite slot width (Fig. 12.1)

Serial number of step (portion between adjacent slots)	Step extent	Function of current ("heights of steps under teeth") $F_{SCR}(x)$
1	$0 \leq x < b_{SLT}$	$J_1(x) = S_1 hx$
2	$b_{SLT} \leq x < t_{SLT}$	J_1
3	$t_{SLT} \leq x < t_{SLT} + b_{SLT}$	$J_1 + J_2(x) = J_1 + S_2 hx$
4	$t_{SLT} + b_{SLT} \leq 2t_{SLT}$	$J_1 + J_2$
5	$2t_{SLT} \leq x < 2t_{SLT} + b_{SLT}$	$J_1 + J_2 + J_3(x) = J_1 + J_2 + S_3 hx$

and height. We will designate the slot pitch as t_{SLT}. By means of this calculation current density, it is easy to calculate the current function of separate steps.

Table 12.4 represents all necessary parameters for MMF investigation, including its harmonic analysis.

Brief Conclusions

1. Investigation methods of damper winding, squirrel cages and excitation winding MMFs are based on representation of periodic (with T period $= \pi D$) distribution curve of current load in the form of harmonic series in complex plane. Thus, it is convenient to present currents in these windings in the form of time dependent complexes.
2. As a result of such representation, the expressions for rotor MMF complex amplitudes acquire a simple physical sense: they correspond to two components of rotor field in the air gap, which differ in amplitude and rotate relative to the rotor in opposite directions. It allows one to develop a general method of MMF investigation for the whole class of short-circuited rotor windings of A.C. machines without restrictions in their construction (for example, for irregular and regular damper winding, asymmetrical squirrel cages).
3. By means of this general method, calculation expressions for MMF complex amplitudes are obtained:

- irregular and regular damper windings;
- asymmetrical squirrel cage (general problem);
- asymmetrical squirrel cage with one damaged bar;
- asymmetrical squirrel cage with three adjacent damaged bars;
- asymmetrical squirrel cage with three damaged bars; two bars nearby, the third—next but one.
- asymmetrical squirrel cage with three damaged bars; three bars, not adjacent.
- squirrel cage without damages;
- excitation winding of salient pole machine;
- electromagnetic screen on pole of high-power low-speed frequency controlled motor.

Analysis of obtained calculation expressions validated the results.

List of symbols

b	Pitch between axes of adjacent bars of short-circuited rotor winding;
$b(x, t)$	Flux density instantaneous values of resulting field in air gap;
b_{SLT}, h	Width and height of rectangular slot;
b_F	Distance between axes of edge bars on adjacent poles $\left(\frac{b_F}{b} > 1\right)$;
b_{OP}, t_{SLT}	Opening width in slot and slot pitch;
$C_1, C_2, C_3, C_4, \ldots$	Constants for calculation of additional currents caused by asymmetry (damage) of squirrel cage;
$C(-n)$, $C(n)$	MMF harmonic amplitudes of n order in expanding step current function $F_{ROT}(x)$;
D	Stator boring diameter;
$F_{ST}(m, Q), F_{ST}(-m, Q)$	MMF harmonic amplitudes of order m corresponding to currents in stator winding of time order Q;
$F_{ROT}(n, \omega_{ROT})$, $F_{ROT}(-n, \omega_{ROT})$	Harmonic amplitudes of spatial order n of direct and additional fields of MMF corresponding to rotor currents with frequency ω_{ROT};
$\underline{F}_{RES,CAG}(n, \omega_{ROT})$, $F_{CAG}(n, \omega_{ROT})$, $\Delta F_{CAG}(n, \omega_{ROT})$	Harmonic amplitude of direct field of order n of MMF of asymmetrical (with damage) squirrel cage, corresponding to resulting current in bars, to the main current of symmetrical cage and additional current, caused by asymmetry (damage) of cage;

$\underline{F}_{RES,CAG}(-n, \omega_{ROT}), F_{CAG}(-n, \omega_{ROT}), \Delta F_{CAG}(-n, \omega_{ROT})$	The same for harmonics of additional field;
$F_{ROT}(x)$	Current function of short-circuited rotor winding, dependence of MMF from on spatial coordinate x along the boring periphery ("MMF step heights under teeth");
$f_{ROT}(x, t)$	Instantaneous values of step function rotor currents
$F_D(x)$	Similar to $F_{ROT}(x)$, but for damper winding MMF;
$F_D(n, \omega_{ROT}), F_D(-n, \omega_{ROT})$	Similar $F_{ROT}(n, \omega_{ROT})$, $F_{ROT}(-n, \omega_{ROT})$, but for damper winding MMF;
$F_{EX}(n, \omega_{ROT}), F_{EX}(-n, \omega_{ROT})$	Similar $F_{ROT}(n, \omega_{ROT})$, $F_{ROT}(-n, \omega_{ROT})$, but for excitation winding MMF;
$F_{SCR}(x)$	Similar to $F_{ROT}(x)$, but for screen on pole;
I_N, J_N	Currents in ring portions (segments) and damper winding bars;
L_{COR}	Active length of stator core;
N	Bar number of short-circuited rotor winding;
n	Number of spatial harmonic of rotor MMF;
N_0	Number of bars of damper winding per pole (squirrel cage on rotor);
p	Number of machine pole pairs;
q_B	Section of damper winding bar;
q_R	Section of ring (segment) between poles;
S_N	Calculation current density in bar with number N;
t	Time
T	Expansion period of MMF and mutual induction flux;
t_S	Slot pitch;
$V_{ROT,1}, V_{ROT,2}$	Linear speeds of direct and additional harmonic field of order n;
$W_{PH}, K_W(m_{EL})$	Number of turns in stator winding phase and its winding factor for harmonic of order m_{EL};
x	Coordinate along stator boring (in tangential direction);
$x_{1,0}; x_{2,1}; \ldots; x_{N,N-1}$	Distance between axes of adjacent bars;
x_0	Distance from the origin of coordinates to axis of the rotor first slot (bar);
δ	Air gap;
$\Delta\varphi$	Phase angle of EMF between two adjacent loops of short-circuited rotor winding;

τ	Pole pitch;
ω_{ROT}	Frequency of EMF and current in rotor loops;
$\Delta\varphi$	Phase angle of EMF between two adjacent loops of short-circuited rotor winding.

References

I. Monographs, Textbooks

1. Demirchyan K.S., Neyman L.R., Korovkin N.V., Theoretical Electrical Engineering. Moscow, St. Petersburg: Piter, 2009. Vol. 1, 2. (In Russian).
2. Kuepfmueller K., Kohn G., Theoretische Elektrotechnik und Elektronik. 15 Aufl., Berlin, New York: Springer. 2000. (In German).
3. Richter R., Elektrische Maschinen. Berlin: Springer. Band I, 1924; Band II, 1930; Band III, 1932; Band IV, 1936; Band V, 1950. (In German).
4. Mueller G., Ponick B., Elektrische Maschinen. New York, John Wiley, 2009. (In German).
5. Schuisky W., Berechnung elektrischer Maschinen. Wien: Springer, 1960. (In German).
6. Mueller G., Vogt, K., Ponick B., Berechnung elektrischer Maschinen. Springer, 2007. (In German).
7. Korn G., Korn T., Mathematical Handbook. New York: McGraw–Hill, 1961.
8. Jeffris H., Swirles B., Methods of Mathematical Physics. Third Edition, Vol. 1 – Vol. 3, Cambridge: Cambridge Univ. Press, 1966.
9. Boguslawsky I.Z., A.C. motors and generators. The theory and investigation methods by their operation in networks with non linear elements. Monograph. TU St.-Petersburg Edit., 2006. Vol. 1; Vol.2. (In Russian).

II. Synchronous Machines. Papers, Inventor's Certificates, Patents

10. Boguslawsky I.Z., Currents and harmonic MMFs in a damper winding with damaged bar at a pole. Power Eng. New York, 1985, № 1.
11. Boguslawsky I.Z., Demirtschyan K.S., Stationaere Stromverteilung in unregelmaessigen und unsymmetrischen kurzgeschlossenen Laeuferwicklungen von Wechselstrommaschinen. Archiv fuer Elektrotechnik, 1992. № 6. (In German).
12. Boguslawsky I.Z., Operating – regime currents of a salient – pole machine. Power Eng. (New York), 1982. № 4.
13. Boguslawsky I.Z., Currents and MMF in a conducting plate in the rotating field of a salient – pole machine. Power Eng. (New York), 1980. № 5.
14. Ferenc S., Pal C., Istvan S., Kaliekas asyncronderudes gyürüszakadaasak szamitages vizsgalata. Elektrotechnika (Hungary), 1982, № 1. (In Hungarian).
15. Polujadoff M., General rotating MMF – Theory of squirrel cage induction machines with non-uniform air gap and several non-sinusoidal distributed windings. Trans AIEE, PAS, 1982.

Chapter 13
Field Harmonics in Air Gap of A.C. Machine in Nonlinear Network

Chapter 13 presents investigation methods of field harmonics in A.C. machine air gap, when operating in nonlinear network. At non-sinusoidal power supply of A.C. machines it is convenient to obtain calculation expressions for rotor and stator field harmonics in air gap using a symbolic method of representation of MMF in the form of time complexes (phasors) in combination with a complex form of representation of harmonic series (Fourier). Thus, for induction machines, harmonic complex amplitudes of field induced by rotor windings in air gap in certain scale virtually repeat their MMF harmonics; the same refers to stator field harmonics.

As is obtained, unlike fields in air gap of salient-pole machines at sinusoidal power supply in nonlinear network, the fields created in air gap by MMF of stator windings, damper winding and rotor excitation winding have peculiarities: for each spatial harmonic in air gap there are two components, which rotate relative to the rotor in the opposite direction.

Rotation speeds of time and spatial harmonic fields of rotor and stator currents are obtained.

Analysis of the obtained expressions for complex amplitudes (phasors) of field harmonics of stator and rotor windings as well as their rotation speeds in air gap allows us to define magnetically coupled loops in stator and rotor for a machine operating in nonlinear network. These are necessary to formulate a system of equations to determine currents and losses in these loops.

Results of investigation performed in this chapter generalize definition stages for magnetically coupled loops in A.C. machine rotor, when operating in nonlinear network.

The content of this chapter is development of the methods stated in [1–3, 13, 14].

I. Boguslawsky et al., *Large A.C. Machines*,
DOI 10.1007/978-4-431-56475-1_13

13.1 Problem Setting

Calculation expressions for MMF complex amplitudes (phasors) for non-sinusoidal power supply of A.C. machines were determined in the previous chapters: stator winding MMF with number of phases m_{PH}, MMF of regular and irregular damper winding and MMF of salient-pole machine excitation winding, MMF of induction machine asymmetrical and symmetric squirrel cage.

It was noted that MMF harmonics of stator and rotor windings with identical spatial period and equal angular speed ω_{BOR} relative to the stator in air gap, determine resulting mutual induction fields in air gap.

Fields in air gap excited by currents in each of listed loops are determined not only by MMF harmonics, but also by other factors: air gap form, saturation level of machine magnetic circuit, tooth zone geometry [3–6], etc. Investigation of fields, excited by rotor and stator windings MMF in machine operation modes, is the object of this chapter. We will solve this problem using the harmonic analysis of magnetic fluxes of mutual induction in air gap; thus, we will determine complex amplitudes (phasors), directions and rotation speeds of separate field harmonics depending on their time and spatial orders [3, 4, 6, 13–15].

For such investigation, it is convenient to use the method developed in concerning transient modes [7] of induction machines [method of rotating field, "Drehfeldtheorie" (in German [5, 8])]. It can be also applied to the investigation of steady-state modes of induction machines at non-sinusoidal power supply, herewith, squirrel cage can be either symmetrical or asymmetrical. Thus, it is not required to include any additional transformations.

However, it cannot be applied to the investigation of steady-state asynchronous modes of salient-pole machines [9] without additional transformations: previously, it was necessary to perform harmonic analysis of mutual induction magnetic fluxes in air gap caused by currents in excitation winding, armatures and damper winding, because magnetic resistances in air gap in longitudinal (d) and cross (q) axes in machines of this kind are different. The problem becomes even more difficult at investigation of steady-state synchronous modes of these machines at non-sinusoidal power supply.

13.2 Initial Data and Their Representation

When solving the problem, determining fields excited by currents in machine rotor and stator loops we accept as initial:

- complex amplitudes (phasors) of MMF harmonics of machine rotor and stator loops;
- equivalent air gap;

- rotor rotation speed (slip);
- number of machine poles 2p.

Let us consider at first some initial data in more detail.

13.2.1 Complex Amplitudes (Phasors) of MMF Harmonics of Machine Rotor and Stator Loops and Their Representation

Each MMF harmonic of order m of stator winding and n—of rotor at non-sinusoidal power supply is obtained for a general case—in the form of two components corresponding to two fields with opposite rotation direction.

Let us consider a small addition into designations of MMF rotor harmonics in this chapter. Let us assume that rotor MMF harmonics are generated by currents in its loops induced by the resulting mutual induction field; it is formed by stator MMF harmonics of order m and rotor MMF harmonics of order n under the condition: $|m| = |n|$. For usability of calculation expressions obtained in this chapter, it is expedient to take into account this order m in the designation of MMF complex amplitudes (phasors) of rotor harmonics, for example, $F_{ROT}(m, n, \omega_{ROT})$, $F_{ROT}(m, -n, \omega_{ROT})$. It additionally indicates the "origin" of currents in rotor loops, determining one or another MMF harmonic. Implicitly, such instruction is already present in calculation expressions for these currents: earlier we obtained expressions with calculation of EMF and currents in rotor loops of m order. However, for the discussion of obtained results in this chapter we need order m in an explicit form.

13.2.2 Equivalent Gap and Its Representation

(a) Induction machine. Air gap δ in machine boring of this type is constant, and we will accept it as equivalent gap δ_{EQ}:

$$\delta_{EQ} = \delta = \text{const.} \tag{13.1}$$

(b) Salient-pole synchronous machine. For this machine the air gap variation δ in the tangential direction along angular coordinate (over stator boring) is determined by the machine cross section. This function $\delta(\varphi)$ satisfies Table 13.1 $(-\pi \leq \varphi \leq \pi)$. In its formulation, it is supposed that the axis of angles origin coincides with rotor cross axis q.

Table 13.1 Variation of air gap $\delta(\varphi)$ of salient-pole machine along angular coordinate

Angular coordinate	Air gap $\delta(\varphi)$	Flux density
$-\pi \le \varphi \le -\pi\frac{1+\alpha}{2}$	$\delta(\varphi) \to \infty$	$B_W(\varphi) \approx 0$
$-\pi\frac{1+\alpha}{2} \le \varphi \le -\pi\frac{1-\alpha}{2}$	$\delta(\varphi) = \delta_{EQ}$	$B_W(\varphi) \neq 0$
$-\pi\frac{1-\alpha}{2} < \varphi \le \pi\frac{1-\alpha}{2}$	$\delta(\varphi) \to \infty$	$B_W(\varphi) \approx 0$
$\pi\frac{1-\alpha}{2} < \varphi \le \pi\frac{1+\alpha}{2}$	$\delta(\varphi) = \delta_{EQ}$	$B_W(\varphi) \neq 0$
$\pi\frac{1+\alpha}{2} < \varphi \le \pi$	$\delta(\varphi) \to \infty$	$B_W(\varphi) \approx 0$

Here α—relative pole width $(\alpha = b_p/\tau)$ where b_p—width of pole shoe, τ—pole pitch [3–5], $\varphi = \frac{2\pi x}{T}$; $B_W(\varphi)$—flux density in air gap in the range of values given in the corresponding line of Table 13.1.

As equivalent air gap δ_{EQ} we accept the following:

$$\delta_{EQ} = \delta_{MIN} + 0.33(\delta_{MAX} - \delta_{MIN}) = \text{const}; \tag{13.2}$$

this ratio for the calculation of equivalent gap δ_{EQ} under the pole shoe is usually accepted in design practice of salient-pole synchronous machines [3–5]; here $\delta_{MAX}, \delta_{MIN}$—maximum and minimum values of air gap under pole.

13.2.3 Rotor Rotation Speed and Slip S_{SL}

Let us represent the expression for slip corresponding to the first time and the first spatial harmonics of the field rotating in the same direction as rotor in the form [4, 6]: $S_{SL} = 1 - \frac{\omega_{REV} p}{\omega_1}$.

Similarly, for the same field rotating in the direction opposite to the direction of rotor rotation, slip S_{SL} is equal to [4, 6]: $S_{SL} = 1 + \frac{\omega_{REV} p}{\omega_1}$.

13.3 Calculation Method of Field Harmonics Excited by Rotor and Stator Winding MMFs

The distribution of magnetic flux density $B_W(\varphi)$ in air gap along the coordinate φ, generated by the stator or rotor winding can be calculated, proceeding from the distribution along this coordinate [1–3]:

- MMF of this winding $F_W(\varphi)$;
- air gap $\delta(\varphi)$:

$$B_W(\varphi) = \frac{\mu_0 F_W(\varphi)}{\delta(\varphi) k_{CAR} k_{SAT}}. \tag{13.3}$$

Here k_{CAR}—Carter's factor [3–6]; k_{SAT}—magnetic circuit saturation factor determined by the influence of resulting flux (mutual induction flux) in air gap. Let us note that the value of k_{CAR} is calculated usually for the mutual induction field determined by first spatial order; with growth of this order its value changes a little, but in practical calculations it is usually neglected. Similarly, k_{SAT} factor is calculated usually for the mutual induction field determined by the first time and first spatial orders; this value if necessary can be clarified by a method of iterations.

Values of flux density $B_W(\varphi)$ according to the ratio (13.3) are given in the last column of Table 13.1.

Let us find calculation expressions for fluxes of mutual induction in air gap excited by rotor and stator windings. For this purpose, it is convenient to use their representation as well as MMF, in the form of harmonic series in complex plane.

13.3.1 Induction Machines

(a) Harmonics of field excited by squirrel cage MMF.

For a machine of this type $\delta(\varphi) = \text{const} = \delta_{EQ}$, therefore each field harmonic in the air gap in certain scale is equal to squirrel cage MMF harmonic.

$$\begin{aligned} B_{ROT}(x, m, n, \omega_{ROT}) = \frac{\mu_0}{\delta_{EQ} k_{CAR} k_{SAT}} \Big[& F_{ROT}(m, n, \omega_{ROT}) e^{\frac{-2j\pi nx}{T}} \\ & + F_{ROT}(m, -n, \omega_{ROT}) e^{\frac{2j\pi nx}{T}} \Big]. \end{aligned} \tag{13.4}$$

Construction peculiarities of induction machine squirrel cage allow us to determine from the ratio (13.4) not only field harmonics with period T_{EL}, but also with period $T = pT_{EL}$, which appear as a result of rotor cage damages.

(b) Field harmonics excited by stator winding MMF.

As well as for squirrel cage field, for stator winding field each field harmonic in certain scale in air gap is equal to its MMF harmonic. With account of Eq. (13.3), we have:

$$\begin{aligned} B_{ST}(x, m, Q_1) &= \frac{\mu_0 F_{ST}(m, Q_1)}{\delta_{EQ} k_{CAR} k_{SAT}} e^{\frac{-2j\pi nx}{T}}, \\ B_{ST}(x, -m, Q_2) &= \frac{\mu_0 F_{ST}(-m, Q_2)}{\delta_{EQ} k_{CAR} k_{SAT}} e^{\frac{2j\pi nx}{T}}. \end{aligned} \tag{13.5}$$

13.3.2 Complex Amplitudes (Phasors) of Field Harmonics Excited by Damper Winding MMF and Excitation Winding MMF of Salient-Pole Synchronous Machine [13–15]

(a) Complex amplitudes (phasors) of rotor field harmonics at $\omega_{REV} = 0$.

For such a machine, the air gap varies according to Table 13.1, and at certain values of angular coordinate (φ) the flux density in air gap $B_W(\varphi)$ as per (13.3) becomes equal almost to zero and then changes its sign. Curve $B_W(\varphi)$ is periodic, and it is convenient to represent it in the form of harmonic series.

Mathematical formulation of this problem is similar to that of the problem to determine MMF harmonics. We determined MMF harmonics proceeding from the expressions found for current functions in rotor loops. These current functions were represented in the form of time complexes (phasors). They vary along the boring under the periodic law and were expressed as harmonics in complex plane. Here we determine the flux density, proceeding from MMF temporary complexes of these loops. It also varies along the boring under the periodic law, and we will also represent it in the form of harmonics in complex plane.

After these preliminary remarks let us find required harmonic series for field harmonics; we should obtain it, proceeding from MMF harmonics and the law of gap variation $\delta(\varphi)$. We give it here after some additional transformations:

$$B_{ST}(\varphi, m, \omega_{ROT}) = \sum_k B_{ROT,1}[F(m, n, \omega_{ROT}), k]e^{-j\varphi k} + \sum_k B_{ROT,2}[F(m, n, \omega_{ROT}), k]e^{j\varphi k} + B_{ROT,0}, \quad \text{where} \quad \varphi = \frac{2\pi n_{EL} x}{T_{EL}}. \tag{13.6}$$

Here k—orders of rotor field harmonics. In this expansion the third complex amplitude (phasor) corresponding to the last summand is equal to zero [1, 2]: $B_{ROT,0} = 0$. For simplification of presentation of complex amplitude (phasor) $B_{ROT}(\varphi, m, \omega_{ROT})$, the expression like (13.6) will further be determined only for its one summand corresponding to one value of orders m, n, k, for example, m = 1, n = 1, k = 1; generally, both summands in Eq. (13.6) should be summarized by values of orders m, n, k of these harmonics; in practical calculations it is usually sufficient to consider three–four first orders.

Flux density complex amplitudes (phasors) corresponding to the first two summands in (13.6) are determined from the expressions [10, 11] similar to (12.4):

$$\begin{aligned} B_{ROT,1}[F(m, n, \omega_{ROT}), k] &= \tfrac{1}{T}\int_{-\pi}^{\pi} B_{ROT}(\varphi)e^{j\varphi k}d\varphi, \\ B_{ROT,2}[F(m, n, \omega_{ROT}), k] &= \tfrac{1}{T}\int_{-\pi}^{\pi} B_{ROT}(\varphi)e^{-j\varphi k}d\varphi, \\ \text{where} \quad T &= 2\pi \end{aligned} \tag{13.7}$$

From these expressions it follows that the complex amplitude $B_{ROT,2}[F(m, n, \omega_{ROT}), k]$ can be obtained from $B_{ROT,1}[F(m, n, \omega_{ROT}), k]$ by substitution of order sign k by the opposite: k by (−k). In further statement, we will accept for these flux densities complex amplitudes (phasors), designations similar to those for MMF:

$$B_{ROT,1}[F(m, n, \omega_{ROT}), k] = B_{ROT}[F(m, n, \omega_{ROT}), k];$$
$$B_{ROT,2}[F(m, n, \omega_{ROT}), k] = B_{ROT}[F(m, n, \omega_{ROT}), -k].$$

In Eq. (13.7) the flux density of $B_{ROT}(\varphi)$ is calculated based on Eq. (13.3) with account of substitution of index "W" by index "ROT". The analytical expression for rotor winding MMF in (13.3) represents harmonic series obtained earlier:

$$F_{ROT}(\varphi) = \sum_{n} F_{ROT}(m, n, \omega_{ROT}) e^{-j\varphi n} + \sum_{n} F_{ROT}(m, -n, \omega_{ROT}) e^{j\varphi n};$$

here harmonics of orders m, n are summarized.

As a result, we find that the problem is reduced to the determination of flux density complex amplitudes (phasors) as:

$$B_{ROT}[F(m, n, \omega_{ROT}), k] = \frac{1}{T} \int_{-\pi}^{\pi} \frac{\mu_0}{\delta_{EQ} k_{CAR} k_{SAT}} \left[F_{ROT}(m, n, \omega_{ROT}) e^{-j\varphi n} + F_{ROT}(m, -n, \omega_{ROT}) e^{j\varphi n} \right] e^{j\varphi k} d\varphi. \tag{13.8}$$

Peculiarity of these analytical expressions consists in the fact that the calculation ratio for complex amplitude (phasor) $F_{ROT}(m, -n, \omega_{ROT})$ can be obtained from the expression for $F_{ROT}(m, n, \omega_{ROT})$ by substitution of order sign by the opposite: n by (−n), and for complex amplitude (phasor) $B_{ROT}[F_{ROT}(m, n, \omega_{ROT}), -k]$—from $B_{ROT}[F_{ROT}(m, n, \omega_{ROT}), k]$ by substitution of sign of order k by the opposite: k by (−k). It significantly facilitates analytical calculations connected with calculation of integrals like (13.7 and 13.8).

Let us find the first summand in Eq. (13.8):

$$B'_{ROT}[F(m, n, \omega_{ROT}), k] = \frac{1}{T} \int_{-\pi}^{\pi} \frac{\mu_0 F_{ROT}(m, n, \omega_{ROT})}{\delta_{EQ} k_{CAR} k_{SAT}} e^{-j\varphi n} e^{j\varphi k} d\varphi.$$

After its transformations with account of values $\delta(\varphi)$ from Table 13.1, we obtain:

$$B'_{ROT}[F(m, n, \omega_{ROT}), k] = \frac{2\mu_0 F_{ROT}(m, n, \omega_{ROT})}{\delta_{EQ} \pi k_{CAR} k_{SAT} (-n + k)} \sin \frac{(-n + k)\pi\alpha}{2} \cos \frac{(-n + k)\pi}{2}.$$

Respectively, second summand in Eq. (13.8) we obtain from the first by substitution of sign at n order by the opposite: n by (−n):

$$B''_{ROT}[F(m,-n,\omega_{ROT}),k]=\frac{2\mu_0 F_{ROT}(m,-n,\omega_{ROT})}{\delta_{EQ}\pi k_{CAR}k_{SAT}(k+n)}\sin\frac{(n+k)\pi\alpha}{2}\cos\frac{(k+n)\pi}{2}.$$

As a result, the flux density complex amplitude (phasor) of the first field component is equal to,

$$B_{ROT}[F(m,-n,\omega_{ROT}),k]=B'_{ROT}[F(m,n,\omega_{ROT}),k]\ +\ B''_{ROT}[F(m,-n,\omega_{ROT}),k] \tag{13.9}$$

As it is noted above, the flux density complex amplitude (phasor) $B_{ROT}[F(m,n,\omega_{ROT}),-k]$—is obtained from $B_{ROT}[F(m,n,\omega_{ROT}),k]$ by substitution of sign at k order by the opposite: k by (−k). We give this expression completely, despite the fact that the result is cumbersome and evident: its separate components will be required further in the analysis of field harmonics in air gap and with account of their interaction.

$$B'_{ROT}[F(m,n,\omega_{ROT}),-k]=\frac{2\mu_0 F_{ROT}(m,n,\omega_{ROT})}{\delta_{EQ}\pi k_{CAR}k_{SAT}(-k-n)}\sin\frac{(-k-n)\pi\alpha}{2}\cos\frac{(-k-n)\pi}{2};$$

$$B''_{ROT}[F(m,-n,\omega_{ROT}),-k]=\frac{2\mu_0 F_{ROT}(m,-n,\omega_{ROT})}{\delta_{EQ}\pi k_{CAR}k_{SAT}(-k+n)}\sin\frac{(-k+n)\pi\alpha}{2}\cos\frac{(-k+n)\pi}{2}.$$

As a result, the flux density complex amplitude (phasor) of the second field component is equal to,

$$B_{ROT}[F(m,n,\omega_{ROT}),-k]=B'_{ROT}[F(m,n,\omega_{ROT}),-k]+B''_{ROT}[F(m,-n,\omega_{ROT}),-k] \tag{13.10}$$

In conclusion of this section it should be noted that for the calculation of field harmonics excited by MMF component in Eq. (13.8) characterized by sign S = 2 or order of "adjacent" harmonic $Q_2 \neq Q_1$, it is necessary in the obtained expressions $B_{ROT}[F(m,n,\omega_{ROT}),k]$ and $B_{ROT}[F(m,n,\omega_{ROT}),-k]$ to replace sign at m order by the opposite (m by −m):

$$B'_{ROT}[F(-m,n,\omega_{ROT}),k]=\frac{2\mu_0 F_{ROT}(-m,n,\omega_{ROT})}{\delta_{EQ}\pi k_{CAR}k_{SAT}(-n+k)}\sin\frac{(-n+k)\pi\alpha}{2}\cos\frac{(-n+k)\pi}{2}.$$

Correspondingly, we obtain the second summand in Eq. (13.10) from the first by substitution of sign at n order by the opposite: n by (−n):

$$B''_{ROT}[F(-m,-n,\omega_{ROT}),k] = \frac{2\mu_0 F_{ROT}(-m,-n,\omega_{ROT})}{\delta_{EQ}\pi k_{CAR} k_{SAT}(k+n)} \sin\frac{(k+n)\pi\alpha}{2} \cos\frac{(k+n)\pi}{2}.$$

As a result, the flux density complex amplitude (phasor) of the third field component is equal to,

$$B_{ROT}[F(-m,n,\omega_{ROT}),k] = B'_{ROT}[F(-m,n,\omega_{ROT}),k] + B''_{ROT}[F(-m,-n,\omega_{ROT}),k]. \tag{13.11}$$

As it was already noted, the flux density complex amplitude (phasor) $B_{ROT}[F(-m,n,\omega_{ROT}),-k]$ can be obtained from $B_{ROT}[F(-m,n,\omega_{ROT}),k]$ by replacement of sign at k order by the opposite: k by (−k):

$$B'_{ROT}[F(-m,n,\omega_{ROT}),-k] = \frac{2\mu_0 F_{ROT}(-m,n,\omega_{ROT})}{\delta_{EQ}\pi k_{CAR} k_{SAT}(-k-n)} \sin\frac{(-k-n)\pi\alpha}{2} \cos\frac{(-k-n)\pi}{2};$$

$$B''_{ROT}[F(-m,-n,\omega_{ROT}),-k] = \frac{2\mu_0 F_{ROT}(-m,-n,\omega_{ROT})}{\delta_{EQ}\pi k_{CAR} k_{SAT}(-k+n)} \sin\frac{(-k+n)\pi\alpha}{2} \cos\frac{(-k+n)\pi}{2}.$$

As a result, the flux density complex amplitude (phasor) of the fourth field component is equal to,

$$B_{ROT}[F(-m,n,\omega_{ROT}),-k] = B'_{ROT}[F(-m,n,\omega_{ROT}),-k] + B''_{ROT}[F(-m,-n,\omega_{ROT}),-k]. \tag{13.12}$$

These general expressions are true when computing the fields in air gap created by currents in rotor loops: in damper winding and squirrel cages with any degree of asymmetry, as well as in excitation winding. Substituting MMF complex amplitudes (phasors) to these expressions, it is easy to obtain in a closed form analytical expressions for flux density complex amplitudes (phasors) corresponding to MMF of listed rotor windings. However, in relation to damper winding in practical calculations it is inexpedient: currents of damper winding contain three components, therefore analytical expressions for MMF complex amplitudes (phasors) and, respectively, flux density are cumbersome. As in modern practice it is more convenient to perform numerical operations with complex numbers (by means of computer), such cumbersome analytical expressions (in a closed form) are less convenient for algorithmization of calculations: they exclude a possibility of stage-by-stage check of results. At the same time, their analysis does not allow one to formulate any additional recommendations, besides known ones [3, 4] in selecting the geometry of the listed windings, for example, for providing field waveform in air gap, close to sinusoidal in operation modes, etc.

Therefore, here we will give the expressions necessary for the calculation realized by numerical methods; we will consider analytical expressions only for special cases, which at the same time will allow us to check validity of obtained calculation expressions.

Let us find excitation winding field harmonics. MMF complex amplitudes (phasors) of excitation winding are obtained in the previous chapter with account of designations accepted in this chapter like:

$$F_{EX}(n, \omega_{ROT}) = \frac{-2jI_{EX}W_{EX}}{\pi n} \sin\frac{\pi n\alpha}{2} \sin\frac{\pi n}{2}.$$

Here n—excitation winding order of MMF spatial harmonic.

To obtain calculation the expression for MMF additional component, it is necessary to substitute in this expression n by (−n); as a result, we obtain:

$$F_{EX}(-n, \omega_{ROT}) = -F_{EX}(n, \omega_{ROT}).$$

Let us use the expressions found in this paragraph to calculate flux density complex amplitudes (phasors), substituting index "ROT" by index "EX":

Let us find the flux density complex amplitude (phasor) of excitation winding field first component $B_{EX}(m, n, k, \omega_{ROT})$.

$$\begin{aligned}
B'_{EX}[F(m, n, \omega_{ROT}), k] &= \frac{2\mu_0 F_{EX}(m, n, \omega_{ROT})}{\delta_{EQ}\pi k_{CAR}k_{SAT}(k-n)} \sin\frac{(k-n)\pi\alpha}{2} \cos\frac{(k-n)\pi}{2} \\
&= \frac{2\mu_0(2I_{EX}W_{EX})}{j\delta_{EQ}k_{CAR}k_{SAT}(k-n)\pi^2 n} \sin\frac{(k-n)\pi\alpha}{2} \cos\frac{(k-n)\pi}{2} \sin\frac{\pi n\alpha}{2} \sin\frac{\pi n}{2}; \\
B''_{EX}[F(m, -n, \omega_{ROT}), k] &= \frac{2\mu_0 F_{EX}(m, -n, \omega_{ROT})}{\delta_{EQ}\pi k_{CAR}k_{SAT}(k+n)} \sin\frac{(k+n)\pi\alpha}{2} \cos\frac{(k+n)\pi}{2} \\
&= \frac{2\mu_0(-2I_{EX}W_{EX})}{j\delta_{EQ}k_{CAR}k_{SAT}(k+n)\pi^2 n} \sin\frac{(k+n)\pi\alpha}{2} \cos\frac{(k+n)\pi}{2} \sin\frac{\pi n\alpha}{2} \sin\frac{\pi n}{2}; \\
B_{EX}[F(m, n, \omega_{ROT}), k] &= B'_{EX}[F(m, n, \omega_{ROT}), k] + B''_{ROT}[F(m, -n, \omega_{ROT}), k].
\end{aligned} \tag{13.13}$$

Complex amplitudes (phasors) of other three flux density components are determined similarly to (13.13), based on the obtained Eqs. (13.9–13.12). In calculation of these complex amplitudes (phasors) from the ratios like (13.7) it is expedient to consider the relationships between complex amplitudes (phasors) of excitation winding MMF obtained in the previous chapters.

We consider a special case: $|m| = |n| = |k| = 1$.

The complex amplitude (phasor) of flux density $B_{EX}[F(m, n, \omega_{ROT}), k]$ of the first component of excitation winding field has the form:

$$
\begin{aligned}
B'_{EX}[F(m,n,\omega_{ROT}),k] &= \frac{2\mu_0 I_{EX} W_{EX}}{j\delta_{EQ} k_{CAR} k_{SAT} \pi^2} \pi\alpha \cdot \sin\frac{\pi\alpha}{2};\\
B''_{EX}[F(m,n,\omega_{ROT}),k] &= \frac{2\mu_0 I_{EX} W_{EX}}{j\delta_{EQ} k_{CAR} k_{SAT} \pi^2} \sin\pi\alpha \cdot \sin\frac{\pi\alpha}{2};\\
B_{EX}[F(m,n,\omega_{ROT}),k] &= B'_{EX}[F(m,n,\omega_{ROT}),k] + B''_{ROT}[F(m,-n,\omega_{ROT}),k]\\
&= \frac{2\mu_0 I_{EX} W_{EX}}{j\delta_{EQ} k_{CAR} k_{SAT} \pi^2} (\pi\alpha + \sin\pi\alpha) \cdot \sin\frac{\pi\alpha}{2}.
\end{aligned}
\tag{13.13'}
$$

Let us determine the flux density complex amplitude (phasor) of excitation winding second field component: $B_{EX}[F(m,n,\omega_{ROT}),-k]$.

$$
\begin{aligned}
B_{EX}[F(m,n,\omega_{ROT}),-k] &= B'_{EX}[F(m,n,\omega_{ROT}),-k] + B''_{ROT}[F(m,-n,\omega_{ROT}),-k]\\
&= \frac{-2\mu_0 I_{EX} W_{EX}}{j\delta_{EQ} k_{CAR} k_{SAT} \pi^2} (\pi\alpha + \sin\pi\alpha) \cdot \sin\frac{\pi\alpha}{2}.
\end{aligned}
\tag{13.14}
$$

Expressions for other two complex amplitudes (phasors) are determined similarly.

Let us note that the obtained expressions for $B_{EX}[F(m,n,\omega_{ROT}),k]$ and $B_{EX}[F(m,n,\omega_{ROT}),-k]$ correspond to complex amplitudes (phasors) in the expansion of pulsating excitation winding field into harmonic series of both rotating fields with account of geometrical dimensions of air gap and pole shoe; they prove validity of these calculation expressions.

It is expedient to present the obtained results in other form, which allows us to give them a bit different physical treatment and to make additional check of results. Taking into account Eq. (13.6) for the special case considered here ($|m| = |n| = |k| = 1$), let us determine the expression for calculating the flux density distribution along stator boring at $0 \le \varphi \le 2\pi$; $\varphi = \frac{2\pi n_{EL} x}{T_{EL}}$.

$$
B_{EX}(\varphi,m,\omega_{ROT}) = B_{EX}[F(m,n,\omega_{ROT}),k]e^{-j\varphi k} + B_{EX}[F(m,n,\omega_{ROT}),-k]e^{j\varphi k}.
$$

We take into account the obtained Eqs. (13.13') and (13.14); it follows from these that

$$
B_{EX}[F(m,n,\omega_{ROT}),k] = -B_{EX}[F(m,n,\omega_{ROT}),-k].
$$

By means of last two ratios, we obtain the distribution of flux density along stator boring like:

$$B_{EX}(\varphi, m, \omega_{ROT}) = -2jB_{EX}[F(m, n, \omega_{ROT}), k] \sin\varphi$$
$$= \frac{-4\mu_0 I_{EX} W_{EX}}{\delta_{EQ} k_{CAR} k_{SAT} \pi^2} (\pi\alpha + \sin\pi\alpha) \cdot \sin\frac{\pi\alpha}{2} \cdot \sin\varphi.$$

Let us note that the reference mark of angles (φ) is superimposed with pole cross axis (q). Respectively, at $\varphi = 0$ (in intersection point of boring circle with cross axis) and $\varphi = \frac{\pi}{2}$ (in intersection point of boring circle with longitudinal axis) we obtain:

$$\text{at } \varphi = 0 : B_{EX}(\varphi, m, \omega_{ROT}) = 0.$$
$$\text{at } \varphi = \frac{\pi}{2} : B_{EX}(\varphi, m, \omega_{ROT}) = \frac{-4\mu_0 I_{EX} W_{EX}}{\delta_{EQ} k_{CAR} k_{SAT} \pi^2} (\pi\alpha + \sin\pi\alpha) \sin\frac{\pi\alpha}{2}.$$

(It is the maximum absolute value of flux density).

Both of these results also prove validity of the obtained calculation expressions [3, 4].

(b) Complex amplitudes (phasors) of rotor field harmonics at $\omega_{REV} \neq 0$.

The expressions found for field harmonics in air gap created by currents in rotor windings allow us to solve several problems of practical interest, for example, to obtain ratios for these harmonic fields in various reference angle systems, and to determine direction and speed of their rotation relative to stator.

Let us consider, for example, variation of their appearance at rotation with rotor speed ω_{REV} in the positive direction of angle reference. Repeating calculations at $\omega_{REV} \neq 0$, it is easy to obtain that for an angle φ relative to the fixed space axis, expressions for field harmonics at $\omega_{REV} \neq 0$ will be transformed in the form:

$$B_{ROT}[F(m, n, \omega_{ROT}, \omega_{REV}), k] = B_{ROT}[F(m, n, \omega_{ROT}), k] e^{jk\omega_{REV} tp},$$
$$B_{ROT}[F(m, n, \omega_{ROT}, \omega_{REV}), -k] = B_{ROT}[F(m, n, \omega_{ROT}), -k] e^{-jk\omega_{REV} tp}. \quad (13.15)$$

These ratios remain true both for positive and negative values of orders m, n.

We write down the expression for flux density complex amplitude (phasor) of the first field component:

$$B^{(I)}_{ROT}[F(m, n, \omega_{REV}), k] = \{B'_{ROT}[F(m, n, \omega_{ROT}), k] + B'_{ROT}[F(m, -n, \omega_{ROT}), k]\} e^{jk\omega_{REV} tp}$$

or

$$B^{(I)}_{ROT}[F(m, n, \omega_{REV}), k] = \left[\frac{2\mu_0 F_{ROT}(m, n, \omega_{ROT})}{\delta_{EQ} \pi k_{CAR} k_{SAT} (k-n)} \sin\frac{(k-n)\pi\alpha}{2} \cos\frac{(k-n)\pi}{2}\right.$$
$$\left. + \frac{2\mu_0 F_{ROT}(m, -n, \omega_{ROT})}{\delta_{EQ} \pi k_{CAR} k_{SAT} (k + n)} \sin\frac{(k+n)\pi\alpha}{2} \cos\frac{(k+n)\pi}{2}\right] e^{jk\omega_{REV} tp}. \quad (13.16)$$

We added the upper index (I) to this flux density component in air gap; in the strict sense, there is no special need in this index because this component is fully characterized by signs of harmonic orders m, n, k. Introduction of this index is expedient because it indicates the speed of this field component in air gap; the calculation expression for it is obtained in the following paragraph. It facilitates the definition of magnetically coupled rotor and stator loops which as it was already noted earlier, are determined by:

- identical orders of spatial field harmonics in air gap;
- identical rotation speeds of these fields relative to stator boring.

Therefore, let us add the upper index to other three components of rotor winding fields as well as to stator winding field components. We write down an expression for flux density complex amplitude (phasor) of the second field component:

$$B_{ROT}^{(II)}[F(m,n,\omega_{REV}),-k]=\left[\frac{2\mu_0 F_{ROT}(m,n,\omega_{ROT})}{\delta_{EQ}\pi k_{CAR}k_{SAT}(-k-n)}\cdot\sin\frac{(-k-n)\pi\alpha}{2}\cos\frac{(-k-n)\pi}{2}+\frac{2\mu_0 F_{ROT}(m,-n,\omega_{ROT})}{\delta_{EQ}\pi k_{CAR}k_{SAT}(-k+n)}\sin\frac{(-k+n)\pi\alpha}{2}\cos\frac{(-k+n)\pi}{2}\right]e^{-jk\omega_{REV}tp}. \tag{13.17}$$

Let us proceed to the calculation of field harmonics excited by MMF component characterized by sign S = 2 or order of "adjacent" harmonic $Q_2 \neq Q_1$. For this purpose it is necessary in the obtained expressions $B_{ROT}[F(m,n,\omega_{ROT}),k]$ and $B_{ROT}[F(m,n,\omega_{ROT}),-k]$ to substitute the sign at order m by its opposite (m by –m):

$$B_{ROT}^{(III)}[F(-m,n,\omega_{REV}),k]=\left[\frac{2\mu_0 F_{ROT}(-m,n,\omega_{ROT})}{\delta_{EQ}\pi k_{CAR}k_{SAT}(k-n)}\sin\frac{(k-n)\pi\alpha}{2}\cos\frac{(k-n)\pi}{2}+\frac{2\mu_0 F_{ROT}(-m,-n,\omega_{ROT})}{\delta_{EQ}\pi k_{CAR}k_{SAT}(k+n)}\sin\frac{(k+n)\pi\alpha}{2}\cos\frac{(k+n)\pi}{2}\right]e^{jk\omega_{REV}tp}. \tag{13.18}$$

Similarly, the fourth flux density component of rotor field has the form:

$$B_{ROT}^{(IV)}[F(-m,n,\omega_{REV}),-k]=\left[\frac{2\mu_0 F_{ROT}(-m,n,\omega_{ROT})}{\delta_{EQ}\pi k_{CAR}k_{SAT}(-k-n)}\cdot\sin\frac{(-k-n)\pi\alpha}{2}\cos\frac{(-k-n)\pi}{2}+\frac{2\mu_0 F_{ROT}(-m,-n,\omega_{ROT})}{\delta_{EQ}\pi k_{CAR}k_{SAT}(-k+n)}\sin\frac{(-k+n)\pi\alpha}{2}\cos\frac{(-k+n)\pi}{2}\right]e^{-jk\omega_{REV}tp}. \tag{13.19}$$

13.3.3 Rotation Speeds $\omega_{BOR,R}$ in Air Gap of Field Harmonic Components Excited by Damper Winding MMF and Excitation Winding MMF of Salient-Pole Synchronous Machine

This paragraph is based on results obtained in Chap. 3.

Let us find calculation expressions for angular rotation speeds $\omega_{BOR,R}$ in air gap of these field components. We assume, thus, that rotor winding MMFs are time complexes (phasors).

The expression $\omega^{(I)}_{BOR,R}$ for the first field component is calculated from the following ratio:

$$\frac{-2\pi k dx}{T} + \omega_{ROT} dt + \omega_{REV} pk dt = 0;$$

Hence we have $\frac{2\pi k}{T} \cdot \frac{dx}{dt} = \omega_{ROT} + \omega_{REV} pk$. We note that $\frac{2\pi k}{T} \cdot \frac{dx}{dt} = \omega_{BOR,R} pk$. Then, the initial equation takes the form: $\omega^{(I)}_{BOR,R} pk = \omega_{ROT} + \omega_{REV} pk$.. For rotor EMF frequency the following is true: $\omega_{ROT} = -\omega_{REV} pk + Q_1 \omega_1$. With account of the last, we obtain: $\omega^{(I)}_{BOR,R} pk = Q_1 \omega_1$. Thus,

$$\omega^{(I)}_{BOR,R} = Q_1 \frac{\omega_1}{pk} \neq f(S_{SL}). \tag{13.20}$$

We try to find the calculation expression for speed $\omega^{(II)}_{BOR,R}$ of the second flux density component. Similarly, we have:

$$\omega_{ROT} dt + \frac{2\pi k dx}{T} - \omega_{REV} pk dt = 0.$$
or
$$\omega^{(II)}_{BOR,R} pk = \omega_{REV} pk - \omega_{ROT}.$$

We use the expression for EMF frequency ω_{ROT} given above and expression for rotor speed rotation $\omega_{REV} = (1 - S_{SL}) \frac{\omega_1}{p}$. After simple transformations, we have:

$$\omega^{(II)}_{BOR,R} = \frac{\omega_1}{pk} [2(1 - S_{SL})k - Q_1] = f(S_{SL}). \tag{13.21}$$

Thus, the speed $\omega^{(II)}_{BOR,R}$ generally depends on slip S_{SL}, that is, on rotor rotation speed ω_{REV}.

Let us consider some special cases:

- Asynchronous mode ($S_{SL} \neq 0$); rotation speed $\omega^{(II)}_{BOR,R}$ of the first spatial and higher time harmonics at m = n=k = 1, $Q_1 > 1, Q_2 > 1$:

$$\omega_{BOR,R}^{(II)} = -\frac{\omega_1}{p}[Q_1 - 2 + 2S_{SL}] = -\frac{\omega_1}{p}(Q_2 + 2S_{SL}).$$

- Synchronous mode ($S_{SL} = 0$); field rotation speed $\omega_{BOR,R}^{(II)}$ of the first spatial and higher time harmonics at m = n=k = 1, $Q_1 > 1, Q_2 > 1$:

$$\omega_{BOR,R}^{(II)} = -\frac{\omega_1}{p}(2 - Q_1) = -Q_2\frac{\omega_1}{p}.$$

We try to find the calculation expression for speed $\omega_{BOR,R}^{(III)}$ of the third field component. Let us take into account that unlike the first two rotor field components excited by stator field time harmonics of order Q_1, the fields of the last two components are excited by stator field time harmonics of order Q_2. The initial equation for calculation $\omega_{BOR,R}^{(III)}$ is as follows:

$$\omega_{ROT}dt - \frac{2\pi k dx}{T} + \omega_{REV}pkdt = 0,$$
or
$$\omega_{BOR,R}^{(III)}pk = \omega_{REV}pk + \omega_{ROT}.$$

Expressions for EMF frequency ω_{ROT} and for rotor rotation speed ω_{REV}, included in it:

$$\omega_{ROT} = pk\omega_{REV} + Q_2\omega_1; \quad \omega_{REV} = (1 - S_{SL})\frac{\omega_1}{p}.$$

Using them, we obtain:

$$\omega_{BOR,R}^{(III)} = \frac{\omega_1}{pk}[2(1 - S_{SL})k + Q_2] = f(S_{SL}). \tag{13.22}$$

We consider some special cases.

- Asynchronous mode ($S_{SL} \neq 0$); rotation speed $\omega_{BOR,R}^{(III)}$ of the first spatial and higher time harmonics at m = n=k = 1, $Q_1 > 1, Q_2 > 1$:

$$\omega_{BOR,R}^{(III)} = \frac{\omega_1}{p}(2 + Q_2 - 2S_{SL}) = \frac{\omega_1}{p}(Q_1 - 2S_{SL}).$$

- Synchronous mode ($S_{SL} = 0$); field rotation speed $\omega_{BOR,R}^{(III)}$ of the first spatial and higher time harmonics at m = n=k = 1, $Q_1 > 1, Q_2 > 1$:

$$\omega_{BOR,R}^{(III)} = Q_1\frac{\omega_1}{p}.$$

Let us proceed to the last expression for speed $\omega^{(IV)}_{BOR,R}$. Similarly to the previous one, the initial equation to calculate $\omega^{(IV)}_{BOR,R}$ takes the form:.

$\omega^{(IV)}_{BOR,R}pk = \omega_{REV}pk - \omega_{ROT}$. Expressions for EMF frequency ω_{ROT} and for rotation speed, coincide with those obtained for $\omega^{(III)}_{BOR,R}$.

As a result, we have:

$$\omega^{(IV)}_{BOR,R} = -Q_2 \frac{\omega_1}{pk} \neq f(S_{SL}). \tag{13.23}$$

13.3.4 *Complex Amplitudes (Phasors) of Field Harmonics Excited by Stator Winding MMF with Account of Cross Section Geometry of Salient-Pole Synchronous Machine at Rotor at Standstill ($\omega_{REV} = 0$) and at Its Rotation ($\omega_{REV} \neq 0$)*

(a) Complex amplitudes (phasors) of stator field harmonics at $\omega_{REV} = 0$.

Let us use general expressions for MMF obtained earlier in Chap. 12.

We begin with the calculation of field harmonics excited by the first MMF component characterized by sign S = 1, for example, order of time harmonic Q_{DIR} and spatial harmonic m_{DIR}; corresponding ratios were given in Chap. 3. According to designations accepted here $Q_{DIR} = Q_1$; $Q_{ADD} = Q_2$.

In the initial Eq. (13.3) for calculation of flux density in air gap, it is necessary to substitute index "W" by index "ST". Let us determine the first summand of complex amplitude (phasor) $B_{STAT}(m, k, Q_1)$:

$$B^{(I)}_{ST}[F(m, Q_1), k] = \frac{2\mu_0 F_{ST,RES}(m, Q_1)}{\delta_{EQ}\pi k_{CAR} k_{SAT}(k-m)} \sin\frac{(k-m)\pi\alpha}{2} \cdot \cos\frac{(k-m)\pi}{2}. \tag{13.24}$$

Thus, harmonics of series characterizing the distribution of the stator winding field first flux density component for sign S = 1 at $\omega_{REV} = 0$ take the form:

$$B^{(I)}_{ST}[F(m, Q_1, x), k] = \frac{2\mu_0 F_{ST,RES}(m, Q_1)}{\delta_{EQ}\pi k_{CAR} k_{SAT}(k-m)} \sin\frac{(k-m)\pi\alpha}{2} \cdot \cos\frac{(k-m)\pi}{2} e^{\frac{-2j\pi kx}{T}}. \tag{13.24'}$$

Respectively, for complex amplitude (phasor) of the second flux density component of the same field we obtain the expression from (13.24) by replacement of sign at k order by the opposite (k by −k):

$$B_{ST}^{(II)}[F(m, Q_1, x), -k] = \frac{2\mu_0 F_{ST,RES}(m, Q_1)}{\delta_{EQ}\pi k_{CAR} k_{SAT}(-k-m)} \sin\frac{(-k-m)\pi\alpha}{2} \cdot \cos\frac{(-k-m)\pi}{2}. \tag{13.25}$$

In this and subsequent expressions it is easy to change to positive both negative signs, in parentheses for orders of spatial harmonics k, m, however, it restricts visualization of correlation of complex amplitudes (phasors) obtained by changing these signs.

Thus, the harmonics of series characterizing the distribution of second flux density component along boring for stator winding field at S = 1 are as follows at $\omega_{REV} = 0$:

$$B_{ST}^{(II)}[F(m, Q_1, x), -k] = \frac{2\mu_0 F_{ST,RES}(m, Q_1)}{\delta_{EQ}\pi k_{CAR} k_{SAT}(-k-m)} \sin\frac{(-k-m)\pi\alpha}{2} \cdot \cos\frac{(-k-m)\pi}{2} e^{\frac{2j\pi kx}{T}}. \tag{13.25'}$$

Further, we find that these two flux density components with rotor rotation ($\omega_{REV} \neq 0$) correspond to stator winding EMF differing in frequency.

Let us proceed to the calculation of flux density harmonics excited by MMF component characterized by another sign (S = 2), for example, with order of "adjacent" time harmonic $Q_{AD} = Q_{DIR} - 2$ and spatial harmonic m_{DIR}; the corresponding ratios were given in the Chap. 3.

As a result, for the third flux density component at $\omega_{REV} = 0$ we obtain:

$$B_{ST}^{(III)}[F(-m, Q_2, x), k] = \frac{2\mu_0 F_{ST,RES}(-m, Q_2)}{\delta_{EQ}\pi k_{CAR} k_{SAT}(k+m)} \sin\frac{(k+m)\pi\alpha}{2} \cdot \cos\frac{(k+m)\pi}{2} e^{\frac{-2j\pi kx}{T}}. \tag{13.26}$$

Respectively, for the fourth flux density component we obtain an expression from (13.26) by substitution of order of k by (–k):

$$B_{ST}^{(IV)}[F(-m, Q_2, x), -k] = \frac{2\mu_0 F_{ST,RES}(-m, Q_2)}{\delta_{EQ}\pi k_{CAR} k_{SAT}(-k+m)} \sin\frac{(-k+m)\pi\alpha}{2} \cdot \cos\frac{(-k+m)\pi}{2} e^{\frac{2j\pi kx}{T}}. \tag{13.27}$$

(b) Complex amplitudes (phasors) of stator field harmonics at $\omega_{REV} \neq 0$.

Let us consider expressions for field harmonics for rotor rotation in positive direction of angle reference φ. It will allow us to determine the direction and rotation speed of field harmonics of various time and spatial orders relative to stator.

Repeating calculations at $\omega_{REV} \neq 0, \quad S_{SL} \neq 0$ it is easy to obtain that for the angle φ relative to the fixed one in the space axis, expressions for MMF harmonics components differing in sign S = 1 will be transformed to the form:

$$B_{ST}^{(I)}[F(m, Q_1, x), k, \omega_{REV}] = \frac{2\mu_0 F_{ST,RES}(m, Q_1)}{\pi\delta_{EQ} k_{CAR} k_{SAT}(k-m)} \cdot \sin\frac{(k-m)\pi\alpha}{2} \cos\frac{(k-m)\pi}{2} e^{-2j\pi n\frac{x}{T}} e^{j(k-m)\omega_{REV} tp}. \tag{13.28}$$

$$B_{ST}^{(II)}[F(m, Q_1, x), -k, \omega_{REV}] = \frac{2\mu_0 F_{ST,RES}(m, Q_1)}{\pi\delta_{EQ} k_{CAR} k_{SAT}(-k-m)} \cdot \sin\frac{(-k-m)\pi\alpha}{2} \cos\frac{(-k-m)\pi}{2} e^{2j\pi n\frac{x}{T}} e^{j(-k-m)\omega_{REV} tp}. \tag{13.29}$$

Respectively, expressions for MMF harmonic components differing in other sign (S = 2), will be transformed in the form:

$$B_{ST}^{(III)}[F(-m, Q_2, x), k, \omega_{REV}] = \frac{2\mu_0 F_{ST,RES}(-m, Q_2)}{\pi\delta_{EQ} k_{CAR} k_{SAT}(k+m)} \cdot \sin\frac{(k+m)\pi\alpha}{2} \cos\frac{(k+m)\pi}{2} e^{\frac{-2j\pi kx}{T}} e^{j(k+m)\omega_{REV} tp}. \tag{13.30}$$

$$B_{ST}^{(IV)}[F(-m, Q_2, x), -k, \omega_{REV}] = \frac{2\mu_0 F_{ST,RES}(-m, Q_2)}{\pi\delta_{EQ} k_{CAR} k_{SAT}(-k+m)} \cdot \sin\frac{(-k+m)\pi\alpha}{2} \cos\frac{(-k+m)\pi}{2} e^{\frac{2j\pi kx}{T}} e^{j(-k+m)\omega_{REV} tp}. \tag{13.31}$$

13.3.5 *Rotation Speeds $\omega_{BOR,ST}$ in Air Gap of Field Harmonic Components Excited by Stator Winding MMF of Salient-Pole Synchronous Machine*

Let us estimate calculation expressions for angular rotation speeds $\omega_{BOR,ST}$ in air gap of stator field components. Thus, we take into account that stator winding MMFs as well as rotor winding MMFs are time complexes (phasors).

The calculation expression $\omega_{BOR,ST}^{(I)}$ for the first flux density component is computed from the ratio: $\frac{-2\pi k dx}{T} + Q_1\omega_1 dt = 0$; hence, we have: $\frac{2\pi k}{T}\frac{dx}{dt} = Q_1\omega_1$.

Let us note that $\frac{2\pi k}{T}\frac{dx}{dt} = \omega_{BOR,ST}pk$.

Thus,

$$\omega^{(I)}_{BOR,ST} = \frac{Q_1\omega_1}{pk} \neq f(S_{SL}). \tag{13.32}$$

The expression for speed $\omega^{(I)}_{BOR,ST}$ coincides with that for speed $\omega^{(I)}_{BOR,R}$.

We find the calculation expression for speed $\omega^{(II)}_{BOR,ST}$ of the second flux density component. Similarly, we have:

$$Q_1\omega_1 dt + \frac{2\pi k dx}{T} - 2\omega_{REV}pk dt = 0,$$
or
$$\omega^{(II)}_{BOR,ST}pk = -Q_1\omega_1 + \omega_{REV}pk.$$

Let us use an expression for rotor rotation speed $\omega_{REV} = \frac{(1-S_{SL})\omega_1}{p}$. After simple transformations, we have:

$$\omega^{(II)}_{BOR,ST} = \frac{\omega_1}{pk}[2(1 - S_{SL})k - Q_1] = f(S_{SL}). \tag{13.33}$$

The expression for speed $\omega^{(II)}_{BOR,ST}$ coincides with that for speed $\omega^{(II)}_{BOR,R}$.

Let us find the calculation expression for speed $\omega^{(III)}_{BOR,ST}$ of the third flux density component. Thus, we assume that unlike the first two components, the fields of the last two components are excited by stator field time harmonics of order Q_2 and have sign S = 2. The initial equation for calculation $\omega^{(III)}_{BOR,ST}$:

$$Q_2\omega_1 dt - \frac{2\pi k dx}{T} + 2\omega_{REV}pk dt = 0,$$
or
$$\omega^{(III)}_{BOR,ST}pk = \omega_{REV}pk + \omega_{ROT}.$$

Using the ratios given earlier, we obtain:

$$\omega^{(III)}_{BOR,ST} = \frac{\omega_1}{pk}[2(1 - S_{SL})k + Q_2] = f(S_{SL}). \tag{13.34}$$

We note that the expression for speed $\omega^{(III)}_{BOR,ST}$ coincides with that for speed $\omega^{(III)}_{BOR,R}$.

Let us proceed to the expression for $\omega^{(IV)}_{BOR,ST}$. The initial equation for calculation $\omega^{(IV)}_{BOR,ST}$ takes the form $\omega^{(IV)}_{BOR,ST}pk + Q_2\omega_1 = 0$.

As a result, we have:

$$\omega_{BOR,ST}^{(IV)} = -\frac{\omega_1}{pk} Q_2 \neq f(S_{SL}). \tag{13.35}$$

We note that expression for speed $\omega_{BOR,ST}^{(IV)}$ coincides with that for speed $\omega_{BOR,R}^{(IV)}$.

13.3.6 *Additional Ratios for Calculation of Complex Amplitudes (Phasors) of Stator Windings at $|m| = |n| = |k| = 1$, Their Check*

The obtained complex amplitudes (phasors) of rotor and stator windings are necessary to form a system of equations of magnetically coupled loops. However, let us additionally check them.

Let us write down expressions for complex amplitudes (phasors) of rotor and stator windings at $|k| = |m| = |n| = 1$ and compare them with known ratios from the theory of two reactions [3, 5, 7].

We consider, at first, the complex amplitude (phasor) $B_{ST}^{(I)}[F(m, Q_1), k]$.

For a special case considered, we have:

$$B_{ST}^{(I)}[F(m, Q_1), k] = \frac{\mu_0 \alpha}{\delta_{EQ} k_{CAR} k_{SAT}} F_{ST,RES}(m, Q_1).$$

The expression for complex amplitude (phasor) of stator winding $B_{ST}^{(IV)}[F(-m, Q_2), k]$ is similar.

For complex amplitude (phasor) $B_{ST}^{(II)}[F(m, Q_1), k]$ we obtain:

$$B_{ST}^{(II)}[F(m, Q_1), k] = \frac{-\mu_0 [F_{ST,RES}(m, Q_1)]}{\delta_{EQ} \pi k_{CAR} k_{SAT)}} \sin(\pi\alpha).$$

The expression for complex amplitude (phasor) of stator winding $B_{ST}^{(III)}[F(-m, Q_2), k]$ is obtained similarly.

Let us find flux densities which are created in air gap MMF $F_{ST,RES}(m, Q_1)$ at $\varphi = \frac{\pi}{2}$ (in intersection point of boring circle with rotor pole longitudinal axis) and at $\varphi = 0$ (in intersection point of boring circle with rotor pole cross axis). We take into account that the reference origin of angles φ is superimposed with rotor pole cross axis ($\varphi = 0$). For determination of flux density, for example, at $\varphi = \frac{\pi}{2}$, it is necessary to multiply the complex amplitude (phasor) $B_{ST}^{(I)}[F(m, Q_1), -k]$ by $e^{\frac{-j\pi}{2}}$ and the complex amplitude (phasor) $B_{ST}^{(II)}[F(m, Q_1), -k]$ by $e^{\frac{j\pi}{2}}$.

We turn our attention to the theory of two reactions [3, 5, 7]. Within this theory, two stator field form factors in air gap are used:

- of longitudinal reaction $K_d = \frac{\pi\alpha + \sin\pi\alpha}{\pi}$;
- of cross reaction $K_q = \frac{\pi\alpha - \sin\pi\alpha}{\pi}$.

They can be obtained if we find respectively half-sum (for $\varphi = 0$) and half-difference (for $\varphi = \frac{\pi}{2}$) of complex amplitudes (phasors) obtained above.

It is also easy to obtain similar results for flux density which creates MMF in air gap $F_{ST,RES}(-m, Q_2)$. It follows from the expressions found.

Let us pay attention to the results obtained for those speeds of field in air gap $\omega^{(II)}_{BOR,R} = \omega^{(II)}_{BOR,ST}$ and $\omega^{(III)}_{BOR,R} = \omega^{(III)}_{BOR,ST}$, which depend on slip S_{SL}; for special case $(|k| = |m| = |n| = 1, Q = 1)$ they are known from the theory of A.C. machines and are connected with occurrence of "monoaxial effect" or "Goerger's effect" [3] for asynchronous start-up of salient-pole synchronous motors.

The provided calculations for complex amplitudes (phasors) of flux density harmonics and rotation speeds in air gap prove validity of calculation expressions obtained in this chapter.

Brief Conclusions [12]

1. For non-sinusoidal power supply of A.C. machines it is convenient to obtain calculation expressions for rotor and stator field harmonics in air gap using a symbolic method of representation of currents and MMF in combination with complex form of representation of harmonic series (Fourier).
2. For induction machines, harmonic complex amplitudes (phasors) of the field created by rotor windings in air gap in certain scale repeat its MMF harmonics; the same refers to stator field harmonics, if their order is lower than that of teeth. Unlike fields in air gap of salient-pole machines at sinusoidal power supply, at non-sinusoidal power supply, the fields created in gap by MMF of stator windings, damper winding and rotor excitation winding have peculiarities: for each spatial harmonic, calculation expressions have two components; physically they correspond to two fields in air gap rotating relative to rotor in opposite directions.
3. Complex amplitudes (phasors) of these field harmonics significantly depend on geometrical dimensions of salient-pole machine cross section (form of air gap, pole shoe, etc.).
4. Rotation speeds of time and spatial harmonic fields of rotor and stator currents are obtained; speeds of stator harmonic fields generally are determined not only by the order of stator current time harmonics, but also by salient-pole rotor rotation speed.
5. Analysis of the obtained expressions for complex amplitudes (phasors) of field harmonics of stator winding and rotor windings, as well as their rotation speeds in air gap allows defining magnetically coupled loops in stator and rotor. They are necessary to formulate a system of equations to determine currents and losses in these loops in nonlinear network.

List of Symbols

$B_{EX}[F(m, n, \omega_{ROT}), k]$	Field harmonic amplitude of excitation winding field in air gap
$B_W(\varphi)$	Flux density in air gap on values φ, determined by currents of corresponding windings
$B_{ROT}[F(m, n, \omega_{ROT}), k]$	Flux density harmonic amplitude of short-circuited rotor winding in air gap
$B_{ST}[F(m, Q), k]$	Flux density harmonic amplitude corresponding to stator currents
$F_{EX}(n, \omega_{ROT})$	MMF harmonic amplitude of excitation winding currents
$F_W(\varphi)$	MMF in the range of values φ, determined by currents in corresponding winding
$F_{ROT}(m, n, \omega_{ROT})$	MMF harmonic amplitude of short-circuited rotor winding
$F_{ST}(m, Q)$	MMF harmonic amplitude of order m corresponding to currents in stator winding of time order Q
k	Order of rotor flux density harmonic
k_{CAR}	Carter's factor
k_{SAT}	Magnetic circuit saturation factor
m	Order of stator MMF harmonics
m_{PH}	Number of stator winding phases
n	Order of rotor MMF harmonics
p	Number of pole pairs in machine
S_{SL}	Slip
t	Time
T, T_{EL}	Period of MMF and fields in air gap
W_{EX}	Number of excitation winding turns (per pole)
α	Relative pole width ($\alpha = b_p/\tau$) where b_p—width of pole shoe, τ—pole pitch
$\delta_{MAX}, \delta_{MIN}$	Maximum and minimum values of air gap under pole
δ_{EQ}	Equivalent air gap
$\delta(\varphi)$	Relationship of air gap and angular coordinate
μ_0	Magnetic permeability of air
φ	Angular coordinate along stator boring $\left(\varphi = \frac{2\pi x}{T}\right)$
$\omega_{BOR,R}$	Angular rotation speed in air gap of rotor field components
$\omega_{BOR,ST}$	Angular rotation speed in air gap of stator field components
ω_1	Network circular frequency
ω_{REV}	Angular speed of rotor rotation
ω_{ROT}	Frequency of rotor current and EMF

References

I Monographs, textbooks

1. Demirchyan K.S., Neyman L.R., Korovkin N.V., Theoretical Electrical Engineering. Moscow, St.Petersburg: Piter, 2009. Vol. 1, 2. (In Russian).
2. Kuepfmueller K., Kohn G., Theoretische Elektrotechnik und Elektronik. 15 Aufl. Berlin, New York: Springer. 2000. (In German).
3. Richter R., Elektrische Maschinen. Berlin: Springer. Band I, 1924; Band II, 1930; Band III, 1932; Band IV, 1936; Band V, 1950. (In German).
4. Mueller G., Ponick B., Elektrische Maschinen. New York, John Wiley, 2009. - 375 S. (In German).
5. Schuisky W., Berechnung elektrischer Maschinen. Wien: Springer, 1960. (In German).
6. Mueller G., Vogt K., Ponick B., Berechnung elektrischer Maschinen. Springer, 2007. 475 S. (In German).
7. Concordia Ch. Synchronous Machines, Theory a. Performance. New York: John Wiley, 1951.
8. Ruedenberg R., Elektrische Schaltvorgaenge. Berlin, Heidelberg, New York: Springer, 1974. (In German).
9. Lyon V., Transient Analysis of A.C. Machinery. New York: John Wiley, 1954.
10. Korn G., Korn T., Mathematical Handbook. New York: McGraw–Hill, 1961.
11. Jeffris H., Swirles B., Methods of Mathematical Physics. Third Edition, Vol. 1 – Vol. 3, Cambridge: Cambridge Univ. Press, 1966.
12. Boguslawsky I.Z., A.C. motors and generators. The theory and investigation methods by their operation in networks with non linear elements. Monograph. TU St.Petersburg Edit., 2006. Vol. 1; Vol.2. (In Russian).

III. Synchronous machines. Papers, inventor's certificates, patents

13. Boguslawsky I.Z., Operating – regime currents of a salient – pole machine. Power Eng. (New York), 1982, № 4.
14. Boguslawsky I.Z., Currents and harmonic MMFs in a damper winding with damaged bar at a pole. Power Eng. (New York), 1985, № 1.
15. Polujadoff M., General rotating MMF – Theory of squirrel cage induction machines with non-uniform air gap and several non-sinusoidally distributed windings. Trans AIEE, PAS, 1982.

Chapter 14
System of Equations for Magnetically Coupled Loops for A.C. Machine in Nonlinear Network

This chapter determines a system of equations for magnetically coupled loops of A.C. machine in nonlinear network. From this system for various operational modes are calculated the values of stator phase voltages and currents, complex amplitudes of resulting field in air gap, and also the distribution of currents in machine rotor loops. As a result, are determined copper losses in these loops, their overheats, core losses and other machine technical and economic indicators. Representation in the form of generalized characteristics of fields in short-circuited rotor loops (damper winding, squirrel cage) allows formulating the system, so that its order does not depend on the number of short-circuited loops in rotor.

For setting a system of equations, there is offered a method selecting time and spatial harmonics based on physical representations determined by non-sinusoidal power supply of machines. It allows us to formulate a basic system of equations considering physical processes in machine caused by higher "adjacent" time harmonics and the first spatial harmonic of resulting field in air gap. A series of higher spatial harmonics for this system formulation is introduced in the calculation by expansion of basic system at the expense of increase in number of unknowns (currents, voltages and complex amplitudes of flux density) with corresponding increase in order of this system. Practical examples are given. The system allows us to determine the mode with reduced values of currents and losses in rotor loops. The content of this chapter is development of the methods stated in [7, 8].

14.1 Problem Setting

In this chapter we formulate a system of equations for magnetically coupled loops of A.C. machines with short-circuited rotor loops for synchronous machines; the simple modification of this system can be used for induction machines also; in this

I. Boguslawsky et al., *Large A.C. Machines*,
DOI 10.1007/978-4-431-56475-1_14

system of equations we take into account currents distribution in damper winding elements or in squirrel cage with damage or without it.

Requirements to the magnetically coupled loops which create the magnetic field in air gap, were given earlier; these loops are determined by:

- identical orders of spatial field harmonics in air gap;
- identical rotation speeds of these fields relative to stator boring.

14.2 Selection Method of Magnetically Coupled Loops for System of Equations

Selection criteria and procedure of stator and rotor magnetically coupled loops for a system of equations can differ; expressions necessary for such selection were obtained in Chap. 3. For example, for a synchronous machine in network with non-sinusoidal voltage and with the frequency of the first harmonic (Q = 1) is f = 50 Hz, and it is sufficient to assume a combination of harmonics: Q = 1, m = 7 and to obtain EMF with frequency f_{ROT} = 300 Hz in rotor loops. Currents at this frequency induce EMF in stator winding loops with frequencies, $f_{ST,1}$ = 50 Hz (Q = 1) and $f_{ST,2}$ = 650 Hz (Q_{DIR} = 13). Rotor and stator loops determined by the harmonic of spatial order m = 7 are magnetically coupled. Such selection should be considered as arbitrary, random: it does not take into account the fact that with growth of time and spatial harmonics orders, the amplitudes of EMF, currents and MMF decrease. In this monograph in selection of magnetically coupled loops we will proceed from physical representations connected with processes in the machine fed by non-sinusoidal power. From regularities determined in Chap. 3, in particular, those fields in air gap determined by time harmonics of orders Q_{DIR}, Q_{AD} and the same spatial order m_{DIR} induce in rotor loops EMF of identical frequency:

$$\omega_{ROT}(Q_{DIR}, m_{DIR}) = \omega_{ROT}(Q_{AD}, m_{DIR}) \tag{14.1}$$

provided that the numbers of both time harmonics (Q_{AD}, Q_{DIR}) satisfy the ratio:

$$|Q_{DIR} - Q_{AD}| = 2m_{DIR}. \tag{14.2}$$

Similarly, it was obtained that

$$\omega_{ROT}(Q_{DIR}, m_{AD}) = \omega_{ROT}(Q_{AD}, m_{AD}) \tag{14.3}$$

provided that the numbers of both time harmonics (Q_{AD}, Q_{DIR}) satisfy the ratio:

$$|Q_{DIR} - Q_{AD}| = 2m_{AD}. \tag{14.4}$$

It is convenient to use these regularities in calculation practice as they allow one to determine in certain sequence the influence of harmonics with the highest amplitude on machine processes, for example, harmonics of order $Q_{AD} = 5$, $Q_{DIR} = 7$ (for machine with number of phases $m_{PH} = 3$), or harmonics of order $Q_{AD} = 11$, $Q_{DIR} = 13$ (for machine with number of phases $m_{PH} = 6$). As a result, for this method of selecting magnetically coupled loops, we obtain two "adjacent" stator loops satisfying the ratios (14.2 or 14.4), and only one rotor loop as per (14.1 or 14.3).

14.3 Features of System of Equations for Magnetically Coupled Loops

A system of equations for magnetically coupled loops for calculation of performance data of DFMs with frequency converter in its rotor was formulated in Chap. 2. Peculiarities of equations of this system consist in the fact that for the determination of current in each phase it is sufficient to specify its impedance as for winding with lumped parameters. It enabled us to determine machine performance data not only for the first time harmonic ($Q = 1$), but also for higher harmonics ($Q > 1$) caused by the frequency converter in rotor circuit. Similar problem was solved in Chap. 4 where the calculation method was stated for performance data of high-power induction motor with short-circuited rotor with nonlinear parameters. Peculiarities of a system of equations for magnetically coupled loops of this motor consist in the fact that the short-circuited rotor winding was represented in the form of equivalent phase, similar to DFMs, therefore, for the determination of its current it is sufficient to specify its impedance as for winding with lumped parameters. As an example of both machines we have provided a concept of generalized characteristic of rotor winding currents and MMFs.

In this chapter let us formulate a system of equations for magnetically coupled loops to solve a more general problem using these characteristics of currents and MMFs. Let us note that it accounts for the distribution of currents in damper winding elements of various construction (regular, irregular) or in squirrel cage (with damage or without it).

For its solution, the followings are assumed:

- machine rotor speed and rotation direction are determined by the first time ($Q = 1$) and the first spatial ($m = 1$) harmonics;
- higher time harmonics differ not only in amplitudes; generally, they can also differ in initial phase angles;
- calculation expressions for flux density complex amplitudes (phasors) in air gap of induction machines can be obtained in two ways: either from expressions for MMF determined for asymmetrical squirrel cage of induction machines in

Chap. 12 or from equations for MMF of damper winding of salient pole machines from the same chapter by setting for it relative pole width $\alpha = 1$;
- for specified constructions of short-circuited rotor windings the number of system equations does not depend on the number of loops in these windings;
- stator winding—three-phase ($m_{PH} = 3$), connection scheme—star. The system of equations for winding with $m_{PH} = 6$ is formulated similarly;
- excitation winding is considered using generalized characteristics, as well as damper winding.

We note that when defining a system of equations, the orders of stator "adjacent" time harmonics are designated by Q_1 and Q_2 ($Q_1 \neq Q_2$); they correspond to signs $S = 1$ and $S = 2$ according to Chap. 3.

14.4 Basic System of Equations for Magnetically Coupled Loops

14.4.1 Formulation of System; Initial Data and Results

Analysis of EMF and currents in magnetically coupled loops performed on the basis of results obtained in the previous chapters specifies ways for practical calculations of machine characteristics in nonlinear network. Each couple of stator loops with two EMFs of various frequencies induced in them by fluxes of "adjacent" time harmonics, and corresponding rotor loops with EMF of only one frequency induced by these fluxes form a group of magnetically coupled loops; this group is connected with other similar groups of loops with common frequency in rotor loops (Table 3.4 in Chap. 3). Practical need to account these groups is determined by their MMF harmonics orders and can be estimated preliminarily. This leads to a practical method of accounting time harmonics of order $Q > 1$ and spatial one of order $m > 1$. For its realization, let us determine a concept on basic system of equations of magnetically coupled loops and further show how on its basis by expanding order of this system, i. e. by increasing number of equations, to consider additional harmonics if they are of practical interest (Appendix 14.1). It should be noted, thus, that when using a basic system of equations, it is possible to estimate intermediate results. For example, in the calculation of losses in loops, it is possible to determine whether there is a need of further increase in harmonics order, or it is possible to finish the calculation with number of harmonics already accounted.

Let us determine a basic system of equations with the following values assumed:

- number of phases $m_{PH} = 3$;
- harmonic amplitude of line voltage (phasor) between phases A and B in network $U_{Q,AB}$ of order Q_1; nonlinear network is supposed to be symmetrical;

- frequency $\omega_{ST} = Q_1\omega_1$ of this voltage harmonic; ω_1—frequency of the first voltage harmonic;
- line voltage harmonic amplitude (phasor) between phases A and B of network $U^{(2)}_{Q,AB}$ of order Q_2;
- frequency $\omega^{(2)}_{ST} = Q_2\omega_1$ of this voltage harmonic;
- rotor rotation speed ω_{REV}; number of pole pairs p;
- order of spatial harmonic m = 1;
- A.C. resistances and leakage reactances of stator windings, short-circuited rotor winding elements, rotor excitation winding (for salient pole machines), and also network elements, external relative to machine terminals;
- geometrical dimensions of machine active part;
- generalized characteristics of currents for each element of rotor loops, generalized characteristics of MMF and fields of currents in these loops.
- The problem consists in determining the following 14 values:
- three amplitudes of phase voltage harmonics $U_{Q,A}, U_{Q,B}, U_{Q,C}$ with frequency $\omega_{ST} = Q_1\omega_1$;
- three amplitudes of phase current harmonics $I_{Q,A}, I_{Q,B}, I_{Q,C}$ with frequency $\omega_{ST} = Q_1\omega_1$;
- three amplitudes of stator phase voltage harmonics $U^{(2)}_{Q,A}, U^{(2)}_{Q,B}, U^{(2)}_{Q,C}$ with frequency $\omega^{(2)}_{ST} = Q_2\omega_1$;
- three amplitudes of stator phase current harmonics $I^{(2)}_{Q,A}, I^{(2)}_{Q,B}, I^{(2)}_{Q,C}$ with frequency $\omega^{(2)}_{ST} = Q_2\omega_1$;
- two flux density amplitude components of resulting field in air gap: $B(m,Q_1)$ and $B(-m,Q_2)$;

In addition, as a result of system solution, the distribution of currents in short-circuited elements of rotor loops is also determined using their generalized characteristics.

For the calculation of machine operation mode, it is necessary to find these 14 unknowns from the system of equations of 14th order for magnetically coupled loop. Let us note that the right part of this system of equations providing a nonzero solution for unknown currents and resulting field flux density values contains line voltages of "adjacent" harmonics: $U_{Q,AB}, U^{(2)}_{Q,AB}, U_{Q,BC}, U^{(2)}_{Q,BC}$. The system can be simplified by forming equations only for one of phases; then the number of unknowns and, respectively, system order can be reduced. However, when defining a system of equations only for one phase, it cannot be used as a basis for solution of number of important practical problems, for example, caused by asymmetry in generator nonlinear load etc. Besides, realization of the system in given form allows us to check in addition correctness of solution results, for example, by checking phase shift angle of currents, shift angle between currents and voltages in each phase, etc. When selecting the type of a system of equations it is considered that its realization assumes a numerical (but not analytical) solution.

14.4.2 Calculation Expressions for Flux Density Harmonics Complex Amplitudes Flux Density (Phasors) of Rotor and Stator Loops $|m| = |n| = |k| = 1$

To write down coefficients of the basic system of equations, we use calculation expressions for complex amplitudes of field harmonics found in the previous chapter. Let us obtain from them calculation expressions for special case – harmonics of orders $|m| = |n| = |k| = 1$.

14.4.3 Calculation Expressions for Complex Amplitudes of Rotor Winding Harmonics Flux Density at $|m| = |n| = |k| = 1$

Based on general expressions found in the previous chapter for flux density harmonics of rotor loops, we obtain:

$$
\begin{aligned}
B^{(I)}_{ROT}(m,n,k,\omega_{ROT}) &= \frac{\mu_0\alpha}{\delta_{EQ}k_{CAR}k_{SAT}}F_{ROT}(m,n,\omega_{ROT}) \\
&\quad + \frac{-\mu_0}{\delta_{EQ}\pi k_{CAR}k_{SAT}}F_{ROT}(m,-n,\omega_{ROT})\sin(\pi\alpha). \\
B^{(II)}_{ROT}(m,n,-k,\omega_{ROT}) &= \frac{-\mu_0}{\delta_{EQ}\pi k_{CAR}k_{SAT}}F_{ROT}(m,n,\omega_{ROT})\sin(\pi\alpha) \\
&\quad + \frac{\mu_0\alpha}{\delta_{EQ}k_{CAR}k_{SAT}}F_{ROT}(m,-n,\omega_{ROT}). \\
B^{(III)}_{ROT}(-m,n,k,\omega_{ROT}) &= \frac{\mu_0\alpha}{\delta_{EQ}k_{CAR}k_{SAT}}F_{ROT}(-m,n,\omega_{ROT}) \\
&\quad + \frac{-\mu_0}{\delta_{EQ}\pi k_{CAR}k_{SAT}}F_{ROT}(-m,-n,\omega_{ROT})\sin(\pi\alpha). \\
B^{(IV)}_{ROT}(-m,n,-k,\omega_{ROT}) &= \frac{-\mu_0}{\delta_{EQ}\pi k_{CAR}k_{SAT}}F_{ROT}(-m,n,\omega_{ROT})\sin(\pi\alpha) \\
&\quad + \frac{\mu_0\alpha}{\delta_{EQ}k_{CAR}k_{SAT}}F_{ROT}(-m,-n,\omega_{ROT}).
\end{aligned}
\tag{14.5}
$$

14.4.4 Calculation Expressions for Complex Amplitudes of Stator Winding Harmonics Flux Density at $|m| = |n| = |k| = 1$

Some of them were already given in Sect. 13.3.6 for their check and verification of correctness. Here let us give calculation expressions completely.

$$
\begin{aligned}
B_{ST}^{(I)}(m,k,Q_1) &= \frac{\mu_0\alpha}{\delta_{EQ}k_{CAR}k_{SAT}}F_{ST,RES}(m,Q_1),\\
B_{ST}^{(I)}(m,-k,Q_1) &= \frac{-\mu_0}{\delta_{EQ}\pi k_{CAR}k_{SAT}}F_{ST,RES}(m,Q_1)\sin(\pi\alpha),\\
B_{ST}^{(III)}(-m,k,Q_2) &= \frac{-\mu_0}{\delta_{EQ}\pi k_{CAR}k_{SAT}}F_{ST,RES}(-m,Q_2)\sin(\pi\alpha),\\
B_{ST}^{(IV)}(-m,-k,Q_2) &= \frac{\mu_0\alpha}{\delta_{EQ}k_{CAR}k_{SAT}}F_{ST,RES}(-m,Q_2).
\end{aligned}
\tag{14.6}
$$

14.4.5 Result Summary: Calculation Expressions for Complex Amplitudes; Field Speeds in Air Gap

To formulate a system of equations of magnetically coupled loops, it is expedient to represent results of investigating fields in the table with indication of rotation speeds in air gap ω_{ROT}. Such a result summary facilitates formation and checking separate equations of system.

Here $B(m, Q_1)$, $B(-m, Q_2)$—complex amplitudes of flux density components of resulting field in air gap. Using this table, it is possible to proceed to the formation of equations. However, it is, as previously, expedient to estimate the ratio between separate components of complex amplitudes.

Note. As it was already stated in Chaps. 4–13, generalized characteristics of currents in short-circuited rotor winding elements, and generalized characteristics of MMF and field of these currents in air gap are not put into square brackets for the purpose to simplify designations: in these chapters, the theory and methods of their investigation are stated. However, in this chapter we start with the formation of a system of equations of magnetically coupled loops; therefore, we will retain designations of these characteristics using square brackets.

14.4.6 Comparative Assessment of Separate Components of Complex Amplitudes (Phasors)

We note first that the obtained results confirm physical ideas of generating fields of higher time harmonics in air gap for rotating salient pole rotor, that is, in case when they move in gap with certain speed and not synchronously with rotor (calculation expressions for these speeds are calculated earlier). Each of expressions for rotor flux density harmonics, for example $\left[B_{ROT}^{(I)}(m,n,\omega_{ROT}),k\right]$, contains two components. At first, let us estimate share of each of them for machine with relative pole width $\alpha \to 1$; in limit this construction of short-circuited winding can be considered as squirrel cage ($\alpha = 1$). Then, the first summand in the expression for

amplitude $\left[B^{(I)}_{ROT}(m,n,\omega_{ROT}),k\right]$ becomes proportional to $\alpha F_{ROT}(m,n,\omega_{ROT}) \rightarrow F_{ROT}(m,n,\omega_{ROT})$; the second—proportional to $\frac{-F_{ROT}(m,-n,\omega_{ROT})}{\pi}\sin(\pi\alpha)$, it has negative phase in comparison with the first one and tends to zero at $\alpha \rightarrow 1$ that proves the obtained results.

It is easy to show that in practical problems [1–3] at relative pole width within $0.667 < \alpha < 0.8$, the absolute value of the second summand is less than the first one, so their ratio makes:

$$\text{at } \alpha < 0.8: \left|\frac{\sin(\pi\alpha)}{\pi\alpha}\right| > 0.234K_f;$$
$$\text{at } \alpha < 0.667: \left|\frac{\sin(\pi\alpha)}{\pi\alpha}\right| < 0.4135K_f,$$

where K_f—ratio of MMFs in corresponding summands; for salient pole machines usually $K_f < 0.5–0.6$.

The same is also true for other expressions for rotor flux density harmonics, for example, $\left[B^{(III)}_{ROT}(-m,n,\omega_{ROT}),k\right]$; the field with this amplitude rotates in air gap with the same speed relative to stator, as $\left[B^{(I)}_{ROT}(m,n,\omega_{ROT}),k\right]$.

Thus, in comparison with induction machines, the field in air gap formed by currents in salient pole machine rotor loops contains additional components determined by the value of relative pole width α; their amplitude is less than that of the main components.

The structure of calculation ratios for complex amplitudes of stator flux density harmonics is obtained in the form similar to that of calculation ratios for rotor. Therefore, the obtained ratios between separate flux density components can be estimated similarly.

14.5 System of Magnetically Coupled Loops Equations [7, 8]

For clarity, equations are formulated for motor mode at $p\omega_{REV} < \omega_1$. At $p\omega_{REV} \geq \omega_1$ and for generator mode they are determined similarly.

14.5.1 Equations for the First System of Loops Determined by EMF Frequency $\omega_{ST} = Q_1\omega_1$

Three equations for voltage $U_{Q,A}$ of phase A, $U_{Q,B}$ of phase B, and $U_{Q,C}$ of phase C are obtained under the second Kirchhoff's law [4, 5]:

$$
\begin{aligned}
&-U_{Q,A} + k_1 I_{Q,A} + k_2 B(m, Q_1) e^{\frac{-j2\pi x}{T_{EL}}} = 0,\\
&-U_{Q,B} + k_1 I_{Q,B} + k_2 B(m, Q_1) e^{\frac{-j2\pi x}{T_{EL}} - \frac{j2\pi}{3}} = 0,\\
&-U_{Q,C} + k_1 I_{Q,C} + k_2 B(m, Q_1) e^{\frac{-j2\pi x}{T_{EL}} - \frac{j4\pi}{3}} = 0.
\end{aligned}
$$

One equation for currents in phases under the first Kirchhoff's law [4, 5]:

$$I_{Q,A} + I_{Q,B} + I_{Q,C} = 0.$$

Two coupling equations between line and phase voltages [4, 5]:

$$U_{Q,A} - U_{Q,B} = \left|U_{Q,AB}\right| e^{\frac{j\pi}{6}}, \quad U_{Q,B} - U_{Q,C} = \left|U_{Q,BC}\right| e^{-\frac{j\pi}{2}}.$$

Here, the following additional designations are accepted:

$$k_1 = R_{ST} K_F(Q_1) + j\omega_{ST} L_{ST}; \quad k_2 = j\omega_{ST} W_{PH} K_{W(m=1)} T_{EL} \frac{L_{COR}}{\pi}.$$

here R_{ST}—A.C. resistance of stator winding phase; $K_F(Q_1)$—Field's factor [1–3] calculated for frequency ω_{ST}; $\omega_{ST} = Q_1\omega_1$—EMF frequency of time harmonic of order Q_1; L_{ST}—leakage inductance of stator phase winding; W_{PH}—number of turns in phase; $K_{W(m=1)}$—winding factor for field harmonic of order m = 1; $T_{EL}\frac{\pi D}{p}$—field harmonic period of order m = 1; D—stator boring diameter; p—number of pole pairs in machine; L_{COR}—core calculation length [1–3].

As a result, we obtain six equations for the first system of loops determined by EMF frequency $\omega_{ST} = Q_1\omega_1$.

14.5.2 *Equations for the $\omega_{ST}^{(2)} = Q_2\omega_1$ Second System of Loops Determined by EMF Frequency*

Three equations for voltage $U_{Q,A}^{(2)}$ of phase A, $U_{Q,B}^{(2)}$ of phase B, and $U_{Q,C}^{(2)}$ of phase C are obtained under the second Kirchhoff's law [4, 5]:

$$
\begin{aligned}
&-U_{Q,A}^{(2)} + k_6 I_{Q,A}^{(2)} + k_7 B(-m, Q_2) e^{\frac{j2\pi x}{T_{EL}}} = 0,\\
&-U_{Q,B}^{(2)} + k_6 I_{Q,\hat{A}}^{(2)} + k_7 B(-m, Q_2) e^{\left(\frac{j2\pi x}{T_{EL}} + \frac{j2\pi}{3}\right)} = 0,\\
&-U_{Q,\tilde{N}}^{(2)} + k_6 I_{Q,\tilde{N}}^{(2)} + k_7 B(-m, Q_2) e^{\left(\frac{j2\pi x}{T_{EL}} + \frac{j4\pi}{3}\right)} = 0.
\end{aligned}
$$

One equation for currents in phases under the first Kirchhoff's law:

$$I^{(2)}_{Q,A} + I^{(2)}_{Q,B} + I^{(2)}_{Q,C} = 0.$$

Two coupling equations between line and phase voltages:

$$U^{(2)}_{Q,A} - U^{(2)}_{Q,B} = \left|U^{(2)}_{Q,AB}\right| e^{\frac{j\pi}{6}} e^{-jT_U}, \quad U^{(2)}_{Q,B} - U^{(2)}_{Q,C} = \left|U^{(2)}_{Q,BC}\right| e^{-\frac{j\pi}{2}} e^{-jT_U}.$$

Here, the following additional symbols are accepted:

$$K_6 = [R_{ST}K_F(Q_2) + R_{LOAD}] + j\omega^{(2)}_{ST}(L_{ST} + L_{LOAD});$$
$$K_7 = j\omega^{(2)}_{ST} W_{PH} K_{W(m=1)} T_{EL} \frac{L_{COR}}{\pi};$$

here R_{LOAD}, L_{LOAD}—respectively A.C. resistance and inductance of load, external relative to machine terminals; $K_F(Q_2)$—Field's factor calculated for frequency $\omega^{(2)}_{ST}$; $\omega^{(2)}_{ST} = Q_2\omega_1$—EMF frequency of time harmonic of order of Q_2; T_U—difference of initial phase angles between line voltages and frequencies ω_{ST} and $\omega^{(2)}_{ST}$.

As a result, we obtain six equations for the second system of loops determined by EMF frequency $\omega^{(2)}_{ST} = Q_2\omega_1$.

14.5.3 *Coupling Equations Between Both Systems of Stator Loops Determined by EMF of These Loops with Frequencies ω_{ST} and $\omega^{(2)}_{ST}$*

Physically, these coupling equations correspond to the Ampere's law [4, 5]: this law establishes a relation between MMF and fluxes in air gap, created by:

- currents in stator loops with frequency ω_{ST}, induced by currents in the same loops with frequency $\omega^{(2)}_{ST}$;
- currents in rotor loops with frequency ω_{ROT}, induced by both rotating resulting fields in air gap.

According to the Ampere's law we have the following two equations; these equations are formulated based on Table 14.1.

The first equation corresponds to the resulting field which rotates in air gap with the speed $\omega^{(I)}_{BOR} = \frac{Q_1\omega_1}{p}$.

$$\begin{aligned} &B_{ST}^{(I)}(m,k,Q_1) + B_{ST}^{(III)}(-m,k,Q_2) + \left[B_{ROT}^{(I)}(m,n,\omega_{ROT}),k\right] \\ &\quad \times B(m,Q_1) + \left[B_{ROT}^{(III)}(-m,n,\omega_{ROT}),k\right] B(-m,Q_2) = B(m,Q_1) \end{aligned} \qquad (*)$$

The second equation corresponds to the resulting field which rotates in air gap with speed $\omega_{BOR}^{(II)} = -Q_2 \frac{\omega_1}{p}$.

$$\begin{aligned} &B_{ST}^{(II)}(m,-k,Q_1) + B_{ST}^{(IV)}(-m,-k,Q_2) + \left[B_{ROT}^{(II)}(m,n,\omega_{ROT}),-k\right] \\ &\quad \times B(-m,Q_2) + \left[B_{ROT}^{(IV)}(-m,n,\omega_{ROT}),k\right] B(m,Q_1) = B(-m,Q_2) \end{aligned} \qquad (**)$$

Let us note that in these coupling equations the value of complex amplitudes $B(m, Q_1), B(-m, Q_2)$ of resulting field in air gap are conditionally presented in the form of the right parts: they are unknown too and are determined from the system of equations. This condition is caused by convenience to show peculiarities of coupling equations with account of higher spatial harmonics in the system of equations of several magnetically coupled loops given in Appendix 14.1.

As a result, we obtain a system of 14 equations with 14 unknowns. It should be noted that generalized characteristics should be included as coefficients in the last two equations corresponding to field currents in rotor loops for example $\left[B_{ROT}^{(II)}(m,n,\omega_{ROT}),-k\right]$. In comparison with the excitation winding closed on the exciter armature resistance, the damper winding plays the main role in the creation of rotor loops field. However, in calculations of salient pole machines, if necessary, it is also easy to consider the influence of excitation winding. For this purpose, it is necessary to find the sum of corresponding generalized characteristics: of short-circuited winding and excitation winding and to use it as coefficient in these two equations instead of generalized characteristic of short-circuited winding. Expressions for generalized characteristics of excitation winding are obtained and analyzed in Chap. 13 for general case and for special case: $|m| = |n| = |k| = 1$.

14.5.4 Peculiarities of Basic System of Equations [6]

One of peculiarity of the presented system of equations for magnetically coupled loops is that the system considers currents distribution in elements of short-circuited rotor loops, for example, of damper winding (regular or irregular). It was achieved by means of generalized characteristics of fields in these short-circuited rotor loops.

Other peculiarity consists in the fact that this system can be formulated in such a way that its order does not depend on the number of short-circuited rotor loops; therefore, it is rather simply realized by a numerical method.

Table 14.1 Flux density complex amplitudes of stator and rotor magnetically coupled loops

Direction of rotor rotation and resulting field in air gap	Rotation speed of resulting field in air gap	Flux density complex amplitude of rotor loops	Flux density complex amplitude of stator loops
Coincides	$\omega_{BOR}^{(I)} = \frac{Q_1\omega_1}{p}$	$\left[B_{ROT}^{(I)}(m,n,\omega_{ROT}),k\right]B(m,Q_1)$ $+\left[B_{ROT}^{(III)}(-m,n,\omega_{ROT}),k\right]B(-m,Q_2)$	$B_{ST}^{(I)}(m,k,Q_1)$ $+B_{ST}^{(III)}(-m,k,Q_2)$
Opposite	$\omega_{BOR}^{(II)} = \frac{-Q_2\omega_1}{p}$	$\left[B_{ROT}^{(II)}(m,n,\omega_{ROT}),-k\right]B(-m,Q_2)$ $+\left[B_{ROT}^{(IV)}(-m,n,\omega_{ROT}),k\right]B(m,Q_1)$	$B_{ST}^{(II)}(m,-k,Q_1)$ $+B_{ST}^{(IV)}(-m,-k,Q_2)$

Let us note that after calculating from this system of equations for flux density complex amplitudes $B(m,Q_1)$ and $B(-m,Q_2)$ of resulting field in air gap, it is also easy to find the distribution of currents in elements of short-circuited rotor loops. For this purpose, it is enough to use generalized characteristics of currents in elements of these loops. This is one more peculiarity of this system.

Selection method of time and spatial harmonics is based on physical representations determined by non-sinusoidal power supply of machines.

It is convenient to use it for compiling a basic system of equations with account of physical processes in machine caused by higher "adjacent" time harmonics and first spatial harmonic of resulting field in air gap. Higher time and spatial harmonics for this system formulation are introduced in the calculation by expansion of a basic system at the expense of increase in number of unknowns (currents, voltages and complex amplitudes of flux density) with corresponding increase in order of this system.

As a result of system solution, are determined: distribution of currents in loops of machine, phase voltages and values of complex amplitudes of resulting field in air gap. It allows one to determine losses in these loops, their overheats, core losses and other technical and economic indicators. The system enables us to determine the mode with reduced values of currents and losses in rotor loops.

Appendix 14.1: Accounting Higher Spatial Harmonics in a System of Equations of Magnetically Coupled Loops

Let us consider a method of expanding the basic system of equations for accounting higher spatial harmonics. We turn our attention, for example, again to Table 3.4 of Chap. 3 where synchronous mode was considered for salient pole frequency-controlled machines. In this table are given four groups of magnetically coupled loops No. 1–No. 4; they are consolidated by common EMF frequency in

rotor loops: $\omega_{ROT} = 6\omega_1$. Loops No. 1 and No. 2 correspond to spatial order $m_{DIR} = 1$, and loops No. 3 and No. 4 to order $m_{DIR} = 7$.

Currents, voltages and complex amplitudes for groups of loops No. 1 and No. 2 are determined by equations of basic system given in Sect 14.5. It contains 14 equations with 14 unknowns and considers spatial harmonics in rotor and stator loops of order $m_{DIR} = 1$ (see 14.5.1–14.5.3). Let us note that the calculation of rotor currents with frequency f = 300 Hz assumes that the distribution of these currents is found for EMF period equal to T; complex amplitudes of MMF and flux density harmonics are found from their distribution curve according to methods given in Chaps. 12 and 13, herewith, expansion period of this distribution curve is also equal to T.

We proceed to groups of loops No. 3 and No. 4 ($m_{DIR} = 7$). Peculiarities of time harmonics of orders Q_{DIR} = 1 and Q_{DIR} = 13 at m_{DIR} = 7 were considered in Chap. 3; the equations defining these peculiarities are marked by sign (*). They consist in the fact that both time harmonics at m_{DIR} = 7 correspond to sign S = 1 entered in Chap. 3. Let us list additional unknowns in determining the spatial harmonic m_{DIR} = 7:

- three phase currents of stator and three phase voltages of stator; their frequency f = 50 Hz. (Q_{DIR} = 1);
- three phase currents of stator and three phase voltages of stator; their frequency f = 650 Hz. (Q_{DIR} = 13);
- two components of complex amplitudes of field induction in air gap.

These 14 unknowns are determined from the system of equations similar to the basic one (see 14.5.1, 14.5.3). Let us note that the calculation of rotor currents with frequency f = 300 Hz assumes that the distribution of these currents is found for EMF period equal to $\frac{T}{m_{DIR}} = \frac{T}{7}$; complex amplitudes of MMF and flux density harmonics are found from their distribution curve according to methods given in Chaps. 12 and 13, herewith, expansion period of this distribution curve is also equal to T/7.

We consider peculiarities of physical process at simultaneous currents flow in groups of magnetically coupled loops No. 1 – No. 4; they are consolidated by common EMF frequency in rotor loops: $\omega_{ROT} = 6\omega_1$, i. e. f = 300 Hz. It is noted above that complex amplitudes of MMF and flux density harmonics in a basic system for group of loops No. 1, No. 2 are found for the expansion period equal to T. However, complex amplitudes of MMF harmonics and of flux density harmonics for currents of this group, are calculated with the expansion period $\frac{T}{m_{DIR}} = \frac{T}{7}$.

As a result, we obtain that in air gap there is the additional resulting field of rotor currents with period equal to T/7. This field corresponds in rotor loops to EMF and currents with frequency f = 300 Hz, which is characterized by two complex amplitudes of flux density.

From this point of view, groups of magnetically coupled loops No. 1 and No. 2 (with stator frequencies f = 250 Hz and f = 350 Hz) and loops No. 3 and No. 4

(with stator frequencies f = 50 Hz and f = 650 Hz) can be considered as electromechanical energy converter.

As stated above it follows that both systems of equations should be added with two more equations; each of them is determined by rotor current with frequency f = 300 Hz in the form of flux density components sum for loop groups No. 1, No. 2 and No. 3, No. 4 with identical period equal to T, T/7. Thus, with account of harmonics of order $m_{DIR} = 7$ we obtain except for 14 unknowns of the basic system additional 16 unknowns; the order of system of equations in comparison with that of the basic is increased to 30.

The stated method of accounting higher harmonics by expansion of the basic system of equations is simple and based on physical representations of processes in machine with non-sinusoidal power supply. Calculation practice shows that before further expansion of this system by including each next group of higher harmonics, it is expedient to make assessment of this expansion. For example, losses in machine rotor and stator windings can be chosen as assessment criteria. Considering that with harmonics order growth, MMF and flux density amplitudes decrease, and the increment of these losses will also decrease; respectively, the expansion extent of basic system of equations is determined in the selection of this criterion by calculation accuracy of losses set preliminarily. This practical assessment allows us to limit the number of harmonics used for the calculation.

Brief Conclusions

1. The system of equations is formulated to calculate operation modes; in its realization are determined values of phase voltages and currents, complex amplitudes of resulting field in air gap, and also the distribution of currents in elements of short-circuited rotor windings of machine (damper winding with damage or without it, etc.). These values allow us to determine losses in rotor and stator loops and other technical and economic indicators.
2. Representation in the form of generalized characteristics of fields in short-circuited rotor loops (damper winding, squirrel cage with demage or without it) enables us to formulate a system so that its order does not depend on the number of short-circuited loops in rotor.
3. For setting a system of equations, the method of selection of time and spatial harmonics based on physical representations determined by nonsinusoidal power supply of machine is offered. It allows us to formulate the basic system of equations considering physical processes in machine caused by higher "adjacent" time harmonics and the first spatial harmonic of resulting field in air gap.
4. Higher spatial harmonics for this system formulation are introduced in the calculation by expansion of the basic system at the expense of increase in number of unknowns (currents, voltages and complex amplitudes of flux density) with corresponding increase in order of this system.

List of symbols

$B(m,Q)$	Flux density amplitude component of resulting field in air gap
$B_{ROT}(m, n, k, \omega_{ROT})$	Flux density harmonic amplitude in air gap of currents in short-circuited rotor winding
$F_{ROT}(m, n, \omega_{ROT})$	MMF harmonic amplitude of currents in short-circuited rotor winding
$F_{ST}(m, Q)$	MMF harmonic amplitude of order m corresponding to currents in stator winding of time order Q
f_{ROT}	Frequency of EMF and rotor currents
f_{ST}	Frequency of EMF and stator currents
$I_{Q,A}, I_{Q,B}, I_{Q,C}$	Harmonic amplitudes of order Q of stator phase current
k	Order of rotor field induction harmonics
k_{CAR}	Carter's factor
k_{SAT}	Magnetic circuit saturation factor
m	Order of stator MMF spacial harmonics
m_{PH}	Number of stator winding phases
n	Order of rotor MMF harmonics
p	Number of pole pairs
Q	Order of stator current time harmonic
$U_{Q,A}, U_{Q,B}, U_{Q,C}$	Amplitudes of machine phase voltage harmonics
$U_{Q,AB}$	Amplitude of line voltage harmonic between phases A and B in network of order Q_1
$U^{(2)}_{Q,AB}$	Amplitude of line voltage harmonic between phases A and B in network of order Q_2
α	Relative pole width
δ_{EQ}	Equivalent air gap
ω_{ROT}	Circular frequency of rotor winding EMF and current
ω_{ST}	Circular frequency of EMF and stator winding currents of order $Q(\omega_{ST} = Q_1\omega_1)$
ω_1	Network circular frequency (frequency of stator current first harmonic)

References

I. Monographs, Textbooks

1. Richter R., Elektrische Maschinen. Berlin: Springer. Band I, 1924; Band II, 1930; Band III, 1932; Band IV, 1936; Band V, 1950. (In German).
2. Schuisky W., Berechnung elektrischer Maschinen. Wien: Springer, 1960. (In German).
3. Mueller G., Vogt, K., Ponick B., Berechnung elektrischer Maschinen. Springer, 2007. 475 S. (In German).

4. Demirchyan K.S., Neyman L.R., Korovkin N.V., Theoretical Electrical Engineering. Moscow, St.Petersburg: Piter, 2009. Vol. 1, 2. (In Russian).
5. Kuepfmueller K., Kohn G., Theoretische Elektrotechnik und Elektronik. 15 Aufl. Berlin, New York: Springer. 2000. (In German).
6. Boguslawsky I.Z., A.C. motors and generators. The theory and investigation methods by their operation in networks with non linear elements. Monograph. TU St.Petersburg Edit., 2006. Vol. 1; Vol.2. (In Russian).

II. Synchronous Machines. Papers, Inventor's Certificates, Patents

7. Boguslawsky I.Z., Magnetically coupled meshes in A.C. machines by non-sinusoidal supply. Power Eng. (New York), 1995, № 2.
8. Boguslawsky I.Z., Generalized characteristics of rotor mesh currents and MMF by A.C. machines. Power Eng. (New York), 1995, № 5.

Chapter 15
Peculiarities of Operation Modes of A.C. Machine with Short-Circuited Rotor Windings at Nonsinusoidal Power Supply

This chapter deals with peculiarities of losses distribution in rotor short-circuited loops obtained based on the investigation of their currents distribution. It is noted that in nonlinear network the distribution of currents and losses in damper winding of salient pole machines depends on the ratio of amplitudes and initial phases of voltage harmonics. If one of voltage amplitudes of two "adjacent" time harmonics is much less than the second, the distribution of currents in such a winding is close to that of currents at asynchronous start-up. Calculation examples are given.

The content of this chapter is development of the methods stated in [3].

15.1 General Comments

In previous chapters it was already noted that admissible power of synchronous or induction machines in network with non-sinusoidal sources is determined usually based on admissible overheats of windings and cores of stator and rotor specified in standards [4–7]. These overheats are determined, generally, by losses in machine windings.

Currents in machine magnetically coupled loops (in stator winding, squirrel cage of induction machine, damper winding and in excitation winding of salient-pole machine) are calculated based on the system of equations for these loops given in Chap. 14. These currents determine main losses in windings.

Additional losses in stator winding and in short-circuited rotor winding bars connected with skin effect are calculated by methods stated in the Chap. 23 of the monograph. There are also given practical examples of their calculation.

Excitation winding overheats of machines by operation in nonlinear network as a rule are not observed in operation practice; they do not exceed usually more than by 5–10 °C overheats for this machine operation in industrial network. It is explained by an application of high-power damper system in the construction of modern salient-pole machines intended for operation in such networks. This system serves

I. Boguslawsky et al., *Large A.C. Machines*,
DOI 10.1007/978-4-431-56475-1_15

as a screen for the excitation winding: cross section of pole bars of this system is usually selected not less than 20 % of cross section of stator winding conductors; cross section of each short-circuited ring or segment between poles is selected not less than 40 % of total cross section of bars of the pole (it was noted in Chap. 12).

Overheats of short-circuited rotor windings (damper winding of salient-pole machine, squirrel cage of induction machine) in standards are not normalized, but in practice their excess more than 160–180 °C is not allowed (smaller value of these two restrictions refers to damper winding); these restrictions are caused by the level of temperature deformations and mechanical stresses in construction elements.

Let us consider peculiarities of operation modes of damper winding and squirrel cage at non-sinusoidal power supply and distinctions of their modes in network with sharp load variation.

Thus, we will consider the results of investigations obtained earlier: at non-sinusoidal power supply EMF and currents of some frequencies ω_{ROT} are induced in rotor cage; each such frequency ω_{REV} is determined by the number of factors: by the first harmonic of network frequency ω_1, orders Q for time and m for spatial harmonics of resulting field in air gap, by rotor rotation speed ω_{REV}, number of machine poles 2p:

$$\omega_{ROT} = f(Q, m, \omega_1, p, \omega_{REV}). \tag{15.1}$$

15.2 Peculiarities of Squirrel Cage Operation Mode ($\omega_{REV} < \omega_1/p$)

In symmetrical squirrel cage of induction machines at the influence of fields of several higher time harmonics from (15.1) $Q_1 = 1, 7, 13, \ldots, 6k + 1$; $Q_2 = 5, 11, 17, \ldots, 6k + 5$ (at $k = 0, 1, 2, \ldots$) there are EMF and currents of several frequencies $\omega_{ROT,1}$, $\omega_{ROT,2}$, … [1, 2].

Losses in squirrel cage from each of frequencies $\omega_{ROT,1}$, $\omega_{ROT,2}$, … are summarized:

$$P_{CAG.RES} = N_0\left[P(\omega_{ROT,1}) + P(\omega_{ROT,2}) + P(\omega_{ROT,3}) + \cdots\right] \tag{15.2}$$

Here N_0—number of bars in squirrel cage, $P(\omega_{ROT,1}), \ldots, P(\omega_{ROT,2}) \ldots$—losses caused by currents of frequencies $\omega_{ROT,1}, \ldots, \omega_{ROT,2}, \ldots$ as per (15.1). Almost a uniform distribution of losses on the rotor periphery in symmetrical cage causes also the uniform distribution of overheats on the rotor periphery and, therefore, temperature deformations and stresses. Such a distribution is interrupted at emergence of asymmetry in cage and results its further damage.

15.3 Peculiarities of Damper Winding Operation Mode ($\omega_{REV} = \omega_1/p$)

In the previous chapters, currents in damper winding elements are found to be distributed depending on bar number N unevenly: the current contains three components, of which only one changes with N under the harmonic law, and two others under aperiodic. Therefore, losses in each of N ($1 \le N \le N_0$) bars on pole are different; the same is also true for ring portions. Respectively, losses in damper winding are also summarized from pair of neighboring harmonics, but separately for each bar, ring portion and segment between poles:

$$\begin{aligned} P_{DRES} = 2p[&P(\omega_{ROT,1}, N_1) + P(\omega_{ROT,1}, N_2) + P(\omega_{ROT,1}, N_3) + \cdots + P(\omega_{ROT,1}, N_0) \\ &+ P(\omega_{ROT,2}, N_1) + P(\omega_{ROT,2}, N_2) + P(\omega_{ROT,2}, N_3) + \cdots + P(\omega_{ROT,2}, N_0) + \cdots]. \end{aligned} \tag{15.3}$$

Here $N = N_1, N_2, \ldots N_0$—numbers of bars and ring portions (segments) on pole.

Uneven distribution of losses on the pole periphery also causes uneven distribution of overheats and, respectively, temperature deformations and stresses.

In Chap. 3 we obtained that in the operation of salient-pole machines in nonlinear network two fields in air gap characterized by various time or spatial harmonics can induce EMF and currents of identical frequency in rotor loops. Among such harmonics the greatest practical interest have "adjacent" time harmonics of orders Q_1, Q_2, for example, harmonics of orders $Q_1 = 7$, $Q_2 = 5$ (order of spatial harmonic $m = 1$) at number of machine phases $m_{PH} = 3$ or harmonics of orders $Q_1 = 13, Q_2 = 11$ ($m = 1$) —at $m_{PH} = 6$. They meet certain conditions given in the same chapter.

For investigation of the working conditions of the damper winding under the joint impact of "adjacent" time harmonics, for example, $Q_1 = 13$; $Q_2 = 11$ with $m = 1$ were calculated the currents and losses in the damper winding of generator 6300 kW, 6.3 kV, $2p = 6$, $m_{PH} = 6$, the number of bars on the pole $N_0 = 8$. The amplitudes of the higher harmonics voltage concerning to the first harmonic were adopted: $\frac{U_{11}}{U_1} = 9\ \%$; $\frac{U_{13}}{U_1} = 7.2\ \%$. Difference in the initial phases of the voltage harmonics $T_U = 0$. The calculations showed that the distribution of currents in the bars when exposed to only one harmonic $Q_2 = 11$ is similar to the current distribution for the asynchronous machines mode and is not similar on the distribution of currents under the combined effect of "adjacent" time-harmonic $Q_1 = 13$; $Q_2 = 11$.

Table 15.1 represents losses in damper winding of the same generator allocated at separate influence of voltage harmonics of order ($Q_2 = 11$, $m = 1$) and ($Q_1 = 13$, $m = 1$), and also at their combined influence ($Q_2 = 11$, $Q_1 = 13$, $m = 1$) for difference of initial phases $T_U = 0$; voltage harmonic structure is given above. From Table 15.1 it follows:

- distribution of currents and losses depends on the ratio of amplitudes of "adjacent" voltage harmonics of orders Q_1, Q_2. This fact influences the distribution of heats, temperature deformations and mechanical stresses in winding elements.

If EMF amplitude of one of "adjacent" harmonics is much less than the second, regularities of currents distribution in damper winding elements at non-sinusoidal power supply and asynchronous mode are almost identical;

- losses in damper winding at non-sinusoidal voltage supply determined by "adjacent" harmonics of orders Q_1, Q_2 at m = 1 exceed total losses at separate power supply of the same harmonics.

15.4 Additional Measures to Decrease Damper Winding Losses in Salient-Pole Machine

Winding with $m_{PH} = 6$ [3] is widely used to reduce losses in rotor loops for synchronous mode of machines in network with non-sinusoidal sources. However, its construction is more complicated than three-phase, and in low-voltage lower power machines (up to 1500–2000 kW) its usage is not always possible. In more detail peculiarities of this winding were given in Chap. 3. There were also stated other measures of reducing additional losses in rotor loops of modern machines in nonlinear network.

At the same time, a certain decrease of losses in damper winding can be obtained if we create the voltage on frequency converter terminals so that voltage phase angles of "adjacent" higher harmonics of order $Q_1 = 7$ and $Q_2 = 5$; $Q_1 = 13$ and $Q_2 = 11$; …, inducing in rotor loops EMF and currents of identical frequency, would be shifted in addition by a certain angle T_U. In practical problems for assessment of the extent of losses decrease, it is expedient to perform a number of alternative calculations at $\pi/2 \leq T_U \leq \pi$. The assessment of losses is given in Table 15.1 for comparison at the combined influence of two "adjacent" time harmonics ($Q_2 = 11$, $Q_1 = 13$, m = 1) in machine at $m_{PH} = 6$ for variants $T_U = 0$ and $T_U \neq 0$. At the combined influence of two "adjacent" harmonics $Q_2 = 5$ and $Q_1 = 7$ in machine at $m_{PH} = 3$ (for variants $T_U = 0$ and $T_U \neq 0$) we obtain the similar results. Let us note that for the determination of losses in rotor loops created in machine by higher time harmonics it is almost sufficient to consider harmonics of the first four orders.

Appendix 15.1

See Table 15.1.

Table 15.1 Comparison of losses in damper winding

Mode of generators	Synchronous	Synchronous	Synchronous	Synchronous
Orders of harmonics	$Q_2 = 11$, m = 1	$Q_1 = 13$, m = 1	$Q_2 = 11$, $Q_1 = 13$, m = 1, $T_U = 0$	$Q_2 = 11$, $Q_1 = 13$, m = 1, $T_U = \pi$
Losses (%)	56.2	25.8	100	74

Brief Conclusions

By operation in nonlinear networks:

1. In an induction machine without cage damage, all its bars are practically in equal thermal and mechanical state: the same refers to ring portions. This state is violated if there is a damage in cage.
2. In salient-pole machines thermal condition of damper winding is caused by uneven distribution of currents and losses in its elements. The law of currents distribution depends on the ratio of amplitudes of "adjacent" harmonics and on the difference of initial phases T_U. If the amplitude of one of these harmonics is much less than the second, the law of currents distribution in nonlinear network approaches that of currents distribution in asynchronous mode.
3. Besides known measures on the reduction of additional losses and overheats in damper winding structural elements given in Chap. 3, reduction of losses can be achieved by a difference increase of "adjacent" harmonics initial phases T_U within the range $\pi/2 \le T_U \le \pi$.

List of Symbols

m	Order of stator MMF spatial harmonics
m_{PH}	Number of stator winding phases
N	Bar number (ring portion or segment) of damper winding or cage rotor
N_0	Number of bars of damper winding per pole or number of bars in squirrel cage
$N = N_1, N_2, \ldots, N_0$	Numbers of bars and ring portions (segments) on pole
$P(\omega_{ROT,1}), \ldots, P(\omega_{ROT,2}) \ldots$	Losses in squirrel cage from currents with frequencies $\omega_{ROT,1}, \omega_{ROT,2} \ldots$
$P_{CAG.RES}$	Total losses in squirrel cage from rotor currents with frequencies $\omega_{ROT,1}, \omega_{ROT,2}, \ldots$
$P_{D.RES}$	Total looses in damper winding with frequencies $\omega_{ROT,1}, \omega_{ROT,2}, \ldots$
p	Number of pole pairs
Q	Order of stator current time harmonic
T_U	Difference of initial phases of two higher "adjacent" voltage harmonics
ω_1	Network circular frequency (frequency of stator current first harmonic)
ω_{REV}	Angular speed of rotor rotation
$\omega_{ROT,1}, \omega_{ROT,2}, \ldots$	Circular frequencies of rotor currents

References

I. Monographs, textbooks

1. Richter R., Elektrische Maschinen. Berlin: Springer. Band I, 1924; Band II, 1930; Band III, 1932; Band IV, 1936; Band V, 1950. (In German).
2. Mueller G., Vogt, K., Ponick B., Berechnung elektrischer Maschinen. Springer, 2007. 475 S. (In German).

II. Synchronous machines. Papers, inventor's certificates, patents

3. Boguslawsky I.Z., Particularity of 6-phases armature winding of A.C. machines with the non-sinusoidal power supply. Power Eng. New York, 1997, No. 5.

III. State Standards (IEC, GOST and so on)

4. GOST (Russian State Standard) R-52776 (IEC 60034-1). Rotating Electrical Machines. (In Russian).
5. IEC 60092-301 Electrical installations in ships. Part 301: Equipment Generators and Motors.
6. Rules and Regulations for the Classification of Ships. Part 6 Control, Electrical, Refrigeration and Fire. Lloyd's Register of Shipping (London). 2003.
7. Russian Maritime Register of Shipping. Vol. 2. Rules for the classification and construction of sea going ships. St. Petersburg. 2003.

Chapter 16
Operation Problems of High-Power AC Machines in Nonlinear Network

Regarding high-power synchronous and induction machines, the method of determination of their admissible power is developed in these chapters for the operation in nonlinear network. The method was checked in bench conditions on generator, 2000 kW, 690 V, 750 rpm (at «Elektrosila» Work, Stock Company "Power Machines" St.-Petersburg). Also we considered a special case representing practical interest—method of determination of generator admissible power for the operation under combined load. Influence of electromagnetic load of generators is investigated on their dynamic characteristics for the operation in autonomous mode (transient voltage deviation at load-off or load-on); practical measures for solution of the problems arising thus are formulated.

The voltage drop ΔU is appeared due to sudden variation of load 500 kVA, by $\cos \varphi = 0.3$ was determined on the bench of «Elektrosila» work. The experimental results are confirmed the validity of the equation, obtained in this chapter for calculation of ΔU, what is comfortable for the practical use.

16.1 General Comments

In recent years in connection with broad application of converting equipments in electrical power systems, these are problems of providing operation modes of high-power AC machines in nonlinear networks, selecting their electromagnetic loads and peculiarities of construction (in comparison with machines intended for linear networks).

Let us consider the main of these problems.

I. Boguslawsky et al., *Large A.C. Machines*,
DOI 10.1007/978-4-431-56475-1_16

16.2 Admissible Power of AC Machines in Nonlinear Network: Determination Methods; Practical Examples [1, 11–13]

Problem formulation

In modern practice high-power AC machines fed from converters of various types are widely used. Along with converters constructed on the principle of pulse-width modulation (PWM) system, frequency converters based on current inverter also find an application in the industry. Their form of stator phase current is considerably different from sinusoidal. Usually, it is characterized by "nonlinear distortion factor" [16–19]. This factor in nonlinear networks usually does not exceed $K_{DIST} < 0.03–0.35$, which exceeds requirements of norms ($K_{DIST} < 0.05$) specified in GOST, IEC standards and Register [16–19]. Therefore, practice defines a problem to determine the admissible power of AC machines for values of K_{DIST} factor exceeding requirements of these norms.

We noted previously that this integrated factor K_{DIST} does not take into account the influence of separate harmonics in current curve on the DC and additional losses in winding and stator and rotor cores and so does not allow one to estimate their thermal condition normalized according to GOST, IEC standards and the Register.

Let us consider peculiarities of calculation method for admissible power P^*_{ADM} of AC machine operating with this converter, proceeding from losses, thermal condition of its stator winding, and also stator and rotor cores. We accept that the real form of phase current differs from sinusoidal; for example, it can be approximately represented by step curve or trapezium of arbitrary form characterized by parameters: by high I (current amplitude), width of bases: bottom $B_{BT} = 0.5T_0$ and top $B_{TP} < B_{BT}, B_{TP} = \text{var}$; here T_0—period equal to 360 electrical degrees.

When determining the admissible power P^*_{ADM}, it is assumed that losses $Q_{AC,N}$, in stator winding for the operation with converter are equal to those $Q_{AC,NET}$ for the operation in parallel with a network of industrial frequency; the same also refers to losses $W_{AC,N}$ in stator and rotor cores for the operation with converter and power supply from the network $W_{TOT,NET}$. AC machine power P^*_{ADM} is determined, proceeding from two conditions: $Q_{AC,N} = Q_{AC,NET}$ and $W_{AC,N} = W_{AC,NET}$. From these equalities we can calculate:

- ratio of the first current harmonic for machine operation with frequency converter to the current amplitude for operation in parallel with industrial frequency network;
- ratio of the first harmonic of resulting flux (mutual induction) in air gap for machine operation with frequency converter to its flux amplitude for operation in parallel with industrial frequency network.

As a result, we have also determined the value P^*_{ADM}.

As examples of this method in Sect. 16.2.4, the value P^*_{ADM} is determined for several current forms (trapezium at $B_{TP} < B_{BT}, B_{TP} = \text{var}$) in the range of stator winding parameters, representing practical interest.

16.2.1 Losses in Stator Winding Carrying Alternating Current Containing a Number of Time Harmonics [1–4]

16.2.1.1 DC Losses

Let us consider a general case, in which the phase current curve contains all odd harmonics of time orders of $N \geq 1$ (in special cases some of these harmonics can be absent). In this chapter the time harmonic order is designated by letter N in contrast to letter Q agreed in other chapters (for example, in Chap. 3): in this chapter Q denotes winding losses.

Then, the DC losses are determined by the following ratio:

$$\sum Q_{DC,N} = Q_{DC,1} \cdots + Q_{DC,5} + \cdots Q_{D.C.,N} + \cdots. \tag{16.1}$$

Expressions for DC losses of separate current harmonics:

$$\begin{aligned} &Q_{DC,1} = 0.5 m_{PH} (K_1 I)^2 R_{PH}; \ldots; \quad Q_{D.C.,5} = 0.5 m_{PH} (K_5 I)^2 R_{PH}; \\ &Q_{DC,N} = 0.5 m_{PH} (K_N I)^2 R_{PH}; \ldots. \end{aligned} \tag{16.1'}$$

Here I—current curve amplitude containing harmonics; m_{PH}—number of phases; $K_1, \ldots, K_1, \ldots, K_N$—expansion coefficients of current curve with harmonics of order $1, \ldots, 5, \ldots, N, \ldots$; R_{PH}—DC resistance of stator winding phase. According to (16.1) and (16.1′), we obtain:

$$\begin{aligned} \sum Q_{DC,N} &= \frac{1}{2} m_{PH} (K_1 I)^2 R_{PH} \left[1 + \cdots + \left(\frac{K_5}{K_1} \right)^2 + \cdots + \left(\frac{K_N}{K_1} \right)^2 + \cdots \right] \\ &= \frac{1}{2} m_{PH} (K_1 I)^2 R_{PH} \sum Q^*_{DC,N}. \end{aligned} \tag{16.2}$$

The sum of the main losses (in relative units) is designated:

$$\sum Q^*_{DC,N} = 1 + \cdots + \left(\frac{K_5}{K_1} \right)^2 + \cdots + \left(\frac{K_N}{K_1} \right)^2 + \cdots. \tag{16.2'}$$

16.2.1.2 Additional Losses

They are determined by the ratio:

$$\sum \Delta Q_{DC,N} = \Delta Q_{DC,1} + \cdots + \Delta Q_{DC,5} + \cdots + \Delta Q_{D.C.,N} + \cdots . \tag{16.3}$$

Expressions for additional losses of separate current harmonics:

$$\begin{aligned} \Delta Q_{DC,1} &= \frac{1}{2} m_{PH} (K_1 I)^2 R_{PH} \Delta K_{F,1}; \ldots; \\ \Delta Q_{DC,5} &= \frac{1}{2} m_{PH} (K_5 I)^2 R_{PH} \Delta K_{F,5}; \ldots; \\ \Delta Q_{DC,N} &= \frac{1}{2} m_{PH} (K_N I)^2 R_{PH} \Delta K_{F,N}; \ldots; \end{aligned} \tag{16.3'}$$

Here $\Delta K_{F,1}; \ldots; \Delta K_{F,5}; \ldots; \Delta K_{F,N}; \ldots$—coefficients of additional losses caused by the skin effect phenomenon in stator winding elementary conductors [2–6]. Calculation expressions of these coefficients for windings of bar and winding types do not coincide. These are given in Chap. 23 in the form convenient for further investigations.

As follows from Chap. 23, the expression $\Delta K_{F,N}$ $(N = 1; \ldots 5; \ldots)$ for windings of both bar and winding types can be presented in the form:

$$\Delta K_{F,N} = \Delta K_{F,1} N^2, \tag{16.4}$$

where $\Delta K_{F,1} = K_{F,1} - 1, \ldots,$ $\Delta K_{F,N} = K_{F,N} - 1;$ $K_{F,1}, \ldots, K_{F,N}$—field's factors for time harmonics of order N [2, 5, 6].

According to (16.3), (16.3) and (16.4) we obtain:

$$\begin{aligned} \sum \Delta Q_{DC,N} &= \frac{1}{2} m_{PH} (K_1 I)^2 R_{PH} \left[\Delta K_{F,1} + \cdots + \left(\frac{K_5}{K_1} \right)^2 \Delta K_{F,5} + \cdots + \left(\frac{K_N}{K_1} \right)^2 \Delta K_{F,N} + \cdots \right] \\ &= \frac{1}{2} m_{PH} (K_1 I)^2 R_{PH} \left(\sum Q^*_{D.C.,N} \right) \end{aligned} \tag{16.5}$$

The sum of the DC losses (in relative units) is expressed as:

$$\sum \Delta Q^*_{DC,N} = \Delta K_{F,1} \left[1 + \cdots + \left(\frac{K_5}{K_1} \right)^2 5^2 + \cdots + \left(\frac{K_N}{K_1} \right)^2 N^2 + \cdots \right]. \tag{16.6}$$

16.2.1.3 AC Losses $Q_{AC,N}$

$$\begin{aligned} Q_{AC,N} &= \sum Q_{DC,N} + \sum \Delta Q_{DC,N} \\ &= \frac{1}{2} m_{PH} (K_1 I)^2 R_{PH} \left[\sum Q^*_{DC,N} + \sum \Delta Q^*_{DC,N} + \right], \end{aligned} \tag{16.7}$$

where $\sum Q^*_{DC,N}$—as per (16.2′),$\sum \Delta Q^*_{DC,N}$—as per (16.6).

Thus, the "distortion factor" usually used in practice for the assessment of current phase form does not determine completely stator winding losses. From Eq. (16.6) it follows that it determines only one component of these losses ($\sum Q^*_{DC,N}$). This coefficient does not determine the second component of losses ($\sum \Delta Q^*_{DC,N}$).

16.2.1.4 Losses in Stator Winding Carrying Sinusoidal Current of Industrial Frequency

DC losses: $Q_{DC,C} = \frac{1}{2} m_{PH} I_C^2 R_{PH}$; here I_C—amplitude of sinusoidal current.

Additional losses: $\Delta Q_{DC,C} = \frac{1}{2} m_{PH} I_C^2 R_{PH} K_{F,1}$.

AC (total) losses:

$$Q_{A.C.,C} = \frac{1}{2} m_{PH} I_C^2 R_{PH} (1 + \Delta K_{F,1}). \tag{16.8}$$

16.2.1.5 Admissible Power of P^*_w, Proceeding from Stator Winding Losses and Its Overheat

Using Eqs. (16.7) and (16.8) for the total losses, we obtain the expression for P^*_w in the form:

$$P^*_w = \sqrt{\frac{1 + \Delta K_{F,1}}{\sum Q^*_{DC,N} + \sum \Delta Q^*_{DC,N}}} \tag{16.9}$$

Calculation expression for power P^*_w is a general one and it allows one to determine the admissible power for AC machine operation in network with frequency converter, proceeding from stator winding losses and overheat at any harmonic structure of phase current.

16.2.2 Losses in Machine Stator and Rotor Core Caused by Mutual Induction Field [2–6] Containing a Number of Time Harmonics

16.2.2.1 EMF and Current Frequencies in Machine Circuits

It should be noted beforehand that for high time harmonics the machine mode is asynchronous. In this mode the stator field of time harmonic of $N_{AD} = 6\,K - 1$ $(K = 1; 2; 3; \ldots)$ order induces in rotor circuits EMF and currents of $f^{ROT}_{N,AD} = (N_{AD} + 1 - s_{N=1})f_{ST,1}$ frequency, while for harmonics of $N_{DIR} = 6\,K - 5$ order the EMF and current frequency in rotor circuits is equal to $f^{ROT}_{N,DIR} = (N_{DIR} - 1 + s_{N=1})f_{ST,1}$. Here $f_{ST,1}$—stator current frequency for N = 1; the slip $s_{N=1}$ for asynchronous machine under normal operating conditions (at N = 1) is usually $s_{N=1} \leq 0.01$; while for synchronous machine $s_{N=1} = 0$.

As for the screening influence of rotor excitation winding in modern generators, the following should be noted:

- semiconductor elements of excitation system usually partly or fully "cut off" a negative half wave of alternating current induced by fields of higher time harmonics, it depends on the winding inductance;
- impedance of this winding is more than that of rotor damper winding. In this regard, the screening influence of excitation winding in comparison with damper winding is small.

16.2.2.2 Mutual Induction Fields of Orders N_{AD} and N_{DIR} in Air Gap. Screening Factors $S_{N,AD}$ and $S_{N,DIR}$

In AC machine the field of rotor currents with frequency $f^{ROT}_{N,AD}$ and stator field of time order N_{AD} (both fields have identical spatial order of "m") generate the resulting field (mutual induction) in air gap. Respectively, it is also characterized by time order N_{AD} and spatial order "m". The same is true for the field of rotor currents with frequency $f^{ROT}_{N,DIR}$ and field of stator time of order N_{DIR}. Let us note that in further calculations fields in air gap at m = 1 are considered. According to the Ampere law [3, 4] MMF of mutual induction field $F^{RES}_{N,AD}$ of order N_{AD} is equal to,

$$F^{RES}_{N,AD} = F^{ROT}_{N,AD} + F^{ST}_{N,AD}. \tag{16.10}$$

For MMF of mutual induction field of order N_{DIR}

$$F^{RES}_{N,DIR} = F^{ROT}_{N,DIR} + F^{ST}_{N,DIR}. \tag{16.11}$$

Here $F_{RES,AD}, \ldots, F^{ST}_{N,DIR}$.—MMF time complexes:$F^{ROT}_{N,AD} = |F^{ROT}_{N,AD}|e^{j\Psi^{ROT}_{N,AD}}$—rotor MMF, $F^{ST}_{N,AD} = |F^{ST}_{N,AD}|e^{j\Psi^{ST}_{N,AD}}$—stator MMF; similarly are determined other MMF complexes of mutual induction field of the order N_{DIR}; $\Psi^{ROT}_{N,AD}$, $\Psi^{ST}_{N,AD}$—phase angles. Each MMF, $F^{RES}_{N,AD}$, $F^{RES}_{N,DIR}$, corresponds to the resulting flux harmonic in air gap determined by the no-load characteristic.

We consider in more detail components of time order N_{AD}. Mutual position in time of vectors $F^{ROT}_{N,AD}$ and $F^{ST}_{N,AD}$ is determined by the ratio [2, 5]: $0.5\pi < |\Delta\Psi^{ROT}_{N,AD}| < \pi$, where $\Delta\Psi^{ROT}_{N,AD} = \Psi^{ROT}_{N,AD} - \Psi^{ST}_{N,AD}$. Thus, these vectors form an obtuse angle between them [2, 5]. Let us use an auxiliary acute angle $\Delta\varphi^{ROT}_{N,AD} = \pi - \Delta\Psi^{ROT}_{N,AD}$. Then, the Ampere law for MMF harmonic amplitudes takes the following form:

$$\left|F^{RES}_{N,AD}\right| = \left|F^{ROT}_{N,AD} - F^{ST}_{N,AD}e^{j\Delta\varphi^{ROT}_{N,AD}}\right|. \tag{16.12}$$

The last expression allows us to estimate the screening influence of rotor currents field harmonics on stator currents field harmonics.

From the viewpoint of this influence let us consider, as previously, differences of physical processes in machine connected with the first and higher time harmonics for non-sinusoidal power supply. For the first MMF harmonic $F^{RES}_{N=1}$ and, respectively, the flux in air gap are determined, proceeding from the voltage set on stator winding terminals [2, 5] so MMF $F^{ST}_{N=1}$ is calculated as the sum of complexes $F^{RES}_{N=1}$ and $F^{ROT}_{N=1}$. However, for stator MMF higher harmonics, $F^{ST}_{N,AD}$ is determined based on the current harmonic amplitude of order $N = N_{AD}$ (according to the harmonic analysis of specified current curve), and MMF complexes $F^{RES}_{N,AD}$ and $F^{ROT}_{N,AD}$ are calculated at slip $S_{N,AD} \approx 1$ [2, 5] so that their sum should be equal to this MMF; in this mode $\Delta\varphi^{ROT}_{N,AD} \approx 0$. According to (16.12), the effectiveness of screening at $S_{N,AD} \approx 1$, $\Delta\varphi^{ROT}_{N,AD} \approx 0$ is determined by a difference between rotor MMF $F^{ROT}_{N,AD}$ and stator MMF $F^{ST}_{N,AD}$ values.

Let us call the relation for $S_{N,AD}$ and a similar relation for $S_{N,DIR}$—screening factors for additional and direct field respectively. We use a relation $S_{N,AD} = \frac{|F^{RES}_{N,AD}|}{|F^{ST}_{N,AD}|}$ for the assessment of screening action of rotor currents field. Previously we noted that it does not remain constant with an increase in harmonic number; depending on this number it changes in limits: $0 < S_{N,AD} < S_1$, where $S_1 = \frac{|F^{RES}_{N=1}|}{|F^{ST}_{N=1}|}$.

For the asynchronous machine, for example, by slip $s_{SL} = 1$, it is easy to obtain calculation values $S_{N,AD}$ for each harmonic $N = N_{AD}$ from machine equivalent

circuit [2, 5]. At $\Delta\varphi \approx 0$ taking into account Eq. (16.12) from equivalent circuit, we obtain the following:

$$S_N \approx \frac{1}{1 + \left| X_{M,N} / Z'_{2,N} \right|}. \tag{16.12'}$$

where $Z'_{2,N} = R'_{2,N} + jX'_{2,N}$; $Z'_{2,N}$—is rotor impedance reduced to stator winding; $R'_{2,N}$ and $X'_{2,N}$—are AC resistance and reactance with account made for skin effect [see Eq. (16.13)]; $X_{M,N}$—reactance of magnetization circuit.

Both values of screening factors $S_{N,AD}$ and S_1 have a clear physical sense.

The first of them gives the quantitative assessment of screening degree of stator currents field harmonics of order $N = N_{AD}$ by rotor currents field harmonics of order $N \approx N_{AD} + 1$ (with frequency $F^{ROT}_{N,AD}$). Therefore, for designing a machine intended for operation with "current" frequency converter it is expedient to select the structure of squirrel cage (damper winding) so that values of the relation of $S_{N,AD}$ were minimum in the range of harmonics $N \approx N_{AD}$. As a result, the machine with these values $S_{N,AD}$ is characterized by minimum values of the following:

- additional losses in stator and rotor cores caused by resulting field harmonics of order $N = N_{AD}$ in air gap;
- EMF harmonics of order $N = N_{AD}$ in stator winding phase and correspondingly harmonics of the same order in phase voltage curve of this machine;
- additional torques at slips by rated power caused by resulting field harmonics of order $N = N_{AD}$ in air gap.

The value $S_{N,AD}$ is influenced by the skin effect in rotor squirrel cage (damper winding) bars: impedance of bar $Z_{BAR,N}$ nonlinearly depends on the frequency of EMF and current in rotor loops:

$$Z_{BAR,N} = R_{BAR,N} K_{F,N} + j2\pi f^{ROT}_{N,AD} L_{BAR,N} K_{X,N}, \tag{16.13}$$

where $R_{BAR,N}$, $L_{BAR,N}$—DC resistance and leakage inductance of bar, $K_{X,N}$—inductance decrease factor, $K_{F,N}$—losses increase factor, field's factor; dependence of factors $K_{X,N}$ and $K_{F,N}$ on frequency f^{ROT}_N is nonlinear and has the form [3, 4, 6, 7]:

$$K_{X,N} \equiv \sqrt{\frac{1}{f^{ROT}_N}}; \quad K_{F,N} \equiv \sqrt{f^{ROT}_{N,AD}}. \tag{16.14}$$

As it follows from both expressions, with a growth in harmonic number N_{AD} the reactance and resistances of short-circuited rotor winding bars increase approximately proportionally to the square root of the number of harmonic N_{AD}. Therefore, MMFs $F^{ROT}_{N,AD}$ and $F^{RES}_{N,AD}$ vary nonlinearly with growth in number N_{AD} according to (16.13) and (16.14).

Analysis for large AC machines (800 kW–10 MW) in the range of frequencies representing practical interest (N_{AD} = 5; N_{DIR} = 7) revealed that in this range $S_{N,AD}$, $S_{N,DIR}$, values vary within the range of $S_N \le 0.12$. According to equations in Sect. (16.2.2.2) they become smaller as far as the harmonic order N becomes higher about in proportion to $\sqrt{N}$.

Let us note that for synchronous machines the relation $\frac{1}{S_1}$ is approximately equal to reactance [2, 5] X_{AD} (p.u.).

Equations (16.10) and (16.11) determine the resulting field Φ_{RES} in machine air gap; it can be represented in the form of harmonic time series of order of N with amplitudes $\Phi_1, \ldots \Phi_5, \ldots, \Phi_N$, herewith, field harmonics of order N_{DIR} from this series (for example, 1; 7; …) rotate in the direction of rotor rotation, and order N_{AD} (for example, 5; 11; …) from this series—in opposite direction.

With account of these results, let us proceed to the calculation of losses in machine cores.

16.2.2.3 Losses in Stator Core

Let us find at first the calculation expression for losses in stator yoke. It is determined by the ratio:

$$\sum W_N^{YOKE} = W_{N=1}^{YOKE} + W_{N=5}^{YOKE} + \cdots + W_N^{YOKE}.$$

Expressions for separate components of losses:

$$W_{N=1} = D_1^{YOKE}\left(B_1^{YOKE}\right)^2 G^{YOKE},\ W_{N=5}^{YOKE} = D_1^{YOKE}\left(B_5^{YOKE}\right)^2 G^{YOKE} 5^{1,3}$$
$$W_N^{YOKE} = D_1^{YOKE}\left(B_5^{YOKE}\right)^2 G^{YOKE} N^{1,3},$$

where D_1^{YOKE}—coefficient determined for the yoke by electrotechnical steel grade, selected by roll direction (for cold-rolled steel), stack assembly technology; G^{YOKE}—yoke weight; $B_1^{YOKE}, \ldots, B_5^{YOKE}, \ldots, B_N^{YOKE}$—calculation flux density in the yoke, determined by harmonics of resulting field Φ_{RES} in air gap: $F_1; \ldots; F_5; \ldots; F_N$. Then flux density values in the yoke: $B_1^{YOKE} = \frac{\Phi_1}{S^{YOKE}}; \ldots B_5^{YOKE} = \frac{\Phi_5}{S^{YOKE}}; \ldots B_N^{YOKE} = \frac{\Phi_N}{S^{YOKE}}$, where S^{YOKE}—calculation section for flux density in the yoke.

With account of last two equations we obtain the calculation expression for losses in the yoke:

$$\sum W_N^{YOKE} = D_2^{YOKE}\Phi_1^2\left[1 + \cdots + \left(\frac{\Phi_5}{\Phi_1}\right)^2 5^{1,3} + \cdots + \left(\frac{\Phi_N}{\Phi_1}\right)^2 N^{1,3}\right], \quad (16.15)$$

where $D_2^{YOKE} = D_1^{YOKE}\frac{G^{YOKE}}{(S^{YOKE})^2}$.

For harmonics of order N = N_{AD} with account of Eqs. (16.13) and (16.14) the following ratio is true:

$$\frac{\Phi_{N,AD}}{\Phi_1} = \frac{K_{SAT1}}{K_{SATN,AD}} \frac{\left|F^{RES}_{N,AD}\right|}{\left|F^{RES}_{1,AD}\right|} = K_{SATN,EQ} \frac{S_{N,AD}}{S_{1,AD}} \frac{\left|F^{ST}_{N,AD}\right|}{\left|F^{ST}_{1,AD}\right|}, \tag{16.15'}$$

where $K_{SAT1}, K_{SAT,AD}$—saturation factors of magnetic circuit of AC machine for harmonics of order N = 1 and N > 1 accordingly and $K_{SAT1} < K_{SATN,AD}$. The factor $K_{SATN,EQ} = \frac{K_{SAT1}}{K_{SATN,AD}}$ for the weak-saturated magnetic circuit of AC machine ($K_{SAT1} \leq 1.15$) is approximately equal to $K_{SATN,EQ} \approx 1$ and for saturated magnetic circuit—$K_{SATN,EQ} < 1$. Assume for the next calculation of the losses in stator and rotor cores ("with reserve"): $K_{SATN,EQ} = 1$.

Ratios in the form (16.15′) are also true for harmonics of order N = N_{DIR} Then the expression for losses $\sum W_N^{YOKE}$ takes the form:

$$\sum W_N^{YOKE} = D_2^{YOKE} \Phi_1^2 \sum W_N^{*ST}. \tag{16.16}$$

Here

$$\sum W_N^{*ST} = 1 + \left(\frac{S_5 K_5}{S_1 K_1}\right)^2 5^{1,3} + \cdots + \left(\frac{S_N K_N}{S_1 K_1}\right)^2 N^{1,3}. \tag{16.17}$$

Equation (16.17) is similar to (16.2) and (16.6); here $K_1, \ldots, K_5, \ldots, K_N$—expansion coefficients of current curve to harmonics series of order $1, \ldots, 5, \ldots, N, \ldots$, which are not multiple to three (star connection of stator winding phases is supposed).

Let us proceed to the calculation expression for losses in stator teeth. It is similar to (16.16):

$$\sum W_N^{TEETH} = D_2^{TEETH} \Phi_1^2 \sum W_N^{*ST}. \tag{16.18}$$

Coefficient D_2^{TEETH} as well as D_2^{YOKE} are based on the consideration of electrotechnical steel grade, roll direction, stack assembly technology, weight of tooth zone and teeth calculation section [6, 7]; the sum $\sum W_N^{*ST}$ is calculated based on (16.17).

16.2.2.4 Losses in Rotor Core

Calculation expressions for losses are similar to (16.16) and (16.18). Differences consist in numerical values for coefficients D_2^{YOKE} and D_2^{TEETH}, and also in the formulation of expression for $\sum W_N^{*ROT}$. It takes the form:

$$\sum W_N^{*ROT} \approx 1 + \left(\frac{S_5K_5}{S_1K_1}\right)^2 6^{1.3} + \cdots + \left(\frac{S_7K_7}{S_1K_1}\right)^2 6^{1.3} + \cdots + \left(\frac{S_{11}K_{11}}{S_1K_1}\right)^2 12^{1.3} + \cdots + \left(\frac{S_{13}K_{13}}{S_1K_1}\right)^2 12^{1.3} + \cdots \tag{16.19}$$

Note. With increasing the order of harmonic N_{AD} and N_{DIR} the exponents may differ from those specified in the Eqs. (16.15) and (16.19). Generally they depend on the type of electrical steel used and can be specified by the manufacturer. On the other hand, with increasing of harmonic order N_{AD} and N_{DIR} the factors determined for the yoke and teeth by the kind of electric steel, the rolling direction and the stacking technology are also changed. Those factors should be measured on the manufacturer's test bench against machines that are similar in design. Nevertheless even with variation of the exponents and factors, the formulas for $\Xi W \times N_{ROT}$ and $\Xi W \times N_{ST}$ are still valid, therefore the above method can still be used for the practical calculations.

This difference is caused by the fact that for "adjacent" harmonics of both orders (for example, $N_{AD} = 5$ and $N_{DIR} = 7$) the frequency of EMF and currents $f_{N,AD}^{ROT}$ and $f_{N,DIR}^{ROT}$ in rotor loops is not equal for the same harmonics to that of EMF and currents in stator loops; expressions for these frequencies are obtained in Sect. 16.2.2.1.

Let us neglect this difference and assume that $\sum W_N^{*ROT} \approx \sum W_N^{*ST}$. Thus, the calculation error in value $\sum W_N^{*ROT}$ makes no more than 3–5 %.

16.2.2.5 Total Losses: Admissible Power Based on Losses in Machine Core and Its Overheats

Summarizing losses in stator and rotor yoke and teeth, we obtain total losses in machine core, when fed from a frequency converter. Equating these losses to those in core for machine operation in industrial network, we obtain the calculation expression for admissible power:

$$P_{COR}^* = \frac{1}{\sum W_N^{*ST}}. \tag{16.20}$$

Here $\sum W_N^{*ST}$—as per (16.17).

The calculation expression for power P_{COR}^* is general and allows one to determine the admissible power for machine operation in network with frequency converter, proceeding from losses and overheat of stator and rotor cores.

Higher time harmonics of mutual induction flux additionally saturate machine core. However, reduction of its first harmonic according to (16.20) usually compensates this saturation, so additional check of magnetic circuit saturation factor, when machine is fed from the frequency converter is usually not required.

16.2.3 Machine Admissible Total Power P_{ADM}

In fractions of rated power determined for machine operating mode in nonlinear network it is found from the following ratio:

$$P^*_{ADM} = P^*_W P^*_{COR}. \tag{16.21}$$

Here P^*_W—as per (16.9), P^*_{COR}—as per (16.20).

16.2.4 Calculation Examples: Determination of Machine Admissible Power P^*_{ADM}

As examples of using Eqs. (16.9–16.21) calculation results of power P^*_{ADM} are given below.

Calculations of power P^*_W are made based on (16.2′), (16.9) for a rectangular and for a trapezium current form with various width of top basis (B_{TB} = var). Three variants of factor ΔK_{F1} are considered:

- $\Delta K_{F,1} = 0.075$ (variant 1);
- $\Delta K_{F,1} = 0.15$ (variant 2);
- $\Delta K_{F,1} = 0.25$ (variant 3 practically with limit values $\Delta K_{F,1}$).

16.2.4.1 Calculation Peculiarities of DC and Additional Losses Based on (16.2′), (16.6), (16.9) for Rectangular Current Waveform (Limit Problem for Trapezium with Equal Top B_{TP} and Bottom B_{BT} Bases: $B_{TP} = B_{BT}$)

$$\sum Q^*_{DC,N} = 1 + \cdots + \left(\frac{1}{5}\right)^2 + \cdots + \left(\frac{1}{N}\right)^2 + \cdots \tag{16.22}$$

Sum of additional losses as per (16.6)

$$\begin{aligned}\sum \Delta Q^*_{DC,N} &= \Delta_{KF,1}\left[\left(\frac{1}{1}\right)^2 (1)^2 + \cdots + \left(\frac{1}{5}\right)^2 (5)^2 + \cdots + \left(\frac{1}{N}\right)^2 N^2 + \cdots\right] \\ &= \Delta_{KF,1}[1 + \cdots + 1 + \cdots + 1 + \cdots].\end{aligned} \tag{16.23}$$

We obtained that DC losses $\sum Q^*_{DC,N}$ as per (16.22) with unrestrictedly large number of expansion terms N have a limit; for example, with account of the first ten expansion terms it is equal to $\sum Q^*_{DC,N} \approx 1.125$.

Additional losses $\sum \Delta Q^*$ as per (16.23) with unrestrictedly large number of expansion terms N for rectangular current waveform, unlike trapezoidal ($B_{TP} < B_{BT}$) have no limit: $\Delta Q_{DC} = \Delta_{KF,1} N$.

Practically, the number of terms (N) in last expression is determined only by the maximum frequency for which field's expressions are correct; it is considered that for elementary conductors dimensions of stator winding usually used in practice they are true at frequencies up to 1000–1200 Hz. With a further increase in current frequency, the $\Delta_{K_F,N}$ error in calculation of additional losses increases, so for the derivation of calculation ratios for $\Delta_{K_F,N}$ with such frequencies it is necessary to investigate more strictly the real field of slot leakage. Practically, this restriction corresponds to values of orders $N < 25$. As an example the first ten harmonics to $N = 19$ are considered (incl.).

According to (16.9) we obtain:

- for $\Delta K_{F,1} = 0.075$: $P^*_w = \sqrt{\frac{1+0.075}{1.125+0.75}} = 0.75$;;
- for $\Delta K_{F,1} = 0.15$: $P^*_w = 0.65$;
- for $\Delta K_{F,1} = 0.25$: $P^*_w = 0.58$.

With account of inductance in the converter circuit, the rectangular current waveform has only theoretical interest: calculations of this current waveform indicate the lower limit of machine power P^*_{ADM}.

According to (16.21) the machine admissible power P^*_{ADM} is equal to,

- for $\Delta K_{F,1} = 0.075$: $P^*_{ADM} = 0.72$;
- for $\Delta K_{F,1} = 0.15$: $P^*_{ADM} = 0.64$;
- for $\Delta K_{F,1} = 0.25$: $P^*_{ADM} = 0.57$.

16.2.4.2 Calculation Results of Power P^*_{ADM} for Trapezoidal Phase Current Waveform with Various Width of Top Basis (B_{TP} = Var) Are Given in Table 16.1

As it follows from calculation results, when the trapezium top basis changes to the value $B_{TP} \leq \frac{2}{3} B_{BT}$, the amplitudes of higher harmonics decrease; it allows us to increase machine power to $P^*_{ADM} \approx 0.93$–0.95.

Note. Calculations P^*_{COR} indicate: Values S_1, $S_{N,AD}$ and $S_{N,DIR}$ confirm the effectiveness of screening influence of squirrel cage currents on stator field higher harmonics. As a result, stator and rotor cores losses of this generator rise only by 3 to 4 % for considered current waveforms in comparison with losses in network operation. Respectively, the power P^*_{COR} makes $P^*_{COR} \approx 0.96$–0.97, which is used in Eq. (16.21) in determination of P^*_{ADM}.

Table 16.1 Power P^*_{ADM} for trapezoidal phase current waveform with various width of top basis (B_{TP} = var)

Trapezoidal form	B_{TB} = 140 el. degr.	B_{TB} = 120 el. degr.	B_{TB} = 100 el. degr.
P^*_{ADM} (var.1/var.2/var.3)	0.9/0.88/0.85	0.93/0.92/0.91	0.95/0.94/0.93

Let us note that unlike P^*_W, the value P^*_{COR} depends on machine equivalent circuit parameters.

16.2.5 *Experimental Determination of Screening Factors $S_{N,DIR}$, $S_{N,AD}$ of Asynchronous and Synchronous Salient Pole Machines*

Values of screening factors $S_{N,DIR}$ and $S_{N,AD}$ form parameters of AC machines, which outline screening features of squirrel-cage rotor circuits (squirrel-cage or damper winding) and their effectiveness. In practical calculations the values of screening factors $S_{N,DIR}$, $S_{N,AD}$ either validate the construction of rotor windings or indicate the necessity for their "strengthening, finishing"; for this reason, their assessment is of practical concern.

Values of screening factors $S_{N,DIR}$ and $S_{N,AD}$ for asynchronous and synchronous salient-pole machines may be obtained by an experiment, for example, during tests on manufacturer's bench. It would be rational to perform tests with the help of one of production machines manufactured at the factory which exhibits:

- much the same level of electromagnetic loads as for similar machine line;
- rotor squirrel cage construction similar for this line of machines, for example, applied materials of its components (copper, aluminum), ratio of basic bar section on a pole to rotor end ring section [2, 5, 7] etc.

Test bench should be equipped with a frequency source of N order harmonic current up to $N \leq 13–17$ and with a synchronous motor for tested machine driving. The motor should be fed by a variable frequency unit that is available as a rule on manufacturer's bench; DC motor may be used instead of synchronous motor. For both cases such a motor should ensure the variation of speed n of tested machine within the range $0.9n_{NOM} \leq n \leq n_{NOM}$.

1. Asynchronous machine.

1.1 Test for determination of MMF $F^{ST}_{N,DIR}, F^{ST}_{N,AD}$ with supply by frequency source of N order harmonic current up to $N \leq 13–17$.

The machine is driven at a speed $n < n_{NOM}$, which corresponds to the slip under rated operating conditions; we have to note that for harmonics of N = 1 order the slip is usually $s_{N=1} \leq 1$ %.

It is supplied with a voltage whose amplitude corresponds to N > 1 order harmonic, for example, $U_N = U_{N=7}$. The amplitude of stator current of N order harmonic is measured as well, for example, $I_N = I_{N=7}$. It should be noted that for harmonics of N > 1 order the slip is $s_N \approx 1$.

As consequence, on the basis of stator current I_N the value of $F^{ST}_{N,DIR}$ will be determined according to Eq. (3.5′) for MMF [2, 5, 7].

The value $F^{ST}_{N,DIR}$, for example, $F^{ST}_{(N=5)}$, shall be determined by an experiment in a similar way.

1.2 Test to specify MMF $F^{RES}_{N,DIR}, F^{RES}_{N,AD}$ with supply from industrial network.

An asynchronous machine is driven at synchronous speed $n = n_{Nom}$, so that for harmonics of N = 1 order the slip makes $s_{N=1} = 0$.

It is fed from an industrial network (N = 1) by U voltage within the range of $0.1U_{NOM} \le U \le 0.7U_{NOM}$, where U_{NOM}—machine rated voltage. During the test for harmonics of N = 1 order one should measure the amplitude of stator current $I_{M(N=1)}$ within the specified voltage range. The non-load characteristic $E_{M(N=1)} = f[I_{M(N=1)}]$ is plotted upon the results of measurements; here $E_{M(N=1)}, I_{M(N=1)}$ are EMF and magnetizing current amplitudes which specify the total field in an air-gap at network frequency. EMF is calculated from the formula: $E_{M(N=1)} = U - I_{M(N=1)}Z_{1(N=1)}$; here $Z_{1(N=1)}$—impedance of stator winding at industrial network frequency (N = 1). The phase angular difference Δφ between voltage U and current $I_{M(N=1)}$ may be taken as equal to Δφ ≈ 90 el. degr. The reactance of magnetizing circuit at this frequency is $X_{M(N=1)} = \frac{|E_{M(N=1)}|}{|I_{M(N=1)}|}$.

At harmonics of N > 1 order the reactance of this circuit is calculated from the expression: $X_{M(N)} \approx NX_{M(N=1)}$ $(K_{SATN,EQ} = 1)$; for example, at N = 7: $X_{M(N=7)} \approx 7X_{M(N=1)}$. Then, for a voltage with amplitude corresponding to harmonic order N, for example, $U_N = U_{(N=7)}$, we shall determine the magnetizing current: $I_{M(N1)} \frac{U_N}{jX_{M(N)} + Z_{1(N)}}$, for example, $I_{M(N=7)} \frac{U_{N=7}}{jX_{M(N=7)} + Z_{1(N=7)}}$, where $Z_{1(N)}$—stator winding impedance at a frequency of N > 1 order.

When calculating the current $I_{M(N)}$ it should be supposed that the phase angular difference Δφ between voltage U_N and current $I_{M(N)}$ is kept equal to Δφ ≈ 90 el. degr.

Finally, on the basis of stator current $I_{M(N)}$ the value of $F^{RES}_{N,DIR}$ will be determined according to Eq. (3.5′) for MMF [2, 5, 7], for example, $F^{RES}_{(N=7)}$. The value $F^{RES}_{N,AD}$, for example, $F^{RES}_{(N=5)}$, shall be determined by an experiment in a similar way (directions of rotor turning when determining MMF $F^{RES}_{N,DIR}$ and $F^{RES}_{N,AD}$—are opposite).

In practice to specify the values $F^{RES}_{N,DIR}$ and $F^{RES}_{N,AD}$ it should be sufficient to choose in a given voltage range 2–3 values, for example, $U = 0.5U_{NOM}$; $U = 0.3U_{NOM}$, because within this range the relationship $E_{M(N=1)} = f[I_{M(N=1)}]$ is linear.

1.3 Now let us calculate screening factors $S_{N,DIR} = \frac{|F^{RES}_{N,DIR}|}{|F^{ST}_{N,DIR}|}$, for example, $S_{N=7} = \frac{|F^{RES}_{(N=7)}|}{|F^{ST}_{(N=7)}|}$ and $S_{N,AD} = \frac{|F^{RES}_{N,AD}|}{|F^{ST}_{N,AD}|}$, for example, $S_{N=5} = \frac{|F^{RES}_{(N=5)}|}{|F^{ST}_{(N=5)}|}$.

2. Synchronous salient-pole machine.

Values of screening factors $S_{N,AD}$ and $S_{N,DIR}$ for synchronous salient pole machine are to be specified in the way similar to that one for asynchronous machine (p. 1).

2.1 Test to determine MMF $F^{RES}_{N,AD}, F^{ST}_{N,DIR}$ with supply from frequency source of N order harmonic current up to $N \leq 13–17$.

The synchronous salient-pole machine is driven at a speed $n = n_{NOM}$, in such a way that the slip is $s_{N=1} = 0$ for N = 1 order harmonic.

It is fed by a voltage with amplitude corresponding to harmonic order N, for example, $U_N = U_{N=7}$. The stator current amplitude of N order harmonic, for example, $I_N = I_{N=7}$ is to be measured. We have to note that for harmonics of N > 1 order the slip makes $s_N \approx 1$.

It would be appropriate to measure the stator current I_N by using a digital oscillograph. This is due to the necessity to ensure $F^{ST}_{N,DIR}$ and $F^{ST}_{N,AD}$ calculation accuracy: the current I_N amplitude varies within the range $I^{MIN}_N \leq I_N \leq I^{MAX}_N$ according to the variation of magnetic conductance in an air-gap along longitudinal and transverse axes. On the basis of both limit amplitude values one can calculate the value of stator current for harmonics of N order:

$$I^{MED}_N = \frac{I^{MAX}_N + I^{MIN}_N}{2}.$$

Thus, relying on stator current I^{MED}_N the value of $F^{ST}_{N,DIR}$ is specified according to Eq. (3.5′) for MMF [2, 5, 7], for example $F^{ST}_{(N=7)}$. The value $F^{ST}_{N,AD}$, for example, $F^{ST}_{(N=5)}$, is to be determined by an experiment in a similar way.

2.2 Determination of MMF $F^{RES}_{N,DIR}, F^{RES}_{N,AD}$.

Methods to determine by an experiment MMFs on manufacturer's bench for synchronous salient pole and asynchronous machines are similar (see p. 1.2). The synchronous salient-pole machine is also driven at synchronous speed $n = n_{NOM}$, so that the slip makes $s_{N=1} = 0$ for N = 1 order harmonic.

However, in contrast to asynchronous machine there is a need to obtain as a result of testing two no-load characteristics $E_{M,(N=1)} = f[I_{M,(N=1)}]$ for synchronous salient pole machine. They differ by amplitude position of stator MMF with relation to both axes of its poles (longitudinal d or transverse q). The first characteristic

should be relevant to first amplitude matching with d axis and to second amplitude matching with q axis.

To perform two tests one should need to equip additionally a test bench with a special synchronous machine, which must provide changing a mutual position of stator winding field with respect to its pole axes. There is a possibility to avoid additional losses if we simulate the field of synchronous salient-pole machine under conditions required to specify MMF $F^{RES}_{N,DIR}, F^{RES}_{N,AD}$; they are the slip $s_{N=1} = 0$ and the absence of eddy currents in its rotor circuits.

When simulating the field the goal is to determine a mutual inductance of three-phase stator winding and rotor pole system (in the absence of current in excitation winding).

To achieve this goal the following is to be set:

- geometrical dimensions of a machine in cross-sectional view (stator core diameters: outer D_A and inside D_{INN}; pole sizes; air gaps under pole δ_{MIN} and on its periphery δ_{MAX} etc.); it should be appropriate to fill in stator slots with ferromagnetic material in order to avoid the slot ripple effect;
- several values of amplitude of first spatial harmonic of stator winding MMF through which the direct current is spread. They must be chosen in a way that the magnetic system of machine remains unsaturated.

The main stages are the following:

- for period $T = \frac{\pi D_{CALC}}{p}$ we specify a harmonic wave of MMF having amplitude F^{RES}; here $D_{CALC} = D_{INN} - \delta_{MIN}$;
- we put the rotor in the first extreme position (when MMF amplitude coincides with d axis of a pole);
- we determine the first harmonic of mutual induction flux Φ_d during period T and its amplitude B_d;
- mutual inductance factor M_d is equal to [3, 4, 8, 9] $M_d = \frac{\Phi_d W_{PH} K_W}{I}$

Here the describing amplitude of current I is specified from (3.5′) accordingly to MMF amplitude F^{RES}. The calculation expression for M_d factor is to be presented in the form as follows:

$$M_d = \frac{B_d}{F^{RES}} m_{PH} (W_{PH} K_W)^2 \frac{TL_{COR}}{\pi^2 p},$$

where $m_{PH} = 3$—number of stator winding phases; L_{COR}—effective length of stator core.

Then, we put the rotor in the second extreme position (MMF amplitude coincides with pole q axis) and we calculate the factor M_q in a similar way. On the basis of both limit values of factors M_d and M_q we will determine the calculation value of mutual induction factor $M_{d,q} = \frac{M_d + M_q}{2}$

At a frequency of N > 1 order the reactance of magnetizing circuit is specified from the expression: $X_{M(N)} = \omega_N M_{d,q}$; for example, at N = 7: $X_{M(N=7)} \approx 7\omega_{(N=1)} M_{d,q}$, where $\omega_{(N=1)}$—network frequency. Then, in a way similar to that one for asynchronous machine for voltage whose amplitude corresponds to N order harmonic, for example, $U_N = U_{(M=7)}$, we may specify the current of magnetization, for example, $I_{M(N=7)} \frac{U_{N=7}}{jX_{M(N=7)} + Z_{1(N=7)}}$, where $Z_{1(N)}$—stator winding impedance at a frequency of N > 1 order. When calculating the current $I_{M(N)}$ it is supposed that in a way similar to asynchronous machines the phase angular difference Δφ between voltage U_N and current $I_{M(N)}$ is equal to Δφ ≈ 90 el. degr.

Thus, according to Eq. (3.5′) the value $F^{RES}_{N,DIR}$, may be specified for MMF [2, 5, 7], for example, $F^{RES}_{(N=7)}$.

The value $F^{RES}_{N,AD}$, for example, $F^{RES}_{(N=5)}$ is to be specified in a similar manner.

In practice to specify the values $F^{RES}_{N,DIR}$ and $F^{RES}_{N,AD}$ it should be sufficient to choose in a given voltage range 2–3 values, for example, $U = 0.5U_{NOM}$; $U = 0.3U_{NOM}$, because within this range the relationship $E_{M(N=1)} = f[I_{M(N=1)}]$ is linear.

2.3 Let us calculate screening factors $S_{N,DIR} = \frac{|F^{RES}_{N,DIR}|}{|F^{ST}_{N,DIR}|}$, for example, $S_{N=7} = \frac{|F^{RES}_{(N=7)}|}{|F^{ST}_{(N=7)}|}$ and $S_{N,AD} = \frac{|F^{RES}_{N,AD}|}{|F^{ST}_{N,AD}|}$, for example, $S_{N=5} = \frac{|F^{RES}_{(N=5)}|}{|F^{ST}_{(N=5)}|}$

Notes.

1. As required, the value of current I^{MED}_N (see p. 2.1) is to be adjusted. To do it, there is a need to get by using a digital oscillograph the relationship $I_N = I(t)$ [$0 \le t \le 0.5T$, where t—time (el. degr.), $T = 2\pi$—period], and then to calculate I^{MED}_N from the following expression:

$$I^{MED}_N = \frac{1}{\pi} \int_0^{\pi} I(t)dt$$

In a similar manner one can adjust the value of mutual inductance $M_{d,q}$ (see p. 2.2). To do this, there is a need to get at simulation the relationship M = M(x) ($0 \le x \le 0.5T$, where x—coordinate, $T = \frac{\pi D_{CALC}}{p}$, and then to calculate $M_{d,q}$ using the expression:

$$M_{d,q} = \frac{2}{T} \int_0^{\frac{T}{2}} M(x)dx$$

2. To determine the mutual induction factor $M_{d,q}$ by using the simulation of field in a machine it should be sufficient to apply one of program packages for electromagnetic field calculation, for example [10].

16.2.6 *Checking of Rotor Short-Circuited Winding of Asynchronous and Synchronous Salient Pole Machines Heating Due to Higher Time Harmonics (N > 1): Losses for Its Calculation; Their Effect on Load of Operating Machines*

In Sect. 16.2.2.1 it is obtained that additional fields in air gap caused by current higher stator harmonics induce in rotor loops EMF and currents with frequencies from 300 Hz to the value somewhat exceeding 1000 Hz.

Additional losses in rotor loops and their overheats for asynchronous machines can be easily determined for each time harmonic from an equivalent circuit [2, 5, 7] at slips $S_{N,DIR} \approx 1$ or $S_{N,AD} \approx 1$. Approximately, the losses $Q_{CAG,N}$ in short-circuited rotor winding from the mutual induction field of order N are determined from the following formula. At N > 1 it is true ("with a reserve") by slip $s \approx 1$: $I'_{2,N} \approx I_{1,N}$ where $I_{1,N}$—stator current harmonic amplitude of order N; as per (16.1′): $I_{1,N} = I_{KN}$, where I—amplitude of phase current; K_N—expansion coefficient of current curve to harmonics series. As a result, we have:

$$Q_{CAG,N} \approx \frac{1}{2} m_{ST} \left(I_{1,N}\right)^2 R'_{2,N}. \tag{16.22′}$$

where $R'_{2,N}$—reduced AC resistance of short-circuited rotor winding.

Additional losses $Q_{D,N}$ in damper winding and its overheats for salient pole machines can be easily determined for the time harmonic at N > 1, slip $s_{SL} \approx 1$ and at small values of screening constants $S_{N,DIR}$ and $S_{N,AD}$ practically from the following ratios.

To determine approximately losses $Q_{D,N}$ one should replace the damper winding by an equivalent squirrel cage having the same sizes of bars and rotor end rings but keeping the following pitches $b_{CAG,EQ}$ between bars $b_{CAG,EQ} = b_D \frac{\tau_p}{b_p}$, where b_D—pitch between damper winding bars; b_p—width of pole; τ_p—pole pitch. When making such a replacement, one should take into account the peculiarities of synchronous machine and its damper winding; in the contrast to asynchronous machine:

- mutual induction fields of "neighbor" harmonics, for example, N = 5 and N = 7 or N = 11 and N = 13 induce in rotor circuits for the first spatial harmonic (m = 1) the currents of the same frequency ω_{ROT}. For example, for harmonics

N = 5 and N = 7: $\omega_{ROT} = 6\omega_{ST}$, for harmonics N = 11 and N = 13: $\omega_{ROT} = 12\omega_{ST}$ (see Chap. 3). Calculations performed for a series of synchronous salient-pole machines have shown that losses $Q_{D,N}$ in damper winding at mutual effect of "neighbor" harmonics, for example, N = 5 and N = 7, are about K_{COM} = 1.3-fold–1.35-fold greater than under their separate effect, for example, N = 5 and N = 7 (see Chap. 15).

- the amplitude of currents in bars of damper winding rotor does not vary according to the harmonic law (see Chaps. 7, 9–11). The analysis of calculation of losses occurred in this type of winding and got for a series of synchronous salient-pole machines by the solution of equation systems (Chap. 14) has shown that in round figures to admissible power at small values of screening factors $S_{N,DIR}$ and $S_{N,AD}$ one may calculate these losses for equivalent squirrel cage using the equation which is similar to (16.22′):

$$\begin{aligned} Q_{D,N} &= \frac{1}{2} m_{ST} K_{COM} K_D \left(I'_{2,N}\right)^2 R'_{2,N} \\ &\approx \frac{1}{2} m_{ST} K_{COM} K_D (I_{1,N})^2 R'_{2,N}, \end{aligned} \tag{16.22″}$$

where $R'_{2,N}$—reduced A.C. resistance of equivalent squirrel cage,

$$K_D = \sum \left[\frac{\left| \frac{E_M}{Z_B K_B} a_0^{N_D} (a_0 - 1) + C_1 a_1^{N_D} (a_1 - 1) + C_2 a_2^{N_D} (a_2 - 1) \right|}{\left| J_{2,EQ(ND)} \right| N_0} \right]^2 .$$

Here the summing is made by numbers N_D of damper winding bars on pole: $N_D = 0; 1; 2; \ldots; nn$ N_{0-1} symbols for E_M, Z_B, K_B, C_1, a_1, C_2, a_2—see Chap. 9

$$a_0 = e^{\frac{-j2\pi m b_D}{T}}, J_{2,EQ(ND)} = \left| J_{2,EQ(ND)} \right| e^{\frac{-j2\pi m b_{CFG,EQ} N_D}{T}},$$

$J_{2,EQ(ND)}$—amplitude of currents in bars of equivalent squirrel cage. EMF amplitude and values of constants C_1, C_2, amplitude of current $J_{2,EQ(ND)}$ are to be specified for the same amplitude of flux density in air gap B_m = idem, for example, at B_m = 1 T, so expressions for currents in the numerator and denominator of equation for factor K_D may be considered as generalized characteristics of these currents. Usually the value of K_D is in an interval of 1.35–1.5.

Let us note that overheats of short- circuited elements in the rotor of asynchronous and salient pole machines are not normalized in GOST and rule of IEC [16–19]. However, the temperature of bars of damper winding of synchronous salient-pole machines is limited under service conditions by the value Θ < 160–180 °C (see Chap. 9); once it is exceeded, winding damages may take place due to

thermal deformations. The same restrictions are set for squirrel cage temperature Θ by asynchronous machine operating practice.

For practical needs the check of winding temperature Θ, specified by losses $Q_{CAG,N}$ or $Q_{D,N}$, is recommended to carry out upon the reduction of rated power according to (16.21).

For practical purposes, screening factors of synchronous salient-pole machine can use approximately Eq. (16.12′), and for losses in stator and rotor cores—Eqs. (16.19) and (16.20) by presentation the damper winding as the equivalent squirrel cage. There is no need to introduce additional factors for calculation while $S_{N,DIR} \le 0.12$ and $S_{N,AD} \le 0.12$ due to $I_{EX,NOM}$ and for realized machines $P^*_{COR} \approx 0.92–0.95$.

For correct designed construction of synchronous machine damper winding ($S_{N,DIR} \le 0.12$, $S_{N,AD} \le 0.12$) the influence of higher harmonics ($N > 1$) on the overheating of the excitation winding is small and can be omitted.

For the synchronous machine if the value of cos φ of the nonlinear load (with $N = 1$) is less than the rated value, the rotor current should be additionally calculated [7]. This current may be greater than the nominal $I_{EX,NOM}$, despite the fact that the power $P^*_{ADM} < 1$. Then the power P^*_{ADM} should be correspondingly reduced further due to overheating of the rotor winding.

If $P^*_{ADM} < 1$ and rotor current $|I|_{EX} < 0.7|I|_{EX,NOM}$, it is usually at $K_{DIST} < 0.35$ overheating of rotor winding meets the requirements of [16].

16.3 Method of Determination Admissible Modes of High-Power Salient-Pole Generator Under Combined Load [11–13]

Modern salient-pole generators are often used at independent power plants marine and stationary, for example, at Nuclear Power Plant. as reserve or emergency power supplies. Usually, they work under a combined load; for example, on vessels they are applied as power supplies of frequency-controlled induction motors for pumps and onboard installations with direct current motor drives (via rectifiers), and also as this generator lighting and heating of the vessel. Let us consider a problem on the determination of admissible operation modes of high-power synchronous salient-pole generator under a combined load rather often provided in circuits of autonomous power plants; part of such a load is characterized by the reduced power factor ($\cos \varphi < 0.8$) and increased values of nonlinear distortion factor K_{DIST} of voltage or current [2, 5, 7].

We express the combined load of such a generator in the form of two equivalent receivers with different parameters. Let us assume that generator ratings, its AC resistance and reactance, and also parameters of both receivers (power factors and nonlinear distortion factors) are set up.

Let us accept for clarity that the nonlinear distortion factor of the first receiver $K_{DIST(1)} < 0.05$, and the second $K_{DIST(2)} > 0.05$. We find a relationship between stator current first harmonic of the second receiver I_2 and the first harmonic of admissible stator current I_{EQ} of generator, whose value is to be determined. Let us designate power factors of both receivers corresponding to the first harmonic of stator currents as cos φ_1 and cos φ_2. We notice that in practice usually the current of "sinusoidal load" I_1, is given, and that of "rectified load" I_2, is to be determined proceeding from parameters of receivers and generator ratings of autonomous power plant. For the first current harmonics we have [3, 4]:

$$I_1 e^{j\varphi_1} + I_2 e^{j\varphi_2} = I_{EQ} e^{j\varphi_E}, \tag{16.24}$$

where values of currents I_1, I_2, I_{EQ}—time complexes (phasors), φ_{EQ}—phase angle between complexes of current I_{EQ} and voltage U of generator.

For receivers with AC resistance and reactance from this equation we obtain an expression for the calculation of value of current of the second receiver:

$$|I|_2 = -|I|_1 \cos(\varphi_2 - \varphi_1) + \sqrt{|I|_{EQ}^2 - |I|_1^2 \sin^2(\varphi_2 - \varphi_1)}. \tag{16.25}$$

Here $|I|_1, |I|_2, |I|_{EX}$—moduli of current values; in the same way are designated moduli of values of EMF, voltages and MMF. Proceeding from conditions of stator winding heating, the following condition should be satisfied:

$$|I|_{EX} < |I|_{NOM}. \tag{16.26}$$

Here $|I|_{NOM}$—rated current modulus of generator stator. According the current I_{EQ} in (16.26) we obtain the amplitude of MMF stator winding F_{EQ}.

The calculation expression for phase angle of this current:

$$\varphi_{QE} = \arccos \frac{|I|_1 \cos \varphi_1 + |I|_2 \cos \varphi_2}{|I|_{EQ}}.$$

Using Eq. (16.25) the current of the second receiver I_2 is determined, if the equivalent current I_{EQ} of generator is known. With the condition (16.26), the additional requirements connected with stator winding overheat and admissible rotor current should be met.

Let us consider the influence of higher time harmonics on stator winding overheat. For this overheat not to exceed admissible, the additional condition should be satisfied:

$$|I|_{EQ}^2 K_{F,1} + |I|_2^2 \left(\sum Q_{DC,N}^* + \sum \Delta Q_{DC,N}^* \right) \le |I|_{NOM}^2 K_{F,1}, \tag{16.27}$$

summation is made over harmonics numbers of order $N > 1$. Usually in the summation it is enough to consider the first three–four current harmonics.

By means of this ratio, the current of the second receiver I_2 is refined with account of higher harmonics, if the equivalent current I_{EQ} of generator is already determined.

For determination of current and overheat of generator rotor winding and excitation system windings it is convenient to use Potier diagram [2, 5, 7], which sets the dependence between excitation current I_{EX}, stator equivalent current I_{EQ} and generator power factor cos φ_{EQ}:

$$|I|_{EX} \sim \frac{1}{WEX} \sqrt{|F|_{MC}^2 + |F|_{EQ}^2 + \frac{2|F|_{MC} + |F|_{EQ}}{1 + \left(\frac{\cos \varphi_{QE}}{X_P + \sin \varphi_{EQ}}\right)^2}}, \tag{16.28}$$

$$|E|_I = |U|_{PH} \cos^2 \varphi_{EQ} + \left(X_P + \sin \varphi_{EQ}\right)^2. \tag{16.29}$$

Here X_P—Potier reactance (p.u.); $|F|_{MC}$—magnetic circuit MMF, determined by EMF $|F|_I$ [7]; $|U|_{PH}$—generator voltage; MMF F_{EQ}–I_{EQ}.

$$|I|_{EX} \leq |I|_{EX,NOM}, \tag{16.30}$$

where $|I|_{EX,NOM}$—generator excitation current by rating power. The last inequality follows from the requirements of providing admissible overheat of generator rotor winding and also excitation system windings.

In general, the determination of generator admissible mode at the combined load is a variational problem (determination of maximum ratio of currents $\frac{|I|_{EQ}}{|I|_{NOM}}$) at set system of restrictions (16.26), (16.27), (16.30).

The problem is formulated as follows.

Given: $|U|_{PH}, |I|_{NOM}, |R|_{PH}, |X|_P, |I|_{EX,NOM}, |I|_1, \cos \varphi_1, \cos \varphi_2, K_{N,2}, K_{N,N}$.

It is necessary to determine $|I|_2$, $|I|_{EQ}$, φ_{EQ}, $|I|_{EX}$ under the condition:

The ratio $|I|_{EQ}/|I|_{NOM}$ with a system of restrictions (16.26), (16.27), (16.30) should be maximum in this variational problem.

Let us state the main stages of problem solution (solution algorithm).

1. We set a current $|I|_{EQ} = K_{EQ}|I|_{NOM}$, where $K_{EQ} < 1$. As the first approach, we assume $K_{EQ} = 0.95$.
2. Let us calculate the current $|I|_2$ and further φ_{EQ} as per (16.25).
3. Let us check the fulfillment of conditions (16.26), (16.27). If they are not fulfilled, the value K_{EQ} should be decreased and items 1, 2 repeated.
4. Let us calculate the current $|I|_{EX}$. as per (16.28), (16.29). If the condition (16.30) is not fulfilled, the value K_{EQ} should be decreased and item 2, 3, 4 repeated.
5. If conditions (16.27), (16.30) are fulfilled, values $|I|_2$, $|I|_E$, φ_E and $|I|_{EQ}$—to be determined

6. At excitation currents $0.7|I|_{EX,NOM} \leq |I|_{EX} < |I|_{EX,NOM}$ and simultaneously at the greater value of K_{DIST} it is expedient to calculate the excitation winding heating with account of additional losses created in rotor loops by fields higher harmonics in stator boring. At currents $|I|_{EX} < 0.7|I|_{EX,NOM}$ for factors $K_{DIST(2)}$ taking place in practice ($K_{DIST} < 0.35$), the excitation winding heating usually does not exceeds the value admissible as per [16].

At achievement of listed conditions, the problem is solved.

The method was checked in bench conditions at the Work "Elektrosila" (St. Petersburg) generator of 2000 kW, 690 V, 2p = 8, intended for drilling rig.

16.4 About the Level of Electromagnetic Load of Modern Salient-Pole Generators and Their Dynamic Characteristics in Independent Mode

16.4.1 General Comments

For the generators of independent power plants working in non-linear circuit have a high level of electromagnetic load ensuring their high technical and economic performance and competitiveness. However, on the way to raise these indicators there are problems caused by modern practice of generators operation in dynamic modes [14, 15]. Decreasing the rated power due to the higher harmonics in a nonlinear network to a value of P^*_{ADM}, according to (16.21), often permits us to solve these problems.

16.4.2 Requirements for Dynamic Modes

At sudden load variations such generators should have certain restrictions for the value of ΔU of transient voltage deviation in comparison with rated. For generators of marine power plants this requirement is formulated in [17–19]: load-on is made from no-load; the value of this load is equal to P_2 = 60 % of rated power of generator S_T (kVA), and its inductive power factor does not exceed cos φ ≤ 0.4; voltage drop ΔU makes ΔU15 %; time T of voltage recover T ≤ 1.5 s, and accuracy—not less than ±3 % of rated voltage. Similar requirements are also imposed in operation to generators of stationary independent power plants.

Figure 16.1 and Table 16.2 represent as illustration a voltage variation curve of generator 625 kVA, 400 V, 1500 rpm at load-on equal to 80 % of its power at cos φ = 0.4.

Providing these requirements for voltage drops often causes problems in designing modern autonomous salient-pole generators for independent power

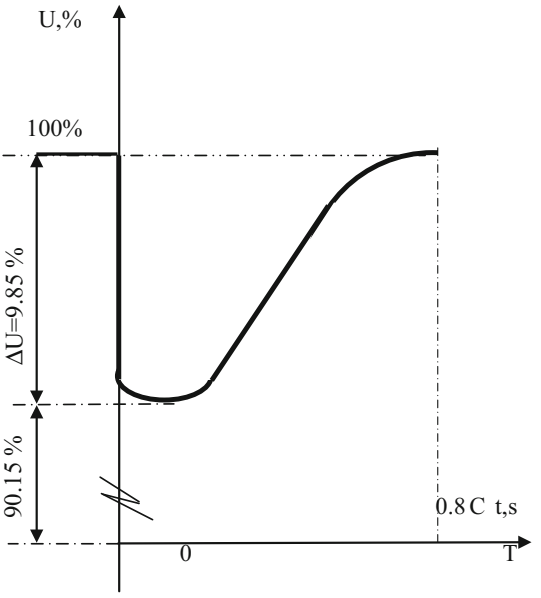

Fig. 16.1 Voltage variation curve ΔU of generator 625 kVA

Table 16.2 Voltage variation ΔU of generator 625 kVA

Reactances	Voltage variation ΔU (%) (load-on 500 kVA = $0.8S_T$; cos φ = 0.3)		Error ε (%)
X'_D = 17 % X''_D = 12 %	9.85 (test)	11.35 (calculation as per [14, 15])	1.5

plants. Let us consider in more detail the reason of their emergence and measure for their solution.

16.4.3 Transient Deviation of Generator Voltage ΔU, Influence of Its Reactances

Analytical investigation of voltage variation process at sudden load variations is performed by several methods [8, 9], for example, on the basis of a system of Park[1] equations. Voltage drop value ΔU at load-on equal to S_T = 100 % (kVA) at inductive cos φ ≤ 0.4 can be calculated from the approximate ratio:

[1]In Russian scientific literature these equations call usually Park–Gorev's equations, according to the well known Gorev's book: "Transients of synchronous machine", Moscow, Gosenergoizdat, 1950, 551 p.

$$\Delta U \approx \frac{X^*}{1+X^*}, \tag{16.31}$$

where X*—calculation reactance: $X''_D \le X^* \le X'_D$; X''_D, X'_D—respectively direct-axis subtransient and transient reactances. The value of transient voltage deviation (drop) is expressed in fractions of generator rated voltage, and values of reactances are expressed in relative units (p.u.) [8].

Thus, the solution of problem on the reduction of voltage dip ΔU is connected with that on the restriction of reactances X''_D and X'_D [2, 5, 7]:

$$X''_D = X_L + \frac{1}{\frac{1}{X_{AD}} + \frac{1}{X_F} + \frac{1}{X_{KD}}}, \tag{16.32}$$

besides

$$X_L = \frac{AS}{B_1} K_{XL}; \quad X_{AD} = \frac{AS}{B_1} K_{XAD}; \quad X_F = \frac{AS}{B_1} K_{XF}; \quad X_{KD} = \frac{AS}{B_1} K_{XKD}; \tag{16.33}$$

here X_L—stator winding leakage inductive reactance; X_{AD}—inductive reactance of direct-axis armature reaction; X_F, X_{KD}—direct axis leakage inductive reactance of excitation winding and damper winding, correspondingly; K_{XL}; K_{XAD}; K_{XF}; K_{XKD}—proportionality factors [7]. In the absence of damper winding ($X_{KD} \to \infty$), we obtain: $X''_D \to X'_D$; AS—stator winding current load, B_1—resulting field flux density amplitude in air gap [2].

Therefore, for the restriction of value X* there are some opportunities to reduce the value of proportionality factors listed in (16.33) or to reduce the ratio AS/B_1.

Let us note that selection of these proportionality factors depends on the ratio AS/B_1.

Calculation practice of modern salient-pole generators for independent power plants confirms that by decreasing proportionality factors in (16.33) due to any change of stator tooth zone geometry, rotor poles and damper winding slots, usually it is possible to obtain the required value of ΔU, if the voltage drop ΔU exceeds restrictions no more than by 5–6 %: ΔE ≤ 5–6 %.

16.4.4 Inductive Resistances and Their Influence on Generator Weight and Dimensional Indicators

Progress in achieving the modern level of technical and economic indicators (efficiency level, minimum weight M_{GEN} and cost) is obtained due to the progress in designing these generators and their production technology, including due to a

rising level of their electromagnetic loads: current load AS and flux density B_1. Let us note that for the last decades we succeeded in increasing the level of these generators approximately by 1.4–1.5 times, generally due to an increase in current load AS. Omitting intermediate calculations, it is easy to obtain the following ratio [7]: $X^* \equiv \Delta U \equiv AS \equiv \frac{1}{M_{GEN}}$.

Thus, modern requirements are to decrease the generator weight and dimensions in conflict to requirements [17–19] on restriction of ΔU.

16.4.5 Problem Solutions: Offers

16.4.5.1 Offers for Newly Manufactured Generators

For newly manufactured generators, it is expedient to bring into compliance the reached electromagnetic load with ΔU voltage drop required in operation, similarly to the case with inductive reactance X'_D of modern turbogenerators in [20]; for each group of generators with power $P_{1,MIN} \le P_1 \le P_{1,MAX}$ it is necessary to determine the admissible value of load $P_{2,MIN} \le P_2 \le P_{2,MAX}$, applied to generators from no-load mode. Thus, it is necessary to consider also reactances of these generators. We note that the number of turbogenerator groups given in the Standard [20], is equal to three. It is expedient to distribute this recommendation also to standards for generators of independent power plants.

16.4.5.2 Offers for Generators Which Are in Operation

For generators in operation, this problem can be solved by a different way. From a group of consumers, it is expedient to allocate, if technologically possible, two–three subgroups differing in degree of their production need. It is easy to automate a sequence of connecting these subgroups (every few seconds). As a result, values of voltage drop $(\Delta U)_{GR} < 15–20$ % required in operation for modern generators and values $X'_D \approx 0.35–0.4$ can be achieved. It is confirmed as follows. In order to connect to the subgroup $P_{2,GR} < P_1$, reactances for subgroup $(X''_D)_{GR}$ and $(X''_D)_{GR}$ are calculated from the ratios:

$$(X''_D)_{GR} = X''_D \frac{P_{2,GR}}{P_{NOM}}; \quad (X'_D)_{GR} = X'_D \frac{P_{2,GR}}{P_{NOM}}. \tag{16.34}$$

Respectively, also the calculation value of inductive reactance $(X^*)_{GR}$ changes:

$$(X^*)_{GR} = X^* \frac{P_{2,GR}}{P_{NOM}}. \tag{16.35}$$

As a result, we obtain: $(\Delta U)_{GR} < \Delta U$.

However, in operation practice it is impossible to exclude such problems, when it is impossible to allocate two–three subgroups of technological consumers. In this case it is expedient to use a method often applied, if necessary, to start the induction motor with high torque M_{MECH} of driving mechanism and with high value of moment of inertia J ("heavy start"); a generator is selected so that its model power P_{MOD} exceeded the rated value: $P_{MOD} > P_{NOM}$; generator model power P_{MOD} is determined so that its reactances provided an application of load with the set value of ΔU.

Note that from the Eqs. (16.34) and (16.35) it follows that decreasing the rated power up to P^*_{ADM} according to (16.21), also allows us to simultaneously reduce the value of ΔU

16.4.6 Additional Requirements to Generators

Additional requirements to generators: necessity to start an induction motor. This requirement is formulated in [16]. Speed-up process of such a motor besides reactances is influenced by the following parameters of generator excitation systems (response speed, forcing rate, etc.), and also load parameters: torque of driving mechanism M_{MECH} and its dynamic moment of inertia J.

Let us note that the motor speed-up process with account of generator parameters is usually calculated using the system of Park equations [8]. For practical calculations in this system it is expedient to present in more detail damper winding loops (in the form of several distributed loops, but not in the form of concentrated loop in each axis); this system should also be added to the equations describing processes in loops of exciter and induction machine.

Brief Conclusions

1. Modern high-power salient-pole generators are often used in systems with combined load, which partly contain frequency converters or rectifiers. Practice moves forward the problem: to determine the admissible power of generators with account of high time harmonics of nonlinear load. Developed method allows solving it using a numerical method with a number of consecutive approximations.
2. Modern highly-used generators of autonomous power plants bring forward requirements of providing performance data in dynamic modes. These requirements contradict to those on reducing generator dimensions and weight, increase of their competitiveness.
3. Some practical solutions of this problem are considered: consecutive start-up of load units, selection of generator with model power exceeding rating power, etc.

List of symbols

AS	Stator winding current load
B_m	Resulting field flux density amplitude in air gap
$B_1^{YOKE}, \ldots, B_5^{YOKE}, \ldots, B_N^{YOKE}$	Calculation flux density in the yoke, determined by resulting field harmonics
D^{YOKE}, D^{TEETH}	Coefficients determined for the yoke or teeth by grade of electrotechnical steel, roll direction (for cold-rolled steel), stack assembly technology
$f_{N,AD}^{ROT}, f_{N,DIR}^{ROT}$	Current frequencies in rotor loops induced by fields of orders N_{AD}, N_{DIR}
$F_{N,AD}^{RES}, F_{N,AD}^{ROT}, F_{N,AD}^{ST}$	MMF of order N_{AD} respectively of resulting field (of mutual induction), rotor and stator fields
$F_{N,DIR}^{RES}, F_{N,DIR}^{ROT}, F_{N,DIR}^{ST}$	The same for MMF of order N_{DIR}
F_{MC}	Magnetic circuit MMF
G_{YOKE}, G_{TEETH}	Weight of yoke, teeth
I	Amplitude of non-sinusoidal current
I_1	First current harmonic of stator "linear load" (of the first receiver)
I_2	First current harmonic of stator "nonlinear load" (of the second receiver)
I_{EX}	Generator excitation current
I_{NOM}	Generator stator rated current
I_{EQ}	First harmonic of generator stator equivalent current
K_1, K_N	Coefficients for harmonics of order N = 1 and N > 1 for expansion of non-sinusoidal current into a series
K_{DIST}	Nonlinear distortion factor
$K_{F,1}, K_{F,N}$	Stator winding field's factors for harmonics of order N
$\Delta K_{F,1}, \Delta K_{F,N}$	Coefficients of additional losses in stator winding for harmonics of order N = 1 and N > 1
K_X	Inductance decrease factor
$K_{XL}; K_{XAD}; K_{XF}; K_{XKD}$	Proportionality factors
m_{PH}	Number of stator phases
N	Order of time harmonic
N_{AD}, N_{DIR}	Order of time harmonic respectively for positive (direct) and additional field
P_{ADM}^*	Admissible total power for machine operation with frequency converter (in p.u.)
P_w^*	Admissible power for machine operation in network with frequency converter, proceeding from stator winding losses and its overheat

P^*_{COR}	The same, proceeding from losses in stator and rotor cores of stator and its overheat
$\sum Q^*_{DC,N}, \sum \Delta Q^*_{DC,N}$	Sum of the main (D.C. losses) and additional losses in winding (in p.u.)
R_{PH}	DC resistance of stator phase
R_{ST}, $L_{ST,N}$	DC resistance and leakage inductance of rotor bar
$S_{N,AD}, S_{N,DIR}$	Screening factors
S_{YOKE}, S_{TEETH}	Calculation cross section of yoke or teeth for flux density calculation
T	Time of voltage recover
T_0 = 360 el. degr.	Period of current (V)
ΔU	Value of generator voltage variation in transient mode
W_{EX}	Number of turns in excitation winding
$W^{YOKE}_{N=1}, W^{YOKE}_{N}$	Losses in yoke from mutual induction fields of order N = 1 and N > 1
$\sum W^{TEETH}_{N=1}, \sum W^{TEETH}_{N}$	Losses in yoke or teeth from mutual induction fields of order N = 1 and N > 1
X''_D, X'_D	Transient and subtransient reactances of generator
X_L	Stator winding leakage reactance
X_{AD}	Inductive reactance of direct-axis armature reaction
X_F, X_{KD}	Direct axis leakage reactance of excitation winding and damper winding, correspondingly
X_p	Potier reactance
$Z_{BAR,N}$	Impedance of rotor bar
$\cos\varphi_{EQ}, \cos\varphi_1, \cos\varphi_2$	Equivalent power factors of receivers, respectively, first and second
$\Psi^{ROT}_{N,AD}, \Psi^{ST}_{N,AD}$ and $\Psi^{ROT}_{N,DIR}, \Psi^{ST}_{N,DIR}$	Phase angles of MMFs $F^{ROT}_{N,AD}, F^{ST}_{N,AD}$ and $F^{ROT}_{N,DIR}, F^{ST}_{N,DIR}$

References

I. Monographs, Textbooks

1. Boguslawsky I.Z., A.C. motors and generators. The theory and investigation methods by their operation in networks with non linear elements. Monograph. TU St.Petersburg Edit., 2006. Vol. 1; Vol.2. (In Russian).
2. Richter R., Elektrische Maschinen. Berlin: Springer. Band I, 1924; Band II, 1930; Band III, 1932; Band IV, 1936; Band V, 1950. (In German).

3. Demirchyan K.S., Neyman, L.R., Korovkin, N.V., Theoretical Electrical Engineering. Moscow, St.Petersburg: Piter, 2009. Vol. 1, 2. (In Russian).
4. Kuepfmueller K., Kohn G., Theoretische Elektrotechnik und Elektronik. 15 Aufl. Berlin, New York: Springer. 2000. (In German).
5. Mueller G., Ponick B., Elektrische Maschinen. New York, John Wiley, 2009. 375 S. (In German).
6. Schuisky W., Berechnung elektrischer Maschinen. Wien: Springer, 1960. (In German).
7. Mueller G., Vogt K., Ponick B., Berechnung elektrischer Maschinen. Springer, 2007. 475 S. (In German).
8. Concordia Ch. Synchronous Machines, Theory a. Performance. New York: John Wiley, 1951.
9. Ruedenberg R., Elektrische Schaltvorgaenge. Berlin, Heidelberg, New York: Springer, 1974. (In German).
10. J.R. Claycomb, Applied Electromagnetics Using Quic Field&MATLAB. Houston Baptist University. 2008

III. Synchronous Machines. Papers, Inventor's Certificates, Patents

11. Boguslawsky I.Z., Problem of the decreasing of additional losses in high power A.C. machines at working in networks with nonlinear elements. News of the Russian Academy of Sciences. Energetika (Power engineering). 2009, № 2, (In Russian).
12. Boguslawsky I.Z., Method of determination of a permissible power of A.C. motor at working in a nonlinear network. Elektrotechnika. № 5, 2009 (in Russian).
13. Boguslawsky I.Z., Permissible regime of the generator under the mixed loading. Elektrotechnika, 1983, № 12, (in Russian).
14. Boguslawsky I.Z., Generators for independent power plants: performance and trends. Archiv fuer Elektrotechnik (El.Eng.), 2006, № 5, Springer Verlag, Berlin.
15. Boguslawsky I.Z., Korchagin N.W., Kroug A.Ja., Popov V.V., Sidelnikov B.V., Rogachevsky W.S., Synchronous generators of stand – alone power stations: dynamic performances and method of their implementation. The Institute of Electrical and Electronics Engineers (IEEE). Proceedings of the international workshop on renewable energy based units and systems. 2006 (REBUS'06).

IV. State Standards (IEC, GOST and so on)

16. GOST (Russian State Standard) R-52776 (IEC 60034-1). Rotating Electrical Machines. (In Russian).
17. IEC 60092-301 Electrical installations in ships. Part 301: Equipment Generators and Motors.
18. Rules and Regulations for the Classification of Ships. Part 6 Control, Electrical, Refrigeration and Fire. Lloyd's Register of Shipping (London). 2003.
19. Russian Maritime Register of Shipping. Vol.2. Rules for the classification and construction of sea going ships. St. Petersburg. 2003, (In Russian).
20. Rotated electrical machines. Turbogenerators. The general technical specifications. GOST 533-2000. Minsk (Belorussia). Interstate council on standardization, metrology and certification, (In Russian).

Chapter 17
Frequency-Controlled Induction Motors in Nonlinear Networks: Assessment Criteria of Higher Harmonics Influence—Method of Criteria Calculation

This chapter presents the criteria for evaluation of the level of their application with account of the harmonic composition of supply voltage, which have been elaborated and proposed for frequency-controlled asynchronous machines. Computational methods have been proposed for criteria identification. The peculiarities of electromagnetic brake operating mode of motors in case of dirty power have been featured. This mode has some distinctions: when an asynchronous motor operates in a linear network under "electromagnetic brake" conditions the drive's energy corresponding to braking torque is converted into electrical power and appears in rotor circuits, but for frequency-controlled asynchronous machines, we have stated that in "electromagnetic brake" mode the energy corresponding to time harmonics of voltage $Q_{AD} = 5, 11, 17, \ldots$ is compensated by that of harmonics of other orders $Q_{DIR} = 1, 7, 13, 19, \ldots$, which comes from the network and appears in rotor circuits.

The content of this chapter is the development of methods stated in [1, 6–21].

17.1 Higher Harmonics and Need of Their Influence Assessment on Machine Modes in Nonlinear Network

The extent of machine electromagnetic load in nonlinear network and, therefore, machine weight, its dimensions and competitiveness can differ at the same voltage and current nonlinear distortion factor $K_{DIST} = \text{idem}$ usually limited to $K_{DIST} < 0.3 \sim 0.35$. It is connected not only with the ratio of amplitudes of various time harmonics of the resulting fields in air gap of three-phase machine in nonlinear network, but also their influence on machine processes. In Chap. 3, fields in air gap contain time harmonics of orders [1–5]:

I. Boguslawsky et al., *Large A.C. Machines*,
DOI 10.1007/978-4-431-56475-1_17

$$\begin{aligned} Q_{DIR} &= 1, 7, 13, 19, \ldots, 6k - 5; \\ Q_{AD} &= 5, 11, 17, 23, \ldots, 6k - 1; \quad (\text{at } k = 1, 2, 3, \ldots). \end{aligned} \tag{17.1}$$

These harmonics differently influence the formation of frequency-controlled machine torque without taken into account the nonlinear distortion factor K_{DIST}. Let us consider this extent of influence of separate higher harmonics in more detail. We note only that in Eqs. (17.1) there are no harmonics, multiple to three: standard star connection of stator winding phases is supposed.

For harmonics of time order of $Q_{AD} > 1$ at restriction of investigation of the first spatial harmonic (m = 1) the direction of their rotation fields is opposite to rotor rotation, so they create "braking" torque. In electrical machine-building practice at sinusoidal power supply (Q = 1, m = 1) the induction motor mode is assumed as "electromagnetic brake" mode, if the stator field rotation direction is opposite to rotor shaft direction [2, 3].

Unlike harmonics of time order $Q_{AD} > 1$, for harmonics of time order $Q_{DIR} > 1$ at m = 1 their direction of fields rotation coincides with that of rotor rotation. At sinusoidal power supply, such operation mode is assumed as "motor".

However, in relation to frequency-controlled induction and salient-pole machines both of these modes at $Q_{AD} > 1$ and $Q_{DIR} > 1$ (at m = 1)—have additional peculiarities. Let us consider them.

17.2 Frequency-Controlled Induction Machines with Short-Circuited Rotor

Such machines with frequency converter in stator circuit are nowadays rather often used in an industry as part of frequency-controlled drives. Methods of analysis of frequency-controlled machines with rotor that contains the phase winding and with converter in its circuit (double fed machines) are considered in [6–9] and in Chapter 2.

17.2.1 Harmonics $Q_{AD} > 1$ (m = 1): Slip S_{AD}, EMF and Current Frequencies $F_{AD,ROT}$ in Rotor Loops. Power Balance in Secondary Loop

Slip S_{AD} and EMF frequencies $f_{AD,ROT}$, for harmonics of orders representing practical interest are compared in Table 17.1. They are found from the ratios:

$$\begin{aligned} S_{AD} &= \frac{Q_{AD} - S_1 + 1}{Q_{AD}}; \quad f_{AD,ROT} = f_1(Q_{AD} - S_1 + 1) = f_1 S_{AD} Q_{AD}; \\ S_1 &= \frac{\omega_1 - p\omega_{REV}}{\omega_1}. \end{aligned} \tag{17.2}$$

Table 17.1 Comparison of parameters for time harmonics of order Q_{AD}

Q_{AD}	S_{AD}	$f_{AD,R}$ (Hz)	P_{EL}^{AD}	$P_{W,R}^{AD}$	P_{W}^{AD}
5	1.198	299.5	0.8347	1.0	–0.1653
11	1.09	599.5	0.9174	1.0	–0.0826
17	1.0582	899.4	0.9450	1.0	–0.0550
23	1.043	1199.45	0.9588	1.0	–0.0412

Here ω_1—circular frequency of network voltage first harmonic $\omega_1 = 2\pi f_1$; for example $f_1 = 50°\text{Hz}$, ω_{REV}—rotor rotation speed, p—number poles pairs. Slip S_1 in Table 17.1 is accepted for certainty equal: $S_1 \approx 0.01$.

Let us consider losses in machine loops, power balance for harmonics of order Q_{AD} and ratios of powers consumed by the motor from network and from shaft at slips $S_{AD} > 1$.

We use the main equations necessary for this mode analysis. We present the active power $P^{AD}(\omega_{REV})$ of time harmonic of order Q_{AD}, consumed from network at rotor shaft rotation speed ω_{REV}, in the form:

$$\begin{aligned} P^{AD}(\omega_{REV}) &= P_{W,ST}^{AD}(\omega_{REV}) + P_{ST}^{AD}(\omega_{REV}) + P_{EL}^{AD}(\omega_{REV}), \\ P_{EL}^{AD}(\omega_{REV}) &= P_{W,R}^{AD}(\omega_{REV}) + P_{W}^{AD}(\omega_{REV}). \end{aligned} \tag{17.3}$$

Here $P_{W,ST}^{AD}(\omega_{REV}) \sim I_1^2 R_1$—losses in stator winding phase; $P_{ST}^{AD}(\omega_{REV}) = P_{FE}(\omega_{REV}) + P_{AD}(\omega_{REV})$—losses which are not proportional to square of currents in machine windings (in stator and rotor cores, additional, etc.). In Table 17.1 it is designated: $P_{EL}^{AD}(\omega_{REV}) \sim I_2^2 \frac{R_2}{S_{AD}}$—electromagnetic power in air gap from network; $P_{W,R}^{AD}(\omega_{REV}) \sim I_2^2 R_2$—losses in rotor equivalent winding; $P_{W}^{AD}(\omega_{REV}) \sim I_2^2 R_2 \frac{1-S_{AD}}{S_{AD}}$—power on motor rotor shaft created by the voltage harmonic of order Q_{AD}; I_2 and R_2 are the current and A.C. resistance of rotor winding equivalent phase reduced to stator winding phase ("dash" signs are omitted).

Powers $P_{EL}^{AD}; P_{W,R}^{AD}; P_{W}^{AD}$ are represented for a comparison in Table 17.1 on the assumption that in this table for each value of slip $S_{AD} > 1$ the common multiplier for three last power components $T = I_2^2 R_2$ is assumed as 100 %: T = 1.

It follows from ratios (17.3) and Table 17.1:

- for harmonics $Q_{AD} > 1$, the slip $S_{AD} > 1$, and with growth in harmonics order the value $S_{AD} \to 1$;
- current frequency in rotor loops is considerable: in rated mode $(S_1 \approx 0.01)$ it is much bigger of the network frequency; this phenomenon has a simple physical interpretation. Occurrence of such frequencies in machines results in emergence of not only additional losses and heatings in rotor loops, but also noise and vibrations. From electrical machine engineering practice it is known that induction machine modes at slips $(S_1 > 1)$ are characterized by emergence of considerable losses and heatings [2, 3] in windings in comparison with modes at

$S_1 \leq 0.01$; these slips occur also in the case under consideration ($S_{AD} > 1$) that reduces the level of electromagnetic load of frequency-controlled machine.

Powers P_{EL}^{AD} and P_W^{AD} do not participate in the creation of net torque, and power P_W^{AD} creates the braking torque. As a result, the working speed of rotor shaft rotation ω_{REV} changes in comparison with the speed when fed from a linear network; power consumed by the motor from a network also changes and, respectively, dependence of electromagnetic torque on slip S_1. Power P_W^{AD} is compensated for frequency – controlled motors not from driving mechanism shaft as at sinusoidal power supply in the mode of "electromagnetic brake", but from the network at the expense of power of harmonics of other orders. This makes a difference of braking mode generated by time harmonics of orders $Q_{AD} > 1$ from the usual braking mode of induction motors (fed from linear network). This peculiarity of physical process in frequency – controlled machines is not taken into account by the factor K_{DIST}.

17.2.2 *Harmonics $Q_{DIR} > 1 = (m = 1)$: Slip S_{DIR}, Frequency of EMF and Currents in Rotor Loops. Power Balance in Secondary Loop*

Slip S_{DIR}, frequency of EMFs and currents for harmonics of orders representing practical interest are compared in Table 17.2, which are found from the ratios (17.4) similar to (17.2):

$$S_{DIR} = \frac{Q_{DIR} + S_1 - 1}{Q_{DIR}}; \quad f_{DIR,ROT} = f_1(Q_{DIR} + S_1 - 1) = f_1 S_{DIR} Q_{DIR}. \quad (17.4)$$

Slip S_1 in Table 17.2 for certainty is also accepted equal to $S_1 \approx 0.01$.

Let us consider losses in machine loops, power balance for harmonics of order Q_{DIR} and ratios of powers consumed by the motor from network and power transferred to shaft at slips $S_{DIR} < 1$.

We use the main equations necessary for analysis of this mode; they are similar to (17.3).

Powers $P_{EL}^{DIR}; P_{W,R}^{DIR}; P_W^{DIR}$ are presented for a comparison in Table 17.2 as well as in Table 17.1 on the assumption that in this table at each slip $S_{DIR} < 1$ for three last components of power, their common multiplier $T = I_2^2 R_2$ (losses in rotor winding $P_{W,R}^{DIR}$) is taken as 100 %: T = 1.

Table 17.2 Comparison of parameters for time harmonics of order Q_{DIR}

Q_{DIR}	S_{DIR}	$f_{DIR,R}$ (Hz)	P_{EL}^{DIR}	$P_{W,R}^{DIR}$	P_W^{DIR}
7	0.8586	300.51	1.1647	1.0	0.1647
13	0.9238	600.470	1.0825	1.0	0.0825
19	0.9479	900.505	1.0550	1.0	0.0550
25	0.9604	1200.5	1.0412	1.0	0.0412

From the ratio (17.4) and Table 17.2 it follows:

- for harmonics $Q_{DIR} > 1$, slip $S_{DIR} < 1$, and with growth in their harmonics order, the value $S_{DIR} \to 1$;
- current frequency in rotor loops as well as at $Q_{AD} > 1$, is practically much more of the network frequency; all remarks concerning the influence of frequencies of such a level on losses and heating, noise and vibrations remain true for harmonics of order $Q_{DIR} > 1$ as well as for harmonics $Q_{AD} > 1$. The remark concerning peculiarities of induction machine modes also remains true at $S_1 \approx 1$ in comparison with its modes at $S_1 \leq 0.01$; these peculiarities also reduce the permissible level of electromagnetic load of a frequency-controlled machine;
- electromagnetic power P_{EL}^{DIR} arriving at air gap from the nonlinear network as well as in the linear network at slip $S_1 < 1$, is spent partially for the rotation of driving mechanism connected to the shaft (power P_W^{DIR}), and partially is dissipated in rotor loops in the form of thermal energy $P_{W,R}^{DIR}$. Thus, unlike the mode with harmonics of order $Q_{AD} > 1$, powers P_{EL}^{DIR} and P_W^{DIR} participate in the generation of net torque. Power P_W^{DIR} at the expense of higher time harmonics of order $Q_{DIR} > 1$ somewhat increases the motor resulting torque, so the working rotor shaft speed ω_{REV} changes towards smaller slips S_1 in comparison with the operation from linear network;
- we should note regularities that occur in comparison with power balance and losses dissipated in machine loops for modes with harmonics of orders Q_{AD} and Q_{DIR}. For example, it follows from a comparison of both tables that at $Q_{AD} = 5$, the value $P_{W,R}^{AD} = -0.1653$, and at $Q_{DIR} = 7$ the value $P_{W,R}^{DIR}$ is equal practically to the same value: $P_{W,R}^{DIR} = 0.1647$. The same occurs for other couples of corresponding harmonics from both tables. It confirms that the power dissipated in rotor loops in braking modes of frequency-controlled motor at $Q_{AD} > 1$, arrives from nonlinear network.

17.2.3 Technical and Economic Indicators Frequency-Controlled Induction Motors [22–26]

17.2.3.1 Quantitative Assessment Criteria of Higher Time Harmonics Influence

From statements in the previous two paras it follows that the nonlinear distortion factor K_{DIST} explicitly does not reflect the quality of electrical energy arriving at stator winding terminals. Therefore, it cannot be used as the only criterion of quality assessment: separate harmonics $Q_{AD} > 1$, $Q_{DIR} > 1$, and also the ratio of their EMF amplitudes play a various role in the power value $P_2(\omega_{REV}) = P_W(\omega_{REV})$ on frequency-controlled motor shaft.

At the same time, operation practice of frequency—controlled induction motors moves forward the problem of assessment of their technical and economic indicators (with account for the quality of fed electrical power [19]).

17.2.3.2 Assessment Methods: Offers and Their Substantiation

Let us consider a number of practical offers on the introduction of such indicators. Calculation methods of these indicators are stated after their formulations (para 17.2.4).

(a) Power factor on shaft $K_{PW.SHAFT}$. Let us designate the ratio of power $P_2(\omega_{REV,NOM})$ of motor in the rated mode to the total power (kVA) $S_T(\omega_{REV,NOM})$ consumed by motor from network in the same mode.

$$K_{PW.SHAFT} = \frac{P_2(\omega_{REV,NOM})}{S_T(\omega_{REV,NOM})}. \tag{17.5}$$

This indicator for rated mode is based on (in comparison with sinusoidal network) the role of the first and higher time harmonics not only in the creation of rated power $P_2(\omega_{REV,NOM})$ by the motor, but also in the consumption of active and reactive powers from network in the rated mode.

In that specific case, at power supply of induction machines from a frequency converter with small value of nonlinear distortion factor $K_{DIST} < 0.1$, the value

$$K_{PW.SHAFT} \approx (\cos\varphi)_{NOM}\eta_{NOM}, \tag{17.6}$$

where η_{NOM}—motor efficiency in rated mode with sinusoidal power supply.

Let us note that the voltage harmonic structure of converter feeding motor usually depends on the drive operation mode; therefore, the factor $K_{PW.SHAFT}$ is formulated as the main characteristic of rated mode (from the viewpoint of influence of higher harmonics on this mode).

(b) Factor of active power $K_{PW.ACT}$. Let us designate the ratio of motor active power $P(\omega_R)$ to the power (kVA) $S_T(\omega_{REV})$ consumed by it from network:

$$K_{PW.ACT} = \frac{P(\omega_{REV})}{S_T(\omega_{REV})}. \tag{17.7}$$

This indicator indicates (in comparison with sinusoidal network) an additional level of motor load with reactive currents caused by higher harmonics of orders $Q_{AD} > 1$, $Q_{DIR} > 1$.

In that specific case, for induction machines fed from a frequency converter with small value of nonlinear distortion factor $K_{DIST} < 0.1$, the value $K_{PW.ACT}$ actually equals to $\cos\varphi$ on motor terminals.

$$K_{PW.ACT} \approx \cos\varphi. \tag{17.8}$$

(c) Motor efficiency factor η_{HARM}. Let us designate the ratio of motor power on the shaft $P_2(\omega_{REV})$ to active power $P(\omega_{REV})$ consumed by it from network.

$$\eta_{HARM} = \frac{P_2(\omega_{REV})}{P(\omega_{REV})}. \tag{17.9}$$

This indicator means (in comparison with sinusoidal network) a function of the first and higher time harmonics not only in the generation by motor of useful power on the shaft, but also in the dissipation of losses in motor loops in the form of thermal energy (including that due to harmonics of order $Q_{AD} > 1$ creating braking torques, and due to harmonics of order $Q_{DIR} > 1$ creating net torques).

In that specific case, at power supply of induction machines from a frequency converter with small value of nonlinear distortion factor $K_{DIST} < 0.1$, the value

$$\eta_{HARM} = \eta, \tag{17.10}$$

where η—motor efficiency with sinusoidal power supply.

(d) Factor of model power K_{MOD}. Let us designate as a factor of model power K_{MOD} the ratio of two motor powers; the first of them (model) corresponds to the operation mode when the motor is fed from a linear network, usually selected as serial from manufacturer's catalog; the second (rated)—corresponds to the motor operation mode with specific mechanism from nonlinear network. For example, for the operation as frequency-controlled motor a serial motor 1000 kW, 6 kV, 750 rpm is selected with regulation limit 1:2 ("down") at constant torque. It is required to determine its power for the operation with this mechanism with account of the influence of the following factors:

- losses and torques from higher harmonics $Q_{AD} > 1$, $Q_{DIR} > 1$;
- reduction of ventilation efficiency by speed regulation.

If as a result of solution of both these problems the following admissible data for this motor were determined: 850 kW, 6 kV, 750 rpm., factor of model power $K_{MOD} = \frac{850}{1000} = 0.85$. We assume the power of serial motor (1000 kW) as model power $P_{2(MOD)}$, and selected motor power (850 kW) for specified operation modes with specific mechanism $P_{2(NOM)}$ as rated power. Thus:

$$K_{MOD} = \frac{P_{2(NOM)}}{P_{2(MOD)}}. \tag{17.11}$$

Usually $K_{MOD} < 1$, but as a rule, it does not mean a decrease in drive technical and economic indicators in the operation with frequency converter in comparison with that in linear network. In practice it often appears that only a frequency-controlled motor with model power greater than rated $P_{2(MOD)} > P_{2(NOM)}$ not only provides a regulation function required by specifications, but also low values of starting current. This allows us to start a driving mechanism with a preset value of moment of inertia, etc.

Let us note that in practice of some unregulated drive cases also other decisions are made; for example, if it is necessary to limit the starting current or it is necessary to start the driving mechanism with high moment of inertia (with electromechanical time constant more than 3–5 s). In this case instead of a semiconductor starting device (for example, frequency converter) the driving motor model power, as in previous case, is sometimes selected: $P_{2(MOD)} > P_{2(NOM)}$. However, based on such decision the need to use a semiconductor starting device is excluded, though the model power of motor selected for this purpose exceeds that with starting device drive in the system. As a result, the cost of electrical equipment set can decrease and its reliability – increase.

Usually, such comparisons necessary for the selection of drive versions are solved in practice by technical and economic analyses. Therefore, the selection of factor K_{MOD} should be supplemented with feasibility study (feasibility report) of selected drive versions with account of cost of separate equipment elements considered in the feasibility report.

We note that in practical calculations to refine admissibility of "heavy start-up" process it is expedient to consider a rise of resistivity in cage elements from temperature and its influence on skin effect in cage bars.

17.2.4 Calculation Peculiarities of Technical and Economic Indicators of Induction Motors in Nonlinear Network

Let us consider a sequence of calculations of these indicators for the main mode: $U_1 = U_{NOM}$.

Initial calculation data assumed as given:

- effective value of the first voltage harmonic $U_1 = U_{NOM}$;
- dependence of power P_{MECH} of driving mechanism on its rotation speed ω_{REV} : $P_{MECH}(\omega_{REV})$;
- relative values of voltage higher time harmonics $\frac{U_5}{U_1}$, $\frac{U_7}{U_1}$, $\frac{U_{11}}{U_1}$, $\frac{U_{13}}{U_1}$, $\frac{U_{17}}{U_1}$, $\frac{U_{19}}{U_1}$;
- equivalent circuit parameters for each harmonic; frequency f_1; number of machine poles 2p;
- rated rotation speed $\omega_{REV,NOM}$; motor rated power.
- To determine:

- motor power P_2 depending on rotation speed ω_{REV} in the range $\omega_{REV} \leq 2\pi f_1/P : P_2(\omega_{REV})$.
- actual motor power and its rotation speed at $U_1 = U_{NOM}$;
- motor technical and economic indicators; $K_{PW.SHAFT}$; $K_{PW.ACT}$; η_{HARM}; K_{MOD}.

Let us state the main stages of problem solution (solution algorithm).
We determine the followings for each value of rotation speed.

(a) Active power consumed from the circuit:

$$P(\omega_{REV}) = P^{AD}(\omega_{REV}) + P^{DIR}(\omega_{REV}). \tag{17.12}$$

Active powers $P^{AD}(\omega_{REV})$, $P^{DIR}(\omega_{REV})$ are calculated directly from equivalent circuits for corresponding harmonics: $Q_{AD} = 5, 11, 17, 23, \ldots$; $Q_{DIR} = 1, 7, 13, 19, \ldots$

Note. In (17.12), the expression for $P^{AD}(\omega_{REV})$ contains the power $P_W^{AD}(\omega_{REV})$ on motor rotor shaft according to (17.3). It creates braking torques and at slips $S_{AD} > 1$ is negative:

$$P_W^{AD}(\omega_{REV}) \sim I_2^2 R_2 \frac{(1 - S_{AD})}{S_{AD}}. \tag{17.3'}$$

This negative sign for P_W^{AD} is given in the last column of Table 17.1 earlier.

(b) Power (kVA) $S_T(\omega_{REV})$ consumed from a network.

Its reactive components are calculated similarly to active ones directly from equivalent circuits for each harmonic.

(c) Losses in windings and in stator and rotor cores (main and additional).

These losses are necessary to compute the machine thermal condition and, therefore, determination of its electromagnetic load level:

$$\begin{aligned} \Delta P_{ACT}(\omega_{REV}) = {} & P_{W,ST}^{AD}(\omega_{REV}) + P_{S,T}^{AD}(\omega_{REV}) + P_{W,R}^{AD}(\omega_{REV}) \\ & + P_{W,ST}^{DIR}(\omega_{REV}) + P_{ST}^{DIR}(\omega_{REV}) + P_{W,R}^{DIR}(\omega_{REV}). \end{aligned} \tag{17.13}$$

(d) Motor power on the shaft $P_2(\omega_{REV})$ depending on the rotation speed in the range $\omega_{REV} \leq 2\pi f_1/p : P_2(\omega_{REV}) = P_W^{DIR}(\omega_{REV}) + P_W^{AD}(\omega_{REV})$ at $Q_{AD} = 5, 11, 17, 23, \ldots$; $Q_{DIR} = 1, 7, 13, 19$.

For checking calculation results the following ratio can be used that is true for each value of speed ω_{REV}:

$$P_2(\omega_{REV}) = P(\omega_{REV}) - \Delta P_{ACT}(\omega_{REV}). \tag{17.14}$$

Here $P(\omega_{REV})$—as per (17.12), $P_{ACT}(\omega_{REV})$—as per (17.13).

After checking (17.14) we plot the power curve on shaft $P_2(\omega_{REV})$ for a number of rotation speed values $\omega_{REV} \leq 2\pi f_1/p$.

Let us determine the point of intersection of curve $P_{MECH}(\omega_{REV})$ and curve $P_2(\omega_{REV})$. The value $P_2(\omega_{REV})$ in the point of intersection of these two curves gives a working point of steady state mode. If the mechanism power $P_{MECH}(\omega_{REV})$ (by speed ω_{REV}) corresponds in intersection point to its rated data, then for motor its power $P_2(\omega_{REV}) = P_2(\omega_{REV,NOM})$ and speed $\omega_{REV} = \omega_{REV,NOM}$. However, if the mechanism power $P_{MECH}(\omega_{REV})$ or speed ω_{REV} in the intersection point does not correspond to its motor rated data, additional measures should be taken in motor control system, for example to increase the supply voltage frequency, etc.

The found values for powers of frequency-controlled motors are sufficient to compute its technical and economic indicators: $K_{PW,SHAFT}$; $K_{PW,ACT}$; η_{HARM}; K_{MOD}.

Thus, both problems formulated above are solved.

We note that in practice for calculation of induction machine performance data we usually use the equivalent circuit of [10, 11] considering the saturation of machine magnetic circuit and skin effect in stator and rotor windings.

Brief Conclusions

1. In modern operation practice of frequency-controlled induction motors the actual problem is development of their electromagnetic load level assessment criteria with account of harmonic structure of supply voltage.
2. Noted are differences of motor "electromagnetic brake" mode with non-sinusoidal power supply from the mode of induction motor "electromagnetic brake" in linear network. The method is developed allowing us to estimate quantitatively how energy of harmonics of order Q_{AD} of frequency-controlled induction motor is compensated by that of harmonics of order Q_{DIR}. Distortion factor K_{DIST} is not based on the fact that at given shaft torque of frequency-controlled induction motor the energy consumed from a network by harmonics of order Q_{DIR} is as high as harmonic voltage amplitude of order Q_{AD}.
3. The offered assessment criteria of high harmonics influence and method of their calculation for frequency-controlled induction motors allow us to consider peculiarities of their modes in nonlinear network.

List of Symbols

f_1	Voltage and current frequency of industrial network
$f_{AD,ROT}$, $f_{DIR,ROT}$	Frequencies of rotor EMF and currents (respectively for time harmonics of order Q_{AD}, Q_{DIR},
I_2	Current in rotor winding equivalent phase reduced to stator winding phase ("dash" sign is omitted)

$K_{PW.ACT}$	Factor of motor active power
K_{MOD}	Factor of motor model power
$K_{PW.SHAFT}$	Power factor on motor shaft
K_{DIST}	Nonlinear distortion factor
m	Order of MMF spatial harmonic of stator field
p	Number of pole pairs
$P^{AD}(\omega_{REV}),\ P^{DIR}(\omega_{REV})$	Motor power (respectively for time harmonic of order Q_{AD}, Q_{DIR}) consumed from network at speed ω_{REV}
$P^{AD}_{W,ST}(\omega_{REV}),\ P^{DIR}_{W,ST}(\omega_{REV})$	Losses in stator winding phase (respectively for time harmonic of order Q_{AD}, Q_{DIR})
$P^{AD}_{ST}(\omega_{REV}),\ P^{DIR}_{ST}(\omega_{REV})$	Losses in stator and rotor cores, additional losses, ventilation losses etc. (respectively for time harmonic of order Q_{AD}, Q_{DIR}), not proportional to square of currents in its windings
$P^{AD}_{EL}(\omega_{REV}),\ P^{DIR}_{EL}(\omega_{REV})$	Electromagnetic power in air gap arriving from network (respectively for time harmonic of order Q_{AD}, Q_{DIR})
$P^{AD}_{W,R}(\omega_{REV}),\ P^{DIR}_{W,R}(\omega_{REV})$	Losses in rotor equivalent winding (respectively for time harmonic of order Q_{AD}, Q_{DIR})
$P^{AD}_{W}(\omega_{REV}),\ P^{DIR}_{W}(\omega_{REV})$	Power on motor rotor shaft (respectively for time harmonic of order Q_{AD}, Q_{DIR})
$P_{MECH}(\omega_{REV})$	Driving mechanism power at speed ω_{REV}
Q_{AD}, Q_{DIR}	Orders of time harmonics of stator EMF and currents
R_2	A.C. resistance of equivalent phase of rotor winding reduced to stator winding phase ("dash" sign is omitted)
$S_T(\omega_{REV})$	Power (kVA) consumed from network at speed ω_{REV}
S_{AD}, S_{DIR}	Slip (respectively for time harmonic of order Q_{AD}, Q_{DIR})
$U_1; U_5; \ldots; U_Q$	Values of voltage time harmonics in nonlinear network
η_{HARM}	Motor efficiency in nonlinear network
η_{NOM}	Motor efficiency in rated mode with sinusoidal power supply
ω_1	Circular frequency of voltage first harmonic and current of network
ω_{REV}	Angular rotor rotation speed

References

I. Monographs, textbooks

1. Boguslawsky I.Z., A.C. motors and generators. The theory and investigation methods by their operation in networks with non linear elements. Monograph. TU St.Petersburg Edit., 2006. Vol. 1; Vol.2. (In Russian).
2. Richter R., Elektrische Maschinen. Berlin: Springer. Band I, 1924; Band II, 1930; Band III, 1932; Band IV, 1936; Band V, 1950. (In German).
3. Mueller G., Ponick B., Elektrische Maschinen. New York, John Wiley, 2009. 375 S. (In German).
4. Demirchyan K.S., Neyman L.R., Korovkin N.V., Theoretical Electrical Engineering. Moscow, St.Petersburg: Piter, 2009. Vol. 1, 2. (In Russian).
5. Kuepfmueller K., Kohn G., Theoretische Elektrotechnik und Elektronik. 15 Aufl. Berlin, New York: Springer. 2000. (In German).

II. Induction machines. Papers, inventor's certificates

6. Boguslawsky I.Z., Research method of regimes of double feed supplied machine with taking into account saturation and higher harmonics. News of the Russian Academy of Sciences. Energetika (Power engineering), 2002, № 1. (In Russian).
7. Boguslawsky I.Z., Double power supplied asynchronous machine with converter in the rotor winding performance investigation method. Proceedings of the Int. Symp.UEES-01. Helsinki. 2001.
8. Boguslawsky I.Z., Danilevich Ja. D., Wind–power and small hydrogenerators designing problems. Proceedings of the IEEE Russia (Northwest Section). International Symposium "Distributed Generation Technology", October 2003.
9. Boguslawsky I.Z., Danilevich Ya.B., Popov V.V., Features of the calculation of electromagnetic loads and the power factor of the rotor of asynchronized synchronous generator at different slips. Proceedings of the Russian Academy of Sciences. Energetika. #6, 2011. (In Russian).
10. Antonov V.V., Boguslawsky I.Z., Savelyeva M.G., Calculation of the characteristics of a powerful induction motor with non-linear parameters. – In the book.: Elektrosila, #35, 1984. (In Russian).
11. Boguslawsky I.Z., Parameters of an equivalent circuit of powerful induction motors at working in nonlinear networks. In book: Problems of creation and maintenance of new electrical power engineering equipment. Department of electrical power engineering problems of Russian Academy of Sciences. St.Petersburg, 2003. (In Russian).
12. Boguslawsky I.Z., Special features of the fields of induction machine with the asymmetrical cage rotor by non-sinusoidal power supply. Power Eng. (New York), 1990, № 2.
13. Oberretl K., Die Oberfeldtheorie des Kaefigmotors unter Beruecksichtigung der durch die Ankerrueckwirkung verursachten Statorstroeme und der parallelen Wicklungszweige. Archiv fuer Elektrotechnik, 1965, № 6.
14. Polujadoff M., General rotating MMF – Theory of squirred cage induction machines with non-uniform air gap and several non-sinusoidally distributed windings. Trans AIEE, PAS, 1982.

15. Vaš P., Analysis of space–harmonics effects in induction motors using N – phase theories. International Conference of Electrical Machines. Brussel, 1978.
16. Vaš P., Altalonositott, egyseges villamosgepelmelet fehlharmonikus jeensegek figyelembevetelere. Elektrotechnika (Hungary), 1980, №9. (In Hungarian).

III. Synchronous machines. Papers, inventor's certificates, patents

17. Boguslawsky I.Z., Harmonic of an armature field and frequencies of currents of rotor contours multiphase salient-pole motor under nonsinusoidal feeding. In books: Problems of creation and maintenance of new electrical power engineering equipment. Department of electrical power engineering problems of Russian Academy of Sciences. St. Petersburg, 2003. (In Russian).
18. Boguslawsky I.Z., Bragin V.I, Danilevich J.B., Demirchjan K.S., Tsatskin A.J., Chernov A. N., The scientific and technical problems of powerful A.C. machines, caused by operation in nonlinear networks. In book.: Proceedings of III International symposium ELMACH − 2000. Moscow. 2000. (In Russian).
19. Boguslawsky I.Z., Kuss G., The level and criteria of estimation of electromagnetic load of A. C. motors in nonlinear networks. Elektrotechnika, 2003, № 10. (In Russian).
20. Boguslawsky I.Z., Magnetically coupled meshes in A.C. machines by non-sinusoidal power supply. Power Eng. (New York), 1995, № 2.
21. Boguslawsky I.Z., Equations system of poliphase A.C. machine by non-sinusoidal power supply. Power Eng. (New York), 1996, № 2.

IV. State Standards (IEC, GOST and so on)

22. GOST (Russian State Standard) R-52776 (IEC 60034-1). Rotating Electrical Machines. (In Russian).
23. IEC 60092-301 Electrical installations in ships. Part 301: Equipment Generators and Motors.
24. Rules and Regulations for the Classification of Ships. Part 6 Control, Electrical, Refrigeration and Fire. Lloyd's Register of Shipping (London). 2003.
25. Russian Maritime Register of Shipping. Vol.2. Rules for the classification and construction of sea going ships. St.-Petersburg. 2003. (In Russian).
26. Rotated electrical machines. Turbogenerators. The general technical specifications. GOST 533-2000. Minsk (Belorussia). Interstate council on standardization, metrology and certification. (In Russian).

Chapter 18
Method of Minimizing Losses in High-Power Low-Speed Frequency-Controlled Motors in Operation Modes at Nonlinear Dependence of Shaft Torque on Rotation Speed

This chapter deals with the problems of operation of frequency-controlled high power synchronous motors with non-linear dependence of torque on shaft speed. The method contributing to minimize losses and enhance the efficiency output under working conditions has been developed. There has been formulated the law of regulating voltage and frequency at rotation speed less than the rated value, as well as criteria ensuring the maximum output under mentioned conditions. A computational example has been shown for the motor of 20 MW, 140 rpm, 11.67 Hz. Upon the level of speed reduction the increase in efficiency output is made from 0.5 to 2 % for this type of motors compared with the usual control laws.

The content of this chapter is the development of methods stated in [6–8].

18.1 Application Areas of High-Power Low Speed Frequency-Controlled Motors

As in various industries and in transport, high-power low speed frequency-controlled motors with shaft torque M = 100–150 T m find now their application, for example, in metallurgy, mining industry, electrical propulsion systems of ice-breakers, ocean liners, etc. [6, 7]. Mass of such machines exceeds 130–140 t. When operating as motors of rolling mills, mine elevators, their rated rotation speed is usually $n_{NOM} \approx 50$ rpm, and power $P_2 \approx 5-7.5$ MW; when using such motors in transport their rated rotation speed is n_{NOM} = 110–150 rpm, and power $P_2 \approx 11-22.5$ MW. Such motors are often made as six-phase ("two stars at angle 30 el. degr.").

Problems of selecting rated voltage U_{NOM} of such machines with winding of this type and with standard three-phase are investigated in [6]; admissible overheats according to [9] and minimum losses in rated mode are accepted as optimization criteria in [6–8]. Problems of ensuring profitability by minimizing losses in

I. Boguslawsky et al., *Large A.C. Machines*,
DOI 10.1007/978-4-431-56475-1_18

operation modes of high-power low speed frequency-controlled motors are considered below.

18.2 Voltage, MMF and Currents in Windings in Operation Modes ($n_{REV} < n_{NOM}$); Mutual Induction Flux in Air Gap

Let us consider the first problem of voltage variation in operation modes, when the motor rotation speed $n_{REV} < n_{NOM}$; respectively, the frequency f_1 of network voltage first harmonic feeding this motor is also less than rated ($f_1 < f_{NOM}$). As optimality criterion for this problem solution let us assume the motor efficiency, and as restrictions—the following: currents in stator I_{ST} and rotor windings I_{EX}, and also the flux of mutual induction Φ in air gap should not exceed values in rated mode.

We note that low speed frequency-controlled motors are usually supplied with separate ventilating equipment so overheats of their windings and stator and rotor core practically do not depend on rotor rotation speed.

Usually in such modes, the voltage $U < U_{NOM}$ is selected for the following condition to be satisfied:

$$U = U_{NOM} \frac{f_1}{f_{NOM}}. \tag{18.1}$$

For low speed frequency-controlled motors (at $f_{NOM} < 16$ Hz) leakage reactance of stator winding is comparable with A.C. resistance, so instead of this ratio a more correct formula is the following: $E = E_{NOM} \frac{f_1}{f_{NOM}}$; here E—stator winding EMF.

From the last expression it follows that at the variation of rotation speed, the mutual induction resulting flux Φ in air gap and motor magnetic circuit saturation remain constant:

$$\Phi = \Phi_{NOM}. \tag{18.1'}$$

In operation practice, the mechanisms driven by low speed frequency-controlled motors differ in dependence of torque on the shaft M_{MECH} on rotation speed n_{REV}. Among them there are mechanisms with quadratic dependence of $M_{MECH} = k_M n_{REV}^2$ (k_M—proportionality factor), for example, exhausters and compressors in metallurgy, screw propellers in shipbuilding. Investigations show that preservation of conditions (18.1) or (18.1′) for low speed frequency-controlled motors coupled with such mechanisms is not always optimum. Thus, the following peculiarities for motor operation modes with such mechanisms are taken into account:

- motor power P_2 on the shaft at the variation of rotation speed n_{REV} varies under the cubic law:

$$P_2 = k_P n_{REV}^3; \tag{18.2}$$

(k_P—factor of proportionality)

- stator current I_{ST} at the variation of voltage according to the ratios (18.1), (18.2) changes under the quadratic law: $I_{ST} \approx k_1 n_{REV}^2$ (k_1—factor of proportionality [1–4]), and short circuit losses Q_{SC} (in stator winding and additional)

$$Q_{SC} = k_Q n_{REV}^4. \tag{18.3}$$

Here k_Q—factor of proportionality [1, 2].

Let us consider the law of MMF and rotor current variation at n_{REV} − var. We represent rotor MMF F_{EX} in the form of two components: Stator MMF F_{ST} and magnetic circuit MMF F_{MC} according Ampere's law:

$$F_{EX} = F_{ST} + F_{MC}. \tag{18.4}$$

Here F_{EX}, F_{ST}, F_{MC}—MMF complex amplitudes (phasors).

We find that the ratio of MMF components in Eq. (18.4) is proportional to motor SCR:

$$SCR \approx \frac{|F_{MC}|}{|F_{ST}|}. \tag{18.4'}$$

Here $|F_{EX}|, |F_{MC}|$—modules of MMF complex amplitudes.

The first component in Eq. (18.4) is determined $|F|_{ST} = k_{F,ST}|I|_{ST} = k_{F,ST}k_M n_{REV}^2$ by stator current; the second component F_{MC}—mutual induction flux Φ in air gap. When meeting conditions (18.1), (18.1′), it does not depend on rotation speed and practically remains constant:

$$|F|_{MC} = k_{F,MC}(|\Phi|). \tag{18.5}$$

Here $k_{F,ST}$—factor of proportionality [1, 2], depend on stator winding data and number of poles in machine; $k_{F,MC}(|\Phi|)$—depend on geometrical dimensions of its active part cross section and mutual induction flux Φ [3].

As a result we obtain that at the reduction of motor rotation speed, the rotor winding MMF and its current decrease much more slowly than in stator, and at rotation speeds $n_{REV} < n_{NOM}$.

18.3 Structure of Losses in Low Speed Frequency-Controlled Motor; Efficiency in Operation Modes ($n_{REV} < n_{NOM}$)

One of the peculiarities of high-power low speed frequency-controlled motors is the structure of losses: the share of short circuit losses Q_{SC} and excitation losses Q_{EX} in rotor winding makes over 85–90 % of total machine losses. Let us consider at first this peculiarity for low-frequency drives of mechanisms with quadratic dependence of $M_{MECH} = k_M n_{REV}^2$.

Analysis of Eqs. (18.1)–(18.5) shows that in operation modes at the reduction of rotation speed $n_{REV} < n_{NOM}$ and, respectively, $f_1 < f_{NOM}$, the short circuit losses sharply decrease in comparison with excitation losses. At the same time, within the specified restrictions for currents in windings and mutual induction flux in air gap, it is possible for each operation mode (P_2 = idem, $n_{REV} < n_{NOM}$) to obtain an approximate equality of losses $Q_{SC} \approx Q_{EX}$. It is easy to show that this equality corresponds to the maximum value of efficiency at low no-load losses that is true at low frequency $f_1 < f_{NOM}$. To provide this equality of losses, it is sufficient instead of the ratio (18.1) and (18.1′) to use the following:

$$U < U_{NOM} \frac{f_1}{f_{NOM}}; \Phi < \Phi_{NOM}. \tag{18.6}$$

At the reduction of flux $\Phi < \Phi_{NOM}$ the value $|F|_{MC} = k_{F,MC}(|\Phi|)$ also decreases in comparison with its value in rated mode (at $\Phi = \Phi_{NOM}$) according to the no-load curve.

At the same time for the selected mode at P_2 = idem, MMF F_{ST} and losses Q_{SC} increase. Compliance with ratios (18.6) leads, therefore, to a change in both components of losses: Q_{SC} and Q_{EX}. At a certain ratio of MMF F_{ST} and F_{EX} for the voltage U according to (18.6) it is possible to obtain an approximate equality of losses Q_{SC}, Q_{EX} and the maximum value of efficiency. Let us note that the frequency-controlled motors usually [7] complete with sensors for monitoring and control of stability angle Θ in real time, that gives the stability in steady-state and transient modes [1–5].

Results of calculation of one of modes of high-power low speed frequency-controlled motors are represented in Table 18.1 (Appendix 18.1) as an example with ratings of 20 MW, 5.8 kV, 140 rpm, f_1 = 11.67 Hz (“Elektosila Work”, Stock Company “Power Machines”, St. Petersburg) designed for liner electrical propulsion systems; at the reduction of rotation speed to n_{REV} = 60 rpm, we obtain the power as per (18.2) P_2 = 1575 kW, U ≤ 2485 V as per (18.6).

It follows from Table 18.1 that in the limits specified by the ratio (18.6), the maximum efficiency takes place at voltage 1860 ≤ U ≤ 1980 V. The dependence of efficiency on voltage is flat.

Nonlinear dependences of windings MMF on rotation speed and losses allow one to find an analytical solution of this problem only approximately: investigation

of maximum efficiency at P_2 = idem, n_{REV} = idem, $U < U_{NOM}\frac{f_1}{f_{NOM}}$. However, its numerical realization makes it possible to obtain practical results with strict accounting of specified nonlinear dependences, and also voltage drop in leakage reactance of stator winding and its A.C. resistance. Solution analysis shows that generally in this nonlinear problem the equality of losses $Q_{SC} \approx Q_{EX}$ can be also true for several values of voltage within the inequality specified as determined in (18.6).

Optimum values of efficiency of the same low speed frequency-controlled motor are given in Table 18.2 (Appendix 18.2) with rated data 20 MW, 5.8 kV, 140 rpm, 11.67 Hz at n_{REV} = var. (in the range $40 \le n_{REV} \le 70$ rpm).

It is expedient to obtain an approximate dependence $U^* = F(n_{REV})^*$ from Table 18.3 (Appendix 18.3) by means of the following functions (with an error no more than 5 % in the calculation of value U^*):

$$\text{(a) } n^*_{REV} = \frac{U^*}{CU^* + B}, \quad \text{herewith, coefficients are equal to } C = 1.2;\ B = 0.35; \tag{18.7}$$

$$\text{(b) } U^* = An^*_{REV} + D\left(n^*_{REV}\right)^2, \quad \text{herewith, coefficients are equal to } A = 0.07;\ D = 1.6; \tag{18.7'}$$

here $U^* = \frac{U}{U_{NOM}}$; $n^*_{REV} = \frac{n_{REV}}{n_{NOM}}$. From Eqs. (18.7) and (18.7′) it follows if the maximum efficiency in operation modes is assumed as optimization criterion, ratios between voltage and frequency in these modes differ from those corresponding to (18.1) and (18.1′).

When using condition (18.6), it is possible to apply an investigation method of maximum efficiency of low speed frequency-controlled motor in operation modes (at $n_{REV} < n_{NOM}$) at other nonlinear dependence of power P_2 on rotation speed n_{REV}.

Appendix 18.1

See Table 18.1.

Table 18.1 Dependence of low speed frequency-controlled motor parameters on stator winding voltage at rotation speed = 60 rpm, f = 5 Hz

U, V	2485	2360	2230	2210	1980	1860	1735	1610
Efficiency (%)	97.4	97.5	97.6	97.7	97.73	97.73	97.70	97.6

Appendix 18.2

See Table 18.2.

Table 18.2 Dependence of efficiency optimum values of low speed frequency-controlled motor on rotation speed

n_{REV}, rpm	70	65	60	55	50	45	40
Efficiency, % [at U as per (18.6) according to offered method]	97.9	97.8	97.7	97.6	97.5	97.3	97
Efficiency, % [at U as per (18.1)]	97.8	97.6	97.4	97.1	96.6	95.9	94.9

Appendix 18.3

See Table 18.3.

Table 18.3 Dependence of optimum values of voltages of low speed frequency-controlled motor on frequency

U, V	2500	2200	1920	1680	1370	1065	870
f_1, Hz	5.83	5.41	5.0	4.58	4.17	3.75	3.34
U^*	0.431	0.3793	0.331	0.2897	0.2361	0.1836	0.15
n^*_{REV}	0.5	0.4637	0.4286	0.3926	0.3574	0.3214	0.2863

Brief Conclusions

1. For the operation of high-power low speed frequency-controlled motors coupled with the mechanism having quadratic dependence of torque on rotation speed, it is possible to find the optimum value of motor efficiency for each speed value. It is achieved by the reduction in mutual induction flux in air gap in comparison with that in rated mode.
2. As the solution of this problem of mode optimization there are the following restrictions: currents in stator and rotor windings, and also mutual induction flux in air gap (extent of magnetic circuit saturation) should not exceed the values corresponding to them in rated operation mode.

List of symbols

E, U EMFs and voltage of the first harmonic of stator winding (E_{NOM}, U_{NOM}—rated EMFs and voltage)

f_1 Frequency of the first harmonic of stator winding voltage and current (f_{NOM}—rated frequency)

F_{EX}	Rotor MMF
F_{ST}	Stator MMF
F_{MC}	Magnetic circuit MMF
I_{ST}, I_{EX}	Stator current (first harmonic) and rotor current
M	Motor shaft torque
M_{MECH}	Torque of drive (torque on the shaft)
n_{REV}	Motor rotation speed (n_{NOM}—rated speed)
P_2	Power on motor shaft
Q_{EX}	Losses in rotor winding (excitation losses)
Q_{SC}	Short circuit losses (in stator winding and additional)
Φ	Mutual induction flux (Φ_{NOM}—rated flux)

References

I. Monographs, textbooks

1. Schuisky W., Berechnung elektrischer Maschinen. Wien: Springer, 1960. (In German).
2. Construction of Electrical Machines. Edited by Kopylov, I.P. - Moscow: Energiya, 1980. (In Russian).
3. Richter R., Elektrische Maschinen. Berlin: Springer. Band I, 1924; Band II, 1930; Band III, 1932; Band IV, 1936; Band V, 1950. (In German).
4. Mueller G., Ponick B., Elektrische Maschinen. New York, John Wiley, 2009. (In German).
5. Kostenko M.P., and Piotrovskiy L.M., Electrical Machines. Vol. 2. Leningrad.: Enirgiya. 1965. (In Russian).

II. Synchronous machines. Papers, inventor's certificates, patents

1. Apevalov V.D., Boguslawsky I.Z., Danilevich Y.B., Korchagin N.V., Popov V.V., Rybin Y.L., Tsatskin A.J., Problems of the creation of powerful A.C. machines. In book: Problems of creation and maintenance of new electrical power engineering equipment. Department of electrical power engineering problems of Russian Academy of Sciences. St.-Petersburg, 2003. (In Russian).
2. Fomin B.I., Makarov N.I., Boguslawsky I.Z., Datzkowskiy L.Kh., Gigulin Yu.V., Krol N.M., Lesokhin A.Z., Powerful synchronous motors for frequency-controlled electrical A.C. drive. Elektrotechnika, 1984, #8. (In Russian).
3. Boguslawsky I.Z., Method of minimizing losses in high-power low-frequency salient-pole motors in operation modes at nonlinear dependence of shaft torque on rotation speed. Izvestiya RAN, Energetika, #5, 2006. (In Russian).

III. State Standards (IEC, GOST and so on)

1. GOST (Russian State Standard) R-52776 (IEC 60034-1). Rotating Electrical Machines. (In Russian).

Chapter 19
Methods of Decreasing Nonlinear Distortion Factor in Voltage Curve of Salient-Pole Generator: Investigation of EMF Tooth Harmonics of Its Multiphase Winding with q per Pole and Phase as Integer

This chapter presents investigation methods of nonlinear distortions of voltage curve of salient pole generator caused by EMF tooth harmonics of its multiphase winding: these EMFs are limited to norms of IEC and GOST [19], and also Marine Register of Russia [20]. Restriction of nonlinear distortion factor (total harmonics distortion—THD) according to these norms is caused by several reasons: interference caused by currents of these harmonics in telephone lines located close to overhead power lines; danger of overvoltages in these overhead power lines connected with resonance phenomenon [1, 2]; additional losses in copper and stator core caused by fields of tooth harmonics; calculation expressions for these tooth EMFs are obtained not only at stator (rotor poles) slots shift in axial direction by one slot division, but also at shift of rotor poles in tangential direction (group or local). Practical examples allowing drawing conclusions on effectiveness of each of these constructive solutions are given.

The content of this chapter is development of the methods stated in [1–7, 15].

19.1 Introduction

In practice of developing modern multipole ($2p > 40$) generators for wind energetics, MHPP (Mini Hydro Power Plant), TEPP (Tidal Electrical Power Plant), powerful diesel power station with low-speed generators 20–25 MW there arises a problem of providing line voltage waveform; this curve should meet requirements of GOST and IEC [19]. It is usually determined at tests in generator no-load mode at bench or installation site. Restriction of nonlinear distortion factor according to these requirements is caused by several reasons:

- disturbances caused by currents in these harmonics in telephone lines located close to high voltage line;

I. Boguslawsky et al., *Large A.C. Machines*,
DOI 10.1007/978-4-431-56475-1_19

- danger of overvoltage in these high voltage lines connected with resonance phenomenon [4, 5].
- additional losses in stator and rotor core, in cooper of windings caused by fields of tooth harmonics;

For providing these requirements some constructive solutions are used in practice [3–8].

When using stator winding with integer $q \leq 3$ slots per pole and phase, they provide application of the following [1–8]:

- skewing of stator slots (or rotor poles) by one stator tooth pitch;
- local or group shift of rotor poles in tangential direction.
- To decrease tooth harmonics EMF, use is also made of stator windings with fractional number q [9].

In practice use of these solutions has several peculiarities:

- stator slot skewing in axial direction is more often used for machines with stator core external diameter 990 mm and less [7, 8]; additional technological difficulties take place, for example, if the stator is made of several sectors, and stator core length exceeds 1000 mm; rotor pole skewing in axial direction is usually used for large-size machines;
- besides such slot skewing in stator (rotor poles), there find application construction with shift of rotor poles in tangential direction. Some modifications of such construction [6, 15, 16] which effectiveness is not identical are known: shift of adjacent poles within every period $T = 2\tau$ (local shift) and shift of adjacent poles within several periods T (group shift); here τ—pole pitch;
- windings with fractional $q < 3$ in comparison with windings with integer q usually contain in MMF curve additional spatial harmonics [3–5], which order $m < p$ (p—order of the main MMF harmonic by expanding into series with the period $T = \pi D$, D—stator boring diameter). Presence of such harmonics ("subharmonics") [9, 10] can cause additional vibrations of stator core and stator frame with amplitude exceeding several times admissible in spite of the fact that amplitude of these MMF harmonics are much less than that of the main harmonic. For elimination of these vibrations, it is necessary to increase generator dimensions and weight due to necessity to increase rigidity of its frame. Selection of $q > 3$ is limited by technological possibility necessary to locate Z slots on stator corresponding to this q; here $Z = 2pm_{PH}q$; m_{PH}—number of generator phases.

At first, we consider a general problem on field of mutual induction tooth harmonics in generator air gap with q as integer. Using the obtained ratios, we find for each of these constructions calculation expressions for EMF tooth harmonics of three-phase winding; it will allow us to estimate effectiveness of each construction. Application of these expressions is followed by examples from practice.

19.2 Tooth Harmonics of Machine with q as Integer: Amplitude of Their Mutual Induction Field in Air Gap in no-Load Mode; Frequency of This Field (Order of Tooth Harmonics)

19.2.1 Problem Formulation

In investigation of mutual induction field of tooth harmonics, we assume that the relation of width b_{SLT} of rectangular stator slot to pitch t_{SLT} is equal to $b_{SLT}/t_{SLT} = 0.5$. In real constructions, this value is smaller [7, 8] and usually is in limits $0.35 < b_{SLT}/t_{SLT} < 0.5$; respectively, the amplitude of tooth harmonics in such constructions is less than at $b_{SLT}/t_{SLT} = 0.5$; therefore, the results of expansion into series obtained in (19.3) are a bit "pessimistic (reserve)"; for "reserve" result let us assume that tooth harmonics in air gap do not fade that is strictly true only in small air gaps and for large pole pitches [9]. Let us assume also that the flux density amplitude in field air gap of tooth harmonics depends linearly on that in excitation winding field air gap.

When studying EMF tooth harmonics of three-phase two-layer winding with integer q in multipole machine we will consider that such two-layer winding contains $2pm_{PH}$ phase zones. Therefore, a machine with such winding can be represented in the form of series set of single ("elementary") machines [3–5]; each formed by one rotor pole pair (p = 1) and phase zones $(2pm_{PH})$ of this winding; it occupies $Z^{EL} = 2m_{PH}q$ slots (further it is accepted for clarity: $m_{PH} = 3$). Number of turns W_{PH}^{EL} in winding phase of this machine (for example, in phase A) is equal to $W_{PH}^{EL} = 2q\frac{S_{TR}}{a}$; respectively, for a group of S^* elementary machines (at $S^* < p$) the number of turns in phase makes $W_{PH}^{S} = W_{PH}^{EL}S^*$; in phase of real machine the number of turns is equal to $W_{PH} = W_{PH}^{EL}p$ (here S_{TR}—number of turns in coil (bar), a—number of parallel branches). One notes also that distribution factors of these winding are identical for the main harmonic (n = 1) and for harmonics of tooth order [3–5]. Chording factor (or pitch factor) K_{DS} of winding for harmonics of this order considered in EMF calculation, according to [3–5], also the winding factor $K_W = K_{DS}K_{CH}$. Therefore, below we will suppose that W_{PH}^{EL} has already included this factor K_W.

It is sufficient to investigate the influence of tooth harmonics of mutual induction field in air gap on the stator winding EMF only for one single ("elementary") machine [7, 8]. It is expedient to study constructions stated above by the same method that allows us to estimate their effectiveness from uniform positions and to make corresponding practical recommendations.

19.2.2 Solution

Let us determine, at first, the field of tooth harmonics $b_z(x,n)$ in stator slot zone; here x—spatial coordinate along stator boring; n—harmonic order. Further, we will consider the influence of rotor field (excitation field), and then, proceeding from the resulting field $b_{Z,0}(x,t,n)$ (mutual induction field in air gap), we will determine EMF frequency and amplitude $e_{Z,0}(x,t,n)$ from tooth harmonics in this stator winding field at no-load; here t—time. In stator tooth zone, let us assume the period T covering three poles for expansion into harmonic series: two edge poles with polarity N and a middle pole with polarity S (see Fig. 19.1). Longitudinal axes of two poles with polarity N (axis d) are designated as A_1A_2 and D_1D_2; period $T = A_1D_1$. Line portions $A_1C_1 = C_1D_1 = \tau = T/2$. In standard rotor constructions for middle pole with polarity S the longitudinal axis (d) coincides with C_1C_2.

However, we will perform these investigations for a more general case: axis C_1C_2 of middle pole is shifted to the position B_1B_2 by the value $D_0 = B_1C_1$, so that line portion $A_1B_1 = \tau_L < \tau$, and line portion $B_1D_1 = \tau_G > \tau$, herewith, $\tau_G + \tau_L = 2\tau = T$. Figure 19.1 shows for clarity the machine tooth zone with q = 2 (machine calculation data are given in Appendix 19.1). It is easy to show that at any q the ratio of period T to pitch t_{SLT} over slots (teeth) makes: $\frac{T}{t_{SLT}} = 6q$; therefore, in Fig. 19.1 at number q = 2 period T corresponds to 12 slot (tooth) pitches. We accept $D_0 = \frac{t_{SLT}}{2}k$, where k = 1, 2, …; thus, we assumed that this value changes depending on pitch t_{SLT} discretely.

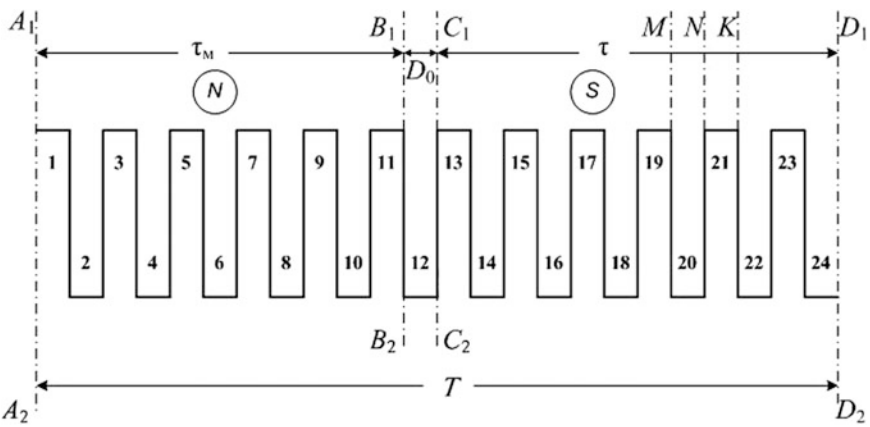

Fig. 19.1 Tooth zone of stator ($A_1D_1 = A_2D_2 = T$; $C_1D_1 = \tau$; $A_1B_1 = \tau_м < \tau$; $B_1C_1 = D_0$ $MK = t_z$; $MN = MK = 0.5 \cdot t_z$

19.2.3 Field of Harmonics $b_{SLT}(x,t,n)$ in Stator Slot Zone

Let us take at first that the generator inductor (rotor) and its armature (stator) are mutually motionless, and rotor poles create in air gap mutual induction field (n = 1) corresponding to the generator no-load EMF, if it rotates with rated speed. In this mode, the flux density under teeth reaches a maximum, and in slot zone is minimum. Let us expand into harmonic series this rectangular induction wave $b_Z(x,n)$ under teeth and slots within the period T. We designate the amplitude of this rectangular flux density wave at $\tau_L = \tau$ as B_Z. Then at $D_0 \neq 0$ on line portion $A_1B_1(\tau_L < \tau)$ it is equal to $\frac{\tau}{\tau_L}B_Z$, and on line portion $B_1D_1(\text{at } \tau_G > \tau)$—respectively —$\frac{\tau}{\tau_G}B_Z$; this amplitude correction is caused [4, 5] by the continuity of magnetic flux (divA = B) on line portion $A_1D_1 = 2\tau$; here A—vector potential of magnetic field [4, 5].

Let us note that, in practice, the flux density amplitude B_Z is determined by relation of slot opening $\frac{b_{SLT}}{t_{SLT}}$ and machine air gap; ratio of B_Z to resulting field flux density amplitude B_{M1} in air gap makes for high-power generators usually: $\frac{B_Z}{B_{M1}} < 0.10 - 0.18$, including for machines with small air gap [9].

We represent the dependence of b(x,n) in the form of series [10–12]:

$$b(x,n) = \sum \left[C(-n)e^{-2j\pi\frac{nx}{T}} + C(+n)e^{2j\pi\frac{nx}{T}}\right]. \tag{19.1}$$

(summation over n). Amplitudes C(–n) and C(+n) are calculated from the ratios:

$$C(-n) = \frac{B_Z}{T}\left[\frac{\tau}{\tau_L}\int_0^{\tau_L} e^{2j\pi\frac{nx}{T}}dx + \frac{\tau}{\tau_G}\int_{\tau_L}^{T} e^{2j\pi\frac{nx}{T}}dx\right]. \tag{19.2}$$

Expression for complex amplitude C(+n) in (19.1) is easy to obtain [10–12] substituting in (19.2) sign at harmonic order n by opposite (n by minus n).

Let us calculate at first the first of integrals for this rotor construction with k = 1 and for stator winding at q = 2, n = 6, q = 12 (Fig. 19.1) in the form:

$$C_1(-n) = \frac{B_Z}{T}\frac{\tau}{\tau_L}\int_0^{\tau_L} e^{2j\pi\frac{nx}{T}}dx = \frac{1}{2j\pi n}B_Z\frac{\tau}{\tau_M}C_1'(-n),$$

where

$$C_1'(-n) = (+1)e^{jn\pi\frac{t_{SLT}}{2\tau}-1} + (-1)\left(e^{2jn\pi\frac{t_{SLT}}{2\tau}} - e^{jn\pi\frac{t_{SLT}}{2\tau}}\right) + (+1)\left(e^{jn\pi\frac{3t_{SLT}}{2\tau}} - e^{2jn\pi\frac{t_{SLT}}{2\tau}}\right)$$
$$+ (-1)\left(e^{jn\pi\frac{4t_{SLT}}{2\tau}} - e^{jn\pi\frac{3t_{SLT}}{2\tau}}\right) + \cdots + (+1)\left(e^{jn\pi\frac{11t_{SLT}}{2\tau}} - e^{jn\pi\frac{10t_{SLT}}{2\tau}}\right)$$

Similarly, for the second integral we have:

$$C_2(-n) = \frac{B_Z}{T}\frac{\tau}{\tau_G}\int_{\tau_M}^{T} e^{2j\pi\frac{nx}{T}}dx = \frac{1}{2j\pi n}B_Z\frac{\tau}{\tau_G}C''(-n)_2,$$

where

$$C''(-n)_2 = (-1)\left(e^{j\pi n\frac{12t_{SLT}}{2\tau}} - e^{j\pi n\frac{11t_{SLT}}{2\tau}}\right) + (+1)\left(e^{j\pi n\frac{13t_{SLT}}{2\tau}} - e^{j\pi n\frac{12t_{SLT}}{2\tau}}\right)$$
$$+ (-1)\left(e^{j\pi n\frac{14t_{SLT}}{2\tau}} - e^{j\pi n\frac{13t_{SLT}}{2\tau}}\right) + \cdots + (-1)\left(e^{j\pi n\frac{24t_{SLT}}{2\tau}} - e^{j\pi n\frac{23t_{SLT}}{2\tau}}\right).$$

After a number of transformations we obtain the complex amplitude C(–n) for this rotor construction (at k = 1 and for stator winding at q = 2, n = 6, q = 12) in the form:

$$C(-n) = \frac{-B_Z}{12j\pi}\left(11\frac{\tau}{\tau_L} + 13\frac{\tau}{\tau_G}\right).$$

Generally, (k > 1, q ≠ 2) the calculation expression for complex amplitude C(−n) is reduced to the following form:

$$C(-n) = \frac{-B_Z}{12j\pi}\left(\frac{\tau}{\tau_L}(6q-k) + \frac{\tau}{\tau_G}(6q+k)\right)$$

(under the following conditions: $m_{PH} = 3$; integer q—is arbitrarily; ratios $\frac{\tau}{\tau_L}$ and $\frac{\tau}{\tau_G}$—are calculated for arbitrarily k, and $\tau_L + \tau_G = 2\tau$). Let us simplify the obtained general expression. Let us write down the ratios for pole pitch τ_L and τ_G of this rotor construction ($D_0 \neq 0$):

$\tau_L = \tau - D_0 = \tau - \frac{t_{SLT}}{2}k = \tau - \frac{\tau}{2}\cdot\frac{1}{3q}k$; then $\frac{\tau}{\tau_L} = \frac{6q}{6q-k}$. Similarly, $\frac{\tau}{\tau_G} = \frac{6q}{6q+k}$.

With account of these ratios we obtain:

$$C(-n) = \frac{-2B_Z}{j\pi n}6q = \frac{(-2)}{j\pi}B_Z; \text{respectively,} \quad C(+n) = \frac{2B_Z}{j\pi}. \tag{19.3}$$

Therefore, both amplitudes do not depend on the parameter k = 1, 2, …, and Eq. (19.3) are true for any ratios of $\frac{\tau}{\tau_L}$ and $\frac{\tau}{\tau_G}$, determined by this parameter:

$$C(-n) \neq f(k); \quad C(+n) \neq f(k). \tag{19.4}$$

Studies similar to Eqs. (19.1)–(19.3) confirm that regularities (19.4) remain true also for values of parameter k < 1. We will use this result in analysis of rotor construction with group pole shift.

Using Eqs. (19.3), let us find the calculation ratio for harmonics field $b_Z(x,n)$ in stator slot zone; with account of (19.3) we obtain (under conditions: $\tau_L = \text{var}, \tau_G = \text{var}, \tau_L + \tau_G = 2\tau$):

$$b(x,n) = \frac{2B_Z}{j\pi}\sum\left(-e^{-2j\pi\frac{nx}{T}} + e^{2j\pi\frac{nx}{T}}\right) = \frac{4}{\pi}B_Z \sin\frac{\pi nx}{\tau}. \tag{19.5}$$

In deriving this expression, it is accepted that generator inductor (rotor) and its armature (stator) are mutually motionless. Let us proceed to generator real operation conditions; we assume that its rotor is stalled, and stator rotates in positive direction of angle reference with rated speed $\omega_{REV} = \frac{\omega_1}{p}$. Then expression for flux density b (x,t,n) takes the form [6]:

$$b(x,t,n) = \frac{4}{\pi}B_Z \sin\left(\omega_Z t - \frac{\pi nx}{\tau}\right). \tag{19.6}$$

where ω_Z—circular frequency of tooth harmonics EMF subject to definition with account for excitation field (rotor field).

19.2.4 Excitation Field $b_{MI}(x)$ (Rotor Field); Resulting Mutual Induction Field (in Air Gap); Flux Density $b_{Z,0}(x,t,n)$ of Tooth Order

Rotor pole shoes are designed so that rotor field $b_{MI}(x)$ varys over a period T under the harmonic law [7–9]. For this purpose, radius R_P of shoe surface is selected smaller than $R_0 = \frac{D}{2} - 2\delta_{MIN}$, so the air gap δ_{MIN} under the pole middle (along axis d) is smaller than at its edges δ_{MAX}, herewith, their ratio [7, 8] makes usually $\frac{\delta_{MAX}}{\delta_{MIN}} = 1.25 - 1.5$. Therefore, with accuracy, sufficient for practice, we assume that for an observer on the rotor the flux density distribution is as follows: $b_{MI}(x) = B_{MI}\cos\frac{2\pi x}{T}$; here B_{MI}—amplitude of this field (reference origin coincides with axis d, i.e. with line A_1A_2), where the value of flux density $b_{MI}(x = 0) = B_{MI}$. With rated line voltage U_L = 1 in the generator mode it is equal to B_{MI} = 1; respectively, flux density B_Z is also determined at U_L = 1. Let us note that for the same observer the stator with its tooth zone rotates relative to rotor with angular speed ω_{REV} so the resulting field of tooth harmonics mutual induction without account of the influence of flux on stator core steel saturation in tooth zone is determined by the following ratio [6]:

$$b_{Z,0}(x,t,n) = \frac{4}{\pi}B_Z \sin\left(\omega_Z t - \frac{\pi nx}{\tau}\right)\cos\frac{2\pi x}{T}. \tag{19.7}$$

Let us represent Eq. (19.7) in the form [10, 11]:

$$b_{Z,0}(x,t,n) = B'_Z \sin\left(\omega_Z t - \frac{\pi(n-1)x}{\tau}\right) + B'_Z \sin\left(\omega_Z t - \frac{\pi(n+1)x}{\tau}\right), \quad (19.8)$$

where $B'_Z = \frac{2}{\pi} B_Z$.

Thus, the field of tooth harmonics mutual induction has two components. These component fields rotate relative to motionless rotor with identical and constant amplitude; they correspond to frequencies ω_Z of tooth EMFs equal respectively to $\omega_Z^{(1)}$ or $\omega_Z^{(2)}$:

$$b_{Z,0}^{(1)}(x,t,n) = B'_Z \sin\left(\omega_Z^{(1)} t - \frac{\pi(n-1)x}{\tau}\right); \quad (19.9)$$

$$b_{Z,0}^{(2)}(x,t,n) = B'_Z \sin\left(\omega_Z^{(2)} t - \frac{\pi(n+1)x}{\tau}\right). \quad (19.10)$$

19.2.5 *Frequencies of Tooth Harmonics $\omega_Z^{(1)}$ and $\omega^{(2)}$; Calculation Expression for Nonlinear Distortion Factor*

Let us determine these EMF frequencies from the condition that at rotation of each field components its angular speed relative to rotor is equal to $\omega_{REV} = \frac{\omega_1}{p}$.

From Eq. (19.9) for the first field component, we obtain:

$\omega_Z^{(1)} dt = \frac{\pi(n-1)dx}{\tau}$; considering that $\frac{dx}{dt} = \frac{\omega_1 \tau}{\pi}$ we obtain:

$$\omega_Z^{(1)} = \omega_1(n-1) = \omega_1(6q-1). \quad (19.11)$$

Similarly, from Eq. (19.10) for the second field component:

$$\omega_Z^{(2)} = \omega_1(n+1) = \omega_1(6q+1). \quad (19.11')$$

The order n of higher harmonics for frequencies of tooth EMFs can be represented also in another form, including the case $m_{PH} \geq 3$:

$$\begin{aligned} n^{(1)} &= 2m_{PH}q - 1, \\ n^{(2)} &= 2m_{PH}q + 1. \end{aligned} \quad (19.12)$$

We will use the obtained ratios (19.9)–(19.12) to calculate EMF $e_{Z,0}(t,n)$ of tooth order in stator winding with integer q for generators of various construction.

Let us write down the calculation expression for nonlinear distortion factor of generator voltage [7–9]. Taking into account Eqs. (19.11) and (19.11′) nonlinear distortion factor for tooth harmonics of generator voltage is calculated from the ratio [19]:

$$K_{DIST}^{(1),(2)} = \sqrt{\left(\frac{E_{Z,0}^{(1)}}{E_0}\right)^2 + \left(\frac{E_{Z,0}^{2}}{E_0}\right)^2}. \qquad (19.12')$$

It should be noted that these harmonics have the greatest influence on the value of the distortion factor. Here E_0—no-load EMF of generator; $E_{Z,0}^{(1)}, E_{Z,0}^{(2)}$—EMFs of tooth harmonics corresponding to frequencies as per Eqs. (19.11) and (19.11′).

19.3 Rotor Construction with Local Shift of Poles in Tangential Direction

19.3.1 Peculiarities of Practical Realization

- in factory conditions, realization of this construction with the value of shift $D_0 = \tau - \tau_L$ or $D_0 = \tau_G - \tau$ can be connected with certain technological difficulties. They depend on the type of fastening of rotor poles. For example, for their fastening on rotor rim it is necessary to perform a precise lay-out for bolts; for small shift values D_0 "close" tolerances for this purpose are required. When fastening poles on shaft by means of "dovetails" or one or several "shanks" [7, 8] the problem becomes even more complicated;
- in realization of this construction it is considered also that the value of pole pitch τ_L or shift D_0 is limited not only by technological capabilities of rotor manufacturing, but also by generator performance data [7–11]. This additional restriction is connected with the uneven distribution of leakage fluxes, closing between adjacent poles N and S within period 2τ; asymmetry in magnetic circuit of rotor poles influences the machine saturation level, especially at operation in modes with generator voltage $U = 1.05_{RAT}$ (according to GOST and IEC [5, 7, 8, 19, 20]);
- for generator operation in case of unsuccessful rotor construction with tangential shift, an increased level of vibrations is possible [10, 17] excluding its operation even in no-load mode. In usual constructions (at $\tau_G = \tau_L = \tau$) phase angle between rotor poles of opposite polarity (N and S) makes $\psi = 180$ el. degr. In the considered construction with such shift ($D_0 \neq 0$) this condition is not met: $\psi \neq 180$ el. degr.; as a result in mutual induction field curve in air gap there appear additional spatial harmonics, including harmonics of order $n < p$, even for stator winding with q as integer. They cause vibrations of stator core and stator frame similar to vibrations which cause harmonics of the same order

(n < p) of stator winding with fractional q [10]. Therefore, the construction of multipole rotor with tangential shift of poles requires an additional analysis of mutual induction field in air gap [1–3, 9] including the determination of amplitude and frequency of "subharmonics".

19.3.2 Tooth Harmonics of EMF $e_{Z,0}(t,n)$ in Stator Winding

Let us assume as calculation unit a group with the following sequence of poles in it: N; S; N. Distance between the first two poles is equal to $\tau_L < \tau$, and between the second and third $\tau_G > \tau$, herewith, $\tau_L + \tau_G = 2\tau$. Let us find previously the flux corresponding to the first field component in air gap:

$$\Phi_{Z,0}^{(1)}(x,t,n) = \int_0^{\tau_L} b_{Z,0}^{(1)}(x,t,n) L_{COR} dx = B'_Z L_{COR} \frac{2\tau}{\pi n^{(1)}} \sin\left(\omega_Z^{(1)} t - \frac{\pi n^{(1)} \tau_L}{2\tau}\right) \sin\frac{\pi n^{(1)} \tau_L}{2\tau}, \quad (19.13)$$

where L_{COR}—calculation length of stator core [7, 8]. Let us accept that this flux corresponds to pole "N".

We note that this flux can be also determined differently as the flux corresponding to the pole "S":

$$\Phi_{Z,0}^{(1)}(x,t,n) = -\int_{\tau_L}^{2\tau} b_{Z,0}^{(1)}(x,t,n) L_{COR} dx. \quad (19.14)$$

Respectively, EMF $e_{Z,0}^{(1)}(t,n)$ with account of the found Eqs. (19.11) and (19.13) for $\omega_Z^{(1)}$ is equal to,

$$e_{Z,0}^{(1)}(t,n) = -W_{PH}^{EL} \frac{d}{dt} \Phi_{Z,0}^{(1)}(x,t,n) = \frac{-4}{\pi^2} W_{PH}^{EL} \omega_1 B_Z \tau L_{COR} \cos\left(\omega_Z^{(1)} t - \frac{\pi n^{(1)} \tau_L}{2\tau}\right) \sin\frac{\pi n^{(1)} \tau_L}{2\tau} = E_{Z,0}^{(1)} \cos\left(\omega_Z^{(1)} t - \frac{\pi n^{(1)} \tau_L}{2\tau}\right), \quad (19.15)$$

where amplitude $E_{Z,0}^{(1)}$ of this EMF in Eq. (19.15) is equal to,

$$E_{Z,0}^{(1)} = \frac{-4}{\pi^2} W_{PH}^{EL} \omega_1 B_Z \tau L_{COR} K_{L.SH}^{(1)}, \quad (19.16)$$

and Factor local shift

$$K_{L.SH}^{(1)} = \sin\frac{\pi n^{(1)}\tau_L}{2\tau}. \tag{19.17}$$

Similarly are determined for the second component in (19.8)–(19.10) the flux $\Phi_{Z,0}^{(2)}(x,t,n)$ and EMF $e_Z^{(2)}(t,n)$;

$$e_{Z,0}^{(2)}(t,n) = E_{Z,0}^{(2)}\cos\left(\omega_Z^{(2)}t - \frac{\pi n^{(2)}\tau_L}{2\tau}\right)K_{L.SH}^{(2)},$$

herewith, EMF amplitudes of both components differ only in Factor $K_{L.SH}^{(2)}$:

$$K_{L.SH}^{(2)} = \sin\frac{\pi n^{(2)}\tau_L}{2\tau}. \tag{19.18}$$

Let us note the following peculiarities of obtained expressions for EMF of tooth harmonics:

- frequencies $\omega_Z^{(1)}$ and $\omega_Z^{(2)}$ of tooth EMFs significantly exceed the network frequency ω_1, however, the amplitude of these EMFs is determined only by frequency ω_1;
- amplitudes $E_{Z,0}^{(1)}$ and $E_{Z,0}^{(2)}$ can be practically changed only by means of poles local shift (Factors $K_{L.SH.}$);
- in the absence of local shift ($\tau_L = \tau_G = \tau$; $D_0 = 0$) Factor $K_{L.SH.} = 1$ for EMF of both frequencies $\omega_Z^{(1)}$ and $\omega_Z^{(2)}$.

It should be also noted that when using both expressions for fluxes (19.13) and (19.14) we obtain the doubled value of phase EMF.

19.3.3 Calculation Example

Let us use generator data from Appendix 19.1. We assume for rotor constructions with local shift the relationship $\frac{\tau_L}{\tau} = \frac{11}{12}$; respectively, $\frac{D_0}{\tau} = \frac{1}{12}$. The value of poles shift is $D_0 = \frac{1}{12}\tau = \frac{t_{SLT}}{2} = 26.2$ mm; such a shift can be realized in practice. Then, as per Eq. (19.12) for $n^{(1)} = 11; n^{(2)} = 13$ we obtain from Eqs. (19.17) and (19.18) $K_{L.SH.}^{(1)} = K_{L.SH.}^{(2)} = 0.1305$. Section 19.2.3 represents usual ratios for the flux density in high-power salient-pole generators: $\frac{B_{SLT}}{B_{MI}} < 0.10 - 0.18$. With account of this

relation, both obtained values for $K_{L.SH.}$ and Eq. (19.12′) it is equal to $K_{DIST}^{(1),(2)} \approx 0.016$, that meets requirements of GOST and IEC ($K_{DIST} \leq 0.05$).

We find that for the selected value $\frac{\tau_L}{\tau} = \frac{11}{12}$, the amplitude of generator first EMF harmonic practically does not decrease, as at n = 1: $K_{L.SH.} \approx 1$.

19.4 Rotor Construction with Group Shift of Poles in Tangential Direction

19.4.1 Peculiarities of Practical Realization

- the following construction of salient-pole rotor with group shift is realized in factory conditions [16] («Elektrosila» Work, Stock Company "Power Machines" St.Petersburg). Poles are subdivided into four groups, each of them contains, respectively, $S_{GR}^{*} = p/G$ pair of poles (for G = 4); the distance between poles in the group is accepted equal to $\tau_L < \tau$. The amplitudes of EMF in the stator winding, are induced by each of these groups are equal, the phases of these EMF are also equal each other;
- group shift has advantages compared to the local one: additional leakage fluxes closing between poles N and S within distance τ_L in design with "group" shift are less as values τ_L can be selected in such a construction only slightly different from pole pitch τ decreases the level of poles saturation caused by additional leakage fluxes between them, especially in operation modes with increased generator voltage (within restrictions of this voltage as per GOST and IEC);
- realization of rotor construction with group shift of poles is connected with additional technological difficulties in comparison with the previous design: at smaller values of shift D_0 more "close" tolerances for this purpose are required for layout;
- construction of multipole rotor with group shift of poles, as well as design with their local shift, needs additional analysis of mutual induction field in air gap [1–3, 9], including the determination of amplitude and frequency of lower spatial harmonics. Unsuccessful multipole rotor design used in practice caused an increased level of generator vibrations [17] excluding its operation even at no-load. Peculiarities of this design are stated in [18]; its analysis in [17] indicated that such vibrations are connected generally with the influence of "subharmonics".

Note: Also for two-layer bar type winding, using in practice for the large generations, we have the relation between the number (W_{PH}) of winding turns, the number of parallel brunches and the number (q) of slots per pole and phase: W_{PH} 2qp/a.

19.4.2 Tooth Harmonics of EMF $e_{Z,0}(t,n)$ in Stator Winding

As calculation unit let us assume a group of $S^*_{GR} = p/G$ poles; distance between poles in the group is accepted equal to $\tau_L < \tau$. Let us find previously fluxes corresponding to the first field component (19.8)–(19.10) in air gap:

$$\Phi_1^{(1)} = \int_{-\tau_L/2}^{\tau_L/2} b_{z,0}^{(1)}(x,t,n) L_{COR} dx = B'_z L_{COR} \frac{2\tau}{\pi n^{(1)}} \sin\frac{\pi n^{(1)}\tau_L}{2\tau} \sin\omega_Z^{(1)} t;$$

$$\Phi_2^{(1)} = \int_{3\tau_L/2}^{5\tau_L/2} b_{z,0}^{(1)}(x,t,n) L_{COR} dx = B'_z L_{COR} \frac{2\tau}{\pi n^{(1)}} \sin\frac{\pi n^{(1)}\tau_L}{2\tau} \sin\left(\omega_Z^{(1)} t - \frac{2\pi n^{(1)}\tau_L}{\tau}\right);$$

$$\Phi_3^{(1)} = \int_{7\tau_L/2}^{9\tau_L/2} b_{z,0}^{(1)}(x,t,n) L_{COR} dx = B'_z L_{COR} \frac{2\tau}{\pi n^{(1)}} \sin\frac{\pi n^{(1)}\tau_L}{2\tau} \sin\left(\omega_Z^{(1)} t - \frac{4\pi n^{(1)}\tau_L}{\tau}\right);$$

$$\Phi_4^{(1)} = \int_{11\tau_L/2}^{13\tau_L/2} b_{z,0}^{(1)}(x,t,n) L_{COR} dx = B'_z L_{COR} \frac{2\tau}{\pi n^{(1)}} \sin\frac{\pi n^{(1)}\tau_L}{2\tau} \sin\left(\omega_Z^{(1)} t - \frac{6\pi n^{(1)}\tau_L}{\tau}\right);$$

$$\ldots$$

Respectively, EMF $e_{Z,0}^{(1)}(t,n)$ in $S^* = S^*_{GR}$ stator winding elements with account of Eq. (19.11) found for $\omega_Z^{(1)}$ is equal to:

$$e_{z,0}^{(1)}(t,n) = -W_{PH}^{EL} \frac{d}{dt}\left[\Phi_1^{(1)} + \Phi_2^{(1)} + \Phi_3^{(1)} + \Phi_4^{(1)} + \ldots\right]. \tag{19.19}$$

After summation of fluxes [12–14] we obtain:

$$e_{Z,0}^{(1)}(t,n) = E_{Z,0}^{(1)} \sin\left[\omega_Z^{(1)} t - \frac{\left(S^*_{GR} - 1\right)\pi n^{(1)}\tau_L}{\tau}\right] \tag{19.20}$$

where the amplitude of phase

$$\left|E_{Z,0}^{(1)}\right| = \frac{4}{\pi^2} W_{PH}^{EL} \omega_1 B_Z \tau L_{COR} G \frac{\sin\frac{S^*_{GR}\pi n^{(1)}\tau_L}{\tau} \sin\frac{\pi n^{(1)}\tau_L}{2\tau}}{\sin\frac{\pi n^{(1)}\tau_L}{\tau}} \tag{19.21}$$

Note: The amplitude E_{PH} of the first harmonic (n = 1) for $S^* = S^*_{GR}$ stator winding elements of generator phase voltage for the low values of D_0 i.e. for $\tau_L/\tau \to 1$, for example $\tau_L/\tau = 119/120$ is equal to the $(2/\pi)\omega_1 W_{PH}^{EL} B_{M1} L_{COR} S^*_{GR}$.

Accordingly the EMF of phase for the harmonic with number n = 1 is equal for this construction $(2/\pi)\omega_1 W_{PH}^{EL} B_{M1} L_{COR} GS_{GR}^*$. Evidently, $W_{PH}^{EL} GS_{GR}^* = W_{PH}$.

Let us determine the group shift distortion factor $K_{DIST}^{(1)}$. As a result, we obtain:

$$K_{DIST}^{(1)} = \frac{2}{\pi}\frac{B_Z}{B_{M1}}\frac{\sin\frac{S_{GR}^*\pi n^{(1)}\tau_L}{\tau}\sin\frac{\pi n^{(1)}\tau_L}{2\tau}}{S_{GR}^*\sin\frac{\pi n^{(1)}\tau_L}{\tau}} \tag{19.22}$$

Similarly to Eqs. (19.20)–(19.22) for harmonics with order $n^{(2)}$ we obtain:

$$K_{DIST}^{(2)} = \frac{2}{\pi}\frac{B_Z}{B_{M1}}\frac{\sin\frac{S_{GR}^*\pi n^{(2)}\tau_L}{\tau}\sin\frac{\pi n^{(2)}\tau_L}{2\tau}}{S_{GR}^*\sin\frac{\pi n^{(2)}\tau_L}{\tau}}.$$

19.4.3 Calculation Example

Let us use generator data from Appendix 19.1. We assume for rotor design with group shift [16] the relation $\frac{\tau_L}{\tau} = \frac{119}{120}; \frac{D_0}{\tau} = \frac{1}{120}$; $S_{GR}^* = 10$. The value of poles shift, is $D_0 = \frac{1}{120}\tau = \frac{1}{20}t_{LST} = 2.62$ mm; such a shift D_0 can be realized in practice at thorough lay-out.

Section 19.2.3 represents conventional ratios for the flux density in high-power salient-pole generators: $\frac{B_{SLT}}{B_{MI}} < 0.10 - 0.18$. With account of this relation, both obtained values for $K_{DIST}^{(1)}$ and $K_{DIST}^{(2)}$ are equal to $K_{DIST}^{(1)} = 0.008$, $K_{DIST}^{(2)} = 0.0068$, $K_{DIST} = 0.0105$, which practically agree with the experiment results for the generator [16] and meets requirements of GOST and IEC ($K_{DIST} \leq 0.05$).

Let us note that for the selected value $\frac{\tau_L}{\tau} = \frac{119}{120}$, the amplitude of generator first EMF harmonic practically does not decrease.

19.5 Generator Construction with Stator Axial Skewing of Stator Core or Rotor Poles

19.5.1 Peculiarities of Practical Realization

Value of bevel size D_0 is usually selected equal to slot pitch t_Z. This choice ($D_0 = t_{SLT}$) is determined by "skewing Factor" K_{SK}. Derivation of this calculation expression is based [5] on analogy with chording Factor of stator winding turn; however as "calculation unit" in the derivation of K_{SK} without winding turn, but with only one of its sides; EMF amplitude and frequencies of tooth order harmonics

thus are not determined [5]; in practical calculations it does not allow us to estimate the value of nonlinear distortion factor K_{DIST} of generator with selected value q.

Appendix 19.2 represents the derivation of calculation expression for generator tooth EMFs with stator slots (rotor poles) skewing. In these derivations are used ratios for mutual induction flux harmonics of tooth order obtained in Sect. 19.2. Taking into account the expression for tooth EMFs, the value of generator nonlinear distortion factor K_{DIST} can be estimated. For a machine with data from Appendix 19.1 it is given in para 19.5.2.

Table 19.1 represents calculations according to Eqs. (19.12) and (A.19.2.4), (A.19.2.6) values of skewing Factor K_{SK} at $\frac{D_0}{\tau_{SLT}} = 1, \frac{D_0}{\tau_{SLT}} = 0.85$ and $\frac{D_0}{\tau_{SLT}} = 1.15$; they correspond to practical values of technological tolerance by value D_0. Calculations are made for the first three values q representing practical interest.

Calculation results for these Factors of K_{SK} confirm that at specified tolerance values effectiveness of skewing remains not for all values of q. Therefore, in construction of production tooling, it is more expedient to provide a possibility of some increase in actual skewing D_0 in comparison with pitch t_{SLT}, but not its reduction.

Let us note that for main EMF harmonic, the skewing Factor at specified values $\frac{D_0}{\tau_{SLT}}$ practically remains equal to $K_{SK}(n = 1, D_0) \approx 1$. We note also that the stator winding MMF at skewing, similar to EMF, changes amplitude by value of K_{SK}; also the phase angle changes similarly to (A.19.2.2) and (A.19.2.5).

19.5.2 Calculation Example

Let us use generator data from Appendix 19.1. From Table 19.1 as per (19.12) for q = 2 at $D_0 = t_{SLT}$ we have $K_{DIST}^{(1)} = 0.0899$; $K_{DIST}^{(2)} = 0.0760$.

Range of $\frac{B_Z}{B_{M1}}$ values for high-power generators is given in Sect. 19.2.3; We accept for clarity the same value of ratio $\frac{B_Z}{B_{M1}}$, as in previous examples (in Sects. 19.3.3 and 19.4.3). Let us estimate the value of nonlinear distortion factor K_{DIST} [3–6]. As a result we obtain that both factors meet requirements of GOST and IEC.

Table 19.1 Skewing Factors K_{SK} for tooth harmonics

Q	$n^{(1)}$, $n^{(2)}$	K_{SK} ($D_0 = t_Z$)	K_{SK} ($D_0 = 0.85t_Z$)	K_{SK} ($D_0 = 1.15t_Z$)
1	5	0.1940	0.3565	0.0434
	7	0.1364	0.0084	0.2085
2	11	0.0899	0.2612	0.0511
	13	0.0760	0.0851	0.1783
3	17	0.0585	0.2303	0.0783
	19	0.0524	0.1126	0.1632

Appendix 19.1

Generator data to compute the nonlinear distortion factor K_{DIST}. P = 8750 kVA; U = 11 kV; f = 50 Hz; diameter of stator boring D = 8 m; active length of stator core L_{COR} = 720 mm; core package width b_{PAK} = 50 mm; m_{PH} = 3; q = 2; number of parallel branches a = 2; number of slots Z = 480.

Appendix 19.2

EMF tooth harmonics $e_{Z,0}(t,n)$ in stator winding with axial skewing of stator core or rotor poles.

Figure 19.2 shows a stator winding turn AGHCA with skewing GB = HF = D_0 relative to machine rotation axis; it coincides with CF; AC = BF = τ. L_{COR}—length of stator core [7, 8] CF = AB = L_{COR}. Let us use at first Eq. (19.9) for the first component of mutual induction flux from para 1:

$$b_{Z,0}^{(1)}(x,t,n) = B'_Z \sin\left(\omega_Z^{(1)} t - \frac{\pi n^{(1)} x}{\tau}\right). \qquad (A.19.2.1)$$

One finds the amplitudes of EMF harmonics of order $n^{(1)}$ induced in turn elements by this mutual induction flux. For this purpose let us divide the length of stator core L_{COR} into N_0 equal elements (at $N_0 \to \infty$); three of them are shown in Fig. 19.2: $CK_3 = K_3H_3 = H_3F$. Respectively, the turn surface is also subdivided into N_0 elements, equal in area, for example, AK_1K_2CA, $K_1H_1H_2K_2K_1$, $H_1GHH_2H_1$. Let us determine the flux $\Phi_{N_{INS}}(n^{(1)})$ of the harmonic of the order $n^{(1)}$, linked with one of elements, for example, $K_1H_1H_2K_2K_1$ having the number $N_{INS}(1 \le N_{INS} \le N_0)$, if viewed from the turn side AC:

$$\Phi_{N_{INS}}^{(1)} = \frac{L_{COR}}{N} \int_{S_3S_2}^{S_3S_1} B'_Z \sin\left(\omega_Z^{(1)} t - \frac{\pi n^{(1)} x}{\tau}\right) dx.$$

Here (Fig. 19.2): $S_3S_2 = D_0 \frac{N_{INS}}{N_0}$; $S_3S_1 = \tau + D_0 \frac{N_{INS}}{N_0}$. With account of these ratios after transformations, we obtain:

$$\Phi_{N_{INS}}^{(1)} = \frac{2B'_Z L_{COR} \tau}{\pi n^{(1)} N_0} \sin\left(\omega_Z^{(1)} t - \frac{\pi n^{(1)}}{2} - \pi n^{(1)} D_0 \frac{N_{INS}}{N_0 \tau}\right).$$

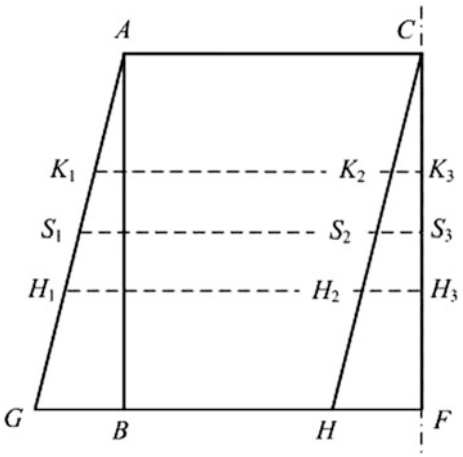

Fig. 19.2 One turn of stator winding (ACHGC) with skewing towards axis direction on the value *HF*

Let us determine the sum of fluxes in all N_0 elements. At $N_0 \to \infty$:

$$\Phi_N^{(1)} = \frac{2B'_Z L_{COR}\tau}{\pi n^{(1)}} \frac{\sin\left(\omega_Z^{(1)}t - \frac{\pi n^{(1)}}{2} - \frac{\pi n^{(1)}D_0}{2\tau}\right)\sin\frac{\pi n^{(1)}D_0}{2\tau}}{\frac{\pi n^{(1)}D_0}{2\tau}}.$$

Accordingly, the EMF with account of the found Eq. (19.11) for $\omega_Z^{(1)}$ is equal to:

$$\begin{aligned} e_{Z,0}^{(1)}(t,n) &= W_{PH}^{EL}\frac{d}{dt}\Phi_N^{(1)} \\ &= \frac{-4}{\pi^2}W_{PH}^{EL}\omega_1 B_Z \tau L_{COR}\cos\left(\omega_Z^{(1)}t - \frac{\pi n^{(1)}}{2} - \frac{\pi n^{(1)}D_0}{2\tau}\right)\frac{\sin\frac{\pi n^{(1)}D_0}{2\tau}}{\frac{\pi n^{(1)}D_0}{2\tau}} \\ &= E_{Z,0}^{(1)}\sin\left(\omega_Z^{(1)}t - \frac{\pi n^{(1)}D_0}{2\tau}\right), \end{aligned} \tag{A.19.2.2}$$

where the amplitude $E_{Z,0}^{(1)}$ of this EMF is equal to:

$$E_{Z,0}^{(1)} = -\frac{4}{\pi^2}W_{PH}^{EL}\omega_1 B_Z \tau L_{COR} K_{SK}^{(1)}, \tag{A.19.2.3}$$

and skewing factor:

$$K_{SK}^{(1)} = \frac{\sin\frac{\pi n^{(1)}D_0}{2\tau}}{\frac{\pi n^{(1)}D_0}{2\tau}}. \tag{A.19.2.4}$$

EMF $e^{(1)}_{Z,0}(t, n)$ and skewing Factor $K^{(2)}_{SK}$ for the second component have the form similar to (A.19.2.2)–(A.19.2.4):

$$e^{(2)}_{Z,0}(t, n) = E^{(2)}_{Z,0} \sin\left(\omega^{(2)}_Z t - \frac{\pi n^{(2)} D_0}{2\tau}\right) K^{(2)}_{SK}, \tag{A.19.2.5}$$

herewith, EMF amplitudes of both components differ only in Factor $K^{(2)}_{SK}$:

$$K^{(2)}_{SK} = \left(\frac{\sin\frac{\pi n^{(2)} D_0}{2\tau}}{\frac{\pi n^{(2)} D_0}{2\tau}}\right). \tag{A.19.2.6}$$

Brief Conclusions

1. In high-power salient-pole generators with stator winding differing in integer number q of slots per pole and phase, in voltage curve there appear additional harmonics [with frequencies $f_Z = (6q \pm 1)50$ Hz] besides the main harmonics (with frequency $f_1 = 50$ Hz). Additional losses and stator core overheats are connected with them; currents of these tooth harmonics can cause interference in telephone lines located close to the high voltage line, and also overvoltages in these high voltage lines due to resonance phenomena. The article presents calculation expressions for tooth EMFs in general case, when within period T (two pole pitch $T = 2\tau$) one of poles is shifted so $\tau_L < \tau$, and $\tau_G > \tau$, herewith, $\tau_L + \tau_G = 2\tau$).
2. Investigated are constructions used in practice, which allow us to reduce the amplitude of these harmonics. Proceeding from the general expression obtained for tooth EMFs, effectiveness of these designs is considered, and ratios are determined for nonlinear distortion factor K_{DIST} whose value is limited by GOST and IEC.
3. Calculation expressions obtained for each of these constructions are applied to the calculation of Factors K_{DIST} corresponding to them; as example, are used generator data 8750 kVA; U = 11 kV; f = 50 Hz.

List of Symbols

a	Number of parallel branches in stator winding
b_{SLT}	Width of rectangular stator slot
b_{PAK}	Width of stator core package
B_{MI}	Flux density amplitudes in excitation field air gap
B_Z	Flux density amplitude in air gap of tooth harmonics field
D	Stator boring diameter
D_0	Local (group) shift of poles, skewing of stator slots (rotor poles)

E_0	Generator EMF amplitude at no-load
$E_{Z,0}^{(1)}, E_{Z,0}^{(2)}$	EMF amplitudes of tooth harmonics corresponding to tooth frequencies
K_{SK}	Skewing factor of stator slots (rotor poles)
K_{DIST}	Harmonic distortion factor
$K_{L,SH}^{(1)}, K_{L,SH}^{(2)}$	Factors of local shift for tooth frequencies $\omega_Z^{(1)}, \omega^{(2)}$
$K_{GR,SH}^{(1)}, K_{GR,SH}^{(2)}$	Factors of group shift for tooth frequencies $\omega_Z^{(1)}, \omega^{(2)}$
L_{COR}	Stator core length
m_{PH}	Number of stator phases
n	Order of flux density harmonic
p	Number of pole pairs
q	Number of slots per pole and phase
R_P	Pole shoe surface radius
S_{TR}	Number of turns in coil (bar)
T	Spatial period of rotor field variation
t	Time
t_{SLT}	Stator slot pitch
U_L	Generator rated line voltage
W_{PH}	Number of turns in stator winding phase (incl. winding factor)
x	Spatial coordinate along stator boring
Z	Number of stator slots
$\delta_{MIN}, \delta_{MAX}$	Air gap under the pole middle (along axis d) and air gap at the edges of pole shoe
τ	Pole pitch
$\omega_Z^{(1)}, \omega_Z^{(2)}$	EMF circular frequencies of tooth harmonics
ω_{REV}	Angular rotation speed
ω_1	Circular network frequency

References

I. Monographs, Textbooks

1. Demirchyan K.S., Neyman L.R., Korovkin N.V., Theoretical Electrical Engineering. Moscow, St.Petersburg: Piter, 2009. Vol. 1, 2. (In Russian).
2. Kuepfmueller K., Kohn G., Theoretische Elektrotechnik und Elektronik. 15 Aufl. Berlin, New York: Springer. 2000. (In German).
3. Richter R., Elektrische Maschinen. Berlin: Springer. Band I, 1924; Band II, 1930; Band III, 1932; Band IV, 1936; Band V, 1950. (In German).
4. Mueller G., Ponick B., Elektrische Maschinen. N.Y., J.Wiley, 2009. - (In German).
5. Voldek A.I., Electrical Machines. Leningrad.: 1974. – 782 c. (In Russian).
6. Bragstad O., Theorie der Wechselstrommaschinen und eine Einleitung in der Theorie der stationaeren Wechselstroeme. Berlin: Springer, 1932. (In German).

7. Construction of Electrical Machines. Edited by of Kopylov, I.P. - Moscow: Energiya, 1980. (In Russian).
8. Mueller G., Vogt, K., Ponick B., Berechnung elektrischer Maschinen. – Springer, 2007. (In German).
9. Boguslawsky I.Z., A.C. Motors and Generators. The Theory and Investigation Methods by Their Operation in Networks with Non Linear Elements. TU St.Petersburg Edit., 2006. Vol. 1; Vol. 2. (In Russian).
10. Detienko F.M., Zagarodnaya G.A. Fastovskiy V.M., Strength and vibration of electrical machines. L.: Energia. 1964 (In Russian).
11. Schuisky W., Berechnung elektrischer Maschinen. Wien: Springer, 1960. (In German).
12. Korn G., Korn T., Mathematical Handbook. New York: McGraw – Hill, 1961
13. Jeffris H., Swirles B., Methods of Mathematical Physics. Third Edition, Vol. 1 – Vol. 3, Cambridge: Cambridge Univ. Press, 1966.
14. Dwight H.B., Tables of Integrals and other mathematical Data. New York: MacMillan Company. 1961.

II. Synchronous Machines. Papers, Inventor's Certificates, Patents

15. Arseniev I.A., Boguslawsky I.Z., Korovkin N.V., Research Methods for the Slot-Ripple EMF in Polyphase Integral Slot Winding. IEEE Russia (Northwest) Section. December, 2012. St.-Petersburg.
16. Tolvinsky V.A., Results of testing of hydrogenerators of the Volkhov hydroelectrical power station. Izvestiya Elektrotoka. 1929, № 6. (In Russian).
17. Koval A.A., Netseevsky A.B., Tsvetkov V.A., On magnetic pull and low freq. vibrations in hydro-generators with in-group pole shift. Electricity. 1988, # 8 (In Russian)
18. Pinsky G.B., Non-uniform arrangement of rotor poles. Papers of Work "Elektrosila". 1979, No. 32 (In Russian)

III. State Standards (IEC, GOST and So On)

19. GOST (Russian State Standard) R-52776 (IEC 60034-1). Rotating Electrical Machines. (In Russian).
20. Russian Maritime Register of Shipping. Vol. 2. Rules for the classification and construction of sea going ships. St.Petersburg. 2003.

Chapter 20
Methods of Decreasing Nonlinear Distortion Factor in Voltage Curve of Double-Fed Machines: Investigation of EMF Tooth Harmonics of Its Multiphase Stator and Rotor Windings with q Per Pole and Phase as Integer

This chapter deals with investigation methods of voltage curve nonlinear distortions for DFMs (in generator mode) caused by the same reasons—EMF tooth harmonics. However, unlike the methods stated in the previous chapter, the influence on EMF tooth harmonics is taken into account not only of stator multiphase winding, but also of rotor winding. This accounting of "bilateral stepped form" considerably complicates the solution: The number of EMF harmonics of various frequencies in voltage curve double-fed generator considerably increases in comparison with salient pole generator. Given here are practical examples, from which it follows that at unsuccessful selection of parameters even of one multiphase winding, for example, of rotor, it becomes inevitable to install filters limiting value of nonlinear distortions in generator voltage curve.

The content of this chapter is development of the methods stated in [1–3, 15, 16].

20.1 Introduction

One of trends in the development of modern power systems is installation of DFMs [17] in these systems, operating in generator mode. In Chap. 2 it has been mentioned that in references [4, 5] these generators are sometimes called ASGs (asynchronized synchronous generators). This name will be also used in this chapter for short. There it is also noted that ASGs are applied in power installations providing constant frequency and amplitude of voltage in network at variable rotation speed of driving motors (diesels, turbines). Depending on the type of these driving motors, their maximum power differs: it is 5–8 MW for wind power and small hydropower plants; 400 MW for large hydrogenerators; 60 MVA for condensers.

In the previous chapter are listed the reasons limiting the value of generator nonlinear distortion factor: interference caused by tooth harmonics currents in telephone lines located close to high voltage transmission lines; danger of

I. Boguslawsky et al., *Large A.C. Machines*,
DOI 10.1007/978-4-431-56475-1_20

overvoltages in these high voltage transmission lines caused by resonance phenomenon [1, 2]; additional losses in copper and core caused by fields of tooth harmonics.

Therefore, in practice of developing modern ASGs as well as salient-pole generators, the problem of providing line voltage waveform is actual; this curve should meet requirements of GOST and IEC [18]. In the previous chapter we considered methods of EMF tooth harmonics calculation for salient-pole generators with unilateral tooth surface (only stator three-phase winding); for these machines the problem of restriction of K_{DIST} value is solved in electrical machine engineering practice by shifting stator slots (rotor poles) by one slot pitch [6–11, 16], or by shifting of poles (local or group) in tangential direction [9, 15], and also application of stator windings with fractional number of slots per pole and phase [6–8].

However, for DFMs differing from salient-pole ones by bilateral tooth surface, the solution of this problem becomes complicated: additional investigation of EMF amplitudes and frequencies induced in stator winding by mutual induction field harmonics is required [16].

20.2 Assumptions

ASGs, unlike multipole synchronous generators, are made structurally not salient-pole: multiphase winding is laid in stator and rotor slots (usually three-phase with integer number q of slots per pole and phase) [6–8], and this number q for stator winding (q_1) and rotor winding (q_2) is not identical: $q_1 \neq q_2$; the stator and rotor cores are laminated; the voltage with slip frequency is applied to rotor slip rings from the frequency converter.

While investigating the influence of stator and rotor harmonics on generator EMF form, let us accept a number of assumptions similar to those accepted in Chap. 19 for salient-pole generators:

- frequencies of tooth harmonics of higher order (over 1000 Hz) have no impact on the conductivity of laminated stator and rotor cores made of electrotechnical steel 0.5 mm thick. With account of the skin effect reducing this conductivity ("reduced sheet thickness" [1, 2] makes over 3.5), the flux density amplitudes of stator and rotor tooth harmonics field in air gap are respectively smaller;
- fields of tooth harmonics do not attenuate in generator air gap; this assumption is true only for small air gaps and large pole pitch [12]. Taking account of this flux density, the amplitude attenuation in field air gap of stator and rotor tooth harmonics is respectively smaller;
- the relation of stator rectangular slot width $b_{SLT,1}$ to tooth pitch $t_{SLT,1}$ is equal to $b_{SLT,1} / t_{SLT,1} = 0.5$. In real constructions this ratio for stator is in a range of $0.35 < b_{SLT,1} / t_{SLT,1} < 0.5$ [10–12]. The same assumptions are accepted also for rotor tooth zone: $b_{SLT,2} / t_{SLT,2} = 0.5$. The flux density amplitudes in field air

gap of stator and rotor tooth harmonics is respectively less than $b_{SLT,1} / t_{SLT,1} = b_{SLT,2} / t_{SLT,2} = 0.5$;

- the flux density amplitude in field air gap of stator and rotor tooth harmonics depends linearly on the flux density amplitude of excitation winding field in gap.
- Note. With these assumptions the calculated value of factor K'_{DIST} of nonlinear distortions is slightly more than the experimental K_{DIST}: the excess is usually $\Delta K_{DIST} = K'_{DIST} - K_{DIST} \leq 0.005$. Practically, it corresponds to an increase in the factor K_{DIST} with possible technological deviations in the process of generator manufacturing (inaccuracy in skewing of slots, etc.).

20.3 Peculiarities of Investigating EMF Tooth Harmonics of ASG Stator and Rotor Three-Phase Windings with Integer Number Q of Slots Per Pole and Phase

In studying ASGs we consider that each of its windings contains $2pm_{PH}$ phase zones, as well as stator three-phase winding of salient-pole synchronous generator. Therefore, ASGs with such stator and rotor windings can be represented in the form of a number of single ("elementary") machines [6–8]; each formed by one pole pair ($p = 1$) and phase zone number $(2m_{PH})$ of this winding. So that, tooth harmonics EMF of ASG mutual induction field (field in air gap) are sufficient to investigate only for one single ("elementary") machine [6–8].

To compute these EMFs the winding factor of such elementary winding for harmonics of arbitrary order can be considered based on [6–8].

20.4 Rotor Fields of and Their Harmonics

20.4.1 Excitation Winding and Field of Its "Winding" Harmonics

An ASG rotor three-phase excitation winding is implemented with the number q_2 usually selected [10–12] by one unit more than for stator winding q_1 ($q_2 > q_1$). The field of this winding (mutual induction field) in rotor coordinates takes the form:

$$b_{MI}(x, n_w) = B_{MI,1}\cos\frac{\pi x}{\tau} + \cdots + B_{MI,n_w}\cos\frac{\pi n_W x}{\tau}; \qquad (20.1)$$

here $0 \leq x \leq \tau$ (reference mark coincides with longitudinal axis d); n_W—order of excitation winding field harmonics; $\tau = T/2$—pole pitch; $B_{MI,1}, \ldots, B_{MI,n}$—amplitudes of harmonics.

Physically, higher harmonics of this excitation field (with amplitude $B_{MI,n}$ at $n_W > 1$) arise in air gap due to the fact that the excitation winding is located discretely on rotor periphery (with current in each slot); they correspond to a step distribution of MMF along the pole pitch (τ) and do not depend on the fact that magnetic resistance of rotor teeth and slots in air gap zone is different. Therefore, these are usually called "winding" ones. Rotation speed of this field relative to the stator is different. The first harmonic of this field (at $n_W = 1$) rotates relative to the stator with synchronous speed $\omega_{REV} = \omega_1/p$ and induces EMF in stator winding, equal to rated voltage. Higher harmonics rotate not synchronously with the first; their amplitude is determined by the current in excitation winding. These harmonics induce in stator winding additional EMFs whose order depends on the value $n_W > 1$. EMF distortion factors from these harmonics are considered in Sects. 20.7 and 20.8.

20.4.2 *Toothed Rotor Form; Fields of Rotor Tooth Harmonics*

To take into account the construction of rotor with tooths form it is convenient to present the excitation winding field as air gap field of salient-pole machines created by the equivalent pole shoe with width $b_p = \tau$. Let us locate slots with bars of equivalent damper winding on such a polar shoe. In synchronous mode currents in these bars are absent. The number of such equivalent rotor slots on each pole is equal to $Z_D = 3q_2$, and slot dimensions are the same as for ASG rotor (slot pitch —$t_{SLT,2}$, slot width—$b_{SLT,2}$). In tooth zone of such a shoe the field has a rectangular waveform with period

$$t_{SLT,2} = \frac{\tau}{Z_D} = \frac{\tau}{3q_2}; \tag{20.2}$$

Physically, higher harmonics of this excitation field arise in air gap due to the fact that magnetic resistance of rotor teeth and slots in the air gap area is deferent, and they do not depend on the fact that the current in rotor slots is absent. Therefore, sometimes these are called "reluctant".

Amplitude of this rectangular wave with the period of (20.2) changes along the pole shoe: it is maximum in the pole middle (in its longitudinal axis zone by relative value $B^*_{MI,1} = 1$) and is minimum at pole edges (in its both cross axes zone) because this field of rotor tooth harmonics is imposed on the field, generated by excitation winding inducing rated voltage in stator winding.

20.4.3 Interaction of the First Harmonic of Mutual Induction Field and Field of Rotor Tooth Harmonics

With account of (20.1), (20.2), the first harmonic of rectangular wave caused by the rotor teeth has the form [16]:

$$b_{SLT,2}(x,n) = \left(B_{SLT,2EQ}B^*_{MI,1}\cos\frac{\pi x}{\tau}\right)\sin\frac{\pi 6q_2 x}{\tau}. \tag{20.3}$$

here $B_{SLT,2EQ}=\frac{4}{\pi}B_{SLT,2}$; relative value of flux density $B^*_{SLT,2}$ for high-power generators usually makes [12]:

$$B^*_{SLT,2} = \frac{B_{SLT,2}}{B_{MI,1}} \leq 0.10 - 0.18. \tag{20.4}$$

Let us note, however, that, in practice, the width of pole shoe in real salient-pole machines is usually $b_p \leq 0.8\tau$, and damper winding bars are usually round, slots—with narrow opening to minimize the influence of damper winding [10–12].

20.5 The First Component of Resulting Mutual Induction Field in Air Gap of Tooth Order

20.5.1 Amplitudes of the First Field Component

Let us determine this component with account of interaction of the following field harmonics in machine air gap:

- rotor tooth harmonics as per (20.3);
- stator tooth harmonics.

In Sect. 20.2 it is accepted ("reserve") that the stator and rotor slot opening of ASG is identical and equal to $\frac{b_{SLT,1}}{t_{SLT,1}} = \frac{b_{SLT,2}}{t_{SLT,2}} = 0.5$. Correspondingly the flux density amplitudes in air gap of tooth harmonics field of stator $B_{SLT,1EQ}$, and rotor $B_{SLT,2EQ}$ determined in ASG no-load mode only by excitation winding field, can also be accepted identical to $B_{SLT,1} = B_{SLT,2} = B_{SLT}$. Correspondingly $B_{SLT,1EQ} = B_{SLT,2EQ} = B_{SLT,EQ}$. Considering the resulting field in stator tooth zone air gap, let us use the results obtained in the previous chapter [9, 15]. We accept, thus, that ASG rotor is stalled, and the stator rotates in positive direction of angle reference with synchronous speed ω_{REV}. Then, we obtain that the first component of resulting mutual induction field in air gap is distributed along the pole pitch as follows [9, 13, 14]:

$$b_{RES,1}(x,t,n) = B^{*}_{MI,1}\cos\frac{\pi x}{\tau}\left(B_{SLT,EQ}\sin\frac{6q_2\pi x}{\tau}\right)\sin\left(\omega_Z t - \frac{6q_1\pi x}{\tau}\right). \quad (20.5)$$

here ω_Z—EMF circular frequency of stator tooth harmonics subject to the definition with account of stator synchronous rotation speed ω_{REV}.

We transform Eq. (20.5); according to [13, 14] we have:

$$\begin{aligned} b_{RES,1}(x,t,n) = 0.25B^{*}_{MI,1}B_{SLT,EQ}\Bigg\{&\cos\left[\omega_Z t - \frac{\pi(6q_1 + 6q_2 - 1)x}{\tau}\right] \\ &+ \cos\left[\omega_Z t - \frac{\pi(6q_1 + 6q_2 + 1)x}{\tau}\right] - \cos\left[\omega_Z t - \frac{\pi(6q_1 - 6q_2 - 1)x}{\tau}\right] \\ &- \cos\left[\omega_Z t - \frac{\pi(6q_1 - 6q_2 + 1)x}{\tau}\right]\Bigg\}. \end{aligned} \quad (20.6)$$

We name the flux density $b_{RES,1}(x,t,n)$ the first component of mutual induction field in air gap of tooth order; it has two indices: the first of them indicates the resulting field ("RES"), and the second—number of component for the designation of flux density. It follows from the ratios (20.6) that it has four components; they rotate relative to the stationary (motionless) rotor with constant amplitude B_Z:

$$B_Z^{(1)} = 0.25B^{*}_{MI,1}B_{SLT,EQ}. \quad (20.7)$$

The field first components take the form:

$$\begin{aligned} b^{(1)}_{RES,1}(x,t,n) &= B_Z^{(1)}\cos\left[\omega_Z^{(1)}t - \frac{\pi(6q_1 - 6q_2 - 1)x}{\tau}\right], \\ b^{(2)}_{RES,1}(x,t,n) &= B_Z^{(1)}\cos\left[\omega_Z^{(2)}t - \frac{\pi(6q_1 + 6q_2 + 1)x}{\tau}\right], \\ b^{(3)}_{RES,1}(x,t,n) &= -B_Z^{(1)}\cos\left[\omega_Z^{(3)}t - \frac{\pi(6q_1 + 6q_2 - 1)x}{\tau}\right], \\ b^{(4)}_{RES,1}(x,t,n) &= -B_Z^{(1)}\cos\left[\omega_Z^{(4)}t - \frac{\pi(6q_1 - 6q_2 + 1)x}{\tau}\right]. \end{aligned} \quad (20.8)$$

These correspond to frequencies ω_Z of tooth EMFs, equal respectively to $\omega_Z^{(1)}, \omega_Z^{(2)}, \omega_Z^{(3)}$ and $\omega_Z^{(4)}$.

20.5.2 Frequencies $\omega_Z^{(1)}, \omega_Z^{(2)}, \omega_Z^{(3)}$ and $\omega_Z^{(4)}$ of EMFs Induced in Stator Winding by the First Component of Field Harmonics

One determines these EMF frequencies from the condition that at the rotation of each field component its angular speed relative to the rotor is equal to $\omega_{REV} = \omega_1 / p$.

From Eq. (20.8) for the first field component we obtain:

$$\omega_Z^{(1)} dt = \frac{\pi(6q_1 - 6q_2 - 1)x}{\tau}. \tag{20.9}$$

With account of $\frac{dx}{dt} = \frac{\omega_1 \tau}{\pi}$, we obtain:

$$\omega_1^{(1)} = \omega_Z |(6q_1 - 6q_2 - 1)|. \tag{20.10'}$$

Similarly to Eq. (20.10′) for other field components of the first field component:

$$\omega_1^{(2)} = \omega_Z |(6q_1 - 6q_2 + 1)|; \tag{20.10''}$$

$$\omega_1^{(3)} = \omega_Z |(6q_1 + 6q_2 - 1)|; \tag{20.10'''}$$

$$\omega_1^{(4)} = \omega_Z (6q_1 + 6q_2 + 1). \tag{20.10''''}$$

The order of higher harmonics for frequencies of stator tooth EMFs can be presented also in other form, including the case $m_{PH} \geq 3$:

$$n_1^{(1)} = |2m_{PH}(q_1 - q_2) - 1|; \tag{20.11'}$$

$$n_1^{(2)} = |2m_{PH}(q_1 - q_2) + 1|; \tag{20.11''}$$

$$n_1^{(3)} = |2m_{PH}(q_1 + q_2) - 1|; \tag{20.11'''}$$

$$n_1^{(4)} = 2m_{PH}(q_1 + q_2) + 1. \tag{20.11''''}$$

20.5.3 EMF Amplitudes $e_1^{(1)}, e_1^{(2)}, e_1^{(3)}$ and $e_1^{(4)}$ Induced in Stator Winding by the First Field Component

Let us note that in the designations of flux density (20.8), frequencies (20.10), order of tooth harmonics (20.11) and further flux (20.12), and EMF (20.13) and (20.14),

upper indices [(1), …, (4)] correspond to the number of field component, and lower to the field harmonic component.

We try to find, as previously, the flux corresponding to the first component $b^{(1)}_{RES,1}(x,t,n)$ in air gap as per (20.8). We accept as previously that the stator winding pitch is shortened (pitch chording is equal β_1); We designate the winding factor [6–8] for the harmonic of order $n^{(1)}$ as $K^{(1)}_{W.ST}$. The flux for the harmonic of order $n^{(1)}$ is equal to,

$$\Phi^{(1)}_{RES,1} = \int_0^{\tau\beta_1} b^{(1)}_{RES,1}(x,t,n)L_{COR}dx = \frac{2\tau B^{(1)}_Z L_{COR}}{\pi n^{(1)}}\sin\left(\omega^{(1)}_Z t - \frac{\pi n^{(1)}\beta_1}{2}\right)\sin\frac{\pi n^{(1)}\beta_1}{2}, \tag{20.12}$$

where L_{COR}—calculation length of stator core [10–12].

Accordingly, EMF $e^{(1)}$ with account of Eqs. (20.10′) for $\omega^{(1)}_Z$ and (20.12) for flux $\Phi^{(1)}_{RES,1}$ of elementary winding is expressed as:

$$\begin{aligned} e^{(1)}_1 &= -W^{EL}_{PH}K^{(1)}_{W,ST}\frac{d}{dt}\Phi^{(1)}_{RES,1} \\ &= -\frac{2}{\pi^2}B^{(1)}_Z\omega_1 W^{EL}_{PH}K^{(1)}_{W.ST}\tau L_{COR}\cos\left(\omega^{(1)}_Z t - \frac{\pi n^{(1)}\beta_1}{2}\right) \\ &= E^{(1)}_1\cos\left(\omega^{(1)}_Z t - \frac{\pi n^{(1)}\beta_1}{2}\right) \end{aligned} \tag{20.13}$$

where the amplitude $E^{(1)}_1$ of this EMF in (20.13) has the form:

$$E^{(1)}_1 = -\frac{2}{\pi^2}B_{SLT}\omega_1 W^{EL}_{PH}K^{(1)}_{W.ST}\tau L_{COR}. \tag{20.14}$$

Other three flux components are calculated similarly, as well as EMF in the phase of elementary stator winding. They differ from (20.13), (20.14) only by orders $n^{(2)}_1, \ldots, n^{(4)}_1$ of tooth harmonics determined based on (20.11′)–(20.11′″) and, respectively, winding factors $K^{(2)}_{W.ST}, \ldots, K^{(4)}_{W.ST}$.

Let us note the following peculiarities of obtained expressions for EMF of tooth harmonics:

- frequencies $\omega^{(1)}_Z, \omega^{(2)}_Z, \omega^{(3)}_Z \omega^{(4)}_Z$ of tooth EMFs significantly exceed the network frequency ω_1, but the amplitude of these EMFs is determined only by frequency ω_1;
- amplitudes of tooth EMFs of the form (20.14) can be changed for the selected stator construction and its tooth zone practically by means of factors $K^{(1)}_{W.ST}, \ldots, K^{(4)}_{W.ST}$.

20.5.4 Nonlinear Distortion Factor $K_{DIST,1}$ of ASG Stator Winding Voltage Caused by the First Component of Mutual Induction Resulting Field in Air Gap of Tooth Order

In Chap. 19 it was already noticed that these harmonics exert the greatest influence on the value of the distortion factor. For determination of this nonlinear distortion factor let us use the calculation expression similar to (19.12′):

$$K_{DIST} = \sqrt{\left[E_1^{(1)*}\right]^2 + \left[E_1^{(2)*}\right]^2 + \left[E_1^{(3)*}\right]^2 + \left[E_1^{(4)*}\right]^2}. \tag{20.15}$$

here $E_1^{(1)*} = \frac{E_1^{(1)}}{E_{MI,1}}$. The amplitude of tooth EMF $E_1^{(1)}$ is calculated based on (20.14).

EMF $E_{MI,1}$ is induced by the first harmonic $B_{MI,1}$ of excitation winding field as per (20.1). It is equal to [6–8]:

$$E_{MI,1} = -\frac{2}{\pi} B_{MI,1} \omega_1 W_{\Phi}^{EL} K_{W.ST} \tau L_{COR}; \tag{20.16}$$

here $K_{W.ST}$—stator winding factor for the calculation of EMF $E_{MI,1}$, it is supposed that the relation $\frac{b_{SLT,1}}{t_{SLT,1}} \to 0$. As a result, we obtain the relation of EMF amplitudes from (20.15) for the harmonic of order $n^{(1)}$:

$$E_1^{(1)*} = \frac{B_{SLT}^*}{\pi} \frac{K_{W.ST}^{(1)}}{K_{W.ST}}. \tag{20.17}$$

Here according to (20.4): $B_{SLT}^* = \frac{B_{Z,SL}}{B_{MI,1}}$.

Expressions for other EMF amplitudes of tooth harmonics in amplitude fractions $E_{MI,1}$ of generator EMF first harmonic have the similar form and differ by winding factors $\left(K_{W.ST}^{(2)}, \ldots, K_{W.ST}^{(4)}\right)$ for tooth harmonics as per (20.11′)–(20.11‴).

20.5.5 Calculation Example

Using (20.10′)–(20.10‴) we determine, at first, EMF tooth frequencies for one of ASG constructions: $q_1 = 2, q_2 = 3$. For such a construction we have $\omega_Z^{(1)} = 2\pi \cdot 250 s^{-1}$; $\omega_Z^{(2)} = 2\pi \cdot 350 s^{-1}$; $\omega_Z^{(3)} = 2\pi \cdot 1450 s^{-1}$; $\omega_Z^{(4)} = 2\pi \cdot 1550 s^{-1}$. Thus, we obtain two components of low frequency (250 Hz and 350 Hz, orders of

tooth harmonics $n^{(1)} = 5, n^{(2)} = 7$) and two components of high frequency (1450 Hz and 1550 Hz, orders of tooth harmonics $n^{(3)} = 29, n^{(4)} = 31$).

Let us determine the nonlinear distortion factor $K_{DIST,1}$ for the first components of this generator as per (20.15) and (20.17); pitch shortening for stator winding is equal to $\beta_1 \approx 0.8$.

This choice is reasonable by the fact that at $\beta_1 \approx 0.8$ we obtain not only the maximum value of winding factor $K_{W.ST}$ included in Eq. (20.16) for EMF $E_{MI,1}$, but also minimum values of winding factors of tooth harmonics $K_{W.ST}^{(1)},\ldots,K_{W.ST}^{(4)}$ included in expressions like (20.14) for EMF $E_1^{(1)}, E_1^{(2)}, E_1^{(3)}, E_1^{(4)}$. Let us refine this value for $q_1 = 2$; diametral winding pitch is equal to $Y = \frac{Z_1}{2p} = 3q_1 = 6$, so that the pitch chording $\beta_1 = \frac{5}{6} = 0.833$. For this chording we have $K_{W.ST} = 0.933$; $K_{W.ST}^{(1)} = \cdots = K_{W.ST}^{(4)} \approx 0.07$.

Let us take for clarity $B_{SLT}^{*} = 0.18$. According to (20.15) and (20.17), we obtain:

$$E_1^{(1)*} = \cdots = E_1^{(4)} \approx 0.0041;\ K_{DIST,1} \approx 0.0085$$

The result meets requirements $(K_{DIST} \leq 0.05)$ GOST and IEC [18] without account of other field higher harmonics in air gap considered in Sects. 20.6 and 20.7.

20.6 The Second Component of Resulting Mutual Induction Field in Air Gap of Tooth Order

20.6.1 Amplitudes of the Second Field Component

We try to determine this component with account of interaction of the following field harmonics in machine air gap:

- first harmonic of excitation winding field as per (20.1);
- stator tooth harmonics.

The solution of the problem to determine this component for ASG practically coincides with that of the similar problem for salient-pole machines; it is stated in the previous chapter [15]. Let us formulate its main results with account of indices, which should correspond to the field component number and ASG rotor and stator construction peculiarities. We accept as in Sect. 20.5.1 that the ASG rotor is motionless (stalled), and the stator rotates in positive direction of angle reference with synchronous speed. The expression for the second components of resulting field takes the form [15] as per (19.7) and (19.8). Let us note that for salient-pole machines there occurs only one component of resulting mutual induction field in air gap of tooth order; for simplicity in the previous chapter it is marked with index "0".

20.6.2 Frequencies $\omega_Z^{(1)}$, $\omega_Z^{(2)}$ of the Second Component of Stator Winding EMF Tooth Harmonics

We try to determine these EMF frequencies as in Sect. 20.5.2 from the condition that at the rotation of each field component its angular speed relative to the rotor is equal to $\omega_{REV} = \frac{\omega_1}{p}$.

According to Eq. (19.11), we obtain for the first component of this field component:

$$\omega_Z^{(1)} = \omega_1(6q_1 - 1). \tag{20.18}$$

For the second component of this field component according to Eq. (19.11′) similar to (20.18):

$$\omega_Z^{(2)} = \omega_1(6q_1 + 1). \tag{20.18'}$$

The order of higher harmonics for frequencies of tooth EMFs can be presented also in the following form, including the case $m_{PH} \geq 3$:

$$n_2^{(1)} = 2m_{PH}q_1 - 1, \tag{20.19}$$

$$n_2^{(2)} = 2m_{PH}q_1 + 1. \tag{20.19'}$$

20.6.3 EMF Amplitudes $e_2^{(1)}$, $e_2^{(2)}$, Induced in Stator Winding by the Second Component of Pole Harmonics

Similarly to (19.15), (19.16) and (20.14) for both EMF components of the second component we obtain:

$$E_2^{(1)} = -\frac{4}{\pi^2} B_{SLT}\omega_1 W_{PH}^{EL} K_{W.ST}^{(1)} \tau L_{COR}. \tag{20.20}$$

EMF amplitude of component $E_2^{(2)}$ differs from (20.20) only by winding factor $K_{W.ST}^{(2)}$; it is calculated for the harmonic of order $n_2^{(2)}$ as per (20.19′).

20.6.4 Nonlinear Distortion Factor $K_{DIST,2}$ of ASG Stator Winding Voltage Caused by the Second Component of Mutual Induction Resulting Field in Air Gap of Tooth Order

Similarly to (20.17) we obtain the relation of EMF amplitudes for both EMF components; for the harmonic of the order $n^{(1)}$:

$$E_2^{(1)*} = \left| \frac{2}{\pi} B_{SLT}^{*} \frac{K_{W.ST}^{(1)}}{K_{W.ST}} \right|. \tag{20.21}$$

The expression for $E_2^{(2)*}$ differs from (20.21) only by the value of winding factor ($K_{W.ST}^{(2)}$ instead of $K_{W.ST}^{(1)}$).

Nonlinear distortion factor $K_{DIST,2}$ is determined similarly to (19.12′) and (20.15).

20.6.5 Calculation Example

According to (20.18) and (20.18′) we first determine EMF tooth frequencies in the same ASG construction, as in the example of Sect. 20.5.5.

For such a construction ($q_1 = 2$) we have $\omega_Z^{(1)} = 2\pi \cdot 650\ s^{-1}$; $\omega_Z^{(2)} = 2\pi \cdot 550\ s^{-1}$. Thus, we obtain two components (with frequency 650 and 550 Hz, orders of tooth harmonics, correspondingly, $n^{(1)} = 13, n^{(2)} = 11$).

As in the example Sect. 20.5.5 for the first component, one accepts that the pitch chording for stator winding $\beta_1 = \frac{5}{6} = 0.833$, and relative value of flux density $B_{SLT}^{*} = 0.18$. For this shortening we have $K_{W.ST} = 0.933$; $K_{W.ST}^{(1)} = K_{W.ST}^{(2)} = 0.933$. Based on (20.21) we obtain $E_2^{(1)*} = E_2^{(2)*} = 0.114$. Result: $K_{DIST,2} = 0.16$.

This result does not meet requirements of [18] GOST and IEC ($K_{DIST} \leq 0.05$); it is easily expected, proceeding from investigation results of distortion factors obtained in the previous chapter. In order to reduce this factor from mutual induction field harmonics of the second order, we need to take additional actions; for example, a change of stator core construction (slot skewing by one slot pitch [6–8, 16], installation of filters).

20.7 The Third Component of Resulting Mutual Induction Field in Air Gap

20.7.1 Amplitudes of the Third Field Component

Let us determine harmonics of this component with account of EMFs induced in stator winding.

Equation (20.1) obtained in Sect. 20.3 indicates rotating field higher harmonics (at $n_W > 1$) created by three-phase excitation current in generator no-load mode. In Sect. 20.4.1 it was already noted that physically the higher harmonics of this field arise in air gap due to the discrete arrangement of winding in slots and, therefore, called "winding"; they rotate not synchronously with its first harmonic. Their rotation speed in air gap relative to stator winding depends not only on the harmonic order n_W, but also on the ASG mode (on slip S_{SL}).

When investigating the influence of amplitude B_{MI,n_W} of these higher "winding" harmonics of rotor field on the generator EMF form, it is supposed that the relation $b_{SLT,1} / t_{SLT,1} \to 0$. This assumption was already used to compute EMF $E_{MI,1}$ as per (20.16); it is induced by the first harmonic $(n_W = 1)$ of the field (20.1) considered.

Amplitudes of flux density higher harmonics $B_{MI,W}$ of this field are determined only by their orders n_W : $\frac{B_{MI,n_W}}{B_{MI,1}} \approx \frac{1}{n_W}$.

20.7.2 EMF Frequencies $\omega_{ST,W}$ in Stator Winding Induced by "Winding" Harmonics of Rotor Field

Harmonics of order n_W induce EMF in stator winding in a wide range of frequencies. Let us write down the expression for their calculation.

For harmonics of order $n_W = 5; 11; 17; \ldots$ in the form:

$$\omega_{ST,W} = \omega_1(n_W - S_{SL}n_W - S_{SL}); \tag{20.22}$$

and for harmonics of order $n_W = 7; 13; 19; \ldots$

$$\omega_{ST,W} = \omega_N(n_W - S_{SL}n_W + S_{SL}); \tag{20.22'}$$

here S_{SL}—slip index at frequency $\omega_{ST,W}$, designates that it refers to the stator winding EMF. Let us note that an ASG works usually at small slips $S_{SL} < 10\,\%$. Table 20.1 gives values of frequencies $f_{ST,W} = \omega_{ST,W} / 2\pi$ at the slip of $S_{SL} = 5\,\%$ in the range of harmonic orders $(5 \le n_W \le 17)$ usually of practical interest.

It follows from Table 20.1 that under certain conditions high order "winding" harmonics of excitation field can induce in stator winding EMF whose frequency is close to the tooth frequency determined by the ratios in Sects. 20.5 and 20.6.

Table 20.1 EMF frequencies in stator winding

N	1	2	3	4	5
n_W	5	7	11	13	17
$f_{ST,W}$, Hz	235	335	520	620	850

N numbers of the third field component

Table 20.1 gives EMF frequencies in stator winding induced by "winding" harmonics of rotor field.

20.7.3 EMF Amplitudes in Stator Winding Induced by "Winding" Harmonics of Rotor Field

The expression for EMF amplitude in stator winding induced by these harmonics has the form [9–12]:

$$E^{(1)}_{MI,n_W} = -\frac{2}{\pi}\frac{B_{MI,1}}{n_W}\omega_1 n^*_W W^{EL}_{PH}\tau L_{COR} K^{(1)}_{W.ST}; \tag{20.23}$$

here $n^*_W = \frac{n'_W}{n_W} < 1$—correction factor considering the slip; $n'_W = n_W - S_{SL}n_W - S_{SL}$ for harmonics of order $n_W = 5; 11; 17; \ldots$ $n'_W = n_W - S_{SL}n_W + S_{SL}$ for harmonics of order $n_W = 7; 13; \ldots; \ldots$; the upper index at stator winding factor $K^{(1)}_{W.ST}$ indicates the number of field component in air gap (Table 20.1), for example, harmonic $n_W = 5$ corresponds to index N = 1, harmonic $n_W = 7$ to index N = 2, etc.; harmonic $n_W = 17$ corresponds to maximum index N = 5. Let us note that at slip S_{SL} = 5 % the value n^*_W in the range of harmonics representing practical interest $(5 \le n_W \le 17)$ is equal to $n^*_W \approx 0.95$.

20.7.4 Nonlinear Distortion Factor $K_{DIST,3}$ of ASG Stator Winding Voltage Caused by the Third Component of Mutual Induction Resulting Field in Air Gap

Similarly to (20.17) for the harmonic of order $n_W = 5$ taking into account (20.16) and (20.23) we obtain:

$$E^{(1)*}_3 = \frac{E^{(1)}_3}{E_{MI,1}} = \frac{n^*_W}{n_W}\cdot\frac{K^{(1)}_{W.ST}}{K_{W.ST}}. \tag{20.24}$$

Expressions for $E_3^{(2)*}, \ldots, E_3^{(5)*}$ differ only by the values of winding factors ($K_{W.ST}^{(2)*}, \ldots, K_{W.ST}^{(5)}$ instead of $K_{W.ST}^{(1)}$).

The nonlinear distortion factor $K_{DIST,3}$ is determined similarly to (19.12′) and (20.15).

20.7.5 Calculation Example

As in examples 20.5.5 and 20.6.5, we accept that the pitch chording for stator winding $\beta_1 = \frac{5}{6} = 0.833$. Then for harmonics given in Table 20.1, we obtain with account of values of EMF $E^{(1)*}, \ldots, E^{(5)*}$: $K_{DIST,3} \approx 0.115$. A decisive role in the value $K_{DIST,3}$ is played by harmonics of order $n_W = 11$ and $n_W = 13$ (numbers of their components N = 3 and N = 4): for them at q = 2 winding factors $K_{W.ST}^{(3)} = K_{W.ST}^{(4)} = K_{W.ST}$ [6–8]. The obtained result ($K_{DIST,3} = 0.115$) does not meet requirements of GOST and IEC [18]; from the example it follows that for the reduction in factor from harmonics of the third mutual induction field component, as well as from the second component, we need additional measures.

20.8 The Fourth Component of Resulting Mutual Induction Field in Air Gap of Tooth Order

20.8.1 Amplitudes of the Fourth Field Component; Frequency EMF

Let us determine this component with account of interaction of the following field harmonics in machine air gap:

- higher ($n_W > 1$) harmonics of excitation winding field as per (20.1);
- stator tooth harmonics.

The solution of the problem to estimate this component for ASG practically coincides with that of the similar problem for the first harmonic motionless (stalled) in Sect. 20.6. Let us accept that ASG rotor is stalled, and the stator rotates at $n_W > 1$ not synchronously with speed $\omega'_{REV} = \omega_1 n_W^* / p$; its rotation direction is determined by the harmonic order n_W in Eq. (20.1).

Taking into account this direction similarly to Eqs. (20.11), (20,18) it is easy to determine the frequency of the fourth field component of corresponding EMFs:

$$\omega_Z^{(1)} = \omega_1 n_W^* |(6q_1 - n_W)|. \tag{20.25}$$

$$\omega_Z^{(2)} = \omega_1 n_W^* |(6q_1 + n_W)|. \tag{20.25'}$$

High frequency EMFs (about 1 kHz) present the greatest practical interest, which are determined based on (20.25′). These EMFs are connected usually with restriction of nonlinear distortion factor value in generators. The reasons causing these restrictions are listed the beginning of Chap. 19 and repeated at the beginning of this chapter.

The order of higher harmonics for EMF tooth frequencies of this component is given by,

$$n_1^{(4)} = 2m_{PH}q_1 - n_W. \tag{20.26}$$

$$n_4^{(2)} = 2m_{PH}q_1 + n_W. \tag{20.26'}$$

20.8.2 EMF Amplitudes Induced in Stator Winding by the Fourth Component of Field Harmonics

Similar to (20.20) for the fourth component we obtain:

$$E_4^{(1)} = -\frac{4}{\pi^2} B_{SLT}\omega_1 \frac{n'_W}{n_W} W_{PH}^{EL} K_{W.ST}^{(1)} \tau L_{COR}. \tag{20.27}$$

Expression for $E_4^{(2)}$ differs from (20.27) only in value of winding factor ($K_{W.ST}^{(2)}$ instead of $K_{W.ST}^{(1)}$).

20.8.3 Nonlinear Distortion Factor $K_{DIST,4}$ of ASG Stator Winding Voltage Caused by the Fourth Component of Mutual Induction Resulting Field in Air Gap of Tooth Order

In the similar way to (20.21) for EMF component of the fourth component determined by the harmonic of order n_W, we obtain:

$$E_4^{(1)*} \approx \frac{2}{\pi} B_{SLT}^* \frac{n'_W}{n_W} \frac{K_{W.ST}^{(1)}}{K_{W.ST}}. \tag{20.28}$$

The expression for $E_4^{(2)*}$ differs from (20.27) only by the value of winding factor ($K_{W.ST}^{(2)}$ instead of $K_{W.ST}^{(1)}$).

So that, the greatest value of EMF relative amplitudes $E^{(1)*}$ and $E^{(2)*}$ depends on the value B_{SLT}^*; it is inversely proportional to the harmonic of order n_W. So, practical interest is represented by harmonics of order $n_W \leq 17$. The nonlinear distortion factor $K_{DIST,4}$ is determined similarly to (19.12′) and (20.15).

Expressions for $E^{(4)*}$ and $E^{(4)*}$ like (20.28) allow us to obtain the "upper" assessment value of factor $K_{DIST,4}$, which is not dependent on the pitch shortening β_1 and number q_1. This highest value of factor $K_{DIST,4}$ is determined, assuming that $K_{W.ST}^{(1)} = K_{W.ST}^{(2)} = K_{W.ST}$; for $n_W \leq 17$ it takes the form:

$$K_{DIST,4}^{MAX} \approx \frac{2}{\pi} \cdot B_{SLT}^* n_W^* \sqrt{2\left[\left(\frac{1}{5}\right)^2 + \left(\frac{1}{7}\right)^2 + \left(\frac{1}{11}\right)^2 + \left(\frac{1}{13}\right)^2 + \left(\frac{1}{17}\right)^2\right]}.$$

At $B_{SLT}^* = 0.18$; $n_W^* = 0.95$ we obtain $K_{DIST,4}^{MAX} = 0.043$.

20.8.4 Calculation Example

As in the example 20.6.5, let us accept for stator winding $q_1 = 2$, and pitch coring $\beta_1 = 5/6 = 0.833$.

For harmonics of order $(5 \leq n_W \leq 17)$ with account of Eqs. (20.26) and (20.26′) we obtain $K_{DIST,4} \approx 0.02$, and this result meets requirements [IV-1] of GOST and IEC ($K_{DIST} \leq 0.05$). We note that in this example $K_{DIST} \ll K_{DIST,4}^{MAX}$.

Thus, the field of higher harmonics $(n_W > 1)$ in (20.1) practically does not influence the ASG voltage waveform; the influence of the first harmonic field $(n_W = 1)$ is the most significant, that is of the second component of mutual induction resulting field in air gap of tooth order. Measures necessary for reduction of factor $K_{DIST,2}$ listed in Sect. 20.6.5 also reduce the value of $K_{DIST,4}$.

Brief Conclusions

1. In high-power DFMs, for example, ASG differing in stator and rotor windings with integer number q of slots per pole and phase [6–8], in voltage curve there appear additional EMFs with frequency exceeding the network frequency. Number of problems is connected with them: Additional losses and stator core overheats; currents of these tooth harmonics can cause interference to the

telephone lines located close to the high voltage line, and also overvoltages in these high voltage transmission lines due to resonance phenomena.

2. As a result of investigation, we obtained calculation expressions for the following amplitudes and frequencies (orders of harmonics):

   2.1 Tooth EMFs with account of bilateral stepped shape—due to slots on stator and rotor.

   2.2 EMF of "winding " harmonics caused by discrete layout of winding in rotor slots.

3. The obtained calculation expressions allow one to calculate nonlinear distortion factor of ASG and to establish a degree of its compliance to requirements of GOST and IEC.
   As an example are calculated nonlinear distortion factors for generator EMF with values $q_1 = 2$, $q_2 = 3$. It is obtained that this generator does not meet the requirements of GOST and IEC; additional actions are required to decrease the nonlinear distortion factor, for example, by a variation of stator core construction (slot skewing by one slot pitch [6–8,15], etc.), installation of filters); also expedient is a thorough selection of stator and rotor winding construction (values q_1, q_2, for pitch chording of these windings, etc.).

List of Symbols

b_{SLT}	Width of slot
B_{MUT}	Amplitude of resulting mutual induction field in air gap (flux of mutual inductance)
b_{MUT}	Instantaneous value of magnetic flux density
b_P	Width of pole shoe
E	Instantaneous value of EMF, induced in the stator winding by the component of field's harmonic
E	Amplitude of EMF
K_{DIST}	Distortion factor
$K_{W.ST}$	Winding factor for stator
L_{COR}	Active length of stator core
m_{PH}	Number of stator phases
n	Order of harmonics
p	Number of pole pairs in machine
q	Number of slots per pole and phase
S_{SL}	Slip
t	Time
t_{SLT}	Stator slot pitch
W_{PH}^{EL}	Number of turns in the phase of elementary (single) winding

x	Coordinate along stator boring (in tangential direction)
Y	Winding pitch
Z	Number of stator slots
τ	Pole pitch
Φ_{RES}	Resulting magnetic flux in the air gap (flux of mutual inductance)
ω_{REV}	Angular rotation speed
ω_1	Circular frequency of rated voltage and current

References

I. Monographs, Textbooks

1. Demirchyan K.S., Neyman L.R., Korovkin N.V., Theoretical Electrical Engineering. Moscow, St.Petersburg: Piter, 2009. Vol. 1, 2. (In Russian).
2. Kuepfmueller K., Kohn G., Theoretische Elektrotechnik und Elektronik. 15 Aufl. Berlin, New York: Springer. 2000. (In German).
3. Boguslawsky I.Z., A.C. Motors and Generators. The Theory and Investigation Methods by Their Operation in Networks with Non Linear Elements. TU St.Petersburg Edit., 2006. Vol. 1; Vol.2. (In Russian).
4. Shakaryan Yu.G., Asynchronized synchronous machines. Moscow: Energoatomizdat, 1986. (In Russian).
5. Zagorskiy A.E., Shakaryan Yu.G., Control of Transients in A.C. Machines. Moscow: Energoatomizdat, 1986. (In Russian).
6. Richter R., Elektrische Maschinen. Berlin: Springer. Band I, 1924; Band II, 1930; Band III, 1932; Band IV, 1936; Band V, 1950. (In German).
7. Mueller G., Ponick B., Elektrische Maschinen. New York, John Wiley, 2009. (In German).
8. Voldek A.I., Electrical Machines. Leningrad: 1974. 782 c. (In Russian).
9. Bragstad O., Theorie der Wechselstrommaschinen und eine Einleitung in der Theorie der stationaeren Wechselstroeme. Berlin: Springer, 1932. (In German).
10. Construction of Electrical Machines. Edited by Kopylov, I.P. Moscow: Energiya, 1980. (In Russian).
11. Mueller G., Vogt, K., Ponick B., Berechnung elektrischer Maschinen. Springer, 2007. (In German).
12. Schuisky W., Berechnung elektrischer Maschinen. Wien: Springer, 1960. (In German).
13. Korn G., Korn T., Mathematical Handbook. New York: McGraw–Hill, 1961
14. Jeffris H., Swirles B., Methods of Mathematical Physics. Third Edition, Vol. 1 – Vol. 3, Cambridge: Cambridge Univ. Press, 1966.

III. Synchronous Machines. Papers, Inventor's Certificates, Patents

15. Arseniev I.A., Boguslawsky I.Z., Korovkin N.V., Research methods for the slot-ripple EMF in polyphase integral slot winding. IEEE Russia (Northwest) Section. December, 2012. St. Petersburg.

16. Boguslawsky I.Z., Dubitsky S.D., Korovkin N.V., Research methods for the slot-ripple EMF in large double-fed machines. IEEE Russia (Northwest) Section. December, 2012. St. Petersburg.
17. Kuwabara T., Shibuya A., Furuta H., Kita E., Mitsuhashi K., Construction and dynamic response characteristics of 400 MW adjustable speed pumped storage unit for Ohkawachi station. IEEE Transactions on Energy Conversion, Vol. 11, No. 2, June 1996.

IV. State Standards (IEC, GOST and so on)

18. GOST (Russian State Standard) R - 52776 (IEC 60034-1). Rotating Electrical Machines. (In Russian).

Chapter 21
Method of Determination Stator Winding MMF at Arbitrary Phase Current Waveform and Unequal Width of Phase Zones (for Investigation of Operational Characteristics of Frequency: Controlled Motors)

In this chapter to study operational characteristics of frequency—controlled motors, there is developed a method of stator winding MMF determination at arbitrary waveform of currents in phases and with unequal phase zone width, for example, for winding implemented with fractional number of slots per pole and phase.

In practice of developing modern frequency—controlled motors, for example, valve intended for various industries, there are problems of studying their operation characteristics (torque, stability limit, efficiency, etc.). They are determined generally by the value of MMF and stator winding field.

In this chapter for the investigation of operational characteristics of frequency—controlled motors there is developed a method to determine this MMF and field generally—in asymmetrical modes; thus, currents in winding phases vary with time with period T_{TIM} under arbitrary periodic (not only harmonic processes), for example, stepwise; for such modes expanding currents into symmetric components are excluded. The method yields construction peculiarities of modern stator windings: various width phase zones that usually take place for multiphase windings with fractional number of slots per pole and phase.

Given here are main stages of this method realization. Practical examples executed for a number of limit problems confirm its correctness. The content of this chapter is development of the methods stated in [1, 2, 10–14].

21.1 Introduction: Problem Formulation

In practice of developing modern frequency-controlled motors, for example, frequency—controlled motors intended for various industries, there are problems of elaborating their operation characteristics (torque, stability limit, efficiency, etc.). They are determined generally by the value of MMF and stator winding field. One of these problems requiring the solution is that of determining this MMF and field generally—in asymmetrical modes, herewith currents in winding phases vary in

I. Boguslawsky et al., *Large A.C. Machines*,
DOI 10.1007/978-4-431-56475-1_21

time with period T_{TIM} under arbitrary (not only harmonic [1–5]) law, for example, stepwise, while the phase zone width of stator winding is different. In one of motor constructions there can be, for example, a mode of variation in time of stator winding currents as follows:

- within period $\Delta t_0 = t_1 - t_0$, instantaneous values of currents in winding phases A, B and C are equal to, i_A = 100 % = const., i_B = 100 % = const, i_C = 0;
- within period $\Delta t_1 = t_2 - t_1$, when the motor rotor turns by an angle $\psi_1 = \frac{\pi}{3}$, instantaneous values of currents in phases A, B and C change: i_A = 0, i_B = 100 % = const, i_C = 100 % = const;
- within period $\Delta t_2 = t_3 - t_2$ when the motor rotor turns by an angle $\psi_2 = \frac{2\pi}{3}$, instantaneous values of currents in phases A, B and C accept the values: i_A = 100 % = const, i_B = 0, i_C = 100 % = const;
- …
- within period $\Delta t_6 = t_7 - t_6$, when the motor rotor turns by angle $\psi_6 = 2\pi$, instantaneous values of currents in phases A, B and C coincide with those of currents at t = 0.

Thus, the variation period of these currents in time is equal to $T_{TIM} = 2\pi$ el. degr., herewith, within this period currents vary not under the harmonic law. Also other modes are possible with similar change of variation in time of currents in stator winding phases. The variation in time of currents i_A, i_B, i_C under arbitrary (not only harmonic) law with period T_{TIM} leads to the fact that the winding MMF also varies in time under arbitrary nonharmonic law with the same period.

This chapter describes a general determination method of stator winding MMF with account of these machine operation modes. It has the non-traditional following peculiarities:

- the method allows us to obtain calculation expressions for MMF of three-phase winding (m_{PH} = 3) with account of time harmonics of order $Q \geq 1$ and spatial harmonics of order $m \geq 1$ without using the method of symmetric components; at $Q > 1$ definition of these components at $m_{PH} = 3$ is caused by certain difficulties;
- it can be applied for the determination of MMF in multiphase machine winding ($m_{PH} > 3$); in similar operation modes for these machines using the method of symmetric components for $Q \geq 1$ meets additional difficulties in comparison with that of MMF harmonics of three-phase winding;
- the method involves construction features of three-phase stator windings of salient-pole and induction machines used in modern practice: stator winding is made six-zone, and for high-power salient-pole machines the winding has usually a fractional number of slots per pole and phase q; herewith, for this q it is often made with phase zones of various width.

Let us turn our attention to these winding construction features. We consider the width of the first of six phase zones (for example, phase A zone) so: b_A; respectively, designations for other zones: $b_{C'}$; b_B; $b_{A'}$; b_C; $b_{B'}$. For such a winding, MMF

(function of stator current) [1–7, 10–12] varies stepwise on the border between two adjacent phase zones. For example, moving along the stator periphery (along coordinate x) from the phase zone of width b_A (with current i_A) towards that with width $b_{C'}$ (with current $(-i_C)$) the function of current [1–3] varies on the border between these zones stepwise by a value $(-i_C)$. When tracing in this direction of all six phase zones, we find that the function of current is stepped; its spatial period generally—for windings with fractional number q [1–3]—is equal to $T_{TG} = \pi D$, where D—stator boring diameter.

The width of these six zones of three-phase winding cannot be identical, for example, to reduce the length of jumpers between these phase zones. Let us indicate the angle $\Delta\alpha_A$ (el. degr.) occupied by such a phase zone with width b_A, in the form:

$$\Delta\alpha_A = \frac{2\pi b_A}{T_{TG}}; \tag{21.1}$$

similarly are given expressions for angles $\alpha_{C'}; \alpha_B; \alpha_{A'}; \alpha_C; \alpha_{B'}$ of other phase zones. With account of (21.1), angles occupied by winding phase zones have the following form:

$$\begin{aligned} \Delta\alpha_A &= \frac{\pi}{3} \pm \Delta\beta_A; \quad \Delta\alpha_{C'} = \frac{\pi}{3} \pm \Delta\beta_{C'}; \quad \Delta\alpha_B = \frac{\pi}{3} \pm \Delta\beta_B; \\ \Delta\alpha_{A'} &= \frac{\pi}{3} \pm \Delta\beta_{A'}; \quad \Delta\alpha_C = \frac{\pi}{3} \pm \Delta\beta_C; \quad \Delta\alpha_{B'} = \frac{\pi}{3} \pm \Delta\beta_{B'}; \end{aligned} \tag{21.2}$$

here $\Delta\beta_A; \Delta\beta_{C'}; \ldots \Delta\beta_B$—additional angles expanding (or narrowing) winding phase zones. Signs at them (±) should be selected to meet the condition:

$$\pm\Delta\beta_A \pm \Delta\beta_{C'} \pm \Delta\beta_B \pm \Delta\beta_{A'} \pm \Delta\beta_C \pm \Delta\beta_{B'} = 0. \tag{21.3}$$

The calculation method of stator winding MMF at arbitrary power supply of its phase zones stated below is true at arbitrary values of additional angles $\Delta\beta_A; \Delta\beta_{C'}; \ldots; \Delta\beta_B$; with account of this condition.

We note that usually in stator winding construction practice these additional angles are accepted equal to,

$$\Delta\beta_A = -\Delta\beta_{C'}; \quad \Delta\beta_B = -\Delta\beta_{A'}; \quad \Delta\beta_C = -\Delta\beta_{B'}. \tag{21.4}$$

Let us write down the calculation expressions for positions of borders between phase zones along the stator periphery (counting from phase zone A):

$$\begin{aligned} &\alpha_A = \Delta\alpha_A; \quad \alpha_{C'} = \Delta\alpha_A + \Delta\alpha_{C'}; \quad \alpha_B = \Delta\alpha_A + \Delta\alpha_{C'} + \Delta\alpha_B; \\ &\alpha_{A'} = \Delta\alpha_A + \Delta\alpha_{C'} + \Delta\alpha_B + \Delta\alpha_{A'}; \quad \alpha_C = \Delta\alpha_A + \Delta\alpha_{C'} + \Delta\alpha_B + \Delta\alpha_{A'} + \Delta\alpha_C; \\ &\alpha_{B'} = \Delta\alpha_A + \alpha_{C'} + \Delta\alpha_B + \Delta\alpha_{A'} + \Delta\alpha_C + \Delta\alpha_{B'} \end{aligned} \tag{21.5}$$

Thus, the stator three-phase winding field and its MMF vary along the stator boring in the form of a step function of current with period T_{TG}, and in time—under arbitrary (not only harmonic) law with period T_{TIM}.

Let us note that the determination of armature reaction MMF of induction and synchronous machines in their operation from industrial network if their width of winding phase zones is identical [1–3], is only a special problem of defining the stator winding MMF of these machines.

Some ways are available for its solution with account of specified peculiarities of machine construction and operation modes.

As previously, we note that for frequency—controlled motors used in an industry, the relation of air gap δ to period T_{TG} is usually $\frac{\delta}{T_{TG}} < 0.0125$; at such values $\frac{\delta}{T_{TG}}$ the attenuation factor [6, 7] of the field in gap $k_{ATT} \approx 1$ for spatial harmonics of order $m < 11$, so this field has practically only radial component.

21.2 Illustration of a Method of Solution for a Particular Case

Method of this problem solution for a special case: motor operation mode—asymmetrical, currents in phases vary under periodic law (with period T_{TIM}), but widths of stator winding phase zones are identical.

Let us estimate this solution in a traditional way, using the method of symmetric components [1–5] not only for the first time harmonic of stator three-phase current, but also for higher ($Q > 1$). Let us note that at $Q > 1$, the argument in both expressions for statement $a = e^{j\frac{2\pi Q}{3}}$ or $a = e^{j\frac{4\pi Q}{3}}$ depends on the number of this harmonic; investigation of this dependence, when expanding into components asymmetrical currents of multiphase stator winding (with number of phases m_{PH} more than three, for example, five, six or nine) meets additional difficulties.

21.2.1 Initial Data

The initial data are,

(a) Currents in phases i_A, i_B, i_C:

$$i_A = \varphi_A(t); i_B = \varphi_B(t); i_C = \varphi_C(t); \tag{21.6}$$

here t—current value of time.

(b) Stator three-phase six-zone winding with phase zones equal in width

$$\begin{aligned}&\alpha_A = \alpha_{C'} = \alpha_B = \alpha_{A'} = \alpha_C = \alpha_{B'} = \frac{\pi}{3}\\&(\text{at } \Delta\beta_A = \Delta\beta_{C'} = \Delta\beta_B = \Delta\beta_{A'} = \Delta\beta_C = \Delta\beta_{B'} = 0).\end{aligned} \tag{21.7}$$

It is found that the method can also be realized for the analysis of motor asymmetrical operation modes with stator winding width of phase zones not identical as per (21.2) and (21.3); its realization for such a winding construction when using traditional methods causes usually additional difficulties.

21.2.2 Solution Stages

The method includes the following stages:

- representation of current in each phase in the form of harmonic series of order Q;
- reduction of each harmonic of order Q of asymmetrical phase currents i_A, i_B, i_C to three systems of symmetrical components of the same order;
- determination of MMF harmonics of time orders $Q \geq 1$ and spatial harmonics of order $m \geq 1$ for each system of currents).

21.2.2.1 Current Time Harmonics

Let us present the phase current $i_A = i_A(t)$ varying in time with period T_{TIM} in the form of time harmonics series [4, 5] of Q order:

$$i_A(t) = \sum I_{A,Q} \sin\left(\frac{2\pi tQ}{T_{TIM}} + \varphi_{A,Q}\right). \tag{21.8}$$

Here, summation is made over the parameter Q; $I_{A,Q}$—harmonic amplitude of order Q; φ_A—phase angle. Also currents $i_B(t)$, $i_C(t)$ can be represented similarly. Generally, harmonics of these currents of the same order Q can be different in amplitude $I_{A,Q} \neq I_{B,Q} \neq I_{C,Q}$; difference of phase angles for currents of these harmonics can also differ: $|\varphi_{A,Q} - \varphi_{B,Q}| \neq |\varphi_{B,Q} - \varphi_{C,Q}|$.

21.2.2.2 Symmetrical Current Components

It is expedient to present a system of phase currents as per (21.8) with amplitudes $I_{A,Q}$, $I_{B,Q}$, $I_{C,Q}$ and with their phase angles $\varphi_{A,Q}$, $\varphi_{B,Q}$, $\varphi_{C,Q}$ to determine the MMF,

generally, in the form of three systems of symmetrical [1–5] components with current amplitudes of direct sequence $\left(I_{A,Q}^{DIR}, I_{B,Q}^{DIR}, I_{C,Q}^{DIR}\right)$, negative sequence $\left(I_{A,Q}^{NEG}, I_{B,Q}^{NEG}, I_{C,Q}^{NEG}\right)$ and currents of zero sequence $(I_{A,Q}^{ZER}, I_{B,Q}^{ZER}, I_{C,Q}^{ZER})$. Let us designate phase angles for currents of each sequence respectively as $\left(\varphi_{A,Q}^{DIR}, \varphi_{B,Q}^{DIR}, \varphi_{C,Q}^{DIR}\right)$; $\left(\varphi_{A,Q}^{NEG}, \varphi_{B,Q}^{NEG}, \varphi_{C,Q}^{NEG}\right)$; $\left(\varphi_{A,Q}^{ZER}, \varphi_{B,Q}^{ZER}, \varphi_{C,Q}^{ZER}\right)$. These current amplitudes and their phase angles are calculated for each sequence from real phase currents determined in (21.6) based on known ratios [4, 5]. For winding construction with isolated neutral, zero sequence currents are usually absent; they arise only in the presence of zero wire or in case of triangle connection of phase windings.

21.2.2.3 Result: Stator Winding MMF Harmonics for Each System of Harmonics Currents at Q ≥ 1 and m ≥ 1 with Account of (21.7). Mutual Induction Fields

Expressions for MMF harmonic of order Q at $\Delta\beta_A = \Delta\beta_{C'} = \Delta\beta_B = \Delta\beta_{A'} = \Delta\beta_C = \Delta\beta_{B'} = 0$ are known [1–3, 7]. For example, for a system of direct sequence currents with amplitudes $I_{A,Q}^{DIR} = I_{B,Q}^{DIR} = I_{C,Q}^{DIR} = I_Q^{DIR}$ it has the form: $F_Q^{DIR} = \frac{3}{\pi} I_Q^{DIR} W_{PH} \frac{K_{W,m}}{pm}$, where W_{PH}—number of turns in winding phase; $K_{W,m}$—winding factor for spatial harmonic of order m; p—number of pole pairs. Similarly, the expression for a system of currents of negative sequence is obtained.

Direct and negative current systems in stator induce currents in rotor loops. Fields generated by stator currents of direct sequence and these currents in rotor loops create torque coinciding with the rotor rotation direction, and the field of negative sequence currents—braking torques.

Thus, this problem solution expects double transformation of currents (expanding phase currents to harmonic series and using the method of symmetrical components for each time harmonic) even for a special case: at $\Delta\beta_A = \Delta\beta_{C'} = \Delta\beta_B = \Delta\beta_{A'} = \Delta\beta_C = \Delta\beta_{B'} = 0$.

21.3 Solution of General Problem

We proceed to the solution of general problem: motor operation mode—asymmetrical, phase currents vary not under periodic harmonic law with period T_{TIM}, and stator winding phase zones differ in width.

As a solution we will not use the method of symmetrical components for the first (Q = 1) and higher (Q > 1) time harmonics of three-phase stator current. Thereby, it is possible to avoid difficulties arising when determining argument of the statement, when using the method of symmetrical components [1–5] of multiphase

currents system, and also summing up MMFs of separate phases for determination of direct and negative sequence MMFs.

The method of this problem solution excludes double transformation of currents as it is made in Sect. 21.2 and in addition it enables us to consider peculiarities of winding construction with various width of phase zones as per (21.2) and (21.3); it is reduced only to the determination MMF by representation of current function [4, 5, 10–12] in winding phases in the form of harmonic series with two variables [8, 9]: by harmonics of orders Q and m. The method includes the following stages [12]:

- determination of analytical expressions for a series of MMF spatial harmonics of order m with period T_{TG} determined by instantaneous values of currents in phases $i_A(t)$, $i_B(t)$, $i_C(t)$ for time intervals $\Delta t_1, \ldots, \Delta t_S, \ldots, \Delta t_V$. For this purpose, MMF step function of winding regardless its phase zone width is represented in the form of a series of spatial harmonics of order m for instantaneous values of currents $i_A(t)$, $i_B(t)$, $i_C(t)$; such a step function can be constructed for any values of these currents in winding phases, that is regardless their variation law within period T_{TIM}. MMF for each spatial harmonic is determined for several time intervals $\Delta t_1, \ldots, \Delta t_S, \ldots, \Delta t_V$ and $\Delta t_S \ll T_{TIM}$. It is supposed that during each of these time intervals Δt_S, current values in phases $i_A(t)$, $i_B(t)$, $i_C(t)$ remain invariable. The number of these time intervals V is determined by the calculation accuracy ε_{CAL} set previously (see Sect. 21.3.4);
- approximation of MMF harmonic values of each order m (their number is equal to V) by means of a series of time harmonics of order Q with period T_{TIM}. Values of these MMF harmonics of order m are considered by the number V as nodes of MMF spatial function.
- Let us consider stages of this method realization in more detail.

Let us note as previously that the spatial harmonic of order m = p for selected period T_{TG} according to Sect. 2.1.1 is the main, of order m < p—the lower, and of order m > p—the higher.

21.3.1 Initial Data

Set in the solution of this problem are:

a) Currents in phases $(i_A, i_B, i_{C\Delta t})$ for a series of time intervals $\Delta t_1, \ldots, \Delta t_S, \ldots, \Delta t_V$. Within each of such intervals they are set constant and equal to,

$$i_A = \varphi_A(t); i_B = \varphi_B(t); i_C = \varphi_C(t), \tag{21.9}$$

b) Three-phase six-zone stator winding with phase zones $\Delta\alpha_A$; $\Delta\alpha_{C'}$; $\Delta\alpha_B$; $\Delta\alpha_{A'}$; $\Delta\alpha_C$; $\Delta\alpha_{B'}$ as per (21.2); position of borders α_A; $\alpha_{C'}$; α_B; $\alpha_{A'}$; α_C; $\alpha_{B''}$ between phase zones along the stator periphery is determined according to (21.5).

c) Stator winding—single-layer with q = 1 slot per pole and phase and pitch shortening $\beta = 1$. We will accept to certainty: p = 1.

However, the generality of solution method stated in Sects. 21.3 and 21.4 is also true for two-layer windings $(S_N = 2)$ at q > 1 and β < 1. At q > 1 the number of current function steps [1–7] respectively increases; correspondingly, amplitudes of spatial harmonics of order m > 1 decrease that is taken into account by the winding distribution factor [1–3, 7]. At β < 1 it is easy to represent the two-layer winding in the form of two single-layer, shifted relative to each other by chording factor [1–3, 7] for the corresponding harmonic of order m.

The solution of the problem is the calculation expression for a series of stator winding MMF spatial and time harmonics F(α,m,t,Q) where $\alpha = \frac{2\pi X}{T_{TG}}$.

21.3.2 *Step Functions of Stator Current: Representation of Each of Them in the Form of Harmonic Series ΣF (α, m, Δt$_S$ = idem)*

One finds the MMF step function $F(\alpha, \Delta t_1)$ [1–5, 10–12] for phase currents $(i_A, i_B, i_C)_{\Delta t_1}$, corresponding to the time interval Δt_1; it can be expanded into harmonic series with period T_{TG}: $F(\alpha, \Delta t_1) = \sum F(\alpha, m, \Delta t_1)$; here summation is performed over the number of harmonics m. Similarly, for time intervals $\Delta t_2, \Delta t_3, \ldots, \Delta t_S, \ldots \Delta t_V$ let us calculate the MMF step functions by number V–1; this function corresponds to the sum of harmonic series terms $\sum F(\alpha, m, \Delta t_S = \text{idem})$. We note that within each of these time intervals V, the currents are constant in amplitude and phase as per (21.9).

21.3.3 *Determination of Amplitude and Phase of Stator Current Step Function in the Form of Series ΣF(α, m, Δt$_S$ = idem) of Spatial Harmonics of Order m*

For a spatial harmonic of order m, the calculation expression for MMF has the form [8, 9]:

$$F(\alpha, m, \Delta t_S = \text{idem}) = |F(\alpha, m, \Delta t_S = \text{idem})| \sin\left(\alpha m + \gamma_{m,S}\right). \tag{21.10}$$

MMF amplitude and its phase angle in space are calculated from the ratios:

$$|F(\alpha, m, \Delta t_S = \text{idem})| = \sqrt{a_{m,S}^2 + b_{m,S}^2}, \quad \gamma_{m,S} = \text{arctg}\frac{a_{m,S}}{b_{m,S}}. \tag{21.11}$$

Indices at coefficients $a_{m,S}$, $b_{m,S}$ and angle $\gamma_{m,S}$ mean: m—order of spatial harmonic, S—time interval Δt_S, determining the value of currents in phases $(i_A, i_B, i_C)_{\Delta tS}$;

$$a_{m,S} = \frac{1}{\pi}\{i_A \sin m\alpha_A + (i_A - i_C)[\sin m(\alpha_A + \alpha_{C'}) - \sin m\alpha_A] + (i_A - i_C + i_B)[\sin m(\alpha_A + \alpha_{C'} + \alpha_B) - \sin m(\alpha_A + \alpha_{C\prime})] + (i_A - i_C + i_B - i_A)[\sin m(\alpha_A + \alpha_{C'} + \alpha_B + \alpha_{A'}) - \sin m(\alpha_A + \alpha_{C\prime} + \alpha_B)] + (i_A - i_C + i_B + i_C)[\sin m(\alpha_A + \alpha_{C'} + \alpha_B + \alpha_{A'} + \alpha_C) - \sin m(\alpha_A + \alpha_{C\prime} + \alpha_B + \alpha_{A'})] + (i_A - i_C + i_B - i_A + i_C - i_B)\cdot [\sin 2\pi m - \sin m(\alpha_A + \alpha_{C'} + \alpha_B + \alpha_{A'} + \alpha_C)]\}, \quad (21.12)$$

$$b_{m,S} = \frac{-1}{\pi}\{[i_A[\cos(m\alpha_A) - 1] + (i_A - i_{C'})][\cos m(\alpha_A + \alpha_C) - \cos m\alpha_A] + (i_A - i_C + i_B)[\cos m(\alpha_A + \alpha_{C'} + \alpha_B) - \cos m(\alpha_A + \alpha_{C\prime})] + (i_A - i_C + i_B - i_A)\cdot [\cos m(\alpha_A + \alpha_{C'} + \alpha_B + \alpha_{A'}) - \cos m(\alpha_A + \alpha_{C\prime} + \alpha_B)] + (i_A - i_C + i_B - i_A + i_C)\cdot [\cos m(\alpha_A + \alpha_{C'} + \alpha_B + \alpha_{A'} + \alpha_C) - \cos m(\alpha_A + \alpha_{C\prime} + \alpha_B + \alpha_{A'})] + (i_A - i_C + i_B - i_A + i_C - i_B)[\cos 2\pi m - \cos m(\alpha_A + \alpha_{C'} + \alpha_B + \alpha_{A'} + \alpha_C)]\}. \quad (21.13)$$

Let us note that the number of calculation expressions like (21.11) is equal to that of time intervals Δt_S into which the time period T_{TIM} is subdivided; this number equal to V.

In Eqs. (21.12) and (21.13) for $a_{m,S}$, $b_{m,S}$ the sum of several currents in brackets is equal to zero; for example, in the last but one summand in brackets is concluded as (i_A–i_C + i_B − i_A + i_C). In it the current sums i_A and (–i_A), i_C and (–i_C) in pairs are equal to zero. All these currents are given in (21.12) and (21.13) only to specify compliance between them and angles occupied by phase zones, for example, between angle $\alpha_{C'}$ and current (–i_C), angle α_B and current (i_B), etc.

This compliance is an additional check of coefficients $a_{m,S}$, $b_{m,S}$.

Equations (21.11)–(21.13) are true for each time interval Δt_S = idem according to condition (21.9).

21.3.3.1 Peculiarity of Calculation Expression for MMF

We, for example, calculate for MMF amplitude $|F(\alpha,m,\Delta t_S = \text{idem})|$ for a series of three consecutive time intervals: $\Delta t_1; \Delta t_2; \Delta t_3$. For time point t = t_0 = 0 we have $t_1 = \Delta t_1$; respectively, the time point $t_2 = \Delta t_1 + \Delta t_2 = t_1 + \Delta t_2$, and time point $t_3 = \Delta t_1 + \Delta t_2 + \Delta t_3 = t_2 + \Delta t_3$. In practical calculations of winding MMF, currents $(i_A, i_B, i_C)_{\Delta tS}$ at time points t_1 and t_2 can remain invariable, and at time point t_3—according to machine operation mode, their value changes; for example, at time points t_1 and t_2 the currents are invariable and equal to i_A = 100 %, i_B = 100 %, i_C = 0; at time point t_3 they vary and are equal to i_A = 0, i_B = 100 %, i_C = 100 %.

Therefore, for this example the following ratios between amplitudes and their phase angles are true:

$$|F(\alpha, m, \Delta t_1)| = |F(\alpha, m, \Delta t_2)| \neq |F(\alpha, m, \Delta t_3)|,\ \gamma_{m,1}(\text{at}\,\Delta t_1) = \gamma_{m,2}(\text{at}\,\Delta t_2) \neq \gamma_{m,3}(\text{at}\,\Delta t_3).$$

Thus, the relations between MMF amplitudes as well as between their phase angles depend on the following:

- machine operation mode (on diagram of relation of phase currents in time),
- value of time intervals Δt_S (sampling increment of variation process in time of phase currents). In more detail the problem on selecting this sampling increment Δt_S is considered in the following para.

21.3.4 Approximation of Stator Current Step Function Harmonics ΣF(α, m, Δt_S = idem) by Means of Time Harmonious Series; Time Harmonics of Order Q ≥ 1

Equations (21.10–21.13) represent calculation expressions for MMF spatial harmonic $F(\alpha, m, \Delta t_S = \text{idem})$ of order m with account of arbitrary variation in time of phase currents $(i_A, i_B, i_C)_{\Delta t}$ provided that within time interval Δt_1 they remain invariable; the same refers to other time intervals $\Delta t_2, \ldots, \Delta t_S, \ldots, \Delta t_V$, and these time intervals satisfy the ratio:

$$\Delta t_1 + \Delta t_3 + \cdots + \Delta t_S + \cdots + \Delta t_V = T_{TIM}. \tag{21.14}$$

It is convenient to consider values of MMF harmonic $F(\alpha, m, \Delta t_S = \text{idem})$ of order m for a sequence of intervals Δt_S as interpolation singular points nodes and to approximate this sequence by means of harmonic series containing harmonics of time order Q [8, 9].

To write down expressions for terms of this harmonic series, let us generalize calculation ratios for time points $t_S(\text{at}\ t_0 = 0)$:

$$\begin{aligned}
t_1 &= \Delta t_1, \\
t_1 &= \Delta t_1 + \Delta t_2 = t_1 + \Delta t_2, \\
&\vdots \\
t_S &= \Delta t_1 + \Delta t_2 + \Delta t_3 + \cdots + \Delta t_S = t_{S-1} + \Delta t_S \\
&\vdots \\
t_V &= \Delta t_1 + \Delta t_2 + \Delta t_3 + \cdots + \Delta t_V = t_{V-1} + \Delta t_V = T_{TIM}.
\end{aligned} \tag{21.15}$$

We calculate the term of harmonic series for time harmonic of order Q at first for the time interval $\Delta t_S = \Delta t_1 = t_1$. The calculation expression has the following form [8, 9]:

$$F(\alpha, m, \Delta t_S = \Delta t_1, Q) = |F(\alpha, m, \Delta t_S = \Delta t_1, Q)| \sin\left(\frac{2\pi t_1 Q}{T_{TIM}} + \gamma_{Q,S}\right). \quad (21.16)$$

here $|F(\alpha, m, \Delta t_S = \Delta t_1, Q)| = \sqrt{\left(a_{Q,S}^2 + b_{Q,S}^2\right)}$—MMF amplitude, $\gamma_{Q,S} = \text{arctg}\frac{a_{Q,S}}{b_{Q,S}}$—its phase angle in time; timepoint t corresponds to the interval $\Delta t_S = \Delta t_1$; $a_{Q,S}$, $b_{Q,S}$—expansion coefficients of harmonic series containing harmonics of time order Q.

Taking account of (21.15), the expressions for coefficients a_Q, b_Q in (21.16) for the time interval $\Delta t_S = \Delta t_1 = t_1$ take the form:

$$\begin{aligned} a_{Q,S} &= \frac{F(\alpha, m, \Delta t_S = \Delta t_1)}{\pi} \int_0^{t_1} \cos\frac{2\pi Q t}{T_{TIM}} dt; \\ b_{Q,S} &= \frac{F(\alpha, m, \Delta t_S = \Delta t_1)}{\pi} \int_0^{t_1} \sin\frac{2\pi Q t}{T_{TIM}} dt. \end{aligned} \quad (21.17)$$

It should be noted that in Eq. (21.17) the time interval $\Delta t_S = \Delta t_1$ for MMF $F(\alpha, m, \Delta t_S = \Delta t_1)$ corresponds to integration limits (0; t_1) as per (21.15); the same is also true for MMF corresponding to other time intervals as per (21.15) for example, for MMF $F(\alpha, m, \Delta t_S = \Delta t_2)$ and integration limits (t_1; t_2), for MMF $F(\alpha, m, \Delta t_S)$ and integration limits (t_{S-1}; t_S).

Let us note also that the number summands in expressions like (21.16) is determined by the number of selected time intervals $\Delta t_1, \Delta t_2, \ldots, \Delta t_S, \ldots, \Delta t_V$.

For practical realization of estimation method to calculate the ratios of MMF time harmonics of order Q of this series, let us, as previously, make some transformations.

With account of (21.14), we have:

$$\frac{2\pi\Delta t_1}{T_{TIM}} + \frac{2\pi\Delta t_2}{T_{TIM}} + \frac{2\pi\Delta t_3}{T_{TIM}} + \cdots + \frac{2\pi\Delta t_S}{T_{TIM}} + \cdots + \frac{2\pi\Delta t_V}{T_{TIM}} = 2\pi.$$

Let us designate separate summands in this expression as:

$$\begin{aligned} &\Delta\psi_1 = \frac{2\pi\Delta t_1}{T_{TIM}}; \quad \Delta\psi_2 = \frac{2\pi\Delta t_2}{T_{TIM}}; \quad \Delta\psi_3 = \frac{2\pi\Delta t_3}{T_{TIM}}; \ldots; \\ &\Delta\psi_S = \frac{2\pi\Delta t_S}{T_{TIM}}; \quad \ldots\Delta\psi_V = \frac{2\pi\Delta t_V}{T_{TIM}}. \end{aligned} \quad (21.18)$$

As a result, we obtain:

$$\Psi_1 = \Delta\Psi_1; \Psi_2 = \Delta\Psi_1 + \Delta\Psi_2 = \Psi_1 + \Delta\Psi_2; \Psi_3 = \Delta\Psi_1 + \Delta\Psi_2 + \Delta\Psi_3 = \Psi_2 + \Delta\Psi_3; \ldots \Psi_S = \Delta\Psi_1 + \Delta\Psi_2 + \Delta\Psi_3 + \cdots + \Delta\Psi_S = \Psi_{S-1} + \Delta\Psi_S;$$
$$\Psi_V = \Delta\Psi_1 + \Delta\Psi_2 + \Delta\Psi_3 + \cdots + \Delta\Psi_V = \Psi_{V-1} + \Delta\Psi_V = 2\pi. \quad (21.18')$$

21.3.4.1 Conditions for Minimum Approximation Error; Expressions for Calculation of Coefficients a_Q, b_Q of Harmonic Series

Let us formulate the conditions necessary to provide the minimum approximation error ε_{CAL} of MMF by means of harmonic series as per (21.17) containing harmonics of time order Q [8, 9].

The first condition determines the relation between time intervals $\Delta t_1, \Delta t_2, \ldots, \Delta t_S, \ldots, \Delta t_V$ as per [8, 9].

The error value ε_{CAL} in MMF calculation is at minimum, if identical time intervals are used for its interpolation:

$$\Delta t_1 = \Delta t_2 = \Delta t_3 = \ldots \Delta t_S \ldots = \Delta t_V = \frac{T_{TIM}}{V}. \quad (21.19)$$

Then, taking into account Eqs. (21.18), (21.18′) and (21.19) we obtain:

$$\Delta\Psi_1 = \Delta\Psi_2 = \Delta\Psi_3 = \ldots = \Delta\Psi_S = \ldots = \Delta\Psi_V = \Delta\Psi = \frac{2\pi}{V}$$

$$\Psi_1 = \Delta\Psi_1 = \frac{2\pi}{V}; \Psi_2 = \frac{2\pi}{V}2; \Psi_3 = \frac{2\pi}{V}3; \ldots; \Psi_S = \frac{2\pi}{V}S; \ldots; \Psi_V = 2\pi. \quad (21.20)$$

Expressions like (21.17) for harmonic series summands and the coefficients a_Q, b_Q with account of (21.20) take the form:

for time interval $\Delta t = t_1 - 0$.

$$a_{Q,S} = \frac{F(\alpha, m, \Delta t_1)}{\pi} \sin Q\Psi_1; \quad b_{Q,S} = \frac{F(\alpha, m, \Delta t_1)}{\pi} \cos(Q\Psi_1 - 1)$$

for time interval $\Delta t = t_2 - t_1$.

$$a_{Q,S} = \frac{F(\alpha, m, \Delta t_2)}{\pi} [\sin(Q2\Psi_1) - \sin(Q\Psi_1)];$$
$$b_{Q,S} = -\frac{F(\alpha, m, \Delta t_2)}{\pi} [\cos(Q2\Psi_1) - \cos(Q\Psi_1)]$$
$$\ldots$$

for time interval $\Delta t = t_S - t_{S-1}$

$$\begin{aligned} a_{Q,S} &= \frac{F(\alpha, m, \Delta t_S)}{\pi}[\sin(QS\Psi_1) - \sin Q(S-1)\Psi_1]; \\ b_{Q,S} &= -\frac{F(\alpha, m, \Delta t_S)}{\pi}[\cos(QS\Psi_1) - \cos Q(S-1)\Psi_1]. \\ &\ldots \end{aligned} \tag{21.21}$$

Let us notice that expressions for harmonics of spatial MMFs $F(\alpha, m, \Delta t_1)$, $F(\alpha, m, \Delta t_2), \ldots, F(\alpha, m, \Delta t_S), \ldots, F(\alpha, m, \Delta t_V)$ of order m in Eqs. (21.17) are as per (21.10) harmonic functions with spatial period T_{TG}.

The second condition determines the number of time intervals $\Delta t_1, \Delta t_2, \ldots, \Delta t_S, \ldots, \Delta t_V$ (number V), by which the time period T_{TIM} is subdivided.

The number of time intervals V should satisfy the following ratio:

$$\left|1 - \frac{|F(\alpha, m, t, Q)|_W}{|F(\alpha, m, t, Q)|_R}\right| < \varepsilon_{CAL}; \tag{21.22}$$

here, MMF amplitude $|F(\alpha, m, t, Q)|_W$ is calculated for the number of time intervals V = W, and MMF $|F(\alpha, m, t, Q)|_R$—for the number of time intervals V = R, herewith, W > R; Let us note that with growth of spatial harmonic order m and time harmonic Q, the number V of time intervals Δt_S increases.

21.3.5 Result: MMF Harmonics of Stator Winding

Equations (21.10)–(21.13) describe amplitudes of MMF spatial harmonics of order m for a number of time interval $\Delta t_1, \Delta t_2, \ldots, \Delta t_S, \ldots, \Delta t_V$, and Eqs. (21.16)–(21.21)—variation of these amplitudes in time in the form of harmonics of order Q for the same values $\Delta t_1, \Delta t_2, \ldots, \Delta t_S, \ldots, \Delta t_V$. It follows from these equations that the winding MMF within period T_{TIM} is determined in the form of a series of summands (number V), each containing the product like $\Delta F_{m,Q,S} \sim \sin(\alpha m + \gamma_{m,S}) \sin\left(\frac{2\pi t_1 Q}{T_{TIM}} + \gamma_{Q,S}\right)$. It can be represented in the form:

$$\Delta F_{m,Q,S} \sim \frac{\cos\left(\frac{2\pi t_1 Q}{T_{TIM}} - \alpha m + \gamma_{Q,S} - \gamma_{m,S}\right) - \cos\left(\frac{2\pi t_1 Q}{T_{TIM}} + \alpha m + \gamma_{Q,S} + \gamma_{m,S}\right)}{2}. \tag{21.23}$$

The first factor in brackets in (21.23) indicates the stator winding field which within time interval Δt_S rotates in the direction of rotor rotation, and the second—in opposite direction. Summing up these numbers we obtain winding MMF in the form:

$$F_{m,Q} = \Delta F_{m,Q,S=1} + \Delta F_{m,Q,S=2} + \cdots + \Delta F_{m,Q,S} + \cdots + \Delta F_{m,Q,V}$$

MMF $F_{m,Q}$ determines both fields of time order $Q \geq 1$ and spatial $m \geq 1$ created by currents in stator winding; when interacting with currents in rotor loops the first creates rotating torque, and the second—braking torque.

21.4 Checking Results: Calculation Example

Let us consider realization peculiarities of stator three-phase winding MMF determination method stated for a specific case:

- currents in three phases vary under harmonic (but not under arbitrary) law with time shift by an angle $\Delta\Psi = \frac{2\pi}{3}$ (el. degr.);
- current amplitudes I_{AMP} in these phases are identical (symmetrical mode);
- width of winding six phase zones is identical; additional angles specified in (21.2–21.4), in the considered special case are equal to zero: $\Delta\beta_A = \Delta\beta_{C'} = \Delta\beta_B = \Delta\beta_{A'} = \Delta\beta_C = \Delta\beta_{B'} = 0$.

Initials for calculation are assumed.

21.4.1 Phase Currents in Stator Winding

$$i_A = I_{AMP}\cos\frac{2\pi t}{T_{TIM}}; i_B = I_{AMP}\cos\left(\frac{2\pi t}{T_{TIM}} - \frac{2\pi}{3}\right); i_C = I_{AMP}\cos\left(\frac{2\pi t}{T_{TIM}} - \frac{4\pi}{3}\right), \tag{21.24}$$

where I_{AMP}—current amplitude; initial phase angles of currents are accepted equal to zero ($\varphi_A = \varphi_B = \varphi_C = 0$).

21.4.2 *Three-Phase Six-Zone Single-Layer Stator Winding with Diametral Pitch and Phase Zones of Equal Width $\alpha_A = \alpha_{C'} = \alpha_B = \alpha_{A'} = \alpha_C = \alpha_{B'} = = \pi/3$; Number q = 1. Position of Borders Between Phase Zones Along the Stator Periphery as Per (21.5): $\alpha_A = \pi/3$; $\alpha_{C'} = 2\pi/3$; $\alpha_B = \pi$; $\alpha_{A'} = 4\pi/3$; $\alpha_C = 5\pi/3$; $\alpha_{B'} = 2\pi$*

Using the method stated, it is necessary to obtain the calculation expression for MMF known [1–3, 7] for this special case of the winding harmonics of order m = 1, Q = 1 like:

$$F = \frac{3}{\pi} I_{AMP} \frac{W_{PH} K_w}{p}. \tag{21.25}$$

Here K_W—winding factor for m = 1.

An example: $W_{PH} = 1$; $K_W = 1$; p = 1.

Let us illustrate peculiarities of the stated determination method for MMF in this example. Primarily, let us assume for simplicity only three time intervals Δt_S (at S = 1; 2; 3): $\Delta t_1 = \Delta t_2 = \Delta t_3 = \frac{T_{TIM}}{3}$; respectively, V = 3.

Solution

Let us determine at first the spatial distribution of MMF for these three time intervals.

For the time point $t = t_0 = 0$ currents in phase zones as per (21.24) are equal to:

$$i_A = I_{AMP}; i_B = -\frac{I_{AMP}}{2}; i_C = -\frac{I_{AMP}}{2}.$$

Let us find the amplitude and phase of spatial harmonic m = 1 for the first time interval $\Delta t_S = \Delta t_1 = t_1$ (at S = 1):

$$F(\alpha, m = 1, \Delta t_1 = \text{idem}) = |F(\alpha, m = 1, \Delta t_1 = \text{idem})| \sin\left(\alpha + \gamma_{m=1,S=1}\right).$$

We calculate for this purpose as per (21.12) and (21.13) coefficients $a_{m=1,\ s=1}$, $b_{m=1,\ s=1}$ and angle $\gamma_{m=1,S=1}$.

$$
\begin{aligned}
a_{m=1,S=1} &= \frac{1}{\pi}\left[I_{AMP}\sin\frac{\pi}{3} + 1.5I_{AMP}\left(\sin\frac{2\pi}{3} - \sin\frac{\pi}{3}\right)\right] \\
&\quad + 1\,I_{AMP}\left(\sin\pi - \sin\frac{2\pi}{3}\right) + (-0\,I_{AMP})\left(\sin\frac{4\pi}{3} - \sin\pi\right) \\
&\quad + (-0.5I_{Amp})\left(\sin\frac{5\pi}{3} - \sin\frac{4\pi}{3}\right) + (0\,I_{AMP})\left(\sin 2\pi - \sin\frac{5\pi}{3}\right)\Bigg] = 0. \\
b_{m=1,S=1} &= \frac{-1}{\pi}\left[I_{AMP}\left(\cos\frac{\pi}{3} - 1\right) + 1.5I_{AMP}\left(\cos\frac{2\pi}{3} - \cos\frac{\pi}{3}\right)\right] \\
&\quad + 1\,I_{AMP}\left(\cos\pi - \cos\frac{2\pi}{3}\right) + (-0\,I_{AMP})\left(\cos\frac{4\pi}{3} - \cos\pi\right) \\
&\quad + (-0.5I_{Amp})\left(\cos\frac{5\pi}{3} - \cos\frac{4\pi}{3}\right) + 0\,I_{AMP}\left(\cos 2\pi - \cos\frac{5\pi}{3}\right)\Bigg] = \frac{-3}{\pi}I_{AMP}. \\
\gamma_{m=1,S=1} &= \operatorname{arctg}\frac{a_{m=1,S=1}}{b_{m=1,S=1}} = 0.
\end{aligned}
$$

Result:

$$
\begin{aligned}
&F(\alpha, m = 1, \Delta t_1 = \text{idem}) \\
&\quad = |F(\alpha, m = 1, \Delta t_1 = \text{idem})|\sin\left(\alpha + \gamma_{m=1,S=1}\right) = \frac{3}{\pi}I_{AMP}\sin(\alpha + 0).
\end{aligned}
$$

Let us find the amplitude and phase of spatial harmonic for the second time interval $\Delta t_S = \Delta t_2 = t_2 - t_1$ (at S = 2).

$$
F(\alpha, m = 1, \Delta t_2 = \text{idem}) = |F(\alpha, m = 1, \Delta t_2 = \text{idem})|\sin\left(\alpha + \gamma_{m=1,S=2}\right)
$$

Currents in phase zones are equal to, $i_A = -0.5\ I_{AMP}$; $i_B = -0.5\ I_{AMP}$; $i_C = I_{AMP}$.

Similarly to the first time interval calculation $\Delta t_S = \Delta t_1 = t_1$ we obtain:

$$
\begin{aligned}
a_{m=1,S=2} &= \frac{1}{\pi}(3 \cdot 0.867)I_{AMP};\ b_{m=1,S=2} = \frac{-1}{\pi}1.5I_{AMP};\ \gamma_{m=1,S=1} = \operatorname{arctg}\frac{a_{m=1,S=2}}{b_{m=1,S=2}} \\
&= \frac{2\pi}{3}.
\end{aligned}
$$

Result:

$$
\begin{aligned}
&F(\alpha, m = 1, \Delta t_2 = \text{idem}) \\
&\quad = |F(\alpha, m = 1, \Delta t_2 = \text{idem})|\sin\left(\alpha + \gamma_{m=1,S=2}\right) = \frac{3}{\pi}I_{AMP}\sin\left(\alpha + \frac{2\pi}{3}\right).
\end{aligned}
$$

We find the amplitude and phase of spatial harmonic for the third (last) time interval $\Delta t_S = \Delta t_3 = t_3 - t_2$ (at S = 3).

$$F(\alpha, m = 1, \Delta t_3 = idem) = |F(\alpha, m = 1, \Delta t_3 = idem)| \sin\left(\alpha + \gamma_{m=1,S=3}\right).$$

Currents in phase zones are equal to,

$$i_A = -0.5 I_{AMP}; i_B = -0.5 I_{AMP}; i_C = I_{AMP}.$$

Similarly to the second time interval calculation $\Delta t_S = \Delta t_2 = t_2 - t_1$ (at s = 2) we obtain:

$$a_{m=1,S=2} = -\frac{1}{\pi}(3 \cdot 0.867) I_{AMP}; b_{m=1,S=2} = \frac{-1}{\pi}(1.5) I_{AMP};$$
$$\gamma_{m=1,S=1} = \text{arctg}\frac{a_{m=1,S=3}}{b_{m=1,S=3}} = \frac{4\pi}{3}.$$

Result:

$$F(\alpha, m = 1, \Delta t_3 = idem) = |F(\alpha, m = 1, \Delta t_3 = idem)| \sin\left(\alpha + \gamma_{m=1,S=3}\right) = \frac{3}{\pi} I_{AMP} \sin\left(\alpha + \frac{4\pi}{3}\right).$$

Thus, we obtain values of harmonic (m = 1) of MMF distribution along the stator periphery (in coordinate $\alpha = 2\pi \frac{x}{T_{TG}}$) for three values (V = 3) of phase currents: for time intervals $\Delta t_S = \Delta t_1 = t_1$ (at S = 1); $\Delta t_S = \Delta t_2 = t_2 - t_1$ (at S = 2); $\Delta t_S = \Delta t_3 = t_3 - t_2$ (at S = V = 3). Within each of these time intervals, MMF amplitude and phase angle do not change.

Let us use these three MMF harmonic values $F(\alpha, m, \Delta t_S = idem)$ of order m = 1 as interpolation points (nodes) and approximate sequence of these three values using harmonic series [8, 9] with harmonics of time order Q. The term of this series corresponding to the harmonic Q = 1, includes three summands (V = 3) as per (21.16):

$$F(\alpha, m, \Delta t_S, Q = 1) = |F(\alpha, m, \Delta t_S, Q = 1)| \sin\left(\frac{2\pi t}{T_{TIM}} + \gamma_{Q=1}\right),$$

where it is consecutive $\Delta t_S = \Delta t_1$; $\Delta t_S = \Delta t_2$; $\Delta t_S = t_3$. Coefficients $a_{Q=1}$ and $b_{Q=1}$ for the calculation of MMF amplitude $|F(\alpha, m, \Delta t_S, Q = 1)|$ and phase angle $\gamma_{Q=1}$ as per (21.21) are equal to,

for time interval $\Delta t_1 = t_1 - 0$.

$$a_{Q=1} = \frac{F(\alpha, m = 1, \Delta t_1)}{\pi} \sin \Psi_1 = \frac{1}{\pi}\frac{3}{\pi} \sin\frac{2\pi x}{T_{TG}} 0.867 I_{AMP};$$
$$b_{Q=1} = \frac{F(\alpha, m = 1, \Delta t_1)}{\pi}(\cos \Psi_1 - 1) = \frac{1}{\pi}\frac{3}{\pi} \sin\frac{2\pi x}{T_{TG}} 1.5 I_{AMP}.$$

Phase angle $\gamma_{Q=1} = \text{arctg}\frac{a_{Q=1}}{b_{Q=1}} = \frac{\pi}{6}$.

Result:

$$F(\alpha, m = 1, \Delta t_1, Q = 1) = \frac{1}{\pi}\frac{3}{\pi}\sqrt{3}\sin\frac{2\pi x}{T_{TG}}\sin\left(\frac{2\pi t}{T_{TIM}} + \frac{\pi}{6}\right)I_{AMP};$$

for time interval $\Delta t = t_2 - t_1$

$$a_{Q=1} = \frac{F(\alpha, m = 1, \Delta t_2)}{\pi}[\sin(2\Psi_1) - \sin(\Psi_1)] = \frac{1}{\pi}\frac{3}{\pi}\sin\left(\frac{2\pi x}{T_{TG}} - \frac{2\pi}{3}\right)\left(-\sqrt{3}\right)I_{AMP};$$

$$b_{Q=1} = \frac{F(\alpha, m = 1, \Delta t_2)}{\pi}[(\cos(2\Psi_1) - \cos(Q\Psi_1))] = \frac{1}{\pi}\frac{3}{\pi}\cos\left(\frac{2\pi x}{T_{SP}} + \frac{2\pi}{3}\right)(0)\cdot I_{AMP}.$$

Phase angle $\gamma_{Q=1} = \text{arctg}\frac{a_{Q=1}}{b_{Q=1}} = -\frac{1}{2}\pi$.

Result:

$$F(\alpha, m = 1, \Delta t_2, Q = 1) = \frac{1}{\pi}\frac{3}{\pi}\sqrt{3}\sin\left(\frac{2\pi x}{T_{TG}} + \frac{2\pi}{3}\right)\sin\left(\frac{2\pi t}{T_{TIM}} - \frac{\pi}{2}\right)I_{AMP};$$

for time interval $\Delta t_3 = t_3 - t_2$

$$a_{Q=1} = \frac{F(\alpha, m, \Delta t_3)}{\pi}(\sin 3\Psi_1 - \sin 2\Psi_1) = \frac{1}{\pi}\frac{3}{\pi}\left[\sin\left(\frac{2\pi x}{T_{SP}} + \frac{4\pi}{3}\right)\right]0.867I_{AMP},$$

$$b_{Q=1} = -\frac{F(\alpha, m, \Delta t_3)}{\pi}(\cos\Psi_1 - \cos 2\Psi_1) = \frac{1}{\pi}\frac{3}{\pi}\left[\cos\left(\frac{2\pi x}{T_{TG}} + \frac{4\pi}{3}\right)\right](-1.5)I_{AMP}.$$

Phase angle $\gamma_{Q=1} = \text{arctg}\frac{a_{Q=1}}{b_{Q=1}} = -\frac{7}{6}\pi$

Result:

$$F(\alpha, m = 1, \Delta t_3, Q = 1) = \frac{1}{\pi}\frac{3}{\pi}\sqrt{3}\sin\left(\frac{2\pi x}{T_{TG}} + \frac{2\pi}{3}\right)\sin\left(\frac{2\pi t}{T_{TIM}} - \frac{7\pi}{6}\right)I_{AMP}.$$

The calculation expression for MMF as a result of approximation on three points is composed of three summands:

$$\begin{aligned} F(\alpha, m = 1, t, Q = 1) &= F(\alpha, m = 1, \Delta t_1, Q = 1) + F(\alpha, m = 1, \Delta t_2, Q = 1) \\ &+ F(\alpha, m = 1, \Delta t_3, Q = 1) = \frac{1}{\pi}\frac{3}{\pi}\sqrt{3}I_{AMP}\left[\sin\frac{2\pi x}{T_{TG}}\sin\left(\frac{2\pi t}{T_{TIM}} + \frac{\pi}{6}\right)\right. \\ &+ \left.\sin\left(\frac{2\pi x}{T_{TG}} + \frac{2\pi}{3}\right)\sin\left(\frac{2\pi x}{T_{TIM}} - \frac{\pi}{2}\right) + \sin\left(\frac{2\pi t}{T_{TG}} + \frac{4\pi}{3}\right)\sin\left(\frac{2\pi t}{T_{TIM}} - \frac{7\pi}{6}\right)\right] \\ &= -\frac{3}{\pi}\left(\frac{1}{\pi}\sqrt{3}\frac{3}{2}\right)\left[\cos\left(\frac{2\pi x}{T_{TG}} - \frac{2\pi t}{T_{TIM}} + \frac{\pi}{6}\right)\right]I_{AMP}. \end{aligned} \tag{21.26}$$

Let us estimate the sampling error using calculation results for V = 3; by a comparison of ratios (21.25) and (21.26) we have:

$$\varepsilon_{CAL} = \left| 1 - \frac{3}{\pi} \frac{\frac{1}{\pi}\sqrt{3}\frac{3}{2}}{\frac{3}{\pi}} \right| = 0.173.$$

This assessment indicates that selection of only three interpolation points (V = 3) is insufficient for the approximation; use of sequence of three spatial MMF of the form $F(\alpha, m, \Delta t_S, Q)$ gives a considerable sampling error even for harmonics of order m = 1, Q = 1.

By means of condition (21.22) it is easy to establish that for this problem the number of points V necessary to satisfy the error $\varepsilon_{CAL} < 1\%$ makes V = 15. The calculation expression for MMF as a result of approximation on fifteen points is obtained in the form:

$$F(\alpha, m = 1, t, Q = 1) = \frac{3}{\pi}\left(\frac{1}{\pi} 0.4158 \frac{15}{2}\right) \cos\left(\frac{2\pi x}{T_{TG}} - \frac{2\pi t}{T_{TIM}} - 1.362\pi\right) I_{AMP}. \tag{21.27}$$

Let us estimate the sampling error for V = 15, using the ratios (21.25) and (21.27):

$$\varepsilon_{CAL} = \left| 1 - \frac{3}{\pi}\frac{1}{\pi} 0.4158 \frac{15}{2} \left(\frac{3}{\pi}\right)^{-1} \right| = 0.0074.$$

In Table 21.1 MMF determination errors are compared using this method subdividing the period T_{TIM} by the following number of time intervals: V = 3 and V = 15(m = 1, Q = 1).

For the number of interpolation points equal to V = 15, we obtained Eq. (21.25) with an accuracy considerably exceeding requirements of practice: MMF calculation error—at most 1 %.

Comparing Eqs. (21.25) and (21.27) it follows:

- The expression known for MMF (21.25) obtained for the special problem (it provides variation of phase currents as per (21.24) under harmonic law and equal width of winding phase zones) contains the coefficient for current harmonic amplitude equal to 3/π;
- in the expression for MMF (21.27) obtained by means of the stated method for general problem (it provides variation of phase currents under arbitrary periodic

Table 21.1 Sampling error of period T_{TIM}

V	Ψ_1 as per (21.20), el. degr.	ε_{CAL} as per (21.22)
3	120	0.173
15	24	0.0074

law, including harmonic one, and arbitrary including identical width of winding phase zones, with account of (21.2) and (21.3), this coefficient is obtained at V = 15 equal to $\frac{3}{\pi}0.9926$.

This result confirms validity of the method.

Brief Conclusions

1. Stated here is a general method of stator winding MMF calculation; for frequency—controlled motors it provides a possibility of phase current variation with period T_{TIM} under arbitrary (not only harmonic) law as well as unequal width of phase zones. In its realization there is no need to use a method of symmetrical components for the first and higher time harmonics of current in stator winding phases. The method allows one to determine instantaneous values of motor electromagnetic moment and its pulsations, efficiency with account of the influence of time and spatial harmonics losses.
2. The method is realized in some stages.
   2.1 Period T_{TIM} of current variation in phases i_A, i_B, i_C is subdivided into several time intervals: $\Delta t_1 = \Delta t_2, \ldots, \Delta t_S, \ldots, \Delta t_V$. Within each of the interval it is supposed that the amplitude and phase angle of currents are invariable.
   2.2 Step function of MMF distribution is determined for each time interval Δt_S along the stator boring periphery (with account of values of currents i_A, i_B, i_C for this time interval). This function is represented for each time interval Δt_S in the form of a series of spatial harmonics of order m. The number of such step functions is equal to V.
   These V values of MMF harmonics of spatial order m are used in the form of approximation points (nodes) with a series of time harmonics of order Q [8, 9]. The number of these points is determined by MMF calculation accuracy ε_{CAL} set previously.
3. The calculation expression for winding MMF within period T_{TIM} contains a series of summands (V); each corresponding to two field components of stator winding: one of them within time interval Δt_S rotates in the direction of rotor rotation.
4. The method can be generalized and used to determine the winding MMF in multiphase machines ($m_{PH} > 3$); in similar operation modes of these machines the use of symmetrical components method for the first and higher time harmonics of stator current meets additional difficulties in comparison with MMF determination for three-phase winding.

List of symbols

$a_{Q,S}, b_{Q,S}$	Coefficients for MMF approximation by Fourier series
b_A, $b_{C'}$; b_B, $b_{A'}$;b_C; b_B	Width of stator winding phase zones
D	Stator boring diameter
$F_Q^{DIR}, F_Q^{NEG}, F_Q^{ZER}$	MMF amplitude of order Q of currents for direct, negative and zero sequences
$i_A(t)$, $i_B(t)$, $i_C(t)$	Instantaneous values of currents in phases A, B, C
$I_{A,Q}$, $I_{B,Q}$, $I_{C,Q}$,	Amplitudes of current time harmonic of order Q in phases A, B, C
$I_{A,Q}^{DIR}, I_{B,Q}^{DIR}, I_{C,Q}^{DIR}$	Harmonics of order Q of currents for positive sequence in phases A, B, C
$I_{A,Q}^{NEG}, I_{B,Q}^{NEG}, I_{C,Q}^{NEG}$	The same for currents of negative sequence
$I_{A,Q}^{ZER}, I_{B,Q}^{ZER}, I_{C,Q}^{ZER}$	The same for currents of zero sequence
K_{AT}	Attenuation factor of electromagnetic wave in machine air gap
$K_{W,m}$	Winding factor for spatial harmonic of order m
m	Order of stator MMF spatial harmonic
p	Number of pole pairs
Q	Order of current time harmonic
q	Number of stator winding slots per pole and phase
S	Time interval Δt_S, defining value of currents in phases (i_A, i_B, i_C) by $S \leq V$
S_N	Number of bars (coils) in slot
t	Value of time
T_{TIM}	Period of phase current variation in time
T_{TG}	Period of winding MMF variation along stator boring (in tangential direction)
V	Number of time intervals into which period T_{TIM} is subdivided
W_{PH}	Number of turns in winding phase
$\Delta\alpha_A, \alpha_C; \alpha_B; \alpha_{A'}; \alpha_C; \alpha_B$	Angles occupied by winding phase zones
$\Delta\beta_A; \Delta\beta_{C'}; \ldots; \Delta\beta_B$	Additional angles expanding (or narrowing) winding phase zones
β	Winding pitch shortening
ε_{CAL}	Accuracy of MMF calculations
$\varphi_{A,Q}, \varphi_{B,Q}, \varphi_{C,Q}$	Initial phase angles of current harmonics of order Q in phases A, B, C
$\varphi_{A,Q}^{DIR}, \varphi_{B,Q}^{DIR}, \varphi_{C,Q}^{DIR}$	Initial values of phase angles of current harmonics of positive sequence
$\varphi_{A,Q}^{NEG}, \varphi_{B,Q}^{NEG}, \varphi_{C,Q}^{NEG}$	The same for currents of negative sequence
$\varphi_{A,Q}^{ZER}, \varphi_{B,Q}^{ZER}, \varphi_{C,Q}^{ZER}$	The same for currents of zero sequence

References

I. Monographs, Textbooks

1. Demirchyan K.S., Neyman L.R., Korovkin N.V., Theoretical Electrical Engineering. Moscow, St.Petersburg: Piter, 2009. Vol. 1, 2. (In Russian).
2. Kuepfmueller K., Kohn G., Theoretische Elektrotechnik und Elektronik. 15 Aufl., Berlin, New York: Springer. 2000. (In German).
3. Richter R., Elektrische Maschinen. Berlin: Springer. Band I, 1924; Band II, 1930; Band III, 1932; Band IV, 1936; Band V, 1950. (In German).
4. Mueller G., Ponick B., Elektrische Maschinen. New York, John Wiley, 2009. 375 S. (In German).
5. Voldek A.I., Electrical Machines. Leningrad: 1974. 782 c. (In Russian).
6. Schuisky W., Berechnung elektrischer Maschinen. Wien: Springer, 1960. (In German).
7. Mueller G., Vogt, K., Ponick B., Berechnung elektrischer Maschinen. Springer, 2007. 475 S. (In German).
8. Korn G., Korn T., Mathematical Handbook. New York: McGraw–Hill, 1961.
9. Jeffris H., Swirles B., Methods of Mathematical Physics. Third Edition, Vol. 1 – Vol. 3, Cambridge: Cambridge Univ. Press, 1966.

II. Induction Machines. Papers, Inventor's Certificates

10. Boguslawsky I.Z., Asymmetrical cage rotor MMF of induction machine. Power Eng. (New York), 1992, № 1.
11. Boguslawsky I.Z., Features of 6 – phases armature winding of A.C. machines with the non-sinusoidal power supply. Power Eng. (New York), 1997, № 5.
12. Boguslawsky I.Z., Ivanov V.G., Rogachevsky V.S., Turusov V.E., Stator winding MMF calculation method at arbitrary phase current waveform and unequal width of phase zones (for research of frequency – controlled motors performance). Science and research magazine of PGSPbPU, 2013, № 6. (In Russian).
13. Polujadoff M., General rotating MMF – Theory of squirrel cage induction machines with non-uniform air gap and several non-sinusoidal distributed windings. Trans AIEE, PAS, 1982.
14. Vaš P., Analysis of space–harmonics effects in induction motors using N–phase theories. International Conf. of Electrical Machines. Brussels, 1978.

Chapter 22
Investigation Method of Transient Modes in Induction Machines with Rotor Cage Asymmetry

This chapter presents investigation methods of transient modes in induction machines with asymmetrical rotor squirrel cage. This asymmetry can arise in the operation (for example, in case of bar breakage, especially at overloads), or in manufacturing (for example, due to low-quality soldering in bar-end ring joint). The solution is represented in the form of investigation of transient modes in two equivalent induction machines with various parameters of secondary loops:

- with symmetrical rotor cage in mutual induction direct field (field in air gap);
- with symmetrical rotor cage in mutual induction additional field (field in air gap);

It is obtained that the mutual inductance of stator and rotor loops as well as impedance of secondary loops of these both equivalent machines is different. Stated here are design ratios for these values of mutual inductance and impedance of secondary loops of both equivalent machines; determined here is interrelation between both mutual induction fields.

The "Theory of rotating field" [1–3] is applied for the determination of currents in rotor and stator loops of these machines in transient modes, because the induction machine is characterized by constant air gap. The method develops this theory in relation to induction machine construction with asymmetrical squirrel cage.

The content of this chapter is development of the methods stated in [1–3, 11–17].

22.1 Introduction: Problem Formulation

The increase of electromagnetic loads in the use of induction motors in operational modes is one of the modern development tendencies; it should also be noted that there is a tendency to use induction machines as generators. In this regard, investigation of operational modes of induction machines is actual.

I. Boguslawsky et al., *Large A.C. Machines*,
DOI 10.1007/978-4-431-56475-1_22

Calculation methods of steady-state modes in A.C. machines with rotor asymmetrical short-circuited loops with regard to the current distribution described in [2, 11, 12, 14–17], in Chaps. 6–10.

We obtained that methods of studying transient modes in these machines include several preliminary stages; they are connected with the calculation of currents distribution in asymmetrical cage elements in steady state conditions as stated in these chapters and with determination of parameters of rotor asymmetrical loops [4–8] in this mode.

Given in realization of these stages, the followings are assumed: machine power, its voltage and power factor (cos φ), slip, geometrical dimensions of machine active part, stator and rotor winding data, impedance of stator winding and rotor symmetrical cage elements, degree of rotor cage asymmetry.

22.2 Calculation of Currents Distribution in Asymmetrical Squirrel Cage Elements

22.2.1 Additional Aperiodic Current Components in Rotor Loops at Occurrence of Rotor Cage Asymmetry

Let us determinate, as the first approximation (K = 1), the flux density amplitude of the main harmonic of resulting mutual induction field (field in air gap) equal to $B^{K}_{RES,DIR}$, corresponding to the operation of induction machine with slip S_{SL}. We accept preliminarily that this resulting field rotates in the same direction as the rotor and induces currents $I_{(N)}$ and $J_{(N)}$ in symmetrical squirrel cage elements containing N_0 bars; the amplitudes of these currents do not depend on the number N of ring (bar) [6, 8]:

$$\left|I_{(N)}\right| \neq f(N); \left|J_{(N)}\right| \neq f(N); \tag{22.1}$$

here $I_{(N)}$—currents in ring portions, $J_{(N)}$—currents in bars. These currents for symmetrical winding are explicitly determined by the flux density $B^{K}_{RES,DIR}$. However, at the occurrence of asymmetry, in squirrel cage elements in ring portions and in bars there arise additional currents [14], depending on the numbers N_P of these asymmetrical elements; Let us designate these currents as $\Delta I_{(N)}$ and $\Delta J_{(N)}$ respectively. They are summarized with currents in ring portions $I_{(N)}$ and bars $J_{(N)}$ before breakage.

Additional currents $\Delta I_{(N)}$ and $J_{(N)}$ vary depending on the cage element number following aperiodic law [14]. The calculation expression for these currents depends on the number P of broken cage elements. For example, with P = 1 for currents $\Delta I_{(N)}$ in ring portions with numbers N = 0; 1; …; $N_P - 1$ it is determined as (N_P—broken bar number):

$$\Delta I_{(N)} = C_1 a_1^N + C_2 a_1^N, \tag{22.2}$$

and with numbers $N_P; N_P + 1; \ldots; N_0 - 1$ it is determined as:

$$\Delta I_{(N)} = C_3 a_1^N + C_4 a_1^N. \tag{22.3}$$

$$\text{Here } a_1 = \frac{2 + \sigma + \sqrt{\sigma^2 + 4\sigma}}{2}; \quad a_2 = \frac{2 + \sigma - \sqrt{\sigma^2 + 4\sigma}}{2}; \quad \sigma = \frac{2Z_R}{Z_B}; \tag{22.3'}$$

Z_R—impedance of ring portions, Z_B—impedance of bar; $C_1; C_2; C_3; C_4$—constants.

Values of these constants $C_1; C_2; C_3; C_4$ are calculated from the system of equations. Its first two equations are obtained from the second Kirchhoff's law [4, 5] for loops containing the broken bar with number N_P; other two equations characterize cage geometry (it is closed). Calculation methods of these constants were considered in detail in Chaps. 7–9.

Additional currents in bars are calculated according to the first Kirchhoff's law [4, 5]:

$$\Delta J_{(N+1)} = \Delta I_{(N+1)} - \Delta I_{(N)}$$

In particular, the current in the broken bar (with number N = N_P) is equal to,

$$\Delta J_{(N=N_P)} = C_3 a_1^{N_P} - C_1 a_1^{N_P - 1} + C_4 a_1^{N_P} - C_2 a_1^{N_P - 1}. \tag{22.4}$$

If the number of broken bars in cage P > 1, the number of unknown values $C_1; C_2; C_3; C_4, \ldots$ in the equations for additional currents respectively increases; the order of system of equations for their definition also increases. It is caused by an increase in number of equations as per the second Kirchhoff's law containing broken bars with number P > 1. As obtained in Chaps. 6–10, generally (at P > 1) the order of such systems $r \leq 2P + 2$; it is equal to the number of unknowns in the equations for currents $\Delta I_{(N)}$. For example, with P = 3, the equations for additional currents $\Delta I_{(N)}$ are determined as follows ($N_{P_1}; N_{P_2}; N_{P_3}$—numbers of broken bars) in this cage:

$$\begin{aligned}
&- \text{ in ring portions with numbers } N = 0; 1; \ldots; N_{P_1} - 1 \\
&\Delta I_{(N)} = C_1 a_1^N + C_2 a_1^N; \\
&- \text{ in ring portions with numbers } N = N_{P_1}; N_{P_1} + 1; N_{P_1} + 2; \ldots; N_{P_2} - 1 \\
&\Delta I_{(N)} = C_3 a_1^N + C_4 a_1^N; \\
&- \text{ in ring portions with numbers } N = N_{P_2}; N_{P_2} + 1; N_{P_1} + 2; \ldots; N_{P_3} - 1 \\
&\Delta I_{(N)} = C_5 a_1^N + C_6 a_1^N; \\
&- \text{ in ring portions with numbers } N = N_{P_3}; N_{P_3} + 1; N_{P_3} + 2; \ldots; N_0 - 1 \\
&\Delta I_{(N)} = C_7 a_1^N + C_8 a_1^N.
\end{aligned} \tag{22.5}$$

In Chap. 7 we find that the number of unknowns (r) can be reduced to r = 2P, if we choose the number (N = 0) with one of the asymmetric (damaged) bars.

22.2.2 Resultant Currents in Ring Portions $\underline{\underline{I}}_{(N)}$ and Bars $\underline{\underline{J}}_{(N)}$ After Breakage

Expressions for resulting currents $\underline{\underline{I}}_{(N)}$ and $\underline{\underline{J}}_{(N)}$ in cage elements after breakage take the form:

$$\underline{\underline{I}}_{(N)} = I_{(N)} + \Delta J_{(N)}; \quad \underline{\underline{J}}_{(N)} = J_{(N)} + \Delta J_{(N)}. \tag{22.6}$$

It should be remarked that with high slips ($S_{SL} \approx 1$), the distribution of resulting currents $\underline{\underline{I}}_{(N)}$ and $\underline{\underline{J}}_{(N)}$ considerably differs from that at low ones, because A.C. resistance and impedance of cage elements increase sharply. Thus, results of investigation method of transient mode in induction machines with asymmetry in cage depend on its impedances in previous steady state mode.

22.3 Calculation of MMF for Asymmetrical Cage Currents

It is convenient to represent stepped current distribution as a stepped curve f(x) in asymmetrical cage bars within $T = \pi(D_{INN} - \delta)$ period in the form of harmonic series in complex plane as per Chap. 12 in the form of two components:

$$f(x) = \sum F_{SEC,DIR} e^{j\frac{-2\pi mx}{T}} + F_{SEC,ADD} e^{j\frac{2\pi mx}{T}}; \tag{22.7}$$

where $\sum F_{SEC,DIR} = \sum \left|F_{SEC,DIR}\right| e^{j(\omega_{SEC} t + \gamma_{SEC,DIR})}$;

$$\sum F_{SEC,AAD} = \sum \left|F_{SEC,DIR}\right| e^{j(\omega_{SEC} t + \gamma_{SEC,ADD})}; \tag{22.8}$$

here the summation is made over the numbers of rotor spatial harmonic n; D_{INN}—stator core internal diameter; $F_{SEC,DIR}, F_{SEC,AAD}$—harmonic complex amplitudes (phasors) of respectively direct and additional rotating MMF of rotor currents; $\gamma_{SEC,DIR}, \gamma_{SEC,ADD}$—phase angles; ω_{SEC}—frequency of EMF and currents in cage elements: $\omega_{SEC} = \omega_1 - \omega_{REV} p = \omega_1 S_{SL}$, where ω_1—network frequency; ω_{REV}—angular speed of rotor rotation; p—number of machine pole pairs; S_{SL}—slip; n—order of spatial harmonic; δ—air gap. Let us note that expanding into series (22.7) with T period, but not with $T_{EL} = T/p$, the main harmonic has order n = p.

Let us concentrate on the investigation of machine processes using this main harmonic. The first component with amplitude $F_{SEC,DIR}$ rotates relative to the stator in the direction of rotor rotation with speed $\omega'_{DIR} = \omega_1/p$, and the second with amplitude $F_{SEC,ADD}$—with speed $\omega'_{ADD} = \left|\frac{\omega_1}{p} - 2\omega_{REV}\right|$. If the slip $S_{SL} > 0.5$, its rotation direction is opposite to the stator field rotation, and if slip $S_{SL} < 0.5$, it coincides with it [6–8]. Thus, the additional field of the main harmonic (of order n = p) can be both direct and reverse depending on the slip.

In practical calculations (22.8), it is expedient to execute an expansion into harmonic series by a numerical method; calculation expressions were given in Chap. 12.

22.4 Calculation of Resulting Mutual Induction Fields (Fields in Air Gap) at n = p

22.4.1 Direct Field

In Sect. 22.2.1 we set previously as the first approximation (K = 1) the flux density amplitude of main harmonic resulting mutual induction field (field in air gap) equal to $B^K_{RES,DIR}$; it was accepted that this resulting field rotates in the same direction as rotor. In this para we will refine the value of amplitude of this flux density $B^K_{RES,DIR}$, so that this mutual induction field matches the value of machine preset rated voltage $U_{STAT.PRESET}$. Then rotor currents and both MMF amplitudes correspond to this voltage according (22.8). The flux density $B^K_{RES,DIR}$ determinates no-load MMF–$F^K_{NO-LOAD,DIR}$:

$$F^K_{NO-LOAD,DIR} = \frac{B^K_{RES,DIR}}{\mu_0}\delta K_{CAR} K_{SAT,DIR}, \tag{22.9}$$

where μ_0—magnetic permeability of air, K_{CAR}—Carter's factor, K_{SAT}—magnetic circuit saturation factor. We should note that for the resulting field with flux density amplitude $B^K_{RES,DIR}$ the saturation factor $K_{SAT,DIR}$ for high-power induction machines is accepted much higher than for synchronous, and makes usually at least $K_{SAT,DIR} = 1.6 - 1.8$.

Using the Ampere's law [4, 5], we obtain an expression for the main harmonic of stator winding MMF: $F^K_{STAT,DIR}$, where the frequency of currents is equal to the network frequency ω_1 as follows:

$$F^K_{STAT,DIR} = F^K_{NO-LOAD,DIR} - F^K_{SEC,DIR}.$$

Here $F_{SEC,DIR}$—as per (22.8), $F^{K}_{NO-LOAD,DIR}$—as per (22.9). From the last expression we determinate the stator current amplitude with network frequency ω_1

$$I^{K}_{STAT,DIR} = F^{K}_{STAT,DIR}\frac{\pi n}{3K_W W_{STAT}}. \tag{22.10}$$

here K_W—winding factor $\left(\text{at}\frac{n}{p}=1\right)$; W_{STAT}—number of turns in stator winding phase. The stator winding phase EMF amplitude induced by the mutual induction field with amplitude $B^{K}_{RES,DIR}$ and frequency ω_1 is equal to,

$$E^{K}_{STAT,DIR} = -j\Phi^{K}_{RES,DIR}\omega_1 K_W W_{STAT}, \tag{22.11}$$

where $\Phi^{K}_{RES,DIR}$—main harmonic of mutual induction flux (flux in air gap):

$$\Phi^{K}_{RES,DIR} = \frac{1}{\pi n} TB^{K}_{RES,DIR} L_{COR}, \tag{22.11'}$$

where L_{COR}—core length. Now, using Eqs. (22.10) and (22.11) it is easy to obtain the following approximation [4, 5] for stator winding phase voltage amplitude:

$$U^{K+1}_{STAT,DIR} = -E^{K}_{STAT,DIR} + I^{K}_{STAT,DIR} Z_{STAT,DIR}, \tag{22.12}$$

where $Z_{STAT,DIR}$—total leakage impedance of stator winding at the frequency equal to ω_1.

The voltage $U^{K}_{STAT,DIR}$ should satisfy the following inequality:

$$\left|\frac{U^{K}_{STAT,DIR}}{U_{STAT.PRESET}} - 1\right| \le \varepsilon_U, \tag{22.13}$$

where $U_{STAT.PRESET}$—preset motor phase voltage, ε_U—preset accuracy of phase voltage calculation; usually in practical calculations it is accepted: ε_U = 2-3 %

The inequality (22.13) is solved using the nonlinear algorithm determined by the ratios (22.2)–(22.12) as follows:

$$U_{STAT,DIR} = f(B_{RES,DIR}). \tag{22.14}$$

As the solution of this algorithm, it is convenient to use one of consecutive approximation methods [9, 10].

After the calculation as per (22.13), the direct field flux density amplitude $B^{\kappa}_{RES,DIR} = B_{RES,DIR}$ (for harmonic of order n = p) is determined by the preset machine voltage, and it is easy to calculate by means of the given ratios the corresponding MMF amplitudes of both fields as per (22.8) and their parameters as well.

22.4.2 Additional Field

To derive Eq. (22.8) we must note that the harmonic of order n = p with amplitude $F_{SEC,ADD}$ rotates relative to the stator with speed ω'_{ADD}. This harmonic induces in stator winding additional EMF $E_{STAT,ADD}$ whose frequency differs from the network frequency $\omega_1 : \omega_{ADD} = \omega_1|1 - 2S_{SL}|$.

Currents $I_{STAT,ADD}$ correspond to additional EMF $E_{STAT,ADD}$ in stator phases. They pass through the network, external relative to machine leads, and are imposed on currents with the frequency ω_1. Usually, in practice when determining these currents, two limiting cases are distinguished for the network feeding motor:

- infinitely power network;
- independent network.

In the first case, it is considered that the network impedance is small relative to that of motor windings, so it is possible to take that the stator winding relative to currents with frequency ω_{ADD} is short-circuited.

In the second case it is supposed that the impedance of external network $Z_{EXT,ADD} \neq 0$.

The additional EMF $E_{STAT,ADD}$ with frequency ω_{ADD} at stator winding terminals is calculated similarly to (22.11) by a method of iterations.

$$E^{(V)}_{STAT,ADD} = -j\Phi^{(V)}_{RES,ADD}\omega_{ADD}K_W W_{STAT}. \tag{22.15}$$

here $\Phi_{RES,ADD}$—main harmonic of mutual induction additional field (flux in air gap) [6–8]; it is calculated by a method of iterations. (V—iteration number):

$$\Phi^{(V)}_{RES,ADD} = \frac{1}{\pi n} TB^{(V)}_{RES,ADD} L_{COR}; \tag{22.15'}$$

here $B^{(V)}_{RES,ADD}$—unknown value of flux density amplitude for V-th iteration.

In case of "infinite" power networks, its currents are determined by the ratio:

$$I^{(V)}_{STAT,ADD} = \frac{E^{(V)}_{STAT,ADD}}{Z_{STAT,ADD}}, \tag{22.15''}$$

where $Z_{STAT,ADD}$—leakage impedance of stator winding at frequency equal to ω_{ADD}. In an independent network these currents $I^{(V)}_{STAT,ADD}$ are determined by the similar ratio:

$$I^{(V)}_{STAT,ADD} = \frac{E^{(V)}_{STAT,ADD}}{Z_{STAT,ADD} + Z_{EXT,ADD}}. \tag{22.15'''}$$

Stator winding MMF $F^{(V)}_{STAT,ADD}$ corresponding to currents in phase $I^{(V)}_{STAT,ADD}$ is equal to,

$$F^{(V)}_{STAT,ADD} = \frac{3}{\pi n} I^{(V)}_{STAT,ADD} K_W W_{STAT}.$$

Using this MMF, according to the Ampere's law we obtain the no-load MMF as follows:

$$F^{(V)}_{NO-LOAD,ADD} = F_{SEC,ADD} + F^{(V)}_{STAT,ADD}. \tag{22.16}$$

The flux density amplitude $B^{(V)}_{RES,ADD}$ of resulting additional field (field in air gap) is determined from the last ratio (22.16) similarly to Eq. (22.9):

$$B^{(V+1)}_{RES,ADD} = F^{(V)}_{NO-LOAD,ADD} \frac{\mu_0}{2\delta K_{CAR} K_{SAT,ADD}}. \tag{22.17}$$

It should be noted that at usual asymmetry levels of squirrel cage for resulting field with flux density amplitude $B_{RES,ADD}$, the saturation factor $K_{SAT,ADD}$ for high-power induction machines is less than $K_{SAT,DIR}$ and usually does not exceed $K_{SAT,ADD} = 1.2 - 1.3$.

Equations (22.15)–(22.17) form a system, where the value $F_{SEC,ADD}$ is preset as per (22.8), and values $F_{NO-LOAD,ADD}, F_{STAT,ADD}, I_{STAT,ADD}, E_{STAT,ADD}, \Phi_{RES,ADD}$ are to be determined provided that flux density amplitudes $B_{RES,ADD}$ as per (22.15′) and (22.17) coincide, when solving this equation by an iteration method. It is possible to refine the values of $B_{RES,DIR}$ and $B_{RES,ADD}$ using this amplitudes. Thereto we have to calculate the current distribution in asymmetrical rotor cage and new values of $F_{SEC,DIR}$ and $F_{SEC,ADD}$.

Note: Interrelation of parameters of direct and additional fields will be considered in Sect. 22.5.3.

22.5 Determination of Mutual Induction Factors and Parameters of Secondary Loops (Rotor) for the Main and Additional Fields

We try to study induction machine transients with asymmetrical rotor squirrel cage, let us use the "Theory of rotating field" [1–3]; expediency of its usage is based on the fact that machines of this type are characterized by constant air gap: $\delta \neq f(x)$ where $0 \leq x \leq T$. The method is based on this theory in relation to the induction machine construction with asymmetrical squirrel cage. For its use, it is necessary to determinate preliminarily mutual induction factors between rotor and stator loops,

and also parameters of secondary loops (rotor) for both fields (direct and additional). In further investigation it is reasonable to replace the real squirrel cage with N_0 bars with equivalent three-phase winding with number of turns in phase $W_{EQ,ROT} = W_{STAT}$ as in stator winding, and the same winding factor K_W. Then we obtain currents in this equivalent winding:

- for direct field: $I_{SEC,DIR} = F_{SEC,DIR} \frac{\pi p}{3 K_W W_{STAT}}$;
- for additional field: $I_{SEC,ADD} = F_{SEC,ADD} \frac{\pi p}{3 K_W W_{STAT}}$,

  for n = p.

22.5.1 Mutual Induction Factor M_{DIR} and Parameters of Secondary Loop (Rotor) for Direct Field

Mutual induction factors of stator and rotor loops at $E_{STAT,DIR}$ as per (22.11):

$$M_{DIR} = \left| \frac{E_{STAT,DIR}}{\omega_1 I_{NO-LOAD,DIR}} \right|, \tag{22.18}$$

where no-load current $I_{NO-LOAD,DIR} = F_{NO-LOAD,DIR} \frac{\pi p}{3 K_W W_{STAT}}$; $F_{NO-LOAD,DIR}$ as per (22.9); EMF of secondary (rotor) loop $E_{SEC,DIR}$, reduced to stator winding EMF is calculated similarly to (22.11): $E_{SEC,DIR} = E_{STAT,DIR}$.

Then, the equivalent impedance of secondary loop corresponding to the direct field ($I_{SEC,DIR}$—as per Sect. 22.5):

$$Z_{SEC,DIR} = \frac{E_{SEC,DIR}}{I_{SEC,DIR}}. \tag{22.19}$$

Components of impedance:

$$Z_{SEC,DIR} = R_{SEC,DIR} + j\omega_{SEC} L'_{SEC,DIR}, \tag{22.19'}$$

where $R_{SEC,DIR}$—A.C. resistance of this loop, $L'_{SEC,DIR}$—its leakage inductance.

22.5.2 Mutual Induction Factor M_{ADD} and Parameters of Secondary Loop (Rotor) for Additional Field

The mutual induction factor between stator and rotor loops at $E_{STAT,ADD}$—as per (22.15):

$$M_{ADD} = \left| \frac{E_{STAT,ADD}}{\omega_{ADD} I_{NO-LOAD,ADD}} \right|, \tag{22.20'}$$

where no-load current $I_{NO-LOAD,ADD} = F_{NO-LOAD,ADD} \frac{\pi p}{3 K_w W_{STAT}}$; $F_{NO-LOAD,ADD}$ as per (22.16); EMF of secondary loop (rotor) $E_{SEC,ADD}$, reduced to stator winding EMF is calculated similarly to (22.15): $E_{SEC,ADD} = E_{STAT,ADD}$.

Then, the equivalent impedance of secondary loop corresponding to the additional field ($I_{SEC,ADD}$—as per Sect. 22.5):

$$Z_{SEC,ADD} = \frac{E_{SEC,ADD}}{I_{SEC,ADD}}. \tag{22.20}$$

Components of impedance:

$$Z_{SEC,ADD} = R_{SEC,ADD} + j\omega_{SEC} L'_{SEC,ADD}, \tag{22.21}$$

where $R_{SEC,ADD}$—A.C. resistance of this loop, $L'_{SEC,ADD}$—its leakage inductance.

22.5.3 *Interrelation of Mutual Induction Factors and Parameters of Secondary Loops (Rotor) for Direct and Additional Fields*

We find the following peculiarity of physical process that is determined by the relation between direct and additional fields of induction machine with asymmetrical rotor cage. By means of the algorithm (22.2)–(22.12) we have determined the main harmonic flux density amplitude of resulting mutual induction field (field in air gap) equal to $B_{RES,DIR}$; they correspond to the operation of induction machine with slip S_{SL}. This slip is determined by impact of two torques on rotor: the main torque corresponding to the flux density $B_{RES,DIR}$, and additional torque corresponding to the flux density $B_{RES,ADD}$ [6–8]. We note that the additional torque is the braking torque. Let us assume that the degree of asymmetry in rotor cage increases, for example, due to an increase in transient impedance in bar-end ring joint. Then the initial slip S_{SL} of induction machine is increased also. As the result EMF and loop impedance of the rotor are changing. This results in changing the variation of currents in its both windings, MMF amplitudes of the main harmonics $F_{SEC,DIR}, F_{SEC,ADD}$ and, respectively, the variation of mutual induction fluxes of both fields in machine air gap.

Therefore, direct and additional mutual induction fields and their parameters in an induction machine with asymmetrical rotor cage are not independent: the current distribution in the asymmetrical rotor cage is determined by the both fields with amplitudes $B_{RES,DIR}$ and $B_{RES,ADD}$.

22.6 Equations for Calculation of Transients in Both Magnetically Coupled Machine Loops

22.6.1 *Equations for Transient Currents in Stator $I_{STAT,DIR}$ and Rotor $I_{SEC,DIR}$ Caused by Direct Field*

According to [1, 3], we write down the equations for both magnetically coupled loops; they are determined as follows:

$$\begin{aligned} L_{STAT,DIR}\frac{di_{STAT,DIR}}{dt} + i_{STAT,DIR}R_{STAT.PH} + M_{DIR}\frac{di_{SEC,DIR}}{dt'} = 0; \\ L_{SEC,DIR}\frac{di_{SEC,DIR}}{dt} + i_{SEC,DIR}R_{SEC,DIR} + M_{DIR}\frac{di_{STAT,DIR}}{dt'} = 0. \end{aligned} \tag{22.22}$$

In the last equations t—own time, and t′—time counted in one loop relative to the second [1, 3]; M_{DIR}—as per (22.18); $R_{STAT.PH}$—A.C. resistance of stator winding phase; $L_{STAT,DIR}$—total inductance of stator phase winding: $L_{STAT,DIR} = L_{STAT,PH} + M_{DIR}$, where $L_{STAT,PH}$—leakage inductance of stator winding phase; $L_{SEC,DIR}$—total inductance of rotor phase loop: $L_{SEC,DIR} = L'_{SEC,DIR} + M_{DIR}$; $R_{SEC,DIR}, L'_{SEC,DIR}$—as per (22.19) and (22.19′).

Let us represent instantaneous values of transient currents $i_{STAT.DIR}, i_{SEC,DIR}$ in the form:

$$i_{STAT,DIR} = I_{STAT,DIR}e^{j(\alpha t + \varphi_{DIR})}; \quad i_{SEC,DIR} = I_{SEC,DIR}e^{j(\beta t + \psi_{DIR})}, \tag{22.23}$$

where $\varphi_{DIR}, \psi_{DIR}$—initial phase angles, α, β—circular frequencies of currents. With account of ratios (22.23), the system of Eq. (22.22) takes the form:

$$\begin{aligned} j\alpha L_{STAT,DIR}I_{STAT,DIR} + I_{STAT,DIR}R_{STAT.PH} + j\alpha M_{DIR}I_{SEC,DIR} = 0; \\ j\beta L_{SEC,DIR}I_{SEC,DIR} + I_{SEC,DIR}R_{SEC,DIR} + j\beta M_{DIR}I_{STAT,DIR} = 0. \end{aligned} \tag{22.24}$$

Directly connected with the time reference system is the relation between frequencies of transient currents in stator α and rotor β as part of Eq. (22.24):

$$\beta = \alpha - \omega_{REV}p. \tag{22.25}$$

Matrix rank r of this system factors equals to r = 2; for transient currents $i_{STAT,DIR}$ and $i_{SEC,DIR}$ in both loops the following is true [9, 10]:

$$\begin{aligned} i_{STAT,DIR} = E_1e^{jY_1t} + E_2e^{jY_2t}; \\ i_{SEC,DIR} = E_3e^{j(Y_1 - \omega_{REV}p)t} + E_4e^{j(Y_2 - \omega_{REV}p)t}; \end{aligned} \tag{22.26}$$

In Eq. (22.26), constants E_1, E_2, E_3, E_4, are determined by initial conditions of transient process, and values $Y = Y_1, Y = Y_2$—attenuation factors of transient currents; these attenuation factors can be obtained from a system of matrix factors (22.24) by substituting the value α by Y. Their calculation matrix takes the form:

$$\begin{matrix} jYL_{STAT,DIR} + R_{STAT.PH} & jYM_{DIR} \\ j(Y - \omega_{REV}p)M_{DIR} & j(Y - \omega_{REV}p)L_{SEC,DIR} + R_{SEC,DIR} \end{matrix} \tag{22.27}$$

Equating the determinant to zero, we obtain according to the matrix rank (r = 2) the equation of the second order relative to the unknown value Y, and, therefore, two values of roots $Y = Y_1$ and $Y = Y_2$; these roots are conjugate [1, 3].

Let us note that constants E_1, E_2, E_3, E_4 are not independent magnitudes; they are connected with the following linear relation:$E_3 = E_1D_3; E_4 = E_2D_4$. To determine constants D_3, D_4, we use the system (22.24). Then, from its second equation, neglecting the value $R_{SEC,DIR}$ in comparison with the value $\beta L_{SEC,DIR}$, we obtain $D_3 = \frac{-M_{DIR}}{L_{SEC,DIR}}$; similarly, from its first equation, neglecting the value $R_{STAT.PH}$ in comparison with the value $\alpha L_{STAT,DIR}$, we obtain $D_4 = \frac{- L_{STAT,DIR}}{M_{DIR}}$.

With considering obtained constants $D_3; D_4$, the calculation expression for current $i_{SEC,DIR}$ is given as follows:

$$i_{SEC,DIR} = \frac{-E_1M_{DIR}e^{j(Y_1-\omega_{REV}p)t}}{L_{SEC,DIR}} - \frac{E_2L_{STAT,DIR}e^{j(Y_2-\omega_{REV}p)t}}{M_{DIR}}. \tag{22.26′}$$

Thus, the task solution for transient currents of stator $i_{STAT,DIR}$ and rotor $i_{SEC,DIR}$ caused by the main field is reduced to that of similar task for transients in induction machines with symmetrical rotor cage, as in detail considered in [1, 3].

22.6.2 *Equations for Transient Currents in Stator $I_{STAT,DIR}$ and Rotor $I_{SEC,ADD}$ Caused by Additional Field*

According to [1, 3], we write down equations for both magnetically coupled loops. They are similar to (22.22), but have some differences characterizing the additional field. So, we will give the equations for both loops with account of these differences; according to [1, 3], the equations are determined as follows:

$$\begin{aligned} L_{STAT,ADD}\frac{di_{STAT,ADD}}{dt} + i_{STAT,ADD}R_{STAT.PH} + M_{ADD}\frac{di_{SEC,ADD}}{dt'} = 0; \\ L_{SEC,ADD}\frac{di_{SEC,ADD}}{dt} + i_{SEC,ADD}R_{SEC.ADD} + M_{ADD}\frac{di_{STAT,ADD}}{dt'} = 0. \end{aligned} \tag{22.22′}$$

In these equations M_{ADD} as per (22.20′); $L_{STAT,ADD}$—total inductance of stator winding: $L_{STAT,ADD} = L_{STAT.PH} + M_{ADD}$, where $L_{STAT.PH}$—leakage inductance of stator winding phase; $L_{SEC,ADD}$—total inductance of rotor phase loop: $L_{SEC,ADD} = L'_{SEC,ADD} + M_{ADD}$; $R_{SEC,ADD}, L'_{SEC,ADD}$—as per (22.21).

Instantaneous values of transient currents $i_{STAT,ADD}, i_{SEC,ADD}$, take the form:

$$i_{STAT,ADD} = I_{STAT,ADD}e^{j(\lambda t + \varphi_{ADD})}; i_{SEC,ADD} = I_{SEC,ADD}e^{\sigma t + \psi_{ADD}}, \qquad (22.23')$$

where λ, σ—circular frequencies of currents.

With account of ratios (22.23′), the system of Eq. (22.22′) takes the form:

$$\begin{aligned} &j\lambda L_{STAT,ADD}I_{STAT,ADD} + I_{STAT,ADD}R_{STAT.PH} + j\lambda M_{ADD}I_{SEC,ADD} = 0; \\ &j\sigma L_{SEC,ADD}I_{SEC,ADD} + I_{SEC,ADD}R_{SEC,ADD} + j\sigma M_{ADD}I_{STAT,ADD} = 0. \end{aligned} \qquad (22.24')$$

Directly connected with the time reference system is the relation between frequencies of transient currents in stator λ and rotor σ as part of Eq. (22.24′):

$$\sigma = |\lambda \pm \omega_{REV}p|. \qquad (22.25')$$

The sign depends on the value of S_{SL}.

Matrix rank r of this system factors is found to be equal to r = 2; for transient currents $i_{STAT,ADD}$ and $i_{SEC,ADD}$ in both loops the following is true:

$$\begin{aligned} i_{STAT,ADD} &= G_1e^{jY_3t} + G_2e^{jY_4t}; \\ i_{SEC,ADD} &= G_3e^{j(Y_3 + \omega_{REV}p)t} + G_4e^{j(Y_4 + \omega_{REV}p)t}. \end{aligned} \qquad (22.26'')$$

In Eq. (22.26′) G_1, G_2, G_3, G_4 are constants determined by initial conditions of transients and values $Y = Y_3, Y = Y_4$—attenuation factors of transient currents; these attenuation factors can be obtained from system matrix factors (22.24′) with substituting the value λ by Y. Their calculation matrix takes the following form:

$$\begin{matrix} jYL_{STAT,ADD} + R_{STAT.PH} & jYM_{ADD} \\ j|Y \pm \omega_{REV}p|M_{ADD} & j|Y \pm \omega_{REV}p|L_{SEC,ADD} + R_{SEC,ADD} \end{matrix} \qquad (22.27')$$

Equating the determinant to zero, we get according to matrix rank (r = 2) the equation of the second order and, therefore, two values of roots $Y = Y_3$ and $Y = Y_4$; these roots are conjugate [1, 3].

Let us show that constants G_1, G_2, G_3, G_4, as well as constants E_1, E_2, E_3, E_4 are not independent values; they are linearly related easily determined similar to Sect. 22.6.1. With account of these linear relations between constants, we obtain the calculation expression for current $i_{SEC,ADD}$:

$$i_{SEC,ADD} = \frac{-G_1 M_{ADD} e^{j(Y_3 + \omega_{REV} p)t}}{L_{SEC,ADD}} - \frac{G_2 L_{STAT,ADD} e^{j(Y_3 + \omega_{REV} p)t}}{M_{ADD}}. \qquad (22.26\square\square\square)$$

As a result, the task solution for transient currents of stator $i_{STAT,ADD}$ and rotor $i_{SEC,ADD}$ caused by additional field as well as tasks for transient currents caused by the direct field is reduced to that of similar task for transients in induction machines with symmetrical rotor cage, as considered in details in [1, 3].

22.7 The Resulting Transient Currents in Windings

Using (22.26) and (22.26′), we obtain:

22.7.1 Currents in Stator Winding

$$i_{STAT.RES}(t) = i_{STAT.DIR}(t) + i_{STAT,ADD}(t).$$

22.7.2 Currents in Secondary Loop (in Rotor)

$$i_{SEC.RES}(t) = i_{SEC.DIR}(t) + i_{SEC,ADD}(t).$$

22.8 Prospects for Using the Method with Account of Rotor MMF Higher Spatial Harmonics, and also for Calculations of Transient Currents in Synchronous Salient Pole Machines with Damper Winding

In the previous paragraphs the investigation of induction machine transient modes was based on only the main MMF harmonic in expansion (22.7). However, the distribution of currents in bars of cage differs from that of harmonics more significant for the greater number of broken bars; there increase the corresponding amplitudes of MMF higher spatial harmonics with growth of number of broken bars. Their accounting is similar to that described for main harmonic. Its peculiarity

for transient currents consists in the fact that each system equation (for example 22.24) has additional summands of the same form. The same is also true for both system equations (for example 22.24′); mutual induction factor and parameters of secondary loop (of rotor) for additional field are calculated from the ratios similar to those given in Sect. 22.5.2.

It should note that the stated method contains all stages necessary for calculating transient currents in synchronous salient pole machines with damper winding; the distribution of currents in this winding in steady state mode also considerably differs from that of the harmonic process, as well as in squirrel cage with broken bars. The calculation method for currents in damper winding, determinations of MMF harmonics and mutual induction fields (with account of air gap variation along pole division) is developed in [11, 12, 14–17], in Chaps. 6–10.

Brief Conclusions

1. To study transients in induction machines with asymmetry in rotor cage, a number of machine parameters should be preliminarily determined: Mutual induction factors between rotor and stator loops and also equivalent parameters of secondary loops (of rotor) for both fields (direct and additional).
2. Calculation of these parameters requires:
   - preliminary calculation of current distribution in asymmetrical cage elements;
   - expansion of the current distribution step curve in bars of rotor periphery of this cage into harmonic series in complex plane;
   - determination of amplitude complex value of MMF direct and additional mutual induction fields (fields in gap).
3. Investigation of transients in induction machine with rotor cage asymmetry is reduced to that of transients in two equivalent symmetrical magnetically coupled loops (of rotor and stator); these two loops are in direct field of mutual induction, and two others—in additional field. Mutual induction factors between rotor and stator loops and also equivalent parameters of rotor and stator secondary loops corresponding to both fields (direct and additional) differ. Therefore, attenuation factors of transient currents are not equal for each of this field.
4. For the investigation of transients in each of these two symmetrical magnetically coupled loops it is expedient to use the “Theory of rotating field” [1, 3]; expediency of its choice is based on the fact that machines are characterized by constant air gap: $\delta \neq f(x)$, where $0 \neq x \leq T$.

List of symbols

$B_{RES,DIR}, B_{RES,ADD}$	FLUX density amplitude in air gap of the main harmonic respectively of direct and additional fields
$C_1; C_2; C_3; C_4$	Constants determined by initial conditions
D_{INN}	Stator core diameter
$E_{STAT,DIR}$	Stator winding phase EMF amplitude induced by direct field of mutual flux density with amplitude $B_{RES,DIR}$ and frequency f_1
$E_{STAT,ADD}$	The same, for additional field with amplitude $B_{RES,ADD}$ and frequency f_{ADD}
$F_{STAT,DIR}, F_{STAT,ADD}$	Amplitudes of MMF harmonics respectively for stator direct and additional fields
$F_{SEC,DIR}, F_{SEC,DIR}$	Amplitudes of MMF harmonics respectively for rotor direct and additional fields
$\Delta F_{SEC,DIR}, \Delta F_{SEC,ADD}$	Amplitudes of MMF harmonics of rotor additional currents respectively for direct and additional fields
$F_{NO-LOAD,DIR}, F_{NO-LOAD,ADD}$	Amplitudes of no-load MMF respectively for direct and additional fields
G_1, G_2, G_3, G_4	Constants determined by initial transient conditions
$\underline{\underline{I}}_{(N)}, \underline{\underline{J}}_{(N)}$	Resulting currents in short-circuited ring portions and in bars (after breakage)
$I_{(N)}, J_{(N)}$	Current amplitudes in short-circuited ring portions and in bars (before breakage)
$\Delta I_{(N)}, \Delta J_{(N)}$	Amplitudes of additional currents in short-circuited ring portions and bars caused by cage asymmetry
$I_{STAT,DIR}$	Stator current amplitude with network frequency ω_1
$I_{STAT,ADD}$	Stator current amplitude with frequency f_{ADD}
$i_{STAT,DIR}, i_{SEC,DIR}$	Instantaneous values of transient currents for direct field respectively in stator and rotor
$i_{STAT,ADD}, i_{SEC,ADD}$	The same for additional field
$J_{(NP)}$	Current amplitude in bar with number N_P before its breakage
K	Iteration number
k_{CAR}	Carter's factor
k_{SAT}	Magnetic circuit saturation factor
k_W	Winding factor
$L'_{SEC,DIR}$	Leakage inductance of secondary loop for direct field
$L'_{SEC,ADD}$	Leakage inductance of secondary loop for additional field
$L_{STAT,DIR}$	Total inductance of stator winding phase for direct field
$L_{STAT,ADD}$	Total inductance of stator winding for additional field

$L_{STAT,PH}$	Leakage inductance of stator winding phase
$L_{SEC,DIR}$	Total inductance of rotor loop for direct field
$L_{SEC,ADD}$	Total inductance of rotor loop phase for additional field
P	Number of broken cage elements
n	Order of spatial harmonic
M_{DIR}	Mutual induction factor between stator and rotor loops for direct field
M_{ADD}	Mutual induction factor between stator and rotor loops for additional field
N_0	Number of bars in cage
N	Number of cage element (bar or ring portion)
N_P	Asymmetrical (broken) bar number
p	Number of pole pairs in machine
$R_{SEC,DIR}$	A.C. resistance of secondary loop for direct field
$R_{SEC,ADD}$	A.C. resistance of secondary loop for additional field
$R_{STAT,PH}$	A.C. resistance of stator winding phase
S_{SL}	Slip
T	EMF expansion period
t	Own time
t'	Time counted in one loop relative to the second
$U_{STAT.PRESET}$	Amplitude of motor preset phase voltage
W_{STAT}	Number of stator winding turns
$Y = Y_1, Y = Y_2$	Attenuation factors of transient currents for the main field
$Y = Y_3, Y = Y_4$	Attenuation factors of transient currents for additional field
Z_R	Impedance of ring portion
Z_B	Impedance of bar
$Z_{STAT,DIR}$	Leakage impedance of stator winding at frequency f_1
$Z_{EXT,ADD}$	Impedance of external network at frequency f_{ADD}
$Z_{STAT,ADD}$	Leakage impedance of stator winding at frequency f_{ADD}
$Z_{SEC,DIR}$	Impedance of secondary loop at frequency f_{SEC} for the main field
$Z_{SEC,ADD}$	Impedance of secondary loop at frequency f_{SEC} for additional field
ΔZ	Increase of bar impedance at its breakage
Z_B	Impedance of unbroken bar
Z_R	Impedance of ring portion
$\gamma_{SEC,DIR}, \gamma_{SEC,ADD}$	Phase angles

ω_{SEC}	Circular frequency of EMF and currents in cage elements
ω_1	Network circular frequency
ω_{REV}	Angular speed of rotor rotation
ω'_{MAIN}	Rotation speed of main field harmonics relative to stator (in direction of rotor rotation)
δ	Air gap
μ_0	Magnetic permeability of air
$\Phi_{RES,DIR}$, $\Phi_{RES,ADD}$	Main harmonic of mutual induction flux (flux in air gap) respectively for direct and additional fields,
φ_{MAIN}, ψ_{DIR}	Initial phase angles
α, β	Frequencies of transient currents respectively for stator and rotor direct field
λ, σ	Frequencies of transient currents respectively for stator and rotor additional field

References

I. Monographs, Textbooks

1. Ruedenberg R., Elektrische Schaltvorgaenge. Berlin, Heidelberg, New York: Springer, 1974. (In German).
2. Boguslawsky I.Z., A.C. Motors and Generators. The Theory and Investigation Methods by Their Operation in Networks with Non Linear Elements. TU St.Petersburg Edit., 2006. Vol. 1; Vol.2. (In Russian).
3. Schuisky W., Berechnung elektrischer Maschinen. Wien: Springer, 1960. (In German).
4. Demirchyan K.S., Neyman L.R., Korovkin N.V., Theoretical Electrical Engineering. Moscow, St.Petersburg: Piter, 2009. Vol. 1, 2. (In Russian).
5. Kuepfmueller K., Kohn G., Theoretische Elektrotechnik und Elektronik. 15 Aufl., Berlin, New York: Springer. 2000. (In German).
6. Richter R., Elektrische Maschinen. Berlin: Springer. Band I, 1924; Band II, 1930; Band III, 1932; Band IV, 1936; Band V, 1950. (In German).
7. Mueller G., Ponick B., Elektrische Maschinen. New York, John Wiley, 2009. - 375 S. (In German).
8. Mueller G., Vogt, K., Ponick B., Berechnung elektrischer Maschinen. Springer, 2007. 475 S. (In German).
9. Jeffris H., Swirles B., Methods of Mathematical Physics. Third Edition, Vol. 1 – Vol. 3, Cambridge: Cambridge Univ. Press, 1966.
10. Korn G., Korn T., Mathematical Handbook. New York: McGraw–Hill, 1961

II. Induction Machines. Papers, Inventor's Certificates

11. Boguslawsky I.Z., Currents in a asymmetric short – circuited rotor cage. Power Eng. (New York), 1982, № 1.

12. Boguslawsky I.Z., Calculating the current distribution on the damper winding of large slow–speed synchronous motors in asynchronous operation. Power Eng. (New York), 1979, № 3.
13. Boguslawsky I.Z., Korovkin N.V., The transient modes of induction machines with asymmetric rotor cage. Proceedings of Russian Academy of Science. Energetika. 2015. № 2. (In Russian).

III. Synchronous Machines. Papers, Inventor's Certificates, Patents

14. Boguslawsky I.Z., Demirtschyan K.S., Stationaere Stromverteilung in unregelmaessigen und unsymmetrischen kurzgeschlossenen Laeuferwicklungen von Wechselstrommaschinen. Archiv fuer Elektrotechnik, 1992, № 6. (in German).
15. Demirchyan K.S., Boguslawsky I.Z., Current flowing in damper winding bars of different resistivity in a heavy-duty low speed motor. Power Eng. (New York), 1980, № 2.
16. Boguslawsky I.Z., Investigation of currents in elements of the regular chain circuit (applying to damper windings of synchronous machines). Elektrotechnika. 2012, № 8. (in Russian).
17. Boguslawsky I.Z., Rogachevsky B.S., Electromagnetic loadings of synchronous machines in asynchronous modes (with taking into account distribution of currents in the damper winding). Elektrotechnika. 2012, № 10. (in Russian).

Chapter 23
Theory and Methods of Investigation of Eddy Currents and Additional Losses in Stator Windings

This chapter develops determination methods of additional losses from eddy and circulating currents in modern stator winding constructions caused by influence of current first and higher time harmonics ($Q \geq 1$). Given here are calculation methods of additional losses and rational selection of construction of bar and coil windings.

For bar windings, the constructions with combined conductors (solid and hollow) are investigated, herewith, their resistivity is different; constructions with incomplete transposition of conductors in slot that is characteristic for high-power multipole machines, for example, diesel—and hydrogenerators; constructions with various height of both bars in slot. Practical recommendations are provided for all these constructions.

For coil windings constructions are investigated for high-power low-voltage machines with small number of turns in each coil. This requires taking into account not only leakage flux from currents in adjacent turns and coils, but also leakage flux from elementary conductors of every turn. Practical examples are given.

Appendices for this chapter are given:

- numerical methods of investigation of skin effect in a rectangular bar of short-circuited rotor winding with account of the variation of its resistivity due to temperature along the slot height. The solution of this problem is connected with modern calculation methods of induction machine starting characteristics;
- analytical design method for circuits of multiphase windings with integer or fractional number of slots per pole and phase q; herewith, this number q can be both more than unity ($q > 1$ usually for electrical machine industry practice), and $q < 1$ (machines with this winding find application in recent years).

I. Boguslawsky et al., *Large A.C. Machines*,
DOI 10.1007/978-4-431-56475-1_23

23.1 Problem Formulation

In present-day practice ensuring the increase of engineering-and-economic performance and competitive growth of high power motors and generators may be realized by upgrading their electromagnetic loads. To achieve this goal, it turns out to be necessary to implement new engineering solutions; at the heart of them are the results of ever-deep investigations of physical processes occurred in machines and their components. Moreover, the study of machine duty conditions will be needed while refining physical and mathematical models of the processes. This is especially important if machine constructions or operating conditions are not standard and the volume of experimental findings is insufficient for practical purposes. For example, in different branches of industry—metallurgy, mining, cement industry, oil and gas production—the utilization of motors and generators operating in networks with non-linear elements (semiconductor frequency convertors) is due to higher-order current harmonics induced in armature winding and respectively to additional losses. To ensure a high level of machine efficiency and overheat according IEC [40] it shall be necessary to carry out further investigations of eddy and circulating currents. The goal of this chapter is to develop efficient methods of additional losses calculation with due account made for higher-order current time harmonics [17–22] and their distribution in slots.

It should be noted that the armature winding (stator winding) is one of machine parts that determines to a great extent the geometry of its active component. A high level of electromagnetic loads of modern machines results in the necessity to carefully choose the rational stator winding construction. At present in line with standard three-phase windings six-phase windings [23–26] are used in machines designed for operation in non-linear networks. Construction method of winding configurations, including fractional per pole and phase, is an open practical issue.

The solution of problems existing in electrical machine engineering requires investigation efforts. In order to cut down additional losses in windings, to minimize machine weight and sizes, the investigations must be continued:

- so that we study eddy currents and losses induced by cross-slot leakage flux in stator windings of various construction: bar windings (with complete or incomplete transposition, with bars of different height in slots etc.), coil windings (with large number of rectangular elementary conductors etc.);
- in order to choose an optimal loss and heating distribution in slots to determine the level of electromagnetic loads of the machine and to identify effective cooling methods;
- to specify methods for the optimal configurations of constructions of polyphase windings with taking into account their features.

This list of problems is in congruence with the content of this chapter.

23.2 Losses and Their Distribution in Bar Stator Windings

23.2.1 Winding Construction Features

Bar stator windings are largely utilized in the practice of electrical machine engineering; generally they are used for large power machines (as a rule, over 3–5 MW). For example, powerful turbine-and water-wheel generators, powerful diesel generators, salient-pole motors are manufactured for various branches of industry—metallurgy, mining, cement etc. In terms of the process-oriented approach manufacturing of bar winding is much more labor intensiveness than that of coil winding. That is why when in practice there is a possibility to manufacture either coil or bar windings, the coil type will be normally chosen. However, while designing unique machines whose maintenance downtimes must be minimum (large power A.C. motors for roll mills, ice-breakers etc.), it should be kept in mind that the bar winding proves to be much less maintenance time consuming. Physical processes of eddy and circulating currents occurrence, their distribution in conductors, computation methods of losses produced by these currents, are closely related to the winding construction features. The following features of bar winding construction are to be mentioned.

1. The bar contains insulated elementary conductors connected in parallel; the length of each elementary conductor makes:

$$L_0 = L_{SLT} + L_S, \tag{23.1}$$

where L_{SLT}, L_S are the length of slot-embedded side and end winding respectively.

Jumper straps between bar elementary conductors are to be placed at winding end parts on either side of the machine.

2. Elementary conductors are transposed along the bar embedded side (along the axis of rotation). In practice the following types of elementary conductor transposition are used in slot-embedded part:

   (a) complete transposition. Its execution is only possible when there is a predetermined combination of bar parameters: number of elementary conductors with bar height, length of stator active part etc.; these parameters must comply with the following criterion [1, 2]:

$$F_0 \le 0.6T_0, \tag{23.2}$$

where $T_0 = \frac{L_{SLT}}{m_B n}$; $F_0 = 2(b_{CON} + a) + 1.73D + 5.36 \times 10^{-3}$; m_B, n—are respectively the number of elementary conductors with bar height and width; b_{CON}—is the width of elementary conductor, a—is the double-sided

thickness of elementary conductor insulation; D—is the thickness of vertical strip in bar between elementary conductors (hereinafter practical units are used in equations: SI system of units).

For a bar with this type of transposition (Fig. 23.1) it is assumed that the machine load current with the amplitude I is uniformly distributed along its conductors in a way that every elementary conductor is flowed by load current of amplitude

$$I_{EL} = \frac{I}{m_B n a_0}, \tag{23.3}$$

where a_0 is the number of winding paths (branches).

This type of transposition is largely applied in electrical machine engineering. In the presentation that follows, unless otherwise specified, it is assumed that a complete transposition of elementary conductors is to be applied while satisfying the conditions of (23.2) and (23.3);

(b) incomplete transposition [17, 20]. It must be performed if it turns out that the condition (23.2) is not met, i.e. $F > 0.6T_0$. Such a configuration is lesser-used in practice as compared to complete transposition. It is used involuntarily when it reveals impossible to perform the complete transposition. For example, in a bar of one of large frequency-controlled motor 7 MW, 12.5 rpm, 6.25 Hz, number of poles 2p = 60 («Elektrosila» Work, Stock Company "Power Machines" St.-Petersburg) all elementary conductors are grouped; each group contains two elementary (t = 2) superimposed conductors as in Fig. 23.2, all groups are transposed between themselves.

We have to remark that the height of a bar with incomplete transposition is somewhat greater than that with complete transposition, the number and sizes of elementary conductors being the same. The load current is uniformly distributed between bar groups; in each group of t conductors flows the current with amplitude

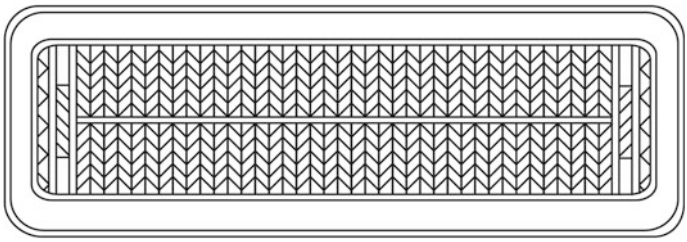

Fig. 23.1 Cross-section of a *bar* with solid elementary conductors (strips are placed in both *bar bases*)

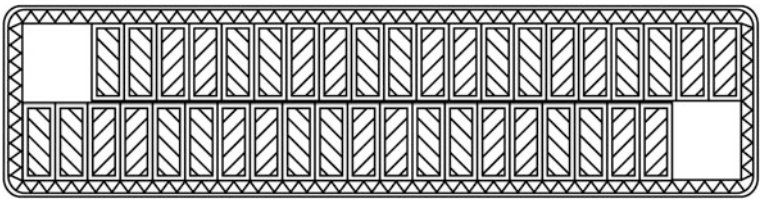

Fig. 23.2 Cross-section of a *bar* with solid elementary conductors (incomplete transposition)

$$I_{EL.GR} = \frac{I}{m_{GR} a_0 n}, \tag{23.3'}$$

where $m_{GR} = \frac{m_B}{t}$, m_{GR}—is the number of groups with bar height.

23.2.2 Sources of Bar Losses: Fundamental Assumptions While Investigating Losses

If a bar primary winding is to be introduced into slots and to make the current with amplitude I and circular frequency ω flow through it, the losses $Q_{A.C.}$ in this winding turn to be larger [3, 4] than those ones $Q_{D.C.}$ at direct current $I_{D.C.}$ flowing around it; in this connection it is assumed that the direct current is of the same effective value that A.C. current ($I_{D.C.} = 0.707I$).

The ratio of losses,

$$K_F = \frac{Q_{A.C.}}{Q_{D.C.}} = 1 + \frac{P_{A.C.}}{Q_{D.C.}} \tag{23.4}$$

is determined by winding parameters and by frequency. Losses $P_{A.C.}$ quantitize the losses increase at alternating current flow around, they are called additional losses, while $Q_{D.C.}$ is called D.C. losses and $Q_{A.C.}$—A.C. losses. K_F is the losses increase factor, or Field's factor [1–7, 20].

The main reason of initiation of additional losses is the slot leakage fluxes that are closed through the tooth, frame yoke and slot space in the tooth zone (Fig. 23.3). They have skin effects in elementary conductors; eddy currents that are resulting from the skin effect play the main role in the value of additional losses $P_{A.C.}$. End part winding leakage fluxes of stator and rotor are also the cause of additional losses occurring in the stator winding. However, as compared to slot leakage fluxes in large scale produced asynchronous and synchronous machines of general purpose application, their influence is not important and in practice they are usually accounted for implicitly. This influence for $Q_{A.C.}$ losses is usually taken into account when dealing with the unique large power electrical machines whose rate

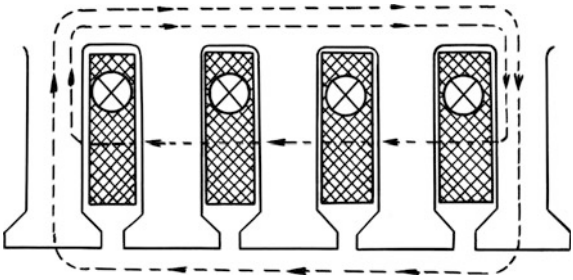

Fig. 23.3 Slot leakage fluxes (number of slots per pole and phase q = 4)

of electromagnetic load is well over that one of asynchronous and synchronous machines of routine production [2].

Several construction measures (transposition in end part etc.) allows a significant reduction of losses from these leakage fluxes. In this section the method of calculation of additional losses in bar windings caused by slot leakage fluxes has been described. The influence of end part coil leakage fluxes on additional losses and the methods of their reduction in large electrical machines is an independent and rather complicated problem related to the development of calculation methods of three-dimensional field. It has been studied in various papers [2–5, 27] etc.

It is common practice to consider a set of assumptions [2–5] at stating the problem related to the calculation of eddy currents and winding losses due to slot leakage flux. They contribute to slightly simplify the solution, but in practice do not introduce any uncertainty on the result. These are the following assumptions:

(a) permeability of steel μ_{FE} in tooth area is taken as $\mu_{FE} = \infty$. For rectangular slot which is of great practical interest, it is assumed that the lines of flux in slot are straight, parallel to its base (Fig. 23.3);
(b) currents of both bars in slots of a double-layer (two-layer) winding with chorded $(\beta < 1)$ or $(\beta > 1)$ lengthened pitches are in phase. In fact, when putting a double-layer winding with $\beta \neq 1$, there are several slots where the both bars belong to different phases; additional losses in bars of such a slot happen to be slightly smaller. This condition may be easily taken into account [1, 5], but in practical calculations it is neglected as a rule and the result is obtained with "some reserve". In practice this is justified because in line with this assumption the influence of end part coil leakage fluxes may be neglected as well.

23.2.3 Problem Setting and Solving Methods

In practice the engineers frequently face the problem of rational choice of stator winding geometry. That is why a clear idea on the features of physical processes in windings with different types of transposition is very important to adopt a proper

solution; insufficiently clear notions of these processes lead sometimes to mistakes that may not always be corrected in practice at the work.

To outline major stages for solving the problem of additional losses and their distribution in double-layer bar winding we shall consider first of all a simple model of a bar with m_B elementary conductors (Fig. 23.1) in height and two elementary conductors in width (n = 2); the transposition is complete.

Let us consider an elementary conductor pth counting from the slot base $(1 \le p \le 2m_B)$. We shall assume that the operational (load) current with amplitude I_{EL} based on (23.3) of this elementary conductor is concentrated in two thin layers BE and CD (Fig. 23.4a) spaced at $h_{EQ} \approx h_{CON}$ (counting along the slot center line); here h_{CON} is the height of elementary conductor. Then the current amplitude in each layer is:

$$I'_{EL} = I_{BE} = I_{CD} = 0.5I_{EL}. \qquad (23.3'')$$

As a result, we replaced an elementary conductor by an equivalent contour BCDE (Fig. 23.4b). In this contour equivalent parallel D.C. resistances of parts BE and CD connected in parallel are equal to:

$$R_{BE} = R_{CD} = \frac{2L_0}{h_{CON} b_{CON} n\sigma} = 2R_{(P)},$$

where σ—is the specific conductivity of elementary conductor, n—is the number of elementary conductors in slot width, b_{CON}—is the width of elementary conductor, h_{CON}—is the height of elementary conductor; $R_{(P)}$—is the D.C. resistance of elementary conductor.

In Fig. 23.4b except for geometric sizes are shown amperemeters A_1, A_2, A_3, A_4 and two keys K. They are presented to outline the difference between the physics of operational and eddy currents. An effective value of operational current $(0.707I_{EL})$ at closed keys K corresponds to the readings of amperemeter A_1 (in circuit section

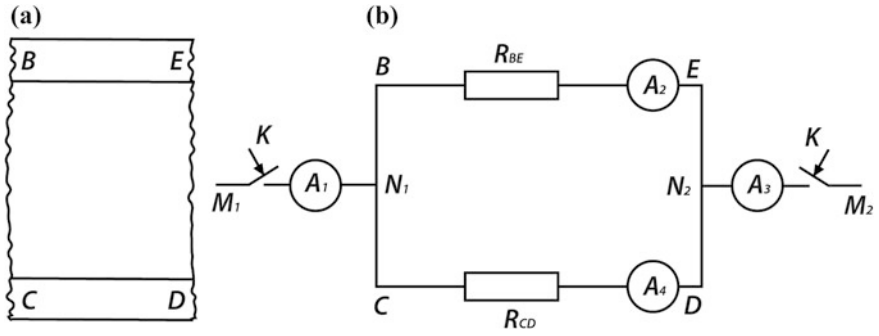

Fig. 23.4 Equivalent concept scheme of eddy currents circulation in elements I′ and I″ of hollow elementary conductor

M_1N_1) and A_3 (in circuit section M_2N_2); the both sections correspond to end part of bars with elementary conductors. In BE and CD circuit sections flows the current I_0, it has two components:

(a) current which is proportional to the machine load current; its amplitude is equal to I'_{EL};
(b) eddy current L_{ED} induced by slot leakage flux, which embraces the contour BCDE:

$$\Phi_P = \Phi_{MUT} + \Phi_S. \tag{23.5}$$

The flux Φ_{MUT} is specified by currents in all conductors $n(p-1)$ arranged below that one under investigation counting from the slot base. This is a mutual flux:

$$\Phi_{MUT} = \mu_0 I_{EL}(p-1)n\lambda_{MUT}, \tag{23.6}$$

where μ_0 is the air permeability, λ_{MUT} is the conductivity for mutual fluxes.

The flux Φ_S is determined by the proper current of pth elementary conductor and is the flux of self-inductance:

$$\Phi_S = \mu_0 I'_{EL} n\lambda_S, \tag{23.7}$$

where λ_S is the conductivity for self-inductance fluxes.

Now we shall note that when considering finite sizes of solid elementary conductor $\lambda_{MUT} \neq \lambda_S$.

Using Maxwell's equation [3, 4], the complex amplitude of eddy current I_{ED} is given by,

$$I_{ED} = -\frac{j\omega\Phi_P}{2R_{BE}} = f\left(I'_{EL}\right), \tag{23.8}$$

where ω is the current circular frequency, $j = \sqrt{-1}$.

Taking into account that eddy currents flow in a closed contour BCDE we shall have for the complex amplitude of resulting current I_0:

for BE section: $I_0 = I'_{EL} - I_{ED}$;
for CD section:

$$I_0 = I'_{EL} + I_{ED}. \tag{23.9}$$

It should be noted that an effective value of eddy current I_{ED} induced by mutual flux corresponds to the readings of amperemeters A_2 and A_4 at open keys; at that, it is assumed that the current I_{EL} according to (23.3) flows through each of remaining elementary conductors $n(p-1)$.

An effective value of resulting current on sections BE and CD is equal to:

$$I_{0,EFF} = 0.707\sqrt{\left|I'_{EL}\right|^2 + |I_{ED}|^2}.$$

This value of resulting current corresponds to the readings of amperemeters A_2 (on section BE) and A_4 (on section CD) at closed keys K.

The losses on sections BE and CD at their flow around by direct current $I_{D.C.}$ $\left(\text{at } I_{D.C.} = 0.707\left|I'_{EL}\right|\right)$ are given by,

$$Q_{D.C.(BE)} = Q_{D.C.(CD)} = 0.5\left|I'_{EL}\right|^2 R_{BE} = \left|I'_{EL}\right|^2 R_{(P)}. \tag{23.10}$$

The losses on the same sections BE and CD at their flow around by the current I_0 are equal to:

$$\begin{aligned} Q_{A.C.(BE)} = Q_{A.C.(CD)} &= 0.5|I_0|^2 R_{BE} = 0.5\left(\left|I'_{EL}\right|^2 + |I_{ED}|^2\right)R_{BE} \\ &= \left(\left|I'_{EL}\right|^2 + |I_{ED}|^2\right)R_{(P)}, \end{aligned} \tag{23.11}$$

at that, $Q_{A.C.(BE)} = Q_{D.C.(CD)} + P_{A.C.(BE)}$, where $Q_{D.C.(BE)}$ following (23.10),

$$P_{A.C.(BE)} = |I_{ED}|^2 R_{(P)}. \tag{23.11'}$$

Thus, the increase in losses of pth elementary conductor is

$$\begin{aligned} K_{(P)} &= \frac{Q_{A.C.(P)}}{Q_{D.C.(P)}} = \frac{\left|Q_{A.C.(BE)} = Q_{A.C.(CD)}\right|}{\left|Q_{D.C.(BE)} = Q_{D.C.(CD)}\right|} \\ &\equiv \frac{\left(2\left|I'_{EL}\right|^2 + |I_{ED}|^2\right)R_{(P)}}{2\left|I'_{EL}\right|^2 R_{(P)}} = 1 + 4\frac{|I_{ED}|^2}{|I_{EL}|^2} \neq f(I_{EL}), \end{aligned} \tag{23.12}$$

where $Q_{A.C.(P)}, Q_{D.C.(P)}$—are losses of pth elementary conductor at its flow around by respectively alternating and direct currents.

The losses increase factor for all p elementary conductors in the slot height ($p = 1, 2, \ldots, 2m_B$) is given by,

$$K_F = \frac{K_{(P=1)} + K_{(P=2)} + \cdots}{2m_B}. \tag{23.13}$$

Now let us summarize the results:

- eddy current of each pth elementary conductor is specified not only by its proper operational current, but also by the operational current of other elementary conductors $n(p - 1)$ in the slot, if we count from its base. This current flows

through pth elementary conductor if it is not even conductively coupled to other elementary conductors n(p − 1) flowed around by load current;

- to calculate eddy currents and losses in pth elementary conductor it will be necessary to find slot leakage fluxes Φ_{MUT} and Φ_S engaged with this elementary conductor.

In the context of what is said above, the problem of losses calculation in the bar may be formulated in the following way.

Let it be given: type of transposition, amplitude of bar operational current I, current circular frequency ω, number and sizes of elementary conductors in slot, number of allocated bars in slot.

It is required to calculate losses in each of slot bars.

From relation (23.12) it follows that to do so it is necessary to find the distribution of eddy currents in an elementary conductor.

Thus being formulated and taking into account the assumptions given in Sect. 23.2.2, the problem may be solved by using a number of analytical and numerical methods.

Usually analytical solutions are based on a set of Maxwell's equations in a differential form which is to be reduced to Helmholtz equation (as a rule one- or two-dimensional [3, 4, 8, 9]); the result of such a solution will be the distribution of complex amplitudes of electric E_M and magnetic H_M magnetic-field strength in height and width of each pth elementary conductor. This solution method is, however, more appropriate for the calculation of A.C. resistance and impedances of solid rectangular bar of the rotor of asynchronous motor. For modern constructions of stator bars, for example with elementary conductors performed with complete or incomplete transposition where besides solid there are hollow elementary conductors, its application results in compound analytical ratios; the features of physical processes are lost to a great extent [28] when the problem is solved by this method. For bars with incomplete transposition by using this method it will be required to solve a more complicated differential equation than that one for complete transposition.

It should be also noted that the use of a set of Maxwell's equations in differential form the current flowing through an elementary conductor is not divided into operational and eddy currents, as it was shown in Sect. 23.2.3: complex amplitudes of E_M and H_M characterize the distribution of resulting current with elementary conductor height [3, 4]. However, in engineering practice such integral notions as "current", "voltage", "EMF", "impedance of circuit section" are used much more frequently than the notion of "complex amplitude of magnetic field"; this may be explained by the fact that integral values are easier to be measured.

In this section it is shown that for elementary conductors of bar winding irrespective of their geometry and bar construction (with solid, hollow, combined, i.e. hollow and solid, elementary conductors) as well as irrespective of the type of transposition (complete or incomplete), the losses and their distribution may be investigated by a general analytical method with the use of integral notions given above. The method does not require any additional assumptions to be introduced,

except for those listed in Sect. 23.2.2, it differs by the clarity of physical notions and results in simple equations obtained in a closed form. Initially the method [10, 29] was used for solid elementary conductors in bar at their complete transposition. Further on, it was developed as applied to the types of modern bar winding constructions: with solid elementary conductors at their incomplete transposition [17, 22] with hollow [8, 9, 30] and combined (hollow and solid) elementary conductors [20–22] at their complete transposition. The results of solution applied constructions of winding mentioned above are understood as particular cases of unique general problem solution; if this is the case of incomplete transposition, there is no need to complicate equations used for investigation of bars with complete transposition.

The method suggests a number of stages to determine eddy currents and losses in elementary conductors. To calculate them it will be necessary to find:

- mutual and self-inductance fluxes; they are determined following the Ampere's law [3, 4] on the basis of operational current, i.e. load current.

The same is done in our case study in Fig. 23.4. At closed keys K starting with operational current I_{EL} in circuit sections M_1N_1 (amperemeter A_1) and M_2N_2 (amperemeter A_2) we determined mutual and self-inductance fluxes Φ_{MUT} and Φ_S following (23.6) and (23.7) to an accuracy of conductivities λ_{MUT} and λ_S;

- eddy currents in each elementary conductor on the basis of found mutual and self-inductance fluxes.

This was done in our study case. Relying on fluxes Φ_{MUT} and Φ_S according to (23.6) and (23.7) we specified the current I_{ED} according to (23.8) in circuit sections BE and CD of loop contour BCDE;

- resulting currents in each elementary conductor; they are to be specified by superposition of operational and induced eddy currents.

This was performed in our study case. In terms of currents I'_{EL} and I_{ED} according to (23.3″) and (23.8) we determined the current I_0 following (23.9) in circuit sections BE and CD of loop contour BCDE;

- refined value of leakage fluxes; it is determined according to the Ampere's law [3, 4] on the basis of resulting current in each elementary conductor and not of operational current as in first iteration.

This refinement was not required to do in our study case due to reasons stated below [see (23.14)];

- losses in terms of found current distributions on elementary conductors cross-section.

This was done in our study case. On the basis of currents I_0, I'_{EL} and I_{ED} we calculated losses $Q_{A.C.}, P_{A.C.}$ following (23.10)–(23.11′) and the factor K_F according to (23.13).

With the use of a set of iterations by the way of reiterating stages mentioned above there are set such values of eddy currents for which their further refinement does not practically lead to losses value changing in elementary conductors. Thus, we obtain the convergence (with a given accuracy) of iterative process of eddy current calculation.

We note that to estimate the field intensity of skin effects in conductor [3, 4] in practical calculations the notion of "reduced height" $K'h_{CON}$ of elementary conductor is to be used, where

$$K' = \sqrt{\frac{\omega \mu_0 \sigma \, b_{CON} n}{2 b_{SLT}}};$$

in [10] it was shown that in case of

$$K'h_{CON} < 1 \tag{23.14}$$

an adjusted distribution of fluxes and currents is not required to be determined. This is a substantial simplification of iterative method: it shall be sufficient to determine eddy currents in each elementary conductor on the basis of operational current only, i.e. upon the results of the first iteration step.

As far as it concerns the sizes of solid copper conductors mostly used in practice, Eq. (23.14) remains true for frequencies up to 650 Hz, while for hollow copper conductors—up to 350 Hz and for hollow steel conductors—up to 7500 Hz.

We note that the eddy current calculated upon the first iteration step is shifted according to (23.5)–(23.8) with respect to the operational current by 90° el. That is why eddy and load current losses may be calculated according to (23.10)–(23.11′) separately. In particular, additional losses $P_{A.C.}$ in bar shall be determined using (23.11′) only by eddy currents in its elementary conductors and by its D.C. resistance.

Note. In conclusion we turn our attention to one further practical pecularities based on investigated physical process of current initiation in winding elementary conductors induced by cross slot leakage flux. In multipole machines with coil winding in case of slot insulation failure, the coil may be sometimes left in slot, but excluded of remained coils in phase, thus creating in one of phase zones a certain asymmetry. If in addition the insulation of some elementary conductors reveals to be damage as well, on the basis of what was said in this section it will follow that the coil elementary conductors are flowed through, even if this coil is excluded of remaining coils of phase zone. Overheats of this type of coils with closed between themselves elementary conductors may be inadmissible. The same is true if the insulation of elementary conductors is damaged in winding bar, not in coil.

23.2.4 General Problem of Eddy Currents and Losses Calculation in Elementary Conductors of the Bar

Now we shall consider a bar made of transposed elementary conductors. Each elementary conductor shall be presented in the form of two elements I′ and I″ spaced at a distance (see Fig. 23.5); electrically the both elements (sections) of this conductor are connected in parallel.

Structurally we may imagine that the elements I′ and I″ are kept at this distance, for example with the help of non-conducting strip. Both elements are not transposed between themselves. Just this condition is the support of common grounds of the general problem:

- at a = 0 it is reduced to the problem with transposed solid conductors in bar;
- at a ≠ 0 but in the case of connecting the both elements I′ and I″ with the help of elements II and III (Fig. 23.5) it is reduced to the problem with hollow conductors in bar;
- at a ≠ 0 but in the case when each element is insulated, it is reduced to the problem with solid conductors at their incomplete transposition [Eq. (23.3′) at t = 2]; here a is the double-sided insulation thickness of elementary conductor; the elements II and III are not available.

Here we shall find eddy currents and losses in bar with elements (sections) I′ and I″.

The both elements placed on the slot bottom (p = 1) and in the second layer (p = 2) are given in Fig. 23.6. The fundamental difference of processes at p = 1 and p = 2 is that at p = 1 eddy currents are induced in conductor sections only by self-induction fluxes, while at p = 2 they are induced both by self- and mutual induction fluxes.

Let us consider the origin of coordinates at the base of each of both sections, so as $Y \leq h_1$, where h_1 is the height of elementary conductor section. The slot field intensity shall be specified following the Ampere's law [3, 4] with account made for assumptions adopted in Sect. 23.2.2.

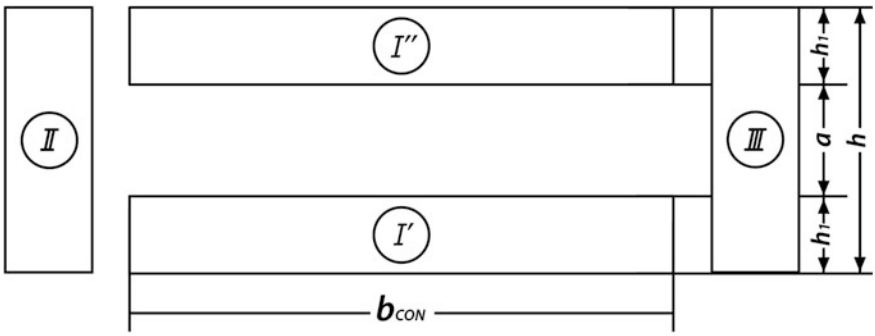

Fig. 23.5 Subdivision of elementary conductor into calculable elements (I′ and I″, II, III)

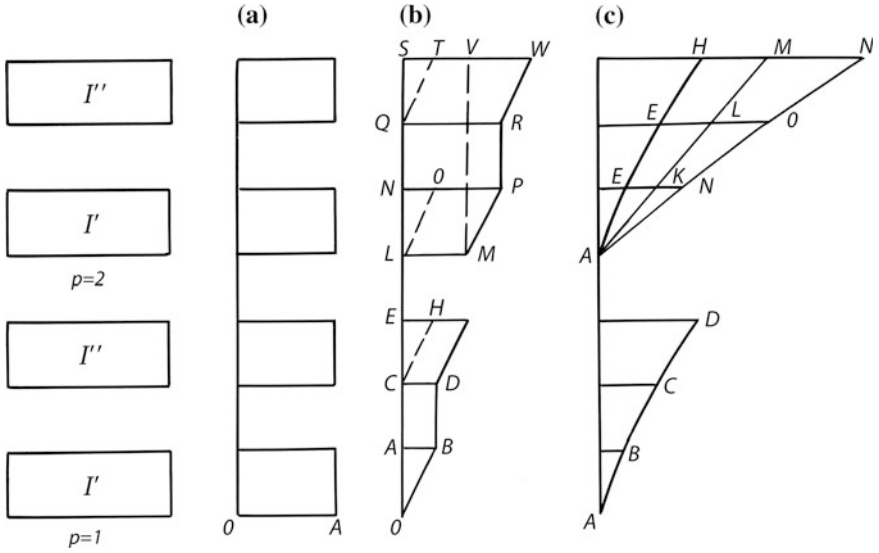

Fig. 23.6 Distribution with height of conductor sections I′ and I″: **a** load current, **b** flux density and **c** leakage flux

The intensity of self-induction field in the slot is obtained:

section I′

$$H'_S = \frac{Jb_{CON}nY}{b_{SLT}}; \tag{23.15}$$

section I″

$$H''_S = \frac{Jb_{CON}(h_1 + Y)}{b_{SLT}}, \tag{23.15'}$$

where J is the density of operational (load) current. $J = \frac{I_{EL}}{S_{MS}}$, where I_{EL} is the load current in elementary conductor according to (23.3); $S_{MS} = 2h_1b_{CON}$ is the cross-section of elementary conductor.

The distribution of self-induction flux with height of conductor sections (per length unit) is the following:

section I′

$$\Phi'_S = \frac{\mu_0 Jb_{CON}nY^2}{2b_{SLT}}; \tag{23.16}$$

section I″

$$\Phi'_S = \frac{\mu_0 J b_{CON} n\left(Yh_1 + 0.5Y^2 + ah_1 + 0.5h_1^2\right)}{b_{SLT}}. \qquad (23.16')$$

Figure 23.6a illustrates the distribution of load current density J with height; here OA ≠ f(Y). Figure 23.6b shows the distribution of leakage field intensity with height of elementary conductor sections I′ and I″ at p = 1; the line OB corresponds to Eq. (23.15) and DK—to (23.15′); the line CH also corresponds to Eq. (23.15); when fitting this line, it is assumed that there is no current in I′ section. The distribution of slot leakage flux is given in Fig. 23.6c; a section of parabolic curve AB corresponds to Eq. (23.16) and section CD—to (23.16′).

Now we shall find the components of eddy currents induced by self-induction flux.

It is evident that the eddy currents flowing on sections I′ and I″ must satisfy the following equation

$$\int_0^{h_1} J''_S dY + \int_0^{h_1} J'_S dY = 0, \qquad (23.17)$$

where J''_S, J'_S are eddy current densities respectively on sections I″ and I′.

A similar ratio has been obtained above for BCDE contour, where eddy currents on sections BE and CD were written in Eq. (23.9) as opposite in sign; they add up to zero (Fig. 23.4, amperemeters A_2 and A_4, open keys K).

Figure 23.7a illustrates the distribution of eddy current density J''_C and J'_C. The equality of areas OBNPO = RSMQR corresponds to Eq. (23.17). From this follows the position of neutral point OP ensuring the equality of these areas

$$OP = \frac{\omega \mu_0 \sigma J b_{CON} n h_1 (a + 1.33h_1)}{2b_{SLT}}$$

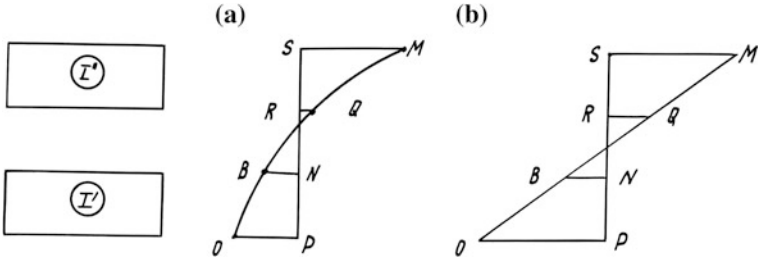

Fig. 23.7 Distribution of eddy current components with height of elements I′ and I″: **a** from self-induction flux and **b** from mutual flux

Taking into account this equation for the density of eddy current induced by self-induction flux, we obtain the following:

section I′

$$J'_S = \frac{j\omega\mu_0\sigma J b_{CON} n\left(Y^2 - ah_1 - 1.33_1^2\right)}{2b_{SLT}}; \tag{23.18}$$

section I″

$$J''_S = \frac{j\omega\sigma\mu_0 J b_{CON} n\left(Y^2 + 2Yh_1 + ah_1 - 0.33h_1^2\right)}{2b_{SLT}}. \tag{23.18′}$$

In Fig. 23.7a a part of parabolic curve OB corresponds to (23.18) and QM—to (4.18′).

Now we shall consider a slot mutual flux. It is determined by the current of all elementary conductors n(p − 1) arranged under investigated one counting from the slot base. The intensity of mutual inductance field in the slot with height of both elements I′ and I″ remains constant:

section I′

$$H_{MUT} = \frac{J b_{CON} n(p-1)2h_1}{b_{SLT}}. \tag{23.19}$$

The distribution of mutual flux with height of conductor sections (per length unit) is given by the following:

section I′

$$\Phi'_{MUT} = \frac{\mu_0 J b_{CON} n(p-1)2Yh_1}{b_{SLT}}; \tag{23.20}$$

section I″

$$\Phi''_{MUT} = \frac{\mu_0 J b_{CON} n(p-1)2h_1(Y + a + h_1)}{b_{SLT}}. \tag{23.20′}$$

In Fig. 23.6b we show the distribution of leakage field intensity with height of conductor sections I′ and I″ at $p \geq 2$ (mutual flux); the parts of a straight line MV correspond to (23.19). In Fig. 23.6c a part of AK line corresponds to (23.20) and of LM line—to (23.20′).

The components of eddy current induced by mutual flux are to be determined in the same way as for the components induced by self-induction flux, here Eq. (23.17) is also valid for it.

Figure 23.7b shows the distribution of eddy current density J_{MUT}. The equality of area OBNPO = RSMQR corresponds here to the equation identical to (23.17). In a similar way, the position of neutral point may be obtained from the following:

$$OP = \frac{\omega\mu_0\sigma J b_{CON} n(p-1)h_1(a+2h_1)}{b_{SLT}}. \tag{23.21}$$

Taking into account this equation for the density of eddy current induced by mutual flux we have:

section I′

$$J'_{MUT} = -j\omega\mu_0\sigma J b_{CON} n(p-1)\frac{\left(4Yh_1 - 2ah_1 - h_1^2\right)}{2b_{SLT}}; \tag{23.22}$$

section I″

$$J''_{MUT} = -j\omega\mu_0\sigma J b_{CON} n(p-1)\frac{4Yh_1 + 2ah_1}{2b_{SLT}}. \tag{23.22'}$$

In a general case the eddy current is determined as self- and mutual induction flux (see Fig. 23.6c, parts AN_1 and ON_2). In this case the equation of eddy current density may be written in the following form:

section I′

$$\begin{aligned} J'_{ED} &= J'_S + J'_{MUT} \\ &= -j\mu_0\omega\sigma J b_{CON} n\left[\frac{Y^2 - ah_1 - 1.33h_1^2 + (p-1)\left(4Yh_1 - 2ah_1 - 4h_1^2\right)}{2b_{SLT}}\right], \end{aligned} \tag{23.23}$$

section I″

$$\begin{aligned} J''_{ED} &= J''_S + J''_{MUT} \\ &= -j\omega\mu_0\sigma J b_{CON} n\left[\frac{Y^2 + 2Yh_1 + ah_1 - 0.33h_1^2 + (p-1)(4Yh_1 + 2ah_1)}{2b_{SLT}}\right]. \end{aligned} \tag{23.24}$$

Equations for J'_{ED} and J''_{ED} contain two terms, where the first does not depend on the number of elementary conductors in the slot and the second corresponding to mutual flux is proportional to (p – 1).

To estimate additional losses, we shall use equations identical to (23.11) and (23.11′) where

$$P_{A.C.} = 0.5\left(b_{CON}\frac{n}{\sigma}\right)\left[\int_0^{b_1}\left|J'_{ED}\right|^2 dY + \int_0^{b_1}\left|J'_{ED}\right|^2 dY\right]. \tag{23.25}$$

According to (23.23) and (23.24) the equation for $P_{A.C.}$ contains three terms; one of them does not depend on $(p-1)$, the second is proportional to $(p-1)$ and the third, $(p-1)^2$.

As the whole, the equation to calculate the losses increase factor in pth conductor is given by based on (23.4):

$$K_{(P)} = 1 + (K')\left\{\left[1.42h_1^4 + a^2h_1^2 + 2ah_1^3\right] + (p-1)^2\left[5.33h_1^4 + 4a^2h_1^2 + 8ah_1^3\right] + (p-1)\left[5.33\ h_1^4 + 4a^2h_1^2 + 8ah_1^3\right]\right\}, \tag{23.26}$$

where K' is obtained according to (23.14).

Now we shall find the losses increase factor K_F for all elementary conductors in slot; their number with height is $m = 2m_B$. Following (23.13) it is equal to $(1 \le p \le m)$:

$$K_F = \frac{K_{(p=1)} + K_{(p=2)} + \cdots + K_{(p=m)}}{m}. \tag{23.27}$$

Let us use the following relations known from mathematics [8]:

$$1 + 4 + 9 + \cdots + (m-1)^2 = \frac{m(m-1)(2m-1)}{6};$$
$$1 + 2 + 3 + \cdots + (m-1) = 0.5m\,(m-1).$$

Then, from Eq. (23.27) we have for K_F

$$K_F = 1 + (K')^4\left[1.42h_1^4 + a^2h_1^2 + 2ah_1^3 + \frac{(m^2-1)\left(5.33h_1^4 + 4a^2h_1^2 + 8ah_1^3\right)}{3}\right]. \tag{23.28}$$

We have to notice that additional losses in elementary conductor sections (I', I'') may also be calculated approximately, if we proceed only from slot mutual fluxes (23.20), (23.20′) and from the density of eddy currents induced by them (23.22), (23.22′). This makes easier to establish calculation equations. Then for all elementary conductors in the slot we have:

$$K_F = 1 + (K')^4 \frac{(m-1)(2m-1)\left(5.33h_1^4 + 4ah_1^2 + 8h_1^3\right)}{6}. \quad (23.29)$$

At $m \to \infty$ Eqs. (23.28) and (23.29) coincide.
Here let us consider particular cases of this problem.

23.2.5 *Bars with Solid Conductors (Complete Transposition): Calculation Example*

We use the results of general problem solution and calculation equations obtained in Sect. 23.2.4 for losses increase factors as applied to the bar construction with solid elementary conductors.

From Eqs. (23.26)–(23.29) we have at a = 0; $2h_1 = h_{CON}$;

(a) for an elementary conductor pth counting from the slot base

$$K_{(P)MS} = 1 + (K'h_{MS})^4[0.09 + 0.333(p-1)^2 + 0.333(p-1)]; \quad (23.30)$$

(b) for all elementary conductors m with slot height [1, 3–5, 20]:

$$K_{F,MS} = 1 + (K'h_{MS})^4\left[0.09 + 0.111(m^2-1)\right]. \quad (23.31)$$

If when calculating losses we consider only mutual fluxes in the slot and densities of eddy currents induced by them, the equation for $K_{F,MS}$ shall take the form:

$$K_{F,MS} = 1 + (K'h_{MS})^4 \frac{(m-1)(2m-1)}{18}. \quad (23.32)$$

Calculation example

There are two bars arranged in the stator slot, each of them contains with height 14 solid elementary conductors transposed between themselves (m = 28). The sizes of elementary conductors and slot width are: $h_{MS} = h_{CON} = 2.5$ mm; $b_{MS} = b_{CON} = 6.5$ mm; $b_{SLT} = 19.5$ mm; n = 2. The machine is operated from the network with sources of non-sinusoidal voltage; the fundamental frequency (g = 1) is f = 43.5 Hz. Let us determine $K_{F,MS}$ for g = 1, g = 5, g = 7.

Solution

For $\sigma = 50 \times 10^6$ S/m we have bassed on (23.14) $K'h_{CON} = 0.189\sqrt{g}$.
For g = 1 we have according to (23.31) and (23.32):

Table 23.1 Results for losses increase factor in a bar with solid conductors (g = 1, g = 5, g = 7)

g	According to (23.31)	According to (23.32)	Error
1	1.111	1.106	0.9950
5	3.790	3.640	0.9600
7	6.462	6.180	0.9560

$$K_{F,MS} = 1 + (0.189)^4[0.09 + 0.111(28^2 - 1)] = 1.111;$$
$$K_{F,MS} = 1 + (0.189)^4 \frac{(28-1)(2 \cdot 28 - 1)}{18} = 1.106. \quad (23.33)$$

Results for g = 1, g = 5, g = 7 are given in Table 23.1. In table the error has been calculated as the ratio of factor $K_{F,MS}$ values obtained following formula (23.32) and (23.31).

It follows from Table 23.1 that even at frequency f ≈ 300 Hz (at g = 7) the error of additional losses calculation does not exceed 5 % with account made of the action of mutual flux only, it is practically admissible.

23.2.6 *Bars with Hollow Conductors (Complete Transposition): Calculation Example*

Now we shall use the results of general problem solution and the design data obtained in Sect. 23.2.4 as applied to the bar construction with hollow conductors. In a hollow elementary conductor (Fig. 23.5) the sections (I', I'') are connected in parallel not only at bar ends (strips in bar heads) but by elements II and III in slot parts. Additional losses for these solid elements shall be calculated on the basis of relations (23.31)–(23.32). D.C. losses in the hollow conductor $Q_{D.C.}$ (losses at direct current flowing around elementary conductor) shall be defined per length unit in a regular manner:

$$Q_{D.C.} = \frac{|J|^2 n S_H}{2\sigma},$$

where $S_H = h_H b_H - a_{CAN} - b_{CAN}$—is the hollow conductor section, h_H—is the hollow conductor height; a_{CAN}, b_{CAN}—are respectively channel height and channel width (Fig. 23.8).

Upon many transformations with allowance for this equation, we shall have for $K_{F,H}$ [20, 30–32]:

(a) for a hollow elementary conductor pth counting from slot base:

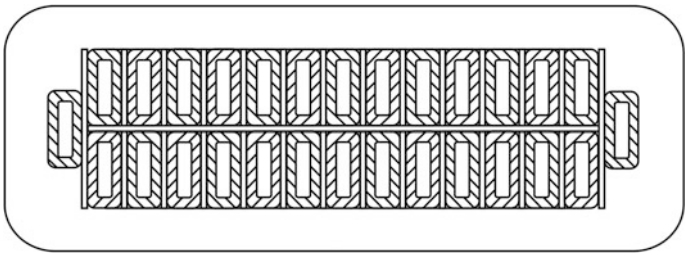

Fig. 23.8 Cross-section of a *bar* with hollow elementary conductors

$$K_{(P)H} = 1 + (K'h_H)^4 \left[0.09 + 0.333(p-1)^2 + 0.333(p-1)\right] \frac{S_H}{S_{H,CONT}} T, \tag{23.34}$$

(b) for all slot elementary conductors m with height

$$K_{F,H} = 1 + (K'h_H)^4 \left[0.09 + 0.111(m^2-1)\right] \frac{S_H}{S_{H,CONT}} T, \tag{23.35}$$

where K'—according to (23.14); factor $T = 1 - \left(\frac{a_{CAN}}{h_H}\right)^3 \frac{b_{CAN}}{b_H}$ characterizes the geometry of a hollow elementary conductor; $S_{H,CONT} = h_H b_H$ is the space occupied by the hollow conductor, where $S_H = h_H b_H - a_{CAN} b_{CAN}$—is the hollow conductor section, h_H—is the hollow conductor height; a_{CAN}, b_{CAN}—are respectively channel height and channel width.

If in the calculation of losses one considers only mutual fluxes in the slot and densities of eddy currents induced by them, the equation for $K_{F,H}$ becomes:

$$K_{F,H} = 1 + (K'h_H)^4 (m-1)(2m-1) \frac{S_H}{S_{H,CONT}} \frac{T}{18}. \tag{23.36}$$

Calculation example

There are two bars placed in stator slot, each of them contains with height 7 hollow elementary conductors transposed between themselves (m = 14). The sizes of elementary conductor and slot are $h_H = 5$ mm, $b_H = 6.5$ mm; n = 2; $a_{CAN} = 2$; $b_{CAN} = 3.5$ mm, $b_{SLT} = 19.5$ mm. The machine is operated from the network having sources of non-sinusoidal voltage; the fundamental frequency (g = 1) is f = 43.5 Hz. Let us determine $K_{F,H}$ for g = 1, g = 5, g = 7.

Solution

For $\sigma = 50 \times 10^6$ S/m we have according to (23.14): $K'h_H = 0.378\sqrt{g}$;

Using (23.34) and (23.35):

$$\frac{S_H}{S_{H,CONT}} = \frac{6.5 \cdot 5 - 2 \cdot 3.5}{32.5} = 0.785,\ T = 1 - \left(\frac{a_{CAN}}{h_H}\right)^3 \frac{b_{CAN}}{b_H} = 1 - \left(\frac{2}{5}\right)^3 \frac{3.5}{6.5} = 0.966.$$

For g = 1 we have according to (23.35):

$$K_{FH} = 1 + (K' h_H)^4 \left[0.09 + 0.111\left(m^2 - 1\right)\right] \frac{S_H}{S_{H,CONT}} T = 1 + 0.378^4 \left[0.09 + 0.111\left(14^2 - 1\right)\right] 0.785 \cdot 0.966 = 1.336.$$

Following Eq. (23.36):

$$K_{F,H} = 1 + (K' h_H)^4 (m - 1)(2m - 1) \frac{S_H}{S_{H,CONT}} \frac{T}{18} = 1 + 0.378^4 (14 - 1)(2 \cdot 14 - 1) \frac{0.785 \cdot 0.966}{18} = 1.302.$$

Results for g = 1, g = 5, g = 7 are given in Table 23.2. In the table the error has been calculated as the ratio of factor $K_{F,H}$ values obtained following the formula (23.36) and (23.35).

It follows from Table 23.2 that even at the frequency f ≈ 300 Hz (at g = 7) the error of additional losses calculation does not exceed 10 % with account of the action of mutual flux only, it is practically admissible.

Note. Two examples given above (Tables 23.1, 23.2) are interesting not only as illustrations of calculation of additional losses in solid and hollow elementary conductors. It is not difficult to note that in the example of Sect. 23.2.5 solid elementary conductors are placed practically in the same slot that hollow elementary conductors in the example given in Sect. 23.2.6. At that, the factors $K_{F,MS}$ are substantially smaller both for fundamental (g = 1) and higher (g > 1) harmonics; the error of calculation following approximate Eq. (23.32) has been reduced.

Here we shall estimate the level of A.C. losses cutting down in the slot part of both bars in the case of hollow conductors replacement by solid.

The A.C. losses for both bar constructions correlate in the following way (at alternating current of the same amplitude flowing around):

Table 23.2 Results for losses increase factor in a bar with hollow conductors (g = 1, g = 5, g = 7)

g	According to (23.35)	According to (23.36)	Error
1	1.336	1.302	0.975
5	9.40	8.55	0.910
7	17.46	15.8	0.905

$$\frac{Q_{A.C.,MS}}{Q_{A.C.,H}} = \frac{K_{F,MS}}{K_{F,H}} \frac{n_H m_H S_H}{n_{MS} m_{MS} S_{MS}}, \tag{23.37}$$

where n_{MS}, n_H—are respectively numbers of elementary conductors with slot width having solid and hollow elementary conductors; m_{MS}, m_H—idem with slot height; S_{MS}, S_H—are respectively sections of solid and hollow elementary conductors.

At g = 1 for two investigated bar constructions we have the following:

$$\frac{Q_{A.C.,MS}}{Q_{A.C.,H}} = \frac{\frac{1.111}{28 \cdot 16.25}}{\frac{1.336}{14 \cdot 25.5}} = 0.653.$$

Such a substantial reduction in A.C. losses in bars is obtained not only due to Field's factor reduction $\left(\frac{1.111}{1.336} = 0.832\right)$ but also due to a considerable increase in total cross section of solid elementary conductors in the slot as compared to hollow elementary conductors $\frac{28 \cdot 16.25}{14 \cdot 25.5} = 1.274$, i.e. due to the reduction of D.C. resistance of a bar with solid elementary conductors and due to overall losses cutting down.

From this example it follows that the use of hollow elementary conductors instead of solid ones is connected not only with the increase of additional but of D. C. losses as well. Their use in first constructions of stator winding of high-voltage turbogenerators with direct cooling has practically resolved the problems related to winding heat. In first constructions of windings with such elementary conductors either oil—dielectric (turbogenerator of 260 mVA of GE Company, USA) or distilled water (turbogenerators of 37.5 mVA of Metro Vickers Company, UK and of «Elektrosila» Work, Stock Company "Power Machines", Russia) have been used as cooling medium. The operation of the above machines has shown that within the constraints imposed by winding overheating, a more efficient bar construction may be used while utilizing both solid and hollow elementary conductors (see Sect. 23.2.8). This circumstance has led to the construction of bar winding with combined elementary conductors. At present it is largely used for other types of machines.

23.2.7 Bars with Incomplete Transposition: Calculation Example

23.2.7.1 Currents Induced by Slot Leakage Fluxes

Let us examine the problem of additional losses calculation in bars with incomplete transposition of solid elementary conductors. We shall assume that the number of elementary conductors in the group t = 2; this type of construction is of great practical interest. To investigate the losses in such a construction it should be

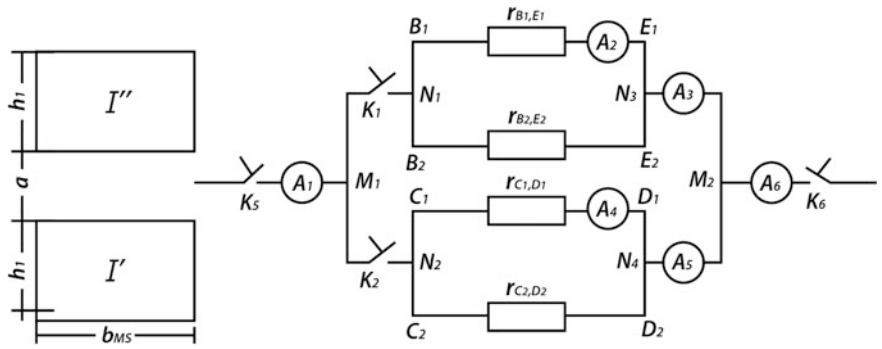

Fig. 23.9 Circuit equivalent diagram of eddy currents circulating in elementary conductors I′ and I″ of slot group of a *bar* with incomplete transposition

appropriate to use the results of investigations carried out in Sect. 23.2.4 where the general problem of losses calculation in sections I′ and I″ of elementary conductor has been preliminarily solved.

In investigated problem these elements I′ and I″ may be considered as both insulated elementary conductors of slot group (at t = 2); the insulation is double-sided in thickness a. If each elementary conductor has such an insulation (Fig. 23.9), the current induced by leakage flux in contour formed by both conductors of group is shorted only through end part. Consequently, it passes not only in slot zone but in end part of every elementary conductor.

To have a conceptual idea on eddy currents initiation in the group containing t elementary conductors, we shall replace each of them by two filaments with current in the same manner as it was done in Sect. 23.2.3.

In Fig. 23.9 its sections B_1E_1 and B_2E_2 correspond to slot part of one elementary conductor and sections C_1D_1 and C_2D_2—of the second one. Sections M_1N_1 and M_2N_2 correspond to both end parts of first elementary conductor and M_1N_2 and M_2N_4—of the second one. The slot leakage flux is embraced by the contour $B_1C_2D_2E_1B_1$ of slot part of a bar. The following current components flow through the sections of M_1M_2:

(a) through sections $M_1B_1E_1M_2$ and $M_1B_2E_2M_2$ of first elementary conductor and through $M_1C_1D_1M_2$ and $M_1C_2D_2M_2$ of second elementary conductor passes the current which is proportional to the machine load current according to (23.3). An effective value of this current corresponds to the readings of amperemeters A_1 and A_6;

(b) in contours $B_1B_2E_2E_1$ of first elementary conductor and in $C_1C_2D_2D_1$ of the second one flow local eddy currents; they are shorted within the slot part of each elementary conductor of group. When opening keys K_1 in circuit M_1N_1, K_2 in circuit M_1N_2 effective values of these eddy currents correspond to the readings of amperemeters A_2 and A_4;

(c) on sections $M_1B_1E_1M_2$ and $M_1B_2E_2M_2$ of first elementary conductor and on $M_1C_2D_2M_2$ and $M_1C_1D_1M_2$ of the second flow the currents circulating on end parts of both elementary conductors through end pieces. When keys K_5 and K_6 are open, the effective values of these currents correspond to the readings of amperemeters A_3 and A_5. In contrast to "local" eddy currents we shall call them circulating currents.

Thus, to calculate additional losses in a bar with incomplete transposition it should be necessary to calculate on the basis of slot leakage fluxes:

- "local" eddy currents in each elementary conductor of slot group;
- circulating currents between elementary conductors of slot group.

23.2.7.2 Derivation of Calculation Equations

In Sect. 23.2.4 we have obtained equations for currents—(23.23) in element I' and (23.24)—in element I'' induced by cross slot leakage flux. These equations have some very interesting features. Let us present each of them as a sum of two components and our attention will be turned to their properties. The current density J'_{ED} is presented a sum in the following:

$$\begin{aligned} J'_{ED} &= J'_{ED.L} + J'_{CIRC}, \\ J'_{ED.L} &= -j\omega\mu_0\sigma J b_{MS} n \frac{Y^2 + 0.33h_1^2 + (p-1)\left(4Yh_1 - 2h_1^2\right)}{2b_{SLT}}, \\ J'_{CIRC} &= -j\omega\mu_0\sigma J b_{MS} n \frac{\left[-ah_1 - h_1^2 + (p-1)\left(-2ah_1 - 2h_1^2\right)\right]R}{2b_{SLT}} \\ &(\text{by } R = 1). \end{aligned} \tag{23.38}$$

In a similar way:

$$
\begin{aligned}
J''_{ED} &= J''_{ED.L} + J''_{CIRC},\\
J''_{ED.L} &= -j\omega\mu_0\sigma J b_{MS} n \frac{Y^2 + 2Yh_1 - 1.33h_1^2 + (p-1)\left(4Yh_1 - 2h_1^2\right)}{2b_{SLT}},\\
J''_{CIRC} &= -j\omega\mu_0\sigma J b_{MS} n \frac{\left[ah_1 + h_1^2 + (p-1)\left(2ah_1 + 2h_1^2\right)\right]R}{2b_{SLT}} (\text{by } R = 1).
\end{aligned}
\tag{23.39}
$$

The components $J'_{ED.L}$ and $J''_{ED.L}$ differ by the following important properties:

$$
\int_0^{h_1} J'_{ED.L} dY = 0; \quad \int_0^{h_1} J''_{ED.L} dY = 0. \tag{23.40}
$$

Physically it means that the eddy currents closed in contours $B_1B_2E_2E_1$ and $C_1C_2D_2D_1$ (Fig. 23.9) correspond to the components $J'_{ED.L}$ and $J''_{ED.L}$. So we shall call them "local" eddy currents.

The components J'_{CIRC} and J''_{CIRC} are different in the following important properties:

(a) the current density in both elementary conductors of slot group with height $0 \le Y \le h_1$ is uniformly distributed (it does not depend on Y):
(b) in both elements I' and I'' currents are equal: $J'_{CIRC} = -J''_{CIRC}$, here

$$
I'_{CIRC} \int_0^{h_1} J'_{CIRC} dY = 0; \quad I''_{CIRC} = \int_0^{h_1} J''_{CIRC} dY. \tag{23.40'}
$$

Consequently, in both elementary conductors of group these currents are equal in value and opposite in sign. This means physically that these currents circulate between elementary conductors of slot group. So, we shall call them circulating currents. Equations for current densities J' and J'' have been obtained on the assumption that currents are closed within the slot part of elementary conductor (R = 1). In the case when the slot leakage flux is distributed along the stator core equal to [1]

$$
L'_{SLT} = L_{SLT} - 0.5 n_C b_C \tag{23.41}
$$

and insulated elementary conductors of group are electrically connected in end part, it should not be difficult to show that in this case the factor is R < 1:

$$R = \frac{L'_{SLT}}{L_0}, \tag{23.42}$$

(n_C, b_C—is the number and the width of channels in stator core).

Thus, at $R < 1$ the circulating current (Fig. 23.9) flowing not only through slot but end parts of both elementary conductors of group corresponds to components J'_{CIRC} and J''_{CIRC} and passes from one elementary conductor to another through end pieces connecting them.

Now we will evaluate A.C. losses in elements I′ and I″ from local eddy and circulating currents. For I′ section additional losses in slot leakage part are equal to:

$$P_{I'} = \frac{b_{MS} L_{SLT} n}{2\sigma} \int_0^{h_1} \left|J'_{ED}\right|^2 dY = \frac{b_{MS} L_{SLT} n}{2\sigma} \int_0^{h_1} \left|J'_{ED.L}\right|^2 dY + \frac{b_{MS} L_{SLT} n}{2\sigma} \int_0^{h_1} \left|J'_{CIRC}\right|^2 dY$$
$$= (P_{I'})_{ED.L} + (P_{I'})_{CIRC}. \tag{23.43}$$

We have to note that during the calculation of $\left|J'_{ED}\right|^2$ the third term appears:

$$\int_0^{h_1} \left|J'_{CIRC} J'_{ED.L}\right| dY = 0.$$

It is identically zero according to (23.40); this makes it possible to calculate separately the losses produced by local eddy and circulating currents.

Let us find equations for losses in the slot part of section I′. After integration of terms in Eq. (23.43) we have:

$$(P_{I'})_{ED.L} = b_{MS} \frac{L_{SLT} n}{2\sigma} |J|^2 (K')^4 \left[0.09 h_1^5 + 1.333 (p-1)^2 h_1^5 + 0.666 (p-1) h_1^5\right], \tag{23.43′}$$

$$(P_{I'})_{ED.L} = b_{MS} \frac{L_{SLT} n}{2\sigma} |J|^2 (K')^4 \left[0.09 h_1^5 + 1.333 (p-1)^2 h_1^5 + 0.666 (p-1) h_1^5\right],$$

$$(P_{I'})_{CIRC} = \frac{1}{2} b_{MS} \frac{L_{SLT} n}{\sigma} |J|^2 (K')^4 \left[2h_1 R^2 \left(ah_1 + h_1^2\right)^2 + 4(p-1)^2 h_1 R^2 \left(ah_1 + h_1^2\right)^2 + 4(p-1) h_1 R^2 \left(ah_1 + h_1^2\right)^2\right]. \quad (23.43'')$$

For I″ section we shall use equations for current densities (23.38) and (23.39); in a similar way we shall obtain:

$$(P_{I''})_{ED} = (P_{I''})_{ED.L} + (P_{I''})_{CIRC},$$

where

$$(P_{I''})_{ED.L} = b_{MS} \frac{L_{SLT} n}{2\sigma} |J|^2 (K')^4 \left[0.756h_1^5 + 1.333(p-1)^2 h_1^5 + 0.666(p-1)h_1^5\right];$$

$$(P_{I''})_{CIRC} = b_{MS} \frac{L_{SLT} n}{2\sigma} |J|^2 (K')^4 [2h_1 R^2 \left(ah_1 + h_1^2\right)^2 + 4(p-1)^2 h_1 R^2 \left(ah_1 + h_1^2\right)^2 + 4(p-1) h_1 R^2 \left(ah_1 + h_1^2\right)^2]. \quad (23.44)$$

General equations for losses in the end part as long as L_S on sections I′ and I″ may be calculated in the same manner.

It is easy to show that at R = 1 the amount of losses due to local eddy and circulating currents on sections I′ and I″ is exactly equal to those obtained in Sect. 23.2.4 for the same sections. This acknowledges the justice of stated calculations.

Let us consider in greater details the physical meaning of equations for components of losses caused by circulating currents. To do so we have to obtain in equation for $(P_{I'})_{CIRC}$ the losses components in another way bearing in mind the following simple physical arguments:

(a) $(P_{I'})_{CIRC,S}$ component. To obtain the current density and additional losses due to self-induction it is sufficient to replace the elements I′ and I″ by infinitely thin filaments with the current combined with their lower bases (counting from the slot base); we assume that the same current flows through these filaments as on respective sections I′ and I″.

For this contour I′–I″ we have the flux density $B_S = \frac{\mu_0 J b_{MS} n h_1}{b_{SLT}}$; flux combined with contour I′–I″: $\Phi_S = \mu_0 J b_{MS} n h_1 = (h_1 + a)\frac{L'_{SLT}}{b_{SLT}}$,density of circulating current induced by self-induction flux:

$$J'_{CIRC,S} = -j\omega\mu_0\sigma J b_{MS} n h_1 = (h_1 + a)\frac{R}{2b_{SLT}}. \tag{23.45}$$

This equation corresponds to the first term in Eq. (23.38) for J'_{CIRC}. Thus, the losses

$$(P_{I'})_{CIRC,S} = b_{MS}\frac{L_{SLT}n}{2\sigma}|J|^2(K')^4 2h_1 R^2\left(ah_1 + h_1^2\right)^2 \tag{23.46}$$

correspond to the first term of Eq. (22.43″);

(b) component $(P_{I'})_{CIRS,MUT}$.

To obtain the current density and additional losses caused by mutual flux we shall replace sections I′–I″ by filaments with current. The flux density in contour I′–I″ from mutual flux is:

$$B_{MUT} = \frac{\mu_0 J b_{MS} n 2h_1(p-1)}{b_{LST}}. \tag{23.47}$$

Mutual flux:

$$\Phi_{MUT} = \mu_0 J b_{MS} n 2h_1(h_1 + a)(p-1)\frac{L'_{SLT}}{b_{SLT}}. \tag{23.48}$$

Density of circulating current induced by mutual flux:

$$J'_{CIRC,MUT} = -\frac{j\omega\mu_0\sigma J b_{MS} n h_1(h_1 + a)(p-1)R}{b_{SLT}}. \tag{23.49}$$

This equation refers to the second term in Eq. (23.38) for J'_{CIRC}. Thus, the losses

$$(P_{I'})_{CIRC} = b_{MS}\frac{L_{SLT}n}{2\sigma}|J|^2(K')^4 4(p-1)^2 h_1 R^2\left(ah_1 + h_1^2\right)^2 \tag{23.50}$$

correspond to the second term of Eq. (2.43″);

(c) component $(P_{I'})_{CIRC,S-MUT}$.

The third term of equation for $(P_{I'})_{CIRS}$ corresponds to a combined action of self- and mutual induction fluxes; it is proportional to the value $(p - 1)$ of degree one:

$$(P_{I'})_{CIRC,S\text{-}MUT} = b_{MS}\frac{L_{SLT}n}{2\sigma}|J|^2(K')^4 4(p-1)h_1R^2\left(ah_1+h_1^2\right)^2. \tag{23.51}$$

Equations for calculation of currents and losses obtained on the basis of pure analysis of distribution of self- and mutual induction field strength coincide completely with those obtained from more simple and physically more clear prerequisites by the way of replacing sections I′ and I″ by filaments with current.

Now we note that for the calculation of current density and losses caused by circulating currents there is no requirement imposed like $K'(h_1+a)<1$ identical to (23.14).

Let us proceed to the calculation of losses increase factor in m_{GR} groups with height making the both slot bars. These losses in slot and end parts are different: in slot part there are eddy and circulating currents, while in end part—only circulating currents (Fig. 23.9).

With the help of obtained calculation equations for additional losses due to "local" eddy and circulating currents it will be fairly simple to calculate this factor: to do so, the above additional losses should be referred to as D.C. losses of the whole bar. As a result we shall have:

- for slot and end parts of both bars in the slot:

$$K_{F,B} \cong 1+\frac{R+3\overline{R}^2}{4}(K'h_{GR})^4\frac{m_{GR}^2}{9}, \tag{23.52}$$

- for slot part of both bars in the slot:

$$K_{F,SLT} \cong 1+\frac{R\left(1+3\overline{R}^2\right)}{4}(K'h_{GR})^4\frac{m_{GR}^2}{9}. \tag{23.53}$$

Here $h_{GR}=2h_1, \overline{R}=R\left(1+\frac{a}{h_1}\right)$, where h_1 is the height of elementary conductor in group (without insulation), a—is a double-sided thickness of elementary conductor insulation.

Equation (23.52) is necessary to calculate losses in the machine and its efficiency factor, while Eq. (23.53)—to calculate overheating of winding slot part with due account made for distribution of losses in some of bars in the slot. The problem of their distribution in the slot has been described in Sect. 23.4.

To verify Eqs. (23.52) and (23.53) let us consider a particular case (complete transposition). In this case we have: $a=0, \overline{R}=R=1$, an equivalent height of elementary conductor is $h_{GR}=h_{MS}$ and their number is respectively $m_{GR}=m$. Taking into account these approximations, we shall have the following:

Table 23.3 Losses increase factors for bar winding with incomplete transposition

g	$K_{F,MS}$ according to (23.52)	$K_{F,SLT}$ according to (23.53)	$K_{F,MS}$ according to (23.31)
1	1.0389	1.0273	1.0241
5	1.9723	1.6835	1.6011
7	2.9057	2.3397	2.1783
11	5.7058	4.3083	3.9090

Eqs. (23.52) and (23.53) coincide with known equations [1, 3–5, 20] for solid conductors (Field's factor) described in Sect. 23.2.5. This confirms the validity of found equations.

For ordinary sizes of copper elementary conductors used in practice Eqs. (23.52) and (23.53) may be used at frequencies $f \leq 650$ Hz; in this case the condition (23.14) is met.

Calculation example

We shall determine additional losses in stator winding of large power frequency-controlled motor (7 MW, 13.1 rpm, 6.55 Hz, number of poles 2p = 60, «Elektrosila» Work, Stock Company "Power Machines", St.-Petersburg) fed by a frequency converter. In current curve of the stator the most significant are harmonics of order g = 5, g = 7, g = 11, circular frequency for g = 1: $\omega = 41.15$ l/s (6.55 Hz). In stator slot there are two bars with height $m_{GR} = 20$ groups of elementary conductors; t = 2. Winding data: $h_1 = 3.55$ mm, $b_{MS} = 9$ mm, $b_{SLT} = 23.2$ mm, $a = 0.30$ mm, n = 2. Now we shall determine losses increase factors for harmonics g = 1, g = 5, g = 7, g = 11, $\sigma = 46 \times 10^6$ S/m.

Solution

For bar construction of this machine R = 0.55. From Eq. (23.53) we have $\overline{R} = 0.5965$. Calculation results according to Eqs. (23.52) and (23.53) are given in Table 23.3.

In Table 23.3 additionally are given losses increase factors calculated using (23.31); they correspond to the bar construction with complete transposition (in the event it may be feasible). Calculation results show that for the same elementary conductors the heating of bar slot part specified in general by factor $K_{F,SLT}$ according to (23.53) remains practically the same when passing to the construction with incomplete transposition and the losses in bars from current high time harmonics determined, as a rule, by factor $K_{F,B}$ according to (23.52), increase when passing to the construction with incomplete transposition.

23.2.7.3 Practical Choice of Elementary Conductors in Slot at Incomplete Transposition

Let us consider the problem which arises usually at designing stator winding in the event when the transposition of all elementary conductors in the bar, whose number with height makes m, fails to be feasible. We determine the height of copper in each group with incomplete transposition, the number of such groups being 0.5 m_{GR} with bar height, under condition that such a winding has the same additional losses $P_{A.C.(GR)}$ and overheating Θ_{GR} in the slot part as those for winding with complete transposition; additional losses $P_{A.C.}$, overheating Θ, height of transposed elementary conductor h_1 and number m are supposed to be known.

Now we shall determine h_{GR} and m_{GR} under the conditions:

$$P_{A.C.(GR)} \leq P_{A.C.}, \tag{23.54}$$

$$\Theta_{GR} \leq \Theta, \tag{23.55}$$

(respective parameters characterizing the winding with incomplete transposition contain symbol "GR"). The first equation indicates practically the equality of additional losses in the slot and end parts of bars at their complete and incomplete transposition and the second one corresponds to the parity of losses in slot part.

An overall height of copper in group h_{GR} at incomplete transposition under condition of (23.54) is:

$$h_{GR} \leq \frac{2h_1}{\sqrt{R + 3\overline{R}^2}}, \tag{23.56}$$

under (23.55)

$$h_{GR} \leq \frac{2h_1}{\sqrt{R(1 + 3\overline{R}^2)}}. \tag{23.57}$$

The number of groups at incomplete transposition under the condition of (23.54) is

$$m_{GR} \leq \frac{1}{2} m_{MS} \sqrt{R + 3\overline{R}^2}, \tag{23.58}$$

under (23.55)

$$m_{GR} \leq \frac{1}{2} m_{MS} \sqrt{R\left(1 + 3\overline{R}^2\right)}. \tag{23.59}$$

Calculation example

At motor designing the following parameters of elementary conductors in slot have been chosen h_{MS} = 1.8 mm, m_{MS} = 44.

It was supposed that in the slot part a complete transposition of elementary conductors may be realized. However, at bar designing it turned out that such a transposition is unfeasible according to (23.2). Let us determine the height of elementary conductors forming a group, and the number of groups at incomplete transposition. Winding data are: b_{MS} = 8 mm, n = 2 mm, b_{SLT} = 20.5 mm, a = 0.27 mm, R = 0.4485, f = 50 Hz, t = 2.

Solution

First we shall specify $\overline{R} = 0.52$. This value is to be updated after determination of h_1.

For Eq. (23.54) from (23.56) and (23.58) we have $h_{GR} \leq 3.15$ mm; $m_{GR} \approx 26$.
For Eq. (23.55) we obtain from (23.57) and (23.59) $h_{GR} \leq 4.0$ mm; $m_{GR} \approx 20$.

Now we will choose h_{GR} = 2.64 mm: the height of each elementary conductor in the group is equal to h_1 = 1.32 mm, the number of groups is m_{GR} = 28.

Let us check the results: $\overline{R} = R\left(1 + \frac{a}{h_1}\right) = 0.4485\left(1 + \frac{0.27}{1.32}\right) = 0.5402$.

Thus, the value $\overline{R}$ was first chosen practically correctly.

23.2.8 *Bars with Different D.C. Resistance of Elementary Conductors: Calculation Example*

Let us consider the problem of calculation of additional losses caused by eddy currents induced by slot leakage cross-flux in elementary transposed conductors of winding bar in the event when the D.C. resistance of these elementary conductors is not the same (Fig. 23.10). The difference may be due to the fact that a part of bar elementary conductors differs by electrical resistivity, cross-sectional area etc.; of practical application are, for example, bar constructions containing solid and hollow elementary conductors whose cross-sectional area is not the same, besides in some

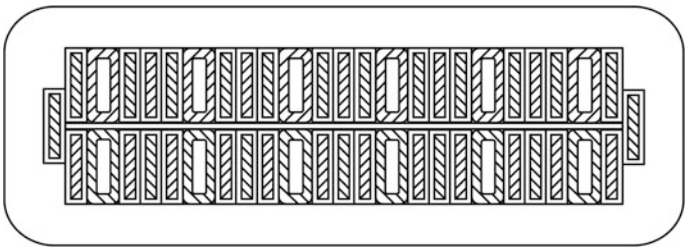

Fig. 23.10 Cross-section of a *bar* with combined elementary conductors (hollow and solid)

of them hollow elementary conductors are made of steel, while solid conductors—of copper [31], so in general case:

$$\sigma_H \neq \sigma_{MS}, \tag{23.60}$$

$$S_H \neq S_{MS}, \tag{23.61}$$

where σ_H, σ_{MS}, S_H, S_{MS} are respectively the specific conductivity of elementary conductor and cross-sectional area of hollow and solid elementary conductors.

In [20, 32] are described the methods to compute additional losses in bars with hollow and solid elementary conductors due to eddy currents induced by slot leakage cross-flux. However, the method described in [32] is valid only for Eq. (23.61), i.e. for constructions where hollow and solid elementary conductors have the same specific conductivity of elementary conductor $(\sigma_H = \sigma_{MS})$; besides, the result has not been reduced to calculation analytic equation (in closed form). In the practice of calculations the absence of such an equation makes it impossible to obtain an analytical dependence between parameters specifying an optimal bar construction. In [33] there is a possibility to specify additional losses subject to both Eqs. (23.60) and (23.61) by using numerical computations. To integrate the results obtained in [34] there have been used methods of similarity law. However, such an integration (in order to have an analytical equation) has been made in [34] only under condition (23.61).

It will be more convenient to subdivide the problem analytical solution dealing with losses $Q_{A.C.}$ in a bar with different resistivity of elementary conductors into several stages [20–22]:

- to determine separately losses in each type of elementary conductors;
- to establish the dependence between leakage fluxes due to currents in each type of elementary conductors in one bar by applying Ampere's law [3, 4].

We make it possible to use the results of first stage and to find additional losses in a bar with combined arrangement of elementary conductors of several types.

Now we shall consider the first stage of problem solution.

The results of investigation of losses due to slot leakage cross-fluxes in bar winding with solid elementary conductors are given in Sect. 23.2.5 [Eqs. (23.30)–(23.32)].

As far as it concerns winding bars with hollow elementary conductors, the results of investigation of losses due to leakage fluxes mentioned above are given in Sect. 23.2.6 [Eqs. (23.34)–(23.36)].

Equations for calculation of losses increase factor in hollow elementary conductor of pth layer and in solid elementary conductor of pth layer are of the same topology. They contain three terms: the first of them does not depend on the number of layers $(p - 1)$; the second is proportional to $(p - 1)$; the third is proportional to $(p - 1)^2$, besides the factors at $(p - 1)$ and $(p - 1)^2$ are the same. Equations for calculation of losses increase factor in a bar with hollow and with solid elementary conductors are of the same topology.

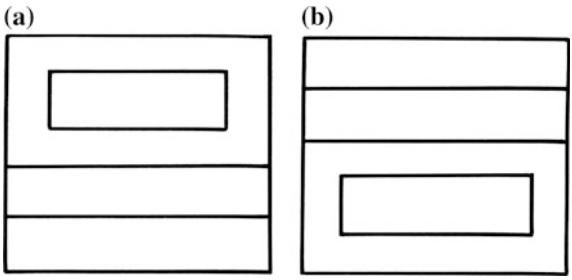

Fig. 23.11 Relative positions of hollow and solid elementary conductors in group

It should be noted that the primary role in origination of losses is attributed to mutual induction slot fluxes specified in Eqs. (23.31), (23.32) and (23.35), (23.36) by terms that are proportional to the number of elementary conductors m. This was backed by examples (Tables 23.1, 23.2).

Equations obtained for calculation of losses increase factors in hollow and in solid elementary conductors make it possible to have at the second stage of solution an equation for calculation of additional losses in bar with combined elementary conductors.

Let us consider a group (Fig. 23.11a, b) containing one hollow and q solid elementary conductors, at that the count of solid elementary conductor in the group if considering from the slot base shall be marked by w (w = 1, 2, 3 …, q). Solid elementary conductors of this group occupy different positions relative to hollow elementary conductor due to the transposition available in slot part. For the first limiting position (a hollow elementary conductor is placed in the group above solid elementary conductors) the intensity of slot cross-field induced by mutual induction in the domain of wth solid elementary conductor is to be specified upon Ampere's law in the form [3, 4]

$$H_{MS,MUT(1)} = \frac{J_H(p-1)nS_H + J_{MS}(p-1)nqS_{MS} + J_{MS}(w-1)nS_{MS}}{b_{SLT}}, \quad (23.62)$$

where J_H, J_{MS} are current densities in cross-sections of hollow and solid elementary conductors, respectively.

From (23.62) it follows that we have established for the first limiting position (Fig. 23.11a) the relation between the intensity $H_{MS,MUT(1)}$ of slot leakage cross-field in the domain of wth solid elementary conductor and currents in both types of bar elementary conductors (hollow and solid).

For the second limiting position (a hollow elementary conductor is placed in group under solid elementary conductors, Fig. 23.11b) we shall obtain in a similar way

$$H_{MS,MUT(2)} = \frac{J_{MS}(p-1)nqS_{MS} + J_{MS}(w-1)nS_{MS} + J_H pnS_H}{b_{SLT}}. \quad (23.63)$$

An averaged value of slot leakage cross field intensity in the domain of wth solid elementary conductor of pth group is:

$$H_{MS,MUT(MED)} = \frac{J_{MS}(p-1)nqS_{MS} + J_{MS}(w-1)nS_{MS} + J_H(p-0.5)nS_H}{b_{SLT}}. \tag{23.64}$$

In a similar way for hollow elementary conductor of pth group in both limiting positions we have:

$$H_{H,MUT(1)} = \frac{J_H(p-1)nS_H + J_{MS}(p-1)nqS_{MS} + J_{MS}nqS_{MS}}{b_{SLT}}, \tag{23.65}$$

$$H_{H,MUT(2)} = \frac{J_{MS}(p-1)nqS_{MS} + J_H(p-1)nS_H}{b_{SLT}}. \tag{23.66}$$

The averaged value of field intensity in the slot in the domain of hollow elementary conductor of pth group is:

$$H_{MS,MUT(MID)} = \frac{J_{MS}(p-1)nqS_{MS} + 0.5J_{MS}qnS_{MS} + J_H(p-1)nS_H}{b_{SLT}}. \tag{23.67}$$

Equations (23.62)–(23.67) contain current densities J_H, J_{MS} in both types of elementary conductors; in [32] it is shown that using (23.14) these current densities may be calculated on the basis of an amplitude I of operational current (load current) in bar, at that it shall be sufficient to assume that this current is uniformly distributed on elementary conductor cross-section. Taking into account the above said we have:

$$\frac{J_H}{J_{MS}} = \frac{\sigma_H}{\sigma_{MS}}. \tag{23.68}$$

The slot leakage field of $H_{MS,MUT(MED)}$ intensity according to (23.64) may be also created only by solid elementary conductors of $(p-1)_{MS,EQ}$ number, if this value is calculated from the equation,

$$\frac{J_{MS}(p-1)_{MS,EQ}nS_{MS}}{b_{SLT}} = H_{MS,MUT(MED)}. \tag{23.69}$$

Taking into consideration of (23.68) we shall have an equivalent number of elementary conductors $(p-1)_{MS,EQ}$ creating the field of $H_{MS,MUT(MID)}$ intensity in the slot having only solid elementary conductors:

$$(p-1)_{MS,EQ} = (p-1)q + w - 1 + \left(p - \frac{1}{2}\right)F = p(q+F) - \left(q + \frac{F}{2} + 1 - w\right), \tag{23.70}$$

where $F = \frac{\sigma_H}{\sigma_{MS}} \frac{S_H}{S_{MS}}$.

In the manner similar to (23.70) we shall obtain an equivalent number $(p-1)_{H,EQ}$ of elementary conductors creating the field of $H_{H,MUT(MED)}$ intensity in the slot having only hollow elementary conductors:

$$(p-1)_{H,EQ} = (p-1) + (p-1)\frac{q}{F} + \frac{q}{2F} = p\frac{F+q}{F} - \left(\frac{q}{2F} + 1\right). \tag{23.71}$$

Let us use the results of the first stage of problem solution.

By using Eq. (23.30) for the losses increase factor $K_{(P)MS}$ and Eq. (23.70) for an equivalent number of solid elementary conductors we shall obtain the losses increase factor for wth solid elementary conductor of pth group of real bar

$$K_{MS,GR(P\cdot W)} = 1 + \left(K'_{MS}h_{MS}\right)^4 \cdot \frac{p(q+F) - \left[\left(q + \frac{F}{2} + 1 - w\right)\right] + \left[p(q+F) - \left(q + \frac{F}{2} + 1 - w\right)\right]^2}{3}. \tag{23.72}$$

By analogy, using Eq. (23.34) for $K_{(P)H}$ and the equivalent number of hollow elementary conductors we shall obtain the losses increase factor for hollow elementary conductor of pth group of real bar

$$K_{H,GR(P)} = 1 + \left(K'_H h_H\right)^4 T \frac{S_H}{S_{H.CONT}} \frac{\left[p\frac{q+F}{F} - \left(\frac{q}{2F} + 1\right)\right] + \left[p\frac{q+F}{F} - \left(\frac{q}{2F} + 1\right)\right]^2}{3}. \tag{23.73}$$

We determine losses in all nqm_{GR} of solid elementary conductors in the slot; here m_{GR} is the number of groups in slot with height. Losses in each solid elementary conductor shall be calculated by Eq. (23.72), at that, a running index of solid elementary conductor in group shall be w = 1, 2, …, q and a running index of group—values p = 1, 2, 3, …, m_{GR}. A calculation equation for losses in solid elementary conductor in slot due to eddy currents induced by slot leakage cross-flux shall be obtained in the form:

$$Q^{(P,W)}_{A.C.MS} = \frac{1}{2}\left(\frac{I_{MS}}{m_{GR}nq}\right)^2 nR_{MS}K_{MS,GR(P,W)}, \quad \text{by } W = 1, 2, \ldots, q, P = 1, 2, \ldots, m_{GR} \tag{23.74}$$

where I_{MS} is the amplitude of operational current (load current) flowing through solid elementary conductors in slot; R_{MS} is the D.C. resistance of solid elementary conductor.

Now we shall determine losses in nm_{GR} hollow elementary conductors in the slot. Losses in each of them are calculated by Eq. (23.73). A calculation equation for losses in hollow elementary conductors in slot due to eddy currents induced by slot leakage cross-flux shall be obtained in the following form:

$$\begin{array}{l} Q_{A.C.H}^{(P)} = \frac{1}{2}\left(\frac{I_H}{m_{GR}n}\right)^2 nR_H K_{H,GR(P)}\,, \\ \text{by } P = 1, 2, \ldots m_{GR} \end{array} \tag{23.75}$$

where I_H is the amplitude of operational current (load current) flowing through hollow elementary conductors in slot; R_H is the D.C. resistance of hollow elementary conductor, at that

$$I_{EL.GR} = I_H + qI_{MS} \tag{23.76}$$

is the load current in a group containing one hollow and q solid elementary conductors.

According to (23.4) an overall losses increase factor is

$$K_{F,COMB} = \frac{\sum_{W=1}^{q}\sum_{P=1}^{m_{GR}} Q_{A.C.MS}^{(P,W)} + \sum_{P=1}^{m_{GR}} Q_{A.C.H}^{(P)}}{Q_{D.C.}}, \tag{23.77}$$

where $Q_{D.C.}$ are losses in groups of elementary conductors at their flow around by direct current.

Taking into account relations (23.74)–(23.77) for some current components and losses we shall have an equation in a closed form for losses increase factors in nm_{GR} slot groups, at that, each group contains one hollow and q solid elementary conductors (in deriving the above equation the terms of second and higher order of infinitesimals have been omitted):

$$K_{F,COMB} = 1 + \Delta K_{EQ}\frac{q + F^3\left(\frac{S_{H,CONT}}{S_H}\right)^3\left(\frac{\sigma_{MS}}{\sigma_H}\right)^2 T}{q + F}, \tag{23.78}$$

where

$$\Delta K_{EQ} = \frac{\left(K'_{MS}h_{MS}\right)^4 m_{GR}^2 (q + F)^2}{9}. \tag{23.79}$$

Equation (23.78) is general and specifies the losses in all elementary conductors in slot due to eddy currents induced by slot leakage cross flux for the bar

construction satisfying the both Eqs. (23.61) and (23.62). This equation [20] has a simple physical conception. The first of multipliers (23.79) corresponds to additional losses in nm_{GR} groups of solid elementary conductors; each group contains q real solid elementary conductors and F equivalent solid elementary conductors replacing one hollow elementary conductor. The second multiplier in (23.78) refers to the influence of existence of these F equivalent solid elementary conductors in each group on additional losses in slot; it does not depend on the number $m_{\Gamma P}$ and frequency ω.

By using the method described above and the relations obtained further it is not difficult to specify additional losses in some bars in slot and in the construction itself where the number of elementary conductors that compose these bars are not the same (for example, the height of solid elementary conductor of upper bar is chosen smaller than that one of lower bar).

Now let us consider three special cases being of particular practical interest.

1st case: $\sigma_H \ll \sigma_{MS}, F \to 0$.

According to (23.78), (23.79) we have:

$$K_{F,COMB} = 1 + \left(K'_{MS} h_{MS}\right)^4 \frac{(m_{GR} q)^2}{9},$$

that practically corresponds to the equation for losses in solid elementary conductors in slot [Sect. 23.2.5, Eq. (23.31)].

2nd case: $\sigma_H \gg \sigma_{MS}$, $K'_{MS} \to 0, F \to \infty$; thus

$$K_{F,COMB} = 1 + \left(K'_H h_H\right)^4 m_{GR}^2 \frac{\frac{S_H}{S_{H,CONT}} T}{9},$$

that practically corresponds to the equation of losses in hollow elementary conductors in slot [Sect. 23.2.6, Eq. (23.35)].

The both limiting cases prove the validity of found Eq. (23.78).

3rd case: $\sigma_H = \sigma_{MS}$

Equations (23.78) and (23.79) are to be simplified:

$$K_{F,COMB} = 1 + \Delta K_{EQ} \frac{q + \left(\frac{h_H}{h_{MS}}\right)^3 T}{q + \frac{S_H}{S_{MS}}}, \tag{23.80}$$

$$\text{where} \quad \Delta K_{EQ} = \frac{(K' h_{MS})^4 m_{GR}^2 \left(q + \frac{S_H}{S_{MS}}\right)^2}{9}.$$

Equation (23.80) is of special practical interest: it is valid for winding bars whose hollow and solid elementary conductors are made of copper.

Calculation example

Table 23.4 Losses increase factors for winding bars with combined elementary conductors of a frequency-regulated drive

g	$K_{F,COMB}(\sigma_H = \sigma_{MS})$	$K_{F,COMB}(\sigma_H \neq \sigma_{MS})$
5	1.298	1.075
7	1.584	1.148
11	2.441	1.365

Table 23.5 Losses ratio $Q^*_{A.C.}$ in bar winding of frequency-regulated drive for versions $\sigma_H \neq \sigma_{MS}$ and $\sigma_H = \sigma_{MS}$

g	5	7	11
$Q^*_{A.C.}$	0.920	0.806	0.620

In stator slots of frequency—controlled drive motor 5.5 MW, 19.2 rpm, the number of poles 2p = 60 [35] has been arranged a double-layer bar winding. Number of elementary conductor groups in slot: with height $m_{GR} = 8$, with width n = 2; slot width $b_{SLT} = 24.5$ mm. Each group contains one hollow and two solid elementary conductors (q = 2). Sizes of hollow elementary conductor: $h_H = 5$ mm, $b_H = 9$ mm; $b_{CAN} = 6$ mm; $a_{CAN} = 2$ mm. Sizes of solid elementary conductor: $h_{MS} = 1.95$ mm; conductivity of both elementary conductors 46×10^6 S/m. A machine is operated by a network containing time harmonics of order g = 5, g = 7, g = 11. Rated frequency (g = 1) f = 9.6 Hz.

The value of factors $K_{F,COMB}$ calculated for g = 5, g = 7, g = 11 for a special case $\sigma_H = \sigma_{MS}$ Eq. (23.80) is given in Table 23.4. Let us note that the values given in this table coincide practically completely with those of calculation of $K_{F,COMB}$ according to [2, 32], method designed only for this special case, and by using the numerical method [33] at $\sigma_H = \sigma_{MS}$; the discrepancy does not exceed 2 %.

Table 23.4 provides the results of calculation of losses increase factor for a construction version where the width of elementary conductor remains the same but the hollow elementary conductor is made of steel ($\sigma_H = 2 \times 10^6$ S/m), at that, in slot with height $m_{GR} = 4$; $h_H = 4.5$ mm; $b_H = 9$ mm, $b_{CAN} = 7.5$ mm; $a_{CAN} = 3$ mm, $h_{MS} = 2.26$ mm, $b_{SLT} = 24.5$ mm, q = 6; so, an overall height of elementary conductors in slot and slot sizes in this version remain practically the same. To calculate $K_{F,COMB}$ a general Eq. (23.78) has been used. The results were verified by a numerical method [33] for $\sigma_H \neq \sigma_{MS}$; the discrepancy does not exceed 2 %.

It should be noted that as compared with the previous case in this construction version the D.C. losses increase in the way that the ratio of losses in winding being flowed by alternating current $Q^*_{A.C.}$ for the construction at $\sigma_H \neq \sigma_{MS}$ and for the construction version at $\sigma_H = \sigma_{MS}$ makes (Table 23.5).

From the table it follows that when the machine is fed by a non-sinusoidal current, approximately equal values of efficiency correspond to windings of both constructions.

At calculation of $K_{F,COMB}$ and $Q^{*}_{A.C.}$ the area of solid elementary conductor S_{MS} and of hollow conductor contour $S_{H,CONT}$ has been specified without taking into account technological rounding, i.e. by rectangular cross-section; with allowance for rounding these areas are approximately smaller by 1–3 %. The error of $K_{F,COMB}$ does not exceed 1 % in this case.

List of symbols

a	Two-sided thickness of insulation of the elementary conductor;
a_0	Number of parallel branches of winding;
a_{CAN}	Height of channel in the hollow conductor;
b_C	Width of channel in the active stator core;
b_{CAN}	Width of channel in the hollow conductor;
b_{CON}	Width of the elementary conductor;
b_H	Width of the hollow elementary conductor;
b_{MS}	Width of the massive elementary conductor;
b_{SLT}	Width of the slot;
B_{MUT}	Flux density corresponds to the mutual induction of leakage flux in the slot with the elementary conductor;
B_S	Flux density corresponds to the self-induction of leakage flux in the slot with the elementary conductor;
F_0	Criteria of transposition quality in the bar winding;
h_{CON}	Height of the elementary conductor;
h_H	Height of the hollow elementary conductor;
h_{MS}	Height of the massive elementary conductor;
H	Magnetic field strength in the slot;
H_H	Magnetic field strength in the slot in the area of hollow conductor of group of conductors;
H_{MS}	Magnetic field strength in the slot in the area of massive conductor of group of conductors;
I	Amplitude of stator current under load;
I_{ED}	Amplitude of eddy current;
I_{EL}	Amplitude of current in the elementary conductor;
$I_{EL,GR}$	Amplitude of stator current in the group of elementary conductors;
J	Current density;
$J_{(CIRC)}$	Current density of circulating current between the elementary conductors;
J_{ED}	Density of eddy current;
J_H	Current density in the hollow conductor;
J_{MS}	Current density in the massive conductor;
K'	The factor of reduction of the height of the elementary conductor to the dimensionless parameter;

$K_{(p)}$	Losses increase factor (Field's factor)
$K_{(p)H}$	Field's factor for the hollow conductor with number p;
$K_{(p)MS}$	Field's factor for the massive conductor with number p;
K_F	Losses increase factor (Field's factor);
$K_{F,MS}$	Field's factor for the bar composed of massive conductors;
$K_{F,H}$	Field's factor for the bar composed of hollow conductors;
L_0	Length of elementary conductor between two end parts;
L_S	Length of end part;
L_{SLT}	Length of slot part of winding without accounting of the channel in the active stator core;
L'_{SLT}	Length of slot part of winding with take into account of the channel in the active stator core;
m	The number of elementary conductors on the height of the bar counting from the bottom of slot;
m_B	The number of elementary conductors in the bar along the height;
m_{GR}	The number of group of elementary conductors along height counting from the bottom of slot;
n	Number of elementary conductors along width of bar;
n_C	Number of channel in stator core;
p	Number of elementary conductor along height of bar counting from the bottom of slot;
$P_{A.C.}$	Additional losses in winding under A.C. current;
q	Number of massive conductors in the group;
$Q_{A.C.}$	Losses in winding under A.C. current;
$Q_{D.C.}$	Losses in winding under D.C. current that is equal to the RMS value of A.C. current;
$Q_{A.C.,H}$	Losses in winding composed of the hollow conductors under A.C. current;
$Q_{A.C.,MS}$	Losses in winding composed of the massive conductors under A.C. current;
R	Ratio between the length of slot part of winding (with accounting of the channel) and length of half-turn;
S_H	Area of hollow conductor;
$S_{H,CONT}$	Area of contour of hollow conductor;
S_{MS}	Area of massive conductor;
T_0	Step of transposition in the bar;
t	Number of elementary conductors in group along height of bar with incomplete transposition;
w	Number of massive conductor in the group;
Y	Coordinate along height of slot (axis of symmetry of rectangular slot);
β	Chording of winding;
θ	Overheat of winding;
λ_{MUT}	Conductivity for the mutual—induction flux;
λ_S	Conductivity for the self-induction flux;

μ_0 Magnetic permeability of air;
μ_{FE} Magnetic permeability of stator core;
σ Electroconductivity of winding conductors;
σ_{MS} Electroconductivity of massive conductors of winding;
σ_H Electroconductivity of hollow conductors of winding;
Φ_P Flux connected with the elementary conductor;
Φ_{MUT} Mutual induction flux connected with the elementary conductor with number p;
Φ_S Self-induction flux connected with the elementary conductor with number p;
ω Circular frequency of EMF and current;

23.3 Numerical Methods of Eddy Current Investigation in Elementary Conductors of Bar Winding

23.3.1 General Observations

A wide utilization of modern computers in electrical machine engineering enables us to determine in a very simple way losses in bar windings of various designs with the help of numerical methods. Numerical iteration methods of calculation of currents induced by alternating magnetic field in a conducting medium have been elaborated in sufficient details last years. They are applied in practice to solve not only one-dimensional but two- and three-dimensional problems [11]. However, investigations show that for rectangular elementary conductors utilized for bar windings and meeting the requirements of (23.14) it will be sufficient to solve one-dimensional problem with accuracy required for practical purposes and to apply assumptions listed in Sect. 23.2.2.

Numerical methods may be of practical interest, for example, in the event when elementary conductors have non-standard geometric shape and analytical equations for calculation of losses in bar having this type of elementary conductors are not available.

For this case study let us consider (within the framework of assumptions given in Sect. 23.2.2) the calculation method of losses in bar winding having hollow and solid elementary conductors transposed between themselves; we shall agree for definiteness that each group contains only one solid elementary conductor (q = 1). This method makes it possible to calculate losses in the case when the resistivity of both elementary conductors in group is different (Eq. 23.60). If there is an analytical solution for losses in bar having these elementary conductors, it is possible to verify the calculation results obtained by numerical methods. The method can be applied within CAE software for A.C. machines having elementary conductors of various shapes and conductivity in stator bar winding.

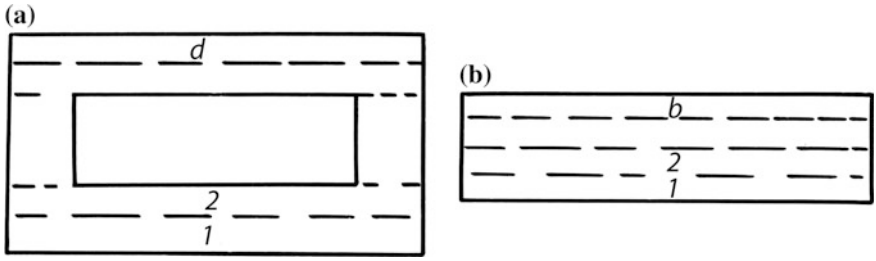

Fig. 23.12 Subdivision of hollow and solid elementary conductors into elements

23.3.2 Problem Statement: Losses in Elements of Hollow and Solid Conductors of Slot Group

Let us subdivide the conductors of slot group into elements: solid elementary conductors—into b elements, a hollow elementary conductor—into d elements (Fig. 23.12). Their number is to be chosen sufficiently large so that the current with height of each elementary conductor could be considered as uniformly distributed with accuracy sufficient for practical calculations, i.e. with accuracy at which $K_{F,COMB}$ is calculated.

We shall symbolize current values in elements of hollow conductor $I_{H(1)}, I_{H(2)}, I_{H(3)}, \ldots, I_{H(d)}$; currents in elements of solid elementary conductor shall be symbolized in a similar way $I_{MS(1)}, I_{MS(2)}, I_{MS(3)}, \ldots, I_{MS(b)}$, I_H—is the current in hollow elementary conductor, I_{MS}—is the current in solid elementary conductor. The same symbols shall be attributed to the elements D.C. resistance of both conductors. Then, for currents, we may write:

$$\begin{aligned} I_{H(1)} + I_{H(2)} + I_{H(3)} + \cdots + I_{H(d)} &= I_H, \\ I_{MS(1)} + I_{MS(2)} + I_{MS(3)} + \cdots + I_{MS(b)} &= I_{MS}, \end{aligned} \tag{23.81}$$

where I_H, I_{MS} are operational (load) currents respectively in hollow and solid elementary conductors of group.

In Eq. (23.76) the following is valid for currents:

$$I_H + qI_{MS} = I_{EL,GR}, \tag{23.82}$$

where $I_{EL,GR}$ is the amplitude of operational current in the group containing one hollow and q solid elementary conductors; in the way similar to (23.3′) we have:

$$I_{EL,GR} \frac{I}{m_{GR} n a_0}.$$

Losses at alternating current flowing-around conductors of slot group shall be written as follows:

- A.C. losses in hollow elementary conductor

$$Q_{H(P)} = \frac{R_{H(1)}\left|I_{H(1)}\right|^2 + R_{H(2)}\left|I_{H(2)}\right|^2 + \cdots + R_{H(d)}\left|I_{H(d)}\right|^2}{2}; \tag{23.83}$$

- A.C. losses in solid elementary conductor

$$Q_{MS(P)} = \frac{R_{MS(1)}\left|I_{MS(1)}\right|^2 + R_{MS(2)}\left|I_{MS(2)}\right|^2 + \cdots + R_{MS(b)}\left|I_{MS(b)}\right|^2}{2}. \tag{23.83'}$$

Losses in the group at alternating current flowing around its elementary conductors:

$$Q_{A.C.(P)} = Q_{H(P)} + qQ_{MS(P)}.$$

Losses at direct current flowing around conductors of slot group (fundamental losses)

$$Q_{D.C.}\frac{R_{GR}\left|I_{EL,GR}\right|^2}{2}, \tag{23.84}$$

where $I_{EL,GR}$—according to (23.82), R_{GR}—is the D.C. resistance of a group of conductors:

$$\frac{1}{R_{GR}} = \frac{1}{R_H} + \frac{q}{R_{MS}}, \quad \frac{1}{R_H} = \frac{1}{R_{H(1)}} + \frac{1}{R_{H(2)}} + \cdots + \frac{1}{R_{H(d)}},$$
$$\frac{1}{R_{MS}} = \frac{1}{R_{MS(1)}} + \frac{1}{R_{MS(2)}} + \cdots + \frac{1}{R_{MS(b)}}.$$

The losses increase factor (Field's factor) $K_{F,COMB}$ for elementary conductors of pth group according to (23.4) is equal to:

$$K_{F.GR(P)} = \frac{Q_{A.C.(P)}}{Q_{D.C.}}. \tag{23.85}$$

The resultant losses increase factor $K_{F,GR}$ shall be calculated in the way similar to (23.27):

$$K_{F.GR} = \frac{K_{F,GR(P=1)} + K_{F,GR(P=2)} + K_{F,GR(P=3)} + \cdots}{m_{GR}}. \qquad (23.85')$$

We see that the problem of specifying losses $Q_{A.C.(P)}$ and factor $K_{F,GR}$ is reduced to that of finding the currents in elements of slot group conductors.

23.3.3 System of Equations for Currents in Elements of Slot Group Conductors. Circuits with Flux Linkage

Elements of all $m_{GR}n$ slot groups form closed circuits with flux linkage. There are several forms of equation system to find currents in these circuits [19, 20, 36]. We shall present it in the form of Kirchhoff's equations for circuits with flux linkage fed by a source with preset voltage. For a bar winding the voltage U between bar ends (strips in end part) for all elementary conductors is the same: U = idem [33].

For notational convenience, it is supposed that the currents in elements of hollow and solid conductors are arranged on their bottom bases. Each system equation shall be written for one conductor element and contains the components of EMF induced by leakage flux of this element (self-induction) and by leakage fluxes of other elements of all slot conductors (mutual induction).

A numerical method using equations for circuits with flux linkage to specify the distribution of currents in them is not a unique method to solve similar problems related to skin effect. In [36] for example, a numerical iterative method is presented as a convenient practical procedure. It was used for the calculation of skin effect in rotor solid bar with account of temperature distribution in it, but it may be also used for the solution of investigated problem.

It is presented in Appendix 1. Due to small sizes of solid and hollow elementary conductors (as compared to the sizes of rotor bar of asynchronous motor) there is practically no need to consider the temperature distribution along the slot center line. However, for generality it is considered when presenting this method in Appendix 1: skin effects may be studied in the same way in the event when the impedance of some conductor elements is not the same due to its geometry as it takes place, for example, in hollow conductor elements belonging with height to different sections (its bases and zone where a cooling channel is arranged).

By using this method, it is not difficult to record an algorithm for calculation of current and additional losses distribution in a group containing solid and one hollow elementary conductors in stator winding bar in the manner similar to that in Appendix 1.

The calculation practice shows that the concordance of factor values $K_{F,GR}$ calculated according to (23.85) and Eqs. (23.78) and (23.79) may be obtained with error less than 2 % if every solid elementary conductor at $K'_{MS}h_{MS} < 1$ is subdivided in height into $b \geq 4$ equal elements. A subsequent increase of the number of elements does not give any adjustment of losses value following (23.85′) but makes

calculations complicated. By analogy, while increasing sequentially the number of elements d of hollow elementary conductor it was established that at $K'_{MS}h_{MS} < 1$ it suffices to specify that $d \geq 5$.

Now let us write the system of Kirchhoff's equations for elements of hollow conductor at d = 5 and of solid elementary conductor at b = 4 [33].

Let us note the coefficients of mutual induction of one element of solid conductor with other element of the same conductor or with an element of other conductor by M_{MS} (with respective counts of these elements) and introduce similar notations (M_H) for coefficients of mutual induction of hollow conductor elements. We shall note by L_{MS} the coefficients of self-induction of solid conductor element (with respective count of this element); similar notations (L_H) shall be introduced for coefficients of self-induction of hollow conductor elements. As before, D.C. resistances of solid conductor elements shall be designated as $R_{MS(1)}, \ldots, R_{MS(4)}$, and of hollow conductor elements as $R_{H(1)}, \ldots, R_{H(5)}$.

Equation for νth element of solid conductor of pth group contains components of EMF caused by the following slot leakage fluxes $(\nu \leq 4, s \leq 4)$:

- flux due to load current $I_{MS(s)}$ in sth element of the same elementary conductor $(s \neq \nu)$

$$\Phi_{MS(\nu,s)} = I_{MS(s)}M_{MS(s,\nu)}; \quad M_{MS(s,\nu)} = M_{MS(\nu,s)}.$$

  For example, at ν = 1 and s = 4 we have:

$$\Phi_{MS(1,4)} = I_{MS(4)}M_{MS(4,1)}; \quad M_{MS(4,1)} = M_{MS(1,4)}.$$

- flux due to current $I_{MS(\nu)}$ in this element with count ν

$$\Phi_{MS(\nu)} = I_{MS(\nu)}L_{MS(\nu)}.$$

  For example, at ν = 1 we have:

$$\Phi_{MS(1)} = I_{MS(1)}L_{MS(1)}.$$

- flux due to current $I_{EL.GR}$ of all $n(p-1)$ groups of conductors arranged under the studied elementary conductor

$$\Phi_{MS(\nu,0)} = I_{EL.GR}n(p-1)M_{MS(\nu,0)}.$$

  For example, at ν = 1 we have:

$$\Phi_{MS(1,0)} = I_{EL.GR} n(p-1) M_{MS(1,0)}.$$

We note that for the second limiting position (Fig. 23.11b) shall be added other terms like

$$\Phi'_{MS(\nu,0)} = I_H M_{MS(\nu,0)}.$$

For example, at $\nu = 1$ we have:

$$\Phi'_{MS(1,0)} = I_H M_{MS(1,0)}.$$

By analogy, the equation for νth element of hollow elementary conductor of pth group contains components of EMF caused by leakage fluxes $(\nu \leq 5) : \Phi_{H(\nu,s)}, \Phi_{H(\nu)}, \Phi_{H(\nu,0)}$. We must note that for the first limiting position (Fig. 23.11a) shall be added other terms:

$$\Phi'_{H(\nu,0)} = I_{MS} M_{H(\nu,0)}.$$

For example, at $\nu = 1$ we have:

$$\Phi'_{H(1,0)} = I_{MS} M_{H(1,0)}.$$

Taking into account these equations for these fluxes the equation for the first element of solid elementary conductor counting from slot base becomes (for the first position in Fig. 23.11a, at $q = 1$):

$$\begin{aligned} &\left[I_{MS(1)}\left(j\omega L_{MS(1)} + R_{MS(1)}\right) + jI_{MS(2)} n\omega M_{MS(1,2)} + jI_{MS(3)} n\omega M_{MS(1,3)}\right. \\ &\quad \left. + jI_{MS(4)} n\omega M_{MS(1,4)}\right] \\ &+ \left[jI_{MS}(p-1) n\omega M_{MS(1,0)} + jI_H(p-1) n\omega M_{MS(1,0)}\right] = U. \end{aligned} \tag{23.86}$$

The first four terms in square brackets correspond to slot leakage fluxes produced by currents in elements of solid conductor of pth group, two other terms in square brackets—to slot leakage fluxes created by currents of $(p - 1)n$ groups arranged under investigated group. The both sums in square brackets are components of voltage in the slot part of elementary conductor from slot leakage fluxes.

In the same way we can write down the other three equations for three remaining elements of solid conductor.

Now let us proceed to equations for hollow conductor elements. With allowances for equations for some components of slot leakage flux we come to the equation for the first element:

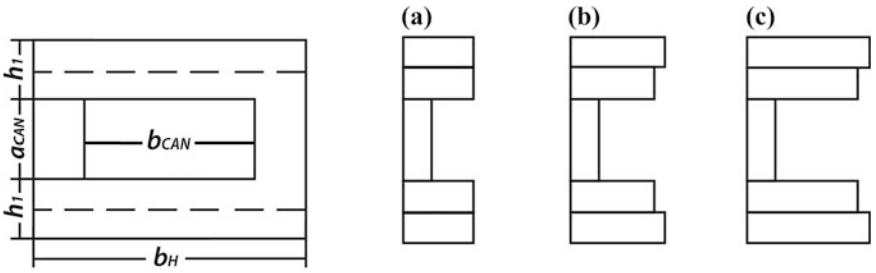

Fig. 23.13 Current distribution profiles with height of hollow elementary conductor. Computation results obtained with the help of numerical method: **a** at p = 1, **b** at p = 5 and **c** p = 15

$$\begin{aligned}&\left[\mathrm{I}_{\mathrm{H}(1)}\left(\mathrm{j}\omega\mathrm{L}_{\mathrm{H}(1)}+\mathrm{R}_{\mathrm{H}(1)}\right)+\mathrm{jI}_{\mathrm{H}(2)}\mathrm{n}\omega\mathrm{M}_{\mathrm{H}(1,2)}+\mathrm{jI}_{\mathrm{H}(3)}\mathrm{n}\omega\mathrm{M}_{\mathrm{H}(1,3)}\right.\\&\quad\left.+\ \mathrm{jI}_{\mathrm{H}(4)}\mathrm{n}\omega\mathrm{M}_{\mathrm{H}(1,4)}+\mathrm{jI}_{\mathrm{H}(5)}\mathrm{n}\omega\mathrm{M}_{\mathrm{H}(1,5)}\right]\\&\quad+\ \left[\mathrm{jI}_{\mathrm{H}}(\mathrm{p}-1)\mathrm{n}\omega\mathrm{M}_{\mathrm{H}(1,0)}+\mathrm{jI}_{\mathrm{MS}}(\mathrm{p}-1)\mathrm{n}\omega\mathrm{M}_{\mathrm{H}(1,0)}+\mathrm{jI}_{\mathrm{MS}}\mathrm{n}\omega\mathrm{M}_{\mathrm{H}(1,0)}\right]=\mathrm{U}.\end{aligned}\tag{23.87}$$

Four other equations for remaining four elements of hollow conductor shall be written in a similar way.

From a system of equations like (23.86) and (23.87) nine currents are to be specified in elements of slot group conductors, while from Eqs. (23.83)–(23.85)—the factor $\mathrm{K}_{\mathrm{F,COMB}}$ for first limiting position.

Four equations for solid conductors of slot group in the second limiting position (Fig. 23.11b) are to be written identically to (23.86). Five equations for one hollow conductor in second limiting position (Fig. 23.11b) are deduced in the way similar to (23.87). For this limiting position from the system similar to the previous one nine currents shall be specified in elements of both conductors and respectively factor $\mathrm{K}_{\mathrm{F,GR}}$. A resulting factor is

$$\mathrm{K}_{\mathrm{F,GR}}=\frac{\mathrm{K}_{\mathrm{F,GR}(1)}+\mathrm{K}_{\mathrm{F,GR}(2)}}{2}.$$

Let us write equations for self- and mutual induction coefficients making part of equation system.

For hollow elementary conductor in Fig. 23.13

$$
\begin{aligned}
&L_{H(1)} = \mu_0 L'_{SLT} \frac{1.667h_1 + a_{CAN}}{b_{SLT}}; \quad L_{H(2)} = \mu_0 L'_{SLT} \frac{1.667h_1 + a_{CAN}}{b_{SLT}};\\
&L_{H(3)} = \mu_0 L'_{SLT} \frac{h_1 + 0.334a_{CAN}}{b_{SLT}}; \quad L_{H(4)} = \mu_0 L'_{SLT} \frac{0.667h_1}{b_{SLT}};\\
&L_{H(5)} = \mu_0 L'_{SLT} \frac{0.167h_1}{b_{SLT}}; \quad \text{where } L'_{SLT} - \text{by } (23.2.41);\\
&M_{H(1,0)} = L_{H(1)}; M_{H(1,2)} = M_{H(2,0)} = L_{H(2)}; M_{H(1,3)} = M_{H(3,0)} = L_{H(3)};\\
&M_{H(1,4)} = M_{H(2,4)} = M_{H(3,4)} = M_{H(4,0)} = L_{H(4)};\\
&M_{H(1,5)} = M_{H(2,5)} = M_{H(3,5)} = M_{H(4,5)} = M_{H(5,0)} = L_{H(5)}.
\end{aligned}
\tag{23.88}
$$

For elements of solid conductor the inductions are to be written in a similar way.

We must note that in equations of EMF (23.86) and (23.87) the influence of leakage flux in end parts may be taken into account.

By way of illustration in Fig. 23.13 we show the current distribution profiles with height of hollow elementary conductor in winding of frequency-controlled motor: (a) for p = 1; (b) for p = 5. Its winding contains $m_{GR} = 8$ groups with height, the sizes of hollow and solid elementary conductors are given in the example of Sect. 23.2; frequency f = 48 Hz (g = 5).

From Eq. (23.85) and from the system of equations like (23.86) and (23.87) there shall be determined the losses and factor $K_{F,GR}$ not only in the bar with hollow and solid elementary conductors but for two special cases when the bar is made either only of solid or only of hollow elementary conductors. For example, in first special case it suffices to set the resistivity of hollow elementary conductors significantly greater than that for solid elementary conductors $(\sigma_H \ll \sigma_{MS})$.

The treatment of calculation results for losses in hollow elementary conductors with various overall sizes and channel dimensions at $\sigma_H = \sigma_{MS}$ shows that the factor K_{FH} may be calculated from relation:

$$
K_{F,H} \approx 1 + \left(K_{F,MS} - 1\right)\left[1 + 3(z+1)^2\right]\frac{1 + \frac{1.15zh_H}{(z+2)b_H}}{0.25(z+2)^4}, \tag{23.89}
$$

where $z = \frac{a_{CAN}}{h_H}$, $K_{F,MS}$ is the losses increase factor of in equivalent solid elementary conductors having the same overall dimensions as hollow conductors; according to (23.31):

$$
K_{F,MS} \cong 1 + \frac{(m^2 - 1)(K'h_H)^4}{9}.
$$

Relations (23.35) and (23.89) provide, for the same bar construction with hollow elementary conductors, the values of $K_{F,H}$ that differ by less than 2 %. This proves the validity of given calculations.

When comparing the results of numerical method of calculation of losses in bar with combined elementary conductors obtained with the help of Eqs. (23.81)–(23.85) and analytical Eqs. (23.78) and (23.79), we may see that the divergence

between them does not exceed 2 % (at $K'_{MS} < 1$, $K'_{H} < 1$), where K'_{MS}, K'_{H} are found following (23.14). This proves once again the validity of performed calculations.

On the basis of what was stated in this section we may see advantages and disadvantages of the numerical method of problem solving as compared with the analytical method.

The fulfilment of problem solving with the help of numerical methods of losses calculation enables us to obtain on the same assumptions the result with the same accuracy that performed by analytical method. It should be noted that when using numerical method there are practically no limitations (within adopted assumptions) imposed on geometric shape of elementary conductors.

In Sect. 23.3.1 we have already found that in engineering practice when designing machines it is important to have not only the numerical result, for example, the value of additional losses in bar with combined elementary conductors, i.e. value $K_{F,GR}$. Equally important is to know what is the influence on the result $\left(K_{F,GR}\right)$ exercised by other parameters characterizing the process, for example, what is its dependence on a_{CAN}, h_H. By solving the problem with the help of numerical methods it comes possible to establish such a dependence in a closed form (like formula) by applying special mathematical methods: law of similarity [12, 13, 34] design of experiments etc. To use these methods it would be necessary to carry out many calculations while changing reference parameters (for example, a_{CAN}, h_H) within the range, which is of practical interest.

List of symbols

a_0	Number of parallel branches in stator winding;
g	Order of temporal harmonic of the current;
$I_{H(1)}$, $I_{H(2)}$, …, $I_{H(d)}$	Amplitude of currents in hollow elementary conductors of group;
$I_{MS(1)}$, $IMS_{(2)}$, …, $I_{MS(b)}$	Amplitude of currents in solid elementary conductors of group;
I_H, I_{MS}	Amplitude of currents respectively in hollow and solid elementary conductors of group;
$I_{EL.GR}$	Amplitude of currents in group containing one hollow and q solid elementary conductors;
$K_{COMB(P)}$	Losses increase factor (Field's factor) for elementary conductors of pth group;
L_{MS}	Self-inductance for solid elementary conductors of group;
L_H	Self-inductance for hollow elementary conductors of group;
M_{MS}	Mutual inductance for solid elementary conductors of group;
M_H	Mutual inductance for hollow elementary conductors of group;

n	The number of elementary conductors at the width of the bar;
$R_{H(1)}$, $R_{H(2)}$, …, $R_{H(d)}$	D.C. resistances in hollow elementary conductors of group;
$R_{MS(1)}$, $R_{MS(2)}$, …, $R_{MS(b)}$	D.C. resistances in solid elementary conductors of group;
R_{GR}	D.C. resistance of the group of elementary conductors;
Φ_H	Leakage flux coupled with hollow elementary conductors of group;
Φ_{MS}	Leakage flux coupled with solid elementary conductors of group.

23.4 Losses Distribution in Bar Winding

23.4.1 Additional Losses Distribution in Winding Turns in Slots

Note. We will use in this para the RMS values for all currents and current densities.

Large power high-voltage machines, for example, diesel generators with low rotational speed, frequency-controlled motors are to be manufactured in some cases with multi-turn bar winding (number of bars in slot being $N > 2$). In some cases they may be produced with coil winding (with number of turns $S_{TR} > 1$). However, on reasons of winding repairability, its manufacturing in the form of bar winding is more preferred and may be unique in case of large sections of turn.

The design of two-pole turbine generators 8–10 MW with rated voltage 6.3 and 10.5 kV with thermosetting insulated two-layer winding developed by the "Electrosila" Work, StockCompany "Power Machines", St. Petersburg, has some special features. In such a machine, the number of effective conductors per stator slot should be at least 4–6. For the winding of coil type, each coil has $S_C = 2–3$ turns per coil. Experience shows that such two-pole coils with winding pitch in

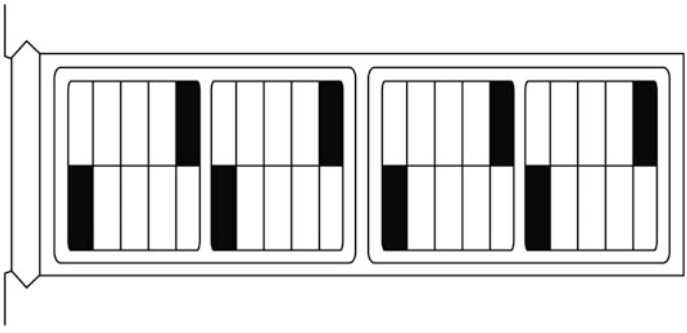

Fig. 23.14 Section of a *double-turn bar*

range of chording $0.8 \le \beta \le 0.833$ are difficult to manufacture and therefore not sufficiently reliable in operation.

For bar-type winding, each bar should contain 2 or 3 turns. Such bars are more complex than one-turn bar, but they are reliable enough in operation. For example, the "Electrosila" Work produced two-pole turbine-type generators up to 6 MW (6.3 kV, cos φ = 0.8) and synchronous motors up to 6 MW (6 kV, cos φ = 0.9) with two-turn bars (N = 4, β = 0.833) and also such turbogenerators of 6 MW (10.5 kV, cos φ = 0.8) and motors of 6 MW (10 kV, cos φ = 0.9) with three-turn bars (N = 6, β = 0.833).

The distribution of power losses over such bars is discussed below.

Figure 23.14 illustrates an example of a double turn bar (N = 4); let us designate the number of layers in turn along of height as m_B, and the total number of layers in slot is always m. The number of elementary conductors per turn of bar winding is $Q' = m_B n$. In practice multi-turn bars contain either N = 4 or N = 6.

Now let us consider the distribution of losses in double-layer winding. We shall do it first for winding with solid elementary conductors. Equation for losses increase factor in pth layer of elementary conductors counting from the slot base becomes according to (23.30):

$$K_{F,MS(P)} = 1 + \frac{(K'h_{MS})^4 (p-1)p}{3}. \tag{23.90}$$

For all Q' of elementary conductors in first turn (M = 1, counting from the slot base) we shall have from (23.90):

$$K_{F,MS(M=1)} = 1 + \frac{1}{m_B}\sum_{p=1}^{m_B}\left(K_{F,MS(p)} - 1\right) = 1 + \frac{(K'h_{MS})^4\left(m_B^2 - 1\right)}{9}.$$

By analogy, for all Q' of elementary conductors of second turn (M = 2):

$$K_{F,MS(M=2)} = 1 + \frac{1}{m_B}\sum_{p=m_B+1}^{2m_B}\left(K_{F,MS(p)} - 1\right) = 1 + \frac{(K'h_{MS})^4\left(7m_B^2 - 1\right)}{9}.$$

For an unspecified M while continuing the summing up it is not difficult to obtain the relation,

Table 23.6 Values of B for M = 1; 2; 3; 4; 5; 6

M	1	2	3	4	5	6
B_M	1	7	19	37	61	91

Table 23.7 Values of factor $K_{F,MS(M)}$ for several turns of bar

M	N = 2	N = 4	N = 6
1	1.083	1.021	1.009
2	1.583	1.146	1.065
3		1.396	1.176
4		1.771	1.343
5			1.56
6			1.843

$$K_{F,MS(M=N)} = 1 + \frac{(K'h_{MS})^4 (B_M m_B^2 - 1)}{9}, \quad \text{where } B_M = M^3 - (M-1)^3. \tag{23.91}$$

For some values of M = 1; 2; 3; 4; 5; 6 B_M values are given in Table 23.6.

So, additional losses in bar turns counting from the slot base satisfy, according to this table, the relation [20, 37, 38]: 1:7:19:37:61:91.

For subsequent calculations it shall be useful to find the relation between the values of factor $K_{F,MS(M=1)}$ of bottom turn of lower bar (M = 1) and factor $K_{F,MS}$ of elementary conductors of the whole slot, i. e. factor for all turns N. By determination of $K_{F,MS(M=1)}$ with allowance for (23.91) we have for $K_{F,MS(M=1)}$:

$$K_{F,MS(M=1)} = 1 + \frac{N(K_{F,MS} - 1)}{B_{(M=1)} + B_{(M=2)} + \cdots + B_{(M=N)}} = 1 + \frac{(K_{F,MS} - 1)}{N^2}. \tag{23.92}$$

Thus, the losses in a turn with number M at its A.C. flow-around are the following [37, 38]:

$$Q_{A.C.(M)} = Q_{D.C.} K_{F,MS(M)} = Q_{D.C.} \left[1 + \frac{(K_{F,MS} - 1) B_M}{N^2}\right], \tag{23.93}$$

where $Q_{D.S.}$—are losses in Mth turn at its flow-around by the direct current, $B_{(M)}$ is based on Table 23.6.

In Table 23.7 as indicated in Eq. (23.93) the values of $K_{F,MS(M)}$ are given for several turns of bar at M = 1; 2; 3; …; 6; they are of practical interest.

When obtaining Table 23.7 an average slot factor $K_{F,MS}$ as specified in (23.93) is equal to $K_{F,MS}$ = 1.333. It follows from the table that the larger the number of turns N in the slot, the higher the level of non-uniformity of losses distribution $Q_{A.C.}$.

Table 23.8 Dependence of losses $Q^*_{TP,BT}$ on an average slot factor $K_{F,MS}$

$K_{F,MS}$	1.1	1.15	1.2	1.25	1.3	1.4
$Q^*_{TR,BT}$	1.146	1.217	1.286	1.353	1.419	1.545

23.4.2 Losses in Several Bars of Double-Layer Winding

The relation of total losses in both slot bars of double-layer winding does not depend on the number of turns N in the slot and is specified only by an average slot factor $K_{F,MS}$. This important conclusion is the result of the following. For a lower bar the A.C. losses

$$\begin{aligned} Q_{A.C.(BT)} &= Q_{D.C.}\left[K_{F,MS(M=1)} + K_{F,MS(M=2)} + \cdots + K_{F,MS(M=0.5N)}\right] \\ &= Q_{D.C.}\left\{0,5N + 0.125N^3\left[K_{F,MS(M=1)} - 1\right]\right\} \end{aligned}. \tag{23.94}$$

Either with allowance of (23.4.3) we have:

$$Q_{A.C.(BT)} = Q_{D.C.}N\left[0.5 + 0.125\left(K_{F,MS} - 1\right)\right]. \tag{23.94'}$$

By analogy, for the upper bar whose turn numbers meet the relations M = 0.5 N + 1; M = 0.5 N + 2;… M = N we have:

$$\begin{aligned} Q_{A.C.(TP)} &= Q_{D.C.}\left\{0.5N + \left(N^3 - 0.125N^3\right)\left[K_{F,MS(M=1)} - 1\right]\right\} \\ &= Q_{D.C.}N\left[0.5 + 0.875\left(K_{F,MS(M=1)} - 1\right)\right]. \end{aligned} \tag{23.95}$$

By consequence, the ratio of total losses in both bars is given by:

$$Q^*_{TP,BT} = \frac{4 + 7\left(K_{F,MS} - 1\right)}{3 + K_{F,MS}}.$$

For example, at average slot factor $K_{F,MS}$ = 1.333 we have $Q^*_{TP,BT}$ = 1.462.

Table 23.8 provides the losses ratio $Q^*_{TP,BT}$ against an average slot factor $K_{F,MS}$.

From Table 23.8 it follows that for machines with high values of $K_{F,MS}$ the matters of upper bar heating may be of great importance.

Table 23.9 Losses ratio $Q^*_{TP,BT}$ in two outer turns against N

N	2	4	6
$Q^*_{TP,BT}$	1.462	1.735	1.826

23.4.3 Losses Ratio in Outer Turns in Slot

Let us specify the losses ratio in outer turns in the slot with numbers M = 1 and $M = N \geq 2$. This problem is more general than that one in the previous section. Its relevance is due to the following. When machines are in short-time overload that is typical, for example, for motors of ice-breakers, roll mills, mine hoists, the winding deformation in the slot is due to the rate of temperature Θ rise in its turns. This rate $\frac{d\Theta}{dt}$ (t—time) is to be determined for copper conductors at adiabatic heating from the following equation [14]:

$$\frac{d\Theta}{dt} \cong \frac{J^2}{200} K_{F,MS}(1 + \rho * \Theta), \left[\frac{^\circ C}{S}\right], \tag{23.96}$$

i.e. it is a function of $K_{F,MS}$; here ρ*—temperature coefficient of conductor resistivity, J [A/mm^2]—is the density of operational current in winding.

We find that in practical calculations at Θ < 100 °C the following relation may be roughly applied:

$$\frac{d\Theta}{dt} \cong \frac{J^2}{175} K_{F,MS}.$$

The factor $K_{F,MS}$ is to be calculated at a temperature under the condition of a strict solution to the problem on adiabatic heating; at this temperature the conductivity σ has been used in the calculation (23.14), (23.31) and (23.32).

At M = 1 and M = N we have:

$$Q^*_{TP,BT} = \frac{1 + \left(K_{F,MS(M=1)} - 1\right)\left[N^3 - (N-1)^3\right]}{K_{F,MS(M=1)}}. \tag{23.97}$$

Table 23.10 Average values of slot factors $K_{F,MS}$

N	2	4	6
$K_{F,MS}$	1.333	1.208	1.186

According to (23.97), Table 23.9 illustrates the losses ratio $Q^*_{TP,BT}$ in two outer turns laid in both bases of slot; an average factor $K_{F,MS}$ is assumed as equal to $K_{F,MS} = 1.333$.

From this table it follows that a multi-turn bar (N > 2) must be designed in such a way that an average slot factor is less than that designed for the standard single-turn bar (N = 2).

Now let us find the equation that determines an average factor $K_{F,MS}$ for elementary conductors in the slot on the basis of a given value of $Q^*_{TP,BT}$. From Eq. (23.97) we obtain:

$$K_{F,MS} = 1 + \frac{Q^*_{TP,BT} - 1}{3\left(1 - \frac{1}{N}\right) - \frac{Q^*_{TP,BT} - 1}{N^2}}. \tag{23.98}$$

In Table 23.10 according to (23.98) we show the values of $K_{F,MS}$ for the slot when $Q^*_{TP,BT} = 1.462$ as given in the previous table for standard double-turn winding (N = 2). Current densities in windings that differ by the number of turns N are supposed to be equal.

It follows from this table that in the multi-turn bar (N > 2) additional losses in the slot must be reduced by 1.5–2 times so as to keep the value $Q^*_{TP,BT}$ at the level which is ordinary for a single-turn bar (N = 2).

With some work it can be shown that obtained equations and losses ratios in winding bars remain true not only for bar constructions with solid elementary conductors, but also for other bar winding constructions (with incomplete transposition, with combined or hollow elementary conductors etc.).

23.4.4 Losses, Overheating and Bar Sizing in Non-standard Design of Stator Double-Layer Winding of Large Modern A.C. Machines

23.4.4.1 Introduction: Problem Statement

As it was mentioned above, the issues of stator winding construction for modern large power AC machines are due to the increase of the rate of their electromagnetic load.

In practice the following problems are put forward, which need to be solved when designing stator winding for these types of machines:

- reduction of losses ratio in both bars;
- reduction of ratio between their heating under steady-state and transient thermal conditions;
- reduction of losses value in slot part of bar.

To solve these problems, it would be appropriate to use a non-standard winding construction with bars of different height. Such a construction is most commonly used in modern practice.

23.4.4.2 Calculation Equations

(a) *Losses in both bars of different height.*

Let us write first calculation equations for losses in bars containing only solid elementary conductors (indirect cooling). It is assumed that there are two bars arranged in the slot; a lower bar (on slot bottom) contains nm_{BT} elementary conductors, at that, n of them are placed in row in one layer; usually [1, 5] n = 2. An upper bar (under wedge) contains respectively nm_{TP} elementary conductors. All elementary conductors in each bar are transposed between themselves [1, 5].

Calculation methods of losses in these bars have been examined in Sect. 23.2.5 for a special case ($m_{BT} = m_{TP}$). Here, we have to repeat only the major results obtained in this section while accounting for the peculiarities of bar construction under consideration.

In a general case we have a ratio $m_{BT} \neq m_{TP}$. In this section the ratios between m_{TP} and m_{BT} (at $m_{TP} + m_{BT} = \text{const}$) will be considered for such bars, and they correspond to the solution of problems laid down above.

Overall A.C. losses (D.C. and additional) in the slot part of each bar of double-layer winding are:

$$\begin{aligned} &\text{-in lower bar: } Q_{BT,SUM} = K_{F,BT} Q_{BT,D.C}; \\ &\text{-in upper bar: } Q_{TP,SUM} = K_{F,TP} Q_{TP,D.C}. \end{aligned} \tag{23.99}$$

Here: $K_{F,BT}$ $K_{F,TP}$ are losses increase factors [1, 5, 6] for lower and upper bars of different height; $Q_{BT,D.C.}$, $Q_{TP,D.C.}$ are D.C. losses in lower and upper bars of slot-embedded part:

$$Q_{BT,D.C.} = I^2 \frac{\rho L_{SLT}}{n m_{BT} b_{CON} h_{BT}}; \quad Q_{TP,D.C.} = I^2 \frac{\rho L_{SLT}}{n m_{TP} b_{CON} h_{TP}}, \tag{23.99'}$$

where I is the rated current in bar; L_{SLT} is the length of slot-embedded part; h_{BT}, h_{TP} are heights of lower and upper elementary conductors; b_{CON} is the width of elementary conductor; ρ is the resistivity of elementary conductor.

On technical reasons they usually choose for both bars the same elementary conductors ($h_{BT} = h_{TP} = h$); then for a general case (at $m_{BT} \neq m_{TP}$) the losses increase factors of both bars may take the form [1, 6]:

$$K_{F,BT} = 1 + D_{F,BT}; \quad K_{F,TP} = 1 + D_{F,TP}, \tag{23.100}$$

where

$$D_{F,BT} = \frac{(K'h)^4 m_{BT}^2}{9}; \quad D_{F,TP} = \frac{7(K'h)^4 m_{TP}^2}{9}; \quad K' = \sqrt{\frac{\omega \mu_0 n b_{CON}}{2\rho b_{SLT}}}. \tag{23.100'}$$

Let us mark with Z the relation between the numbers of elementary conductors:

$$Z = \frac{m_{BT}}{m_{SUM}}, \tag{23.101}$$

where $0 < Z < 1$; $m_{SUM} = m_{TP} + m_{BT}$—is the total number of layers occupied by elementary conductors in both slot bars (in the direction of its line of symmetry).

With allowance of Eqs. (23.99)–(23.101) we shall have the equation for A.C. losses in each bar with solid elementary conductors for a general case (at $m_{BT} \neq m_{TP}$):

$$\begin{aligned} &\text{in lower bar:} \\ &Q_{BT,SUM} = I^2 \frac{(1 + D_{F,SUM} Z^2)\rho L_{SLT}}{Z n m_{SUM} S}; \\ &\text{in upper bar:} \\ &Q_{TP,SUM} = I^2 \frac{\left[1 + D_{F,SUM}(1-Z)^2\right]\rho L_{SLT}}{(1-Z) n m_{SUM} S}. \end{aligned} \tag{23.102}$$

Here S is the section of elementary conductor,

$$D_{F,SUM} = K_{F,SUM} - 1 = \frac{(K'h)^4 m_{SUM}^2}{9}, \tag{23.103}$$

$K_{F,SUM}$ are the losses increase factors for all nm_{SUM} elementary conductors in the slot.

It should be noted that the values of $K_{F,SUM}$, $D_{F,SUM}$ do not depend on the values of Z; they are specified only by the total number of elementary conductors m_{SUM} in the slot.

In practice for machines with indirect cooling the value of $D_{F,SUM}$ is within a range (at Z = 0.5) of $0.05 < D_{F,SUM} \leq 0.33$; sometimes it is taken a little bit larger for high-power turbogenerators: $D_{F,SUM} < 0.4$.

Now let us examine the peculiarities of losses calculation in slot-embedded part of bars with solid and hollow elementary conductors (with direct water cooling) [20, 21]. We shall assume that the lower bar of winding contains $nm_{GR,BT}$ groups of elementary conductors; for bar construction of such a winding the following is usually true: n = 2. The upper bar contains respectively $nm_{GR,TP}$ groups of elementary conductors. Each group in both bars contains one hollow and q solid elementary conductors (usually q = 2 or q = 3). In a general case:

$m_{GR,BT} \neq m_{GR,TP}$. All elementary conductors of each bar are transposed between themselves [1, 5]. For technical reasons usually for both bars they choose the same elementary conductors both hollow and solid. Calculation methods for losses in bars are studied in Sect. 23.2.6 for a special case $(m_{GR,BT} = m_{GR,TP})$. Here, we have to repeat only the major results obtained in this section, while accounting for peculiarities of bar construction under consideration.

In general case $(m_{GR,BT} \neq m_{GR,TP})$ for losses $Q_{BT,SUM}$, $Q_{TP,SUM}$ in the slot-embedded part of both bars Eq. (23.102) remain valid when being updated by the following:

$D_{F,SUM}$ value is to be calculated from (23.79)

$$D_{F,SUM} = K_{F,SUM} - 1 = \Delta K_{EQ} \frac{q + F^3 \left(\frac{S_{H,CONT}}{S_H}\right)\left(\frac{\sigma_{MS}}{\sigma_H}\right) T}{q + F}, \qquad (23.103')$$

where $\Delta K_{EQ} = \left(K'_{MS} h_{MS}\right)^4 \frac{m_{GR}^2 (q+F)^2}{9}$, h_{MS} is the height of solid elementary conductor; K' is according to (23.100′); σ_H, σ_{MS} are electric conductivities of hollow and solid elementary conductors; $m_{GR,SUM}$ is the total number of layers occupied by groups in both bars in the slot (in the direction of its line of symmetry); S_H, S_{MS} is the section of hollow and solid elementary conductors; $F = \frac{\sigma_H/\sigma_{MS}}{S_H/S_{MS}}$; $S_{H.CONT} = h_H b_H$—is the space occupied by hollow conductor contour (circuit); $T = 1 - \left(\frac{a_{CAN}}{h_H}\right)^3 \frac{b_{CAN}}{b_{CON}}$; $b_{CAN}, b_{CON} = b_H$ is the channel width in hollow conductor and respectively the width of conductor; h_H, a_{CAN} is the height of hollow conductor and of channel, respectively. It should be noted that in some constructions solid and hollow elementary conductors are made with different conductivities $(\sigma_H \neq \sigma_{MS})$; the value of Z is calculated from (23.101′):

$$Z = \frac{m_{GR,BT}}{m_{GR,SUM}}, \qquad (23.101')$$

where $0 < Z < 1$; $S = S_H + qS_{MS}$.

In practice for machines with direct water cooling the value of $D_{F,SUM}$ is within a range (at $Z = 0.5$): $0.4 < D_{F,SUM} \leq 0.8$.

From obtained design data it follows that for winding construction with direct cooling the values of $K_{F,SUM}, D_{F,SUM}$ do not depend on the values of Z; they are specified by the total number of elementary conductors $m_{GR,SUM}$ in the slot. Similar results have been obtained for winding with indirect cooling.

The A.C. losses in both winding bars with direct and indirect cooling are:

$$\begin{aligned} Q_{SUM,Z} &= Q_{BT,SUM} + Q_{TP,SUM} \\ &= \frac{I^2 \rho L_{SLT}}{n m_{GR,SUM} S} \left[\frac{1 + 7D_{F,SUM}(1-Z)^2}{(1-Z)} + \frac{1 + D_{F,SUM} Z^2}{Z} \right] \end{aligned} \qquad (23.104)$$

the value of S is calculated from equation: $S = S_H + qS_{MS}$ is the section of elementary conductors of slot group.

According to this equation you will find below the dependence of losses in slot on the relation Z = var (at $0 < Z \leq 1$): $Q_{SUM,Z} = f(Z)$. In practical calculations it would be useful to find a specific value of these losses (in p. u.) by calculating beforehand the relation of losses $Q_{SUM,Z}$ specified by Eq. (23.104) at Z = var against losses $Q_{SUM,Z=0.5}$ specified by the same equation at Z = 0.5:

$$Q^*_{SUM,Z} = \frac{Q_{SUM,Z}}{Q_{SUM,Z=0.5}} = \frac{1 + D_{F,SUM}Z^2}{4Z(1 + D_{F,SUM})} + \frac{1 + D_{F,SUM}7(1 - Z)^2}{4(1 - Z)(1 + D_{F,SUM})}. \quad (23.105)$$

From this equation it follows that relative losses $Q^*_{SUM,Z}$ may be determined only by two variables: $D_{F,SUM}$ according to Eqs. (23.103) or (23.103′) and Z according to Eqs. (23.101) or (23.101′).

(b) *Overheating and its relationship at different sizes of both bars in slot*

We shall study the overheating for different operating conditions.

Calculation equations for transient conditions

When changing load conditions for winding with indirect cooling it is usually assumed [14] that the overheating of winding at $\frac{t}{T_\Theta} = 0.1-0.2$ varies following the adiabatic relation (t—time, T_Θ—time constant of thermal process in winding). For further calculations, one may admit that this assumption is also true for a winding with direct water cooling. Then for lower bar the rate of its overheating variation Θ_{BT} is equal to [14]:

$$\frac{d\Theta_{BT}}{dt} = Q_{BT,SUM}\frac{a_2^2 - a_1^2}{C_{CON}G_{BT}}, \quad (23.106)$$

where C_{CON} is the specific heat of copper; G_{BT} is the weight of copper in bar; a_2, a_1 are the current values in bar before load conditions are changed and after such a change (in fractions of rated current), respectively. By analogy with Eq. (23.106), the equation for upper bar overheating variation $\frac{d\Theta^*_{TP,BT}}{dt}$ may be written.

In practical calculations it would be useful to find the overheating ratio under transient conditions for both bars $\Theta^*_{TP,BT}\frac{\Theta_{TP}}{\Theta_{BT}}$; taking into account Eqs. (23.102) and (23.106) we have:

$$\frac{d\Theta^*_{TP,BT}}{dt} = \frac{Q_{TP,SUM}}{Q_{BT,SUM}} \cdot \frac{G_{BT}}{G_{TP}}. \quad (23.107)$$

(c) *Calculation equations for steady-state conditions*

Indirect cooling. The value Θ_B of overheating of each winding bar in these operating conditions contains three components [1, 5, 14] of temperature difference between the elementary conductor and cooling gas in machine air gap; Θ_{INS} is the temperature difference in slot insulation, Θ_{CR}—in stator core, Θ_{CNV}—is the convective temperature drop between stator core surface and cooling gas.

The component Θ_{INS} for lower bar is equal to:

$$\Theta_{INS,BT} = \frac{Q_{BT,SUM} D_{INS}}{\lambda_{INS} F_{BT}} = \frac{Q_{BT,SUM}}{\Lambda_{INS,BT}}, \tag{23.108}$$

where $\Lambda_{INS,BT}$ is the thermal conductivity of slot insulation; D_{INS} is the one-sided thickness of slot insulation; λ is the specific thermal conductivity of insulation; F_{BT} is the cooling surface of lower bar. By analogy with (23.108) the equation may be written for the component $\Theta_{INS,TP}$ of upper bar. For lower bar the conductivity for thermal fluxes in the direction of slot base and in the direction of inter-bar insulation is considerably less than that in the direction of active steel teeth; for upper bar the conductivity in the direction of wedge is also considerably less than that one in the direction of teeth. Taking into account the above said, we shall have for both bars: $F_{BT} \approx 2L_{SLT}m_{BT}h$, $F_{TP} \approx 2L_{SLT}m_{TP}h$, then the slot insulation conductivity is equal to:

$$\Lambda_{INS,BT} = \frac{\lambda 2 L_{SLT} m_{BT} h}{D_{INS}}; \Lambda_{INS,TP} = \frac{\lambda 2 L_{SLT} m_{TP} h}{D_{INS}} \tag{23.108'}$$

For two other components of heat drop $(\Theta_{CR}, \Theta_{CNV})$ equations similar to (23.108) shall be valid. For example, for lower bar:

$$\Theta_{CR,BT} = \frac{Q_{BT,SUM}}{\Lambda_{CR,BT}}, \quad \Theta_{CNV,\ BT} = \frac{Q_{BT,SUM}}{\Lambda_{CNV,BT}},$$

where $\Lambda_{CR,BT}, \Lambda_{CNV,BT}$ are thermal conductivities for fluxes in core and from the surface of stator core in cooling gas.

For upper bar calculation relations are identical.

As a result, the value of overheating Θ_B of each bar shall have the form:

$$\Theta_{B,BT} = \frac{Q_{BT.SUM}}{\Lambda_{BT}}, \quad \Theta_{B,TP} = \frac{Q_{TP.SUM}}{\Lambda_{TP}},$$

where Λ_{BT}, Λ_{TP} are equivalent slot thermal conductivities for thermal fluxes of lower and upper bars respectively.

It may be shown [1, 4, 5] that an equivalent thermal conductivities for core package $\Lambda_{CR,BT}$ obtained from the equivalent thermal circuit is formed by a series of conductivities; some of them are proportional to lower bar height $H_{BT} = hm_{BT}$, for example, stator core conductivity in the area of teeth; however, others of them are not a function of the height H_{BT}, for example, stator core conductivity in the

area of yoke. In a similar way, an equivalent conductivity $\Lambda_{CNV,BT}$ obtained from the equivalent thermal circuit does not practically depend on the height H_{BT} at calculations of the component Θ_{CNV} of convective temperature drop, practically does not depend on the height H_{BT}. These regularities remain true for conductivities in components of temperature drops in upper bar whose height is proportional to $H_{TP} = hm_{TP}$.

Now we shall consider the following two limiting cases for both bars in slot.

In the case $\Lambda_{BT} = f(H_{BT}), \Lambda_{TP} = f(H_{TP})$ we have:

$$\left[\Theta^*_{TP,BT}\right]_I = \frac{Q_{TP.SUM}}{Q_{BT.SUM}} \cdot \frac{m_{BT}}{m_{TP}}. \tag{23.109}$$

In the case $\Lambda_{BT} \neq f(H_{BT}), \Lambda_{TP} \neq f(H_{TP})$ we have:

$$\left[\Theta^*_{TP,BT}\right]_{II} = \frac{Q_{TP.SUM}}{Q_{BT.SUM}}. \tag{23.109'}$$

A real relation $\left[\Theta^*_{TP,BT}\right]_{MID}$ of both bars overheating is within the range:

$$\left[\Theta^*_{TP,BT}\right]_I < \left[\Theta^*_{TP,BT}\right]_{MED} < \left[\Theta^*_{TP,BT}\right]_{II}. \tag{23.110}$$

We shall note that the overheating component Θ_{INS} may reach approximately 50 % of bar overheating.

Direct water cooling. In winding construction with direct water cooling the temperature of bars [1, 5, 14] is specified by water overheating in hollow conductors, under steady state conditions it may be regulated by water flow through the winding [39]; the component of convective temperature drop between the wall of hollow conductor channel and the water is insignificant and this component may be neglected.

Usually both winding bars (upper and lower) are connected hydraulically in a series, for example, in the construction of turbogenerators of $P \leq 300-500$ MW rated power; for machines of rated power, for example, for turbogenerators of $P \geq 500$ MW rated power the bars are usually connected hydraulically in parallel.

Calculations equations for an average bar overheating are the following:

at hydraulic coupling of both bars in parallel:

$$\Theta_{TP} = \frac{Q_{TP.SUM}}{2C_W L_{TP}}; \quad \Theta_{BT} = \frac{Q_{BT.SUM}}{2C_W L_{BT}}; \tag{23.111}$$

Table 23.11 Bars of equal height Z = 0.5: $Q^*_{TP,BT} = f(D_{F,SUM})$

$D_{F,SUM}$	0.4	0.6	0.8	1.0
$Q^*_{TP,BT}$	1.545	1.783	2.0	2.2

at hydraulic coupling of both bars in a series when the upper bar is connected to a cold water collecting channel (version 1):

$$\Theta_{TP} = \frac{Q_{TP.SUM}}{2C_W L_{TP}}; \quad \Theta_{BT} = \frac{Q_{TP.SUM} + 0.5Q_{BT.SUM}}{C_W L_{BT}}; \tag{23.111'}$$

at hydraulic coupling of both bars in a series when the lower bar is connected to a cold water collecting channel (version 2):

$$\Theta_{TP} = \frac{\frac{1}{2}Q_{TP.SUM} + Q_{BT.SUM}}{C_W L_{TP}}; \quad \Theta_{BT} = \frac{Q_{BT.SUM}}{2C_W L_{BT}}, \tag{23.111'}$$

where C_W is the water specific heat; L_{TP}, L_{BT}—are water flows through each bar; at both bars hydraulic coupling in the series: $L_{TP} = L_{BT} = L$.

The values of $\Theta^*_{TP,BT}$ are given in Sect. 23.4.4.3 with account of various versions of hydraulic bar coupling.

23.4.4.3 Practical Results Bar Sizing, Relations Between Bar Losses and Between Their Overheating

The service experience has shown that long-run displacement of bars relative to each other and relative of the slot gives the failure of their insulation. Such displacements are due to different losses and overheating of upper and lower winding bars.

(a) Bar sizing and relations between bar losses

Losses $Q_{TP.SUM}$ and $Q_{BT.SUM}$ in the winding of standard design with equal height of upper and lower bars ($Z = 0.5$) are different; thus their overheating is different too. In Table 23.11 the relation $Q^*_{TP,BT} = \frac{Q_{TP.SUM}}{Q_{BT.SUM}} = f(D_{F,SUM})$ of losses is given according to Eqs. (23.102) and (23.103) at $Z = 0.5$ and at $0 \le D \le 1$.

From Eqs. (23.85), (23.86), (23.102) and (23.103) it follows that for machines with indirect cooling in a limiting case (at $D_{F,SUM} = 0.33$) losses relation in bars makes $Q^*_{TP,BT} = 1.462$ and for machines with direct water cooling in a limiting case (at $D_{F,SUM} = 0.8$) this relation according to these equations and Table 23.11 makes $Q^*_{TP,BT} = 2.0$. These results prove the necessity to take for A.C. large power machines additional measures so as to reduce losses relation at $Z = 0.5$.

Table 23.12 Equal losses in both bars in slot $Q^*_{TP,BT} = 1; Z = f(D_{F,SUM}); Q_{SUM,Z} = f(D_{F,SUM})$

$D_{F,SUM}$	1.0	0.8	0.6	0.40	0.2	0
Z	0.1423	0.1758	0.1171	0.3069	0.41	0.5
$Q^*_{SUM,Z}$	1.7924	1.6191	1.4186	1.2076	1.0502	1.0

Table 23.13 Bars of different sizes (Z = var): $Q^*_{SUM,Z} = f(Z)$, $Q^*_{TP,BT} = f(Z)$, $T^*_{TP,BT} = f(Z)$, $\Theta^*_{BT,TP} = f(Z)$ at $D_{F,SUM} = 0.33$ and $D_{F,SUM} = 0.80$

$D_{F,SUM} = 0.33$				$D_{F,SUM} = 0.80$			
Z	$Q^*_{SUM,Z}$	$Q^*_{TP,BT}$	$T^*_{TP,BT}$	$Q^*_{SUM,Z}$	$Q^*_{TP,BT}$	$T^*_{TP,BT}$	$\Theta^*_{BT,TP}$
0.5	1.0	1.4611	1.4611	1.0	2.0	2.0	2.5
0.48	1.0087	1.3977	1.2901	1.0142	1.9596	1.8089	2.5112
0.46	1.0198	1.3367	1.1387	1.0302	1.9182	1.6340	2.5213
0.44	1.0334	1.2777	1.0039	1.0481	1.8751	1.4733	2.5333
0.42	1.0497	1.2203	0.8837	1.0679	1.8300	1.3252	2.5464
0.40	1.0687	1.1641	0.7761	1.0898	1.7825	1.1883	2.5610
0.38	1.0908	1.1088	0.6796	1.1140	1.7322	1.0616	2.5773
0.36	1.1163	1.0541	0.5929	11.1406	1.6787	0.9443	2.5957

In general case (at Z = var) the relation between losses in upper and lower bars has the form according to (23.103), (23.104):

$$Q^*_{TP,BT} = \frac{1 + D_{F,SUM}7(1-Z)^2}{1 + D_{F,SUM}Z^2} \cdot \frac{Z}{1-Z} \cdot \tag{23.112}$$

From this equation it follows that the value $Q^*_{TP,BT}$ is determined only by two variables: $D_{F,SUM}$ according to (23.103) or (23.103′) and Z according to (23.101) or (23.101′).

Let us find the first with the help of (23.112) the sizes of each of bars for the case when their losses relation $Q^*_{TP,BT} = 1$ (equal losses in both bars); after transformation of (23.112) we shall have: $D_{F,SUM} = \frac{2Z-1}{(1-Z)(8Z^2-7Z)}$. This cubic equation has the solution at $D_{F,SUM} \geq 0$ only in cases when the relation Z is within the range: $0 \leq Z \leq 0.5$ and at $0.875 < Z < 1.0$; the last variation range is of no practical interest. The results of calculation of values Z within the range of $0 \leq Z \leq 0.5$ are shown in Table 23.12. Additionally relative values of losses $Q^*_{SUM,Z}$ obtained from Eq. (23.105) are shown in this table.

From Table 23.12 it follows that total losses in slot $Q^*_{SUM,Z}$ at $Q^*_{TP,BT} = 1$ and $Z \neq 0.5$ are significantly larger than in the standard winding (at Z = 0.5). Taking into consideration the losses of machine efficiency and the increase of winding overheating, one may conclude that the winding construction for which $Q^*_{TP,BT} = 1$, is not useful. In practice they adopt usually a compromise decision where the values $Q^*_{SUM,Z} \rightarrow 1$ and $Q^*_{TP,BT} \rightarrow 1$. Normally the losses increase $Q^*_{SUM,Z}$ is limited by $Q^*_{SUM,Z} \leq 1.05 - 1.10$ (with allowance of the possibility of efficiency factor decreasing).

While solving the problem related to the choice of sizes for both bars it is assumed that slot sizes and relevant value of $D_{F,SUM}$ as well as an assumed level of losses $Q^*_{SUM,Z} \leq 1.05 - 1.10$ are practically specified. In this case the following problem solution will be the most convenient.

- from Eqs. (23.105) and (23.112) to calculate relations, $Q^*_{SUM,Z} = f(Z)$, $Q^*_{TP,BT} = f(Z)$. Using these relations:
- to choose a given range of the value of relative losses $Q^*_{SUM,Z}$ and relevant equations;
- to specify for this value of Z the losses relation $Q^*_{TP,BT}$.

Relations $Q^*_{SUM,Z} = f(Z)$, $Q^*_{TP,BT} = f(Z)$, for limiting values of $D_{F,SUM} = 0.33$ and $D_{F,SUM} = 0.80$ are given as an example in Table 23.13.

Bar Sizing and Relations Between Bar Overheating

Transient conditions

The following Eqs. (23.106) and (23.107) have been obtained for these conditions in the previous section. The relationship between the rate of overheating variation $\frac{d\Theta^*_{TP,BT}}{dt}$ and the relation Z may be obtained from these equations with due account of losses (23.102) in both bars:

$$\frac{d\Theta^*_{TP,BT}}{dt} = Q^*_{TP,BT}\frac{Z}{1-Z},$$

or

$$\frac{d\Theta^*_{TP,BT}}{dt} = \frac{1 + D_{F,SUM}7(1-Z)^2}{1 + D_{F,SUM}Z^2} \cdot \frac{Z^2}{(1-Z)^2}. \qquad (23.107')$$

When performing practical calculations it may be possible to calculate beforehand from Eq. (23.107′) the relations $\frac{d\Theta^*_{TP,BT}}{dt} = f(Z)$ for each value of $D_{F,SUM}$. These relations for limiting values of $D_{F,SUM} = 0.33$ and $D_{F,SUM} = 0.80$ are given in Table 23.13 as an example in the form of $T^*_{TP,BT} = f(Z)$.

Steady state conditions: Indirect cooling

A calculation equation for the first limiting case $\left[\Theta^*_{TP,BT}\right]_I$ may be taken from Eq. (23.109); it coincides with (23.107′). The relation $\left[\Theta^*_{TP,BT}\right]_I = f(Z)$ for a limiting value of $D_{F,SUM} = 0.33$ (indirect cooling) is given as an example in Table 23.13 in the form of $T^*_{TP,BT} = f(Z)$.

A calculation equation for the second limiting case $\left[\Theta^*_{TP,BT}\right]_{II}$ can be obtained from Eq. (23.109′); it coincides with Eq. (23.112). The relation $\left[\Theta^*_{TP,BT}\right]_{II} = f(Z)$ for a limiting value $D_{F,SUM} = 0.33$ is given as an example in Table 23.13 in the

form of $Q^*_{TP,BT} = f(Z)$. Real values of medium overheating $\left[\Theta^*_{TP,BT}\right]_{MED}$ are shown in Table 23.13 at Z = idem between values $T^*_{TP,BT}$ and $Q^*_{TP,BT}$.

Steady state conditions: Direct cooling

- *The both bars are hydraulically coupled in parallel*

The relation of overheating $\Theta^*_{TP,BT} = \frac{\Theta_{TP}}{\Theta_{BT}}$ in both bars has been obtained after the transformation of calculation Eq. (23.111):

$$\Theta^*_{TP,BT} = Q^*_{TP,BT}\frac{L_{BT}}{L_{TP}} = Q^*_{TP,BT}\frac{m_{GR,BT}}{m_{GR,TP}}\cdot\frac{V_{BT}}{V_{TP}} = Q^*_{TP,BT}\frac{Z}{1-Z}\cdot\frac{V_{BT}}{V_{TP}}$$
$$= Q^*_{TP,BT}\frac{Z}{1-Z}V^*,$$

where $V^* = \frac{V_{BT}}{V_{TP}}$, V_{BT}, V_{TP} is the velocity of cooling water in respective bars. If we assume that $V^* \approx 1$, equation $\Theta^*_{TP,BT} = f(Z)$ coincides with (23.107′). For a limiting value $D_{F,SUM}$ = 0.8 (direct cooling) it is given as an example in Table 23.13 in the form of relation $T^*_{TP,BT} = f(Z)$.

- *The both bars are hydraulically connected in series*

The relation of overheating $\Theta^*_{TP,BT} = \frac{\Theta_{TP}}{\Theta_{BT}}$ in both bars has been estimated after the transformation of calculation Eqs. (23.111) and (23.111′) in the form:

for version 1:

$$\Theta^*_{TP,BT(1)} = \frac{\frac{1}{2}Q_{TP,SUM}}{Q_{TP,SUM} + \frac{1}{2}Q_{BT,SUM}} = \frac{Q^*_{TP,BT}}{2Q^*_{TP,BT}+1};$$

It should be noted that with such a scheme the overheating of upper bar is less than that of lower bar, so $\Theta^*_{TP,BT(1)} < 1$:

for version 2:

$$\Theta^*_{TP,BT(2)} = \frac{\frac{1}{2}Q_{TP,SUM} + Q_{BT,SUM}}{\frac{1}{2}Q_{BT,SUM}} = Q^*_{TP,BT} + 2;$$

We should note that with such a scheme the overheating of upper bar is greater than that of lower bar, so $\Theta^*_{TP,BT(2)} > 1$.

When comparing relations $\Theta^*_{TP,BT(2)}$ and $\frac{1}{\Theta^*_{TP,BT(1)}}$ we find that the version 1 of connection is more preferable: $\frac{1}{\Theta^*_{TP,BT(1)}} < \Theta^*_{TP,BT(2)}$ at any values of within the range $1 < Q^*_{TP,BT} < 2$, which is of practical interest. The results of calculation of relation $\Theta^*_{BT,TP} = \frac{1}{\Theta^*_{TP,BT(1)}} f(Z)$ for $D_{F,SUM}$ = 0.8 are given as an example in Table 23.13.

From the solution of given equations and from Table 23.13 it follows that the values $\Theta^*_{BT,TP} = f(Z)$ in the domain of relative losses $1.0 < Q^*_{SUM,Z} < 1.1$ do not practically vary: $\Theta^*_{BT,TP} \approx 2.5$.

Unlike the bars with indirect cooling these values of relation $\Theta^*_{BT,TP}$ for a bar with direct water cooling are ordinary and needs some measures to be taken so as to ensure the operational reliability of winding with this system of cooling: by regulating cooling water, the consumption according to the generator loading low overheating of both winding bars is kept constant [39].

Practical limits are discussed of parameter variation of windings with direct and indirect cooling. Limit values of bar relative height Z and limit values of relative losses $Q^*_{TP,BT}$, $Q^*_{SUM,Z}$ and overheating $T^*_{TP,BT}$, $\Theta^*_{BT,TP}$ are shown in Table 23.13.

On the basis of calculation results in Table 23.13 it is easy to set the regularities defining dependences of relative values $Q^*_{SUM,Z}, Q^*_{TP,BT}$ $T^*_{TP,BT}$, $\Theta^*_{BT,TP}$ on $D_{F,SUM}$ and Z.

Calculation Example 1. Let it be given the following: the slot of generator stator with indirect cooling may contain $nm_{SUM} = 2.92$ elementary conductors (with allowance for slot insulation); these elementary conductors have the losses increase factor equal to $K_{F,SUM} = 1 + D_{F,SUM} = 1.38$. It is required to specify the sizes of both bars in the slot under the condition that $Q^*_{SUM,Z} \leq 1.04$.

According to Eq. (23.105) for $D_{F,SUM} = 0.38$ and $Q^*_{SUM,Z} \approx 1.04$ we may have Z = 0.4348 (at $m_{BT} = 2{\cdot}92{\cdot}0.4348 = 2{\cdot}40$; $m_{TP} = 2{\cdot}52$). An adjusted value of $Q^*_{SUM,Z}$ is equal to $Q^*_{SUM,Z} = 1.0395$; from Eq. (23.112): $Q^*_{TP,BT} = 1.3276$; from Eq. (23.107′): $T^*_{TP,BT} = 1.0213$. These values correspond to limiting values given in Table 23.13 at $D_{F,SUM} = 0.33$.

Note: For $D_{F,SUM} = 0.38$ and $Z = 0.5$ (standard winding construction) according to given equations we shall have $Q^*_{TP,BT} = T^*_{TP,BT} = 1.5205$. As compared to this construction when choosing the winding with the found value of Z = 0.4348 (non-standard design) the reduction of value $Q^*_{TP,BT}$ makes: $\frac{1.3276}{1.5205} = 87.35\ \%$; of value $T^*_{TP,BT} = \frac{1.0213}{1.5205} = 67.2\ \%$.

Calculation Example 2. We give the following: the slot of generator stator with direct cooling may contain $nm_{GR,SUM} = 2{\cdot}20$ groups of hollow and solid elementary conductors (with allowance of slot insulation); these groups of elementary conductors have the losses increase factor equal to $K_{F,SUM} = 1 + D_{F,SUM} = 1.571$. Winding bars are hydraulically connected in parallel; $V^* = 1$. It is necessary to specify the sizes of both bars in slot under the condition that $Q^*_{SUM,Z} \leq 1.085$.

Following Eq. (23.105) for $D_{F,SUM} = 0.571$ and $Q^*_{SUM,Z} \approx 1.08$ we shall have Z = 0.4 (at $m_{GR,BT} = 2{\cdot}20{\cdot}0.4 = 2{\cdot}8$, $m_{GR,TP} = 2{\cdot}12$). An adjusted value of $Q^*_{SUM,Z}$ is equal to $Q^*_{SUM,Z} = 1.081$; from Eq. (23.112): $Q^*_{TP,BT} = 1.4898$; from Eq. (23.107′): $T^*_{TP,BT} = 0.9932$. Found values correspond to limiting values given in Table 23.13 at $D_{F,SUM} = 0.8$.

Note: $D_{F,SUM} = 0.571$ and $Z = 0.5$ (standard winding design) according to given equations we shall have $Q^*_{TP,BT} = T^*_{TP,BT} = 1.7495$. As compared to this

Table 23.14 Minimum losses in both bars in slot: $Z = f(D_{F,SUM})$, $Q^*_{SUM,Z} = f(D_{F,SUM})$

$D_{F,SUM}$	0.4	0.5	0.6	0.7	0.8
Z	0.5719	0.5881	0.6032	0.6172	0.6303
$Q^*_{SUM,Z}$	0.9843	0.9773	0.9098	0.9619	0.9536

construction when choosing the winding with the found value of Z = 0.4 (non-standard design) the reduction of value $Q^*_{TP,BT}$ makes: $\frac{1.4898}{1.7495}$ = 85.16 %; of value $T^*_{TP,BT} = \frac{0.9932}{1.7495}$ = 56.8 %.

It follows from both examples that the reduction of overheating $T^*_{TP,BT}$ in comparison to the standard winding design (Z = 0.5) makes 70 % (irrespective of the mode of winding cooling), at that, for winding with direct cooling the value $T^*_{TP,BT}$ makes $T^*_{TP,BT} \approx 1$.

23.4.4.4 Reduction of Losses in Both Winding Bars

In 23.4.4.2 there have been mentioned some peculiarities of winding with direct cooling (the practice of water consumption regulation in terms of generator loading [39] with the aim to keep a specified level of winding overheating, a low level of this overheating as compared to the winding with indirect cooling etc.). With allowance of this consideration it would be useful to examine the problem related to losses reduction in both bars in slot.

This problem may be solved with the help of Eq. (23.105). For losses $Q^*_{SUM,Z}$ in both bars in slot at arbitrary relation of Z, we shall have:

$$\frac{1 + D_{F,SUM} 7(1 - Z)^2}{1 - Z} + \frac{1 + D_{F,SUM} Z^2}{Z} = \min$$

or after transformation:

$$\frac{1}{(1 - Z)^2} - \frac{1}{Z^2} = 6D_{F,SUM}. \tag{23.113}$$

It follows from this equation that minimum losses are specified only by variables $D_{F,SUM}$ and Z. In Eq. (23.113) there exists such a solution within the range of $0.5 < Z < 1.0$ (in contrast to the problem of Sect. 23.4.4.3). The results of problem solving within $0.4 < D_{F,SUM} < 0.8$ being of practical interest are given in Table 23.14.

The maximum reduction of losses in both winding bars at $Z > 0.5$ is less than 5 %; the utility of using the winding of such a construction ($Z > 0.5$) is to be specifically considered for each generator with due account of the value of its

current load, relative value of winding losses as compared to other components of losses in generator, value of its efficiency etc.

Brief Conclusions

1. For the construction of stator winding with both indirect gas and direct water cooling its parameters: $Q^*_{TP,BT}$ (losses relation in upper and lower bars), $Q^*_{SUM,Z}$ (relative value of losses in both bars in slot), $T^*_{TP,BT}$, $\Theta^*_{TP,BT}$ (relation of upper and lower bars overheating) are specified only by two variables: $D_{F,SUM}$ (total number of elementary conductors in slot) and the relation Z of the number of elementary conductors (or groups) in both slot bars.
2. The values $D_{F,SUM}$ and Z comprised in obtained equations for calculation of parameters $Q^*_{TP,BT}$, $Q^*_{SUM,Z}$, $T^*_{TP,BT}$, $\Theta^*_{TP,BT}$ are the defining criteria. For both stator winding constructions the values of parameters $Q^*_{TP,BT}$, $T^*_{TP,BT}$ are smaller with criteria Z changing in range $0.4 < Z < 0.5$ than at $Z = 0.5$.
3. For a winding with direct cooling minimum values of losses in both slot bars are obtained at values of criteria Z within $0.572 < Z < 0.63$ (at $0.4 < D_{F,SUM} < 0.8$).

List of symbols

b_{CON}	Width of elementary conductor;
b_{SLT}	Width of slot;
C_{CON}	Specific heat of conductor;
C_W	Specific heat of distillate;
G_{BT}, G_{TP}	Respectively weight of copper of lower and upper bars of double-layers winding;
$h_{BT} = h_{TP} = h$	Respectively height of elementary conductor of lower and upper bars of double-layers winding;
I	Amplitude of stator current under load;
J	Current density in winding conductor;
K′	Factor of reduction of the height of the elementary conductor to the dimensionless parameter;
$K_{F,MS(P)}$	Field's factor of massive conductor in the p-th layer of multiturn bar winding counting on the bottom of slot;
$K_{F,MS(M=1)}$, $K_{F,MS(M=2)}$, $K_{F,MS(M=3)}$, …., $K_{F,MS(M=N)}$	Field's factors of massive conductor in bars with number M = 1, M = 2, M = 3, …., M = N for multiturn bar winding;
$K_{F,MS}$	Field's factor for multiturn bar winding (for all turns in the slot);
$K_{F,BT}$	Field's factor for lower bar of double-layer winding with different height of bars;
$K_{F,TP}$	Field's factor for upper bar of double-layer winding with different height of bars;

L	Distillate consumption in lower and in upper bars hydraulically connected serially;
L_{BT}, L_{TP}	Respectively distillate consumption in lower and upper bas hydraulically connected parallel;
L_{SLT}	Length of slot part of winding without accounting of the channel in the active stator core;
M	The number of elementary conductors on the height of the bar counting from the bottom of slot;
m_{TP}	Number of elementary conductors in upper bar of double-layer winding;
m_{BT}	Number of elementary conductors in lower bar of double-layer winding;
m_{SUM}	Number of elementary conductors in upper and lower bars of double-layer winding (general number of elementary conductors in slot);
n	Number of elementary conductors along width of slot;
N	Number of loops in slot of multiturn bar winding;
q	Number of massive conductors in group;
$Q_{A.C.(BT)}$	Losses in lower bar of multiturn bar winding (in the bar on the bottom of slot by M = 1) under A.C. current;
$Q_{A.C.(TP)}$	Losses in upper bar of multiturn bar winding (in bar under wedge by M = N) under A.C. current;
$Q_{BT.\ D.C.}$	D.C. losses in lower bar of double-layer winding with different height of bars;
$Q_{TP.\ D.C.}$	D.C. losses in upper bar of double-layer winding with different height of bars;
$Q_{SUM,Z}$	A.C. losses in lower and upper bars of double-layer winding with different height of bars;
$Q^*_{SUM,Z}$	Ratio between A.C. losses in both bars of double-layer winding with difference in height of bars ($Z \neq 0.5$) to A.C. and losses in lower and upper bars of double-layer winding with identical height of bars ($Z = 0.5$)
$Q^*_{TP.BT}$	Ratio between the losses in extreme (M = N and M = 1) turns multiturn bar winding;
$Q_{BT.SUM}$	A.C. losses in lower bar of double-layer winding with different height of bars;
$Q_{TP.SUM}$	A.C. losses in upper bar of double-layer winding with different height of bars;

S, S_H, S_{MS}	Respectevely area of group contained massive and hollow conductors and area of massive and hollow conductors;
$S_{H,CONT}$	The area occupied by the contour of the hollow conductor;
t	Time;
$T_{TP,BT}$*	Ratio of temperature of upper bar to the temperature of lower bar for the extreme case of heat-transfer under indirect cooling;
V_{BT}, V_{TP}, V*	Distillate velocities in the channels of upper and lower bars and ration of these velocities;
Z	Ratio of number of elementary conductors (or group of elementary conductors) in upper bar to full of they number in the slot;
θ	Overheating of winding;
Θ_{TP}	Overheating of upper bar;
$\Theta_{TP,BT}$*	Ratio of overheatings of upper bar and lower bars;
Θ_{INS}	Temperarute drop in slot insulation of bar;
Θ_{CR}	Temperarute drop in stator core;
Θ_{CNV}	Convective temperarute drop from the surface;
λ_{INS}	Heat conductivity of slot insulation;
Λ_{BT}, Λ_{TP}	Respectevely equivalent of thermal of slot conductivity for thermal stream of upper and lower bars;
ρ	Specific resistance;
σ_{MS}	Electroconductivity of massive conductors of winding;
σ_H	Electroconductivity of hollow conductors of winding.

23.5 Additional Losses in Coil Winding

23.5.1 Design Features

When establishing the relations for calculation of eddy currents and additional losses one should take into account the following design features of coil winding. As a rule, the winding is a two-layer ensemble (Fig. 23.15) and the number of turns (effective conductors) in coil is $S_C < 10$. The number of elementary conductors with height of effective conductor is not usually large ($N_0 < 6$–8). In powerful low-voltage machines, like motors and diesel generators of 1600–2000 kW, there are stator windings as a coil with $S_C = 2$ and even $S_C = 1$, while the number N_0 reaches $N_0 = 8$. From the point of view of calculation of eddy and circulating currents in elementary conductors the significant factor is that in bar winding the

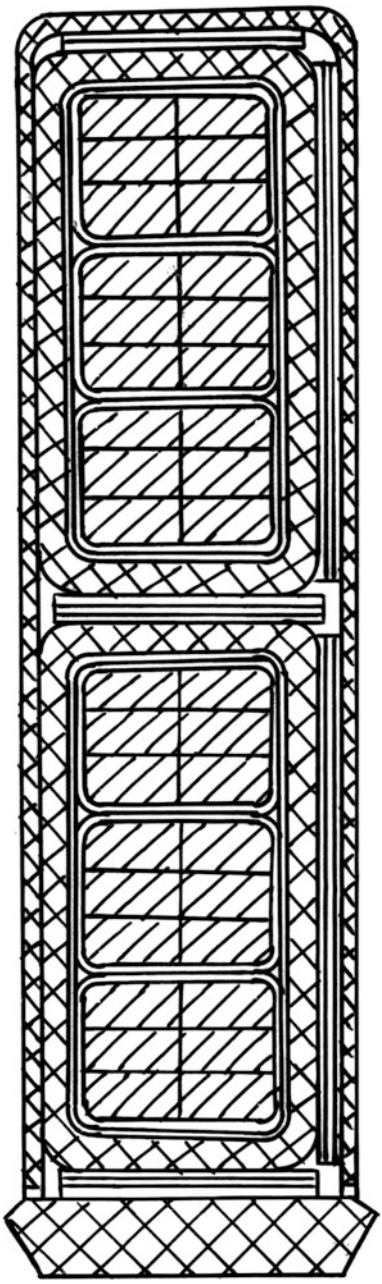

Fig. 23.15 Section of turns in coil winding

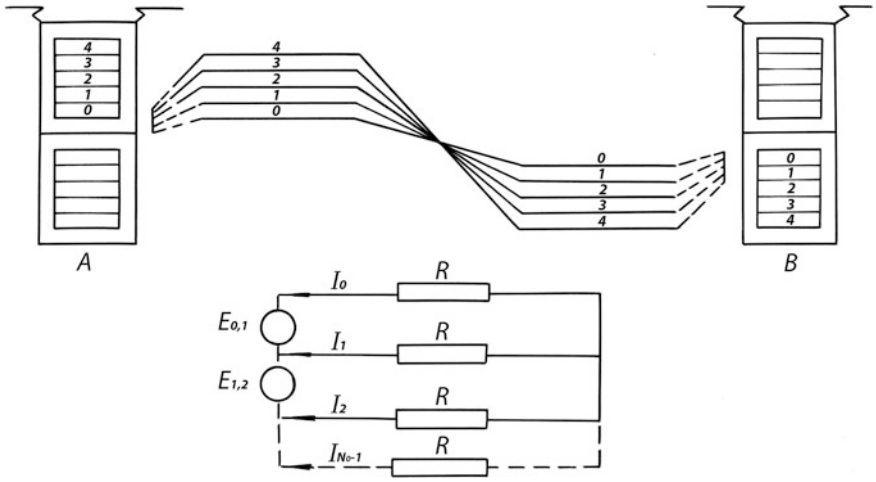

Fig. 23.16 Circuits of elementary conductors in coil winding

length of each elementary conductor connected in parallel is equal to the length L_0 according to (23.1); in coil winding this length is $2S_C$ times greater:

$$L_0' = (L_{SLT} + L_S)2S_C, \tag{23.114}$$

where L_{SLT}, L_S are respectively the lengths of slot and end parts of winding.

We should notice that in modern large A.C. machines the length of end part accounts for a sizable proportion of slot length.

The absence of transposition in slot part is the difference between coil- and bar-types windings. The reduction of additional losses level may be reached in this winding by natural transposition in end part: the process of manufacturing the coil supposes that elementary conductors in both turn sides occupy different positions in height (see Fig. 23.16). For example, if an effective conductor (turn) contains with height five elementary conductors, then counting from the slot base their numbers for one side of turn correspond to the sequence N = 0, 1, 2, 3, 4 and for the second side—N = 4, 3, 2, 1, 0. This sequence may be different for the second side of turn if there is an additional twisting of turn elementary conductors in end part. This may result in additional mutual displacement of turn elementary conductors with height. Let us note that in usual practice for large power machines (over 200 kW) such a twisting in end part is not performed as a rule.

23.5.2 Fundamental Assumptions

When setting the problem of calculation of additional losses in coil winding the same assumptions shall be taken into consideration that those ones for bar windings. They have been stated in Sect. 23.2.2.

23.5.3 Approaches to Solve the Problems of Additional Losses Caused by Slot Leakage Flux

In Fig. 23.16 an example is presented, composed of two slots (A and B) with single-turn coils. Slots A and B are spaced from each other along a bore at winding pitch $y = \beta\tau$, where β is pitch chording [1, 5] and τ is pole pitch. The coil contains with height five elementary conductors ($N_0 = 5$). Their relative position in both slots is schematized in Fig. 23.16. Let us consider two arbitrary conductors, for example, with numbers N = 2 and N = 3 in turn. They are insulated and closed by strips at turn ends; the distance between strips makes L_0' according to (23.114). These two conductors form a circuit, which is located in leakage field. Such a circuit in coil winding is similar to that formed by elementary conductors of slot group in bar winding at their incomplete transposition. The investigations of currents induced by slot leakage flux in the coil winding circuit give the same results that the currents in a circuit formed by elementary conductors of group at their incomplete transposition in bar; eddy currents are partially completed within the slot part of each elementary conductor ("local" currents) and partially between these conductors through strips (circulating currents).

The singularities of both currents have already been examined in Sect. 23.2. Particularly, "local" eddy currents meet the requirements of Eq. (23.40) and circulating currents—of (23.40′); that is why the losses caused by each of these currents may be calculated separately.

Additional losses due to "local" eddy currents are to be calculated from Eqs. (23.31) or (23.32). For this reason in future we shall consider the problem related only to circulating currents.

To calculate additional losses due to circulating currents it would be necessary to find first their distribution along all elementary conductors of a turn.

To that end, one should find beforehand the currents in each pair of elementary conductors, for example, elementary conductors with numbers N = 2 and N = 3, N = 2 and N = 1, N = 2 and N = 4 etc. and then, using the method of superposition we find the resulting current in each elementary conductor and subsequently additional losses in turn. To find this resulting current at arbitrary number N_0 of elementary conductors with turn height is an intricate problem though not complicated. In the next section we propose a more convenient method of problem solving related to the distribution of circulating currents in elementary conductors of coil winding.

23.5.4 Distribution of Circulating Currents

23.5.4.1 Special Case

Let us consider first a specific problem: we shall investigate the distribution of currents in coil with the number of turns $S_C = 1$ and the number of elementary conductors in turn with height $N_0 = 5$ in Fig. 23.16. Let us present these conductors of section $Q_{MS} = b_{MS}h_{MS}n$ in the form of fibres concentrated in lower base of elementary conductors (counting from slot base). According to Kirchhoff's second law let us write down the equation for a circuit formed by elementary conductors with numbers N = 0 and N = 1 (see Fig. 23.16).

$$I_0R_{MS} - I_1R_{MS} = E_{0,1}, \tag{23.115}$$

where $R_{MS} = \dfrac{L'_0}{b_{MS}h_{MS}n\sigma}$—D.C. resistance of elementary conductor.

The EMF $E_{0,1}$ in the circuit (0.1) has several terms. This is explained by the fact that turn sides are laid in two slots and occupy there with height different position. Therefore, leakage fluxes combined with the circuit (0.1) in slots are not equal.

The leakage flux combined with the circuit (0.1) in one of slots (A) is equal to [1, 3, 4]:

$$\Phi_{A(0,1)} = \frac{(I_0 + I_{EL,T})\mu_0 L'_{SLT}(h_{MS} + a)}{b_{SLT}}, \tag{23.116}$$

where $I_{EL,T}$—is the load current of a turn, L'_{SLT}—according to (23.41).

The leakage flux combined with the same circuit in the second slot (B) is equal to [1, 3, 4]:

$$\Phi_{B(0,1)} = \frac{(I_4 + I_3 + I_2 + I_1)\mu_0 L'_{SLT}(h_{MS} + a)}{b_{SLT}}. \tag{23.116'}$$

Thus, the EMF $E_{0,1}$ determined by these fluxes with account made for the direction of execution of the contour is the following:

$$E_{0,1} = -\frac{j\omega\mu_0 L'_{SLT}}{b_{SLT}}(h_{CON} + a)\left[\left(-I_0 - I_{EL,T}\right) + (I_4 + I_3 + I_2 + I_1)\right]\cdot \tag{23.117}$$

Here $h_{CON} = h_{MS}$, a—double-sided insulation thickness of an elementary conductor, the current $I_{EL,T}$ is the load current in turn

$$I_{EL,T} = \frac{I}{a_0},$$

where I—is the rated current in stator winding, a_0—is the number of parallel branches of winding.

Equations according to the Kirchhoff's second law for the next circuit formed by elementary conductors with numbers N = 1 and N = 2 shall be written in a similar way (Fig. 23.16):

$$I_1 R_{MS} - I_1 R_{MS} = E_{1,2}, \tag{23.115'}$$

where

$$E_{1,2} = -\frac{j\omega \mu_0 L'_{SLT}}{b_{SLT}} (h_{MS} + a)\left[(-I_0 - I_1 - I_{EL,T})(I_4 + I_3 + I_2)\right]. \tag{23.117'}$$

Now we shall find the difference between the left and right parts of Eqs. (23.115) and (23.115′). As the result we shall have:

$$R_{MS}(I_0 - 2I_1 + I_2) = E_{0,1} - E_{1,2}. \tag{23.118}$$

Let us proceed to a more general problem ($S_C > 1$). Equations of the type (23.118) may be deduced for each of two adjoining circuits formed by conductors with numbers N, N + 1, and N + 2.

$$I[N+2] - 2I[N+1] + I[N+0] = \frac{E[N,N+1] - E[N+1,N+2]}{R_{MS}} \tag{23.119}$$

(at $N \leq N_0 - 2$).

Equations of the type (23.118) and (23.119) are difference equations of second order, nonhomogeneous; analytical methods of their solution are known [8, 9].

In general case expressions for EMF are more complicated than those for $E_{0,1}$, $E_{1,2}$ because each circuit in slot does not occupy one position but by S_C times more; as a consequence, the number of terms in parentheses in (23.117) and (23.117′) for EMF E[N, N + 1] or identical increases by S_C times.

When establishing equations to compute circulating currents distribution in elementary conductors of a turn in practice in expressions for EMF of the type (23.117) and (23.117′) one may neglect [1, 5] leakage fluxes created by load currents in elementary conductors of the turn under consideration. For example, in our problem in Eqs. (23.117) and (23.117′) for $E_{0,1}$,$E_{1,2}$ they neglect currents $I_0, I_1, \ldots, I_4$ and consider that the leakage flux is generated only by adjoining turn with load current in turn $I_{EL,T}$. This may be justified if $S_C > 2$ and $N_0 \leq 5$. In this particular case Eq. (23.118) takes the form:

$$I[N+2] - 2I[N+1] + I[N+0] = 0. \tag{23.119'}$$

This is the difference equation of second order [8, 9]. To solve it let us lay down two boundary conditions.

The first condition is similar to (23.115). It follows from Kirchhoff's equation for two adjoining elementary conductors in turn base (effective conductor). Counting the elementary conductor numbers from slot base we shall have

$$I[N+2] - I[N+1] = \frac{E[N+2, N+1]}{R_{MS}}, \tag{23.120}$$

where $E[N+2, N+1] = -\frac{j\omega\mu_0 L'_{SLT}}{b_{SLT}}(h_{MS} + a)S_C^2 I_{EL,T}$; R_{MS}—according to (23.115).

The second boundary condition is the following:

$$I_0 + I_1 + I_2 + \cdots + I_{N_0-1} = I_{EL,T}. \tag{23.121}$$

However, the second boundary condition may be written in another way. To do so, let us assume that $I_{EL,T} = 0$. Then the currents $I_0 + I_1 + I_2 + \cdots + I_{(N_0-1)}$ are circulating currents only.

The solution of difference Eq. (23.119′) with allowance of boundary conditions (23.120) and (23.121) for circulating currents (for the second boundary condition it is assumed that $I_{EL,T} = 0$) has the following form:

$$I_{CIRC(N)} = -\frac{E[N+2, N+1](2N - N_0 - 1)}{2R_{MS}}. \tag{23.122}$$

In particular, for first three elementary conductors according to (23.122) we shall have:

$$\begin{aligned} I_{CIRC(0)} &= -\frac{E[N+2, N+1](-N_0 - 1)}{2R_{MS}}, \\ I_{CIRC(1)} &= -\frac{E[N+2, N+1](1 - N_0)}{2R_{MS}}, \\ I_{CIRC(2)} &= -\frac{E[N+2, N+1](3 - N_0)}{2R_{MS}}. \end{aligned} \tag{23.122'}$$

Now let us verify the validity of Eq. (23.119′). With allowance of (23.122′) we shall have:

$$I_{CIRC(2)} - 2I_{CIRC(1)} + I_{CIRC(0)} = 0.$$

The resulting current in each elementary conductor will be described in this case in the following way:

$$I_N = I_{EL} + I_{CIRC(N)}, \tag{23.123}$$

where $I_{CIRC(N)}$—from (23.122′), $I_{EL} = \frac{I_{EL,T}}{N_0}$.

It follows from this special case that circulating currents change linearly as a function of the number N.

23.5.4.2 General Case

Let us proceed to a general problem when $S_C > 1$, at that the number of elementary conductors N_0 with turn height is significant $(N_0 > 5)$ so it will be impossible to neglect leakage fluxes due to currents of these elementary conductors [18].

We shall assume that an effective conductor of double-layer coil winding is located in the upper layer counting from the slot base. Therefore S_C effective conductors of lower and $p - 1$ upper $(1 \le p \le S_C)$ layers are arranged under it. The total current under effective conductor counting from the slot base makes

$$I_{EL,M} = I_{EL,T}\left(S_C e^{j\varphi} + p - 1\right). \tag{23.124}$$

It should be noticed that for effective conductor of lower layer we have respectively

$$I_{EL,M} = I_{EL,T} e^{j\varphi}(p - 1). \tag{23.124'}$$

Here φ—phase angle between currents of both turns in slot.

The current $I_{EL,M}$ determines the intensity of mutual induction field linked with conductors under consideration.

To set the equation let us assume first of all that the second part of effective conductor under consideration which belongs to the respective slot spaced from the first at winding pitch and does not cross over the slot leakage flux. Therefore, circulating currents due to this slot leakage flux are absent in elementary conductors of a turn. Let us write in an integral form the first Maxwell's equation [1, 3–5] for two adjoining in height elementary conductors with numbers (N + 0) and (N + 1) counting from the effective conductor base $(N = 0, 1, \ldots, N_0 - 1)$

$$\begin{aligned} H_{(N+0)} &= \frac{I_1 + I_2 + I_3 + \cdots + I_{N+0} + I_{EL,M}}{b_{SLT}}, \\ H_{(N+1)} &= \frac{I_1 + I_2 + I_3 + \cdots + I_{N+1} + I_{EL,M}}{b_{SLT}}. \end{aligned} \tag{23.125}$$

According to the second Maxwell's equation [1, 3–5] we have:

$$\begin{aligned} I_N - I_{N+1} &= -\frac{j\omega\mu_0 L'_{SLT} H_{(N+0)}(h_{MS}+a)}{R_{MS}}, \\ I_{N+1} - I_{N+2} &= -\frac{j\omega\mu_0 L'_{SLT} H_{(N+1)}(h_{MS}+a)}{R_{MS}} \end{aligned} \tag{23.126}$$

where R_{MS}—according to (23.115).

Now let us deduct term by term in (23.126) one equation from another, with allowance of (23.125) we shall have:

$$I[N+2] - (2+d_0)I[N+1] + I[N+0], \tag{23.127}$$

where $d_0 = \frac{j\omega\mu_0\sigma L'_{SLT} h_{MS}(h_{MS}+a)b_{MS}n}{L'_0 b_{SLT}}$ and L'_{SLT}—according (23.41).

The current changes as a function of the conductor number N and this takes the following form [8, 9]:

$$I_N = C_1 a_1^N + C_2 a_2^N, \tag{23.128}$$

where C_1, C_2—are constants specified by boundary conditions and the values a_1, a_2 are [8, 9].

$$a_{1,2} = \frac{2+d_0 \pm \sqrt{d_0(d_0+4)}}{2}. \tag{23.128'}$$

Let us write one of Eqs. (23.126) for two adjoining elementary conductors in turn base $I_0(1+d_0) = I_1 - d_0 I_{EL,M}$.

With allowance of (23.128) we have:

$$C_1(1+d_0-a_1) + C_2(1+d_0-a_2) = -I_{EL,M} d_0. \tag{23.129}$$

We shall use this equation as the first boundary condition.

It will be convenient to present the second boundary condition in the form:

$$I_1 + I_2 + I_3 + \cdots + I_{N_0-1} = I_{EL,T}, \tag{23.130}$$

where $I_{EL,T}$—is the load current in turn. With due account of (23.128) we shall have:

$$\frac{C_1\left(a_1^{N_0}-1\right)}{a_1-1} + \frac{C_2\left(a_2^{N_0}-1\right)}{a_2-1} = I_{EL,T}. \tag{23.130'}$$

From Eqs. (23.129) and (23.130′) the constants C_1 and C_2 are to be calculated. Their form is slightly simplified if we use the Vieta's theorem [8, 9] for roots a_1 and a_2 of characteristic equation corresponding to (23.127).

Table 23.15 Current distribution in elementary conductors at $S_C = 2$ and $S_C = 1$

S_C	N	$\lvert I_N \rvert$	φ'	I_{MED}
2	0	26.915	322.60	
	1	24.578	342.34	
	2	26.747	9.37	25
	3	34.761	34.02	
1	0	9.376	292.85	
	1	9.448	300.00	
	2	9.873	313.70	
	3	9.111	331.80	
	4	13.610	350.90	12.5
	5	17.550	8.66	
	6	23.022	24.61	
	7	30.161	39.39	

This method may be used to calculate the current distribution in elementary conductors in general case, when the coil contains S_C turns connected in series. Let us find the current distribution in elementary conductors of such a winding. With allowance of their mutual position at both sides of turn the basic equation will take the form [20, 22]:

$$I[N+2] - (2 + 2d_0S_C)I[N+1] + I[N+0] = 0.$$

The first boundary condition shall be written as follows:

$$C_1(1 + 2d_0S_C - a_1) + C_2(1 + 2d_0S_C - a_2) = I_{EL,T}d_0S_C + d_0I_{EL,T}M_C. \quad (23.131)$$

For the design which is commonly used in practice (without twisting of elementary conductors in end part) the factor M_C is equal to $M_C = S_C^2$.

Using these boundary conditions (23.130) and (23.131) we estimate the factors C_1 and C_2 we have the expression for the current in each of N_0 elementary conductors:

$$I_N = \frac{(a_1 - 1)a_1^N I_{EL,T}\frac{(S_C + M_C)\left(1 - a_2^{N_0}\right)}{2S_C} - 1}{a_2^{N_0} - a_1^{N_0}} + \frac{(a_2 - 1)a_2^N I_{EL,T}\frac{(S_C + M_C)\left(a_1^{N_0} - 1\right)}{2S_C} + 1}{a_2^{N_0} - a_1^{N_0}}. \quad (23.132)$$

It should be noted that the currents calculated according to (23.132) are complex (phasor) numbers.

Table 23.15 provides as an example the distribution of current in elementary conductors of winding turn when the number of turns in slot makes four ($S_C = 2$) and two ($S_C = 1$) the number of parallel winding paths $a_0 = 8$ corresponds to the first version of winding of frequency-controlled motors and $a_0 = 4$ corresponds to

the second one. In first version $N_0 = 4$ and in second $N_0 = 8$ respectively. The load current in turn is assumed to be equal to $I_{EL,T} = 100$ relative units (p.u.). If the current is uniformly distributed through elementary conductors (frequency $\omega \to 0$) the average current in I_{MED} makes 25 p.u. in the first version and 12.5 p.u. in the second one.

In Table 23.15 is also given for checking [1, 5] the phase angle (φ') for the current in each elementary conductor. From this table it follows that with S_C number and consequently parallel winding paths a_0 increase, and the distribution of current in elementary conductors appears to be more uniform. The relation of maximum current value in elementary conductor to minimum value makes only 1.41 for = 2 S_C and for = 1 S_C—much larger: 3.31. The nature of current distribution changes as well.

23.5.5 Losses Due to Circulating Currents and Losses Distribution in Winding Turn

23.5.5.1 General Case

The losses increase factor in turn according to (23.4) is calculated from the equation:

$$K_F = N_0 \frac{|I_0|^2 + |I_1|^2 + \cdots + |I_{N_0-1}|^2}{|I_{EL,T}|^2}. \tag{23.133}$$

23.5.5.2 Special Case: $S_C \leq 4$

If we neglect leakage fluxes caused by currents in some elementary conductors, we shall easily have a simple analytical expression for losses and their distribution. Let us use Eq. (23.122).

Additional losses in Nth conductor of the coil due to the circulating current $I_{CIRC(N)}$:

$$P_{A.C.,N} = \frac{|I_{CIRC(N)}|^2 R_{MS}}{2},$$

Table 23.16 Losses increase factor K_F for g = 1, g = 5, g = 7

g	K_F according to (23.133) and (23.132)	K_F according to (23.134)
1	1.113	1.1108
5	3.334	3.769
7	4.578	6.428

Table 23.17 Distribution of circulating currents in elementary conductors ($S_C = 2$, $N_0 = 6$)

N	g = 5	g = 7
0	36.51+j·36.45	47.23+j·41.84
1	30.08+j·16.44	36.90+j·16.47
2	20.76+j·1.740	22.51+j·0.22
3	11.13−j·9.31	8.060−j·10.49
4	3.14−j·9.31	−3.790−j·19.20
5	−1.81−j·26.93	−10.9−j·28.84

where R_{MS}—according to (23.115).

Additional losses in all coil turns:

$$P_{A.C.} = P_{A.C.(0)} + P_{A.C.(1)} + P_{AC(2)} + \cdots + P_{A.C.(N_0-1)}.$$

Using these equations we shall obtain the losses increase factor:

$$K_F = 1 + \frac{P_{A.C.}}{Q_{D.C.}} = 1 + (K' h_{MS})^4 \left(1 + \frac{a}{h_{MS}}\right)^2 S_C^2 N_0^2 \frac{N_0^2 - 1}{12} \left(\frac{L'_{SLT}}{L_0}\right)^2, \quad (23.134)$$

where K'—according to (23.14), L_0—according to (23.1), L'_{SLT}—according to (23.41). Usually it is assumed that

$$N_0^2 - 1 \cong N_0^2; \quad a = 0. \quad (23.135)$$

As a rule, Eq. (23.134) is used with given approximations (23.135) for practical calculations [1, 5]. For elementary conductor sizes used in practice Eq. (23.134) with allowance of (23.135) for frequencies 150–200 Hz and $N_0 \leq 4$ may give the following results with significant error as compared to those obtained following the formula (23.134) for the same $N_0 \leq 4$.

It should be noted that the reduction of factor K_F according to (23.133) or (23.134) while keeping a certain ratio of winding parameters may be successively gained by increasing the number of its parallel paths under the condition $\frac{S_C}{a_0}$ = const, as it is proved in Table 5.1. However, this measure results in bad slot filling and, consequently, in D.C. losses increase. This number of parallel brunches has to correspond to that of machine poles.

Example

A double-layer coil winding is placed in the stator slot, with the number of turns being $S_C = 2$. Turns contain elementary conductors $N_0 = 6$; $n = 2$. Their sizes are: $b_{MS} = 4.75$ mm; $h_{MS} = 2.24$ mm; $a = 0.22$ mm; slot width $b_{SLT} = 14$ mm; radial channels—not available; ratio $\frac{L'_{SLT}}{L_0} = 0.3861$; frequency $f = 50$ Hz; $\sigma = 57 \times 10^6$ S/m.

It is required to find the factor K_F of losses increase in the coil winding for current harmonics of order $g = 1$, $g = 5$, $g = 7$.

Calculation results are given in Table 23.16.

Note.

The temperature for the value of σ is usually chosen according to the class of winding insulation.

From Table it follows that the account of elementary conductor leakage flux influence results in the fact that additional losses in turn become not proportional to the current frequency like this is the case in a bar of asynchronous motor with deep slots rotor [1, 5].

By way of evidence of the validity of results given in Table 23.16 we shall show an estimated distribution of circulating currents in elementary conductors that have been obtained at g = 5 (f = 250 Hz) and at g = 7 (f = 350 Hz) from Eq. (23.132). The results of current calculation are given in Table 23.17.

In the calculations the operational (load) current in turn is assumed to be equal to $I_{EL,T}$ = 100 p.u. From Table it follows:

- the amount of currents in elementary conductors meets the requirements of Eq. (23.121), that proves the validity of obtained results;
- with an increase in harmonics order g the level of non-uniformity of current distribution in coil elementary conductors becomes greater. In this way the value of factor K_F is increased.

23.6 Questions for Self-Testing

1. What is the reason of eddy and circulating currents occurring in elementary conductors of bar and coil windings?
2. What are fundamental measures to be taken to cut down additional losses?
3. Why do the currents circulating between elementary conductors appear in bar winding with incomplete transposition and in coil winding?
4. There is a double-layer winding with two-turn bars arranged in slots. What are the relations between additional losses in turns of both bars?
5. A double-layer bar winding with mica insulation has been placed in stator slot of the motor; the slot width is 20.2 mm. The bar contained 52 solid elementary conductors (m = 26, n = 2), their sizes are: h_{MS} = 1.5 mm, b_{MS} = 7.1 mm. When the thinner thermosetting insulation has been chosen, there were arranged 34 elementary conductors (m = 17, n = 2), with their sizes being h_{MS} = 2.5 mm, b_{MS} = 7.5 mm. In what way did winding losses change: (a) additional; (b) total.
6. Estimated losses (D.C. losses and additional) for coil winding of insulation class B make 86 kW, $K_{F,MS}$ = 1.227. It is required to determine losses (D.C. and additional) when changing the insulation class F [40].

Note. By A.C. resistance of winding calculation we use the temperature 75 °C (for “B” type winding insulation) or 115 °C (for “F” type winding insulation).

7. If an asynchronous motor is fed from a frequency converter, winding losses lead to 115 kW and $K_{F,MS} = 1.17$ (at 40 Hz). It is required to specify winding losses at 55, 70 and 88 Hz.
8. What must be the ratio of additional to D.C. losses in bar winding with hollow elementary conductors so that their amount was minimum? Is the result valid yet, if elementary conductors in bar are solid or combined (hollow and solid)?

Argument. A.C. losses $Q_{A.C.(H)}$ in winding with hollow elementary conductors are equal to,

$$Q_{A.C.(H)} \sim 0.5 I_{PH}^2 R_{PH} K_{F,H} m_{PH} \sim \frac{K_{F,H}}{m_H n S_H},$$

where m_{PH}—number of phases, I_{PH}—phase current, R_{PH}—D.C. resistance of winding phase, m_H—number of elementary conductors in bar.

Taking into account this relation, we have:

$$Q_{A.C.(H)} \sim \frac{1 + m_H^2 \upsilon}{m_H \omega'},$$

where υ, ω'—constants of proportionality.

Setting to zero the losses derivative $Q_{A.C.(H)}$ upon m, we have:

$$K_{F.H} \sim 1 + m_H^2 \upsilon = 2.$$

It should be noted that this result does not depend on the type of elementary conductors in bar (hollow, solid, combined) because this type of elementary conductors is taken into account only by constants υ and ω'.

As the consequence, the minimum losses in slot for bar winding take place when the Field's factor is $K_F = 2$, and here additional losses are equal to D.C. ones.

Let us note, however, the following conditions examined earlier:

- at $K_F = 2$ the relation of A.C. losses in upper (M = 2) and lower (M = 1) bars makes 2.2 according to (23.97), at that, the dependence $Q_{A.C.} = f(m)$ is flat in $K_F = 2$ zone. These two boundary conditions lead to the choice of values K_F:
  (a) up to $K_{F,MS} < 1.30$–1.33 for machines with solid elementary conductors (indirect cooling). At large values of $K_{F,MS}$ there are difficulties occurring with upper bar cooling;
  (b) up to $K_{F,COMB}$ 1.65–1.7 for machines with combined elementary conductors (direct water cooling). The choice of larger values ($1.8 < K_{F,COMB} < 2$) does not practically influence the value of A.C. losses reduction in stator winding but results in increased consumption of copper and stator core.

List of symbols

a	Thickness of elementary conductor insulation;
a_0	Number of parallel brunches of stator winding;
b_{MS}	Width of massive elementary conductor in turn;
b_{SLT}	Width of slot;
$E_{0,1}$, $E_{1,2}$, $E_{2,3}$	EMF between elementary conductors in the turn of winding;
h_{MS}	Heght of massive elementary conductor in turn;
$I_{CIRC(N)}$	Circulation current between elementary conductors of turn;
I_{EL}	Load current in elementary conductor of turn;
$I_{EL,M}$	Load current in M turns of slot (counting value of M from the bottom of slot);
$I_{EL,T}$	Load current of winding turn;
K_F	Field's factor of bar winding;
L_0'	Length of elementary conductor between two end parts of stator winding;
L_S	Length of end part of bar;
L_{SLT}	Length of slot part of bar;
m	Number of elementary conductors in the slot along on the heigth;
N_0	Number of elementary conductors in turn;
$P_{A.C.,N}$	Additional losses in Nth elementary conductor of winding turn under circulation current ($N \leq N_0$);
$P_{A.C.}$	Additional losses in all elementary conductors of winding turn under circulation current;
$Q_{D.C.}$	Losses in coil by D.C. current;
$Q_{A.C.}$	Losses in coil by A.C. current;
R_{MS}	D.C. resistance of massive elementary conductor in the winding turn;
R_{PH}	D.C. resistance of stator winding phase;
S_C	Number of turns in coil ($S_C = S_{TR}$);
W_{PH}	Number of turns in winding of a stator phase;
μ_0	Magnetic permeability of air;
φ	Phase angle;
$\Phi_{A(0,1)}$, $\Phi_{B(0,1)}$	Leakage flux connected with loop (0, 1) for two slots of winding (A and B);
ω	Circular frequency of stator current.

Appendix 1: Method of Skin Effect Computation in Rotor Bars of Large Power Asynchronous Motor with Allowances for Temperature Distribution Therein

Rotor bars of large power asynchronous squirrel-cage motors (torque on the shaft $M_0 \geq 5 \times 10^3$ Nm) are often made square or trapezoidal. The practice shows that the characteristic $M_0 = f(n)$ of powerful asynchronous motor with squirrel-cage

rotor obtained on bench during its service after lengthy standstill is different from the $M_0 = f(n)$ measured immediately after its rated duty (n—rotation speed). In particular, this relates to deep bar rotors and may be explained by different action of skin effect in bars under specified conditions. At motor running up the temperature in bars depends significantly on previous service conditions. The distribution of temperature with height of a bar influences the eddy currents distribution in it and, consequently, the value of its resistance and inductive reactance, these values determining the relation $M_0 = f(n)$. Making allowance of the fact that the starting torque on the shaft is usually specified in specifications, in practice it is often necessary to refine the parameters of motors.

Algorithms for the calculation in this appendix are convenient additionally to use in the factory in the design of high-power induction motors with heavy start-up. For example, as is presented in the method of designing asynchronous machines, in Chap. 4.

Calculation equations for rectangular slot. To derive the equation characterizing the distribution of current with bar height with taking account of the function $\rho(y)$, it will be more convenient to use the numerical method based upon the use of Maxwell's equations in an integral form (y—coordinate: $0 \leq y \leq h$; h—bar height, ρ—resistivity). We shall use the assumptions adopted as a rule for calculations of skin effect in slots [1, 3–5]. Let us assume, in particular, that the steel permeability $\mu_{FE} = \infty$ and field lines are straight, parallel to slot base; taking into account this assumption the current density shall vary only with height h.

Let us consider first a rectangular slot. We shall divide a rectangular bar in height into N equal elements. Their number is specified by the accuracy of calculation of bar resistance and reactance, for practical problems it mostly makes $N < 200–300$ and more. The current S_M within each Mth element will be considered as placed in its lower base as an infinite thin layer. Let us write the first Maxwell's equation for neighboring elements in slot base:

$$H_1 = \frac{S_1}{b_{SLT}}; \quad H_2 = \frac{S_1 + S_2}{b_{SLT}}; \tag{A.23.1.1}$$

(b_{SLT}—slot width, H_1, H_2—magnetic field strength in the first and second slot elements).

Then for Mth element ($1 \leq M \leq N$) counting from the slot base:

$$H_M = \frac{S_1 + S_2 + \cdots + S_M}{b_{SLT}}. \tag{A.23.1.1'}$$

Let us describe in an integral form the second Maxwell's equation for neighboring elements in the slot base:

$$S_1 R_1 - S_2 R_2 = -j\omega\mu_0 H_1 h_M L_{COR}; \tag{A.23.1.2}$$

$$S_2R_2 - S_3R_3 = -j\omega\mu_0 H_2 h_M L_{COR}. \qquad (A.23.1.2')$$

where h_M is the height of Mth element of bar; L_{COR}—is the length of rotor core; ω—is the circular frequency; μ_0—the air permeability; R_1, R_2, R_3—are resistances.

Now we shall deduct from Eq. (A.23.1.2) term-by-term Eq. (A.23.1.2′):

$$S_3R_3 - 2S_2R_2 + S_1R_1 = j\omega\,\mu_0 S_2 L_{COR}\frac{h_M}{b_{SLT}}. \qquad (A.23.1.3)$$

For elements (M + 2), (M + 1) and (M + 0) after transformation, we shall have respectively:

$$\begin{aligned} &S[M+2] - S[M+1]\left(2R_{(M+1)} + j\omega\mu_0\frac{L_{COR}h_M}{b_{SLT}}\right)\frac{1}{R_{(M+2)}} \\ &\quad + S[M+0]\frac{R_{(M+0)}}{R_{(M+2)}} = 0;\ (M = 1, 2, \ldots, N-2) \end{aligned} \qquad (A.23.1.4)$$

We find that Eq. (A.23.1.4) at $R_{(M+2)} = R_{(M+1)} = R_{(M+0)}$ corresponds completely to that of the propagated wave (Helmholtz's equation [3, 4]), characterizing the plane-wave propagation in a conducting medium, if the strength of electric and magnetic fields vary sinusoidally. Its difference approximation for three points is given in Note.

We shall also note that Eq. (A.23.1.4) may be obtained from an equation system for magnetically connected meshes [3, 4]; these equations contain coefficients for self- and mutual induction, calculation expressions for which are given in [33]. When calculating these coefficients one should take that the current S_M is presented as an infinite thin layer in lower base of each of N elements. This assumption is considered true as in practical calculations the height of Mth element makes less than 1 % of bar height.

Let us write boundary conditions for the solution of (A.23.1.4). According to the order of difference equation, there are two conditions. We shall use as the first Eq. (A.23.1.2):

$$S_2 = S_1\left(\frac{R_1}{R_2} + j\omega\mu_0\frac{L_{COR}h_M}{b_{SLT}R_2}\right). \qquad (A.23.1.5)$$

The sum of the currents $S_1, S_2, \ldots, S_M$ is equal to:

$$\sum_{M=1}^{N} S_M = I, \qquad (A.23.1.6)$$

where I—load current of bar.

This relation shall be used as the second boundary condition.

To solve the difference Eq. (A.23.1.4) it would be convenient to apply one of sweep method modifications. For S_1 we shall set an initial approximation

$$S_1^{(k=1)} = \frac{I}{2N}. \qquad (A.23.1.5')$$

The calculation of current values S in the elements is to be presented in the form of the following computing sequence (algorithm).

1. We set $S_1 = S_1^{(k=1)}$.
2. We calculate S_2 according to (A.23.1.5); $S_3, S_4, \ldots, S_N$ according to (A.23.1.4);

$$I^{(k)} = \sum_M S_M.$$

3. If $\left|\frac{I^k}{I} - 1\right| > \varepsilon$, then it is required to calculate a new approximation for S_1: $S_1^{(k=2)} = S_1^{(k=1)} \frac{I^k}{I}$ and proceed to p. 2, if $R_M \neq f(N)$ i.e. $\rho \neq f(y)$. However, when the temperature along of height of the bar is changed we have to use in general case for calculation $S_1^{(k=2)}$ one of the methods [8, 9] for the determination of the roots of nonlinear equations of the form $I^{(k)} = f[S_1^{(K)}]$ provided that: $\sum_M S_M = I$.

Otherwise, the calculation of currents in elements is completed and one can specify losses increase factor (Field's factor) K_F and factor K_X—inductance decrease factor. For practical calculations $\varepsilon \approx 1 \times 10^{-5}$.

Both factors at ρ = var shall be determined by relations

$$K_F = \frac{|S_1|^2 R_1 + |S_2|^2 R_2 + \cdots + |S_N|^2 R_N}{|I|^2} \cdot \frac{1}{R_{EQ}},$$

where R_{EQ}—is the D.C. resistance of a bar;

$$\frac{1}{R_{EQ}} = \sum \frac{1}{R_M}; \qquad (A.23.1.7)$$

$$K_X = \frac{L_{A.C.}}{L_{D.C.}} = 3\frac{|S_1|^2 + |S_1 + S_2|^2 + \cdots + |I|^2}{N|I|^2}. \qquad (A.23.1.7')$$

Here $L_{A.C.}$, $L_{D.C.}$—is the inductance of a bar respectively with allowance of skin effect and at uniform distribution of current with bar height.

Estimation of maximum error. The error of solution (A.23.1.4) by a numerical method in terms of bar division into N elements is to be conveniently estimated at

$$R_M = \text{con st} = \frac{\rho L_{COR}}{b_M h_M}, \quad b_M\text{—width of Mth bar element.}$$

In this case the error is maximum as the current distribution with conductor height at R_M = const shows a more pronounced activity of skin effect than at $R_{(M+2)} > R_{(M+1)} > R_{(M+0)}$. The solution of difference Eq. (A.23.1.4) at R_M = const is identical to (23.127).

An analytical solution for S(y) at ρ = const is given for example in [3, 4]. Its comparison with (A.23.1.4) allows determining the number N corresponding to a specified error.

The choice of the number of elements (N) is closely related to the value of relative error when specifying the factors K_F and K_X. The practice of calculation of current distribution S_M has shown that if we assume that a relative error in calculation of K_F is approximately 5 % that is sufficient for engineering calculations, then the minimum number of N elements may be found from relation

$$N > 15h\sqrt{\frac{\omega\mu_0}{2p_1} \cdot \frac{b_M}{b_{SLT}}}. \qquad \text{(A.23.1.8)}$$

Here ρ_1 corresponds to M = 1.

This number N is an initial approximation to determine the number of elements.

Within the limits of this algorithm (p. 1–p. 3) it is easy to specify after p. 2 for each element M of a bar the values of resistivity ρ in relation to the temperature Q_M:

$$\rho(M, \Theta) = \rho_0(1 + \rho^* \Theta_M). \qquad (*)$$

In problems of practical importance such a refinement is necessary first of all to define the parameters of squirrel-cage rotor of the machine operating under conditions of abrupt change in loading (run-up, reverse operation etc.).

In general case to take into account the dependence (*) we have to solve the equation:

$$\frac{d\Theta_M}{dt} = \frac{Q_M - Q_{COND,M} + \Delta Q_{M+1,M} - \Delta Q_{M,M-1}}{CG_M}. \qquad (**)$$

Here Q_M—losses, found in a layer with number M (M ≤ N), $Q_{COND,M}$—losses taken from the layer into rotor teeth by heat transfer and then into air gap by convection; $\Delta Q_{M+1,M}$, $\Delta Q_{M,M-1}$—inlet and outlet losses respectively for a layer with number M, C—specific heat of a conductor; G_M—weight of Mth layer of a bar. (In a particular case on the condition of adiabatic heating usually $Q_{COND,M} \approx 0$).

Thus, to refine the parameters of rotor the proposed algorithm provides the solution of two problems at each step of integration Δt:

- current distribution over cross-section of a bar;

- calculation of the values of specific resistivity of each of M (M ≤ N) elements (layers) of a bar when calculating the distribution.

Considering the flat nature character of variation of temperature $\Theta_M(t)$ on time t it should be sufficient to apply the Euler method [8, 9] for integration of this equation; the integration step Δt is to be taken according to [8, 9]. Initial conditions to solve this equation are to be specified by motor operating conditions:

- under no load conditions (after sustained service interruption), $Q_M = Q_0 =$ const, (at M = 1; 2; …; N), here Q_0—ambient air temperature;
- under hot start-up conditions (without sustained service interruption, subsequent loading change) Q_M = f(M), (at M = 1; 2; …; N).

These values of Q_M have been already specified by the solution of Eq. (**) for the previous operating mode.

It should be noted that there is a certain relation [8, 9] between number of bars' elements N in Eq. (A.23.1.8) and the integration time step Δt of differential Eq. (**).

Peculiarities of calculations for trapezoidal bar. Now let us consider the peculiarities of calculation of skin effect in trapezoidal bar at ρ = var. To calculate skin effects in such a bar at ρ = var. we shall use traditional assumptions [3, 4]. Let us consider first neighboring elements in slot base. According to Maxwell's equations, we have by analogy with (A.23.1.1), (A.23.1.2) and (A.23.1.2′):

$$\begin{aligned} S_2R_2 - S_1R_1 &= +j\omega\mu_0 S_1 L_{COR}\frac{h_1}{a_1'};\\ S_3R_3 - S_2R_2 &= +j\omega\mu_0 (S_2 + S_1) L_{COR}\frac{h_2}{a_1'}. \end{aligned} \tag{A.23.1.9}$$

The values a_1', a_1' are calculated by the center line of elementary trapezoid.

Now we shall deduct the second equation from the first one:

$$S_3R_3 - 2S_2R_2 + S_1R_1 = +j\omega\mu_0\left[(S_2 + S_1)\frac{h_2}{a_2'} - S_1\frac{h_1}{a_1'}\right]L_{COR}. \tag{A.23.1.10}$$

Equation (A.23.1.10) is significantly simplified if we introduce therein additional conditions:

$$\frac{h_2}{a_2'} = \frac{h_1}{a_1'} = \text{const}.$$

In this case Eq. (A.23.1.10) takes the form of (A.23.1.3). Consequently, in order to have in general case at $1 \le M \le N$ the calculation equation in the form of (A.23.1.4), it is necessary to subdivide the bar in height so that the height of its elements is different $(a_M = b_M)$:

$$\left.\begin{aligned}\frac{h_1}{b_1} = \cdots = \frac{h_M}{b_M} \cdots = \frac{h_N}{b_N} = p,\\ \frac{h_2}{h_1} = \cdots = \frac{h_M}{b_{(M-1)}} = \cdots = \frac{b_N}{b_{(N-1)}} = \delta.\end{aligned}\right\}$$

The values $b_1, b_2, \ldots, b_M, \ldots, b_N$ are calculated by center line of elementary trapezoid.

The values δ and p are calculated from relations:

$$\delta = \sqrt[N]{1 - \frac{2h}{b_{BT}}} \cdot \mathrm{tg}\varphi, \quad \mathrm{tg}\varphi = \frac{b_{BT} - b_{TP}}{2h}; \quad p = \frac{1-\delta}{1+\delta}\mathrm{ctg}\varphi,$$

where b_{BT}, b_{TP}—is the width of lower and upper bases of trapezoidal bar (counting from slot base).

Note. The Helmholtz's equation for plane-wave [3, 4] at sinusoidal variation in time of electric and magnetic fields strength is:

$$\frac{d^2E}{dy^2} = kE, \quad \text{where } k = j\frac{\omega\mu_0}{\rho} \cdot \frac{b_M}{b_{SLT}}.$$

Its difference approximation [3, 4] by three equidistant points:

$$\frac{E[M+2] - 2E[M+1] + E[M+0]}{h_M^2} = j\frac{\omega\mu_0}{\rho} \cdot \frac{b_M}{b_{SLT}} E[M+1].$$

After transformation we have:

$$E[M+2] - E[M+1]\left(2 + j\omega\mu_0 \frac{h_M^2 b_M}{\rho b_{SLT}}\right) + E[M+0] = 0.$$

This equation corresponds to (A.23.1.4) at $R_{(M+2)} = R_{(M+1)} = R_{(M+0)}$.

List of symbols

b_{SLT}	Slot width;
C	Specific heat of conductor;
G_M	Weight of Mth bar element (M ≤ N);
h_M	High of Mth bar element (M ≤ N);
$H_1, H_2, \ldots, H_M$	Strength of magnetic field in slot in boundaries of Mth bar element of rotor (M ≤ N);
h	High of rotor bar;
I	Amplitude of bar current under load condition;
K_F	Losses increase factor (Field's factor);
K_X	Factor of inductance decrease of bar;
L_{COR}	Length of rotor core;

$L_{A.C.}$	Inductance of bar with take onto account of skin effect;
$L_{D.C.}$	Inductance of bar without take onto account of skin effect;
M	Number of bars element (M ≤ N);
N	Number of elements along of the height of a bar;
$Q_{COND,M}$	Losses taken from layer into rotor teeth by heat transfer and then into air gap by convection;
Q_M	A.C. loses in Mth element of bar;
$R_1, R_2,\ldots,R_M$	D.C. resistivity of bar elements;
R_{EQ}	D.C. resistivity of bar;
$S_1, S_2,\ldots, S_M$	Currents in bar elements;
y	Coordinate along the axis of symmetry of the slot;
ε	Error of calculating;
μ_0	Permeability of air;
θ	Temperature of winding;
ρ	Resistivity of conductor;
ρ*	Temperature factor of the increasing of the specific resistance;
ω	Circular frequency of rotor current

Appendix 2: Analytical Method of Designing Polyphase ($m_{PH} \geq 3$) Stator Winding with an Arbitrary Fractional Number Q of Slots Per Pole and Phase

Introduction: Fundamental assumptions

The issues of development of common methods for designing and investigating fractional q windings (q < 1, q > 1) are of practical interest for machines with $m_{PH} \geq 3$ over a wide range of rated power (0.5 kW–25 MW), including machines working with nonlinear network.

It is has been already mentioned (see Chap. 19 etc.) that MMF of stator windings with q fractional, especially at its small values, for example, q < 3, usually contains, as compared to MMF with integer q, additional space harmonics [1, 3–5]. The order of these space harmonics is m < p (p—number of pole pairs and order of fundamental MMF harmonic at series expansion with period being T = πD; D—stator bore diameter). The presence of this type of harmonics ("subharmonics" [8]) may cause additional vibrations of stator core and stator frame with amplitude being several times larger than an admissible value [15], though amplitudes of MMF harmonics are much less than the fundamental harmonic amplitude. To eliminate vibrations one should increase overall dimensions and weight of a generator owing to the necessity to strengthen its frame.

For this reason, on the practical level of multipole synchronous machine designing it becomes necessary when selecting the design of stator winding to examine carefully all options of stator windings with optional q number, so as to preclude additional vibrations of stator coreand frame. In this context, a need was

created to develop an analytical method of designing polyphase ($m_{PH} \geq 3$) stator winding with an arbitrary fractional number q of slots per pole and phase. There has been given a detailed account of it in [26]; in the same place, there have been described procedures validating this analytical method to design a series of winding structures.

By applying the results of such a design for a selected type of winding construction it will not be difficult to perform the analysis of MMF harmonics and to specify the amplitude and phase of its space harmonics, including those of space order m < p. The method to plot a stream step function required for such an analysis of MMF harmonics has been described in Chap. 12 with respect to the analysis of MMF of windings dropped in rotor slots; it may be used without being modified to solve this problem. It should be noted that in practice in multipole machines in order to reduce the length of jumpers between winding phase bands the jumpers are used to connect "outsider" phase bands in case when their own bands are "far"; this adversely affects the harmonic composition of winding MMF.

Let us investigate first the peculiarities of the topology of a double-layer winding with fractional q; at that, we shall assume that the count of upper bar (coil) coincides with slot number. The characteristics of single-layer winding with fractional q have been additionally studied. It is assumed that modern armature windings with phase number equal to m have $2m_{PH}$ phase zones. The q number is given in the form:

$$q = \frac{Z}{2pm_{PH}} = E + \frac{F}{H}, \tag{A.23.2.1}$$

$F < H$, $H \neq m_{PH}G$, where G = 1.2, …

Problem setting

When investigating the topology of fractional q winding and designing it the following problems [1, 5, 6] should be solved [26]:

- to set a phase zone for each bar (coil) (for example, A);
- to determine the sequence of bar (coil) connections in phase zone;
- to determine the sequence of phase zone connection, for example, star connection.

To solve the above problems it should be sufficient to determine the sequence R of bar (coil) counts in the form as follows:

$$R = \{n_D, n_E, \ldots, n_J, \ldots, n_L, \ldots, n_H\} \tag{A.23.2.2}$$

of this winding. The sequence R contains Z bar (coil) counts which are preliminarily in (A.23.2.2) placed in an arbitrary order, for example, in the form: $n_D = 1$, $n_g = 2$, …, $n_H = Z$. In this case the phase angle is between voltage vectors of bars (coils) laid down in neighboring slots [1, 5]

$$W = 360\frac{m'p}{Z} = 180\frac{m'}{m_{PH}q}. \quad (A.23.2.3)$$

However, between bar (coil) counts in sequence (A.23.2.2) there are some regularities that are to be investigated in [26]. As a result of this investigation, the subsequent sections contain the following regularities [24–26] allowing the solution of set problems:

(a) A fractional q winding contains a specified series of sequences: $R = \{R_1, R_2, \ldots, R_J, \ldots, R_K\}$.

At designing a fractional q winding it turns out to be necessary to determine the topology and the configuration of only one sequence (unitary winding R_J). The configuration of other K–1 sequences may be determined from the sequence of unitary winding R_J with the help of parameters S, K, T whose equations have been obtained in [26].

(b) A unitary winding contains one or several components, for example, for a unitary winding R_J the following is true: $R_J = \{R_J(1), R_J(2), \ldots, R_J(V), \ldots\}$.

The number of components of unitary winding $R_J(V)$ is equal to the parameter B_0 whose expression has been found in [26].

At designing a fractional q winding it turns out to be necessary to determine the topology and the configuration of only one component $R_J(V)$ making part of unitary winding R_J.

Configurations of other components of unitary winding may be specified from the component $R_J(V)$ configuration with the help of parameter D_B [26].

(c) A unitary winding components may be presented in the form:

$$R_J(V) = \{n_E, n_P, n_U, n_V, \ldots, n_H,\}, \quad (A.23.2.4)$$

at that, the difference between phase angles of voltage vectors of bars (coils) with counts n_P and n_E, ..., n_H and n_V, for each fractional q winding is minimum. In this case such a winding has a maximum distribution coefficient. Correspondingly, the difference of counts of these bars (coils) is constant and equal to the parameter Y:

$$|n_P - n_E| = \cdots = |n_H - n_V| = Y. \quad (A.23.2.5)$$

It should be noted that the difference Y is equal to the resulting fractional q winding pitch [1, 5, 6]. It follows from this that the count sequence in the component of unitary winding $R_J(V)$ corresponds to the sequence of bar (coil) connections in its configuration.

Expressions for parameters Y, D_B have also been found in [26].

(d) A unitary winding contains all m_{PH} phases (A, …, C, …) of armature winding: $R_J(V) = \{R_J(A), \ldots, R_J(C), \ldots\}$.

At designing a fractional q winding it turns out possible to determine its topology and configuration with the help of parameter K_Z [26] on the basis of the topology and configuration of only one of its phase zones, for example A.

From these regularities of fractional q winding it follows that in order to investigate the winding topology and to determine its configuration it should be necessary to find calculation relations for parameters S, T, K, B, D_B, Y, K_Z.

In [26] are obtained the calculation relations for these parameters and in detail is expounded the method of designing of the winding with their using. In the same place are presented the practical examples of designing.

Brief Conclusions [16]

1. To calculate the current distribution in the elementary conductors of coil winding it is convenient to use difference equations [8, 9]. They yield the solution for currents in a closed form.
2. In the coil-type winding of large A.C. machines the transposition of elementary conductors takes place usually only at the end parts. The transposition is formed during the coils manufacture.
3. In case of a large number of elementary conductors in the turn, not only the leakage flux of "neighbouring" turns in a slot should be taken into account, but also the leakage flux of the elementary conductors comprising the turn.
4. To reduce eddy currents and A.C. losses in the coil type winding the number of elementary conductor layers in the turn should be less than 5–6.

List of symbols

A, B, C, …	Winding phases;
B_0	Number of components of unit winding;
b_{SLT}	Slot width;
K	Number of sequences in winding;
K_Z	Winding parameter;
m_{PH}	Number of phases;
m'	Order of field spatial harmonic in air gap;
$n_D, n_g, \ldots, n_j$	Numbers of bars (coils);
p	Number of pole pairs;
q	Number of slots per pole per phase;
R	Sequence of bar (coil) numbers;
S	Winding parameter;
T	Number of bars (coils) of unit winding, its period;
W, W_M	Phase angles (el. degr.);
Y	Resulting winding pitch;
Z	Number of slots

References

I. Monographs

1. Construction of Electrical Machines. Edited by Kopylov, I.P. Moscow: Energiya, 1980. (In Russian).
2. Turbogenerators. The calculation and constructing. Edited by Ivanov N.P. and Lyuter R.A. Leningrad, Energiya, 1967. (In Russian).
3. Demirchyan K.S., Neyman L.R., Korovkin N.V., Theoretical Electrical Engineering. Moscow, St.Petersburg: Piter, 2009. Vol. 1, 2. (In Russian).
4. Kuepfmueller K., Kohn G., Theoretische Elektrotechnik und Elektronik. 15 Aufl. Berlin – New – York: Springer. 2000. (In German).
5. Mueller G., Vogt K., Ponick B., Berechnung elektrischer Maschinen. – Springer, 2007. (In German.).
6. Mueller G., Ponick B., Elektrische Maschinen. New York, John Wiley, 2009. (In German).
7. Mueller G., Ponick B., Grundlagen elektrischer Maschinen. Springer, 2005. (In German).
8. Korn G., Korn T., Mathematical Handbook. New – York: McGraw – Hill, 1961.
9. Jeffris H., Swirles B., Methods of mathematical Phisics. Third Edition, Vol. 1 – Vol. 3, Cambridge: Cambridge Univ. Press, 1966.
10. Hawkins C.C., The Dynamo, Its Theory, Design and Manufacture. Vol. III (Alternators). Isaac Pitman & Sons. London, 1925.
11. Silvester P.P., Ferrari R.L., Finite Elements for Electrical Engineers, Cambridge University Press 3 Ed., 1996.
12. Huntley H.E., Dimensional Analysis. Dover Publications. New York. 1967.
13. Finney, D. J., An Introduction to the Theory of Experimental Design. The University of Chicago Press, Chicago 1960.
14. Gotter G., Erwaermumg und Kuehlung elektrischer Maschinen. Berlin (Goettingen), Heidelberg: Springer, 1954. (In German).
15. Detienko F.M., Zagarodnaya G.A. Fastovskiy V.M.. Strength and vibration of electrical machines. L.: Energia. 1964 (In Russian).
16. Boguslawsky I.Z., A.C. motors and generators. The theory and investigation methods by their operation in networks with non linear elements. Monograph. TU St.-Petersburg Edit., 2006. Vol. 1; Vol.2. (In Russian).

II, III. Induction and synchronous machines. Papers, inventor's certificates

17. Boguslawsky I.Z., Additional losses in a bar windings of under incomplete transposition, Izvestiya RAN, Energetika, #1, 1995. (in Russian).
18. Boguslawsky I.Z., Method for calculating circulation currents in elementary conductors of a stator winding. Power Eng. (New York), No.2, 1982.
19. Boguslawsky I.Z., Demirchyan K.S., Chechurin V.L., et al., The problems of MMF and losses calculating in salient-pole machines. Proceedings Trudy LPI, 1979. #367 (in Russian).
20. Boguslawsky I.Z., Berechnung der Zusatzverluste in den Staendrwicklungen von modernen Wechselstrommaschinen. Archiv fuer Elektrotechnik (El. Eng.), 1994, No. 5, Springer Verlag, Berlin. (In German).
21. Boguslawsky I.Z., Additional losses due to eddy current in bar with different resistance of elementary conductors. Izvestiya RAN, Energetika, 1991, #4, (in Russian).

22. Boguslawsky I.Z., Untersuchung einer unkonventionellen Zweischichtwicklung fuer moderne Generatoren: Verluste, Erwaermungen und Abmessungen der Staebe. Archiv fuer Elektrotechnik (El. Eng.), 2002, No. 1, Springer Verlag, Berlin. (In German).
23. Boguslawsky I.Z., Winding factors of the 12-phase winding with fractional q for the synchronous slow-speed machines. Elektrotechnika, #7, 1976. (In Russian).
24. Boguslawsky I.Z., Twelve – zone stator winding with fractional number of slots per pole and phase for large slow – speed machines. Elektrotechnika, #1, 1978. (In Russian).
25. Boguslawsky I.Z., Features of 6 - phases armature winding of A.C. machines with the non-sinusoidal power supply. Power Eng. (New York), 1997, No. 5.
26. Boguslawsky I.Z., Kuss G., Investigation of the structure m - phase stator winding with a fractional number q. Proceedings of the Russian Academy of Sciences. Energetika, #5, 1998. (In Russian).
27. Bobkov Yu.A., Determination of parameters of compensated transposition schemes in end part of turbogenerator winding bars. Electrichestvo. 1990 #3, (In Russian).
28. Schoenfeld R., Untersuchung der Stomverdraengung und Berechnung der Widerstandsverhaeltnisse fuer Hohlleiter - Roebelstaebe. Wiss. Zeitschrift der TH Dresdn. Heft 6. 1957. (In German).
29. Taylor U., Eddy Currents in Stator Windings. Tr. AIEE. 1928.
30. Khutoretzkiy G.M., Boguslawsky I.Z., Additional losses in stator wonding of turbogenerator. Izvestiya VUZ. Elektromechnika. 1962. #8, (In Russian).
31. Neidhoefer G., Innenkuehlung von Roebelstaeben und Massnahmen zur Verminderung der Zusatzverluste. Sonderadruck aus Scientia Electrica. #14. 1968. (In German).
32. Hoercher F., Asztalos P., Zusaetzliche Verluste in Hohleitern. Bull. Der Firma Ganz. #2. 1965. (In German).
33. Boguslawsky I.Z., Dyachenko G.I., Shlendov V.D., Computation of additional losses on eddy current in winding collected on hollow and massive conductors. Electrotehnicheskaya promyshlennost, #271, Moscow.: Informelektro, 1966, (In Russian).
34. Boguslawsky I.Z., Derevitzkiy L.G., Generalization on the basis of similarity theory results of the additional losses calculation in the Rebel's bars. Electrotehnicheskaya promyshlennost, #3241, Moscow.: Informelektro, 1966, (In Russian).
35. Fomin B.I., Makarow N.I., Boguslawsky I.Z., Datskovsky L.Ch., Powerfull synchronous motors for controlled A.C. electrical drives. Sov. Electr. Eng., 1984, #8.
36. Boguslawsky I.Z., Skin effect in the bars of powerful induction motor with take into account of the temperature distribution in bars. Electrichestvo, #9, 1981, (In Russian).
37. Boguslawsky I.Z., A losses distribution in two-turns bar of double-layer winding of large motor. Elektrotechnika, 1984, #10, (in Russian).
38. Boguslawsky I.Z., Additional losses in multiturn bar winding. Elektrotechnika, 1989. #2 (In Russian).
39. Liese M., Stabtemperaturueberwachung: ein Baustein der Betriebsdiagnose zur bedarfgefuehrten Revision von Turbogeneratoren. Siemens Power Jornal (Zeitschrift des Bereichs Energieerzeugung – KWU) #3, 1995. (In German).

IV. State Standards (IEC, GOST and so on)

40. GOST (Russian State Standard) R - 52776 (IEC 60034-1). Rotating Electrical Machines. (In Russian).